UNIVERSITY OF SOUTHAMPTON

NATURAL AND ENVIRONMENTAL SCIENCE

National Oceanography Centre

Taxonomy, palaeobiogeography and relationships of cryptoclidid plesiosaurs from the Slottsmøya Member, Agardhfjellet Formation, central Spitsbergen

by

Aubrey Jane Roberts

A dissertation submitted to the University of Southampton in accordance with the requirements for award of the degree of Doctor of Philosophy in the Department of Ocean and Earth Science

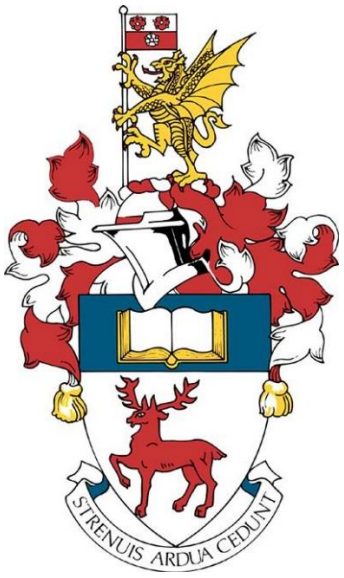

May 2017

UNIVERSITY OF SOUTHAMPTON

ABSTRACT

NATURAL AND ENVIRONMENTAL SCIENCE

Ocean and Earth Science

Thesis for the degree of Doctor of Philosophy

TAXONOMY, PALAEOBIOGEOGRARPHY AND RELATIONSHIPS OF CRYPTOCLIDID PLESIOSAURS FROM THE SLOTTSMØYA MEMBER, AGARDHFJELLET FORMATION, CENTRAL SPITSBERGEN

by Aubrey Jane Roberts

The Late Jurassic – Early Cretaceous marine reptiles of the Boreal Region, have been understudied due to limited access and poor preservation of material. Large-scale excavations in the Late Jurassic – earliest Cretaceous Slottsmøya Member of the Agardhfjellet Formation (central Spitsbergen), have resulted in the description of the first Mesozoic marine reptile Lagerstätte from the Boreal Region. Novel excavation and preparation techniques have been developed to tackle the preservation in permafrost and Arctic settings, which are documented for the first time in this work. Among the 58 collected individuals of ichthyosaurians and plesiosaurians, numerous cryptoclidid plesiosaurs are present. Cryptoclididae is a species rich clade of Middle Jurassic – Early Cretaceous long-necked plesiosaurians best known from the mid- to high-latitude regions of the Northern Hemisphere. The primary aims of this study are to describe and interpret two exceptionally preserved cryptoclidid specimens from the Slottsmøya Member. Analysis of the first specimen enabled a taxonomic clarification of *Colymbosaurus*. The second specimen is recognised as a new genus and species that preserves, for the first time, cranial material of a Late Jurassic cryptoclidid and is described with the aid of computed tomography. Phylogenetic work includes the addition of new phylogenetic characters, as well as numerous changes to the character states for individual taxa. The resulting phylogenetic trees, provides a new interpretation of the intrarelationships of the Cryptoclididae. This phylogenetic work along with comparable work performed on ophthalmosaurid ichthyosaurs, in conjunction with palaeobiogeographic methods to further our understanding of marine reptile distributions and diversity in the Boreal Region. The results from this study, presents a complex relationship with the distributional patterns of these animals through seaways, being in part, dependent on changes in eustatic sea level and tectonic development of the Northeast Atlantic.

Table of Contents

List of Tables

List of Figures

Appendix 5

Appendix 6

Appendix 7

List of Accompanying Materials

Appendix 1: Additional information for the introduction

Appendix 2: Published paper Delsett et al., 2016

Appendix 3: Supplementary information for Chapter 2

Appendix 4: Published paper Roberts et al., 2017

Appendix 5: Supplementary phylogenetic information for Chapters 2, 3 and 4

Appendix 6: Supplementary information for Chapter 3

Appendix 7: Supplementary information for Chapter 4

Appendix 8: Published paper Delsett et al., 2017

DECLARATION OF AUTHORSHIP

I, AUBREY JANE ROBERTS declare that this thesis "Taxonomy, Palaeobiogeography and relationships of cryptoclidid plesiosaurs from the Slottsmøya Member, Agardhfjellet Formation, central Spitsbergen" and the work presented in it are my own and has been generated by me as the result of my own original research.

I confirm that:

1. This work was done wholly or mainly while in candidature for a research degree at this University;
2. Where any part of this thesis has previously been submitted for a degree or any other qualification at this University or any other institution, this has been clearly stated;
3. Where I have consulted the published work of others, this is always clearly attributed;
4. Where I have quoted from the work of others, the source is always given. With the exception of such quotations, this thesis is entirely my own work;
5. I have acknowledged all main sources of help;
6. Where the thesis is based on work done by myself jointly with others, I have made clear exactly what was done by others and what I have contributed myself;
7. Parts of this work have been published as: Chapter 2 is published as Roberts et al., (2017), Journal of Vertebrate Paleontology. Published supplementary material for this thesis is available in appendices 2 (Delsett et al., 2016) and 8 (Delsett et al., 2017). The phylogenetic characters (1-270) in Appendix 5, have been published in Benson and Druckenmiller (2014).

Signed: .....

Date: .....

Acknowledgements

First of all, I would like to thank my supervisor Dr. J. H. Hurum for giving me the opportunity to work on this project and participate in the Svalbard marine reptile excavations. His enthusiasm for research and fieldwork persuaded me to study vertebrate palaeontology. Dr. Hurum has given me values and knowledge that I will treasure for the rest of my career. I also wish to thank my co-supervisor Dr. P. S. Druckenmiller, for fruitful discussions, plesiosaur skull preparation, skype conversations at crazy hours and great assistance in paper writing. I wish to thank my previous supervisor Dr. G. J. Dyke for guidance, opportunities and support. In addition, I wish to thank my supervisor Dr. Ian Harding and panel chair Dr. Jessica Whiteside for guidance and advice, throughout this project. I also would like to thank Dr. Darren Naish for introducing me to the University of Southampton, as well as numerous discussions on marine reptiles. I also wish to thank M. Smith, for assisting the VP PhD students during our time here at the National Oceanography Centre.

I would like to give a special thanks to all the volunteers, technicians, researchers and students that participated in the excavation of the specimens included in this thesis (Ø. Enger, E. M. Knutsen, M. Høyberget, S. Larsen, L. Kristiansen, T. Wensås, L. Novis, N. Munthe-Kaas, H. A. Nakrem, J. Rousseau, L. Liebe Delsett, E. Tundstad and B. Lund). I am eternally grateful to ML. Knudsen Funke, who taught me the art of fossil preparation and for assisting me along with V. Engelschiøn Nash, M. Koevoets and C. Ekeheien in preparing the specimens described in this thesis. I would like to thank O. Katsamenis for access to the µ-vis visualization laboratory at the University of Southampton and Ø. Hammer and B. Cordonnier for assistance with CT scanning and interpretation in Oslo.

In particular I would like to extend my gratitude to my co-students in Southampton (J. Lawrence Wujek, E. Martin-Silverstone, R. Gandola, L. Muscutt, A. Irwin, J. Hansford and E. Newham) and in Oslo (L. Liebe Delsett, K. Hyrniewicz and M. Koevoets), for sharing this experience and helping each other through the trials of thesis writing. The fossil collectors along the Dorset coast (P. Howe, R. Edmonds, S. Etches and C. Moore), have my sincere gratitude for showing me their collections and for discussion. I warmly thank my dear friend and amazing artist E. van Hulsen for painting and drawing one of the plesiosaur specimens included in this thesis. I would also like to thank other students and researchers that have been supportive, shared ideas and assisted me during my PhD (D. Foffa, J. Liston, D. Legg, V. Fischer, M. S. Fernández, M. O'Sullivan, R. B. J. Benson and

D. Lomax). In particular, I would like to thank my dear friend and co-author of the field blogs V. Engelschiøn Nash, for keeping me digging even in the toughest conditions and for assisting with last minute editing. Last but not least I would like to thank L. Liebe Delsett, for our amazing team work and discussions on marine reptiles and for sharing ideas.

This project was funded by NERC, the University of Southampton and the University of Oslo with a grant from Tullow Oil. The fieldwork leading to this study was financed by Exxon Mobil (2007-2011), Fugro (2007, 2009-2011), Spitsbergen Travel (2007-2012), The Norwegian Petroleum Directorate (2007-2008), Hydro (2007), The Norwegian Research Council (2007), The Norwegian Ministry of Education and Research (2007), StatoilHydro (2008), Brian Snyder (2010), OMV (2009-2012), Nexen (2010-2011, Tullow Oil (2012) and National Geographic (2009-2011). Travel grants for research trips and conferences from PalAss (2014) and Synthesys (2014), were of great assistance for this project.

I want to thank all the institutions, curators and researchers for hosting me or supplying me with information: NHMUK (Sandra Chapman), MOZ and MLP (M. Fernandez), CAMSM (M. Riley), LEICS (M. Evans), GLAHM (N. Clark), NOTNH (A. Smith), OUM (E. Howlett), YORKM (S. King), UWM (L. Vietti), Copenhagen (G. Cuny), PETRM (G. Wass), MANCHM (K. Sherburn), DONMG (D. Lomax), CASP (S. Kelly), Glasgow Museum RC (A. Ainsworth), and NMS (S. Walsh).

I wish to thank my parents (Jayne and Andrew Roberts), for financial, academic and moral support, this project would not have been possible without you. I wish to thank extended family and close friends (S. Trice and J. Brown) for help and encouragement during my time as a PhD student. My eternal gratitude and love goes to M. Leach, who kept me fed, reasonably healthy and has been so patient during the final stages of my degree.

Finally, I wish to dedicate this thesis to my late grandfather Commander Anthony James Roberts OBE, RN, for the inspiration to be an explorer.

Definitions and Abbreviations

GAI, Geographic area of interest

MPT, Most parsimonious tree

PAE, Parsimony analysis of endemicity

OTU, Operational taxonomic unit

UK, United Kingdom

µCT, Micro computed tomography

Institutional Abbreviations

BRSMG, Bristol City Museum and Art Gallery

CAMSM, Sedgwick Museum of Earth Science, Cambridge University, Cambridge, United Kingdom

GLAHM, Hunterian Museum, University of Glasgow, United Kingdom

GMLU, Geological Museum of the University of Lodz, Poland

LEICS, Leicester New Walk Museum, United Kingdom

MANCH, Manchester Museum, United Kingdom

MGUH, Geological Museum, Copenhagen, Denmark

NHMUK, Natural History Museum, London, United Kingdom

NOTNH, Wollaton Hall, Nottingham, United Kingdom

OUM, Oxford University Museum of Natural History, United Kingdom

PETRM, Peterborough Museum, United Kingdom

PMO, Paleontological Museum Oslo, University of Oslo, Norway

PMU, Paleontological Museum of Uppsala, Museum of Evolution, Uppsala, Sweden

SVB, Svalbard Museum, Longyearbyen, Norway

UNIS, University Centre in Svalbard, Norway

UW, University of Wyoming, United States

YORKM, York Museum and Art Gallery, United Kingdom

Introduction

Introduction

The main purpose of this doctoral research is the description of two well-preserved plesiosaur specimens from the Late Jurassic – earliest Cretaceous Slottsmøya Member of Spitsbergen (Svalbard). Using phylogenetic analysis and palaeobiogeographic methods, these two specimens are put into a global perspective and thereby increase our knowledge about the distribution and taxonomic diversity of Boreal marine reptiles during this interval.

1.1 General introduction to plesiosaurs: their palaeobiology, ecology and evolutionary history

Plesiosaurs are a clade of secondarily marine reptiles, which inhabited marine and some lacustrine environments during the Mesozoic Era (Kear, 2006; Taylor and Cruikshank, 1993). They are a derived clade within Sauropterygia (Owen, 1860); a group which encompasses plesiosaurs and their Triassic relatives, the pistosaurids, placodonts, pachypleurosaurs and nothosaurs (Storrs, 1993). The earliest unambiguous remains of plesiosaurs are known from the latest Triassic (Rhaetian) (Storrs, 1994; Taylor and Cruikshank, 1993), although a possible specimen has been described from the Norian of Russia (Sennikov and Arkhangelsky, 2010). This group shares a close phylogenetic relationship with pistosaurids, a group of Triassic stem sauropterygians known chiefly from China, Nevada and Europe (Cheng et al., 2006; Rieppel et al., 2002). By the Early Jurassic, plesiosaurs had diversified into multiple clades, size ranges and morphotypes and attained a worldwide distribution (Benson et al., 2012; Thulborn and Warren, 1980). Fossilised remains of this group are known from every continent including high latitude areas and even fresh water deposits (Hurum et al., 2012; Kear, 2006). Plesiosaurs did not survive the K-Pg extinction event, suggesting an overall lineage temporal span of around 138 Ma (Storrs, 1997).

Traditionally, Plesiosauria was split into two major groups based on their basal body morphology; Pliosauridae and Plesiosauridae (Figure 1). Plesiosauridae were characterised by their large number of cervicals and small cranium (A), whereas Pliosauridae had fewer cervical vertebrae and a large macropredatory

cranium (B). In recent years, the use of phylogenetic analyses, has shown that these two different body plans evolved independently multiple times (O'Keefe, 2001). However, the terms pliosauromorph and plesiosauromorph, are commonly used in the literature when referring to body plan type (Ketchum and Benson, 2010).

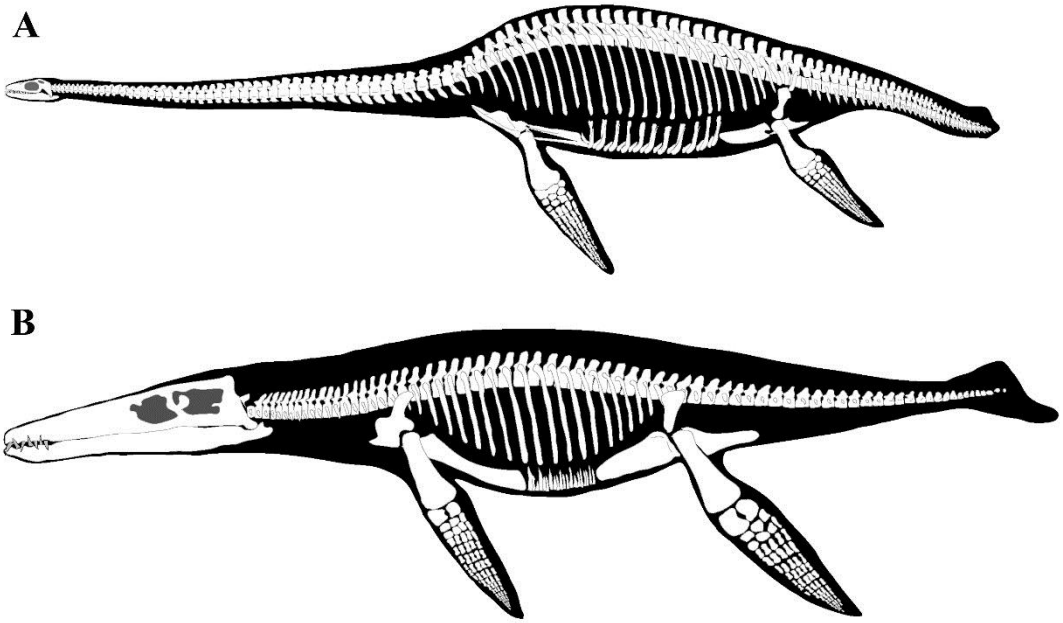

Figure 1: The two different body plans present in plesiosaurians. **A**, a plesiosauromorph type, with a long neck and small cranium in respect to body size (based on PMO 224.248). **B**, a pliosauromorph type, short neck and large head in respect to body size (modified from Knutsen, 2012).

Being obligate marine tetrapods, derived plesiosaurs show significant adaptations to marine life. These include posterodorsally retracted external nares, reduced epipodials, evidence of live birth and the unique use of four similarly sized hydrofoil-shaped limbs for forward propulsion (Cruickshank et al., 1991; Halstead, 1989; Massare, 1994; O'Keefe and Ciappe, 2011). Hypotheses regarding plesiosaur feeding preferences are commonly reflected by their body plan: the pliosauromorph type has been suggested to feed on larger prey ranging from fish to other reptiles, while the plesiosauromorph type has been suggested to feed on smaller and/or soft prey in the water column or in soft sediments (Massare, 1987; Noè et al., 2017).

The general ontogenetic stage of individual plesiosaurs is easily recognised, by the definitions suggested by Brown (1981) and are followed in this thesis:

juveniles are distinguished by the lack of fusion along the neurocentral suture between the neural arches and vertebral centra, adults show fusion between the neural arches and centra, whereas old adults show additional fusion of limb elements and other features of advanced ossification (e.g. distinct distal facets on the propodials).

1.2 Plesiosaurian phylogenetic relationships

Early attempts to classify and separate Plesiosauria into different families, were largely based on the two different body plans. The early and subsequent work is well summarised in Ketchum and Benson (2010). The last major pre-cladistic classification of plesiosaurs by Brown (1981), split Plesiosauria into Plesiosauroidea and Pliosauroidea. Plesiosauroidea included three families; Plesiosauridae, Elasmosauridae and Cryptoclididae, whereas Pliosauroidea included a single family Pliosauridae.

Following the first phylogenetic studies of Plesiosauria (e.g.Bardet and Godefroit, 1998; Carpenter, 1999; Hampe, 1992; O'Keefe, 2001), a new understanding was reached of the convergent evolution that took place in the different lineages. Numerous problematic clades of plesiosaurs have had enigmatic relationships to other groups, with the most discussed of these being the polycotylids and leptoclidids. These two Cretaceous groups include taxa with a pliosauromorph body plan and were previously defined as pliosauroids. These two groups have since been placed inside Plesiosauroidae as their pliosauromorph condition was found to be convergent with Pliosauroidae (O'Keefe, 2001). More recently, the phylogenetic research by Benson and Druckenmiller (2014) has started to build a consensus on our understanding of general relationships between the major clades of plesiosaurs (Figure 2). Benson and Druckenmiller (2014) placed these two groups (Leptocleidia = Leptocleididae + Polycotylidae) plesiosaurs as a sister clade to elasmosaurids, creating a new clade (Xenopsaria) to encompass them (Figure 2). Improvements on the phylogenetic work for individual clades have been made for pliosaurids (Benson et al., 2013; Fischer et al., 2015) and cryptoclidids (Benson and Bowdler, 2014; Roberts et al., 2017). Other researchers have proposed alternative phylogenetic trees for Xenopsaria with different taxa and characters included, yielding marginally

different and often poorly resolved results (Sachs et al., 2016; Sachs and Kear, 2015, 2017). This illustrates that although the intra-relationships of plesiosaurs is approaching a consensus, further detailed work is required to increase the resolution for some clades. One of the focus points of this thesis, is the phylogenetic position and interrelationships of the clade Cryptoclididae, a group of long-necked plesiosauroids. The phylogenetic work and data included in this thesis, builds upon the published dataset and character list published in Benson and Druckenmiller (2014) available on Dryad (http://datadryad.org/resource/doi:10.5061/dryad.v843v) with numerous additions and changes.

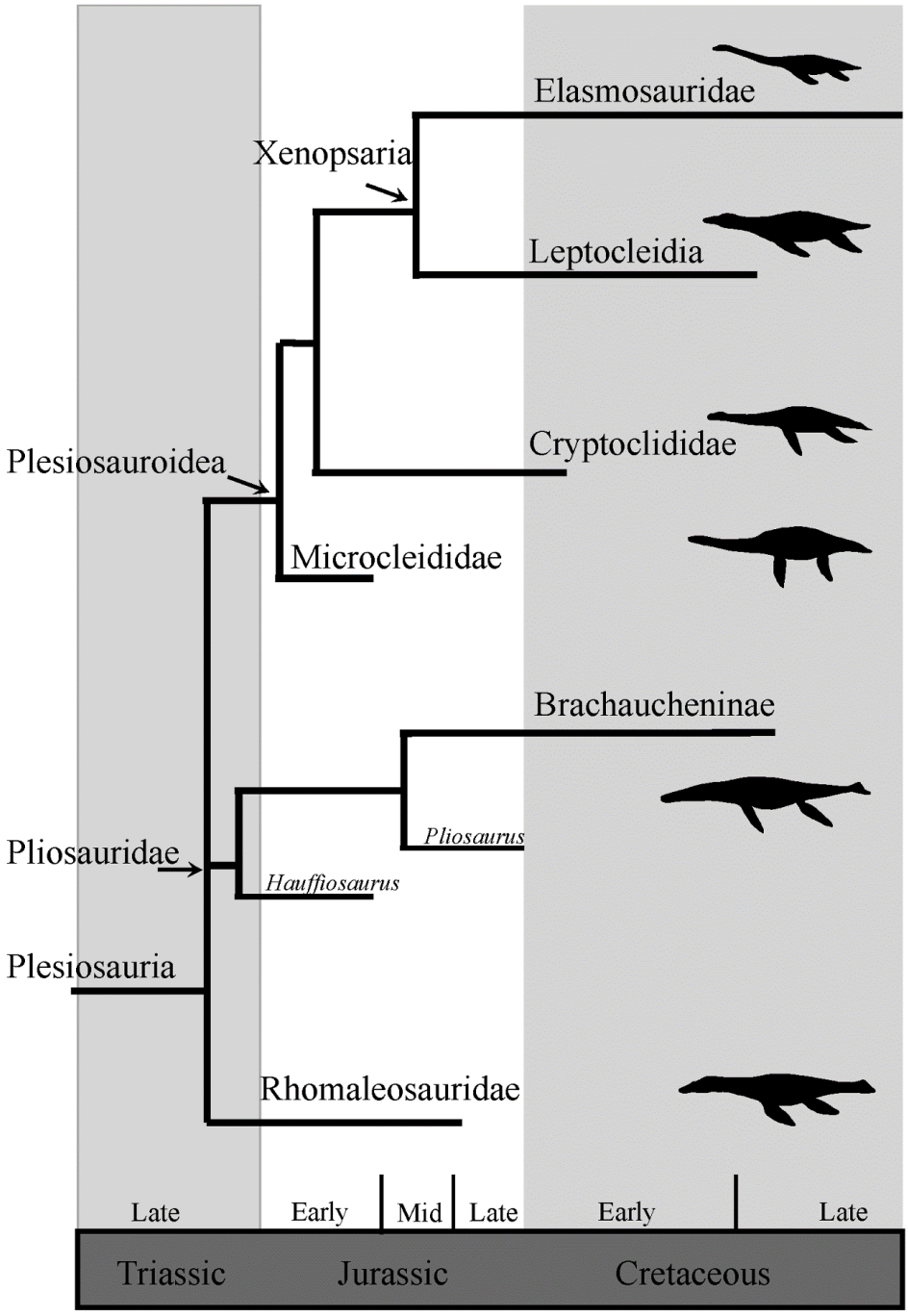

Figure 2: A generalised view of general plesiosaur phylogenetic relationships and body shape, simplified from Benson and Druckenmiller (2014).

1.2.1 The Middle Jurassic – Early Cretaceous – a time of change

The Middle – Late Jurassic represents a time of change for plesiosaurians, with the dominating groups of the Early – early Middle Jurassic (e.g. rhomaleosaurids and microcleidids) replaced by new clades (pliosaurids and cryptoclidids) (Benson and Druckenmiller, 2014). During the Late Jurassic a high taxonomic diversity of plesiosaurs was recorded, although predominantly documented from the northern hemisphere (Chapter 4, this volume). Another faunal change continued at the Jurassic – Cretaceous transition, resulting in a substantial loss in taxonomic diversity of cryptoclidid plesiosaurs with only one described taxon surviving into the Cretaceous (*Abyssosaurus nataliae*; Benson and Druckenmiller, 2014; Berezin, 2011a). Pliosaurids also suffered a loss in disparity following the Jurassic – Cretaceous transition, with only a single clade (Brachaucheninae) enduring till the Late Cretaceous (Benson and Druckenmiller, 2014). The Early Cretaceous saw the appearance of new groups of plesiosaurs, the xenopsarians, with their earliest representatives known from the Berriasian of Europe (Sachs et al., 2016). This clade continued to diversify until the final extinction of plesiosaurs at the Cretaceous – Palaeocene boundary (Benson and Druckenmiller, 2014; Serratos et al., 2017).

1.3 The Cryptoclididae: a long-known yet enigmatic plesiosaurian family

Since its initial description, the Middle Jurassic – Early Cretaceous plesiosauroid family Cryptoclididae (Williston, 1925), has been referred to numerous placements in Plesiosauria. The family has been incorporated into the Elasmosauridae, based on the similarities chiefly from the post-cranial skeleton (Brown, 1981; Ketchum and Benson, 2010). In some cases, some cryptoclidid taxa were grouped with elasmosaurids (Cimoliasauridae), in a sister-group relationship to polycotylids (Schumacher, 2007). With the increase of characters in phylogenetic data matrices and the addition of more complete specimens with cranial data and new taxa, the Cryptoclididae was re-established as its own family as a sister group to Xenopsaria (Elasmosauridae + Leptocleidia; Benson and Druckenmiller, 2014) and is the only long-necked plesiosauroid clade present in the Late Jurassic.

Cryptoclididae has been defined on primarily post-cranial synapomorphies, following Benson and Bowdler (2014), including (but not limited to); the morphology of the cervical vertebral, coracoid and epipodials. This thesis has added several possible synapomorphies for this clade (Chapter 3, this volume), although due to the lack of cranial material, it is uncertain if these are present in all taxa.

In previous work, Cryptoclididae has been split into two subclades, although one of these is yet to be formally named. The named subclade, the Colymbosaurinae [Benson and Bowdler, 2014] is a cryptoclidid subfamily, including all the known plesiosauroid taxa from the Slottsmøya Member of Spitsbergen alongside taxa from the UK, North America and Russia. This subfamily is solely defined by postcranial synapomorphies, as cranial material is poorly known from this group (Benson and Bowdler, 2014). Due to the small number of synapomorphies described for this clade, and that these are not present or preserved in all taxa, the subfamily is poorly supported by the phylogenetic analyses on Plesiosauria (Roberts et al., 2017; Chapter 2, this volume).

The cryptoclidid material from the Late Jurassic – Early Cretaceous (Volgian) Slottsmøya Member of Spitsbergen, represents a large fraction of the cryptoclidid taxa described from this interval. The incorporation of the new specimens from there (this volume), altered our understanding of cryptoclidid intrarelationships. The new taxon *gen. et species nov.* (Chapter 3, this volume) preserved a significant amount of cranial material and postcranial material and displayed numerous postcranial features, some of which are synapomorphies for Colymbosaurinae. When the new taxon was incorporated into a phylogenetic analysis, most of this subfamily was shifted elsewhere in the strict consensus tree (Chapter 3, this volume). This shows that the original configuration of this subclade is poorly supported and could be subject to conflicting phylogenetic characters (cranial vs. post-cranial).

1.3.1 The cryptoclidid fossil record and historical collections

Cryptoclididae has a long historical record in Europe due to the Middle to Late Jurassic clay quarries in the south and midlands of England. During Victorian times, numerous collectors donated and sold vast amounts of specimens to primarily

(but not limited to) UK museums. Among these, the "Leeds collection" yielded a significant amount of cryptoclidid plesiosaur specimens from the Callovian Oxford Clay Formation (min. 60 diagnosed specimens; J. Liston *pers. comm.*). These collections have proven valuable for researchers, in building an understanding of the interspecific diversity and ontogenetic change in cryptoclidid plesiosaurs (Brown, 1981). This thesis includes comparisons to cryptoclidid specimens held in 13 museum collections from the Oxford Clay and Kimmeridge Clay Formations, resulting in the documentation of over 200 individual cryptoclidid specimens from these formations. This material is the most extensive collection available for comparison with the Slottsmøya Member cryptoclidids. Although not as rich and extensively collected as the Oxford and Kimmeridge Clay Formations, several localities outside Europe bear cryptoclidid material including the Sundance Formation (USA) and several formations in Russia.

Figure 3: The worldwide distribution of cryptoclidid fossils (Middle Jurassic – Early Cretaceous), based on published and undescribed material. For references on different localities, see table Appendix 1, Table A1.1.

Equatorial and Southern hemisphere cryptoclidids

Cryptoclidid specimens from the southern hemisphere are rare and at present are only known from the Callovian – Kimmeridgian interval. Specimens referred to cf. *Muraenosaurus* and cf. *Cryptoclidus* from the early Callovian of Argentina (Chacaico Sur), although undiagnostic, share affinities to taxa from the Callovian

Oxford Clay Formation of Europe (Gasparini and Spalletti, 1993). *Vinialesaurus caroli*, a taxon described from cranial and anterior cervical material from Cuba, comes from the Jagua Vieja Member (middle-late Oxfordian) of the Jagua formation (Gasparini et al., 2002). Unfortunately, the specimen is poorly preserved and is therefore usually excluded from phylogenetic analyses (Benson and Druckenmiller, 2014).

From the Late Jurassic, a series of cervical centra discovered in the Katrol Formation (Kimmeridgian) of the Kutch province in India, have been referred to Cryptoclididae indet. (Bardet et al., 1991). In addition, a single plesiosauroid vertebra has been described from the Late Jurassic – Early Cretaceous part of the Chichali Formation of Pakistan (Buffetaut, 1981). This specimen could represent a cryptoclidid vertebra, but poor preservation and stratigraphic control of the specimen's origin means a diagnosis beyond Plesiosauroidea cannot be made. The significance of some of the material, is that it shows the presence of cryptoclidids in the southern Tethys during the Late Jurassic.

Oxford Clay Formation

The Oxford Clay Formation stretches from the Callovian to Oxfordian (Cox et al., 1992). The majority of the marine reptile material comes from the Callovian Peterborough Member, although some fragmentary material is available from the Oxfordian (Benton and Spencer, 1995). Several genera and species of cryptoclidids are known from the Peterborough Member of the Oxford Clay Formation; *Cryptoclidus*, *Muraenosaurus* and *Tricleidus* (Andrews, 1910; Martill et al., 1994). Of these three genera, *Cryptoclidus* and *Muraenosaurus* are the most commonly represented among the preserved material. Although previously synonymised with *Muraenosaurus* (Brown, 1981), '*Picrocleidus*' may represent an additional genus. More recent research has pointed out that there are some major morphological and phylogenetic differences between *Muraenosaurus* and the holotype of '*Picrocleidus*', warranting redescription (Benson and Druckenmiller, 2014). All of these taxa are described from partial cranial and postcranial material (Brown, 1981), with the most extensive of these being *Cryptoclidus eurymerus* including complete cranial material available in museums and private collections (Andrews, 1910;

Brown, 1981; Brown and Cruickshank, 1995). Other marine reptiles described from the Peterborough Member include thalattosuchians (teleosaurids and metriorhychids), pliosauroids and ichthyosaurs (Andrews, 1913; Ketchum and Benson, 2011; Moon and Kirton, 2016). The largest collection of Oxford Clay Formation marine reptiles is held at the Hunterian Museum, Glasgow (UK).

Sundance Formation

The Sundance Formation stretches over the Middle to early Late Jurassic of Wyoming and South Dakota. The Redwater Shale Member (informal member: Oxfordian) is part of the Upper Sundance Formation (Imlay, 1980; Pipiringos, 1968). Several marine reptile taxa have been described from the member, including an ichthyosaur (*Ophthalmosaurus natans*), a pliosauroid (*Megalneusaurus rex*) and two cryptoclidid taxa (*Tatenectes laramiensis* and *Pantosaurus striatus*) (Massare et al., 2014). Of the cryptoclidid plesiosaurs, *Tatenectes laramiensis* is the most known, with five referred specimens (O'Keefe and Street, 2009; O'Keefe and Wahl, 2003b). One of the specimens (UW 24215) of *T. laramiensis* preserves cranial material, although this is too poorly preserved to be described and compared to other more complete taxa in detail (Buchy et al., 2006a).

Kimmeridge Clay Formation

While not as articulated as the Oxford Clay Formation plesiosauroids, marine reptile remains are also common in the Kimmeridge Clay Formation. This formation is exposed and well-studied in southern and eastern England, but is also present in northern France (Boulonnais). In the UK, the Kimmeridge Clay Formation covers the Kimmeridgian and Tithonian (Morgans-Bell et al., 2001), including numerous horizons shown to bear marine reptiles and other vertebrate material (Grange et al., 1996; Martill et al., 2006). All of the marine reptile finds appear to come from the shales, although this is not always clear for historic specimens (Benton and Spencer, 1995). Marine reptile material is most common in the *autissiodorensis*, *hudlestoni* and *pectinatus* zones, with some rare material from the *pallasiodes* and *rotunda* zones. Isolated plesiosaur bone elements can be find throughout the entire succession (S. Etches *pers. comm*.).

Benson and Bowdler (2014) suggested that more taxonomic diversity of cryptoclidids is present in the Kimmeridge Clay than previously understood. To date, two (widely accepted) cryptoclidid genera have been described from the formation; *Kimmerosaurus* and *Colymbosaurus* (Brown, 1981). *Kimmerosaurus langhami* is currently known from a partial skull and cervical vertebrae from the *pectinatus* zone (Tithonian: Brown et al. 1986) and a currently undescribed specimen from below the *mutablis* zone from Wiltshire (Grange et al., 1996). However, the Wiltshire material cannot be located at the BRSMG and it is unknown how diagnostic the material is (D. Foffa *pers. comm.*). *Colymbosaurus* is chiefly known from postcranial material, and is by far the most common cryptoclidid taxon in the Kimmeridge Clay Formation (Benson and Bowdler, 2014). Brown (1981), argued that these two genera could be synonymous as they lacked significant overlapping material. This has later been dismissed by further descriptions of *Colymbosaurus* material (Benson and Bowdler, 2014; Knutsen et al., 2012c) and the work in this thesis (Chapter 2, this volume; Roberts et al., 2017). A third species is possibly present described as '*Plesiosaurus*' *mansellii* (Hulke, 1870), but this specimen requires redescription (Benson and Bowdler, 2014; Roberts et al. 2017). The type specimen of '*P.*' *mansellii* is interpreted to come from the *scitulus* zone (Benton and Spencer, 1995).

Numerous specimens of other marine reptiles, ichthyosaurs (*Nannopterygius enthekiodon*, *Brachypterygius extremus*, *Ophthalmosaurus icenicus*), thalattosuchians (*Steneosaurus*, *Geosaurus*, *Machimosaurus*, *Dakosaurus*) and pliosaurids (*Liopleurodon*, *Pliosaurus*), are also found throughout the formation (Benson et al., 2013; McGowan and Motani, 2003; Moon and Kirton, 2016; Young and Steel, 2014; Young et al., 2014; Young et al., 2015).

Russian Cryptoclidids

Excavation and description of Middle – Late Jurassic marine reptile material has a long history in Russia (Storrs et al., 2000), although many of the early specimens were described in Russian and not figured. The majority of the historical specimens were recovered as chance occurrences in quarries and oil shale mines, or as float in the Volga and Moscow River basins (Storrs et al., 2000). Bogolyubov (1911) named several new plesiosaur taxa based on fragmentary specimens, all of

which have been considered *nomina dubia* (Storrs et al., 2000). However, recent efforts have been made to redescribe historical specimens in addition to new material (Arkhangelsky et al., *in press*; Zverkov et al., 2015). Some of the material in Bogolyubov (1911) has been redescribed and assigned to *Colymbosaurus* indet. (Arkhangelsky et al., *in press*). A more complete cryptoclidid (*Abyssosaurus nataliae*), from Chuvashia was described in Russian (Berezin, 2011b) and in English (Berezin, 2011a), represents the only cryptoclidid specimen described from the upper Hauterivian (Cretaceous).

The Slottsmøya Member (Agardhfjellet Formation) of Spitsbergen (Svalbard)

The plesiosaur material described in this thesis derives from the Late Jurassic – earliest Cretaceous Slottsmøya Member of central Spitsbergen. As a marine reptile Lagerstätte, the Slottsmøya Member preserves the richest and best-preserved specimens of plesiosaurians and ichthyopteygians worldwide during the Tithonian – Berriasian (Volgian) interval (Delsett et al., 2016). Extensive sampling in this region has led to a large collection held at the University of Oslo Natural History Museum and the Svalbard Museum. Details and previous research on this member is found in section (1.5).

1.4 The Late Jurassic – Early Cretaceous Boreal Region

The Late Jurassic – Early Cretaceous Boreal Sea, consisted of a wide epicontinental sea between 300 – 600 m in depth (Dypvik and Zakharov, 2012). Palaeotemperature estimates from isotope analysis from the Boreal Region during the Tithonian – Valanginian show a colder water temperature (5 – 10°C, King Carls Land, Ditchfield, 1997; 13 – 16°C, Spitsbergen, Hammer et al., 2011), in comparison to estimates for Europe (13.9 – 19.8°C, Gröcke et al., 2003). Although some of the variation from the different Boreal sections can partially be ascribed to the different organisms the isotopes were sampled from (e.g. pelagic cephalopods vs. bottom dwelling brachiopods), some could suggest temporal/regional fluctuations in climate and sea temperature in the Late Jurassic Boreal Sea. The colder temperatures of the Boreal Sea, may have been responsible for the lack of thalattosuchian and testudine fossils in the region (Chapter 4, this volume).

1.4.2 Spitsbergen

The Svalbard archipelago (Norway) is located between 74° and 81° north and 10° and 35° east and includes numerous islands, the largest of which is Spitsbergen (Figure 4). Svalbard has exposures of strata ranging from Archean to Quaternary in age (Harland, 1997), giving a detailed account of the history of life with numerous and important animal and plant fossils, particularly from the Mesozoic (Hurum et al., 2012; Hurum et al., 2016; Kear et al., 2016; Launis et al., 2014). During the Mid to Late Mesozoic, Svalbard was positioned at a relatively high latitude of approximately 60-70° North (Ditchfield, 1997) and was part of the Boreal Region. The Jurassic-Cretaceous outcrops are largely constrained to central and southern Spitsbergen (Parker, 1967). As the geological setting of Spitsbergen in the Late Jurassic – Early Cretaceous is covered in the individual introductions to the chapters and in Delsett et al., 2016 (Appendix 2), only a general summary of the geological setting and current research on the Agardhfjellet Formation will be given here.

Central Spitsbergen (Nordenskiöld Land), includes a mountain range between Sassendalen and Adventdalen with large and accessible outcrops of Mesozoic strata (Hurum et al., 2012). The Agardhfjellet Formation constitutes sedimentary rocks between Mid Jurassic – Early Cretaceous in age, based on macrofossils (Wierzbowski et al., 2011), foraminifera (Hjálmarsdóttir et al., 2012; Nagy and Basov, 1998), palynology (Bjærke, 1980; Dalseg et al., 2016) and high resolution organic carbon-isotope stratigraphy (Koevoets et al., 2016). The Agardhfjellet Formation consists of four members: Based on the organic carbon isotope data and diagnostic ammonites both from field collecting at Janusfjellet and from drill cores made by Longyearbyen (central Spitsbergen), ages of the individual members can be estimated: the Oppdalen Member (Mid Jurassic), the Lardyfjellet Member (early Oxfordian – earliest late Kimmeridgian), the Oppdalsåta Member, (late Kimmeridgian – earliest Tithonian) and the Slottsmøya Member (Tithonian – Berriasian or Volgian)(Koevoets et al., 2016).

Figure 4: A map of Svalbard with the settlements marked as dots and the field site marked as a star.

Sedimentology and depositional environment of the Slottsmøya Member

Recent research on the depositional environment and fauna of the Slottsmøya Member, contributes to our understanding of this high latitude environment at the Jurassic – Cretaceous boundary (Hurum et al., 2012). The Slottsmøya Member represents approximately 12 million years of deposition, with a thickness ranging between 70 – 100 m (Delsett et al., 2016; Dypvik et al., 1991; Hammer et al., 2011). Previously the Slottsmøya Member was considered to be Volgian in age (Dypvik et al., 1992; Mørk et al., 1999), but new descriptions of macrofossils (ammonites) and agglutinated foraminifera suggest an Early Volgian to Late Ryazanian (Tithonian –

Berriasian) age for the member (Hjálmarsdóttir et al., 2012; Wierzbowski et al., 2011). The abundance of plant debris and dinoflagellates, as well as the sequence stratigraphy, indicate an initial transgressive sequence in the oldest section of the member, followed by a regression into the Early Cretaceous (Dalseg et al., 2016; Koevoets et al., 2016).

The Slottsmøya Member largely consists of grey shales, often weathered into paper shale and widespread dolomite and siderite interbeds and nodules (Collignon and Hammer, 2012). The depositional environment is interpreted to have been dysoxic with periodic oxygenation of the bottom water, with a low sedimentation rate (Collignon and Hammer, 2012). Two sideritic storm deposits are present which serve as marker beds throughout central Spitsbergen: The oldest, used as a marker bed (0 m on the log, "Echinoderm bed"; Rousseau and Nakrem, 2012). A secondary, younger marker bed, the *Dorsoplanites* bed, is present in the upper-most section of the member (27 m) and defined by a high abundance of the perispinctid Middle Volgian ammonite *Dorsoplanites* sp. (Collignon and Hammer, 2012; Delsett et al., 2016).

Numerous hydrocarbon seep carbonate bodies can be found in the upper-most section of the Slottsmøya Member (Hammer et al., 2011). Invertebrate fossils are numerous in the seep bodies, showing a high diversity assemblage of bivalves, brachiopods, gastropods, serpulids, with rare occurrences of cephalopods, sponges, echinoids, crustaceans, scaphopods and vertebrate material (Hryniewicz et al., 2015). In addition, occurrences of sunken driftwood are common in and surrounding the seep carbonate bodies (Hryniewicz et al., 2015). This fauna includes few seep obligate taxa (7.8 % of total abundance), which is consistent with a shallow epicontinental sea palaeoenvironment during deposition (Hryniewicz et al., 2015).

1.5 The Slottsmøya Member fauna

1.5.1 Fossil marine reptiles from Svalbard: a historical context

Marine reptile excavations on the island of Spitsbergen in the Archipelago of Svalbard (Norway) have a long history starting in the 1860s. The first expeditions explored Triassic outcrops and several specimens of primitive ichthyopterygians

were found and described (Hulke, 1873; Yakovlev, 1903). Material from later expeditions included a single pliosaurid centrum described by Wiman (1914), which shared similarities with *Peloneustes* (Lydekker, 1889). These specimen, along with additional material from these early expeditions have since been redescribed (Kear and Maxwell, 2013; Maxwell and Kear, 2013). A fieldtrip in 1931 by a team of American medical doctors excavated a partial skeleton of a plesiosaurian from the Slottsmøya Member, Agardhfjellet Formation in central Spitsbergen. The specimen was donated to the University of Oslo Natural History Museum and later described as a new taxon of cryptoclidid plesiosaur; '*Tricleidus' svalbardensis* (Persson, 1962). Other isolated material was later described by Ginsburg and Janvier (1974). In 2001, a group of students and researchers from the University Centre in Svalbard (UNIS) discovered a partial skeleton of a plesiosaur in the Slottsmøya Member outcrop on the slopes of Janusfjellet, which was later excavated by the University of Oslo, Natural History Museum in 2004 (Hurum et al., 2012). This expedition gave rise to a series of yearly excavations (2006-2012) in the region by the University of Oslo, resulting in a total of 58 excavated specimens of marine reptiles in addition to the historical material (List available in Appendix A1, Table A1.1).

The macro vertebrate material recovered from the Slottsmøya Member is fragile and in some cases extremely fractured. New methods were developed over the past few years during the preparation of the plesiosaurian and ichthyopterygian material. These methods combined with µComputed Tomography (µCT), are presented as a separate methods chapter (Chapter One, this volume).

1.5.1 The Cryptoclidid taxa of the Slottsmøya Member

Of the 58 collected marine reptile specimens, 26 are plesiosauroid plesiosaurs (Figure 5). In a PhD thesis completed by Knutsen (2012a), and in resulting papers (Knutsen et al., 2012a, c, d) three novel taxa of cryptoclidid plesiosaurs were described and '*Tricleidus' svalbardensis (*1931 specimen) along with additional material was referred to *Colymbosaurus svalbardensis* (Figure 5). Of the cryptoclidid genera described from the Slottsmøya Member in Knutsen (2012), *Spitrasaurus* is by far the most complete. This genus includes two taxa, *S. larseni* and *S. wensaasi*, both of which are represented by juvenile type specimens (Knutsen

et al., 2012d). Despite the problematic ontogenetic state, this genus is easily differentiated from all other cryptoclidids with the most striking feature being the length of the neck (60 cervical vertebrae in *S. wensaasi*). *Djupedalia* is a monotypical taxon, with a single species *D. engeri* described from a juvenile individual (Knutsen et al., 2012a). *D. engeri* can be differentiated from *Spitrasaurus* and other penecontemperanous taxa by unique features of the braincase, cervical vertebrae and limbs (Knutsen et al., 2012a, d).

An additional cryptoclidid from the Slottsmøya Member was published by Kear and Maxwell (2013), as a historical specimen held in the Wiman collection at the Evolution Museum in Uppsala, Sweden. This specimen was suggested to be *Colymbosaurus svalbardensis*, but based on the research presented in Chapter 2 (this volume), is not referable to the genus. In addition, this specimen was heavily reconstructed and therefore most elements are hard to describe with confidence. Nonetheless, this does not contract from the historical significance of this specimen.

The material included in this thesis includes two partial skeletons of adult cryptoclidid plesiosaurs, which have been systematically described and compared to other cryptoclidid taxa. These two specimens represent two of the most complete plesiosaur specimens remaining to be formally described from the Slottsmøya Member material held at the Natural History Museum, Oslo.

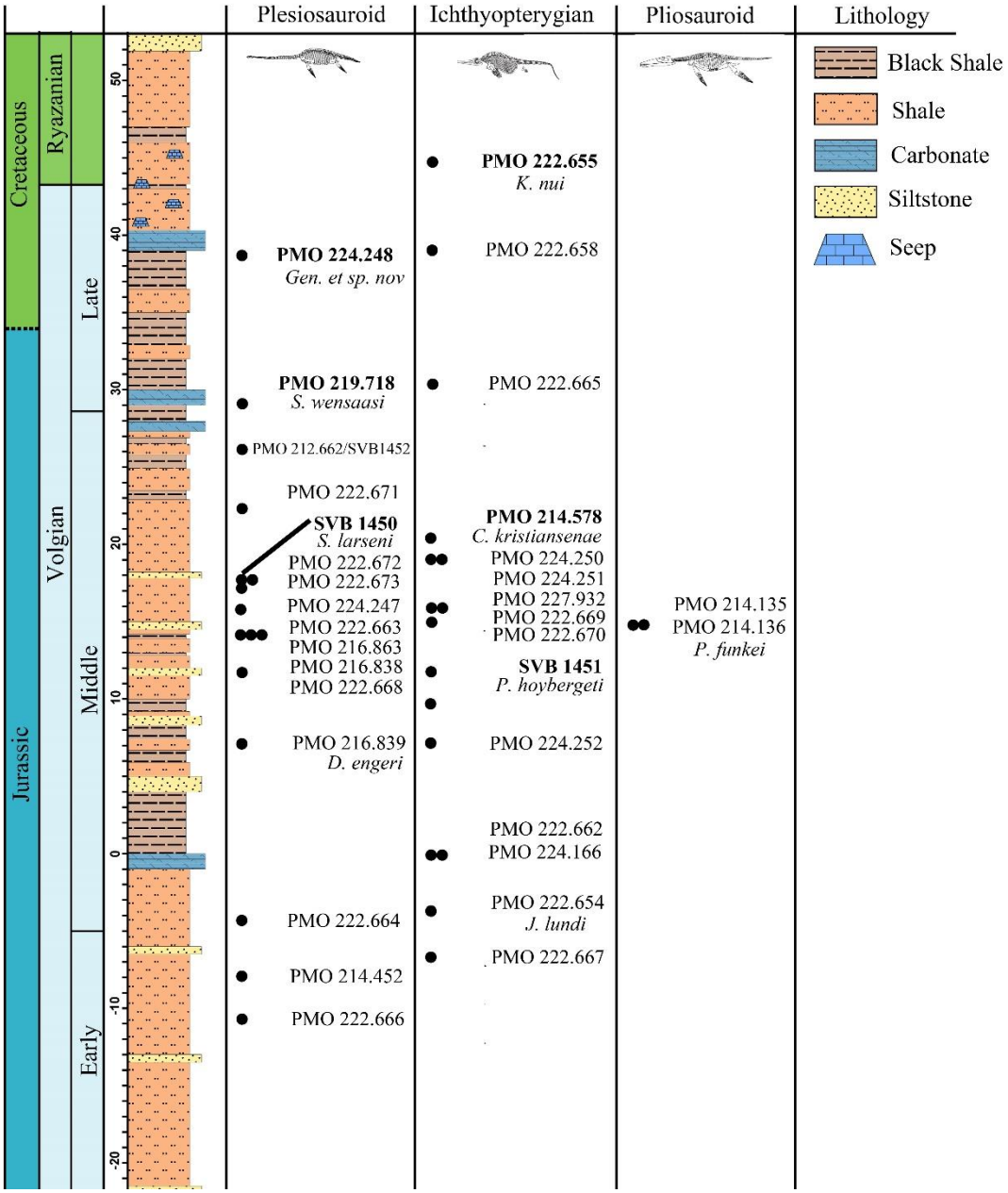

Figure 5: The stratigraphic placement of the collected marine reptile specimens from the Slottsmøya Member (2004-2012). Holotype specimens are marked in bold. See Appendix 1, Table A1.2 for specimen references.

1.5.2 Other macrofossil material from the Slottsmøya Member

The Slottsmøya Member is not only rich in cryptoclidid plesiosaur material, but also a number of ichthyopterygian, pliosaurid and macro invertebrate fossils. Ichthyopterygian fossils are numerous, with over 30 specimens collected in 2004-2012, ranging from partial to near-complete skeletons (Appendix 1, Table A1.2). Of these, four new genera and taxa have been described; *Cryopterygius kristiansenae*, *Janusaurus lundi*, *Palvennia hoybergeti* and *Keilhauia nui* (Delsett et al., 2017; Druckenmiller et al., 2012; Roberts et al., 2014). *C. kristiansenae*, *P. hoybergeti* and *J. lundi* all derive from the Tithonian deposits of the Slottsmøya Member, whereas *K. nui* represents the most complete ichthyosaur from the Berriasian stage (Delsett et al., 2017).

In addition to the cryptoclidid plesiosaur material, three pliosaurid specimens were excavated. Two of these have been described and referred to the new species *Pliosaurus funkei* (Knutsen et al., 2012b). The specimens were referred to the genus *Pliosaurus* on the basis of the shared morphology. The undescribed specimen consists of a single tooth from Janusfjellet.

The macro-invertebrate assemblage of the Slottsmøya Member has been described based on material from methane seeps (Hryniewicz et al., 2014; Sandy et al., 2014; Vinn et al., 2014; Wierzbowski et al., 2011), CO2 drill cores (Koevoets et al., *in prep*.), storm deposits (Rousseau and Nakrem, 2012) and exposed material from the black shales (Hammer et al., 2013). The majority of the invertebrate material is preserved either in sideritic storm deposits, in the hydrocarbon seep carbonates interbeds or in the hydrocarbon seep carbonates themselves (Hammer et al., 2011). The rarity of well-preserved invertebrate fossils in the black shales, has resulted in some problems with correlating the Slottsmøya Member succession with other contemporaneous localities (Wierzbowski et al., 2011). However, with high resolution organic carbon-isotope stratigraphy completed for the Agardhfjellet Formation, further correlations with other units in the Barents Sea and the Russian Platform can continue (Koevoets et al., 2016).

An echinoderm Lagerstätte close to the base of the Slottsmøya Member, represents a low diversity assemblage from the early middle Volgian (~middle

Tithonian, Rogov, 2004). The material includes one crinoid and one echinoid identified to genus level, as well as several new species of asteroids and ophiuroids currently under description (Rousseau and Nakrem, 2012). The excellent preservation of these usually fragile specimens, suggest a rapid burial event and is interpreted to be a storm deposit (Brett and Baird, 1986; Rousseau and Nakrem, 2012).

Although rare in exposures, teleost material has been recovered from the CO2 drill cores by Longyearbyen of the Slottsmøya member, is possibly referable to the Jurassic taxon *Leptolepis sp.* (Koevoets et al., *in prep*).

1.5.3 Palaeobiogeographic implications of the Spitsbergen material

Currently, all the Slottsmøya Member marine reptile taxa are endemic (found in one location), either at a species or generic level (Roberts et al., 2014). However, recent descriptions of Russian Boreal and Sub-Boreal ichthyosaurians have questioned this (Zverkov et al., 2015). While this may be the case, the limited overlapping diagnostic cranial material between Russian and Slottsmøya Member ichthyosaur taxa make referals questionable at this time (Chapter Four, this volume). Differing from the Late Jurassic ichthyosaurians, some of the Slottsmøya Member plesiosaurians share similarities with the Tethyan fauna, at least on a generic level (Knutsen et al., 2012b, c; Roberts et al., 2017). This raises new questions relating to the palaeobiogeography and evolutionary rates of marine reptiles spanning the Jurassic – Cretaceous boundary (Chapter 4, this volume).

1.6 Phylogenetic methods

For the ease of the reader, a general introduction to the use of phylogenetic methods used in this thesis is presented here. The data matrix of phylogenetic character states utilised in chapters of this thesis derive from a matrix published by Benson and Druckenmiller (2014), consisting of 80 operational taxonomic units (OTUs) and 270 characters. Of the 270 characters, 140 are cranial features and the remaining 130 post-cranial features (see Appendix 5 for character list). In this thesis the "wildcard" or "rogue" taxa identified in Benson and Druckenmiller (2014), were also removed from the analyses. Two taxa were added to this matrix, along with additional characters and numerous changes to character scores for cryptoclidid taxa

(See Chapters 2 and 3; Appendix 5). A couple of revisions of the matrix were published during the period of this doctorate (Benson et al., 2013; Fischer et al., 2015; Serratos et al., 2017), however these were not incorporated as these did not change the phylogenetic position or intrarelationships of the Cryptoclididae family. As one of the supervisors on this project (P. S. Druckenmiller) was one of the original creators of the matrix, the edited scores and character updates were made in accordance to the taxonomic purpose of the character.

The original analysis by Benson and Druckenmiller (2014) utilised the combined approach of ratchet and TBR (tree bisection reconnection). The parsimony ratchet method is most commonly used for analysis of large data sets, such as genetic data (Nixon, 1999), whereas TBR is a heuristic search where parts of the tree are separated and then reconnected to different parts of the tree. The data matrix was compiled and edited using Mesquite (Maddison and Maddison, 2017) and the phylogenetic program used for all the analyses was TNT (Trees with New Technology V 1.5; Goloboff and Catalano, 2016). In TNT the parsimony ratchet method includes several steps: starting by generating a Wagner tree, followed by branch swapping. Subsequently, a subset of random characters are given additional weight (determined by user, default is 4 in TNT V. 1.5) and branch swapping (TBR) is performed on the reweighted matrix, keeping one or multiple trees. The matrix is then reweighted back to the original weights and TBR is performed on the current tree. This is commonly done 50 – 200 times (iterations), although in some cases (e.g.Benson and Druckenmiller, 2014) fewer iterations have been used. In TNT (v. 1.5) an additional round of TBR can be performed on the resulting most parsimonious trees (MPTs) from the ratchet analysis. This is recommended as it gives a more accurate reflection of the number of MPTs, than using just the ratchet analysis (Nixon, 1999).

Tree support can be estimated by using bremer support and/or bootstrap values. Bootstrapping is a resampling method, which assess the repeatability of the consensus tree; generating a measure (%) of probability that the consensus tree represents the true phylogeny (Hillis and Bull, 1993). This method gives an indication of how well supported individual nodes are by the characters. A low

bootstrap value for a node indicates that few character support that node (Hillis and Bull, 1993). The use of 2000 replicates in bootstrap resampling is recommended to get good estimates, although fewer replicates (100-500) can give an indication (Efron et al., 1996). An alternative method, Bremer support (decay index) can be used to illustrate the character support at nodes, by showing the number of steps required to create a polytomy at nodes in most parsimonious trees (Bremer, 1994).

In analyses with a low number of characters relative to number of taxa (typical of fossil data), missing data can affect tree resolution (Wiens and Morill, 2011). However, research has indicated that the percentage of incompleteness in an individual taxon is not exclusively responsible for affecting tree resolution, rather it is the taxonomic importance of the characters it can be scored for (Wiens, 2006): the smaller number of characters, the more problematic missing data is for tree resolution. For Mesozoic marine reptiles, there are several cases where additional material has resulted in additional scored characters for certain taxa, which has drastically changed their phylogenetic placement (e.g. *Libonectes morgani*; Sachs and Kear, 2015; *Arthropterygius chrisorum*; Fernández and Maxwell, 2012).

1.7 The aims and significance of this study

Few Upper Jurassic – Lower Cretaceous cryptoclidid plesiosaur assemblages beyond fragmentary material are available and are predominantly from the Tethyan region. During this interval, the interrelationships, distribution and taxonomic turnover of cryptoclidids are poorly understood (Benson and Druckenmiller, 2014). The aim of this study is to describe two exceptionally preserved Upper Jurassic – Lower Cretaceous plesiosaur specimens from the Slottsmøya Member, Agardhfjellet Formation of central Spitsbergen (Svalbard) and how these two specimens increase our understanding of this enigmatic group in a global context.

The first chapter describes the materials and methods used for the manual and virtual preparation of the specimens described in this thesis. During the time period of this doctoral research, preparation methods were tried and adapted for the highly-fractured material from the high Arctic. These are documented and shown, as future reference for others wishing to collect marine reptile fossils from high latitudes.

Chapter 2 describes a new specimen (PMO 222.663) of *Colymbosaurus svalbardensis,* which is the only genus of cryptoclidid found to be present in multiple regions during the Late Jurassic. As such, this genus is important for understanding the distribution of cryptoclidids into the Boreal Sea from the Tethyan region. A new cryptoclidid genus and species from the Jurassic – Cretaceous boundary described in Chapter 3, increases our understanding of which cryptoclidid lineages continued into the Cretaceous and radically changed the cryptoclidid phylogenetic tree topology. These specimens have been incorporated into a large dataset of phylogenetic characters, from original and existing work, to further understand the relationships of the Cryptoclididae with other plesiosauromorph plesiosaurs. This phylogenetic work, in addition to similar work on ophthalmosaurid ichthyosaurs was time-calibrated in order to compare diversification and distribution events to climatic and eustatic sea level changes (Chapter 4, this volume). Furthermore, palaeobiogeographic methods were tested for the first time on marine reptile clades from the Late Jurassic. This work places the Boreal plesiosaurs in a global perspective and maps our current knowledge on the palaeobiogeography of marine reptiles during the Late Jurassic – Early Cretaceous.

1.8 Contributions to the articles and appendices

Chapter one: The preparation methods were tested by M-L. K. Funke and A. J. Roberts. The µCT tomography and preparation of the specimen for analysis was done by A. J. Roberts and B. Cordonnier (in acknowledgements), with assistance from Hammer (in acknowledgments). The manuscript was written by A. J. Roberts, with minor edits from J. H. Hurum and M-L. K. Funke. Percentage of work 85 % A. J. Roberts, 10 % M-L. K. Funke and 5 % J. H. Hurum. *Publication status:* Planned for submission to the Geological Curator (GCG)

Chapter two: Preparation of the specimen done by A. J. Roberts, aided by V. Engelschiøn Nash and M-L. K. Funke (acknowledgements). Paper written by A. J. Roberts with major edits from P. S. Druckenmiller and minor edits by L. L. Delsett and J. H. Hurum. Collections visited by A. J. Roberts for comparative material. Photographs of specimen and figures made by A. J. Roberts (Figure 2 made by L. L. Delsett and A. J. Roberts). Changed scorings for taxa and phylogenetic analysis was performed by A. J. Roberts. Supplementary data compiled by A. J. Roberts. Percentage of work 80 % A. J. Roberts, 10 % P. S. Druckenmiller, 5 % L. L. Delsett and 5 % J. H. Hurum. Reviewers (F. R. O'Keefe and P. Vincent) contributed to minor edits on the article (in acknowledgements). *Publication status:* Published. Roberts et al. 2017. Journal of Vertebrate Paleontology 37: DOI: 10.1080/02724634.2017.1278381. Supplementary data published online, but also included in Appendix 3. Original article in Appendix 4.

Chapter three: Preparation of the specimen done by A. J. Roberts, aided by P. S. Druckenmiller, M-L. K. Funke, V. Engelschiøn Nash and M. Koevoets (acknowledgements). The µCT tomography was performed by B. Cordonnier and A. J. Roberts. The manuscript was written by A. J. Roberts with main edits by P. S. Druckenmiller and minor edits by L. L. Delsett, J. H. Hurum and B. Cordonnier. Collections visited by A. J. Roberts for comparative material. Photographs of specimen and figures made by A. J. Roberts. New characters, changed scorings for taxa and phylogenetic analysis was performed by A. J. Roberts. Supplementary data compiled by A. J. Roberts. Percentage of work 80 % A. J. Roberts, 8 % P. S.

Druckenmiller, 4 % B. Cordonnier, 4 % L. L. Delsett and 4 % J. H. Hurum. *Publication status:* Planned for submission to PeerJ

Chapter four: Initial idea and manuscript written by A. J, Roberts with minor edits from I. C. Harding and J. H. Hurum. Suggestions from L. L. Delsett, D. Foffa, P. S. Druckenmiller and V. E. Nash were incorporated (acknowledgments). All analyses, figures and supplementary material were compiled/made by A. J. Roberts. Percentage of work 90 % A. J. Roberts, 5 % I. Harding, 4 % J. H. Hurum, 1 % other suggestions from multiple persons (in acknowledgements). *Publication status:* Planned to be incorporated into a larger study including other marine reptile clades.

Appendix 1: Supplementary information for the introduction, including an updated list from Delsett et al. (2016) of the Slottsmøya Member marine reptile specimens.

Appendix 2: Published version of Delsett et al., (2016), describing the depositional environment, taphonomy and diagenesis of the Slottsmøya marine reptile Lagerstätte. A. J. Roberts contributed to the preparation of nine of the included specimens. A. J. Roberts contributed to making and updating previous illustrations and taphonomic descriptions of the plesiosaurian specimens and the holotype specimen of ichthyosaur *Janusaurus lundi*. In addition, A. J. Roberts assisted Ø. Hammer on the computer tomography in order to make Figure 8.

Appendix 3: Supplementary information for Chapter 2. Figures and tables were made by A. J. Roberts. The phylogenetic data matrix was edited by A. J. Roberts from the published matrix by Benson and Druckenmiller (2014).

Appendix 4: Published version of Chapter 2, Roberts et al., 2017.

Appendix 5: Supplementary information for the phylogenetic analyses run in Chapters 2, 3 and 4, with information regarding new characters and changes in character states of cryptoclidid taxa. A shortened version of the original Benson and Druckenmiller (2014) character list is provided, as well as detailed descriptions of the new characters used in Chapters 3 and 4.

Appendix 6: Supplementary figures and tables for the description of PMO 224.248 in Chapter 3, written and made by A. J. Roberts.

Appendix 7: Supplementary information for Chapter 4, including the collected occurrence data, data matrices, R scripts and an additional figure. All data was collected, presented and analysed by A. J. Roberts.

Appendix 8: The published version of Delsett et al., 2017. A. J. Roberts contributed to the conceptualization and manuscript editing and performed the phylogenetic analysis.

Chapter 1

Excavation, virtual and manual preparation techniques for the high Arctic, Late Jurassic – Early Cretaceous Slottsmøya Member marine reptiles

Excavation, virtual and manual preparation of the high Arctic, Late Jurassic – Early Cretaceous Slottsmøya Member marine reptiles

Roberts, A. J. [1 2], Funke, M. L. K. [2] and J. H. Hurum [2]

[1] Ocean and Earth Science, University of Southampton, Southampton, United Kingdom

[2] Natural History Museum, University of Oslo, Oslo, Norway

Abstract

The recent excavation of nearly 60 marine reptile specimens from the Slottsmøya Member, central Spitsbergen (Svalbard, Norway), has led to the testing of numerous preparatory methods and novel excavation techniques. Key results of this work show that the use of the temporary adhesive Mowilith, a polyvinalacetate, represents a good alternative to paraloid-type temporary adhesives for extremely fractured material. Permanent cyanoacryloid adhesives used on the material have successfully stabilized the specimens from damage, although significantly cleaning prior to application is required for a lasting effect. Finally, we present the case study of a plesiosaur skull, where computed tomography was utilised to further the preparation of the specimen. Computed tomography images aided to locate the borders of the bone material allowing for more of the surrounding matrix to be removed without damage. The utilisation of computer tomography provides a virtual preparation alternative, for particularly fragile specimens.

Introduction

Between 2004-2012, eight seasons of extensive fieldwork in the Late Jurassic – Early Cretaceous black shales of the Slottsmøya Member of the Agardhfjellet Formation in the central Spitsbergen Sassenfjord area, have yielded numerous skeletal remains of plesiosaurs and ichthyosaurs (Druckenmiller et al., 2012; Knutsen et al., 2012a, b, c, d; Roberts et al., 2014; Roberts et al., 2017). The specimens from this member display different states of preservation and vary substantially in completeness, erosional stage and mineralisation (Delsett et al., 2016; Kihle et al., 2012). Field seasons in the high Arctic (78º N) are short, as the

localities are mostly snow free for approximately four weeks a year. The fractured condition of the fossils offers multiple excavation and preparatory challenges, as numerous types of adhesives and encasing materials fail to work optimally under these conditions (-5 – 10+ C^{o}). As such, many new and old techniques have been tested during the preparation of these specimens, some of which could prove useful for future excavation and preparation of material from the Polar Regions. Here we present the challenges with excavating and preparing these specimens, as well as our solutions to surmounting them.

Preservation

Marine reptiles found in organic-rich shale, such as the Posidonienschiefer in Holzmaden (Germany), are usually compressed and distorted (Martill, 1993 and references therein). Similar to the Posidonienschiefer, the Slottsmøya Member has a comparable matrix and degree of compaction, but displays a higher sedimentation rate (Delsett et al., 2016). As a result, many of the marine reptile specimens have not undergone compaction to a similar degree as fossils from the Posidonienschiefer. Research has indicated that the presence of early pore mineralisation (permineralisation) by barite ($BaSO_4$) and calcite ($CaCO_3$), could be responsible for the relatively three-dimensional preservation observed in many of the specimens (Delsett et al., 2016; Kihle et al., 2012). The documented presence of *in situ* cold seep carbonates in the upper section of the Slottsmøya Member (Hammer et al., 2011), could be the mechanism for the remobilisation of barite into the vascular bones of the marine reptiles (Delsett et al., 2016).

The key difference between excavating and preparing macro-vertebrate fossil material from high latitude versus low latitude areas is the presence of permafrost. The lack of vegetation in these environments, results in exposure of fossil material to a high rate of climatic erosion. Due to the freeze-thaw processes in the active layer of the permafrost, most of the specimens have undergone congelifraction (fragmentation by freeze-thaw processes in the active layer of the permafrost). The main types of preservation states for the Slottsmøya Member material are the following (Figure 1.1): (A) subjected to congelifraction, particularly in the black shales; (B) covered in secondarily formed gypsum and iron oxides in the black shales; (C) partially or completely in siderite nodules and (D) several of these states

can occur simultaneously in the same specimen. In addition, some of the specimens that were found exposed on the surface have been subject to significant environmental erosion.

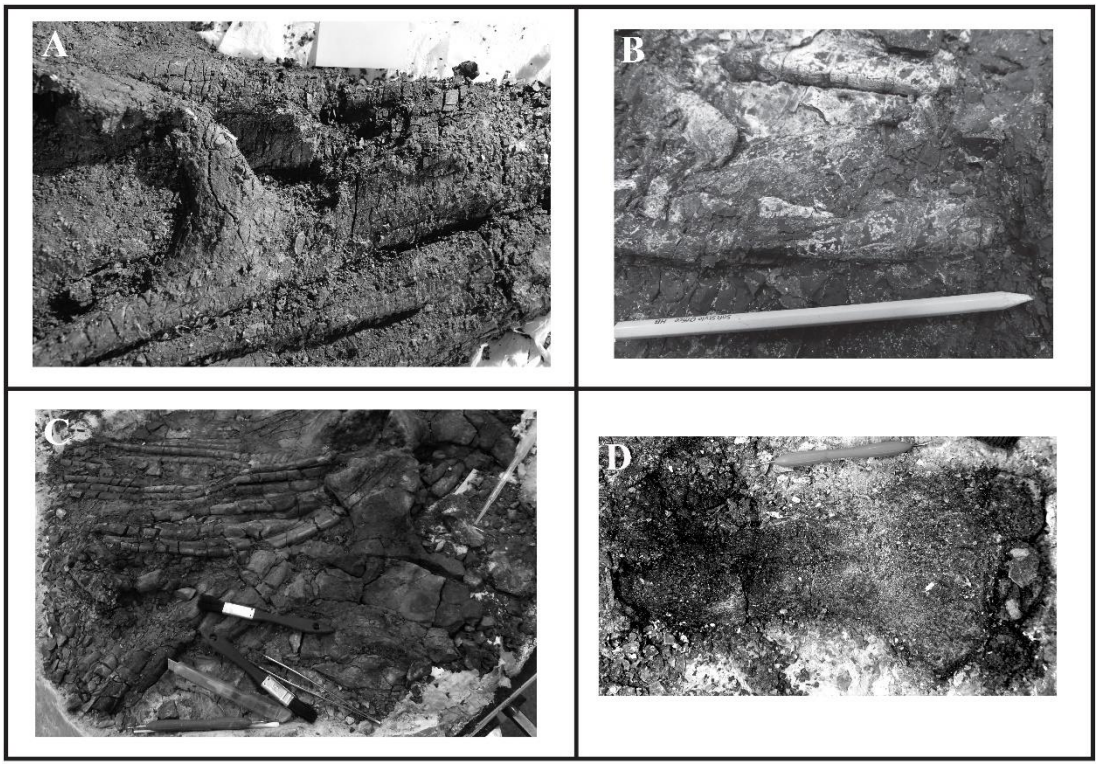

Figure 1.1: Different types of preservation in the Slottsmøya Member marine reptiles. **A**, Extreme fracturing from freeze-thaw processes on an ichthyosaur skull (PMO 222.654); **B**, gypsum covering bone elements of an ichthyosaur skull (PMO 222.669); **C**, preservation in siderite-rich matrix (PMO 222.669); **D**, extreme fracturing from weathering and congelifraction and covering from gypsum flakes on a plesiosaur humerus (PMO 224.248).

Excavation

During the excavation of the specimens, traditional excavation tools such as hoes, spades and jack hammers, as well as the more unorthodox equipment such as chainsaws, were used to cut away the permafrost and expose the specimens. When exposed, toilet paper (minimum 5-ply) was dampened with water to form a papier-mâché cover preventing moisture loss and creating a strong, yet pliable barrier between the plaster and bone (Figure 1.2A). Attempts at using aluminium foil as a boundary caused significant damage to the specimens over time, as the aluminium foil disintegrates in the low pH environment of pyrite-rich organic shale.

Plaster (Giluform 250) was used to make the jackets, coupled with inlaid burlap and metal rods to strengthen the packaging. This type of plaster works well in cold environments (-5 – 5+ C°), although requires to be hand-held in place along the undercut sides during hardening (Figure 2B-C). Alternative packaging, such as expanding spray foam where tried with less success. The area surrounding the specimen is first trenched, then after the application of the top jacket, undercut. The plaster jackets are separated from the ground using custom-made 0.5-1m long chisels. Theses chisels are driven in under the top jacket until they almost form a floor supporting the brittle shale (Figure 2D-E). These are struck in place and then rope is tied around the ends, enabling the jacket to be flipped manually (Figure 2D) and preventing the specimen and matrix from falling out of the bottom of the jacket. As the matrix is often frozen (permafrost) during collection, the matrix and bone-material is easily held in place by the chisels.

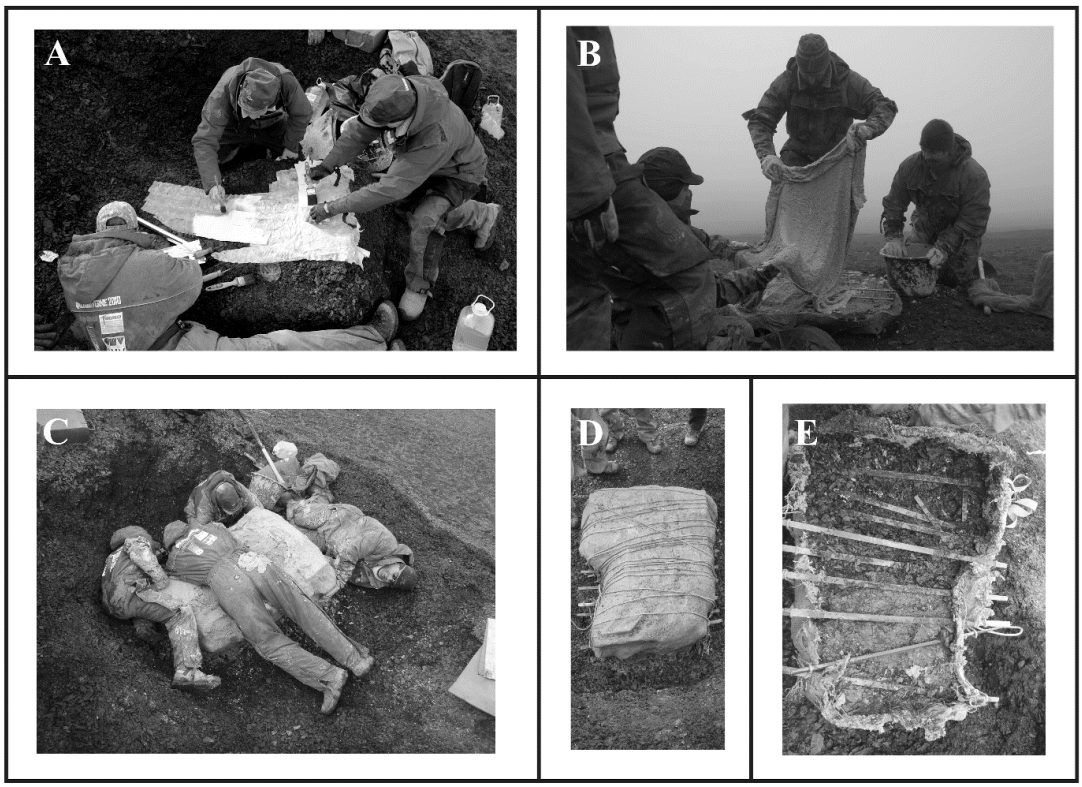

Figure 1.2: The excavation process of Spitsbergen Jurassic marine reptiles. **A,** The application of dampened toilet paper. **B**, The application of plaster-saturated burlap. **C**, The plaster is held in place during hardening. **D**, The plaster jackets are separated from the ground by chisels and rope is used to secure them. **E**, the plaster jacket after flipping. Photos courtesy of Erik Tunstad.

Due to the limited weight feasible for helicopter-removal, the size and weight of the plaster jackets had to be restricted. After turning the plaster jackets, the chisels were taken out, so the jacket weight could be reduced by manual removal of matrix. Larger sections of the skeletons had to be split, and the jackets were separated by documenting and carefully removing bones between them. After the specimens were transported to the laboratory in Oslo, they had to thaw and dry for at least six months before preparation can be commenced. The method for making the plaster jackets in the field, is also used in the laboratory to flip between the different sides of the specimens.

Preparation and conservation

The preparation time for the complete specimens is estimated to be between 800-2000 hours, depending on the size and preservation of the individual specimen. All the specimens were prepared mechanically and no acid preparation was used. Larger and/or fragile specimens were prepared directly *in situ* in the plaster jackets, whereas some small or well-preserved specimens were removed element-by-element from the jacket for preparation. The tools used for the preparation of the Slottsmøya vertebrate fossils depends on the type of surrounding matrix and the preservation of bone elements. For tough siderite- and gypsum covered specimens, utility knives, dental tools and air scribes are required. For cleaner and better-preserved material, removing the matrix, cleaning with ethanol and stabilising elements with temporary adhesive is usually sufficient. Other techniques, such as sandblasting with sodium bicarbonate and in some cases iron powder, can be applied to fragile material after stabilising with fluid permanent adhesive. As in all fossil preparation (López-Polin, 2012), several stages are involved in the preparation of the Slottsmøya Member marine reptiles, including A) initial cleaning, B) stabilisation and C) restoration

Initial cleaning

The cleaning process involves the manual removal of the surrounding matrix, dust, gypsum and siderite from the specimens. As the matrix is fragmented due to congelifraction, in most cases it was easy to remove excess matrix using smaller brushes and tweezers. After exposure of the bone surface, cotton buds dipped in 96% ethanol was found to be an efficient way of removing dust and gypsum flakes from the fractured bone surface. This technique cannot be used on the specimens covered

in large amounts of gypsum and siderite, as this material is often too strongly attached to the bone surface (Figure 1.3). However, the application of ethanol, can help loosen tight-fitting matrix for manual cleaning with scalpels. In an ichthyosaur specimen (PMO 222.669), the majority of the bone elements where covered in a thick layer of gypsum which could not be manually removed without damaging the bone surface (Figure 1.1B). In this instance, sandblasting using bicarbonate powder removed most of the gypsum without damaging the bone surface. An alternative gypsum dissolution method developed and described in detail in Knutsen (2012), is to submerge bone elements in saltwater solution for 1-3 days at 25 °C. Knutsen (2012), tested this method on an ichthyosaur paddle (PMO 214.578), which succeeded in removing gypsum crystals on the bone surface and between fractures. However, this method cannot be used on highly fractured and fragile material, as the gypsum crystals in many cases participate in holding the fractured bone elements together.

One of the plesiosaur specimens (PMO 216.839) displayed a different preservation type to the other material: the bones were covered in gypsum, siderite and jarosite ($KFe^{3+}{}_3(SO_4)_2(OH)_6$), a hydrous sulphate of potassium and iron. The vascular spaces inside some of the bone elements, included numerous pyrite crystallisations. To limit the amount of future pyrite decay, this specimen had to be significantly cleaned prior to adhesive application and remains under close observation.

In a plesiosaur specimen (PMO 222.663), a large amount of siderite was present in the surrounding matrix and on the bone elements, resulted in a combination approach of sandblasting with bicarbonate powder, air scribes and scalpels to reveal the bone surface. In most cases, this combination approach has proven to be the most efficient method of cleaning the Slottsmøya Member bone material.

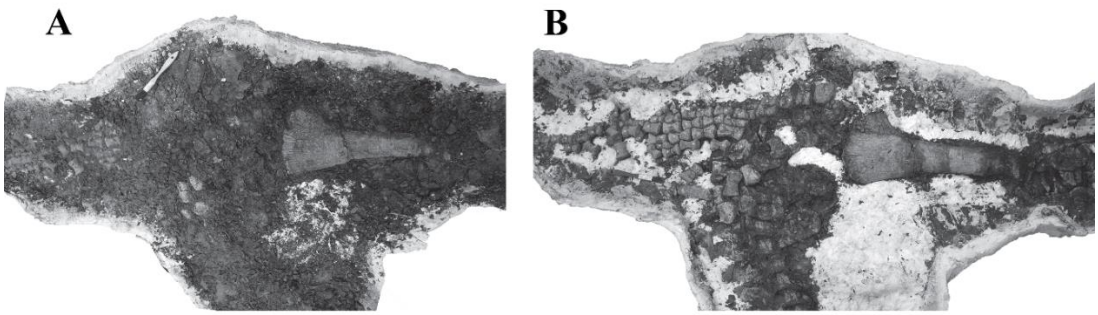

Figure 1.3: A plesiosaur hind limb and caudal vertebrae. **A**, before and **B**, after initial cleaning. The shale is heavily fragmented and easy to remove. The preparation time between the photos is a week. Note the brush for scale.

Stabilisation

Following the initial cleaning process, the specimens require stabilisation. As most specimens have undergone significant congelifraction, use of a temporary adhesive was required. The temporary adhesive used for stabilisation is a polyvinylacetate (PVAC) "Mowilith", which is sometimes used during preparation in Germany (Lippmann, 1986; Wadewitz, 1977), but is to our knowledge rarely used elsewhere in Europe. This polyvinylacetate is commonly dissolved in a solution of acetone, but can also be dissolved into 96% ethanol over several days, a less detrimental solution for the user. Viscous solutions are mixed as 1:2 (Mowilith granules: ethanol) and additional ethanol can be added to the solution to the required viscosity. A higher concentration is used for surface stabilising and a thinner solution for stabilising deeper into the bone. Mowilith can easily be removed for the bone surface by the application or submersion in ethanol and is therefore an effective stabiliser on the fractured material from Spitsbergen. In larger and tightly packed specimens such as the plesiosaurs PMO 222.663 (*Colymbosaurus svalbardensis*) and PMO 224.248, temporary and permanent adhesives were used to avoid three-dimensional elements collapsing when removing underlying matrix or to remove bone elements for permanent reconstruction. In addition to functioning as a stabiliser, Mowilith can also be used in the final stages of preparation as a coating. Used as a coating, this product has so far prevented additional fracturing and acts as basic seal to atmospheric changes.

Restoration

After an extended period of drying/hardening following the Mowilith application (minimum 24 hours), individual bone elements were stable enough to be moved or repositioned for the final restoration process. Gypsum and calcite mineralisation between fractures had to be removed and the broken edges cleaned completely, to allow for the application of adhesive (Figure 1.4). Due to the sheer number of fractures, temporary adhesive solutions such as Paraloid B72 were tried and deemed insufficient as the glued fractures could not support any weight strain. As a result, a number of permanent adhesives are used to reconstruct the elements.

For gluing major fractures that need to be able to bear some weight strain, the preferred adhesive is Jurassic Gel, made by Paleobond®. This adhesive can also be used to fill internal missing fragments of material, and can be matted (to avoid reflection in photographs) by gently brushing acetone or gently sandblasted with bicarbonate powder over the dried adhesive. Other more fluid permanent adhesives were utilised in areas with small micro-factures or to glue smaller fragments of bone: ethyl-cyanoacrylate "Geodur" ® (three types, viscous, medium and fluid). These are usually applied using a pipette for increased accuracy and to avoid excess adhesive. All these permanent adhesives require the use of a hardener (Loctite 7452 activator idh. No. 88224). A penetrating adhesive (Paleobond® Penetrant Stabilizer PB002-12), can be used on heavily weathered and micro-fractured bone elements and tooth enamel. This adhesive successfully stabilised fragile and/or porous elements (e.g. ichthyosaur phalanges and teeth), and has so far stopped additional fracturing, rendering the specimen stabile enough for handling. This penetrating adhesive should be left to dry a minimum of 24 hours.

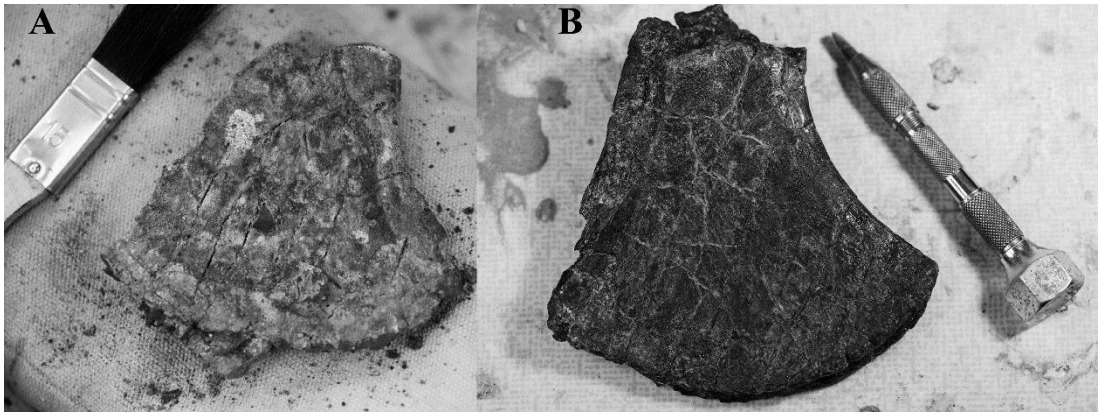

Figure 1.4: Clavicle of *Djupedalia engeri* (PMO 216.839). **A**, before cleaning, stabilisation and restoration; **B**, result after the completed preparation.

Some of the partially prepared specimens have been subject to further damage over time, by pyrite decay and secondarily formed gypsum crystallisation. One of these, the holotype of *Cryopterygius kristiansenae* (PMO 214.478), was originally only prepared from one side and required further conservation of the opposite side. When the specimen was flipped, cleaning and stabilisation of this side was performed. Areas which had been reached by Mowilith during the initial preparation, appeared in better condition than other areas. The removal of the siderite-rich matrix covering the bone elements and the application of Mowilith solution appears to have slowed this process down considerably. However, the specimen will require observation over time to see if these methods help in the long-run. A summary of the use of the different methods based on the general preservation types, can be found in Table 1.1.

	Preservation type			
Method	*Siderite surrounding specimen*	*Gypsum flakes on surface*	*Gypsum and compact shale*	*Fracturing*
Manual cleaning with tweezers	x	x	x	x
Sandblasting with bicarbonate	x	x	x	
Ethanol clean using cotton buds		x		x
Application of Mowilith for stabilisation	after matrix removal	after matrix removal	after matrix removal	x
Manual preparation using air scribes and scalpels	x	only if necessary	x	
Use of penetrating permanent adhesive	after cleaning and matrix removal	after cleaning and matrix removal	after cleaning and matrix removal	x
Use of thicker permanent adhesives	after cleaning and matrix removal	after cleaning and matrix removal	after cleaning and matrix removal	for larger factures
Application of Mowilith for conservation	x	x	x	x

Table 1.1. A general summary of the methods used for the individual preservation types.

The use of computed tomography (CT) prior to complete preparation

For the past 40 years, Computed tomography (CT) has been used to obtain three-dimensional information on fossil specimens (Conroy and Vannier, 1984; Jungers and Minns, 1979). Significant changes and improvement to CT scanning technology and computer visualisation has made CT work easier, faster and work at a higher resolution (Cnudde and Boone, 2013; Sutton, 2008; Sutton et al., 2014). Virtual preparation is a technique that can be used on fragile specimens, or where the matrix is hard to visually differentiate from the bone. As shown by Larkin et al. (2010), CT or X-ray radiography can be a useful method of determining boundaries during the preparation of marine reptiles. In some cases, particularly in the preparation of cranial material, where bone elements can be extremely thin and often over/underlap each other, CT scanning can be used to interpret the extent of bone material and underlying bone elements.

For the fragile cranium of PMO 224.248, a cryptoclidid plesiosaur from Svalbard; µCT scanning was performed before and after complete preparation. The scanner used on the material was a Nikon XT H 225 ST at the University of Oslo, Natural History Museum, Norway. In some areas of the cranium of PMO 224.248, the matrix was particularly hard and firmly attached to the bone resulting in some

damage during early preparation. Due to this issue, the decision to scan prior to any further preparation, was made.

The CT machine's ability to penetrate fossil specimens depends on the density, thickness and mineralisation of the specimen, as well as the contrast to the surrounding matrix (Cnudde and Boone, 2013). Therefore, the individual preservation of any specimen must be taken into account when using filters and beam energy settings. A major limitation of CT scanning is usually the size of the specimen itself, as few scanners can accommodate large specimens and even then, objects often have to be scanned in sections (e.g. Larkin et al., 2010). The cranium of PMO 224.248, was scanned in three sections due to the limited range of view in the scanner (10x10 cm). The scans were later meshed together during post-processing to form a single high-resolution scan.

Due to the size-issue, the cranium had to be positioned snout-up in the µCT scanner in a secured cradle. Trials were completed using two different types of cradles: the first cradle made from plaster and the second using a dense foam material (Ethafoam). Although, the resulting µCT images for the plaster cradle were sufficient to utilise the images as a basic visual aid in manual preparation. The plaster cradle caused a loss of resolution as the dense material was harder to penetrate by the X-rays and some of the bone material displayed a similar density to the plaster. This resulted in additional effort to segment out the plaster cradle during post-processing. Following this attempt, Ethafoam was cut to fit the cranium and lined with a thin mat of cotton wool covered by plastic foil (Figure 1.5). This cradle method secured the specimen, is light-weight and also cut a significant amount of post-processing time, due to the low-density support material.

Figure 1.5: The skull of PMO 224.248 in the Ethafoam cradle used for the µCT scan. The skull is 22.5 cm in total length.

The manual preparation of the cranium of PMO 224.248 was performed using µCT images as a reference, allowing for safe matrix removal without causing damage to underlying bone elements (Figure 1.6). Areas such as the palate, alveoli, basicranium and external naris were further prepared using this method. This method was crucial to avoiding damage to the thin bone walls of the alveoli and the palate, which were barely visible using a hand lens (Figure 1.7). As the posterior section of the cranium was generally uncompressed, removal of matrix in some areas could cause collapse. To avoid this, a virtual preparation of the braincase was completed using Aviso Fire (FEI Company, V.8). The resulting three-dimensional model included most of the necessary taxonomic information (Chapter 3, this volume), deeming further manual preparation an unnecessary risk.

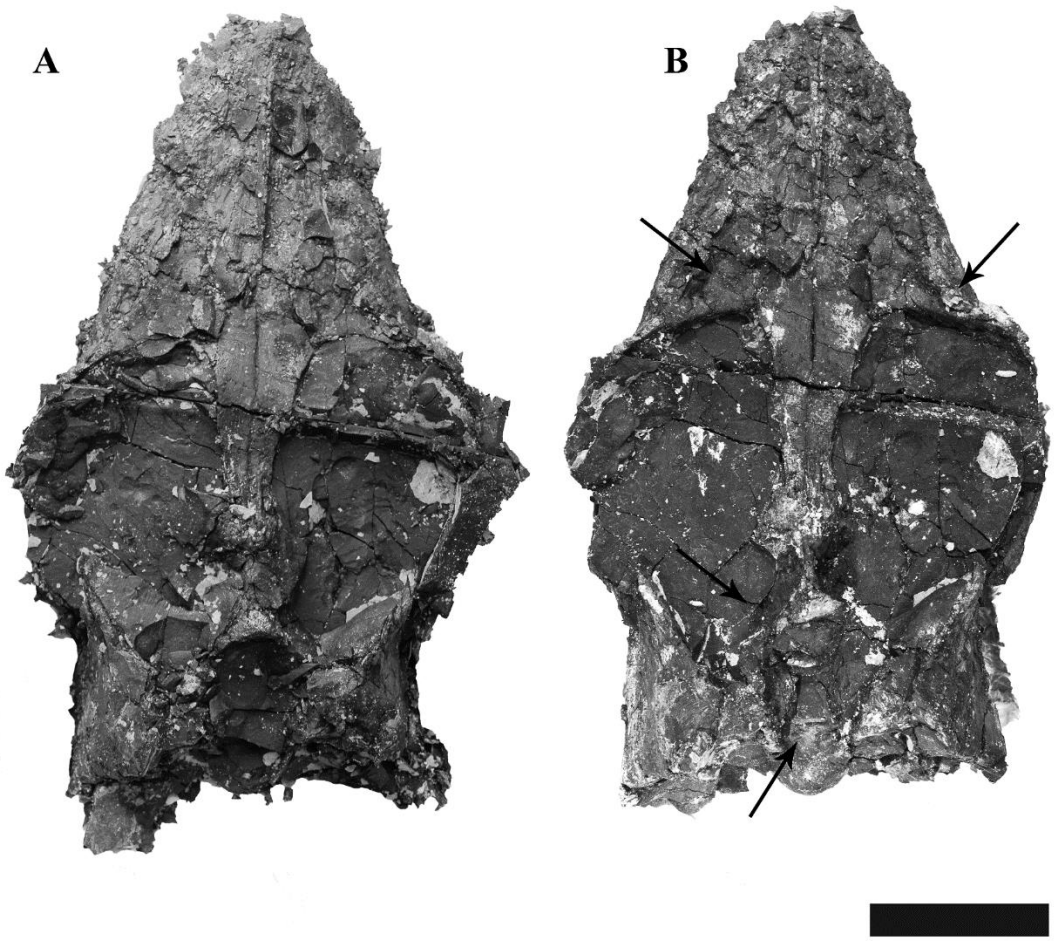

Figure 1.6. The cranium of PMO 224.248 in dorsal view. A, before and B, after computed tomography was used to assist the final preparation. The arrows indicate regions where the CT scans where used as a "guide" to bone element depth. Scale equals 5 cm.

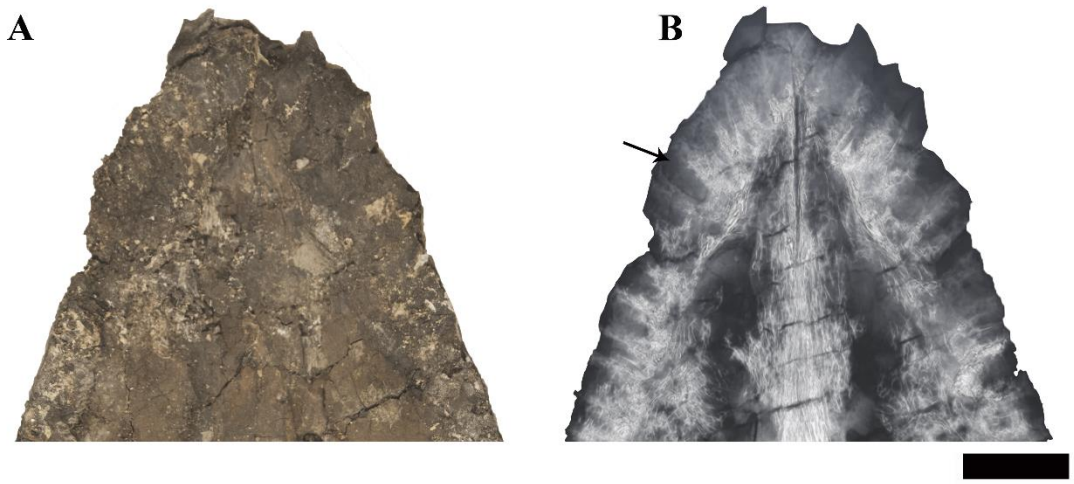

Figure 1.7: The prepared snout of PMO 224.248 in ventral view. **A**, a photograph; **B**, the µCT scan of the same area. Note the light-coloured barite and/or calcite filling the vascular canals in the bone. Scale bare equals 2 cm.

Discussion

Temporary adhesives used for conservation and stabilisation processes are most commonly vinyl (e.g. Mowilith) or acrylic (e.g. Paraloid B72) consolidants. The temporary adhesives Mowilith and Paraloid B72 are both stable and are to a degree reversible, however Paraloid B72 is more frequently used and has a long history of use in museums outside Germany (e.g. Carpenter and Radley, 2010; Padilla et al., 2010; Sassoon et al., 2010). Similar to Paraloid B72, Mowilith has documented advantages and disadvantages and in the literature, has seemed to perform equally to Paraloid B72. Mowilith has been shown not to influence oxygen isotope analysis, if removed prior to sampling (Stephan, 2000). However, similar substances have been shown to influence ^{14}C analysis (Law et al., 1991). Another study testing multiple temporary adhesives dissolved in acetone (Paraloid B72, Primal AC61 and Mowilith) showed that these can distort surface traits using an optical or electron microscope (Fernández-Javlo and Monfort, 2008). For the plesiosaur cranium PMO 224.248, we found no visible artefacts using Computed Tomography from Mowilith application, suggesting the distortions are only visible on the surface. Based on our observations, Mowilith has been more successful in stabilising highly fractured material such as Figure 1.1A. Unlike Paraloid B72, Mowilith can be easily mixed with ethanol, rather than acetone, making the solution less harmful to the technicians. In addition, similar to the use of Paraloid B72

(Larkin et al., 2010), the use of Mowilith has not also restricted the detrimental effects from atmospheric changes (e.g. Pyrite decay) affecting the prepared specimens over the past decade. The prepared specimens will remain under close observation to see if the stabilising effect of the Mowilith deteriorates in future.

The use of cynoacryloids as permanent adhesives on fossil material has been debated. This is predominantly due to the near irreversibility of the substances and the unknown strength duration of the individual types have not been subject to long historical use (Shelton and Chaney, 1994). Temporary adhesives are usually more pliable and are unsuitable for bearing weight strain in significantly fractured, three-dimensional material. For some of the Slottsmøya Member specimens, the use of cynoacryloids was necessary to be able to study and move the specimens without permanent damage. Although if it can be avoided we recommend not to use these substances, due to their almost irreversible nature. However, for elements that are required to be bear weight strain and remain stable, they are indispensable.

While vertebrate palaeontologists frequently use CT methods and radiography to interpret internal and hidden bone structures, there are also multiple advantages of using CT to virtually prepare specimens. These include the reduction in damage to fragile and thin bone elements by over preparation and being able to visualise the extent and depth of the individual bone elements. In our experience, the µCT images have proven central for not only the taxonomic description of the internal cranial anatomy of PMO 224.248 (Chapter 3, this volume) and has avoided the manual preparation of certain areas altogether. In addition, the CT images have also helped in further understanding the topology of the palate and braincase of the specimen during manual preparation. In these regions, the bone material is often extremely thin and fragile and utilising CT images served as a guide to judge the margins of the individual elements. A problematic issue with CT scanning on partially or completely compressed material, is that images in the cross sectional dimension often have numerous artefacts and are not as clear as other dimensions. This is because the scanner has to penetrate a thicker section of bone and/or matrix. Some of these artefacts (e.g. ring artefacts) can be reduced or removed during post-processing, or can minimised by utilising different filters. The continually improved resolution of Computed Tomography, can be used to avoid destructive sampling, over-preparation and for describing microanatomy fossil material (Sutton et al.,

2014; Takeda et al., 2016). We hope that this provides a reference for other researchers wanting to excavate and work on fossil vertebrate material from high-latitude regions.

Acknowledgements

B. Lund, V. Engelschiøn Nash, E. M. Knutsen, P. S. Druckenmiller and M. Koevoets are thanked for assistance during the preparation of the specimens discussed in this paper. Erik Tunstad and Bjørn Funke are thanked for photographs of the preparation and excavation.

Chapter 2

Osteology and relationships of *Colymbosaurus* Seeley 1874, based on new material of *C. svalbardensis* from the Slottsmøya Member, Agardhfjellet Formation of central Spitsbergen

Submitted to Journal of Vertebrate Paleontology on June 3, 2016; accepted October 31, 2016, published online March 8, 2017. Published version available in Appendix 4

Authors: Roberts, A. J., Druckenmiller, P. S., Delsett, L. L. and Hurum, J. H.

Osteology and relationships of *Colymbosaurus* Seeley 1874, based on new material of *C. svalbardensis* from the Slottsmøya Member, Agardhfjellet Formation of central Spitsbergen

Authors: Roberts, A. J. [1 2], Druckenmiller, P. S. [3 4], Delsett, L. L. [2] and J. H. Hurum[2]

[1]The National Oceanography Centre, University of Southampton, Southampton, Hampshire SO14 3ZH, United Kingdom, ajr1g13@soton.ac.uk;

[2]Natural History Museum, University of Oslo, 0562, Norway, l.l.delsett@nhm.uio.no, j.h.hurum@nhm.uio.no;

[3]University of Alaska Museum, 907 Yukon Drive, Fairbanks, Alaska, 99775, psdruckenmiller@alaska.edu;

[4]Department of Geoscience, University of Alaska Fairbanks, 900 Yukon Drive, Fairbanks, Alaska, 99775.

Abstract

Colymbosaurus is a genus of long-necked plesiosaurian represented by two valid species; *C. megadeirus* from the Upper Kimmeridge Clay Formation (Kimmeridgian–Tithonian) of the United Kingdom and *C. svalbardensis* from the Slottsmøya Member of the Agardhfjellet Formation (Tithonian–Berriasian) of Svalbard, Norway. Due to the lack of complete and articulated skeletons and a near absence of cranial material, *Colymbosaurus* has been problematic to morphologically characterize. Here, we describe, and conduct a phylogenetic analysis on an informative new specimen referable to *C. svalbardensis* from the Slottsmøya Member, PMO 222.663, which preserves a large portion of the axial and appendicular skeleton. The new material contributes important new osteological data for the species and together with an extensive examination of congeners in British museums, clarifies the diagnostic characters of the genus. We provide two new diagnostic characters of the epipodials for the genus and re-evaluate the utility of an anteroposteriorly oriented bisecting ridge on the distal end of the propodials. We also

present two new diagnostic features for *C. svalbardensis* regarding the neural canal and femoral morphology. A phylogenetic analysis recovers a monophyletic and well-supported genus *Colymbosaurus*. The new specimen of *C. svalbardensis* confirms that this species is not synonymous with other described Slottsmøya Member plesiosauroids, demonstrating considerable diversity of the clade at high latitudes close to the Jurassic–Cretaceous boundary.

Introduction

Plesiosauria is a clade of secondarily aquatic reptiles that inhabited the Mesozoic seas (Taylor and Cruickshank, 1993). Their earliest remains are known from the Late Triassic (Norian; Sennikov and Arkhangelsky, 2010) and by the Early Jurassic, plesiosaurians had a world-wide distribution and diversified into several clades exhibiting a wide range of morphotypes (Bardet et al., 2014; Benson et al., 2012; Ketchum and Benson, 2010). In the wake of recent broad scale phylogenetic studies (Benson and Druckenmiller, 2014; Druckenmiller and Russell, 2008; Ketchum and Benson, 2010; O'Keefe, 2001) there is increasing consensus regarding the taxonomic relationships among major plesiosaurian clades. However, relationships within these clades remain problematic. One major small-skulled, long-necked plesiosauroid clade is Cryptoclididae, known from the Callovian (Middle Jurassic) to the latest Hauterivian (Early Cretaceous) (Benson and Druckenmiller, 2014). Cryptoclidids are predominantly northern hemispheric in distribution, with the majority of specimens found in the Oxford and Kimmeridge Clay Formations of the U.K. (Gasparini et al., 2002). Recognizing synapomorphies for Cryptoclididae has proven challenging, as many of the described taxa either lack overlapping material or are described from juvenile specimens (Benson and Bowdler, 2014; Brown, 1981; Knutsen et al., 2012a, c, d; O'Keefe et al., 2011). Following Benson and Druckenmiller (2014), cryptoclidid synapomorphies include large orbits and external nares, a small vertical jugal, the lack of a prefrontal, a strongly emarginated cheek and reduced tooth ornamentation. Ten cryptoclidid genera are currently recognized (Benson and Druckenmiller, 2014); *Abyssosaurus* (Berezin, 2011a), *Colymbosaurus* (Seeley, 1874a), *Cryptoclidus* (Phillips, 1871), *Djupedalia* (Knutsen et al., 2012a), *Kimmerosaurus* (Brown, 1981), *Muraenosaurus* (Seeley, 1874b), *Pantosaurus* (Marsh, 1893), *Spitrasaurus* (Knutsen et al., 2012d), *Tatenectes* (Knight, 1900) and *Tricleidus* (Andrews, 1909). Other provisionally valid

cryptoclidids also included in the Benson and Druckenmiller (2014) analysis include *Picrocleidus beloclis* (Andrews, 1910) and '*Plesiosaurus*' *mansellii* (Hulke, 1870).

Colymbosaurinae (Benson and Bowdler, 2014) is a cryptoclidid subclade diagnosed soley on postcranial features due to the paucity of cranial material for this group (Benson and Bowdler, 2014). Seven species are referred to this subclade, including British (*Colymbosaurus megadeirus*; Benson and Bowdler, 2014), North American (*Pantosaurus striatus*; Marsh, 1893; O'Keefe and Wahl, 2003b) and Russian (*Abyssosaurus nataliae*; Berezin, 2011a) taxa. Notably, all four of the plesiosauroids currently described from the Upper Jurassic Slottsmøya Member Lagerstätten of Spitsbergen (*Colymbosaurus svalbardensis*, *Djupedalia engeri*, *Spitrasaurus larseni* and *S. wensaasi*; Knutsen et al., 2012a, c, d) are also members of this clade.

The high Arctic island of Spitsbergen, part of the Norwegian Svalbard archipelago, has yielded many important remains of marine reptiles from the Upper Jurassic Slottsmøya Member of the Agardhfjellet Formation. At present, a total of three new monospecific genera of ichthyosaurs and two new genera and four species of plesiosaurians have been described, all of which are endemic to this region (Delsett et al., 2016; Hurum et al., 2012). The first cryptoclidid described from the Slottsmøya Member Lagerstätten was '*Tricleidus*' *svalbardensis* (Persson, 1962). An additional 23 cryptoclidid skeletons were excavated between 2004 and 2012 from the Slottsmøya Member. Based on new morphological data derived from some of this material, Knutsen et al. (2012c) referred the holotype specimen of '*Tricleidus*' *svalbardensis* (PMO A27745) to the British Kimmeridgian genus *Colymbosaurus* along with two other partial postcranial skeletons (PMO 216.838, PMO 218.377).

Despite being known from numerous specimens in the Kimmeridge Clay Formation and now the Slottsmøya Member of Spitsbergen, *Colymbosaurus* has proven difficult to diagnose, in part due to the near absence of cranial remains and a scarcity of associated material. This problem was further compounded by the suggestion that *Colymbosaurus* is synonymous with *Kimmerosaurus langhami* (Brown, 1981; Brown et al., 1986) also from the Kimmeridge Clay Formation, an idea that is now discounted (Benson and Bowdler, 2014). Recently, Benson and Bowdler (2014) re-examined and re-diagnosed this taxon on the basis of three

diagnostic characters: 1) a postaxial flange bearing a single large postaxial ossicle facet of sub-equal size to the other epipodial facets; 2) an anteroposteriorly oriented ridge bisecting the distal facets on the propodials; 3) cervical vertebrae which are slightly anteroposteriorly shorter than dorsoventrally high and lack a lateral ridge. Here, we describe the most complete Slottsmøya Member specimen referable to *Colymbosaurus svalbardensis*, PMO 222.663. The new material from the Slottsmøya Member and a re-examination of additional material from the Kimmeridge Clay Formation permit a revaluation of diagnostic characters for both the genus and *C. svalbardensis.*

Geological Setting

The Slottsmøya Member is the uppermost of four members of the Agardhfjellet Formation that spans a Middle Jurassic to Lower Cretaceous marine succession on Spitsbergen. The Agardhfjellet Formation is separated from the overlying Lower Cretaceous Rurikfjellet Formation by a regionally recognizable layer known as the Myklegardfjellet Bed (Dypvik et al., 1991)(Figure 2.1). The Slottsmøya Member consists of 55–70 m of dark grey to black silty mudstone, which is often weathered into paper shale. There are discontinuous silty beds with associated siderite and dolomite interbeds and siderite nodules, some of which are interpreted as storm deposits (Rousseau and Nakrem, 2012).

The Slottsmøya Member represent approximately 12 million years of deposition spanning the upper Tithonian to the lower Berriasian (Hammer et al., 2012). As summarized in Delsett et al. (2016), detailed stratigraphic and isotopic work has divided the member into lower (-22–0 m), middle (0–27 m) and upper (27–52 m) units (Figure 2.2), using a distinctive echinoderm bed (‘yellow layer’) as a lower marker bed (0 m; Rousseau and Nakrem, 2012) and the *Dorsoplanites* layer as a second, stratigraphically higher marker bed (27 m; Collignon and Hammer, 2012; Hammer et al., 2012; Hjálmarsdóttir et al., 2012; Nagy and Basov, 1998). The specimen described here (PMO 222.663) is from the middle unit (Figure 2.2), a particularly fossiliferous stratigraphic interval (~14 m) from which six ichthyosaurs and six plesiosaur specimens have been excavated (Delsett et al., 2016). PMO 216.838, the recently referred specimen of *Colymbosaurus svalbardensis* (Knutsen et

al., 2012c) was also found at this same interval. However, the exact stratigraphic position of the holotype specimen (PMO A27745) is unknown.

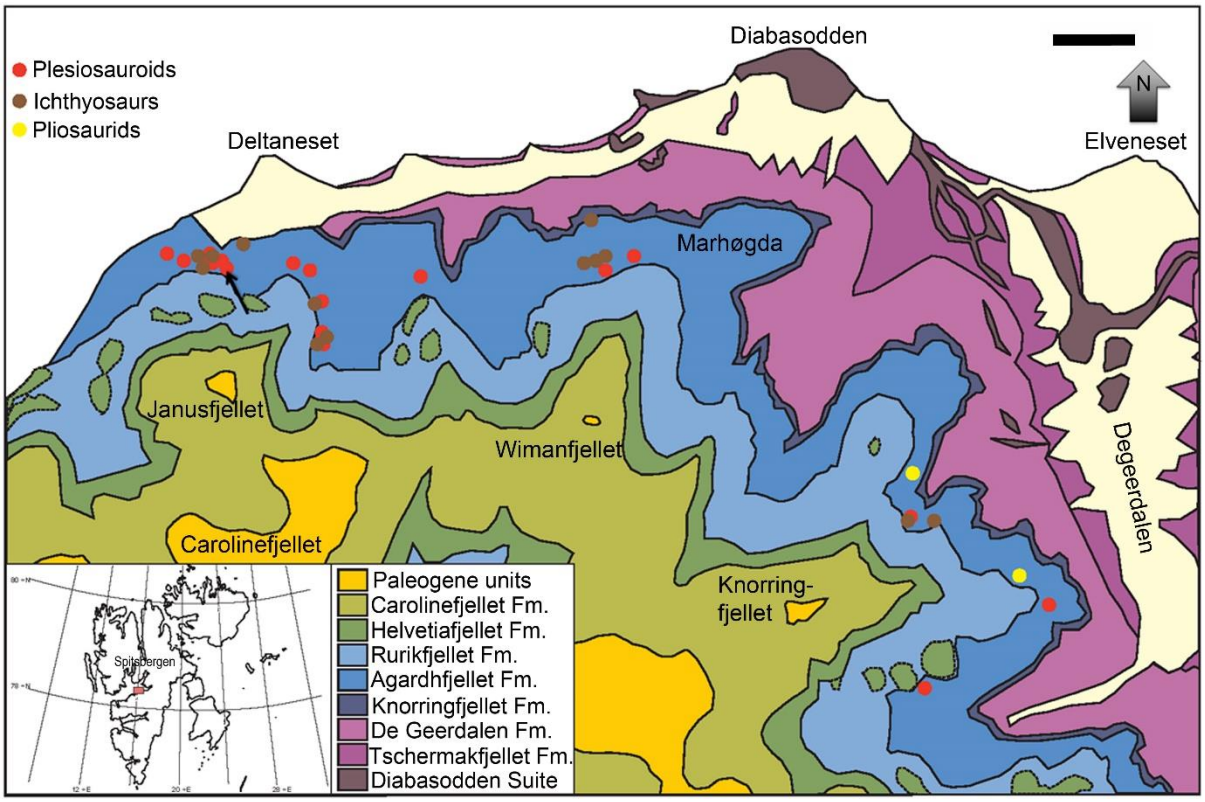

Figure 2.1: Geological map of study area, including the Agardhfjellet Formation and excavation sites. The black arrow indicates the location of PMO 222.663. (Modified from Dallmann et al., 2001; Hurum et al., 2012). Scale bar equals 1 km.

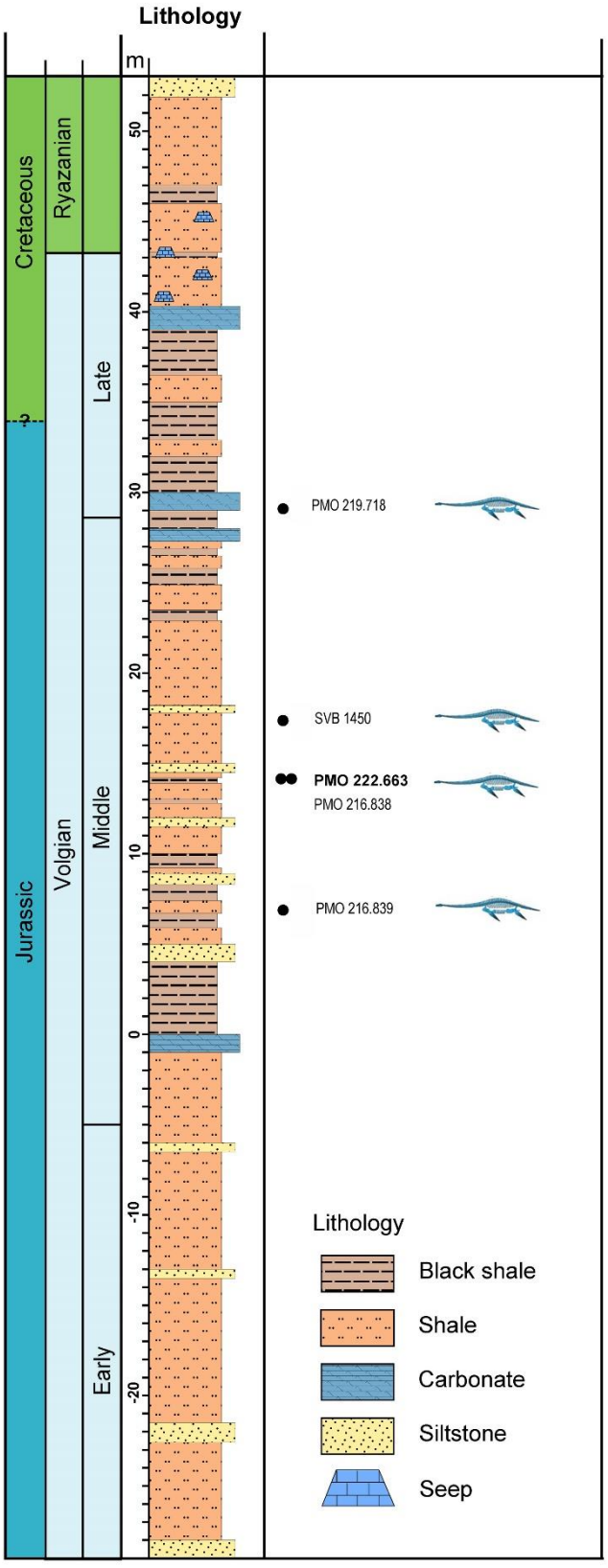

Figure 2.2: stratigraphic position of PMO 222.663 compared to the referred specimen of *Colymbosaurus svalbardensis* (PMO 216.838) in bold, *Spitrasaurus* (PMO 219.718, SVB 1450) and Djupedalia (PMO 216.839). Modified from Delsett et al. (2016).

Institutional Abbreviations—**CAMSM**, Sedgwick Museum of Earth Science, Cambridge University, Cambridge, U.K.; **GLAHM**, The Hunterian Museum, University of Glasgow, U.K.; **LEICS**, Leicester New Walk Museum, U.K.; **MANCH**, The Manchester Museum, U.K.; **NHMUK**, Natural History Museum, London, U.K.; **NOTNH**, Wollaton Hall, Nottingham, U.K.; **OUM**, Oxford University Museum of Natural History, U.K.; **PETRM**, Peterborough Museum, U.K.; **PMO**, Paleontological Museum Oslo, University of Oslo, Norway; **PMU**, Paleontological Museum of Uppsala, Museum of Evolution, Uppsala, Sweden; **SVB**, Svalbard Museum, Longyearbyen, Norway; **YORKM**, York Museum and Art Gallery, U.K..

Materials and Methods

PMO 222.663 was excavated on the mountain of Janusfjellet over two field seasons (2010–2011). The specimen was mechanically prepared using air scribes, air abrasion and small manual tools (Chapter 1, this volume). In addition to this new specimen, the holotype of *Colymbosaurus svalbardensis* (PMO A 27745) and the two previously referred specimens (PMO 216.838 and PMO 218.377; Knutsen et al., 2012c) were re-examined in the course of this study. In addition to the *Colymbosaurus svalbardensis* material, Kimmeridge Clay Formation specimens were also examined in several U.K. museums. Two of these specimens, NHMUK R10062 and OUM J.3300, are reasonably complete and can be referred to *Colymbosaurus*. To add to the diagnostic features defined by Benson and Bowdler, (2014), 22 propodials referred to or with similar morphology to *Colymbosaurus* were examined and measured (Appendix 3, Table A3.1). The majority of these are from the Kimmeridge Clay Formation held in U.K. museums, save PMO 222.663 and the holotype of *Colymbosaurus svalbardensis* (PMO A27745) from Spitsbergen (Knutsen et al., 2012c). All specimens that were included in this study, with the exception of CAMSM J68344, are from a mature ontogenetic stage. Some specimens include several propodials (OUM J.3300, PMO 222.663, MANCH LL.5513/MANCH LL.5514) and were examined to assess variation in humeri and femora. More propodial material resembling *Colymbosaurus* is available in private collections and in unregistered material at other museums; these were examined but not included in this study. Whenever possible, the presence or absence of the distal

anteroposteriorly oriented ridge, used as one of the diagnostic features by Benson and Bowdler, (2014), was recorded and defined by a distinct ridge extending on both epipodial facets.

Systematic Palaeontology

SAUROPTERYGIA Owen, 1860

PLESIOSAURIA de Blainville, 1835

PLESIOSAUROIDEA Gray, 1825

CRYPTOCLIDIDAE Williston, 1925

COLYMBOSAURINAE Benson and Bowdler, 2014

COLYMBOSAURUS Seeley, 1874a

Type Species—*Colymbosaurus megadeirus*

Valid Referred Species—*Colymbosaurus svalbardensis* (Persson, 1962)

Occurrence—Upper Jurassic; Kimmeridge Clay Formation, Kimmeridgian–early Tithonian, U.K.; Agardhfjellet Formation, Tithonian–early Berriasian, Svalbard, Norway.

Amended Diagnosis—A large cryptoclidid with the following features: mid-cervical vertebrae marginally anteroposteriorly shorter than dorsoventrally tall and lacking a longitudinal ridge on the lateral surface (modified from Benson and Bowdler, 2014); middle caudal centra subrectangular due to a flat ventral surface, with widely-spaced chevron facets; propodials with a large posterodistal expansion at least twice as large as the preaxial expansion, bearing a single postaxial ossicle facet of subequal size to the epipodial facets (modified from Benson and Bowdler, 2014); ulna conspicuously anteroposteriorly wider than the radius and proximodistally short; fibula symmetrically pentagonal in outline having equally long pre- and postaxial margins and with facets subequal in length for the fibulare and astragalus.

Referred Material—NHMUK R10062, a partial skeleton including cervical, dorsal and caudal vertebrae, dorsal ribs, a coracoid, ischium and pubis, and

a right humerus and some associated limb elements; OUM J.3300, an incomplete skeleton including a partial right mandible, cervical, dorsal, and caudal vertebrae, partial pectoral girdle, four propodials and disarticulated limb elements.

Remarks—NHMUK R10062 has not been previously described in detail, but was informally referred to *Colymbosaurus* by Brown (1984). OUM J.3300 is currently undescribed, but can be confidently referred here to *Colymbosaurus*.

NHMUK R10062 is one of the most complete specimens referable to *Colymbosaurus*. The preserved mid-dorsal vertebra exhibits a tall neural canal similar to *Colymbosaurus svalbardensis*. The mid-caudals are pentagonal in anterior view, with widely spaced chevron facets as in *Colymbosaurus.* No anteroposteriorly oriented ridge is visible on the distal articular surface of the humerus, similar to some propodials of *Colymbosaurus megadeirus* (Benson and Bowdler, 2014). For this reason, Benson and Bowdler (2014) referred NHMUK R10062 to Plesiosauroidea *incertae sedis*. The ilia of NHMUK R10062 are nearly identical to those found in PMO 222.663 in their general morphology. They share a sub-equal expansion of the dorsal end and are mediolaterally compressed.

OUM J.3300 is the only *Colymbosaurus* specimen to have cranial material, consisting of a partial right mandible along with several possible cranial fragments and the majority of the postaxial skeleton. OUM J.3300 is referred to *Colymbosaurus* on the basis of mid-cervical vertebrae that are marginally anteroposteriorly shorter than dorsoventrally tall and lack a longitudinal ridge on the lateral surface. The specimen shares the morphology of the postaxial expansion of the propodials with *Colymbosaurus*, the ulna is conspicuously anteroposteriorly wider than the radius and proximodistally short, and the fibula is pentagonal with sub-equally large facets for the astragalus and fibulare.

COLYMBOSAURUS SVALBARDENSIS (Persson, 1962)

(Figures 2.3–11)

Holotype—PMO A27745

Referred Material—PMO 222.663 is an incomplete, partially articulated skeleton preserving 14 dorsal and three sacral vertebrae, a nearly complete caudal

series, coracoids, partial interclavicle-clavicle complex, both ilia, four propodials, most of the epipodials and several more distal limb elements. Other referred material includes PMO 216.838 and PMO 218.377 (Knutsen et al., 2012c).

Amended Diagnosis—A species of *Colymbosaurus* with four sacral vertebrae (three in *C. megadeirus*). Differs from *Colymbosaurus megadeirus* in having proximodistally shorter epipodials in the hind limb (tibia, fibula length/width ratio) (Knutsen et al., 2012c), a dorsoventrally taller neural canal on the mid-dorsal vertebrae (at least twice as tall as wide), a more gracile femoral shaft (PMO 216.838 is excluded here due to preservation), and the posterior margin of the ischium is abruptly squared-off and relatively broad (Knutsen et al., 2012c).

Diagnostic Remarks of PMO 222.663—PMO 222.663 is referred to *Colymbosaurus* on the following basis: (1) the middle caudal centra are subrectangular due to a flat ventral surface, with widely spaced, low chevron facets located ventrolaterally; (2) the propodials possess a large posterodistal expansion at least twice as large as the preaxial expansion, and bear a single postaxial ossicle facet of subequal size to the epipodial facets; (3) the ulna is conspicuously anteroposteriorly wider than the radius; (4) the fibula is symmetrically pentagonal in outline with subequal facets for the fibulare and intermedium. PMO 222.663 shares important features with the holotype of *Colymbosaurus svalbardensis* (PMO A27745) and is referred to this taxon on the basis of possessing a neural canal of the middle dorsal vertebrae that is at least twice as tall as wide (maximum internal height/maximum internal width) and relatively short epipodials (tibia length/width ratio).

Occurrence—Upper Jurassic Slottsmøya Member of the Agardhfjellet Formation (upper Tithonian–lower Berriasian). PMO 222.663 was found 14 m above the ‘yellow layer’ marker bed and 13 m below the *Dorsoplanites* marker bed (Delsett et al., 2016); locality coordinates 33x E518470 N8696400.

Taphonomy—PMO 222.663 consists of a partial axial skeleton with an associated nearly complete appendicular skeleton (Figure 2.3). Similar to most of the marine reptile material from the Slottsmøya Member, the specimen has undergone congelifraction (fragmentation due to repeated freeze-thaw cycles) and compaction

in certain areas (Delsett et al., 2016). Cranial material, as well as cervical and anterior dorsal vertebrae are not preserved. In total, 14 partial dorsal vertebrae are preserved, six of which remain in a single articulated series. A total of three compressed sacrals is also present, of which only one preserves an entire neural spine and seven sacral ribs suggesting the presence of a forth sacral vertebrae. In addition, there are 24 caudal vertebrate, ten of which are articulated. The majority of these vertebrae are eroded and lack part, if not all, of the neural spine and transverse process. The left pectoral girdle is displaced and lying partially below the right and is preserved in a more sideritic shale compared to the remainder of the skeleton, resulting in differential compaction of the skeleton in this region. Both femora are preserved, although the left femur is crushed at its proximal end and near the postaxial flange. The right femur has been displaced and shifted 180 degrees relative to the rest of the paddle. The distal limb elements are well-preserved and partially articulated in the hind limbs.

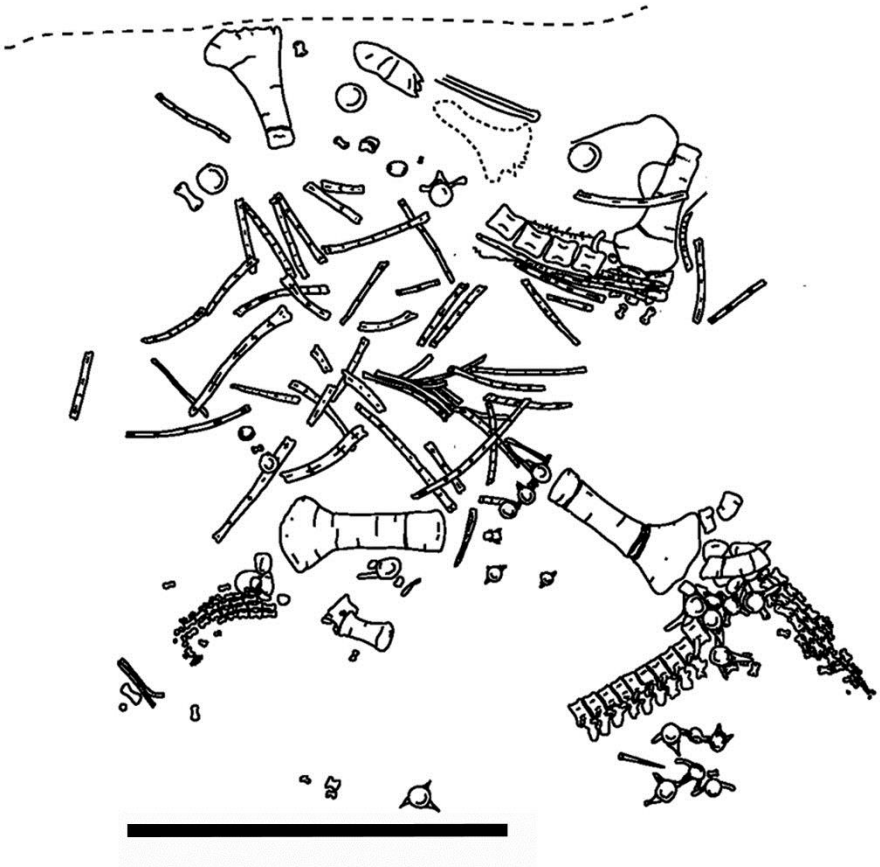

Figure 2.3: Quarry map of PMO 222.663, modified from Delsett et al., (2016). Dashed line indicates erosional slope. Scale bar equals 1 m.

Ontogenetic State

PMO 222.663 is considered an adult on the basis of fused neurocentral sutures throughout the entire preserved portion of the vertebral column, fused caudal ribs and distinct and well formed epipodial facets on the propodials (Brown, 1981). Compared to the syntypes of *Colymbosaurus megadeirus*, PMO 222.663 appears to be slightly smaller based on the size of the vertebrae and propodials (Benson and Bowdler, 2014).

Description and Comparisons

Axial Skeleton

Dorsal Vertebrae—Due to compression of the dorsal vertebrae in PMO 222.663, only certain aspects of the morphology can be described in detail (Figure 2.4A–E). The centra are slightly wider than tall in anterior view, similar to *Tatenectes laramiensis* and NHMUK R10062 (*Colymbosaurus* indet.; Brown, 1984; O'Keefe et al., 2011), whereas the centra dimensions in *Muraenosaurus leedsii* are more equidimensional (Andrews, 1910; Brown, 1981).

As in *Colymbosaurus svalbardensis* the neural canal of PMO 222.663 is significantly taller than wide (Figure 2.4D, E), although in PMO 222.663 some of this could be attributed to distortion (Knutsen et al., 2012c). This condition differs from the circular neural canal observed in Kimmeridge Clay Formation cryptoclidids (Benson and Bowdler, 2014; AJR, *pers. obs.*, CAMSM J35344 and OUM J.3300). The combined mediolateral width of the zygapophyses is narrower than the centrum, as in *Colymbosaurus megadeirus* (Benson and Bowdler, 2014). Based on the single, undistorted neural arch base, PMO 222.663 lacks an anteroposterior constriction at the base of the neural spine as in all other cryptoclidids (Benson and Druckenmiller, 2014). In the mid-dorsal vertebrae (Figure 2.4E), the transverse processes are placed dorsally with respect to the neural canal, and gradually shift ventrally in more posterior vertebrae. In anterior view, the transverse processes are inclined at 30–40° with respect to the horizontal plane, as in the holotype of *Colymbosaurus svalbardensis* (Knutsen et al., 2012c). Due to crushing, it is impossible to see if the transverse processes sweep posteriorly in lateral view. The rib facets appear oval and are dorsoventrally taller than anteroposteriorly long, but this could be a taphonomic artefact. The posterior-most dorsal vertebra is more circular than the more anterior

vertebrae and has short rectangular-shaped transverse processes in anterior view, but is still separated from the centrum (Figure 2.4C).

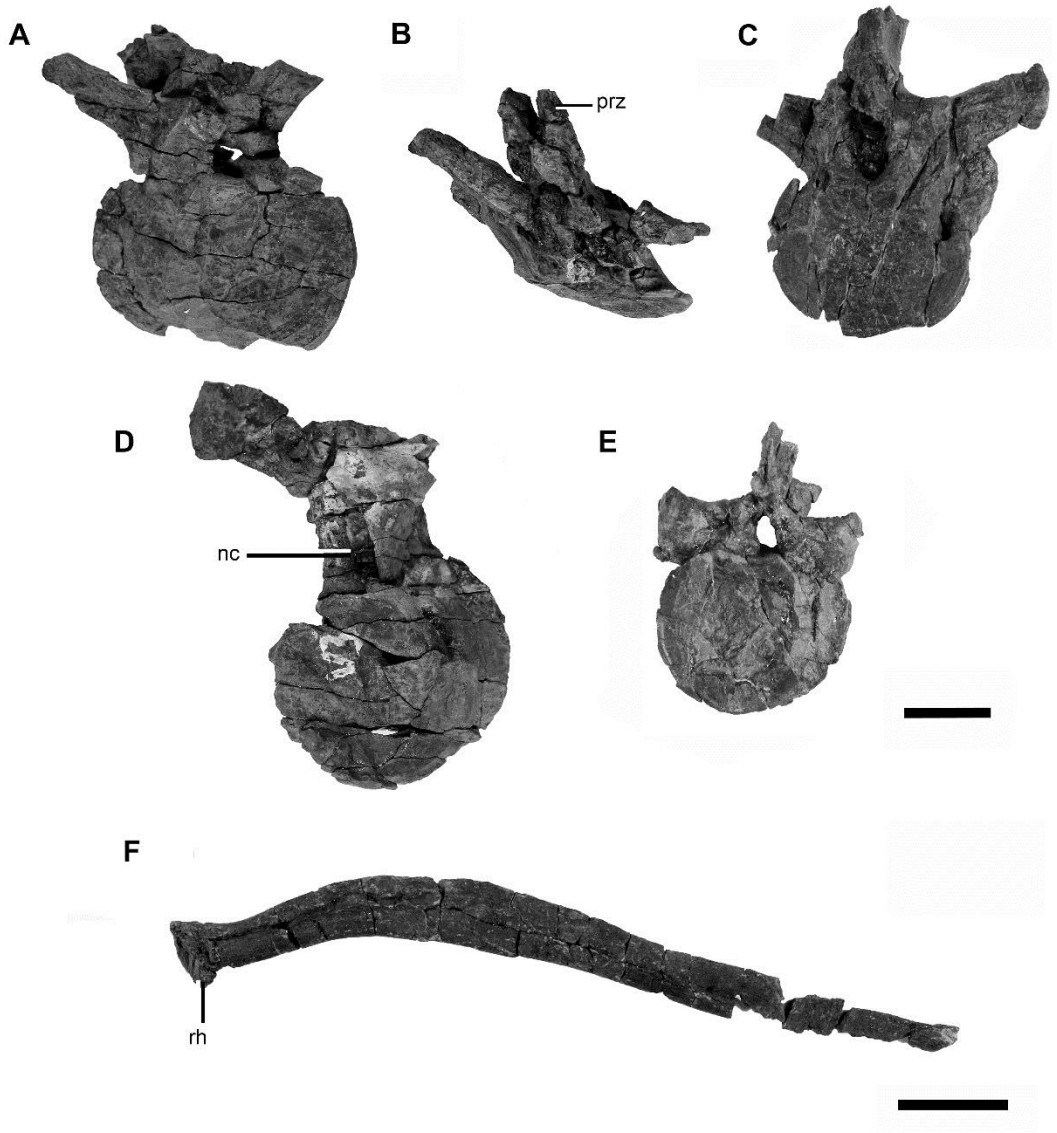

Figure 2.4: Dorsal vertebrae and a partial dorsal rib of PMO 222.663. **A**, mid-dorsal vertebrae in posterior and **B**, dorsal views; **C**, anterior/mid-dorsal in anterior view; **D,** mid-dorsal in anterior/posterior? view; **E**, posterior-most dorsal in posterior view; **F**, a right dorsal rib in posterior view. **Abbreviations: nc**, neural canal; **prz**, prezygapophysis; **rh**, rib head. Scale bars equal 2 cm (A–E**)**; 5 cm (F).

Sacral Vertebrae—Three sacral vertebrae are preserved in PMO 222.663 (Figure 2.5A–C) and were identified as those vertebrae in which the centrum and neural arch both contribute to the sacral rib facet (Benson and Bowdler, 2014). However, this state can be difficult to determine in well-ossified adults, such as

PMO 222.663, where the neurocentral sutures are fused and the centra poorly preserved. Three pairs of sacral ribs were also identified in PMO 222.663, although an additional sacral rib may also be present (see below). Thus, four sacral vertebrae may have been present, but poor preservation and disarticulation in this area makes it difficult to confirm. Four sacrals are present in the holotype of *Colymbosaurus svalbardensis* (PMO A 27745) and *Tatenectes laramiensis* (Knutsen et al., 2012c; O'Keefe et al., 2011), while three are found in *C. megadeirus* (Benson and Bowdler, 2014).

The order of the sacral vertebrae in PMO 222.663 can be determined by the position of the sacral rib facets, along with other associated vertebrae (O'Keefe et al., 2011). The first sacral was identified by the more dorsal position of the rib facets, in respect to the other sacral vertebrae (Figure 2.5A). In posterior view the centrum is mediolaterally wider than dorsoventrally tall. The vertebra interpreted as being the second or third sacral has a more ventrally-positioned rib facet than the first (Figure 2.5B). The morphology of the sacral rib facets on this vertebra are subcircular rather than dorsoventrally long and anteroposteriorly short, as in the sacrals of one of the syntypes in *Colymbosaurus megadeirus* (CAMSM J63919) and NHMUK R10062 (Benson and Bowdler, 2014). The posterior-most sacral is the best preserved of the three and was found in articulation with the first caudal vertebra (Figure 2.5C). The neural spine is dorsoventrally shorter and nearly anteroposteriorly as long as the centrum, with a slightly posteroventrally sloping apical margin. As in most cryptoclidids the sacral neural spines are positioned dorsally from the centrum (O'Keefe et al., 2011). This morphology differs from *Pantosaurus striatus*, where the neural spines are significantly posteriorly inclined (Wilhelm and O'Keefe, 2010). A partial sacral rib was found in articulation with this vertebra (Figure 2.5C).

PMO 222.663 preserves seven partial to complete sacral ribs. Four are complete, two other proximal rib fragments remain in articulation with the centra, and one is incomplete. The most gracile sacral rib (Figure 2.5D) was found adjacent to the second or third sacral vertebra, is straight and trilobate-shaped in cross section proximally and becomes more oval in cross section distally. The other sacrals are straight and elongate and exhibit nearly equal expansion of both the proximal and distal ends. The sacral ribs (Figure 2.5E, F and G, H) are interpreted as two sets, as these were found in close proximity to each other. Each of the sacral ribs preserved

in PMO 222.663 are proximodistally extended and exhibit nearly equally expanded proximal and distal ends. This differs from the spatulate sacral ribs found in *Tatenectes laramiensis* and *Pantosaurus striatus*, which have anteroposteriorly expanded distal ends in dorsal view (O'Keefe et al., 2011; Wilhelm and O'Keefe, 2010). Additionally, PMO 222.663 also differs from *Cryptoclidus eurymerus*, in which the proximal end is dorsoventrally thicker than the distal end (Brown, 1981).

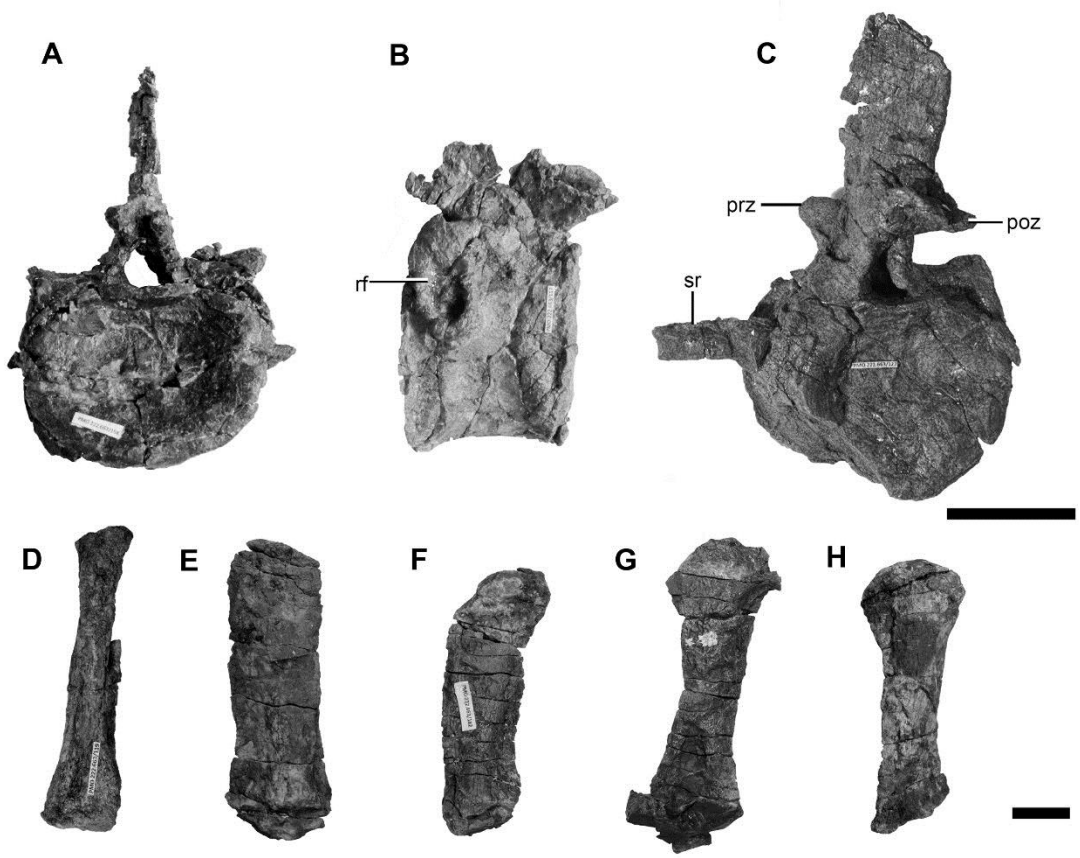

Figure 2.5: Sacral vertebrae and ribs of PMO 222.663. **A**, first sacral vertebra in posterior view; **B**, second or third sacral vertebra in lateral view; **C**, posterior sacral vertebra in posterolateral view; **D–H**, sacral ribs. **Abbreviations: poz**, postzygapophysis; **prz**, prezygapophysis; **rf**, rib facet; **sr**, sacral rib. Scale bar equals 5 cm (A–C) and 2 cm (D–H).

Caudal Vertebrae—The 24 caudal vertebrae preserved in PMO 222.663 represent the most complete plesiosauroid tail known from the Slottsmøya Member, and consist of an articulated anterior series, and several disarticulated mid- and posterior caudals (Figure 2.6). In general morphology, the centra are pentagonal and mediolaterally wider than dorsoventrally tall, as in the holotype for *Colymbosaurus svalbardensis* (PMO A27745) and *C. megadeirus* (Benson and Bowdler, 2014;

Knutsen et al., 2012c). Paired subcentral foramina are present ventrolaterally. All caudals possess chevron facets, except the first centrum preserved in the series. Similar to the holotype of *C. svalbardensis* (Knutsen et al., 2012c) the chevron facets are triangular in ventral view, with the apex pointing anteriorly (Figure 2.6B), in contrast to oval facets seen in *C. megadeirus* (Benson and Bowdler, 2014). The facets slightly protrude from the ventral surface, but are recessed in PMU 24781, an historical specimen from the Slottsmøya Member, suggested to resemble *Colymbosaurus* by Kear and Maxwell, (2013). As in both *C. svalbardensis* and *C. megadeirus,* the chevron facets are shared between adjacent vertebrae (Figure 2.6E). An anterior ridge on the chevron facet is present in *C. megadeirus* and also NHMUK R10062 (AJR, *pers. obs*.), but is absent in PMO 222.663.

The neural arches on the anterior caudal vertebrae are well preserved (Figure 2.6A). These are posteriorly angled, so the posterior margin of the neural spine is dorsal to the anterior third of the succeeding centrum, similar to the holotype specimen of *Colymbosaurus svalbardensis* (PMO A27745; Knutsen et al., 2012c). The neural spine is slightly taller than the dorsoventral height of the centrum (Table 2.1). On the sixth vertebra in the articulated caudal series, an anteriorly oriented process extends from the pedicel of the neural arch; this structure may be a taphonomic artefact or possibly a pathology (Figure 2.6E). This process is fused to the pedicel, and appears broken distally (Appendix 3, Figure A3.1). The caudal ribs are fused to the centra and are gracile. The ribs terminate in a sharp point, which differs from the spatulate morphology observed in *Cryptoclidus eurymerus* (PETRM R283).

The two posterior-most caudals differ significantly from the rest of the series. The central are fused via the caudal ribs and part of the neural canal floor (Figure 2.7). The posterior-most vertebra is compressed so that the posterior face of the centrum is angled posterodorsally, and the chevrons are fused to the centrum. Unlike the fused posterior caudal vertebrae in *Cryptoclidus eurymerus* NHMUK R8575, those of PMO 222.663 bear caudal ribs, although in the posterior-most vertebra these are significantly reduced. A neural arch is not present, as is often the case in posterior vertebrae (Wilhelm, 2010). This structure may represent a pygostyle-like structure similar to that seen in the posterior caudal series of various plesiosaurians outside Cryptoclididae, such as *Albertonectes* and *Rhomaleosaurus zetlandicus*,

(Kubo et al., 2012; Smith, 2013). The presence of a fused pygostyle structure in adults has also been suggested to be a synapomorphy of Cryptoclididae (Benson and Druckenmiller, 2014).

The morphological variation throughout the caudal series also provides insight into the possible presence of a tail bend in PMO 222.663. Caudal series are well known from three genera of cryptoclidids; *Cryptoclidus* (e.g., NHMUK R 8575), *Muraenosaurus* (e.g., NHMUK R2864) and *Pantosaurus* (USNM 536965; Wilhelm, 2010; Wilhelm and O'Keefe, 2010). The latter has a slight downward bend of the tail starting at the fourth caudal, indicating a tail bend (Wilhelm and O'Keefe, 2010). The presence of a tail bend is difficult to confirm in PMO 222.663 due to the vertebral compression. However, the neural spines angle posteriorly from the mid-caudal vertebrae, resulting in a slight ventral displacement of the vertebrae (Figure 2.6E). Following Smith (2013), this morphology could be indicative of a downward tail bend in PMO 222.663.

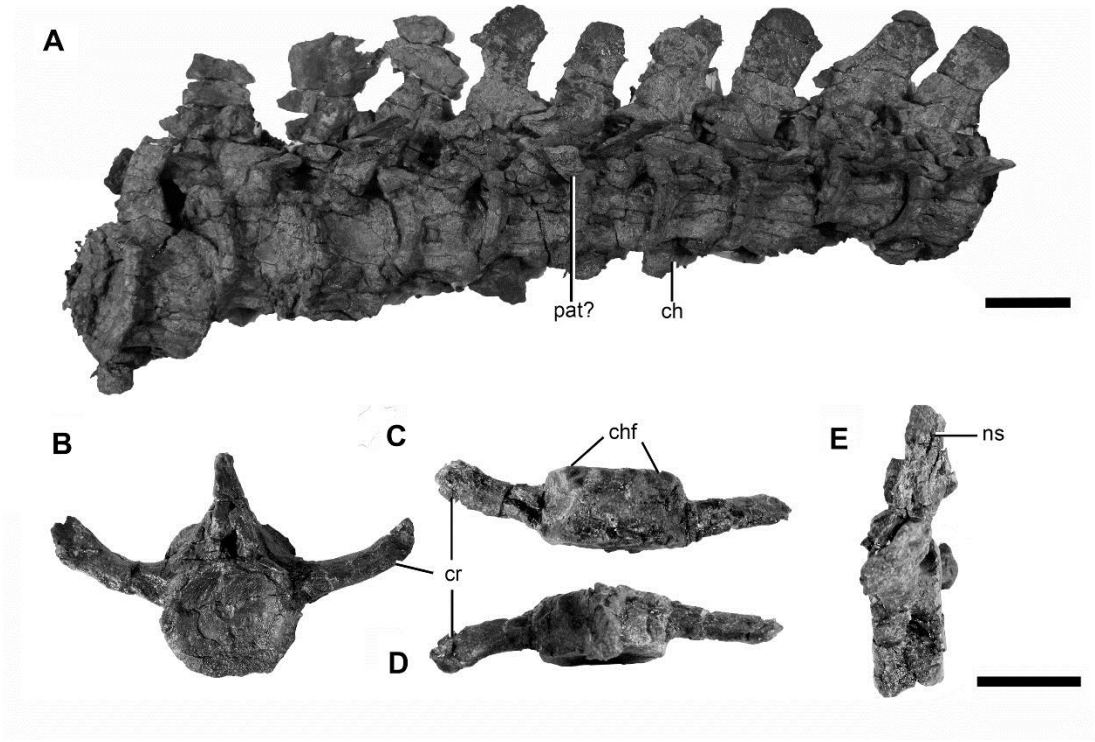

Figure 2.6: Selected caudal vertebrae of PMO 222.663. **A**, the articulated anterior caudal series; **B**, a mid-caudal vertebra in anterior, **C**, ventral **D**, and dorsal views; **E**, mid-caudal in lateral view. **Abbreviations**: **ch**, chevron; **chf**, chevron facet; **cr**, caudal rib; **ns**, neural spine; **pat?**, pathology?. Scale bar equals 5 cm.

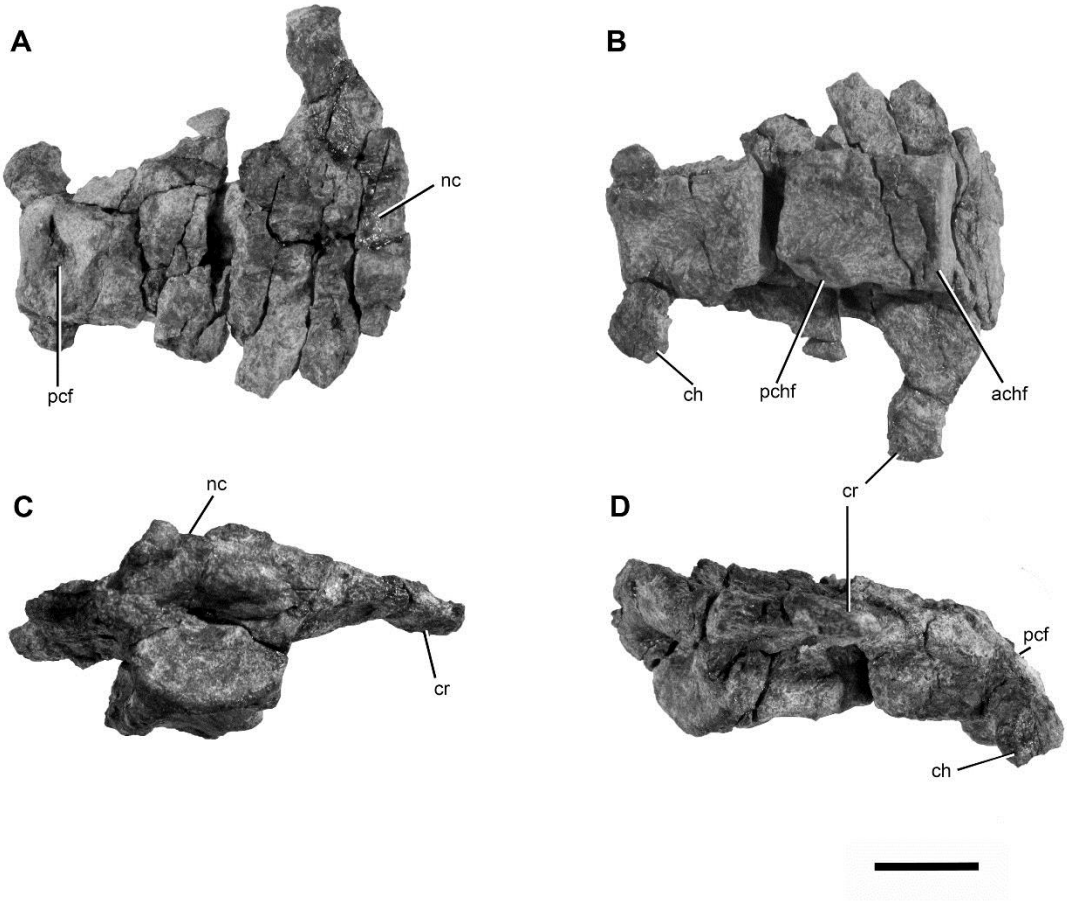

Figure 2.7: Two posterior-most caudal vertebrae of PMO 222.663 in **A**, dorsal, **B**, ventral, **C**, anterior and, **D**, lateral views. **Abbreviations: achf**, anterior chevron facet; **ch**, chevron; **cr**, caudal rib, **nc**, neural canal floor, **pcf**, posterior centrum face, **pchf**; posterior chevron facet. Scale bar equals 2 cm.

Dorsal Vertebrae	DV Height (centrum)	AP Length	ML Width (centrum)	NS Height
Mid-dorsal	7	6	9.2	x
Posterior-most dorsal	7.6	*3.2	9.2	1.9
Sacral Vertebrae				

Anterior-most				
Sacral	6.7	*3.5	9.1	4.9
2/3rd Sacral	*7.4	*5.9	x	x
Posterior-most				
Sacral	7.1	x	8.0	7.1
Caudal Vertebrae				
Anterior-most				
Caudal	7.0	*2.9	8.7	7.3
Mid-caudal	5.4	x	6.3	5.9
Posterior caudal	2.8	*3.0	3.0	x

Table 2.1: Selected axial skeleton measurements for PMO 222.663. * indicates that the number could be wrong, due to compression, x indicates missing data. **Abbreviations: AP**, anterior-posterior, **DV**, dorsal-ventral, **ML**, medial-lateral, **NS**, neural spine.

Dorsal Ribs and Gastralia—Numerous disarticulated dorsal ribs and rib fragments are preserved in PMO 222.663. Five complete or near-complete ribs are preserved, all of which have single-headed proximal ends (although crushed). A single proximal end of an un-distorted rib is preserved, bearing an oval facet for articulation with the transverse process (Figure 2.4F). The ribs are bilobate in cross section and gradually become more oval-shaped distally. The most-complete and undistorted dorsal rib from PMO 222.663 is likely from the mid-dorsal region and measures approximately 50 cm in total length, lacking the distal-most end. This is slightly longer than those in *Colymbosaurus* indet. (NHMUK R10062; 40–47 cm), which has approximately the same overall body size. The ribs of PMO 222.663 are strongly curved throughout, differing from the weaker curvature observed in NHMUK R10062 (AJR, *pers. obs.*), *Djupedalia engeri* and *Tatenectes laramiensis* (Knutsen et al., 2012a; O'Keefe et al., 2011).

Several complete gastralia are preserved in PMO 222.663, along with several other probable fragments. These are dorsoventrally curved as in *Cryptoclidus* and

Muraenosaurus (Andrews, 1910; Brown, 1981) and have grooves along the articulating surfaces of the adjacent gastralia. The majority of these are proximodistally short, curved and tapering, similar to those preserved in other cryptoclidids (Andrews, 1910; O'Keefe et al., 2011). There is no obvious evidence that these are pachyostotic as seen in *Tatenectes laramiensis* (O'Keefe and Street, 2009; O'Keefe et al., 2011).

Appendicular Skeleton

Pectoral Girdle—A partial pectoral girdle is preserved in PMO 222.663, consisting of an incomplete clavicle-interclavicle complex and coracoids (Figure 2.8). The fragments interpreted to be the clavicle-interclavicle complex are partially fused, making interpretation difficult (Figure 2.8C-D). This complex is rarely preserved in Late Jurassic cryptoclidids and tentative identifications are based partly on morphology and their proximity to other pectoral elements (Brown, 1981). The nearly complete left clavicle is wing-like, with a smooth ventral surface and a pitted dorsal surface, presumably for articulation with the scapula. The interclavicle is fully fused to the clavicles and appears as a bulge on the visceral surface between the two clavicles. On the left clavicle, the anterior margin is convex and the posterior margin is concave. The medial margin is straight and tapered towards the midline and approaches, but does not contact the right clavicle. The lateral margin is more gently rounded than that seen in *Cryptoclidus eurymerus* and *Tricleidus seeleyi* (Andrews, 1909; Brown, 1981). Clavicle-interclavicle complexes are only known from three other Kimmeridgian–Tithonian cryptoclidids and only a single plate-like element is known from the Oxfordian cryptoclidid *Tatenectes laramiensis* (O'Keefe and Street, 2009). In NHMUK R10062 (Brown, 1984) the clavicles differ from those of PMO 222.663 in being triangular and having a foramen perforating one of the elements. The clavicle or interclavicle element preserved in *T. laramiensis* is more square and anteroposteriorly longer in dorsal view than the short and wide element seen in PMO 222.663. However, in the holotype of *Djupedalia engeri* (PMO 216.839) the partial clavicle closely resembles the nearly complete clavicle of PMO 222.663 in being 'wing-like' with a concave anterior margin (Knutsen et al., 2012a).

Portions of the left and right coracoids are preserved and dorsoventrally compressed, obscuring their individual morphology (Figure 2.8B). However, they

preserve complimentary portions allowing a more complete reconstruction of their overall shape (Figure 2.8A). The element interpreted as the right coracoid, based on its close association with the right humerus, consists of much of the anterior end, including part of the medial symphysis and glenoid. The left coracoid consists primarily of the lateral margin. There is no clear evidence for the presence of an anteromedial process, but this area is damaged and could have been lost. In anterior view, the region between the glenoid and medial symphysis appears level. The anteroposteriorly oriented platform on the ventral surface of the coracoids observed in other colymbosaurines such as *Colymbosaurus megadeirus* (and possibly *Abyssosaurus*; Benson and Bowdler, 2014), is not present. *Spitrasaurus wensaasi* and *Djupedalia engeri* also lack this trait, although the holotype specimens are not fully mature (Knutsen et al., 2012a, d).

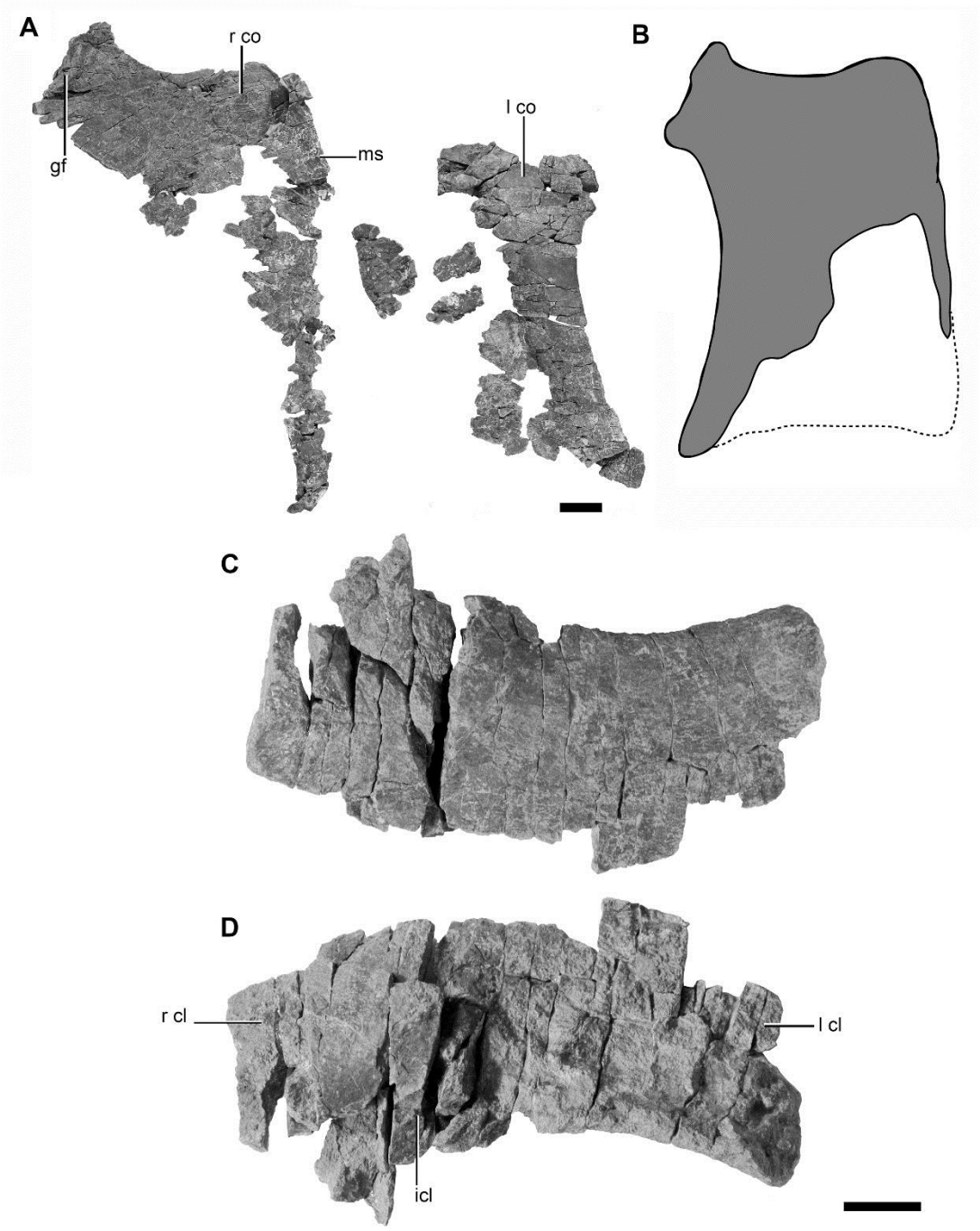

Figure 2.8: The pectoral girdle of PMO 222.663. **A**, the preserved coracoid material reconstructed in approximate life position in ventral view; **B**, reconstructed single coracoid based on the preserved portions of the right and left elements; **C**, clavicle-interclavicle complex in visceral and, **D** anteroventral views. **Abbreviations: gf**, glenoid facet; **icl**, interclavicle; **l cl**, left clavicle; **l co**, left coracoid; **ms**, medial symphysis; **r cl**, right clavicle; **r co**, right coracoid. Scale bar equals 5 cm (A–B); 2 cm (C–D**)**.

Humerus—The identity and orientation of the humerus is based on the posterior location of the tuberosity relative to the capitulum. The humeri are well-preserved but the proximal regions of the right and to some degree the left humerus are dorsoventrally compressed (Figure 2.9). The description is largely based on the better preserved left humerus (Figure 2.9B–F). In dorsal view, the humeral shaft constricts immediately distal to the proximal head, remains consistently broad for the first one third of the shaft and then expands distally. Compared to the femur, the humerus is proximally wider, proximodistally shorter, and possesses a more robust shaft (Table 2.2). In posterior view the dorsal surface of the humerus is convex along the length of the element and flat to slightly concave along the ventral surface. The postaxial margin of the shaft exhibits coarse rugosities along the majority of its length, with the exception of the postaxial flange. There is a single foramen perforating the left humerus mid-shaft along the postaxial surface that is absent in the right humerus, probably due to deformation in this limb (Figure 2.9C). Based on a comparison of the relatively smooth bone surface on the right humerus, in addition to CT scans of the left taken in this region, the 'swelling' on the left humerus is likely pathological in origin.

The distal articular surface bears three facets for the radius, ulna and a postaxial ossicle, respectively, the largest being for the ulna. In contrast, there are two epipodial facets in *Muraenosaurus leedsii* and four in *Pantosaurus striatus* (Andrews, 1910). In dorsal view, the postaxial flange is considerably more developed than the preaxial flange. A reduced preaxial flange is also present in the referred specimen of *Colymbosaurus* (NHMUK R31787), although the postaxial flange is missing (Benson and Bowdler, 2014). In OUM J.3300 (*Colymbosaurus* indet.), the distal margin is similar to that seen in PMO 222.663 in having a reduced preaxial flange and an enlarged postaxial flange. The greatly expanded postaxial morphology seen in PMO 222.663 differs from that seen in Callovian cryptoclidids where the pre- and postaxial flanges are significantly expanded (Andrews, 1910; Brown, 1981). *Spitrasaurus larseni* and *Djupedalia engeri* are also subequally expanded, although this could be due to their younger ontogenetic state (Knutsen et al., 2012a, d).

The right humerus of PMO 222.663 preserves the complete distal edge and lacks an anteroposteriorly oriented bisecting ridge on the distal epipodial facets,

previously considered as a diagnostic character for *Colymbosaurus* (Benson and Bowdler, 2014). The distal end of the right humerus is partially fused with the ulna; however, a groove is absent on the proximal articular surface of the right radius, suggesting the corresponding ridge on the humerus is absent (Benson and Bowdler, 2014). As in other specimens of *Colymbosaurus*, the ulnar facet of PMO 222.663 is anteroposteriorly longer than the radius, similar to *C. megadeirus* (Benson and Bowdler, 2014). The long ulnar facet preserved in *C. megadeirus* and *C. svalbardensis* differs from other cryptoclidids such as *Pantosaurus striatus*, *Cryptoclidus eurymerus* and *Muraenosaurus leedsii*, in which the radial facet is relatively longer (O'Keefe and Wahl, 2003b).

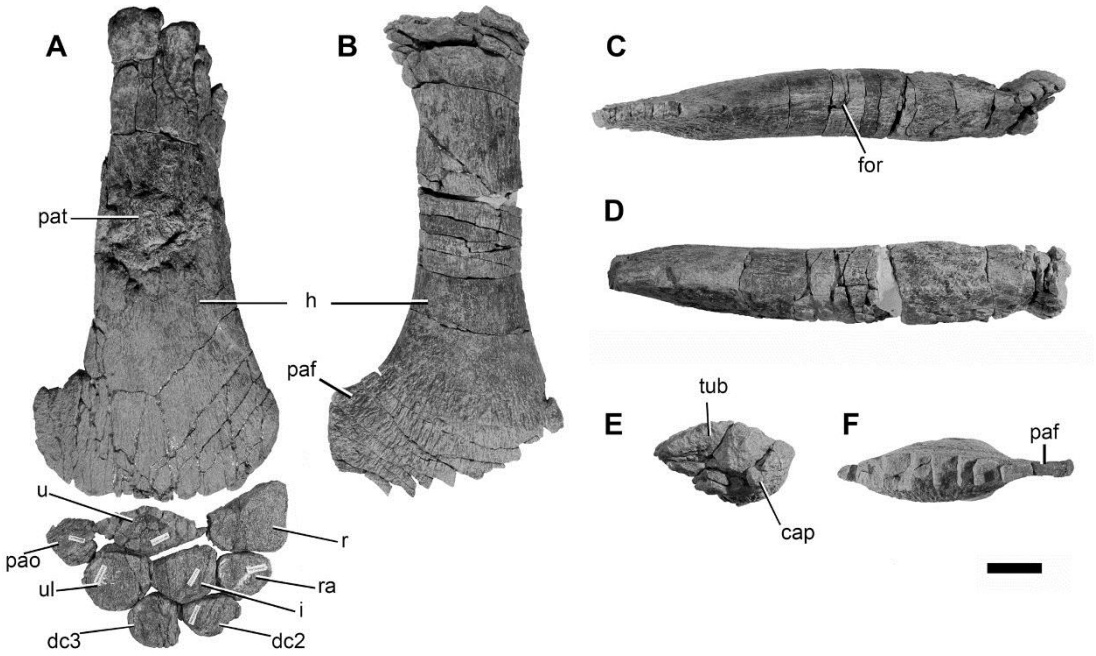

Figure 2.9: Humeri and proximal forelimb elements of PMO 222.663. **A**, right humerus and proximal forelimb elements articulated as found, in dorsal view; **B**, left humerus in ventral, **C**, anterior and **D**, posterior views, **E**, proximal and, **F**, and distal ends the left humerus. **Abbreviations: cap**, capitulum; **dc2**, second distal carpal; **dc3**, third distal carpal; **for**, foramen; **h**, humerus; **i**, intermedium; **paf**, postaxial flange; **pao**, postaxial ossicle; **pat**, pathology, **r**, radius; **ra**, radiale; **tub**, tuberosity; **u**, ulna; **ul**, ulnare. Scale bar equals 5 cm.

Epipodials and mesopodials—There are three elements in the epipodial row, the radius, ulna and a postaxial accessory ossicle, which were preserved in articulation with the right humerus (Figure 2.9A). An epipodial foramen (spatium

interosseum) is absent in PMO 222.663, unlike Oxford Clay Formation cryptoclidids where an epipodial foramen is present between the radius and ulna (Andrews, 1910). The radius is trapezoidal in dorsal view, being proximodistally shorter along the posterior margin and in proximal view evenly thick dorsoventrally. The radius is slightly longer than the ulna proximodistally, but approximately 25 % shorter anteroposteriorly (Table 2.2). This morphology is similar to that seen in OUM J.3300 (*Colymbosaurus* indet.), but differs from *Spitrasaurus wensaasi*, *Djupedalia engeri* and *Pantosaurus striatus* where in dorsal view, the radius is twice or more the size of the ulna in volume (Knutsen et al., 2012a, d; O'Keefe and Wahl, 2003b). Alternatively, in *Muraenosaurus leedsii* and *Cryptoclidus eurymerus*, the radius is proximodistally longer than the ulna, but nearly identical in anteroposterior width (Brown 1981). The ulna of PMO 222.663 is anteroposteriorly wider than proximodistally long in dorsal view and has a diamond shape. OUM J.3300 exhibits a similarly anteroposteriorly elongate ulna, although it is not as pointed as in PMO 222.663. These proportions differ from the proximodistally long ulna of *Pantosaurus striatus* and *Tatenectes laramiensis* (O'Keefe and Street, 2009; O'Keefe and Wahl, 2003a; O'Keefe and Wahl, 2003b). The ulnae in *Djupedalia engeri* and *Spitrasaurus larseni* are too poorly ossified for comparison (Knutsen et al., 2012a, d).

A postaxial ossicle is preserved in articulation with the humerus and other epipodials in PMO 222.663. This element was positioned directly posterior to the ulna and articulated to the ulnare, giving the element a more distal position than expected for this element. A partial postaxial ossicle is also preserved in *Abyssosaurus nataliae* and resembles the triangular morphology seen in PMO 222.663 (Berezin, 2011a). Although a facet for a postaxial ossicle is present in the forelimb of *Pantosaurus striatus* and *Tatenectes laramiensis*, the element is not preserved in the holotypes or referred specimens (O'Keefe and Street, 2009; O'Keefe and Wahl, 2003b). A limb element sharing the same morphology as the postaxial ossicle in PMO 222.663 is preserved in OUM J.3300; however, it is not in articulation and whether this postaxial ossicle is from the forelimb or the hind limb cannot be determined.

There are three elements in the proximal mesopodial row, the radiale, intermedium and ulnare. The radiale is rounded in dorsal view, and the smallest of the three. It has four facets for the radius, intermedium, and first and second carpals.

The intermedium and the ulnare are fused, a feature that has been observed in other adult cryptoclidids (Caldwell, 1997). Given that these elements are dorsoventrally compressed, the fusion could also be possibly taphonomic. The intermedium has six facets for the radius, radiale, ulna, ulnare and second and third carpals. The ulnare has five facets for the intermedium, ulna, postaxial accessory ossicle, the third carpal and the fifth metacarpal. In the distal mesopodial row, the second and third carpals were identified in articulation with the right paddle. Other fragmentary disarticulated metapodial and phalangeal elements were preserved in association with both forelimbs. There is no evidence for a preaxial row as seen in *Spitrasaurus* (Knutsen et al., 2012d).

	PD Length	Proximal AP Width	Distal AP Width	min. shaft AP width
Left Humerus	41	11.5	*20.1	8.3
Right Humerus	43.7	11.5	22,2	9.5
Left Femur	44.2	10.5	*16.2	6.8
Right Femur	45	*5.7	19.9	*5.7

	Max. AP Length	Max. PD Length	Min. PD Length	DV Proximal Thickness
Right Humerus Elements				
Radius	8.1	6.1	2.5	2.1
Ulna	9.9	4.9	0	x
Post ax. os.	4.5	4.3	x	x
Right Femur Elements				
Tibia	7.1	5.1	3.9	3.1

Fibular	8.1	5.5	x	3.6
Post ax. os.	3.8	*4.8	x	2.2
Left Femur				
Elements				
Tibia	7.6	5.3	x	3.1
Fibular	3.1	5.2	x	2.9
Post ax. os.	3.9	4.9	x	x

Table 2.2: Selected measurements of the appendicular elements of PMO 222.663. * indicates that the number could be wrong, due to compression, x indicates missing data. **Abreviaciones: AP**, anterior-posterior, **DV**, dorsal-ventral **PD**, proximal-distal.

Pelvic Girdle

Ilium—Both ilia are preserved in PMO 222.663 and were found in the vicinity of their respective limbs (Figure 2.10). Other elements of the pelvic girdle were not preserved. The ilia have undergone mediolateral compression, particularly in the right ilium. However, as the ilia of PMO 222.663 are compressed and are incomplete in the holotype specimen of *C. svalbardensis* (PMO A27745), detailed comparative remarks are not possible. In lateral view, the dorsal expansion is only slightly anteroposteriorly wider than the acetabular end, similar to isolated ilia and more complete specimens from the Kimmeridge Clay Formation (e.g., NHMUK R10062; OUM J.3300; CAMSM J29896; CAMSM J29897). In lateral view, the dorsal margin has subequal anterior and posterior expansions. This differs somewhat from the asymmetrically shaped dorsal portion of the ilium preserved in the holotype of *Colymbosaurus svalbardensis* (PMO A 27745), and the more rounded dorsal end of *Tatenectes laramiensis* and *Pantosaurus striatus* (Knutsen et al., 2012c; O'Keefe et al., 2011; Wilhelm and O'Keefe, 2010). The anterior margin is concave and display more of the acetabular facet in medial view, as in the majority of cryptoclidids (Andrews, 1910; AJR, pers. obs., NHMUK R7428). The anterior margin differs somewhat in the holotype of *C. svalbardensis*, where the preserved acetabular end and shaft is straight. A midshaft tubercule is absent in PMO 222.663, similar to other specimens of *C. svalbardensis* (Knutsen et al., 2012c), but differing

from numerous penecontemporaneous specimens from the Kimmeridge Clay Formation (CAMSM J29896; CAMSM J29897) as well as PMU 24781 from the Slottsmøya Member (Kear and Maxwell, 2013) that possess this feature. The torsion of the shaft seen in *Cryptoclidus eurymerus*, *Tatenectes laramiensis* and *Muraenosaurus leedsii*, could not be observed in PMO 222.663 due to crushing (Andrews, 1910; Brown, 1981; O'Keefe et al., 2011).

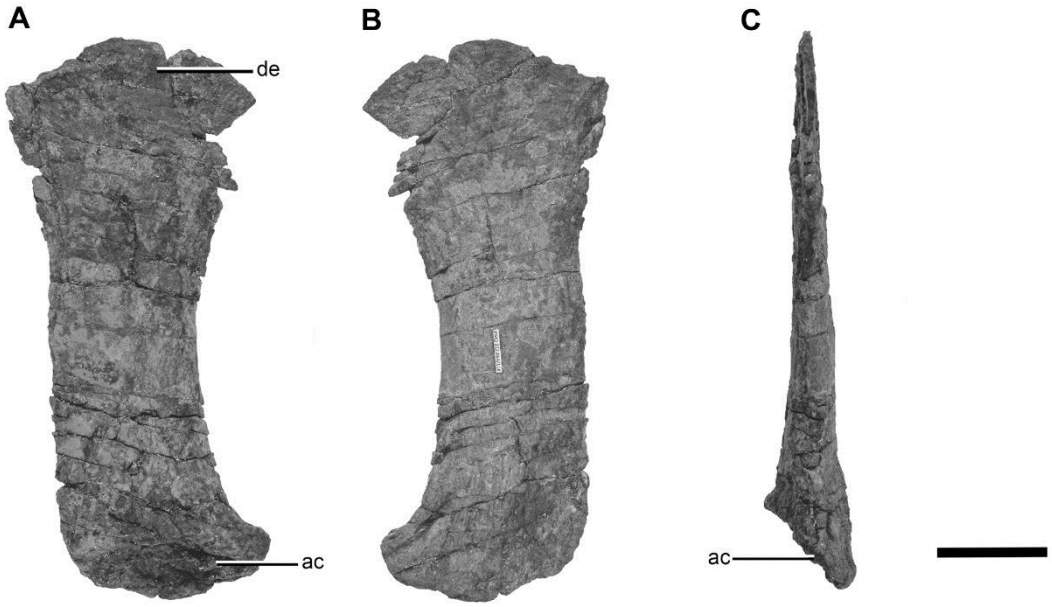

Figure 2.10: Left ilium of PMO 222.663 in **A**, medial, **B**, lateral and, **C**, posterior views. **Abbreviations: ac**, acetabular facet; **de**, distal expansion. Scale bar equals 5 cm.

Femora—Both hind limbs are well preserved and the majority of the preserved elements are articulated (Figure 2.11). In proximal view the trochanter is situated directly dorsal to the capitulum. As in *Colymbosaurus svalbardensis*, the femur of PMO 222.663 retains the same anteroposterior width until approximately midway along the shaft where it begins to expand (Knutsen et al., 2012c) (Table 2.2). The femoral shaft of PMO 222.663 does not constrict immediately distal to the capitulum (possibly a taphonomic artefact), although there is a slight constriction in the holotype specimen of *C. svalbardensis* (Knutsen et al., 2012c). This differs from *C. megadeirus* and *Muraenosaurus leedsii,* where a clear constriction is present (Andrews, 1910; Brown, 1981; Benson and Bowdler, 2014).

The distal end of the femur bears three distinct facets for the tibia, fibula and a postaxial ossicle. This differs from PMU 24781, which bears an additional single pre- and postaxial facet, and '*Plesiosaurus' mansellii*, which has two postaxial facets (Hulke, 1870). The tibial and fibular facets are clearly demarcated and pitted, and are subequal in anteroposterior length, as in *Abyssosaurus nataliae* (Berezin, 2011a), but unlike the larger tibial facet seen in PMU 24781 and in the other referred specimens of *Colymbosaurus svalbardensis* (Kear and Maxwell, 2013; Knutsen et al., 2012c). As in all material referred to *C. svalbardensis* and PMU 24781, an anteroposteriorly oriented ridge bisecting the distal femoral facets is absent in PMO 222.663, unlike some specimens of *C. megadeirus* (Benson and Bowdler, 2014; Knutsen et al., 2012c). Distally, the femur has a well-developed straight edged postaxial flange, which is angled more posterodistally than in the humeri. The postaxial flange has a relatively shorter postaxial facet than in the humerus.

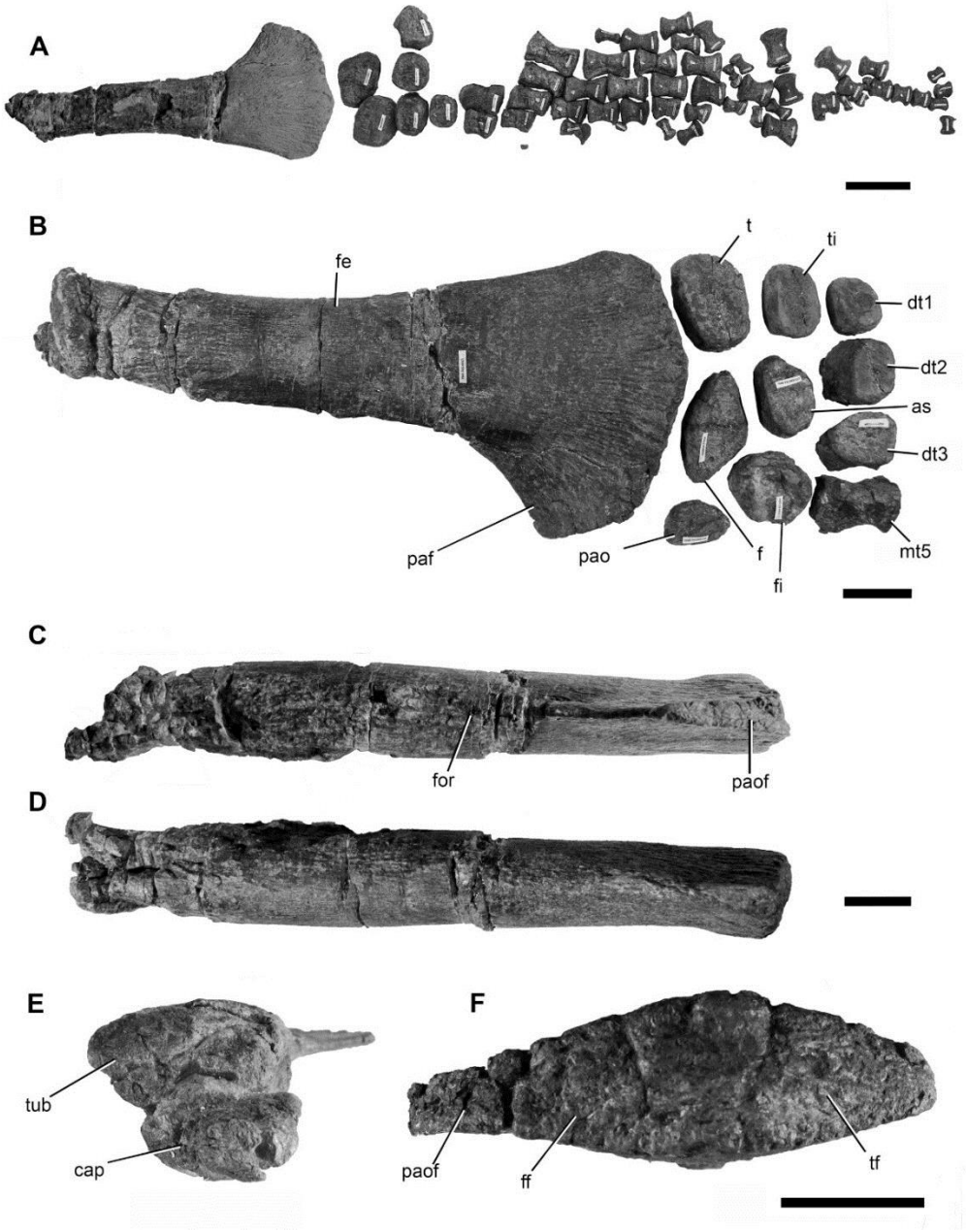

Figure 2.11: Right hind limb of PMO 222.663. **A**, right paddle as preserved in ventral view; **B**, the right femur, epipodials, tarsals and IV metatarsal in dorsal view (reconstructed), **C**, The right femur in posterior view, **D**, anterior, **E**, proximal and, **F**, distal views. The identification and position of elements in B is based on the more complete paddles of the holotype specimen of *C. svalbardensis* (PMO A27745). **Abbreviations**: **as**, astragalus; **cap**, capitulum; **dt1**, first distal tarsal; **dt2**, second distal tarsal; **dt3**, third distal tarsal; **dt4**, forth distal tarsal; **f**, fibula; **fe**, femur; **ff**, fibula facet; **fi**, fibulare; **for**, foramen; **mt5**, fifth metatarsal; **paf**, postaxial flange; **pao**, postaxial ossicle; **paof**, postaxial ossicle facet; **t**, tibia; **tf**, tibia facet; **ti**, tibiale; **tub**, tuberosity. Scale bar equals 10 cm (**A)**; 5 cm (**B–F**).

Epipodials and Mesopodials—There are a total of three elements in the epipodial row, the tibia, fibula and a single postaxial ossicle, as in *Colymbosaurus svalbardensis*, *C. megadeirus*, *Djupedalia engeri* and *Spitrasaurus* (Benson and Bowdler, 2014; Knutsen et al., 2012a, c, d), but unlike the two observed in *Cryptoclidus eurymerus*, *Muraenosaurus leedsii* and *Tatenectes laramiensis* (Andrews, 1910; Brown, 1981; O'Keefe and Street, 2009). A preaxial epipodial element is not present in either hind limb. The tibia and fibula are nearly equidimensional, and are both anteroposteriorly wider than proximodistally long (Table 2.2). The tibia is suboval in dorsal view, with four facets for the femur, fibula, astragalus and tibiale, the largest of which is for the femur. Unlike the well demarcated astragalar facet of the tibia in both species of *Colymbosaurus*, the astragalar facet of PMO 222.663 is diminutive on the right and indistinguishable from the facet for the tibiale on the left (Benson and Bowdler, 2014; Knutsen et al., 2012c). The fibula is triangular in dorsal view and bears five facets, the longest for the femur, two short facets for the tibia and the postaxial ossicle, respectively, and two subequal facets for the astragalus and fibulare. The postaxial ossicle is triangular and is similar to that seen in the forelimb (Figure 2.11B). This element was removed during excavation of the right hind limb, but is preserved articulated on the left. Only an external mould of the postaxial ossicle is known in NHMUK R40640 (*Colymbosaurus* indet; Brown, 1981; Knutsen et al., 2012c), which has three subequally-sized facets for the femur, fibula and fibulare. Previously, the postaxial ossicle of *C. svalbardensis* was known from the hind limbs of the additional referred specimens, but not the holotype (PMO A 27745; Knutsen et al., 2012c). The postaxial ossicle of PMO 222.663 is identical to that in other referred specimens to *C. svalbardensis* (PMO 218.377; PMO 216.838), being triangular and bearing two facets, with the smallest for the fibula.

Three proximal mesopodial elements are preserved; the fibulare is the largest while the somewhat smaller astragalus and tibiale are similar in size, consistent with other specimens of *Colymbosaurus svalbardensis* (Knutsen et al., 2012c). The fibulare and tibiale are suboval in outline, being anteroposteriorly wider than proximodistally long. The fibulare in *C. svalbardensis* is distinct in being anteroposteriorly broader and bearing two offset distal facets, while *C. megadeirus* has a single distal facet for the fifth metatarsal (Benson and Bowdler, 2014; Knutsen

et al., 2012c). The first distal tarsal appears similar to other cryptoclidids, being small and bearing three facets. Based on the proximal position of the fifth metatarsal in PMO 222.663, it is possible that this element is shifted entirely into the mesopodial row, as in *Djupedalia engeri* and *C. svalbardensis* (Knutsen et al., 2012a, c).

Metapodials and Phalanges—Five digits are preserved in the hind limb of PMO 222.663. The proximal edges of the metapodials of the hind limb are more convex in dorsal view compared to those in the forelimb. The phalanges are robust with flat articular surfaces, which become more convex in dorsal view distally throughout the hind limb. The distal-most elements are oval to lunate in dorsal view. The longest digit (the third) has a minimum of 11 articulated phalanges and a large number of disarticulated smaller ones distal to the articulated series (Figure 2.11A).

Discussion

Phylogenetic Analysis

A modified version of the data matrix of Benson and Druckenmiller (2014) (also used by Benson and Bowdler, 2014) was used in this analysis (Appendix 3, Supp. Data 2, 3). First, we attempted to replicate the results of the original analysis (Benson and Druckenmiller 2014), which was conducted in PAUP* (Swofford, 2003), using TNT (V1.1) (Goloboff et al., 2010). The matrix was built in Mesquite (V.3.10; Maddison and Maddison, 2016). In order to most closely replicate the original search algorithm, run in PAUP*, a New Technology Search was performed in TNT using a combination of both ratchet and TBR (see Appendix 3 for specific settings). All characters are unordered and equally weighted and the same wildcard taxa were removed as in Benson and Druckenmiller (2014). *Yunguisaurus* was defined as the outgroup taxon (Cheng et al., 2006). The search resulted in fewer MPTs (2016) than in the original analysis, but with the same number of steps (1289) and the strict consensus recovered the same topology (CI = 0.304; RI = 0.661).

To the Benson and Druckenmiller (2014) matrix were added the scores for two new OTUs, *Colymbosaurus svalbardensis*, based solely on the holotype specimen, and PMO 222.663. Additionally, a small number of scores for other cryptoclidid taxa were modified (Appendix 3, Supp. Data. 2). A second matrix was also prepared that combined the scores for *C. svalbardensis* and PMO 222.663 as a

single OTU (Appendix 3, Supp. Data 3). Bremer support and a bootstrap percentages were performed in TNT. Bremer support values are presented in Figure 2.12; however, bootstrap values for all nodes within Cryptoclididae were less than 50% and are not shown.

The analysis of the first matrix yielded 576 MTPs with 1290 steps. The strict consensus tree recovered PMO 222.663, *Colymbosaurus svalbardensis* and *C. megadeirus* in a polytomy and as the sister taxon to (*Spitrasaurus* spp. + *Djupedalia* + *Abyssosaurus*) within Colymbosaurinae (Figure 2.12A). The analysis of the second matrix yielded 576 MPTs, with 1289 steps and the strict consensus tree recovered the same topology, with *C. svalbardensis* (composite scoring) and *C. megadeirus* as sister taxa (Figure 2.12B). The topology for the other cryptoclidids was identical to that presented in Benson and Bowdler (2014).

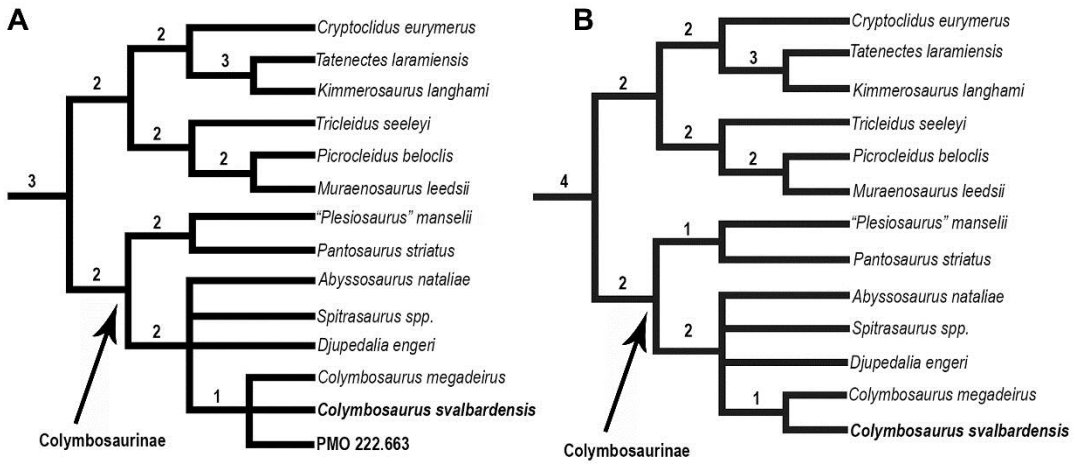

Figure 2.12: The results of the phylogenetic analysis of Cryptoclididae. **A**, strict consensus of 576 MPTs with PMO 222.663 and *Colymbosaurus svalbardensis* scored as a separate OTUs (CI = 0.304, RI = 0.661); **B**, strict consensus of 576 MPTs, with a composite scoring of PMO 222.663 and *Colymbosaurus svalbardensis* (CI = 0.303, RI = 0.663). Bremer support values are given above the internodes.

Diagnostic Characters of *Colymbosaurus*

Multiple Kimmeridge Clay Formation specimens that have been or are possibly referable to *Colymbosaurus* exhibit a large amount of variation in several

aspects of their morphology. This variation must be taken into account when re-evaluating diagnostic features of the genus.

Characters relating to the length to height ratio and the lack of a lateral ridge on the cervical vertebrae (Character 153 and 154, respectively; Benson and Druckenmiller, 2014) have been studied in *Colymbosaurus megadeirus* (Benson and Bowdler, 2014), but are currently unknown in *C. svalbardensis* (including PMO 222.663). With regards to cervical length to height dimensions, there is a greater degree of intraspecific variation in this character than was previously recognized, particularly regarding which region of the cervical series is measured. In NHMUK R10062 the preserved anterior and posterior cervical vertebrae have a length to height ratio < 0.7, but the ratio increases slightly in the mid-cervical vertebra. In OUM J.3300 and the syntype CAMSM J.29596–29691, J.59736–J.59743 (referred to in Benson and Bowdler, 2014 as CAMSM J.29596ect.) this ratio is close to 1.0 in the anterior cervicals, and this value steadily decreases to 0.8 in the mid-cervical vertebrae. This illustrates that more consistent results are found when measurements are limited to the mid-cervical series where there is less variation among specimens referred to *Colymbosaurus*.

One of the most variable features of the genus relates to the morphology of the postaxial flange of the propodials (Figure 2.13), defined in the diagnosis of Benson and Bowdler (2014:1054) as; "propodials with a large posterodistal expansion bearing a postaxial ossicle facet of subequal size to the epipodial facets". Most other colymbosaurines, including *Abyssosaurus nataliae*, *Spitrasaurus wensaasi*, *S. larseni*, *Djupedalia engeri* and *'Plesiosaurus mansellii'*, also possess a postaxial flange (Berezin, 2011a; Hulke, 1870; Knutsen et al., 2012a, c, d). Thus, to help further distinguish *Colymbosaurus* from other penecontemporaneous taxa we have modified the diagnosis to denote; 'an extended postaxial flange, which is significantly larger than the preaxial flange, bearing a single postaxial ossicle facet of subequal size to the epipodial facets'. Further, the specification of a single postaxial ossicle facet distinguishes *Colymbosaurus* from the taxonomically problematic material of '*P.*' *mansellii* (NHMUK PV OR40106), which also has a large postaxial flange but bears discrete facets for two postaxial accessory ossicles on the humerus (Hulke, 1870).

The presence of an anteroposteriorly oriented ridge bisecting the distal articulating facets of the propodials, has also been used as a diagnostic character of *Colymbosaurus* (Benson and Bowdler, 2014; Brown, 1981). An anteroposteriorly bisecting ridge on the distal end of the propodials is observed on the propodials of numerous specimens of *Colymbosaurus* including *C. 'richardsoni'* (NHMUK R1682) and *Colymbosaurus* indet. (OUM J.3300 and NHMUK R31787; Benson and Bowdler, 2014). However, the bisecting ridge shows varying degrees of anteroposterior exposure on other '*Colymbosaurus*-like' propodials from the Kimmeridge Clay Formation, including some which appear to lack the ridge altogether. Eighteen propodials (isolated and associated) from the Kimmeridge Clay Formation were examined in the course of this study that have been either referred to *Colymbosaurus* or otherwise resemble *Colymbosaurus* on the basis of overall propodial morphology or associated material. The left humerus and right femur of PMO 222.663, left femur of PMO 216.838 and the right femur of PMO A27745 were also included for comparison. Of the 22 propodials examined, nine had a well-defined anteroposteriorly oriented ridge present on both epipodial facets, four had a ridge on one of the epipodial facets and nine lacked the ridge altogether (Appendix 3, Table A3.1). Additionally, MANCH LL.5513–14, which preserves both femora, had a recognizable ridge on the left femur, but not on the right.

After re-examination of PMO 218.377, one of the referred specimens of *Colymbosaurus svalbardensis* (Benson and Bowdler, 2014)(Figure 3.10A), the presence of an anteroposteriorly oriented bisecting ridge on the distal humeral facets is equivocal. This ridge is also clearly absent in all other propodials of specimens referable to *C. svalbardensis*, including PMO 222.663. The potential utility of this feature also needs to be taken into the light of other factors, including taphonomic compression (CAMSM J29739, NHMUK R6317) and ontogenetic and/or individual variation (MANCH LL.5513–14). A similar feature has also been observed in other uncompressed cryptoclidids propodials from the Oxford Clay Formation (CAMSM J67072, GLAHM V1807, MANCH LL.14975, LEICS 413.1956/40, NOTNH FS5879) and a non-cryptoclidid propodial from the Kimmeridge Clay Formation (OUM J.13837). These observations suggest that the presence of an anteroposteriorly oriented bisecting ridge may prove valuable in a broader evolutionary context. Given that this character is equivocal on the holotype of *C. svalbardensis* (PMO A 27745)

and in two of the referred specimens of *C. svalbardensis* (PMO 222.663, PMO 216.838) and is variable in extent and presence in Kimmeridge Clay Formation specimens of *Colymbosaurus*, we do not consider this to be a reliable diagnostic character for the genus. However, it is possible that the presence of this feature could be diagnostic at a less inclusive taxonomic level, possibly for *C. megadeirus*.

Based on a broad examination of material from both the U.K. and Svalbard, we provide new diagnostic features for *Colymbosaurus* relating to the morphology of the mid-caudal vertebrae and the ulna and fibula.

As described above, the middle caudal centra of *Colymbosaurus* are subrectangular due to the presence of a flat ventral surface with widely spaced, low chevron facets located ventrolaterally (Benson and Druckenmiller, 2014). The middle caudal centra of *Colymbosaurus* are distinctive among cryptoclidids in that their chevron facets project slightly from the ventral surface and are not positioned in a deep groove (PMU 24781) or are not significantly venterolaterally projecting (e.g., *Cryptoclidus eurymerus*; Andrews, 1910; Kear and Maxwell, 2013). The mid-caudal centra in *Colymbosaurus* also have a flat ventral margin in anterior view, compared to the more rounded morphology in *Cryptoclidus eurymerus*, *Muraenosaurus leedsii* and *Pantosaurus striatus* (Andrews, 1910; Wilhelm and O'Keefe, 2010).

In referred specimens of *Colymbosaurus* where an ulna is present (PMO 222.663; OUM J.3300), the element is conspicuously anteroposteriorly wider than the radius, and proximodistally short. This differs from the ulna in *Muraenosaurus leedsii*, *Pantosaurus striatus*, where the ulna is significantly anteroposteriorly shorter than the radius and to '*Plesiosaurus*' *mansellii*, where the ulna is subequal length to the radius (Andrews, 1910; Hulke, 1870; O'Keefe and Wahl, 2003b).

A unique morphology of the fibula is also observed in *Colymbosaurus megadeirus* (CAMSM J29654–91; CAMSM J59736–43), *Colymbosaurus* indet. (OUM J.3300), and *C. svalbardensis* (PMO A27745; PMO 216.383; PMO 218.377; PMO 222.663) in which this element is pentagonal to nearly triangular, with symmetrical preaxial and postaxial margins. The fibula lacks a spatium interosseum and has subequal facets for the fibulare and intermedium, differentiating *Colymbosaurus* from all other cryptoclidids. This particular morphology is noted in Knutsen et al. (2012a) as one of the characters justifying the referral of the *C.*

svalbardensis material to *Colymbosaurus*. Although some specimens of *Cryptoclidus eurymerus* also exhibit a pentagonal fibula, these are anteroposteriorly longer than those seen in *Colymbosaurus* and possess a clear spatium osseum (Andrews, 1910; Brown, 1981).

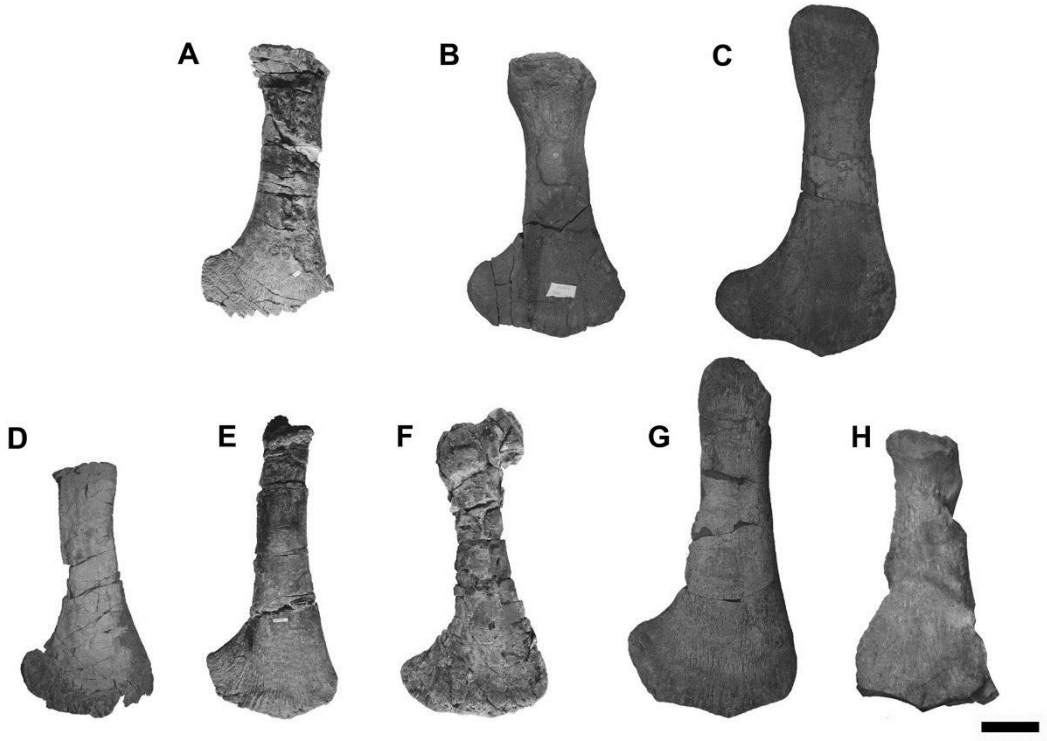

Figure 2.13: Humeri (upper row) and femora (bottom row) of referred specimens of *Colymbosaurus*. **A**, left humerus (reversed) of PMO 222.663 (*C. svalbardensis*), **B**, right humerus of NHMUK 10062 (*Colymbosaurus* indet.; photo used with permission); **C**, right humerus of OUM J.3300 (*Colymbosaurus* indet.); **D**, right femur of PMO A 27745 (holotype of *C. svalbardensis*); **E**, right femur of PMO 222.663 (*C. svalbardensis*); **F**, left femur of PMO 216.839 (C. svalbardensis) **G**: right femur of OUM J.3300 (*Colymbosaurus* indet.); **H**. right femur of CAMSM H29654 (*C. megadeirus*). Scale bar equals 5 cm.

New Autapomorphies for *Colymbosaurus svalbardensis*

In addition to the holotype specimen, PMO A27745, Knutsen et al. (2012c) also included PMO 216.838 and PMO 218.377 in the hypodigm of *Colymbosaurus svalbardensis*. The inclusion of the new specimen described here, PMO 222.663 (also found at nearly the exact same stratigraphic horizon as PMO 216.838),

provides the opportunity to recognize two additional autapomorphies from the dorsal vertebrae and hind limbs.

The neural canal of the dorsal vertebrae in the holotype specimen and PMO 222.663 is conspicuously ovate and dorsoventrally taller than wide when compared to the more rounded, equidimensional neural canals observed in *Colymbosaurus megadeirus* and other plesiosauroids from the Kimmeridge Clay Formation (Benson and Bowdler, 2014; AJR, *pers. obs.* OUM J.55482). The presence of this character in multiple specimens suggests this is not simply a taphonomic artefact but is the true morphology and can be recognized as a new autapomorphy of the species. A second possible autapomorphy pertains to the relative anteroposterior expansion of femoral head relative to the femoral shaft, as seen in either dorsal or ventral view (Figure 2.13). In all specimens of *C. svalbardensis*, the anteroposterior width of the femoral shaft is nearly the same as that of the proximal end. In contrast, the anteroposterior width of the shaft is conspicuously less that of the proximal end in *Colymbosaurus* material from the Kimmeridge Clay (NHMUK R31787; OUM J.3300; NHMUK 10062; Benson and Bowdler, 2014). Furthermore, this feature also does not seem to be the result of a taphonomic bias given that a marked constriction between the humeral head and shaft is present in the newly referred specimen of *C. svalbardensis*, PMO 222.663.

The Affinities of NHMUK R10062 to *Colymbosaurus svalbardensis*

NHMUK R10062, a partial skeleton including much of the vertebral column and associated girdle and limb elements, was originally named *Colymbosaurus 'portlandicus'* by Brown (1984) and was subsequently referred to Plesiosauroidea incertae sedis by Benson and Bowdler (2014). Based on the newly amended diagnosis, NHMUK R10062 shares three diagnostic features of *Colymbosaurus* and can be referred to this taxon: (1) the mid-caudals are pentagonal in anterior view, with widely-spaced chevron facets; (2) the humerus has a large postaxial expansion at least twice as large as the preaxial expansion, bearing a single postaxial ossicle facet of subequal size to the epipodial facets; and (3) although the ulna is not preserved, the ulnar facet on the humerus is longer than the radial facet.

It is noteworthy that NHMUK R10062 also shares several features with *Colymbosaurus svalbardensis*. The neural canal of the mid-dorsal vertebrae is taller

than wide, although not to the degree as observed in specimens of *C. svalbardensis* from the Slottsmøya Member (Knutsen et al., 2012c). Additionally, it shares the same morphology of the posterior margin of the ischium, which is abruptly squared-off and mediolaterally broad. This suggests that NHMUK R10062 is potentially referable to *C. svalbardensis* and as such, represents the first specimen of this taxon occurring in the upper Kimmeridge Clay Formation. However, in the absence of additional overlapping material, we refrain from formally referring the specimen to *C. svalbardensis.*

Survival of Colymbosaurinae into the Cretaceous

The Slottsmøya Member of central Spitsbergen preserves a high diversity of colymbosaurine plesiosauroids (*Djupedalia engeri*, *Spitrasaurus larseni*, *S. wensaasi* and *Colymbosaurus svalbardensis*) that lived close to or likely across the Jurassic–Cretaceous boundary at high paleolatitudes (>60°; Torsvik et al., 2002). The taxon composition differs from the slightly older Kimmeridge Clay Formation in the U.K. where non-colymbosaurine plesiosauroids are also found (e.g., *Kimmerosaurus*). Given that the stratigraphically youngest known colymbosaurine is *Abyssosaurus* from the Early Cretaceous of boreal Russia (Berezin, 2011a), and that colymbosaurines are the only known plesiosauroids from the high latitude deposits of the Slottsmøya Lagerstätte, we propose that this clade may have persisted across the Jurassic–Cretaceous boundary in the Boreal Realm. Ongoing studies relating to the stratigraphy, diversity and phylogenetic relationships of cryptoclidids from the Slottsmøya Lagerstätte and other sites are needed to better understand the timing and nature of extinctions for the clade at the Jurassic–Cretaceous boundary (Benson and Druckenmiller, 2014).

Acknowledgments

The authors thank S. Chapman (NHMUK), M. Riley (CAMSM), E. Howlett (OUM), K. Sherburn (MANCH), A. Smith (NOTNH), S. King (YORKM), M. Evans (LEICS), N. Clark (GLAHM) and G. Wass (PETMG) for access to collections. We acknowledge the reviewers F. R. O'Keefe and P. Vincent for their helpful comments on the manuscript. We thank R. B. J. Benson for comments on an earlier version of the manuscript, D. Legg for advice on using TNT and S. Etches for access to his collection. G. J. Dyke, E. M. Knutsen, A. H. Roberts, J. S. Roberts, A. Smith, D.

Foffa and R. Forrest are thanked for helpful discussion. M-L. Funke and V. E. Nash are thanked for their assistance in the preparation of PMO 222.663. Permission to use a photograph of NHMUK 10062 was granted and the copyright of the image retained by the London Natural History Museum, U.K. The Governor of Svalbard provided excavation permits 2006/00528-24 and 2006/00528-32. Fieldwork for the excavation of PMO 222.663 in 2010 and 2011 was funded by Exxon Mobil, Fugro, Spitsbergen Travel, OMV, Nexen and National Geographic (EC0425_09, EC0435_09). AJR is funded by NERC, GSNOCS University of Southampton and Tullow Oil. LLD is supported by a PhD grant from the Ministry of Education and Research via the Natural History Museum, University of Oslo.

Chapter 3

A new plesiosaurian from the Slottsmøya Member (Volgian) of Spitsbergen, with insights into the cranial anatomy of cryptoclidids using Computed Tomography

A new plesiosaurian from the Slottsmøya Member (Volgian), with insights into the cranial anatomy of cryptoclidids using Computed Tomography

Authors: Roberts, A. J. [1 2], Druckenmiller, P. S.[3 4], Cordonnier, B. [5], Delsett, L. L. [2] and J. H. Hurum[2]

[1]The National Oceanography Centre, University of Southampton, Southampton, Hampshire SO14 3ZH, United Kingdom

[2]Natural History Museum, University of Oslo, 0562, Norway

[3]University of Alaska Museum, 907 Yukon Drive, Fairbanks, Alaska, 99775,

[4]Department of Geoscience, University of Alaska Fairbanks, 900 Yukon Drive, Fairbanks, Alaska, 99775

[5]Physics of Geological Processes, Institute of Geosciences, University of Oslo, Norway

Abstract

Cryptoclidids are a major clade of plesiosauromorph plesiosaurians best known from the Middle – Late Jurassic, but little is known regarding their turnover into the Early Cretaceous. Of thirteen known cryptoclidid taxa, only five preserve cranial material and only one taxon has a complete, but compressed cranium. Thus, the lack of knowledge of the cranial anatomy of this group may hinder the understanding of phylogenetic intrarelationships, which are currently predominantly based on postcranial data. Here we present a nearly complete adult cryptoclidid specimen (PMO 224.248) representing a new taxon from the latest Jurassic – earliest Cretaceous part of the Slottsmøya Member, of central Spitsbergen. PMO 224.248 preserves a complete cranium, partial mandible, complete and articulated cervical, pectoral and anterior-mid dorsal vertebral series, along with the pectoral girdle and anterior propodials. High resolution micro computed tomography (µCT) methods were utilised to reveal new data on the cranial anatomy of this specimen. New internal features of the braincase and palate found using computed tomography, were also confirmed present in other cryptoclidid specimens. Phylogenetic analysis including new characters, presents a new tree topology for the Cryptoclididae and

particularly for the subfamily Colymbosaurinae These results show that at least two cryptoclidid lineages were present in the Boreal Region during the Late Jurassic – Early Cretaceous and that representatives from these two lineages crossed the Jurassic – Cretaceous boundary at mid-high latitudes.

Introduction

Plesiosaurs are a group of secondarily aquatic reptiles that predominantly inhabited marine environments during the Mesozoic era. During the Jurassic, the plesiosaur fossil record reveals a worldwide distribution and high level of morphological disparity (Benson et al., 2012). As with all other marine reptile groups, plesiosaur taxonomic diversity was heavily affected by eustatic sea-level changes during the Jurassic – Cretaceous transition (Tennant et al., 2016b), with the decline and replacement of some Jurassic clades by Xenopsaria (Benson and Druckenmiller, 2014). The Middle Jurassic – Early Cretaceous plesiosauroid family Cryptoclididae, is a species-rich clade primarily known from the Northern Hemisphere. The majority of the specimens derive from the Oxford and Kimmeridge Clay Formations of the UK. The recent recovery and description of numerous cryptoclidid specimens from the Slottsmøya Member of the Agardhfjellet Formation (central Spitsbergen), now constitute a major component of overall Boreal plesiosaurian richness from the Tithonian-Berriasian interval (Druckenmiller et al., 2012; Knutsen et al., 2012a, b, c, d; Roberts et al., 2017).

The Cryptoclididae is split into two subfamilies, the Colymbosaurinae [Benson and Bowdler, 2014] and another clade yet to be formally named. The Colymbosaurinae, previously included all the described plesiosauroid taxa from the Slottsmøya Member (*Djupedalia engeri*, *Spitrasaurus wensaasi*, *S. larseni*, *Colymbosaurus svalbardensis*), in addition to *Abyssosaurus nataliae*, *Pantosaurus striatus* and *Colymbosaurus megadeirus* (Benson and Bowdler, 2014). The Colymbosaurinae share multiple postcranial synapomorphies as limited cranial material is available from the incorporated taxa. Although rare for cryptoclidids, the specimen described here (PMO 224.248) preserves a complete cranium and represents a new genus and species of cryptoclidid plesiosaur. PMO 224.248 was excavated from the Slottsmøya Member, Agardhfjellet Formation of central Spitsbergen, from a section encompassing the Jurassic – Cretaceous boundary. The specimen represents the fourth and youngest cryptoclidid genus described from the

Slottsmøya Member. This new taxon not only added significant information on cranial morphology for cryptoclidids, but also yields new insights to their limited turnover into the Cretaceous and phylogenetic inter-relationships.

Geological Setting

The Agardhfjellet Formation encompasses a thick succession of Middle Jurassic to Lower Cretaceous sedimentary rocks. The formation comprises four members; Oppdalen Member, Lardyfjellet Member, Oppdalsåta Member and the Slottsmøya Member. The Slottsmøya Member (Volgian) consists of dark-grey to black silty mudstone, which is often weathered into paper shale. There are discontinuous silty beds, with siderite concretions, in addition to siderite and dolomite interbeds. The Slottsmøya Member is overlain by the Lower Cretaceous Myklegardfjellet Bed, which define the base of the Rurikfjellet Formation (Dypvik et al., 1991).

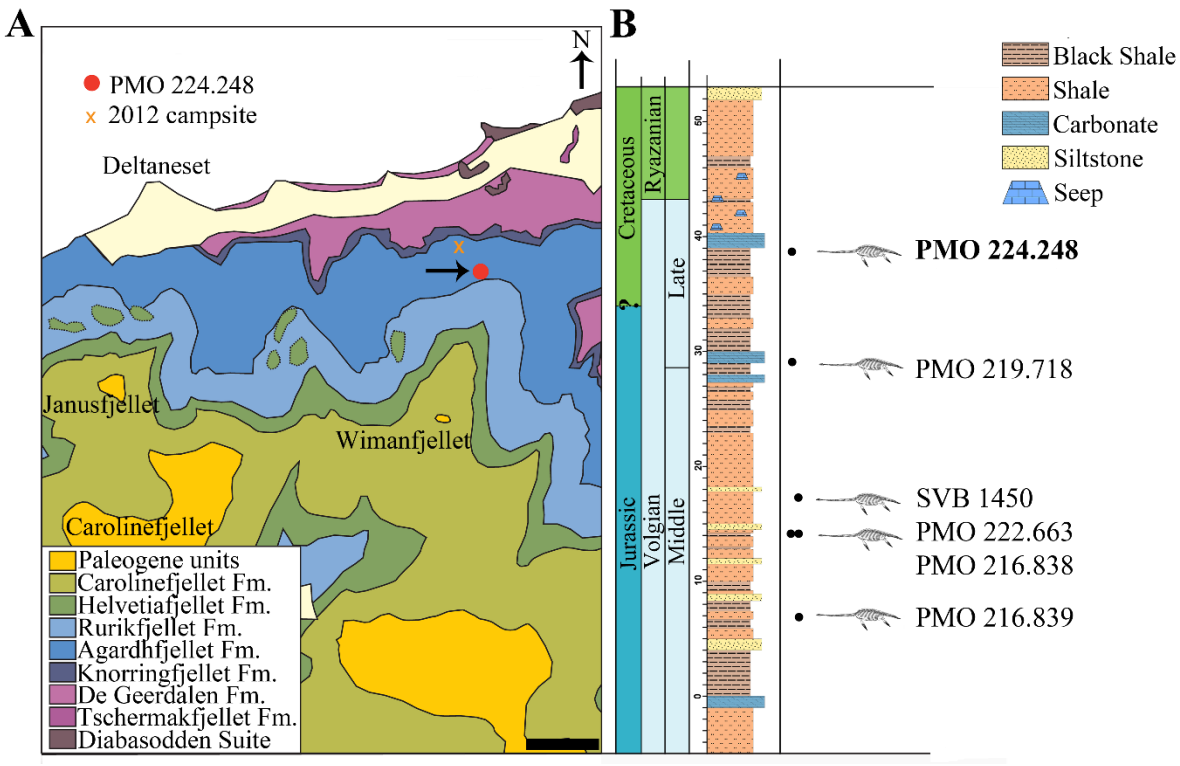

Figure 3.1: Map of locality and stratigraphy of the Upper Jurassic (middle Volgian) to the Early Cretaceous part of the Slottsmøya member of the Agardhfjellet Formation (the lowest unit not included, see text) with described cryptoclidid positions. **A**, Geological map of the field site in central Spitsbergen. The arrow points to the excavation site of PMO 224.248 (Modified from Dallmann et al., 2001

and Hurum et al., 2012). Scale bar equals 1 km. **B**, The stratigraphic position of PMO 224.248 (in bold) in relation to the other described cryptoclidids specimens (PMO 219.718 – *Spitrasaurus wensaasi*; PMO 222.663, PMO 216.838 – *Colymbosaurus svalbardensis*; PMO 216.839 – *Djupedalia engeri*; SVB 1450 – *Spitrasaurus larseni*). Note the uncertain position of the Jurassic – Cretaceous boundary. Modified from Delsett et al. 2015).

The Slottsmøya Member was deposited in an open marine environment under dysoxic conditions (Collignon and Hammer, 2012). These marine deposits represent approximately 12 million years of deposition from the upper Tithonian (uppermost Jurassic) to the lower Berriasian (lowermost Cretaceous; Hammer et al., 2012). The member has been divided into three units; a lower (-22-0m), middle (0-27m) and an upper condensed unit (27-52? m) (Collignon and Hammer, 2012). The specimen (PMO 224.248) described in this paper derives from the upper condensed unit (at 38.5 m), so it is hard to pinpoint whether this specimen derives from the Lower Cretaceous or the Upper Jurassic sediments. However, the seeps overlying the specimen in the stratigraphy are determined to be from the Early Cretaceous (Hryniewicz et al., 2012).

Materials and Methods

Measurements

Measurements were taken using a calliper or tape measure for longer measurements (>15 cm). For some of the braincase elements that were obscured by matrix or another element, measurements were taken using the CT scan images.

µCT methodology

The cranium, left mandible, 8th cervical vertebra and possible gut contents were scanned using µ-Computer Tomography (µCT) and the University of Oslo Natural History Museum (Økern Campus). Figures of the volume renderings of the complete posterior of the skull and 8th cervical vertebra are shown in the supplementary materials (Appendix 6, Figures A6.2, A6.6). Due to the size limitations of the scanner, three separate scans of the cranium (posterior, middle and anterior), were taken and then merged together to form a single high-resolution scan. For the cranium: a total volume of 7 274 887 cm^3 was acquired using a Nikon XT H

225 ST desktop CT scanner, with a spatial resolution equal to a voxel size of 0.0753767 mm^3. A 2mm copper filter was utilised. For each scan, tomographic acquisition was performed under step rotation with an exposure time of 2000 ms, the beam energy was 180 keV and 3016 projections were taken over 360º. For the left mandible, two CT scans were performed and then merged. These consisted of 1583 projections taken over 360°, with an exposure time of 1000 ms. The 8^{th} cervical vertebra was scanned with 3016 projections taken over 360°, with 1000 ms exposure.

Manual segmentation of the braincase was performed with the 3D analysis software Aviso Fire (V. 8.1) and Fiji (ImageJ) at the University of Southampton µ-vis (Muvis) Digital Visualisation Laboratory. The automatic segmentation of the complete cranium was pre-processed with a growing algorithm developed by CB in MATLAB (V. 2016b). This eliminated some of the surrounding and internal matrix from the volume rendering using differences in density.

Institutional abbreviations

CAMSM, Cambridge Sedgewick Museum, Cambridge, United Kingdom; **NHMUK**, Natural History Museum, London, United Kingdom; **MGUH**, Geological Museum, Copenhagen, Denmark; **PETMG**, Peterborough Museum and Art Gallery, United Kingdom; **PMO**, Palaeontology museum, Natural History Museum, Oslo, Norway; **OUM**, Oxford University Museum, United Kingdom; **SVB**, Svalbard Museum, Norway; **UW**, University of Wyoming, Wyoming, United States of America.

Systematic Palaeontology

Sauropterygia Owen, 1860

Plesiosauria de Blainville, 1835

Plesiosauroidea Welles, 1934

Cryptoclididae Williston, 1925

Gen et species nov.

Holotype: PMO 224.248

Occurrence: The holotype specimen PMO 224.248 was excavated from the north-facing slopes of Wimanfjellet (Mt. Wiman), from the upper part of the Slottsmøya Member, Agardhfjellet Formation, central Spitsbergen: GPS coordinates UTM 33X E523620 N8696396 (Figure 3.1). The specimen was located 38.5 m above the yellow storm deposit marker bed (0m in log), and is late Volgian (latest Tithonian/ early Berriasian) in age.

Differential diagnosis

A moderately sized cryptoclidid plesiosaur (estimated body length of 5.0-5.5 m), possessing the following autapomorphies unique among Plesiosauria (*) and Cryptoclididae (**) and unique character combinations: premaxilla bears 6 alveoli (5 in *Tricleidus seeleyi* and *Muraenosaurus leedsii*); medial margin of premaxilla terminates anterior to the posterior margin of external naris**; maxilla bears an estimated 16 alveoli (18 in *Cryptoclidus eurymerus*; 15 in *Tricleidus seeleyi*); frontal twice as long as parietal (subequal or less in *Cryptoclidus eurymerus* and *Muraenosaurus leedsii*); frontal participates in the medial and posterior margins of the external naris (participates posteriorly in *Muraenosaurus leedsii*); presence of an interfrontal vacuity (absent in *Muraenosaurus leedsii*); low but narrow sagittal crest (flat and broad in *Kimmerosaurus*); quadrate articulates anterolaterally to the pterygoid (posteromedially in *Tricleidus seeleyi* and *Muraenosaurus leedsii*); lateral cotyle of quadrate larger than medial cotyle (reversed in *Spitrasaurus larseni*); basioccipital tubera broad and flattened (circular in *Kimmerosaurus langhami* and *Cryptoclidus eurymerus*); basioccipital tubera triangular in ventral view, following the anteromedial process of pterygoid anteriorly (cylindrical with finished bone anteriorly in *Kimmerosaurus langhami*); exoccipital does not contribute to occipital condyle (contributes in *Kimmerosaurus langhami* and *Cryptoclidus eurymerus*); posteromedian ridge on supraoccipital absent (present in *Kimmerosaurus langhami* and *Muraenosaurus leedsii*); palatine and vomer excludes maxilla from internal naris (maxilla participates in *Muraenosaurus leedsii*); vomer excluded from anterior interpterygoid vacuity (participates in *Muraenosaurus leedsii* and *Cryptoclidus eurymerus*); anteromedial process of pterygoid reaches parabasisphenoid (absent in *Cryptoclidus eurymerus*); dentary with a mediolaterally extended alveolar surface and with laterally shifted, labially inclined alveoli (no mediolateral extension and alveoli positioned centrally in *Tricleidus*); deep glenoid facet of the mandible,

constituting over half the dorsoventral height of the mandible (relatively shallow in *Colymbosaurus spp.*, *Cryptoclidus eurymerus* and *Kimmerosaurus langhami*); retroarticular process slightly dorsally inclined (significantly inclined in *Spitrasaurus larseni*); faint longitudinal ridged teeth, distinct on labial side (distinct on lingual side in *Muraenosaurus leedsii* and *Cryptoclidus eurymerus*; ridging absent in *Kimmerosaurus langhami*); slightly recurved tooth crowns (significantly recurved in *Spitrasaurus larseni* and *Kimmerosaurus langhami*); hypophyseal eminence present on ventral surface of atlas (ventral keel in *Cryptoclidus eurymerus*, *Muraenosaurus leedsii* and *Tricleidus seeleyi*); atlantal rib present (absent in *Colymbosaurus megadeirus*); 50 cervical vertebrae (32 in *Cryptoclidus eurymerus*; 44 in *Muraenosaurus leedsii*; 41 in *Colymbosaurus megadeirus*; 60 in *Spitrasaurus wensaasi*); cervical centra are slightly amphicoelous (conspicuously concave in *Djupedalia engeri* and *Kimmerosaurus langhami*); 8th cervical with anteroposteriorly long postzygapophyses, close to the length of centrum (*); anterior-most cervical neural spines low and posteriorly angled (straight in *Kimmerosaurus langhami*); cervical prezygapophyses unfused anteriorly and fused posteriorly (unfused throughout in *Cryptoclidus eurymerus* and completely fused in *Spitrasaurus* spp. and *Djupedalia engeri*); postzygapophyses fused along the midline (unfused in posterior-most cervicals in *Djupedalia engeri*); lateral ridges present on mid-posterior cervicals (absent in *Colymbosaurus megadeirus*, *Cryptoclidus eurymerus*, *Djupedalia engeri*, *Kimmerosaurus langhami* and *Tricleidus seeleyi*); posterior cervical – anterior dorsal ribs with a distinct longitudinal ridge (**); dorsal vertebral rib facets dorsoventrally taller than wide (circular in *Tatenectes laramiensis*); dorsal process of scapula short and reduced (tall and extensive in *Abyssosaurus nataliae* and *Djupedalia engeri*); extended anteromedial process of coracoid (reduced in *Colymbosaurus megadeirus* and *Abyssosaurus nataliae*); humeri significantly larger than femora (femora larger than humeri in *Djupedalia engeri*, subequal in *Colymbosaurus svalbardensis*); sigmoid humerus in dorsal view (**); forelimbs with three to four distal articular facets (two in *Cryptoclidus eurymerus* and *Muraenosaurus leedsii*); radius slightly larger than ulna (anteroposteriorly shorter in *Colymbosaurus svalbardensis*).

Taphonomy

The specimen is well-preserved and fully articulated, with the exception of the skull and distal phalangeal elements (Figure 3.2). The cranium had drifted 20 cm away from its original position, and the majority of the phalanges had drifted from the limbs and were not preserved in articulation. The posterior region of the skeleton was eroded from the sacral region, although a partial left hindlimb and femora fragments were recovered. From the position of the skeleton, it can be inferred that PMO 214.248 had a ventral landing.

PMO 224.248 preserves a complete skull, although it is dorsoventrally crushed and damaged in places. The cranium could not be completely prepared from the matrix, as the bones where significantly fractured. The braincase was partly disarticulated due to the crushing, with the supraoccipital pushed down into the foramen magnum. The majority of the cervical vertebrae are missing portions of the right cervical rib and neural spines, due to crushing and/or pre-burial erosion. The posterior-most cervicals were disarticulated and crushed by the overlying pectoral girdle. The pectoral and anterior dorsal vertebrae are partly crushed and distorted by the overlying pectoral girdle. Most of the neural arches are missing from the dorsal vertebrae, as these were exposed to post-diagenetic erosional processes.

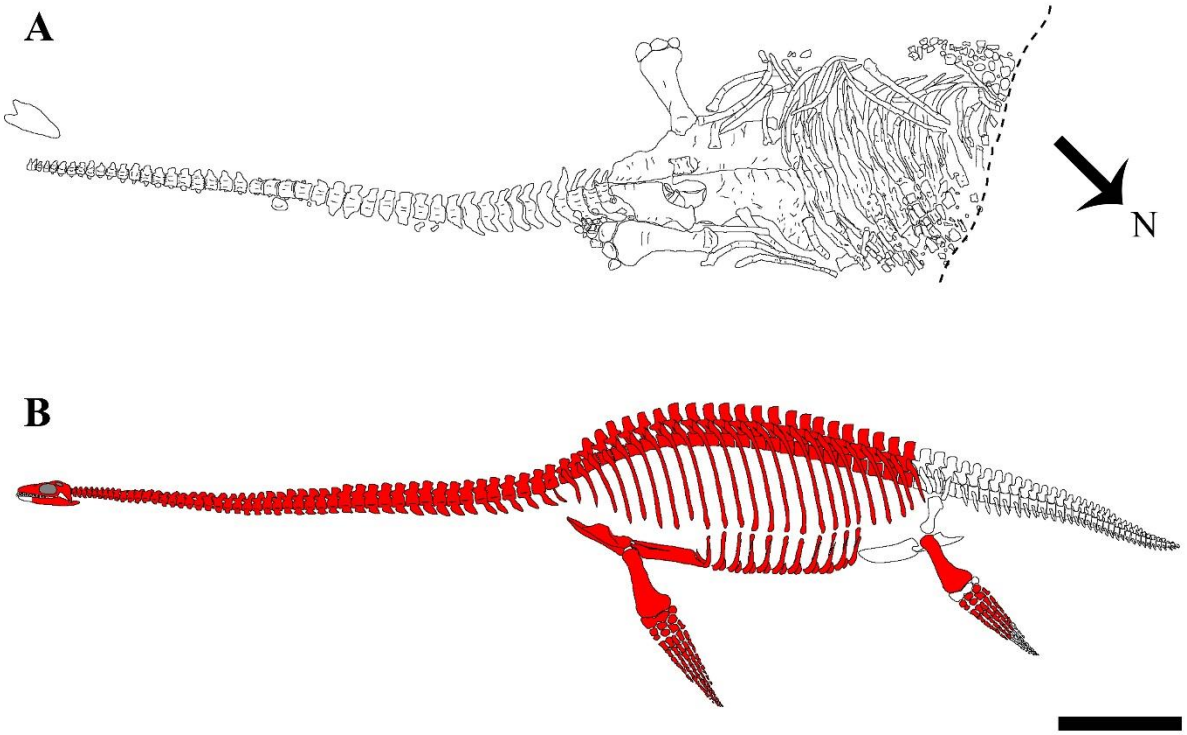

Figure 3.2: Quarry map and reconstruction of PMO 224.248. **A**, drawing from a combination of field and laboratory drawings in ventral view (modified from Delsett et al., 2016); **B**, skeletal reconstruction of PMO 224.248, where red indicates preserved elements. Scale bar equals 50 cm.

Ontogeny

PMO 214.248 is interpreted to be an adult based on its large size and presence of fused neurocentral sutures throughout the preserved vertebral column (Brown, 1981). Other indicators of mature stage of are the fusion along the medial facet of the coracoids and well-formed distal facets of the humeri (Brown 1981).

Description and comparison with other cryptoclidid taxa

Cranium

The temporal fenestrae are conspicuously small relative to the size of the orbits, being roughly ~17 % of total skull length, whereas the orbit constitutes ~29 % of total skull length. The tooth row extends around 75 % of the total skull length. For selected measurements of the cranium see Appendix 6, Table A6.1. The cranium is

presented in dorsal (Figure 3.3) and ventral (Figure 3.4) views, as well as a reconstructed image (Figure 3.5).

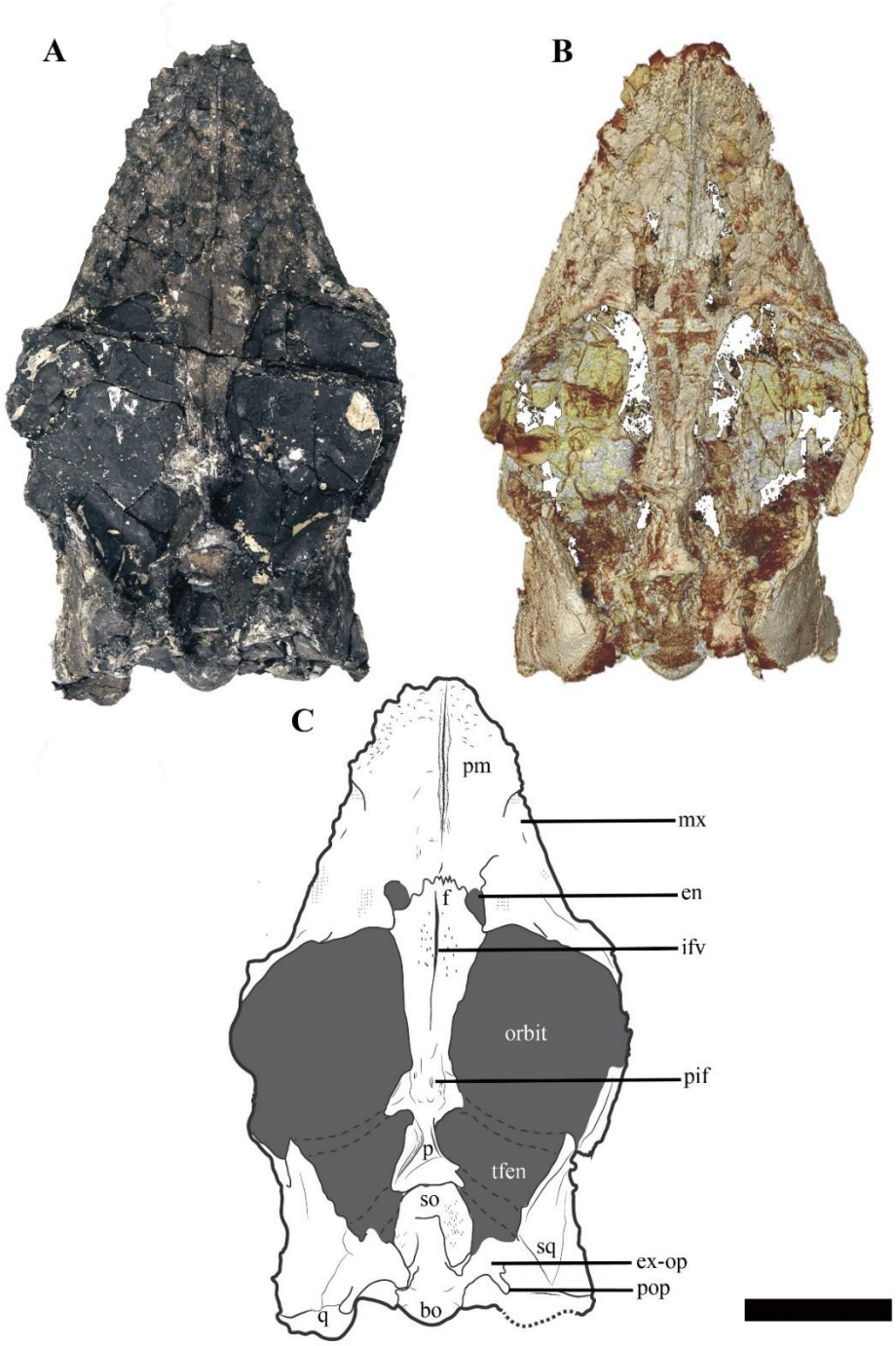

Figure 3.3: The cranium of PMO 224.248 in dorsal view. **A**, photo, **B**, µCT reconstruction and **C**, interpretation. **Abbreviations: bo**, basioccipital; **en**, external naris; **ex-op**, exoccipital-opisthotic; **f**, frontal; **ifv**, interfrontal vacuity; **mx**, maxilla; **p**, parietal; **pif**, pineal foramen; **pm**, premaxilla; **pop**, paraoccipital process; **q**, quadrate; **so**, supraoccipitial; **sq**, squamosal; **tfen**, temporal fenestra. Scale bar equals 5 cm.

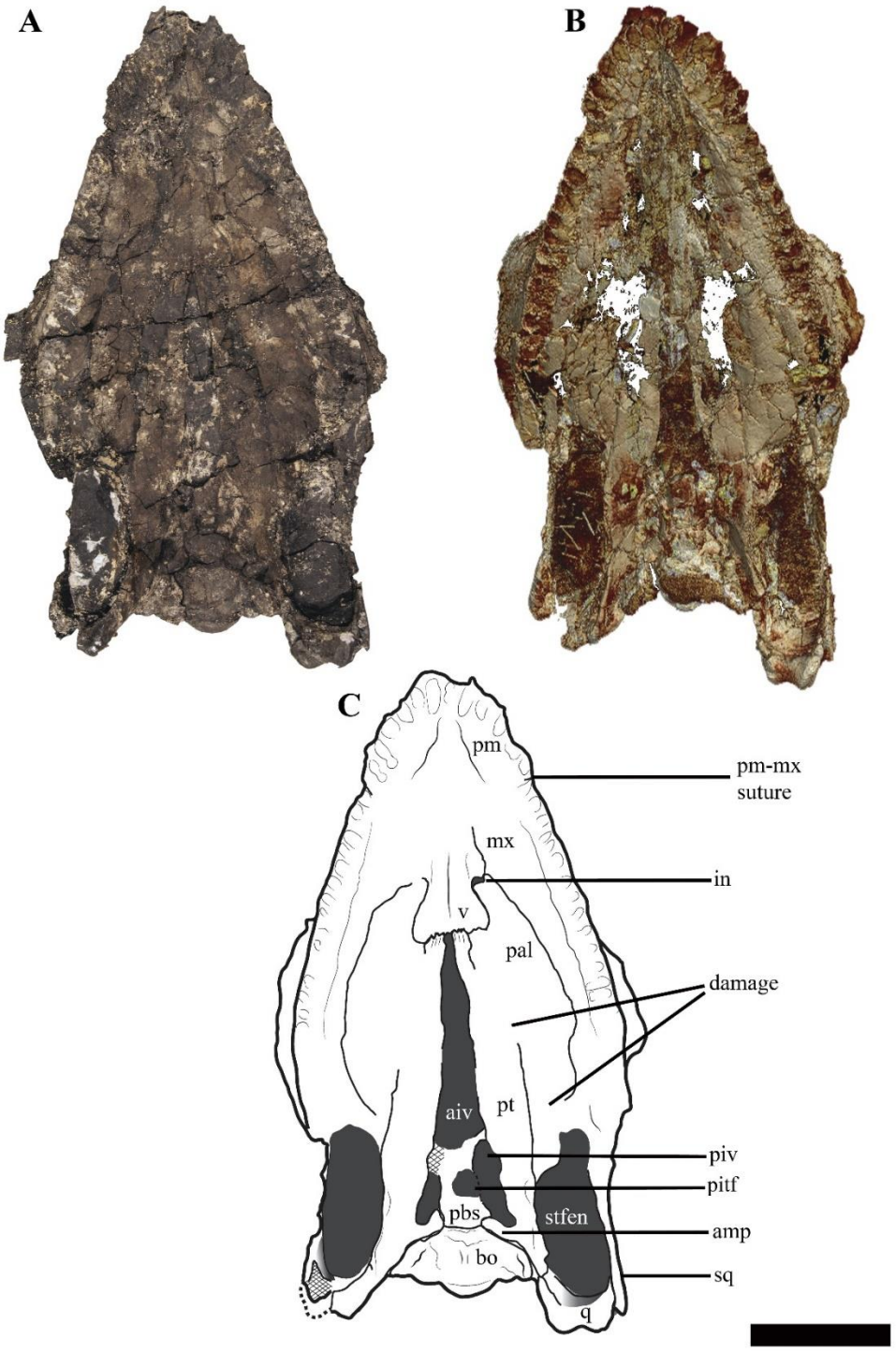

Figure 3.4: The cranium of PMO 224.248 in palatal view. **A**, photo, **B**, µCT reconstruction and **C**, interpretation. **Abbreviations: aiv**, anterior interpterygoid vacuity; **bo**, basioccipital; **in**, internal naris; **mx**, maxilla; **pal**, palatine; p**bs**, parabasisphenoid **pitf**, pituitary fossa; **piv**, posterior interpterygoid vacuity; **pm**, premaxilla; **pt**, pterygoid; **q**, quadrate; **sq**, squamosal; **stfen**, subtemporal fenestra; **v**, vomer. Scale bar equals 5 cm.

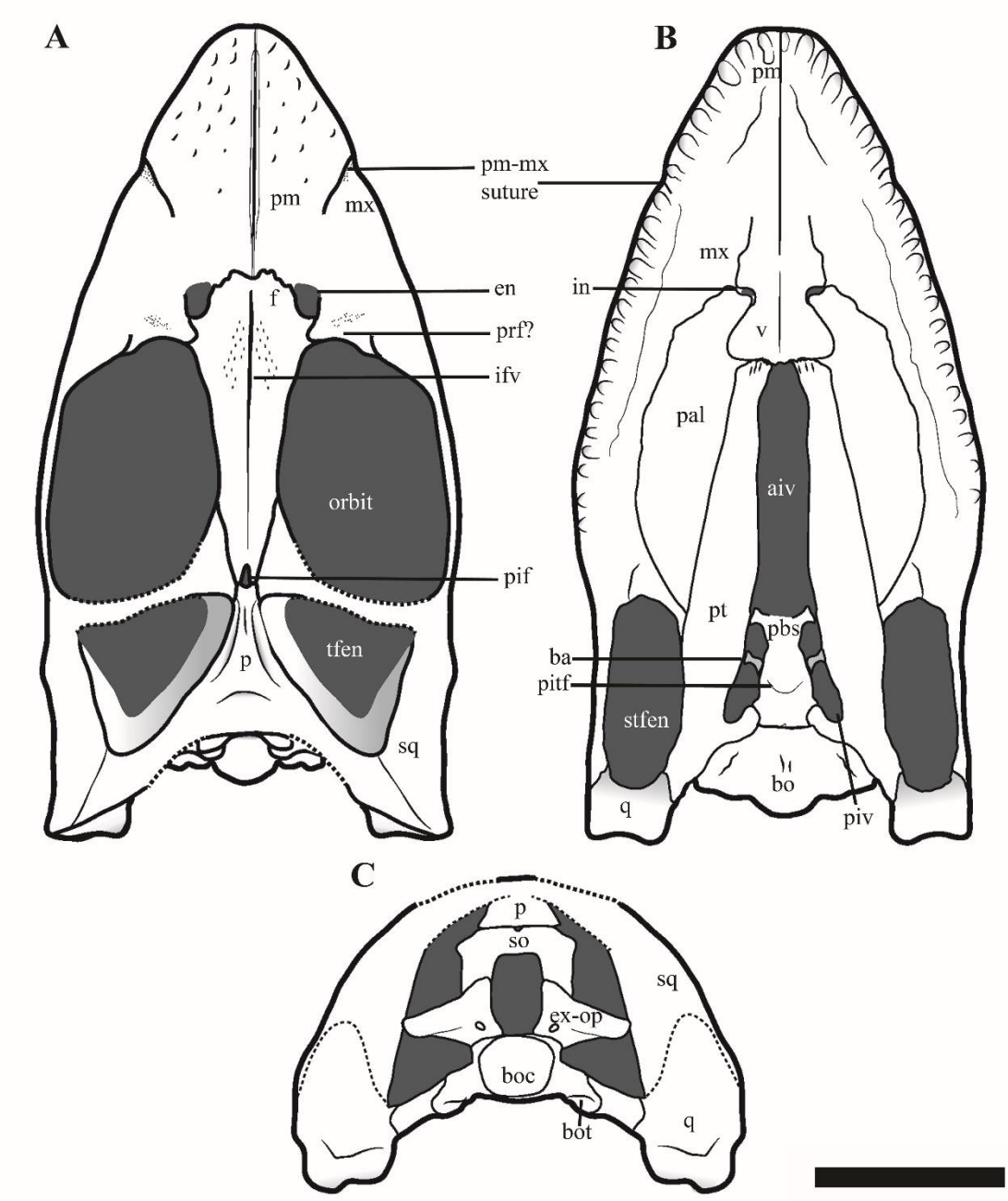

Figure 3.5: Reconstructions of the cranium of PMO 224.248. **A**, dorsal, **B**, palatal and **C**, posterior views. **Abbreviations: aiv**, anterior interpterygoid vacuity; **ba**, basal articulation; **bo**, basioccipital; **boc**, basioccipital condyle; **bot**, basioccipital tuber; **en**, external naris; **ex-op**, exoccipital-opisthotic; **f**, frontal; **ifv**, interfrontal vacuity; **in**, internal naris; **mx**, maxilla; **p**, parietal; **pal**, palatine; **pbs**, parabasispenoid; **pif**, pineal foramen; **pitf**, pituitary fossa; **piv**, posterior interpterygoid vacuity; **pm**, premaxilla; **pt**, pterygoid; **q**, quadrate; **so**, supraoccipital; **sq**, squamosal; **stfen**, subtemporal fenestra; **tfen**, temporal fenestra; **v**, vomer. Scale bar equals 5 cm.

Premaxilla—The premaxilla forms the majority of the dorsal and lateral surfaces of the rostrum anterior to the orbit (Figure 3.3). As with all cryptoclidids (that preserve cranial material), the rostrum is relatively short (Andrews, 1910; Brown and Cruickshank, 1994), having a preorbital to total skull length ratio of 0.43. Similar to *Muraenosaurus leedsii*, the dorsal surface of the premaxilla is rugose, forming numerous low and sharp crests (Andrews, 1910). The premaxillae form a narrow ridge that extends along most of the rostral midline. The anterior portion of the premaxilla-maxilla suture is visible in dorsal view, extending from the rostral margin towards the external naris. The external nares of PMO 224.248 are positioned immediately anterior to the orbital margin, being relatively more posterodorsally placed than in *M. leedsii*. In PMO 226.248, the dorsomedial processes of the premaxilla terminate anterior to the posteromedial margin of the external naris, forms only the anterior and anteromedial borders of the external naris, an autapomorphy of this taxon. In *Cryptoclidus eurymerus* the morphology of this region is ambiguous (in PETMG R.283.412); however, it has been reconstructed with the premaxillae excluded from most of the medial margin of the external naris by the frontal (PETMG R.283.412; Brown and Cruickshank, 1994). This morphology is not homologous with the condition where the anterior flange of the frontal, excludes the premaxilla from the external naris in some rhomaleosaurids (Smith and Benson, 2014). In *M. leedsii* and *Tricleidus seeleyi*, the premaxillae form the medial margin of the external nares and either terminate at or continue past the posterior margin of the external nares (Andrews 1910; Brown, 1981). The µCT images confirms that the premaxilla overlaps the anterior portion of the frontal and that this sutural contact lies approximately in line with the external naris, as in *C. eurymerus* (PETMG R.283.412; Andrews, 1910; Brown and Cruickshank, 1994). Furthermore, in PMO 224.248 the premaxilla-frontal suture is embayed anteriorly along the midline with the longest dimension of the premaxilla occurring in the parasagittal plane. In contrast, the dorsomedial process of the premaxillae taper posteriorly along the midline in *C. eurymerus* and *M. leedsii*.

Among cryptoclidids the number of premaxillary alveoli is constrained between 5-8 teeth on each side (Brown, 1981). Based on µCT images (Figure 3.4B), the premaxilla of PMO 224.248 have a total of six alveoli on each side, the same

number as *Cryptoclidus eurymerus* (Brown and Cruickshank, 1994), but greater than that observed in *Muraenosaurus leedsii* (five: Brown, 1981) and less than that suggested for *Kimmerosaurus langhami* (minimum eight: Brown, 1981). The first and sixth alveoli are noticeably smaller in all dimensions than the other premaxillary alveoli, which are otherwise similar in size. The premaxillary-maxillary suture is visible in ventral view, just posterior to the sixth alveolus (Figure 3.4-5).

Maxilla—The maxilla of PMO 224.248 forms the ventral rim and most of the anterior margin of the orbit. The prefrontal-maxilla suture is equivocal due to significant breakage in this region. The lateral surface of the maxilla is lightly pitted and rugose, but not to the same extent as the premaxilla. In ventral view the alveoli are partially obscured by matrix, but can be counted using µCT images, showing a maximum of 16 alveoli when taking damage on both sides into account. This is less than *Cryptoclidus eurymerus* (18; Brown, 1981), but similar to other Oxford Clay Formation cryptoclidids (16 in *Muraenosaurus leedsii*; 15 in *Tricleidus seeleyi*; Brown, 1981). The maxillary alveoli vary only slightly in size and morphology, with the larger labiolingually expanded alveoli located more anteriorly and smaller, more rounded alveoli posteriorly. We interpret that the slight asymmetry regarding maxillary alveolus size present in PMO 224.248, is likely due to variation in tooth replacement stage. This morphology differs from *T. seeleyi*, where clear heterodonty is present (Brown, 1981). As in *C. eurymerus* (PETMG R.283.412), the posterior extent of the maxillary tooth row in PMO 224.248 terminates in line with the position of the postorbital bar and is positioned considerably higher than the glenoid fossa in lateral view.

Ventrally, the maxilla approaches and nearly contributes to the margin of the internal naris, but is excluded by the palatine-vomer contact, similar to *Cryptoclidus eurymerus* (Andrews, 1910). This morphology differs from *Muraenosaurus leedsii* where the premaxilla and maxilla contribute to the anterior and lateral margins of the internal naris respectively (Andrews, 1910; Brown and Cruickshank, 1994).

Prefrontal—The region anterior to the orbit in PMO 224.248 is difficult to interpret, due to poor preservation. Two possible sutures that could represent the lateral and medial margins of a prefrontal, with the position of these sutures confirmed by differences in bone orientation using µCT images (Appendix 6, Figure

A6.1). Using these margins, the prefrontal would be constrained to a small wedge-shaped section directly anterior to the orbital rim, separated from the external naris by a dorsal process of the maxilla. The element is thickened along the orbital margin and posterodorsally overlaps the frontal in a pointed process. The prefrontal is rarely described in Callovian cryptoclidids, with the exception of *Muraenosaurus leedsii* (Andrews, 1910; Brown, 1981). This has been attributed to either poor preservation of this area in most specimens, or because the element is indiscernible due to fusion with the maxilla (Brown, 1981; *pers. obs.* PSD).

Frontal—In PMO 224.248, the anteroposterior length (measured along the midline) of the frontal is 2.3 times longer than the length of the parietal, whereas in other taxa the relative lengths are nearly the same (= ~0.9 *Cryptoclidus eurymerus* PETMG R.283.41; = ~1 *Cryptoclidus eurymerus* NHMUK R2860; = ~0.8 *Muraenosaurus leedsii* using Andrews, 1910; = ~1.4 *Tricleidus seeleyi* NHMUK R3539). Anteriorly, the frontal participates in the medial and posterior margins of the external naris. In *M. leedsii*, the frontal participates in the margin of the external naris, but lacks the same degree of anterior extension seen in PMO 224.248 (Andrews, 1910). As in *M. leedsii*, the greatest mediolateral width of the frontal occurs directly in line with the anterior margin of the orbit, in contrast to *C. eurymerus* where this occurs more posteriorly along the middle orbital margin (Andrews, 1910; Brown and Cruickshank, 1994). At the point of articulation with the parietal the mediolateral width of the element is roughly a third of the maximum mediolateral width. Along the dorsal margin of the orbit, the frontal has a concave margin, differing considerably from the straight frontal margin of *Muraenosaurus* specimens (*M. leedsii*; NHMUK R.2678) and from *C. eurymerus*, where it is convex (*C. eurymerus*; PETMG R.283.412). The relationships of the postfrontal and postorbital to the skull roof are not preserved.

The frontals vary in the degree to which they contact one another along the dorsal midline. At their anterior- and posterior-most ends (adjoining the premaxillary and parietal contacts, respectively), the frontals are fully in contact and fused along the midline. However, along the remainder of their length they lack a firm midline contact and enclose a narrow and elongate slit-like opening, referred to here as the interfrontal vacuity. This vacuity is not homologous to the "frontal foramen" observed near the anterior margin of the frontal in some polycotylids, which is not

located along the midline (Carpenter, 1996). However, this vacuity does bear some resemblance to the dorsomedian frontal foramen described in *Brancasaurus brancai* (Sachs et al., 2016). The most conspicuous development of the interfrontal vacuity occurs in the anterior half of the frontals where it can be recognised by having smooth, finished bone medially and a slight concavity following the midline. An interfrontal vacuity is also clearly present in several other cryptoclidids (e.g. *Kimmerosaurus langhami*; *Tatenectes laramiensis*; *Tricleidus seeleyi*; possibly *Cryptoclidus eurymerus*) and could represent a new synapomorphy for a subclade of Cryptoclididae (see Discussion). The dorsal surface of the frontal in PMO 224.248 is generally smooth, but is textured with a few small indentations adjacent to the interfrontal vacuity.

The morphology of the ventral surface of the frontal in PMO 224.248 is visible in the µCT images and tapers medially in cross section. On the ventral surface of the frontal in *Kimmerosaurus langhami*, *Cryptoclidus eurymerus* and *Muraenosaurus leedsii* a trough is present on either side of the interfrontal vacuity or frontal midline. In *K. langhami* these are clearly seen, starting posteriorly in line with the pineal foramen and terminate at the preserved anterior end of the frontal (*pers. obs.* AJR NHMUK R8431). These structures are absent in *Tricleidus seeleyi* and PMO 224.248 based on the µCT images.

The frontal-parietal suture is somewhat obscured in dorsal view due to gypsum mineralization and the presence of rugosities in the anterior portion of the parietal. However, µCT images show that the posterior margin of the frontal interdigitates with the anterior margin of the parietal and that the frontal envelopes the anterior rim and most of the lateral rims of the pineal foramen (Figure 3.6).

Parietal—The anterior extent of the parietal lies approximately in line to the level of the temporal bar. In dorsal view, the parietal bears a mediolaterally narrow sagittal crest that is slightly flattened dorsally, exhibiting an intermediate condition between the tall and sharp crest seen in *Cryptoclidus eurymerus* (Brown and Cruickshank, 1995) and the broad, flat sagittal crest seen in *Kimmerosaurus langhami* (Brown, 1981). In lateral view, the apex of the sagittal crest is straight and gently inclines posterodorsally. In contrast, this morphology differs from the dorsally

convex sagittal crest seen in *C. eurymerus*. The squamosal-parietal contact is indiscernible.

The µCT images reveal the presence of two large dorsoventrally oriented fossae in the parietals that open onto the posteroventral surface, but do not extend to the dorsal surface (Figure 3.6). This feature is also present in another undescribed Slottsmøya Member cryptoclidid (PMO 212.662). In *Kimmerosaurus langhami* (NHMUK R.8431), these parietal fossae are likely absent, as they are not visible on the ventral surface (Brown, 1981). In *Cryptoclidus eurymerus* (NHMUK R.2860) and *Muraenosaurus leedsii* (NHMUK R.2422) the parietals are partly obscured by the supraoccipital and parietal fossae cannot be identified. Although the function of these fossae is currently unclear, CT scanning of additional specimens could infer whether this is a cryptoclidid feature or more constrained to a specific clade.

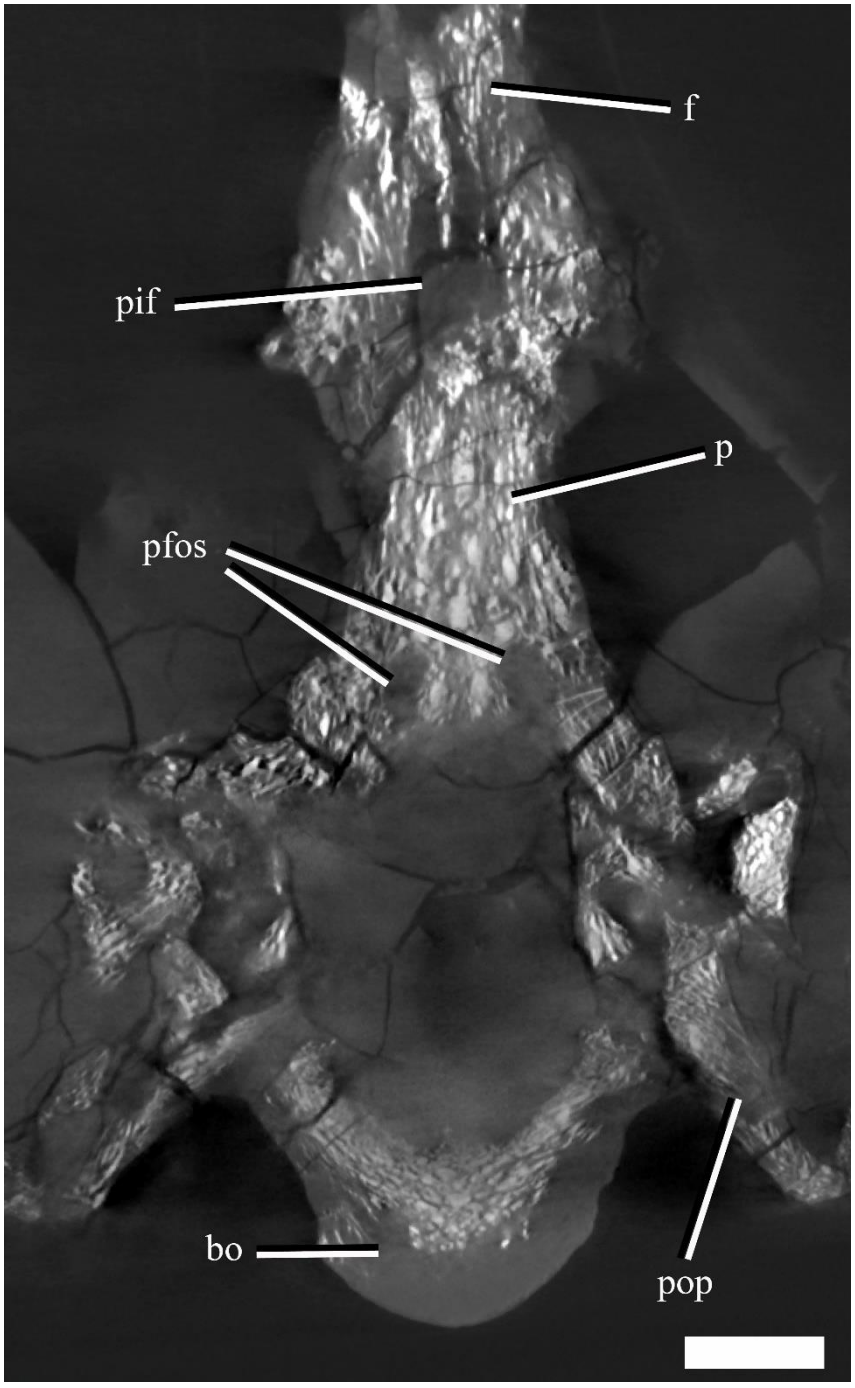

Figure 3.6: A µCT slice (cross section) of the posterior part of the skull roof and braincase of PMO 224.248, illustrating the parietal fossae and pineal foramen. **Abbreviations: bo**, basioccipital; **f**, frontal; **p**, parietal; **pfos**, parietal fossae; **pif**, pineal foramen; **pop**, paraoccipital process. Scale bar equals 1 cm.

Squamosal—In lateral view, the suspensorium is near vertically inclined, although the dorsal half of the squamosal dorsal ramus is inflected abruptly anteriorly (Appendix 6, Figure A6.2). The squamosal bears a dorsoventrally tall

anterior ramus which curves slightly medially, following part of the temporal fenestra anterior margin. The ventromedial process of the squamosal is short, extending ventrally to roughly half the dorsoventral length of the quadrate shaft. The dorsal margin of the squamosal-quadrate suture is visible in posterior view, where a small groove is present (Figure 3.7). However, this suture could not be located dorsally in µCT scan images (Appendix 6, Figure A6.2). The relationships between the squamosal and the jugal and postorbital cannot be discerned due to poor preservation in this area.

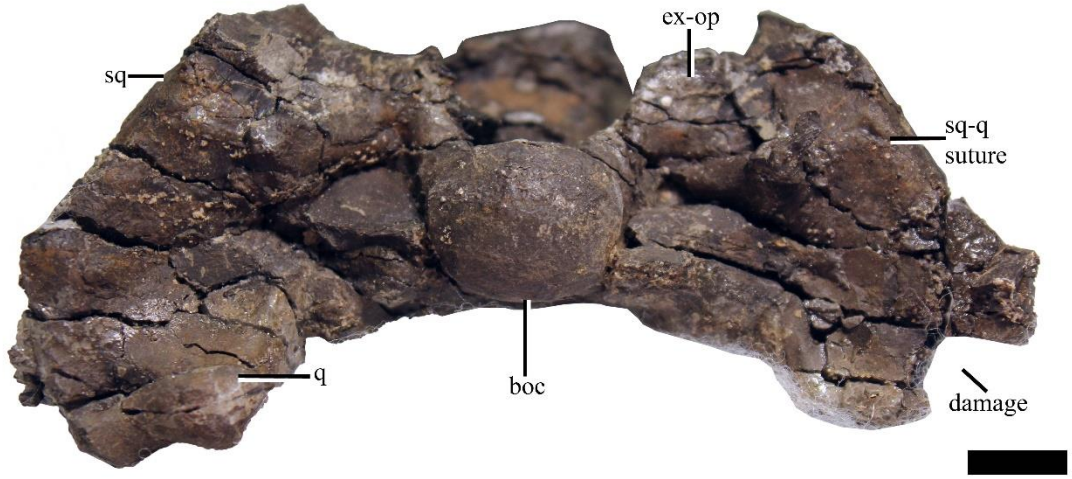

Figure 3.7: The cranium of PMO 224.248 in posterior view. **Abbreviations: boc**, basioccipital condyle; **ex-op**, exoccipital opisthotic; **q**, quadrate; **sq**, squamosal. Scale bar equals 1 cm.

Quadrate—Due to a fracture running along the middle of the right quadrate, the left quadrate is better preserved. Similar to *Djupedalia engeri* and *Kimmerosaurus larseni*, the lateral cotyle of the quadrate condyle in PMO 224.248 is slightly larger in anteroposterior length and dorsoventral extent than the medial cotyle. This differs from *Spitrasaurus larseni*, where the opposite state is present (Knutsen et al., 2012d). There is no indication of a quadrate foramen.

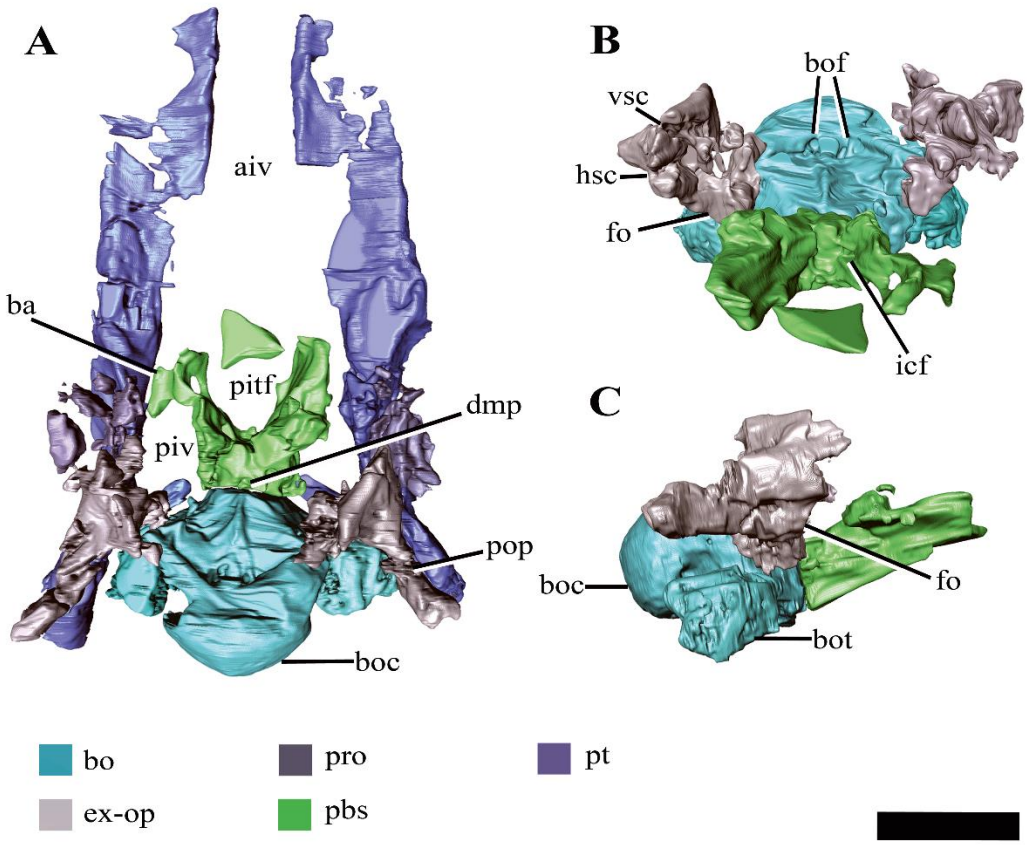

Figure 3.8: Surface reconstruction of the braincase and pterygoids of PMO 224.248 using the µCT images. In **A**, dorsal, **B**, anterodorsal and **C**, lateral views. **Abbreviations: aiv**; anterior interpterygoid vacuity; **ba**, basal articulation; **bo**; basioccipital; **boc**, basioccipital condyle; **bof**, basioccipital foramina; **bot**, basioccipital tuber; **dmp**, dorsal median pit; ex-**op**; exoccipital-opisthotic; **fo**; fenestra ovalis; **hsc**, horizontal semicircular canal; **pbs**, parabasisphenoid; **pitf**, pituitary fossa; **piv**, posterior interpterygoid vacuity; **pop**, paraoccipital process; **pro**, prootic; **pt**, pterygoid; **vsc**, vertical semicircular canal. Scale bar equals 2 cm.

Basioccipital—The anterior and dorsal surfaces of the basioccipital of PMO 224.248 are obscured by matrix and other skull elements, but can be described fully using the µCT segmentation (Figure 3.8). The occipital condyle lacks both a notochordal pit and a constriction on the dorsal and ventral surfaces; however, a slight constriction is visible on the lateral surfaces. As in *Spitrasaurus larseni*, the exoccipital facets reach, but do not contribute to the occipital condyle (Knutsen et al., 2012d). In contrast, the exoccipitals in *Kimmerosaurus langhami* and in some specimens of *Cryptoclidus eurymerus* form a portion of the condyle (Andrews, 1910; Brown, 1981). In posterior view, the condyle is mediolaterally wider than

dorsoventrally tall. The height-to-width ratio (H/W) of the condyle (~0.82) is comparable to that of *Spitrasaurus larseni* (0.8) and *Kimmerosaurus langhami* (0.85) (Knutsen et al. 2012d), but differ from *Muraenosaurus leedsii* and *T. seeleyi* that possess more circular condyles (H/W ~1).

Similar to *Tricleidus seeleyi* and another undescribed Slottsmøya Member cryptoclidid specimen (PMO 212.662), the basioccipital tubera of PMO 224.248 are dorsoventrally flattened and triangular in general outline as seen in ventral view and their ventral surfaces are gently concave in occipital view (Appendix 6, Figure A6.2). The entire anterolateral margin of the tubera meet and run parallel to the pterygoid extending to the basisphenoid margin. This morphology contrasts to the pillar-like (circular in cross section) and laterally-facing tubera in *Cryptoclidus eurymerus* and *Kimmerosaurus langhami (*Andrews, 1910; Brown, 1981). In addition to this morphology, *K. langhami* displays finished bone along the posterolateral basioccipital margin between the basisphenoid facet and tubera (Brown, 1981; Brown and Cruickshank, 1994).

The posterior floor of the foramen magnum is visible, forming part of a shallow but mediolaterally broad concavity between the two exoccipital-opisthotics. Anteriorly, there is a low anteroposteriorly oriented ridge that terminates near the contact with the basisphenoid (Figure 3.8B). Two paired foramina open on to the dorsal surface of the basioccipital and extend into the body of the element, where they are visible in the µCT images, but terminate before reaching the ventral surface. Similar to *Kimmerosaurus langhami*, the ventral surface of the basioccipital is relatively flat, with a short anteroposteriorly oriented median ridge that terminates at the rim of the anterior margin (Brown, 1981).

Parabasisphenoid—A clear demarcation between the parasphenoid and basisphenoid of PMO 224.248 is indiscernible. In dorsal view on the posterior margin of the body of the parabasisphenoid, a small fossa is present along the suture with the basioccipital (‘dmp’, Figure 3.8A). This structure appears homologous with the “dorsal median pit” described in *Muraenosaurus leedsii* (Andrews, 1910), hypothesised to mark the embryonic basicranial fenestra. However, the foramen present in PMO 224.248, is significantly reduced in comparison to *M. leedsii* (Andrews, 1910). A deep fossa is present on the anterior margin of the basisphenoid

body interpreted to be the pituitary (or hypophyseal) fossa, similar to that described in *Tricleidus seeleyi*, *Kimmerosaurus langhami* and *M. leedsii* (Andrews, 1910; Brown et al., 1986). The ventral floor of the pituitary fossa, including parts of both the basisphenoid and parasphenoid (Andrews, 1910), is missing likely due to taphonomic loss. In lateral view the internal carotid foramen is visible opening into the pituitary fossa (not visible on right). In dorsal view on the posterior margin of the parabasisphenoid, a small fossa is present along the suture with the basioccipital. In palatal view, the basal articulation of plesiosauroids is often visible in ventral view through the posterior interpterygoid vacuity (Buchy et al., 2006a). In PMO 224.248, the basal articulation is visible on the µCT scans and is better preserved on the left side and positioned dorsally in respect to the rest of the palate

The parabasisphenoid bears posterolaterally located facets for the anteromedial process of the pterygoid similar to *Tricleidus seeleyi*, but in contrast to *Muraenosaurus leedsii* and *Cryptoclidus eurymerus* where the pterygoid simply articulates to the basioccipital tuber (Andrews, 1910; Brown, 1981). In *T. seeleyi*, the pterygoid facets of the parabasisphenoid are circular in outline and are slightly anterolaterally projecting, whereas in PMO 224.248 the facet surface appears uniform and triangular in shape in the µCT images. The presence of a pterygoid facet on the body of a parabasisphenoid is also present in another Slottsmøya Member cryptoclidid (PMO 212.662) and has been suggested to be present in *Kimmerosaurus langhami* (NHMUK R10042; Benson and Druckenmiller, 2014, Appendix S2). That a minimum of three cryptoclidid taxa share this palatal configuration over a long temporal span (Callovian – Volgian), suggests that this morphology is more widespread in cryptoclidids than previously believed.

Anteriorly, the parabasisphenoid is very thin and somewhat damaged, making this region difficult to segment out of the µCT images. The anterior portion (parasphenoid) separates the pterygoids along the midline and forms the entire posterior margin of the anterior interpterygoid vacuity, but lacks a projecting cultiform process, like that seen in some polycotylids and basal plesiosaurians (Buchy et al., 2006a; Carpenter, 1996; O'Keefe, 2001; Vincent and Benson, 2012). The anterior margin of the posterior interpterygoid vacuity is formed by a lateral extension of the parabasisphenoid.

Exoccipital-opisthotic—Both exoccipital-opisthotics are preserved in partial articulation, but are damaged and displaced venterolaterally due to compression. As only the posterior view is visible on the specimen (Figure 3.7), the following description is largely based on µCT images (Figure 3.9).

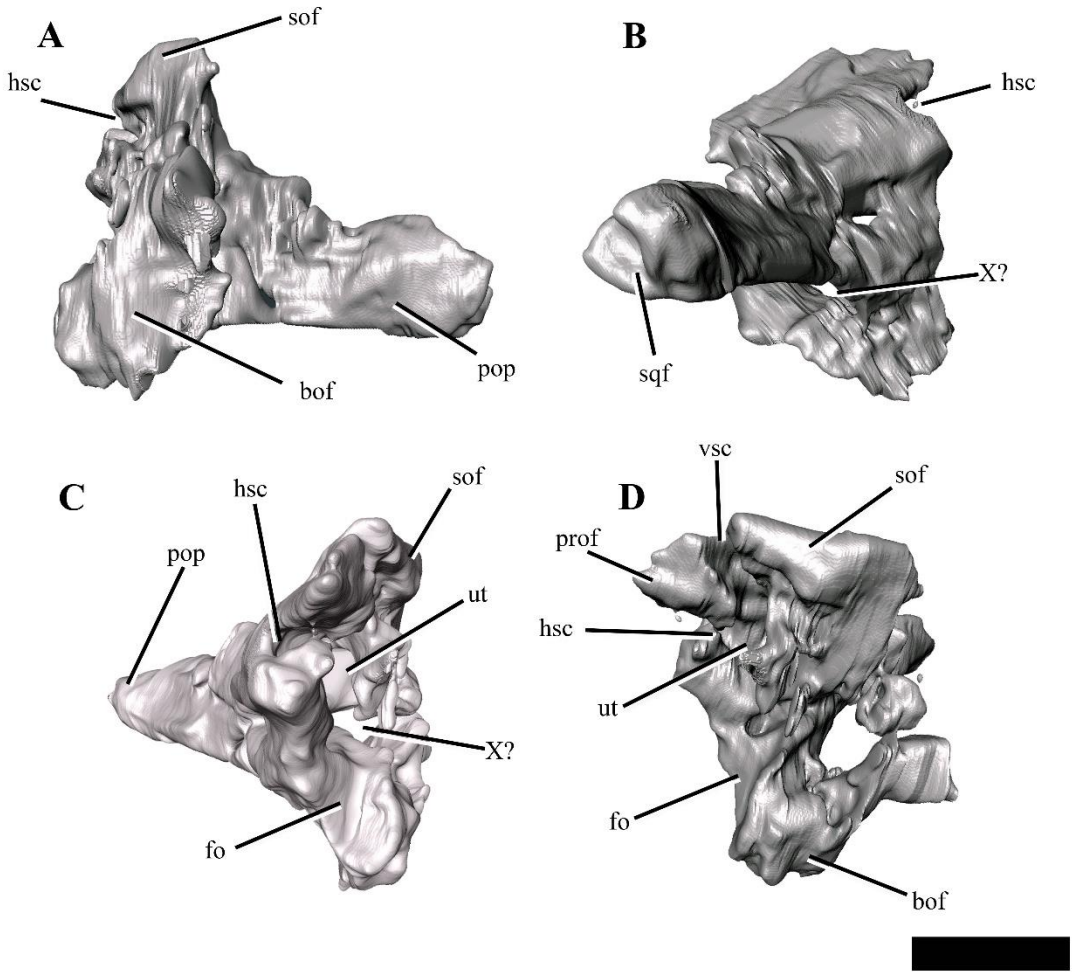

Figure 3.9: The right exoccipital-opisthotic of PMO 224.248 segmented out from µCT images. In **A**, posterior, **B**, lateral, **C**, anterior and **D**, medial views. **Abbreviations: bof**, position of basioccipital facet; **fo**, position of fenestra ovalis; **hsc**, horizontal semicircular canal; **pop**, paraoccipital process; **prof**, position of prootic facet; **sof**, position of supraoccipital facet; **sqf**, position of squamosal facet; **ut**, utriculus; **vsc**, posterior vertical semicircular canal; **X**, position of cranial nerve openings. Scale bar equals ~1 cm

The body of the exoccipital-opisthotic is dorsoventrally taller than mediolaterally wide. In posterior view, the paraoccipital process is visible extending laterally from the body of the element. The cross sectional shape of the paraoccipital

process shaft is dorsoventrally taller than wide. Similar to *Muraenosaurus leedsii*, the length of the paraoccipital process is close to the dorsoventral height of the exoccipital, in contrast to *Tricleidus seeleyi* and *Djupedalia engeri*, which have more elongate paraoccipital processes (Andrews, 1910; Brown, 1981; Knutsen et al. 2012a). As in *Kimmerosaurus langhami* and *Cryptoclidus eurymerus*, the paraoccipital process is expanded distally where it contacts the squamosal (Brown, 1981).

On the medial surface, a large anteroposteriorly oriented cavity is present at the centre of the exoccipital-opisthotic body. Although the structure is distorted, it may represent the recess for the utriculus as described for *Muraenosaurus leedsii* and *Tricleidus seeleyi* (Andrews, 1910). Two semicircular canal openings are visible in medial view: a dorsally orientated vertical posterior semicircular canal and a horizontal anterior semicircular canal. The posterior vertical semicircular canal is positioned just anterior to the supraoccipitial facet and runs ventrally into a cavity interpreted to be for the utriculus, similar to *Kimmerosaurus langhami* and *Cryptoclidus eurymerus* (Andrews, 1910; Brown, 1981). The horizontal anterior semicircular canal is located directly ventral to most of the prootic facet and opens posteriorly into the utricular cavity.

In lateral view (Figure 3.9B), a large foramen could either be for the exit for cranial nerve X, or may be formed of multiple cranial nerve openings which have merged due to crushing. The posterior portion of the fenestra ovalis is located along the anterior margin of the exoccipital, ventral to anterior horizontal canal and the prootic facet.

Supraoccipital—The supraoccipital remains in articulation with the parietal, but has rotated anteriorly so that its posterior surface faces dorsally. The element is anteroposteriorly thickest at the exoccipital-opisthotic facet and thins dorsally. Compared to the relative dorsoventral height of the exoccipital-opisthotic, the supraoccipital contributes roughly half of the total height of the foramen magnum. The foramen magnum appears to be oval in shape, unlike the more hour-glass outline seen in *Kimmerosaurus langhami* (Brown et al., 1986). PMO 224.248 lacks a posteromedian ridge on the supraoccipital, as seen in *K. langhami* and *Muraenosaurus leedsii* (Brown et al., 1986). A small foramen located on the midline

of the dorsal border with the parietal, a feature that is also present in *C. eurymerus* (Brown, 1981, Figure 2), but notably absent in *M. leedsii* and possibly *K. langhami* (Brown, 1981; Brown et. al, 1986; AJR *pers. obs.* NHMUK R.10042).

Prootic—Two crushed and slightly disarticulated elements visible anterior to the exoccipital-opisthotics in the µCT images, are interpreted to be the prootics (Figure 3.8). The elements are too distorted to warrant further description.

Vomer—The anterior extent of the vomers in PMO 224.248 is unclear, however they are mediolaterally narrowest anteriorly. Posterior to the internal nares, the vomer expands in mediolateral width, becoming broadest near their posterior margin, similar to that observed in *Muraenosaurus leedsii* (Andrews, 1910). The left and right vomers are in full contact along, although unfused along the midline and the ventral surface is convex and lacks ornamentation. This differs from the clear fusion seen in *Vinialesaurus caroli* (Gasparini et al., 2002) and partial fusion and ridged ventral surface in an undescribed juvenile Callovian cryptoclidid specimen (NHMUK R 2853; *pers obs.* AJR). As in most other cryptoclidids, the vomer forms the medial and at least part of the anterior border (Andrews, 1910). As in some other plesiosauroids that preserve this region (e.g. *M. leedsii*; Andrews, 1910), the vomers have posterolaterally expanded margins that partially lie ventral to the palatines, an orientation confirmed by the µCT images in cross section. The posterior contact with the pterygoids consists of an interdigitating suture. The vomer forms the anterior border of the anterior interpterygoid vacuity, in contrast to *M. leedsii* and *Cryptoclidus eurymerus* where the pterygoids meet anteriorly along the midline and exclude the vomer from participation in margin of the anterior interpterygoid vacuity (Andrews, 1910; Brown and Cruickshank, 1994).

Palatine—The palatine of PMO 224.248 form the posterolateral border of the internal naris. As is typical of cryptoclidids, the palatines do not meet anteriorly along the midline, but are separated anteriorly by the vomer (Buchy et al. 2006a). Similar to *Cryptoclidus eurymerus* and *Muraenosaurus leedsii* a suborbital fenestra is absent (Andrews, 1910; Brown and Cruickshank, 1994). The posterior margin of the palatines are presumed to terminate at the anterior margin of the ectopterygoid, although it is difficult to discern the nature of this contact due to poor preservation in this area. The ectopterygoid area lacks a boss or flange of the pterygoid.

Pterygoid—The pterygoid is mediolaterally narrow anteriorly and gradually increases in width posteriorly, as in *Cryptoclidus eurymerus* and *Muraenosaurus leedsii* (Andrews, 1910; Brown, 1981; Brown and Cruickshank, 1994). The anterior region of the pterygoids are separated along the midline, by a prominent and mediolaterally broad anterior interpterygoid vacuity. The mediolaterally broad morphology of the anterior pterygoid vacuity is similar to *Tricleidus seeleyi* and does not narrow anteriorly to the same degree as in *Muraenosaurus leedsii* (Andrews, 1910).

The pterygoid forms the lateral margins of the posterior interpterygoid vacuity, which is anteroposteriorly short compared to *Cryptoclidus eurymerus* and *Muraenosaurus leedsii* (Andrews, 1910; Brown, 1981). The pterygoids do not meet along the midline posterior to the posterior interpterygoid vacuity, as is the case in some leptoclidid and polycotylid plesiosaurs (e.g. *Edgarosaurus muddi*, *Umoonasaurus demoscyllus*; Druckenmiller, 2002; Kear et al., 2006). The posterior interpterygoid vacuity is located entirely posterior to the anterior margin of the subtemporal fossa, as in *Tricleidus seeleyi* (Andrews, 1910).

As in *Tricleidus seeleyi*, the pterygoid bears a narrow, prong-like anteromedial process (basisphenoid process of the pterygoid; Andrews 1910), that contacts the parabasisphenoid. The anteromedial process parallels the anterolateral margin of the basioccipital, but does not form a distinct facet for it. The anteromedial process in PMO 224.248 is similar in relative length to that of *T. seeleyi*; however, it differs from *T. seeleyi* in being anteromedially curved rather than straight and greater in dorsoventral height (based on CT imaging) in lateral view (Andrews, 1910).

The quadrate ramus of the pterygoid deflects posterolaterally towards the pterygoid ramus of the quadrate and is dorsoventrally taller than wide. The pterygoid forms a broad medially facing facet for the quadrate, similar to *Kimmerosaurus langhami* (Brown, 1981).

Mandible—Each mandibular ramus is disarticulated from the cranium and the anterior portions of each are missing, including the symphyseal region (Figure 3.10). Based on corresponding measurements from the upper jaws, the left mandible lacks the anterior 10.5 cm of the ramus, providing an estimated total mandibular length of 27 cm.

The left mandible, which is more complete and the basis for the following description, preserves the dentary, splenial, angular, surangular and articular (see Appendix 6, Figure A6.3 for images). The Meckalian canal is visible on the left mandible, suggesting that the prearticular and splenial are damaged. A disarticulated element either representing the prearticular or splenial is present adjacent to the right mandible (Appendix 6, Figure A6.4). There is no visible facet or suture on the surangular for the coronoid, as seen clearly in *Tricleidus seeleyi* (Andrews, 1910; Brown, 1981).

In dorsal view, the alveolar row is laterally positioned relative to the parasagittal long axis of the ramus, resulting in a mediolaterally expanded dorsal portion of the dentary that preserves fourteen alveoli (inferred from µCT images). The alveoli are strongly labially angled (~60° from the parasagittal plane), which increases slightly anteriorly. This differs from the more dorsally-directed alveoli in *Tricleidus seeleyi* (Andrews, 1910). In dorsal view, only a couple of the primary alveoli for the replacement teeth are visible, as these are partially covered by matrix. The mediolateral expansion of the dentary preserves finished bone medial to the alveoli, contributing to at least a third of the lateromedial width of the dentary dorsal surface. Ventrally, the mediolateral expansion abruptly decreases in width. In cross section, the anterior portion of the element (at the mid-point of the dentary), is subtriangular due to the expanded mandibular dorsal surface. Similar expanded mediolateral dorsal surfaces, are also observed in *Spitrasaurus larseni*, *Djupedalia engeri* and *Muraenosaurus leedsii* (Andrews, 1910; Knutsen et al. 2012a, d). In *Kimmerosaurus langhami* a mediolaterally expansion of the dentary is present although possibly due to taphonomy in one of the referred specimens (NHMUK R.10042; *pers. obs.* AJR), but appears absent on the holotype specimen (Brown 1981). This morphology differs from the other taxa, where a mediolateral expansion is either missing entirely (*Tricleidus seeleyi*), or a lateral expansion is only present on the posterior half of the dentary (*Cryptoclidus eurymerus*; '*Picrocleidus*' *beloclis*) and lacks the abrupt ventral constriction observed in PMO 224.248, *S. larseni* and *Muraenosaurus leedsii* (Andrews, 1910; Brown, 1981; Knutsen et al., 2012d). This feature is proposed as a new phylogenetic character (see Discussion).

The lateral surface of the dentary is gently striated. Dorsomedially, a partial suture between the splenial and dentary is visible. Posteriorly, there is no clear suture

between the dentary and surangular. The angular-surangular suture is partly visible in lateral and medial views. In *Kimmerosaurus langhami* and *Cryptoclidus eurymerus* the ventral margin of the angular is convex ventral to the glenoid, becoming concave anteriorly along the ventral margin (Brown, 1981; Brown and Cruickshank, 1994). This morphology is reduced in PMO 224.248 and *Tricleidus seeleyi*, where the ventral margin of the angular is almost straight, with a slight convexity in line with the articular (Andrews, 1910; Brown, 1981). The surface of the glenoid is slightly undulated posteriorly and dorsoventrally deep, being over half the dorsal-ventral height of the mandible. This is distinct from the shallow and smooth articular facet of *Colymbosaurus* (OUM J.3300; Chapter 2, this volume), *Cryptoclidus eurymerus*, *Muraenosaurus leedsii* and *Kimmerosaurus langhami* (Brown, 1981; Roberts et al., 2017).

In PMO 224.248, the retroarticular process is uniform in dorsal-ventral thickness until it reaches the posterior terminus. The retroarticular process is nearly twice as long as it is dorsoventrally tall, in contrast to the even longer than tall retroarticular process in *Spitrasaurus larseni* (Knutsen et al. 2012d) and *Muraenosaurus leedsii* (Andrews, 1910). The process is dorsally inclined at ~15º with respect to the longitudinal axis of the mandibular ramus. This is significantly less than the in strong inclination seen in *S. larseni* (35º) and greater than *Colymbosaurus indet.* (OUM J. 3300; ~9°) and *Tricleidus seeleyi* (10º). There is no mediolateral deflection of the retroarticular process.

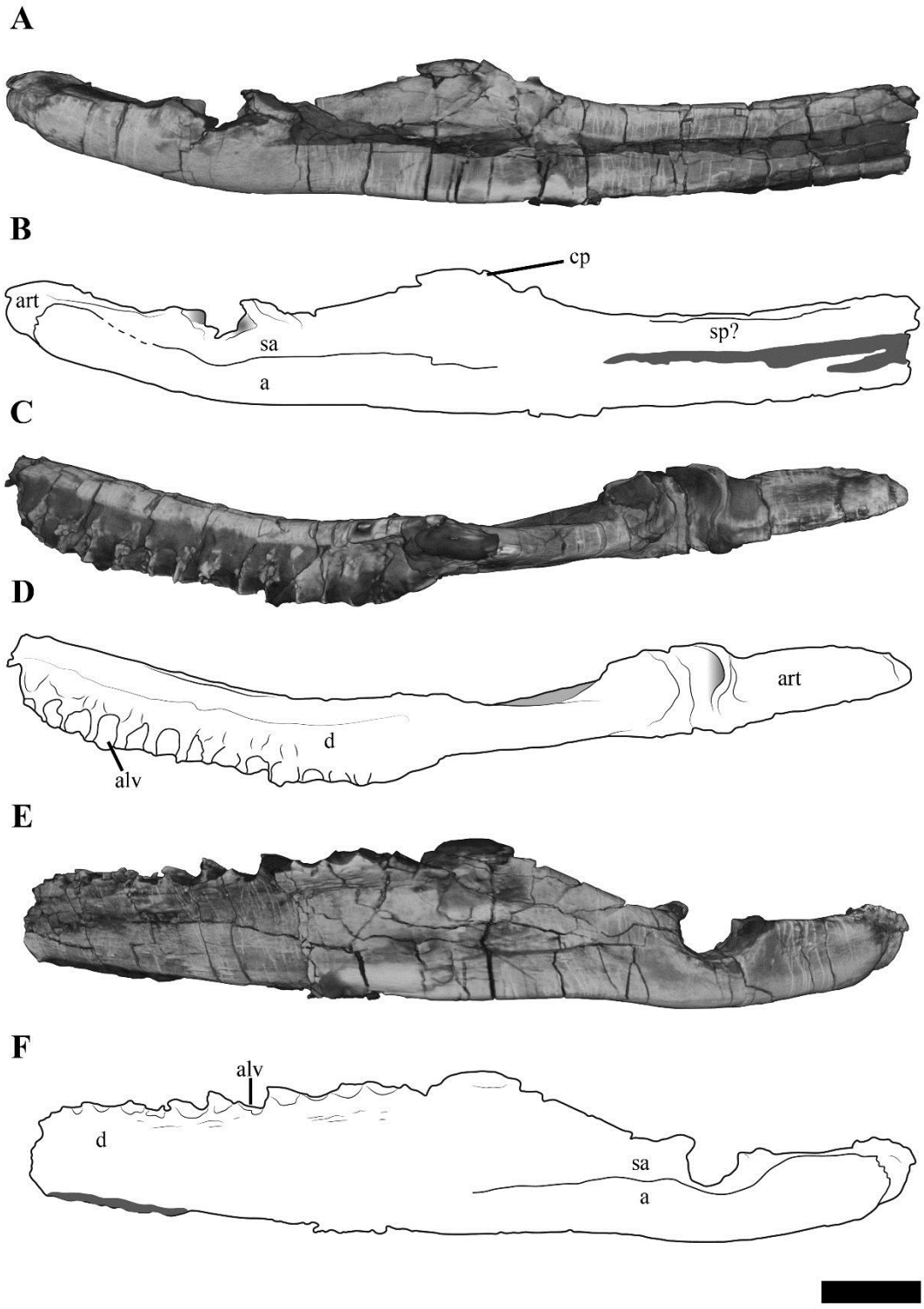

Figure 3.10 – The left mandible of PMO 224.248 shown as the computed tomography surface rendering and interpretations. In **A-B**, medial, **C-D**, dorsal and **E-F**, lateral views. **Abbreviations: a**, angular; **alv**, alveolus; **art**, articular; **cp**, coronoid process; **d**, dentary; **sa**, surangular; **sp**, splenial. Scale bar equals 1 cm.

Dentition—Eight partial to complete but displaced teeth, along with several fragments were found adjacent to the anterior region of the skeleton. Fully erupted teeth are absent in all of the dentigerous portions preserved in PMO 224.248, but several unerupted replacement teeth are visible *in situ* on the µCT images. The individual teeth vary slightly in size, but not morphology, indicating that the minor size difference represents stages of tooth replacement and not heterodonty as suggested by the alveoli. The crowns are gracile in comparison to the more robust teeth in *Tricleidus seeleyi* and *Cryptoclidus eurymerus* (Brown 1981). The largest and most complete tooth preserved (Figure 3.11A), measures ~4 cm in length from apex of the crown to the root. In axial (mesial/distal) view, the complete tooth (Figure 3.11A), is lingually curved along the crown, straightens out at the start of the root and terminates in a slightly lingually curved root terminus. This morphology differs from the significantly lingually curved teeth of *Kimmerosaurus langhami* (75º; Brown, 1981) and *Spitrasaurus larseni* (Knutsen et al., 2012d). The enamelled crown represents a third of the total length of the tooth and displays a gradual transition to the root. A smaller, but fractured tooth (Figure 3.11B-E), bears fine longitudinal ridges on the enamel, which gradually fades towards the apex. The ridging is most prominent on the labial side, unlike the prominently lingually ridged teeth of *Muraenosaurus leedsii* and *Cryptoclidus eurymerus* (Brown, 1981). On some teeth, the axial (mesial?/distal?) margin of the crown bears a more pronounced enamelled ridge. This ridge could represent the edge of a partial wear facet, as it has no distinct shared morphology between teeth and has a variable presence on the preserved tooth crowns (Appendix 6, Figure A6.5). Close to the tip of the crown, the labial side is flattened compared to the convex lingual surface resulting in a D-shaped cross section, similar to *Spitrasaurus larseni* and some elasmosaurids (Knutsen et al., 2012d; Sato et al., 2006). This morphology differs from the more oval-shaped cross section in *K. langhami*, *M. leedsii* and *C. eurymerus* (Brown 1981). The shaft of the root is subcircular in cross section and slightly expanded in diameter with respect to the crown, by a gently undulating surface which decreases in width towards the root terminus. One of the teeth (Appendix 6, Figure A6.5), has a clear reabsorption facet on the lingual side of the root. The root terminus is straight and abrupt, whereas other cryptoclidids show a more gradual reduction in diameter at the root terminus (e.g. *K. langhami* and *C. eurymerus*; PETMG R.283.412).

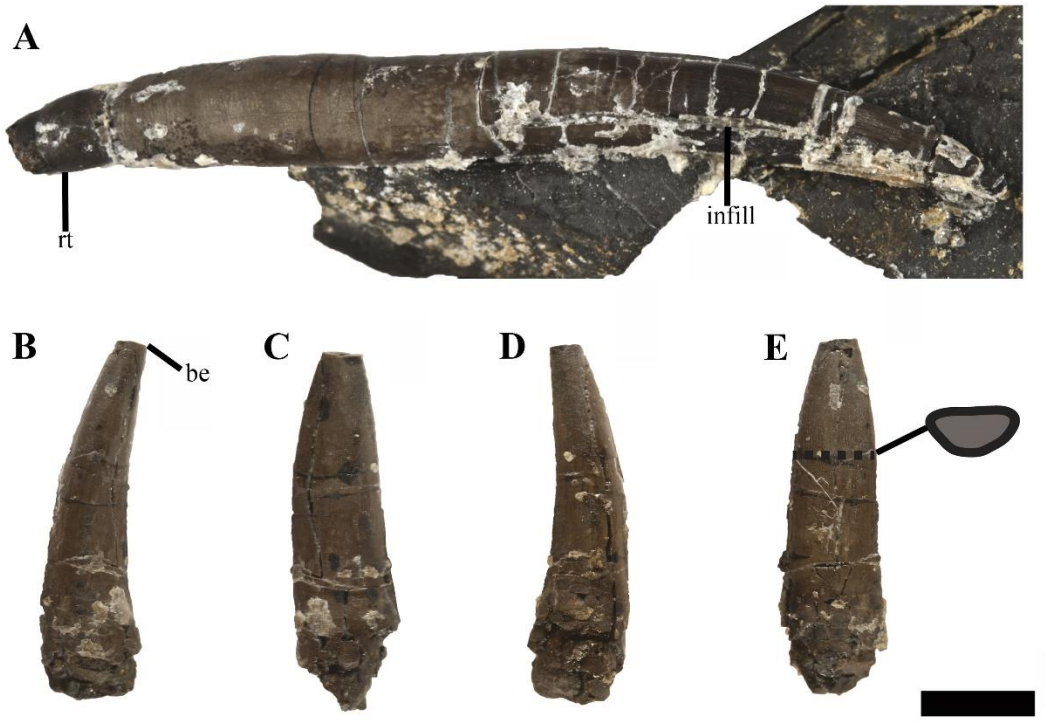

Figure 3.11: Isolated teeth from PMO 224.248. **A**, the most complete tooth in axial view; **B-E**, an incomplete tooth **in B, D** axial, **C**, lingual and **E**, labial views with a cross section of the tooth. **Abbreviations: be**, broken edge; **rt**, root tip. Scale bar equals 0.5 cm.

Axial skeleton

Fifty cervical vertebrae are preserved in PMO 224.248, including the atlas-axis complex. This is greater than the Callovian cryptoclidids; *Cryptoclidus eurymerus* (32; Brown, 1981) and *Muraenosaurus leedsii* (44; Brown, 1981) and some Tithonian – Early Cretaceous taxa; *Colymbosaurus megadeirus* (41; Benson and Bowdler, 2014), *Abyssosaurus* (44-51?; Berezin, 2011a), *Djupedalia engeri* (>40; Knutsen et al. 2012X). PMO 224.248 preserves fewer cervical vertebrae than that described in *Spitrasaurus wensaasi* (60; Knutsen et al., 2012d), In total, the neck of PMO 224.248 is estimated to be ~2 m in length including the preserved intervertebral spacing prior to preparation. Selected measurements from the axial skeleton can be found in Appendix 6, Table A6.2.

Atlas-axis—Reflecting the advanced ontogenetic status of PMO 224.248, the atlas-axis complex is completely fused, however part of the suture between the atlas and axis centrum are visible. The complex is approximately twice as

anteroposteriorly long as mediolaterally wide, whereas in *Spitrasaurus larseni* and *Colymbosaurus megadeirus*, the complex is only slightly anteroposteriorly longer than wide (Benson and Bowdler, 2014; Knutsen et al., 2012d). The long and narrow morphology of the atlas-axis in PMO 224.248 is more similar to that of *Muraenosaurus leedsii* and some elasmosaurids, such as *Aristonectes parvidens* (Andrews, 1910; Brown, 1981; Gasparini et al., 2003).

In anterior view, the atlantal cup is concave and subcircular in outline. No suture is visible to confirm atlantal centrum (odontoid) participation in the ventral portion of the atlantal cup, a feature common in cryptoclidids, including C*olymbosaurus megadeirus* and *Spitrasaurus* (Benson and Bowdler, 2014; Knutsen et al., 2012d). Ventrally, the atlantal intercentrum forms a low anteroventrally directed hypophyseal eminence, similar to *C. megadeirus*, *Spitrasaurus* and *Abyssosaurus nataliae* (Benson and Bowdler, 2014; Berezin, 2011a; Knutsen et al., 2012d), that is positioned in the anterior half of the element, although this is positioned more centrally in *C. megadeirus* (Benson and Bowdler, 2014). This morphology differs from the ventral keel formed by the ventral surface of the atlas present in the Oxford Clay Formation cryptoclidids and elasmosaurids (Andrews, 1910; Gasparini et al., 2003).

As in most cryptoclidids (exception, *Colymbosaurus megadeirus*) an atlantal rib is present and is set posteriorly on the atlas centrum (Benson and Bowdler, 2014). The axial rib is single-headed and occupies most of the ventrolateral length of the axial centrum, where it is fused. This differs from *C. megadeirus*, where the axial rib is borne partly on the posterolateral portion of the atlantal centrum (Benson & Bowdler, 2014). The ventral surface of the axis is generally concave, with a rounded, low and anteroposteriorly orientated ridge running from the anterior edge of the axis. The neural arch of the atlas-axis complex is fused and bears a dorsoventrally short, but anteroposteriorly elongate neural spine.

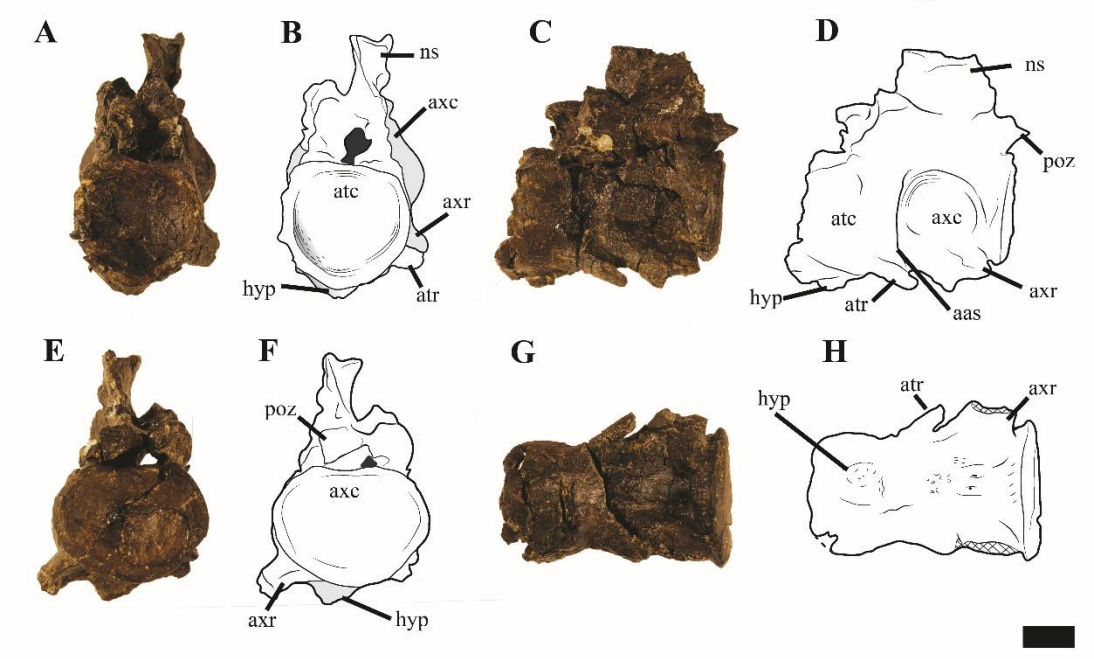

Figure 3.12: Photos and interpretations of the atlas-axis complex of PMO 224.268. In **A-B**, anterior, **C-D** lateral, **E-F** posterior and **G-H**, ventral views. **Abbreviations: aas**, atlas-axis suture; **atc**, atlas centrum; **atr**, atlantal rib; **axc**, axial centrum; **axr**, axial rib; **hyp**, hypophyseal ridge; **ns**, neural spine; **poz**, postzygapophysis. Scale bar equals 1 cm.

Cervical vertebrae (3-50)—The articular surfaces of the centra are weakly amphicoelous, although not to the degree of concavity observed in *Kimmerosaurus langhami* (Brown et al., 1986). The anterior cervical vertebrae are mediolaterally wider than anteroposteriorly long (Appendix 6, Table A6.2). This relationship shifts gradually in the mid-cervical region as, the length to width ratio steadily decreases posteriorly. The posterior cervical vertebrae (~35 – 50) are mediolaterally wider than anteroposteriorly long, unlike the more equal dimensions seen in *Cryptoclidus eurymerus* (Andrews, 1910) and a partial cryptoclidid specimen from Greenland (MGUH 28378; Smith, 2007).

The lateral surfaces of the anterior centra are conspicuously concave, becoming more convex posteriorly in the series (Figure 3.13). A structure that could represent a weak lateral ridge is present in some of the mid-posterior cervical vertebrae in PMO 224.248 and is visible in the 32nd to the 38th cervical vertebra (Figure 3.14). This should not be confused with the raised convex dorsal margin of the rib facet. This transverse ridge crosses the lateral surface of the centrum,

positioned in between the neural ach pedicles and rib facet. A lateral ridge may have been present in more anterior/posterior vertebrae, but cannot be unambiguously identified due to the preservation. In *Spitrasaurus*, a lateral ridge is present throughout most of the cervical series, located dorsal to the cervical rib facet (Knutsen et al. 2012d). The ventral surface of the anterior – middle cervical vertebrae bear paired foramina separated by a sharp ridge in the anterior cervicals, which disappears posteriorly in the series. The presence of a ventral ridge is shared with some cryptoclidids (e.g. *Tricleidus seeleyi*; Andrews, 1910), but is completely absent in *Colymbosaurus megadeirus* (Benson and Bowdler, 2014).

In dorsal view, the prezygapophyses are mediolaterally narrower than the width of the centrum and positioned directly above the centrum, similar to *C. megadeirus*, *Abyssosaurus nataliae* and *Djupedalia engeri* (Benson and Bowdler, 2014; Berezin, 2011a; Knutsen et al., 2012a). Similar to *Kimmerosaurus langhami* (Brown et al., 1986), in the anterior-most cervicals (3^{rd}-6^{th}) of PMO 224.248, the prezygapophyses are separate along their entire length. However, in the following cervicals the prezygapophyses partially fuse medially along the anteroventral margin and from around the 15^{th} cervical the prezygapophyses are completely medially fused. This morphology differs from *Spitrasaurus* spp. and *Djupedalia engeri*, where the prezygapophyses are either partially or completely ventrally fused throughout the entire neck (Knutsen et al., 2012a, d). In *Cryptoclidus eurymerus* the prezygapophyses remain unfused (Andrews, 1910; Brown, 1981). As in *Spitrasaurus*, the postzygapophyses are fused throughout the entire cervical series and extend posterior to the posterior margin of the centrum. In PMO 224.248, the length of the postzygapophyses varies throughout the series and in some regions significant posterior elongation is preserved: on the 8^{th} cervical, the postzygapophysis length approaches the anterior-posterior length of the entire centrum (Figure A6.6). When articulated with the 9^{th} cervical, there is a larger intervertebral space in between the two centra, than in preceding and following cervical vertebrae. Based on studies of sauropod dinosaurs, this could represent an area of more flexibility in the neck (Taylor and Wedel, 2013; see Discussion).

The neural spines in the anterior-most cervical vertebrae are low (3-10), anteroposteriorly extended and angled posteriorly, positioned over the postzygapophyses. Where the neural spine is completely preserved, the dorsal

margin is slightly rounded. This morphology differs from the relatively straight, tall and dorsally flattened margins of the neural spines of the anterior-most cervical vertebrae in *Kimmerosaurus langhami*, *Spitrasaurus* and *Djupedalia engeri* (Brown et al., 1986; Knutsen et al. 2012 a, d). In the 7th cervical, the neural spine is less than half the dorsoventral height of the centrum, when measured from the top of the postzygapophyses. The anterior – mid cervical (10-18) neural spines are posteriorly shifted; so the middle of the dorsal margin of neural spine is positioned directly over the posterior margin of the centrum (Figure 3.13F). In lateral view the neural spines are triangular to trapezoid in outline, becoming more rectangular posteriorly and increase in height. The neural spines on the posterior cervicals are anteroposteriorly long, dorsally flattened and more centred over the centrum. Although positioned more centrally, the posterior margin of the neural spine still reaches the anterior half of the next centrum due to the anteroposterior length of the neural spine (Figure 3.14). Some of the mid and the posterior cervicals show a mild anterior inclination of the neural spine. This morphology is comparable to that seen in *Spitrasaurus wensaasi* and "*Picrocleidus*" *beloclis*, however the neural spines of PMO 224.248 do not consistently angle anteriorly as in *Spitrasaurus* spp. (Knutsen et al. 2012d). The neural canal is oval in anterior view.

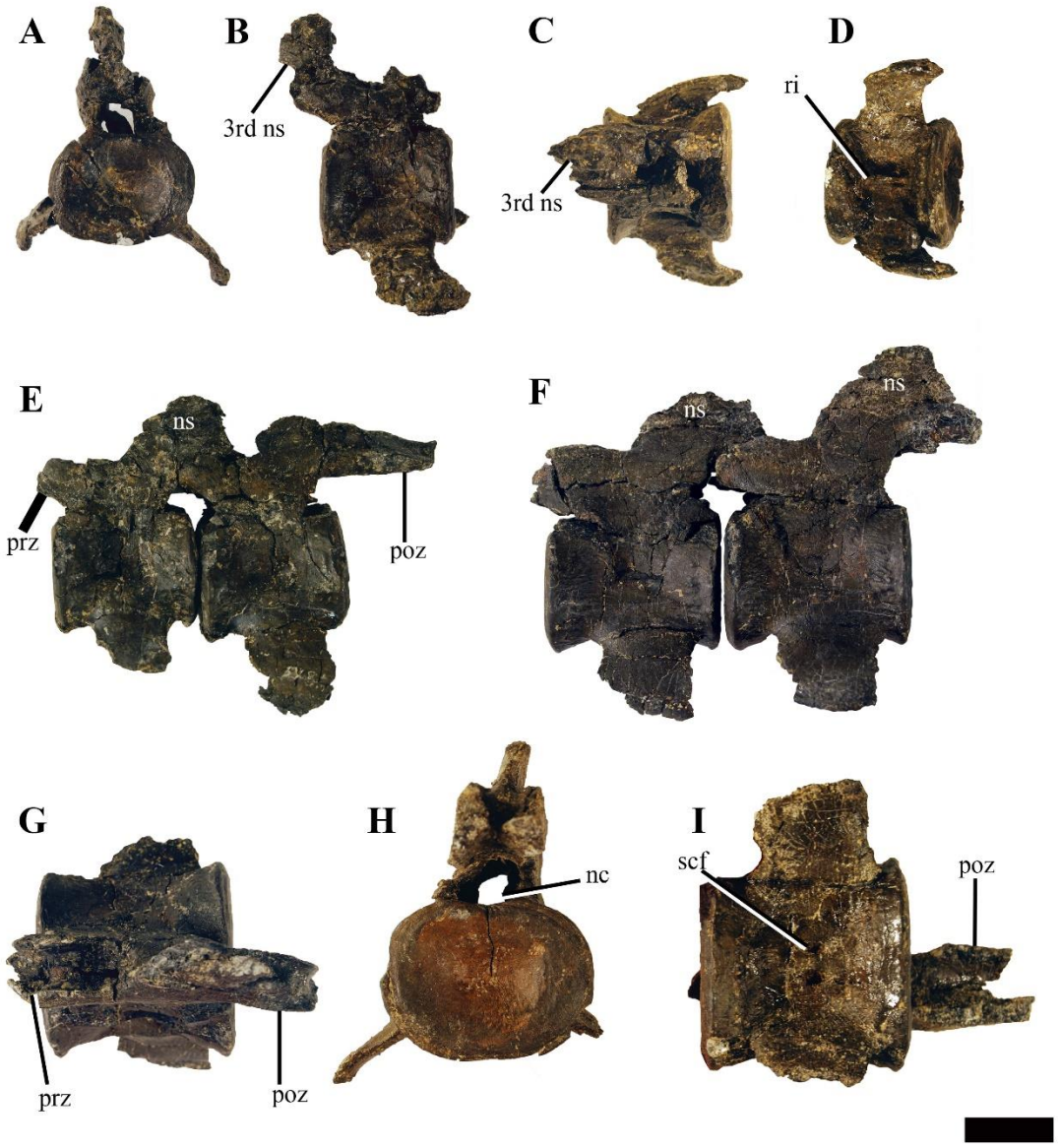

Figure 3.13: Selected anterior – mid cervical vertebrae of PMO 224.248. The 4th cervical vertebrae in **A**, anterior; **B**, lateral; **C**, dorsal and **D**, ventral views. **E**, the 7th and 8th articulated cervical vertebrae in lateral view. **F**, the articulated 14th and 15th cervical vertebrae in lateral view. **G**, the 15th cervical in dorsal view. The 17th vertebrae in **H**, anterior and **I**, ventral views. **Abbreviations: 3rd ns**, neural spine from the 3rd cervical vertebrae; **nc**, neural canal; **ns**, neural spine; **poz**, postzygapophyses, **prz**, prezygapophyses, **ri**, ventral ridge; **scf**, subcentral foramina. Scale bar equals 2 cm.

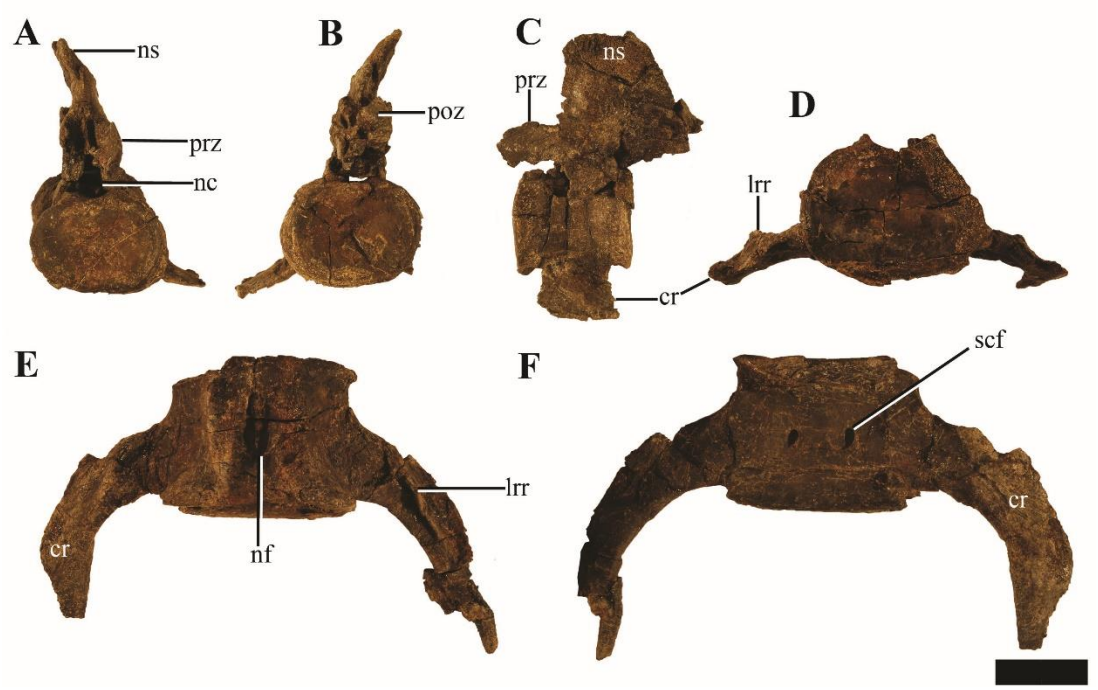

Figure 3.14: Two posterior cervical vertebrae from PMO 224.248. The 29th cervical vertebra in **A**, anterior; **B**, posterior and **C**, lateral views. The 44th cervical vertebra in **D**, anterior; **E**, dorsal and **F**, ventral views. **Abbreviations: cr**, cervical rib; **lrr**, longitudinal rib ridge; **nc**, neural canal; **nf**, nutritive foramina; **ns**, neural spine; **poz**, postzygapophyses; **prz**, prezygapophyses; **scf**, subcentral foramina. Scale bar equals 4 cm.

Cervical ribs—The cervical rib facets receive single-headed ribs, which are fused to the centrum throughout the entire series (Figures 3.13-14). In the anterior cervicals, the cervical ribs are relatively short, hatchet-shaped, due to a small anterior process and terminate laterally in a posterodistal point. In the mid-cervical vertebrae, the anterior process is further reduced, gradually increasing in prominence in the posterior cervicals. This differs from *Djupedalia engeri*, where the anterior process on the cervical ribs is clearly present in the entire cervical series (Knutsen et al., 2012a). In the mid-cervicals, the ribs are distally short and lack anterior/posterior curvature. From the 40th cervical, the ribs start to elongate exceeding the length of the centrum. Similar to *Djupedalia engeri*, the posterior cervical ribs become anteroposteriorly narrower and curve posteriorly (Knutsen et al. 2012a). This morphology differs from MGUH 28378 (*Cryptoclididae* indet.), where the posterior cervical ribs are straight and to *Spitrasaurus wensaasi*, where they are only slightly posteriorly curved (Knutsen et al., 2012d; Smith, 2007). From the 44th cervical and

posteriorly, the cervical ribs bear a longitudinal dorsally positioned ridge, starting from the proximal head and terminating around the midpoint of the rib shaft, an autapomorphy of this taxon. This longitudinal ridge is also present on the pectoral and anterior dorsal ribs and could represents a muscle attachment (Noè et al., 2017).

Pectoral vertebrae—At least two pectoral vertebrae (Figure 3.15 A – F) can be unambiguously identified (*sensu* Sachs et al., 2013), with the possibility of a third (Figure 3.15G). As in *Colymbosaurus megadeirus* (Benson and Bowdler, 2014), the centra are significantly mediolaterally wider than dorsoventrally tall in anterior view (Appendix 6, Table A6.2), although this may be partially due to taphonomic compression. As in *Cryptoclidus eurymerus*, pectoral vertebrae 1 and 2 have clear circular rib facets and the subcentral foramina are widely spaced compared to the cervicals (Brown, 1981). The neural arch is poorly preserved and cannot be described in detail. A third poorly preserved vertebra could represent the third pectoral (Figure 3.15G). This element was slightly disarticulated posteriorly from the two pectorals and located just posterior to the medial symphysis of the scapula during preparation. The neural arch and centrum contribute to the dorsoventrally tall and laterally extended rib facet, which almost forms a transverse process on the right side. This rib facet morphology is also present in the pectoral and sacral vertebrae of *Colymbosaurus megadeirus* (CAMSM J.29640; Benson and Bowdler, 2014). As such the location and similar morphology to other posterior pectorals in *Colymbosaurus*, supports the argument that this element can be identified as the third pectoral vertebrae.

Several pectoral ribs are preserved, either in articulation with or adjacent to the pectoral vertebrae. These share the same morphology as the posterior cervical ribs, but are more distally extended.

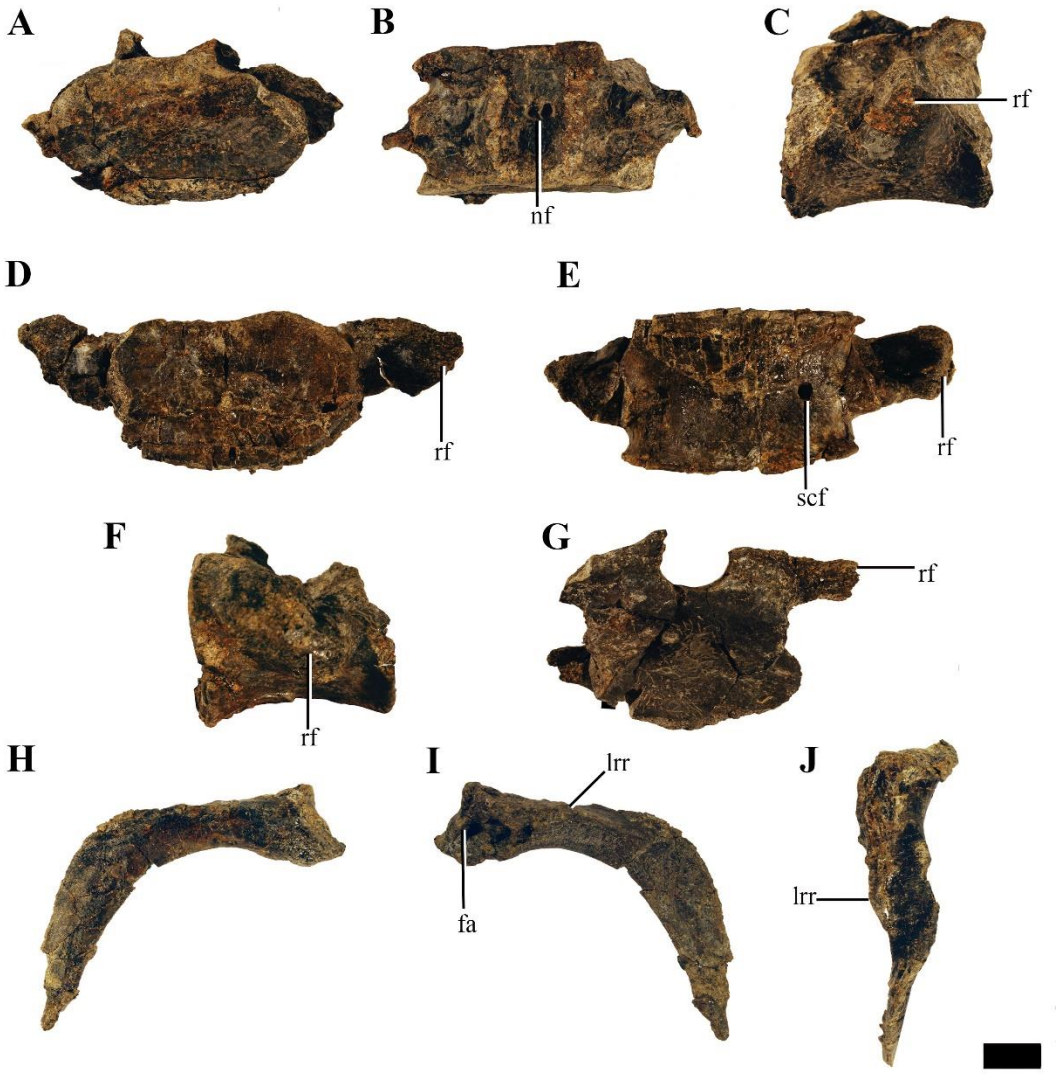

Figure 3.15: Pectoral vertebrae and pectoral ribs of PMO 224.248. The 1st pectoral in **A**, anterior; **B**, dorsal and **C**, lateral views. The 2nd pectoral in **D**, anterior, **E**, ventral and **F**, lateral views. **G**, the 3rd pectoral vertebrae in posterior view. The 1st pectoral rib in **H**, anterior; **I**, posterior and **J**, dorsal views. **Abbreviations: fa**, facet for the pectoral rib; **lrr**, longitudinal rib ridge; **nf**, nutritive foramina; **rf**, rib facet; **scf**, subcentral foramen. Scale equals 2 cm.

Dorsal vertebrae—Ten dorsal vertebrae are preserved, however the posterior-most of these are poorly preserved and some are fused together by diagenesis (Figure 3.16). The dorsal vertebrae are mediolaterally narrower than the posterior-cervical and pectoral vertebrae but not to the degree as in *Spitrasaurus wensaasi* (Knutsen et al., 2012d). The neural arches are crushed and the transverse processes flattened; however taking into account the shape of the dorsal rib heads

and deformation of the transverse process, the rib facets are dorsoventrally taller than wide, being oval in outline as in *Spitrasaurus wensaasi* (Knutsen et al., 2012d). This contrasts to the more circular dorsal rib facets described in *Tatenectes* and most Oxford Clay Formation cryptoclidids (Andrews, 1910; O'Keefe et al., 2011). The anterior dorsal centra preserve either singular or paired subcentral foramina on the ventrolateral surface.

Figure 3.16: Dorsal vertebrae and ribs of PMO 224.248. The 1st dorsal vertebrae in **A**, anterior and **B**, ventral views. The 2nd dorsal vertebrae in **C**, anterior; **D**, lateral and **E**, ventral views. The 3rd dorsal vertebrae in **F**, anterior and **G**, ventral views. Scale equals 2 cm. **H**, a right anterior dorsal rib head in proximal view. **I**, a complete rib in anterior view. **Abbreviations: ph**, proximal head; **lrr**, longitudinal rib ridge; **scf**, subcentral foramina; **tp**, transverse process. Scale equals 5 cm.

Dorsal ribs—The majority of the dorsal ribs are incomplete due to erosion of the exposed fossil. Two ribs remain complete, but somewhat crushed; an anterior- (Figure 3.16I) and a mid-dorsal rib. The rib heads are robust and single headed with an oblong ovoid facet (Figure 3.16H), being dorsoventrally taller than anteroposteriorly wide as in *Colymbosaurus megadeirus* (Benson and Bowdler, 2014) and a specimen referable to *Muraenosaurus* (NHMUK R.2427). The mid-dorsal rib was in partial-articulation with the 5th dorsal vertebrae and measures to be 66.5 cm in actual length. This rib is curved along the proximal half of the shaft and then straightens out towards the expanded distal end. On the proximal end, a ridge is present on the posterolateral margin. The cross section is subcircular in shape along most of the shaft, but increases in mediolateral width proximally. A groove is present on the posterior surface of the proximal and distal regions of the rib. On the anterior dorsal ribs a longitudinal ridge is present, as described for the posterior cervical- and pectoral ribs.

Gastralia—The gastral basket of PMO 214.248 is well-preserved, with at least ten sets of gastralia identified. These form a tight gastral basket, where the first set butts against the posterior margin of the coracoid. Each set contains a medial gastralium, which in turn articulates with 2-3 lateral gastralia on either side. Some of the gastralia are partly fused, which attribute to the sideritic cement (possibly gut content, see discussion) covering the dorsal surface.

Appendicular skeleton

Clavicle and interclavicle—Two clavicles and an interclavicle are preserved in articulation with the scapula. Due to the hard matrix in this region, it was not possibly to separate the elements from the scapula and overlying vertebrae. The clavicles (dorsal to interclavicles) are only visible in cross section, are dorsoventrally thin and are reduced in comparison to the interclavicle, as in *Muraenosaurus leedsii* (Andrews, 1910; Brown, 1981). The interclavicle forms the anterior-most margin of the pectoral girdle along the midline, resembling the triangular element present in *Muraenosaurus leedsii* (Andrews, 1910; Brown, 1981).

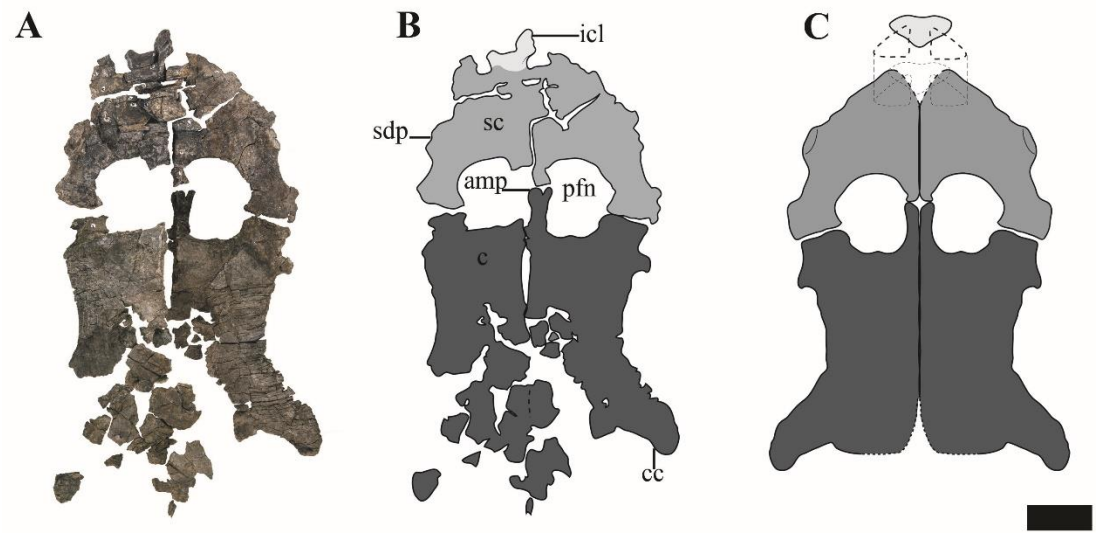

Figure 3.17: The pectoral girdle of PMO 224.248. **A**, the complete pectoral girdle; **B**, interpretation and **C**, reconstruction. Abbreviations: **amp**, anteromedial process of the coracoid; **c**, coracoid; **cc**, coracoid cornu; **icl**, interclavicle; **pfn**, pectoral fenestra; **sc**, scapula. Scale equals 5 cm.

Scapula—The scapulae of PMO 224.248 are preserved in articulation with the rest of the pectoral elements and humeri (Figure 3.17). Selected measurements of these elements can be found in Appendix 6, Table A6.3. The anterior and medial margins of the scapulae are difficult to interpret, due to poor preservation and crushing by overlying elements (clavicles, interclavicle). As in all adult cryptoclidids with the exception of *Abyssosaurus nataliae*, the scapulae meet ventromedially along most of the medial margin to the posteromedial process, forming a dorsoventrally thickened symphysis (Andrews, 1910; Berezin, 2011a; O'Keefe and Street, 2009). The posteromedial process of the scapula contacts the anteromedial process of the coracoid along an ovate facet, producing a complete pectoral bar.

PMO 224.284 bears a short and broad dorsal process, in contrast to cryptoclidids from the Oxford Clay, where the extension of the dorsal process can exceed half the total anteroposterior length of the element (Andrews, 1910). This morphology also differs from *Abyssosaurus nataliae* and *Djupedalia engeri*, where the dorsal process forms a large part of the anterior portion of the element, being both anteroposteriorly extensive and dorsally extended (Berezin, 2011a; Knutsen et al., 2012a). The glenoid region is dorsoventrally thickened in comparison to the rest of the element and bears a facet for the glenoid and coracoid that are subequal in

length, similar to that observed in *Abyssosaurus nataliae* (Berezin, 2011a), but differing from that seen *Cryptoclidus eurymerus* and *Djupedalia engeri*, where the coracoid facet is the larger of the two facets (Andrews, 1910; Knutsen et al., 2012a) and to *Spitrasaurus wensaasi* where the coracoid facet is significantly smaller (Knutsen et al., 2012d) . In PMO 224.248, the glenoid facet is deeply concave, whereas the coracoid facet is nearly flat, but rugose.

Coracoid—Both coracoids were articulated, although somewhat fragmented posteriorly and medially. The coracoids bear a large anteromedial process, which has a slight bifurcation anteriorly, extending further anteriorly than the scapular facet. The anteromedial process forms most of the medial margin of the ovate pectoral fenestrae are, differing from *Colymbosaurus megadeirus* and *Abyssosaurus nataliae* where this margin is mainly formed by the scapula (Benson and Bowdler, 2014; Berezin, 2011a) and *Tatenectes laramiensis* where both contribute equally (O'Keefe and Street, 2009). The anterior portion of the medial symphysis is dorsoventrally thickened in comparison to the rest of the element, creating a shelf along the anterior margin (posterior from the pectoral fenestra), as in most derived plesiosauroids (Benson and Bowdler, 2014). The ventrally projecting medial symphysis of the coracoids in PMO 224.248 articulate along the medial symphysis so that the ventral margins, form an angle close to 180°. In anterior view the dorsal margins are nearly uniform. The almost uniform dorsal surface in PMO 224.248, could be due to taphonomic dorsoventral compression. This morphology is similar, although less angled than the more dorsolaterally orientated coracoids of *Cryptoclidus eurymerus* (Andrews, 1910; AJR *pers. obs.* NHMUK R2616) and *Colymbosaurus megadeirus* (Benson and Bowdler, 2014; Roberts et al., 2017). The medial symphysis continues posteriorly throughout the preserved medial margin of the coracoid. The lateral margin of the coracoid is concave and terminates posterolaterally in a distinct posteriorly curved cornu, which just exceeds the lateral margin of the glenoid in the parasagittal plane. The posterior margin is concave and a groove is present medial to the cornu, possibly to articulate with the anterior gastralia.

Humerus—Both humeri are predominantly uncrushed and well-preserved, except for the tuberosity which is crushed on both (See Appendix 6, Table A6.5 for measurements). In dorsal view, the proximal portion of the humerus is angled slightly anteriorly, resulting in a sigmoidal shape in dorsal view similar to some

leptoclidids and polycotylids (Hampe, 2013). Ventrally, a prominent rugosity is present near the proximal end, forming the dorsoventrally thickest point of the humerus (Figure 3.18). As in *Djupedalia engeri*, the anteroposterior shortest point is just proximal to the ventral rugosity, after which the humeral shaft gradually distally expands in anteroposterior width (Knutsen et al., 2012a). This morphology differs from the more distally constricted morphology observed in *Spitrasaurus*, *Muraenosaurus leedsii*, *Tricleidus seeleyi*, *Pantosaurus striatus* and *Cryptoclidus eurymerus*, where the shaft is anteroposteriorly shortest towards the midshaft and anteroposteriorly expanded at the proximal and distal ends (Andrews, 1910; Benson and Bowdler, 2014; Brown, 1981; Knutsen et al., 2012d; O'Keefe and Wahl, 2003b). Posteriorly, there are at least three nutritive foramina perforating the posterior surface near the mid-point of the shaft, an uncommon trait in cryptoclidids, but it is also observed in *Spitrasaurus wensaasi* (Knutsen et al., 2012d).

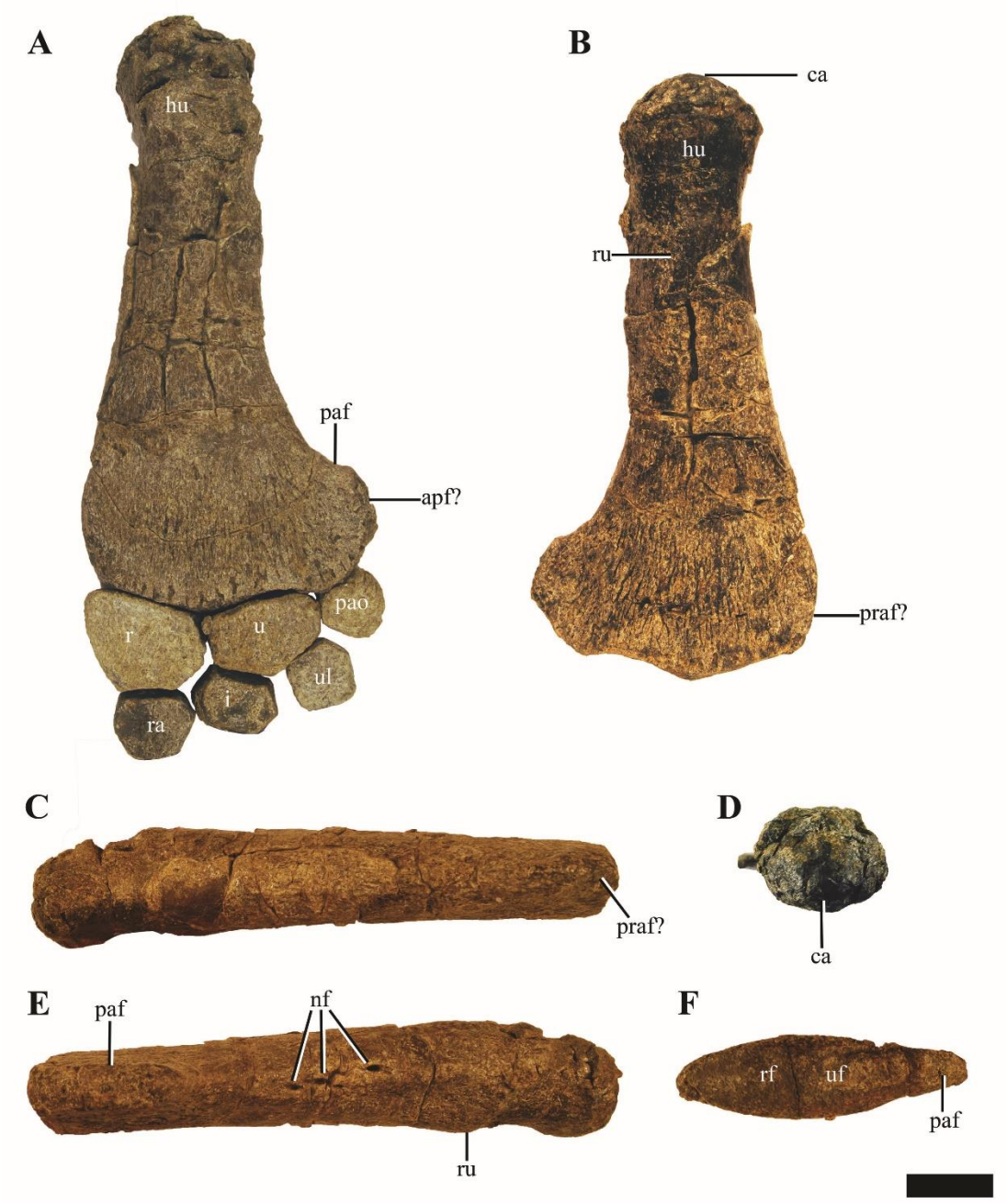

Figure 3.18: The left humerus and proximal limb elements of PMO 224.248. **A**, the left forelimb with the proximal elements articulated in dorsal view. The left humerus in **B**, ventral; **C**, anterior; **D**, proximal; **E**, posterior and **F**, distal views. **Abbreviations; apf**, additional postaxial facet; **ca**, capitilum; **hu**, humerus; **i**, intermedium; **nf**, nutritive foramina, **paf**, postaxial flange; **pao**, postaxial ossicle; **praf**, preaxial facet; **r**, radius; **ra**, radiale; **rf**, radius facet; **ru**, rugosity; **u**, ulna; **uf**, ulna facet; **ul**, ulnare. Scale bar equals 5 cm.

Distally, there is little to no preaxial expansion. A large, posteriorly expanded postaxial flange is present, although not to the same degree as seen in

Colymbosaurus svalbardensis (Knutsen et al., 2012c; Roberts et al., 2017). PMO 214.248 lacks an anteroposteriorly oriented bisecting ridge on the distal epipodial facets, as observed in some specimens of *Colymbosaurus megadeirus* (Benson and Bowdler, 2014). The distal articular end of the humerus bears three conspicuous convex facets for; the radius, ulna and a postaxial accessory element. Along the anterior margin, a rugosity is present, possibly representing a facet for a preaxial accessory element found in articulation on one of the limbs (Appendix 6, Figure A6.7). The postaxial flange has at least one facet angled posterodistally, although a secondary postaxial facet could be present directly posteriorly. Whether this posterior-most facet is an actual facet or for connective tissue attachment is equivocal, as no element was found in articulation with this facet. The distal facet morphology in PMO 224.248 differs from the two distal facets seen in *Muraenosaurus leedsii* and *Tricleidus seeleyi* (Andrews, 1910), the three seen in *Colymbosaurus* (a single postaxial ossicle facet; Roberts et al., 2017) and the four seen in '*Plesiosaurus*' *mansellii* (two postaxial facets; Hulke, 1870).

Epipodials and mesopodials—The radius, ulna and postaxial ossicle element are diagenetically fused to each other, as is the radius partially to the humerus. In addition, the right forelimb preserves an *in situ* oval preaxial element found adjacent to the preaxial facet (Appendix 6, Figure A6.8). In proximal view, there is a shallow groove present on the radius and ulna for articulation with the convex distal margin of the humerus. An epipodial foramen (*spatium interosseum*) is absent, unlike in the Oxford Clay Formation cryptoclidids, with advanced ossification ("old" adults) in *Cryptoclidus eurymerus* (Andrews, 1910; Brown, 1981).

The radius is the largest of the epipodial elements, being slightly anteroposteriorly wider and proximodistally longer than the ulna. This differs from *Colymbosaurus svalbardensis*, where the radius is proximodistally longer, but anteroposteriorly shorter than the ulna (Roberts et al., 2017) and *Spitrasaurus spp.*, *Djupedalia engeri* and *Pantosaurus striatus*, where the radius is at least twice the size of the ulna in all dimensions (Knutsen et al. 2012 a, d; O'Keefe and Wahl, 2003b). In dorsal view, the outline of the radius has a convex anterior margin which slopes posterodistally, resembling that of *Spitrasaurus larseni* (Knutsen et al., 2012d). In proximal view the radius is dorsoventrally thickest posteriorly and

thinnest along its anterior margin. The radius has four dorsoventrally thick facets for the humerus, ulna, intermedium, radiale and an anterior facet for a preaxial ossicle (Appendix 6, Figure A6.9). The facet for a preaxial accessory element is shared on between the radius and radiale anterior margins, as described for *Spitrasaurus larseni* (Knutsen et al., 2012d). Two small elements, although disarticulated adjacent to the right forelimb along the preaxial margin, could represent part of an anterior accessory row (Appendix 6. Figure A6.8).

The ulna is anteroposteriorly wider than proximodistally long, although significantly less than the extremely anteroposteriorly elongated ulna observed in *Colymbosaurus svalbardensis* (Roberts et al., 2017). As in *Pantosaurus striatus* (O'Keefe and Wahl, 2003b), the ulna of PMO 224.248 has five facets; with the largest facet for the humerus, two smaller anterior and posterior elements for the radius and postaxial ossicle respectively, and two distal facets of subequal size for the intermedium and ulnare.

The postaxial ossicle has three facets for the humerus, ulna and ulnare, and is convex along its posterior margin. As the postaxial element was fused to the ulna, it is possible to reconstruct its position relative to the humerus accurately. Based on this interpretation, the preserved postaxial element, occupies only a small portion of the postaxial margin of the humerus. This is somewhat different from "*Plesiosaurus" mansellii*, where the postaxial elements occupy the entire distal postaxial margin (Hulke, 1870).

The mesopodial elements were partially articulated and identified either by their position relative to the epipodial elements or their morphology. In both forelimbs all the mesopodial elements are preserved and their small size suggests the presence of significant connective tissue during life. The radiale is the largest of the three and bears five facets; the largest for the radius, the smallest for the intermedium, two facets for the 1st and 2nd distal carpal and a facet along the anteroproximal margin for a preaxial ossicle. The intermedium bears six facets: two proximal facets for the radius and a longer facet the ulna and three smaller facets for the ulnare, 3rd distal carpal and radiale. The ulnare is bears five facets: two proximal subequal facets for the ulna and postaxial ossicle and three subequal facets for the intermedium, 3rd carpal and 2nd post axial element.

Metacarpals and phalanges—The metacarpals were disarticulated; the distal carpals are small and their articulation to the rest of the limb uncertain. Two of the carpals are proximodistally reduced and rounded in dorsal outline. This morphology differs from the more elongated and angular distal carpals seen in most cryptoclidids (*Colymbosaurus svalbardensis*, *Cryptoclidus eurymerus*, *Muraenosaurus leedsii*, *Tricleidus seeleyi*; Andrews, 1910; Brown, 1981; Roberts et al., 2017). A possible 5th metacarpal was identified based on the unusual morphology of the element, and on its proximal position and articulating elements. This element seems to be nearly entirely shifted into the distal carpal row.

Twenty-nine phalanges/metacarpals are preserved in the right forelimb and twenty-two phalanges/metacarpals are present in the left forelimb. Many of these were removed during excavation, although their location was noted. The proximal phalanges are hourglass-shaped, with flat articular surfaces, whereas the more distal phalanges of the 2nd or 3rd dactyl row, are proximodistally shorter and more compact, similar to that observed in *Colymbosaurus svalbardensis* (Roberts et al., 2017).

Femora—Fragments of the femora from PMO 224.248, were located downslope from the skeleton. These consist of fragments of distal, mid-shaft and proximal sections. The femur sections where identified based on the amount of weathering, as the left limb was partly preserved with the rest of the body and thereby less weathered. The partial femur interpreted as the left, consists of a distal end, shaft fragments and part of the proximal end (Appendix 6, Figure A6.10). The bone texture and shape suggest that the femur had a postaxial flange, which is not preserved. On the distal fragment of the left femur, part of the distal surface is preserved. This is smooth and slightly convex. When comparing the femoral sections to the complete humeri in PMO 224.248, it is clear that the femora were smaller than the humeri based on anteroposterior length of the proximal and distal ends, as well as the shaft cross section.

Hind limb elements—Distal elements from the left hind limb was preserved in PMO 224.248 and are partially articulated although heavily weathered (Appendix 6, Figure A6.11). The meso- and metatarsals are present, in addition to several phalanges. Five mesopodial elements are preserved in left hind limb, representing

the fibulare, astragalus, tibiale and the two distal tarsal elements. The 5th metatarsal appears to be entirely shifted into the distal tarsal row. Several complete and partial phalanges are preserved. As seen in *Colymbosaurus*, the largest element in dorsal view of the mesopodial elements is the fibulare (Knutsen et al., 2012c; Roberts et al., 2017). The fibulare has six facets, with the largest being for the fibula. Along the posterior margin of the fibula there are two facets, one proximally for the postaxial ossicle and another distally possibly for a second ossicle. The astragalus is oval in outline, but bears a proximal convexity, to separate the facets for the fibula and tibia. The element is dorsoventrally thicker than proximodistally long (excluding the proximal surface convexity). The tibiale is the smallest of the three elements and bears five facets: a proximal facet for the tibia, two short proximal facets for the astragalus and second distal tarsal, a long distal facet for the first distal tarsal and a short anterior facet, possibly for a preaxial row. The distal lengths of the tibia and fibula can be estimated, based on the close articulation between the tibiale, astragalus and fibula. This suggests that at least, the distal anteroposterior extent of the fibula, appears to be longer than that of the tibia. Four metatarsals are preserved; the second, third, fourth and possibly the fifth. As in most cryptoclidids, the forth metatarsal is the largest (Knutsen et al., 2012c).

Discussion

Phylogenetic implications and the interrelationships of cryptoclidids

PMO 224.248 was scored into the data matrix of Roberts et al., (2017), edited from Benson and Druckenmiller (2014). Three new characters were added, totalling in a matrix including 273 unordered morphological characters and 76 OTUs. Additional modifications to the character states of individual cryptoclidid taxa are available in Appendix 5. The three new characters (Characters 271-273) were created on the basis of variation in some features in Cryptoclididae and describe two cranial and one post-cranial feature (discussed more fully below). Information on how to recognise the individual character states for these new characters are available in Appendix 5.

Character 271: Frontal, inter-frontal vacuity—frontals are loosely connected along the midline (0); frontals are partially separated along the midline by an

interfrontal vacuity (1). Absent, frontals split entirely or partially by posterior process of the premaxilla or completely fused (?).

Character 272: Dentary, mediolateral expansion of the dorsal surface—No mediolateral expansion (0); a small lateral expansion, often posteriorly; (1) a mediolateral expansion of the dorsal mandibular surface is present, resulting in a laterally shift of the alveoli (2).

Character 273: Morphology of the fibula—Lunate, close to or as proximodistally long as wide and distal facet (0); pentagonal anteroposteriorly wider than long, with equally sized distal facets for fibulare and astragalus (1). Edited from character 92 in (Smith, 2007b).

The analysis was performed in TNT (V.1.5) (Goloboff and Catalano, 2016) using the new technology search (Ratchet), combined with Tree bisection reconnection (TBR). The analysis used 1000 iterations, with 10 random addition sequences and 10 random seed. All trees were kept and auto constrain turned off and all characters were equally weighted. *Yunguisaurus* was defined as the outgroup taxon (Cheng et al., 2006). The bremer function in TNT (V 1.5), was used to calculate bremer supports. The scripts stats.run was used to calculate CI and RI. The complete consensus tree for Plesiosauria is available in Appendix 5, Figure A5.4. Bootstrap resampling (1000 replications), was also performed (Appendix 5, Figure A5.5).

Results of the phylogenetic analysis

The strict consensus tree of 144 MPTs (most parsimonious trees) shows the monophyly of Cryptoclididae is relatively well supported (Figure 3.19) with a decay index of four, as found in Benson and Bowdler (2014).

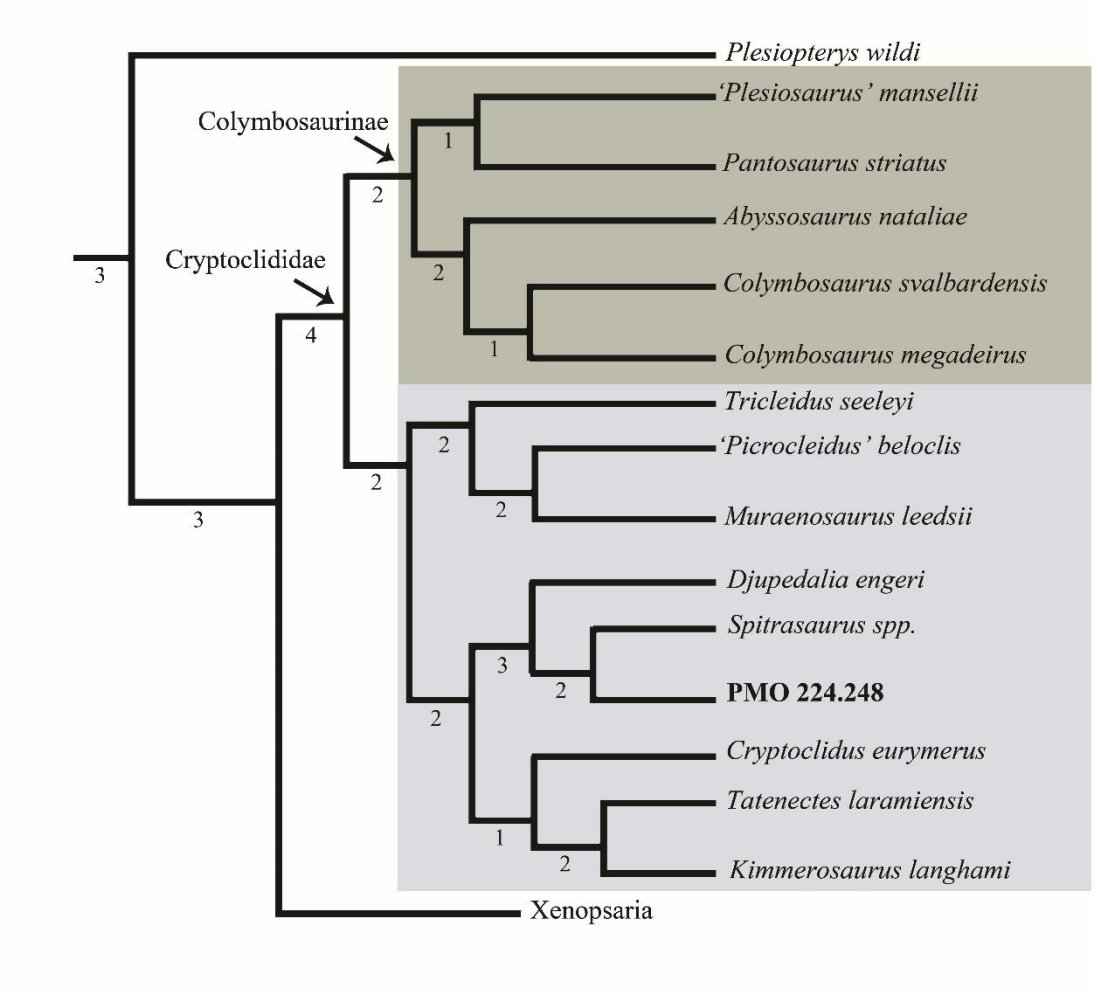

Figure 3.19: Strict consensus tree of 144 MPTs with a tree length of 1318 (CI= 0.300 and RI = 0.664). Bremer support is shown below the clade branches. The complete tree for Plesiosauria is available in Appendix 5, Figure A5.4.

Cryptoclididae is supported by the following seven synapomorphies (character number/state): (144/1) the atlantal centrum participates in the anterior rim of the atlantal cup (state 0 *Tatenectes laramiensis*); 202/0 the anterolateral margin of the scapula is flat/gently convex; (235/1), in the forelimb the digits/tarsal/carpal axis extends posterodistally relative to propodial long axis because proximodistal length of radius/tibia is substantially greater than that of the ulna/fibula; (245/1), the preaxial expansion on the distal margin of the humerus is smaller than the postaxial expansion (2 in *Cryptoclidus eurymerus* and ambiguous between 1&2 in *Spitrasaurus sp.*); (255/3), ratio of tibia length to maximum width is >0.75 (state 1 in *Pantosaurus striatus* and state 2 in *Colymbosaurus megadeirus*); (261/2), an epipodial foramen is absent (state 0 in *Muraenosaurus leedsii*, 1 in '*Picrocleidus'*

beloclis and *Tricleidus seeleyi*, 1&2 in *Cryptoclidus eurymerus* depending on ontogeny, ambiguous in *Abyssosaurus laramiensis*); (262/1), the ratio of maximum radius length to maximum ulna length is between 1.4-1.7 (state 0 in PMO 224.248, state 2 in *Cryptoclidus eurymerus*). All of these synapomorphies are solely postcranial, due to the lack of complete and/or well-preserved cranial material in this clade. The synapomorphies found here are somewhat different to those found in Benson and Bowdler, (2014); where only one of these characters (144) was recovered as a synapomorphy in this analysis. PMO 224.248 can be referred to the family Cryptoclididae on the basis of sharing three of seven synapomorphies (two could not be scored for PMO 224.248).

As found in Benson and Bowdler (2014), Cryptoclididae is split into two subclades, one of which has been formally named as Colymbosaurinae. In Benson and Bowdler (2014), this subfamily includes *Colymbosaurus*, *Spitrasaurus*, *Djupedalia engeri*, *Pantosaurus striatus*, *"Plesiosaurus" mansellii* and *Abyssosaurus nataliae*. As cranial material for these taxa is either limited or unavailable, the synapomorphies include only post-cranial features. This is problematic, as there could be a conflicting signal between cranial and post-cranial characters in the data matrix. PMO 224.248 could be scored for a significant number of cranial and post cranial characters in the matrix and share three of the five Colymbosaurinae synapomorphies described in Benson and Bowdler (2014). The addition of this new taxon to the data set, along with the three new characters, created a new topology for the cryptoclidid clade. Although the two major subclades are still present, the Slottsmøya Member taxa *Spitrasaurus spp.*, *Djupedalia engeri* and PMO 224.248 were removed from the Colymbosaurinae subfamily and placed as a sister group to *Cryptoclidus eurymerus*, *Tatenectes laramiensis* and *Kimmerosaurus langhami*. Although this configuration is supported with higher Bremer support values than those reported in Benson and Bowdler (2014), most of the internal structure of the cryptoclidid tree was not retained after running a resampling bootstrap analysis (see Appendix 5, Figure A5.5). However, this analysis does show that a revision is required of the diagnostic features of Colymbosaurinae in light of the new taxon (PMO 224.248). As a result, four synapomorphies for the reduced Colymbosaurinae clade were recovered: (197/0) the anteromedial margin of the coracoid does not contact the scapula; (209/2), the coracoid anteromedial process

is short and subtriangular; (224/1), the anteroposterior width of the ilium is expanded, between 1.5-2.0 times the minimum anteroposterior width of the shaft and (256/1), the anterior margin of the radius is straight or convex.

Although the precise position of PMO 224.248 as sister taxon to *Spitrasaurus* spp. is weakly supported (Bremer Support =2), the clade incorporating *Djupedalia engeri*, *Spitrasaurus* spp. and PMO 224.248 receives higher support (Bremer Support = 3). This clade is shares three synapomorphies: (152/5) the number of cervicals is between 50-60; (157/2) the anterior cervical neural spines are inflected anterodorsally (ambiguous in PMO 224.248) and (234/1), the presence of preaxial ossicles. The separation of this Slottsmøya Member restricted clade from Colymbosaurinae, shows that at least two separate clades of cryptoclidids were present in the Boreal region during the Late Jurassic – Early Cretaceous.

The effect of the new characters

Interfrontal vacuity—Through examination of cryptoclidid specimens where the dorsal/ventral surface of the frontal is visible, an interfrontal vacuity along the frontal midline is clearly present in several taxa. In *Tricleidus seeleyi* (Appendix 5, Figure A5.1B) and *Kimmerosaurus langhami* the medial margin of the frontal is slightly concave and has finished bone along the entire surface indicating the presence the interfrontal vacuity (AJR *pers. obs*.; NHMUK R3539; NHMUK R.8431). In *Cryptoclidus eurymerus*, the presence of this feature is ambiguous on the neotype (NHMUK R2860). In a referred specimen (PETMG R.283.412; Brown and Cruickshank, 1994), the elements are loosely sutured and a small vacuity could be present. Due to this *C. eurymerus* is scored for states 0 and 1 in the matrix. A similar situation is present in *Tatenectes laramiensis* (UW 24215 being poorly preserved, the medial surface of the frontal in a specimen of *Tatenectes laramiensis* (UW 24215) is smooth, indicating that a vacuity could be present (O'Keefe and Wahl, 2003a). This structure may not be limited to cryptoclidids, as a similar feature is observed in a xenopsarian: the Berriasian taxon *Brancasaurus brancai* preserves a small dorsomedian foramen along the frontal midline anterior to the pineal foramen (Sachs et al., 2016). Due to the ambiguous placement in *T. laramiensis* and *Cryptoclidus*, as well as its presence in a xenopsarian, this character was not recovered as a synapomorphy for Cryptoclididae or subclade. However, if additional

cranial material becomes available for some of these taxa, this character could represent a future cranial synapomorphy for Cryptoclididae, or the currently unnamed subfamily (non-colymbosaurines). However, the interfrontal vacuity found in *B. brancai* requires further study, to identify if this feature is homologous with the interfrontal vacuity found in some cryptoclidids.

Mediolateral expansion of the dentary—A difference in the morphology of the dorsal (tooth bearing) surface of the dentary is observed between some cryptoclidid taxa and other members of Plesiosauria. In Early Jurassic taxa (exception: *Plesiopterys*), pliosauroids and xenopsarians, there is no mediolateral expansion of the dorsal dentary surface: the lateral and medial surfaces are uniform and the alveoli are centred over the mandible. When present a mediolateral expansion, gives the mandible a subtriangular shape in cross section. This feature can be scored as present for the majority of non-colymbosaurine cryptoclidids (exception *Tricleidus seeleyi*). although, in some taxa (*Cryptoclidus*), only a partial lateral expansion of the dentary is present posteriorly, or ambiguous between referred specimens possibly due to preservation (*Kimmerosaurus langhami*). Although, not recovered as a synapomorphy in this analysis, with the addition of new material this feature could represent a synapomorphy for the unnamed subfamily of cryptoclidids (non-colymbosaurines).

Fibula morphology—In previous work, this character has been combined with the character describing radius morphology due to their morphological similarity (Smith, 2007, character 92). However, these are not homologous and should not be combined and differences between the ulna and fibula are evident in some cryptoclidid taxa (e.g. *Colymbosaurus svalbardensis*). In the resulting consensus tree, state (1) of this character was recovered as a synapomorphy for Cryptoclidia (Cryptoclididae + Xenopsaria).

Palaeobiological implications

Feeding ecology

The preserved cranium of PMO 224.248, displays relatively large orbits relative to the temporal fenestrae (anteroposterior length of orbit/anteroposterior length of temporal fenestra = ~1.7) in comparison with other cryptoclidid taxa preserving cranial material (*Cryptoclidus eurymerus*, ~0.93; *Muraenosaurus leedsii*,

~0.58). In comparison the orbit anteroposterior length/total cranial length in PMO 224.248 (0.29), is comparable to other cryptoclidid plesiosaurs (*Cryptoclidus eurymerus* ~0.21; *Muraenosaurus leedsii*, ~0.17). This could imply that the cranial size was not enlarged to accommodate a larger orbit, the temporal region was reduced to increase orbital size. On an absolute scale, the size of the orbit (Appendix 6, Table A6.1) in PMO 224.248, is not significantly large in comparison to other contemporaneous marine reptiles such as ophthalmosaurid ichthyosaurs. For ophthalmosaurids, eye size can be estimates using the scleral ring (Fernández et al., 2005). The enlarged orbit/cranium size for ophthalmosaurids, has been suggested to have been an adaptation for deep-diving (Motani et al., 1999). Enlarged eyes accommodates additional photoreceptive cells and has additional area for light intake, thereby increasing the capability of the animal to see in low-light conditions (e.g.deep or murky water; Motani et al., 1999). Scleral rings are rarely preserved in plesiosaurs, and so an accurate estimate for eye size is currently unavailable. Nevertheless, the enlarged orbit in PMO 224.48 may have been an attempt at a similar palaeobiological adaptation at a cost of reduced area for adductor muscular attachments. However, the reduced adductor area may also be related to feeding ecology.

The mediolateral expansion of the mandible dorsal surface, displays an almost lateral exit angle for the teeth from the alveoli in PMO 224.248 and is extremely similar to the morphology seen in *Spitrasaurus larseni* (Knutsen et al., 2012d). In PMO 224.248 the cross section the maximum diameter of one of the crowns (at crown-root transition) is ~5.5 mm and is somewhat larger to that described for *K. langhami* and *S. larseni* (<5 mm; Brown, 1981; Knutsen et al., 2012d). Some of the teeth of PMO 224.248 show wear facets, indicating a tight fit between the lower and upper jaw teeth. This differs from the teeth described for *Kimmerosaurus langhami*, where no abrasion or wear is visible on the crowns (Brown, 1981). The preserved teeth of PMO 224.248 are not as recurved as those in *S. larseni* and *K. langhami*, and therefore probably displayed a more protruding dentition than these taxa. Although evolved independently, this morphology is similar to, but not as extreme as the laterally facing alveoli of the elasmosaurid *Aristonectes parvidens* (Gasparini et al., 2003) (Gasparini et al., 2003). This gracile and trap-like dentition in combination with the enlarged orbit relative to temporal

fenestral size, suggests that PMO 224.248 may have fed on small, unarmoured prey from the water column or sea floor and the enlarged orbits may have increased visual acuity in these environments (Figure 3.20) (Massare, 1987; Noè et al., 2017).

Implications for neck flexibility in cryptoclidids

Despite sharing the same plesiosauroid body form, cryptoclidids display high disparity in the number and morphology of the cervical vertebrae between genera. Noè et al., (2017), used two taxa of cryptoclidid plesiosaurs (*Muraenosaurus*, *Tricleidus* and *Cryptoclidus*), to illustrate neck flexibility and function, although did not provide any quantitative analysis. For elasmosaurids, the number of cervical vertebrae has been demonstrated to have had multiple independent reductions over time (Serratos et al., 2017), contra to previous research (Sachs et al., 2013). Although the number of cervical vertebrae is unknown for a significant fraction of Late Jurassic – Early Cretaceous cryptoclidid taxa, PMO 224.248 and the Slottsmøya Member genera *Spitrasaurus* and *Djupedalia*, have an increased number of cervicals (character 152/5-6) in comparison to the ancestral state in the subclade (152/3-4). This demonstrates that the number of cervical vertebrae appears to increase over time at least in one clade of cryptoclidids, with the highest number recorded in the Slottsmøya Member (Upper Jurassic) taxon *Spitrasaurus wensaasi* (60: Knutsen et al., 2012d). This suggests that selection pressure towards an extended cervical series was prominent among cryptoclidids, although probably connected to feeding, locomotion and/or respiration, the functionality of this feature is not entirely clear (e.g. Andrews, 1910; Brown 1981; McHenry et al., 2005).

In cryptoclidids, the variation in the dimensions of the centra and morphology of the neural arch throughout the cervical series is considerable. In the cervical centra of *Colymbosaurus megadeirus* and *Tricleidus seeleyi* the mediolateral width always exceeds than the dorsoventral height, and the dorsoventral height is subequal or more than the anteroposterior length (Andrews, 1910; Benson and Bowdler, 2014). In PMO 224.248, *Muraenosaurus leedsii* and *Spitrasaurus larseni* the cervicals are mediolaterally wider than dorsoventrally taller, but anteroposteriorly longer than dorsoventrally tall (Brown, 1981; Knutsen et al., 2012d). The elongated cervical vertebrae in these longer-necked taxa may function to increase stiffness in the cervical series to counter the increased number of cervical

vertebrae, or alternatively could serve as additional means to increase total neck-length (Noè et al., 2017). Extended cervical postzygapophyses observed in some sections of the neck in PMO 224.248, has been inferred to increase neck flexibility in some sauropods (Taylor and Wedel, 2013): where the extended pre- and postzygapophyses increase intervertebral spacing, giving more flexibility. This indicates that the flexibility of the cryptoclidid neck is more complex and regional than presented in Noè et al., (2017). Further studies utilising biomechanical functional analyses such as finite element analysis (FEA) in combination with muscular reconstruction, could be useful to more accurately reconstruct neck flexibility.

Gastroliths in cryptoclidids

The posterior region of the gastral basket, was covered in a rusted silt layer in PMO 224.248. Considering this predominately silty matrix includes a large number of small worn pebbles (gastroliths) and bone fragments, the presence of stomach content is likely. The gastroliths are small ranging from <2cm in diameter and are significantly smaller than those described from Late Cretaceous plesiosaurs (Cicimurri and Everhart, 2001; Everhart, 2000). A section of the layer along with a section of the underlying gastralia were µCT scanned, revealing a large amount of material embedded in the matrix. To our knowledge, this is the first time gastroliths have been described for cryptoclidid plesiosaurs. The material requires further analysis to derive the source of the gastroliths and the origin of the bone material, which is beyond the scope of this paper.

Figure 3.20: A reconstruction of PMO 224.248 in its natural environment. Illustration by Esther van Hulsen.

Concluding remarks

PMO 224.248 represents the temporally youngest occurrence of a plesiosaur from the Slottsmøya Member (Agardhfjellet Formation) of central Spitsbergen. This specimen will represent the forth taxon described from the member, although several other cryptoclidid specimens remain to be described. PMO 224.248 is one of the few cryptoclidids with detailed cranial osteology available, providing much needed morphological information for understanding the intrarelationships of cryptoclidids. In addition, this specimen uniquely preserves a complete cervical series found in articulation, offering future opportunities to test current hypotheses on plesiosaur neck-flexibility and evolution. As the specimen was found in the section encompassing the Jurassic – Cretaceous boundary and likely Berriasian in age, PMO 224.248 along with the Russian *Abyssosaurus nataliae* represent the only cryptoclidid genera from the Early Cretaceous. The phylogenetic results of this study indicate that two separate clades of cryptoclidids crossed the Jurassic – Cretaceous boundary in the Boreal region of Spitsbergen and the sub-Boreal region of Russia.

Acknowledgements

The authors wish to thank the museum curators and researchers that assisted AJR during collection visits; S. Chapman and L. Steel (NHMUK), M. Riley (CAMSM), E. Howlett (OUM), M. Evans (LEICS), M. Fernández (MOZ, MLP), G. Wass (PETMG), N. Clark (GLAHM), G. Cuny (MGUH), K. Sherburn (MANCH), L. A. Vietti (UW). D. Foffa, S. Etches, V. E. Nash, D. Legg, A. S. Smith, V. Fischer, J. Wujek, E. M. Knutsen and E. Martin-Silverstone are thanked for discussion. M-L K. Funke, C. Ekeheien, M. Koevoets and V. E. Nash are thanked for assistance during the preparation of the specimen. Ø. Hammer is thanked for assistance with the computed tomography and O. Katsamensis is thanked for access to the visualisation laboratory (µ-vis) in Southampton. The Willi Hennig Society is acknowledged for their sponsorship of TNT (Trees with New Technology). Gratitude is warranted to all the volunteers of the Spitsbergen Mesozoic Research Group, who participated in the 2012 excavations. The authors warmly thank the palaeoartist Esther van Hulsen for illustrating PMO 224.248.

Chapter 4

The distribution and cladogenesis of Mid Jurassic (Callovian) to Early Cretaceous (Valanginian) Boreal plesiosaurs and ichthyosaurs

The distribution and cladogenesis of Mid Jurassic (Callovian) to Early Cretaceous (Valanginian) Boreal plesiosaurs and ichthyosaurs

Authors: Roberts, A. J.[1 2] , Harding, I. C. [1] and J. H. Hurum[2]

[1]Ocean and Earth Science, University of Southampton, National Oceanography Centre Southampton, European Way, Southampton, Hampshire SO14 3ZH, United Kingdom, ajr1g13@soton.ac.uk;

[2]Natural History Museum, University of Oslo, 0562, Norway, j.h.hurum@nhm.uio.no;

Abstract

With the recent increased sampling of Mesozoic marine reptile specimens in high latitude regions, greater geographic coverage enables a more comprehensive assessment of their palaeobiogeography. Here we present a review of the global distribution of plesiosaur and ichthyosaur taxa described during the Mid Jurassic – Early Cretaceous and discuss these data in the context of sea level and climatic variations. We present the first quantitative assessment of the biogeographic distribution of plesiosauroid plesiosaur and ophthalmosaurid ichthyosaur clades by employing ancestral states analysis using *BioGeoBEARS*. The data have also been subject to parsimony analysis of endemicity and distance measures. Geographic regions of interest were chosen based on the regional occurrence of the taxa included, depending on the analysis. Although only partly successful, these analyses show that moderate-high plesiosaurian and ichthyosaurian taxonomic exchange took place between most geographic regions of interest during this interval. Furthermore, the ancestral states analysis indicates that derived clades of plesiosauroids including the elasmosaurids, cryptoclidids and leptoclidids likely stemmed from a sub-Boreal ancestor based on the available data. In contrast, the ophthalmosaurid distributions are far more complex, reflected upon the wider distribution. Of the six models available in *BioGeoBEARS*, the DEC+J model (diversification, extinction, cladogenesis and founder-event) fitted the data significantly better than the other

models and display a large founder-event component. Cladogenesis events coincide with global sea-level highstands (transgressive events), and thus the opening of seaways between Tethys, Panthalassa and the Boreal Sea may have been the driver for the founder effect in these clades. In turn, the apparent increased provincialism and endemism of some Boreal marine reptile clades during the Tithonian could in part be coupled with the latest Jurassic regression. As previously documented for other extant and extinct taxa, we suggest that a wider geographic distribution may have the potential to increase temporal ranges for cryptoclidid plesiosaurs and ophthalmosaurid ichthyosaurs. However, additional data particularly from other clades and groups of marine reptiles is required to further test this hypothesis.

Introduction

Over the past century numerous descriptions of Mesozoic marine reptile fauna have increased our knowledge on their diversity, palaeobiology and distributions. The predominantly pelagic ichthyosaurs and plesiosaurs displayed a world-wide distribution by the Early Jurassic, which continued until their final extinction (Bardet et al., 2014). Ichthyosaurs and plesiosaurs show numerous specialised marine adaptations that allow for high dispersal potential (Bernard et al., 2010; Fischer et al., 2011b; Motani, 2002), such as live birth (O'Keefe and Ciappe, 2011), dorsally placed external nares (Cruickshank et al., 1991), increased growth rate (Houssaye, 2013) and a hydrodynamic body shape (Buchholtz, 2001). While other contemporary marine reptiles such as the thalattosuchian clades also shared most of these adaptations, in contrast to ichthyosaurians and plesiosaurians they were unable to colonise high latitude regions during the Jurassic (Massare et al., 2014; Tennant et al., 2016a); indeed, thalattosuchians appear to either have been very rare in- or were unable to colonize the Boreal Region, possibly as a result of the cooler climate or high-latitude seasonality documented during this interval (Ditchfield, 1997; Hammer et al., 2001; Žák et al., 2011).

The Mid – Late Jurassic is a significant time interval to examine marine reptile palaeobiogeographic distributions: the opening up of new seaways during the break-up of the supercontinent Pangaea presented new opportunities for marine macrofaunal migration, allowing access to regions previously separated by the supercontinent (Bardet et al., 2014). The formation of the Caribbean (Hispanic) Corridor enabled marine faunal exchange between the sub-Boreal Western Tethyan

region and Panthalassa during the Jurassic, is well-documented by macro- and microfossils (Aberhan, 2001; Barrientos-Lara et al., 2016; Gasparini, 1996; Gasparini and Fernández, 2005; Iturralde-Vincent, 2003). During the same period, the opening of the Northeast Atlantic and other confluent seaways over Western Russia (Russian Platform) offered opportunities for fauna to migrate between the northern Boreal Realm and the Tethyan Ocean (Bardet et al., 2014; Zverkov et al., 2015).

Although the increased numbers of described Mesozoic marine reptile species have generated opportunities for reconstructing their palaeobiogeographical distributions, studies have so far been either on a general overview (Bardet et al., 2014), or have focused specifically Triassic and Jurassic marine reptile clades (Arkhangelsky, et al., *in press*; Rieppel, 1999; Sander and Faber, 1998; Zverkov et al., 2015). Of these studies only Arkhangelsky et al., (*in press*), discuss the distributional patterns of multiple contemporaneous marine reptile clades for restricted time slices (‘temporal bins’). Many ichthyosaurian and plesiosaurian genera were present in a number of regions during the Late Jurassic, but in the Boreal Sea, high taxonomic diversity, apparent provincialism and endemism has been suggested for some clades of plesiosaurian and ophthalmosaurid ichthyosaurs (Figure 4.1; Roberts et al., 2014; Chapter 3, this volume). By providing seaways that linked the Panthalassic and Tethyan Oceans, the Boreal Sea is an important locality for understanding plesiosaurian and ichthyosaurian palaeobiogeography, due to the considerable Late Jurassic species richness of these groups described from this region (Hurum et al., 2012; Chapter 3, this volume). However, the high number of marine reptile taxa from this region, is mainly due to the considerable number of single occurrences (holotype only) and often endemic (restricted to one locality) taxa described from the Slottsmøya Member Lagerstätte of Spitsbergen (Svalbard). Although a restricted Late Jurassic Boreal province of Boreal marine reptiles has been suggested, no quantitative analysis has been provided in support or against this hypothesis (e.g. Paparella et al., 2016; Zverkov et al., 2015).

Few studies (aside from Fischer et al., 2016, Tennant et al., 2016b) which examine the distribution and diversity of ichthyosaurians and plesiosaurians have included discussion of eustatic sea level change and/or tectonic movements in any detail, nor have they provided the quantitative analysis usually employed in

biogeographical analyses of invertebrates (e.g. Aberhan, 2001). Although some efforts have been made in understanding the latitudinal gradients seen in some marine reptiles (Crocodylifoms; Tennant et al., 2016a). No Late Jurassic marine reptile palaeobiogeographic investigation has as yet provided distance matrix, ancestral states analysis or other quantitative measures to illustrate genera or taxa shared between palaeogeographic regions. Thus, in order to assess the palaeobiogeography of marine reptiles during the splitting of Pangaea, we have collected published (89) and unpublished (3) taxonomic data from the Callovian – Valanginian interval (Appendix 7, Tables A7.1-3). For the first time for Late Jurassic marine reptiles, we use classical palaeobiogeographic methods and ancestral states analysis to better quantify the temporal distributions of plesiosaurians and ichthyosaurians. These distributions are discussed alongside palaeoclimatic and eustatic sea level changes to better understand abiotic influences on distributional patterns. Furthermore, such analyses can provide insight into the origination of certain clades, how biogeographic distributions influence taxon survivability (speciation and extinction rates) (Brown and Kodric-Brown, 1977), and the hypothesized Boreal provincialism of some marine reptile groups during the Late Jurassic.

The palaeogeography of the Boreal Region during the Callovian – Valanginian

During the Mesozoic, the Boreal Sea was present in what is today the Arctic region (Figure 4.1). This shelf sea was connected to the Panthalassic and Tethyan oceans through multiple, fluctuating seaways (Zakharov et al. 2002). The Northeast Atlantic and the shallow epicontinental sea covering part of the western Russian Platform (Middle Russian Sea; Arkhangelsky et al., *in press*), intermittently connected the Boreal Sea to the Tethys during the Jurassic and Cretaceous (Rogov, 2012, 2013; Rogov et al., 2008; Sahagian et al., 1996). The Mesozoic Boreal Sea and the present-day Arctic Ocean were and are heavily influenced by the connecting water masses (Shimada et al., 2006; Zhang et al., 1998): by currents passing through these connecting seaways, influence temperature, salinity and climate (Korte et al., 2015; Shimada et al., 2006; Zhang et al., 1998). During the Mesozoic, the formation of north – south orientated seaways established routes for marine faunal exchange

between the northern (Boreal) and southern (Tethyan) realms (Doré, 1991; Dunton, 1992; Sahagian et al., 1996; Wierzbowski and Rogov, 2011). In this study, the Boreal Realm is used to encompass the entire region surrounding the Mesozoic palaeo-Arctic and its marine fauna (Zakharov et al., 2002). The Boreal Mesozoic marine macrofauna (both invertebrate and vertebrate) had an almost circumpolar distribution (Zakharov, 1987; Zakharov and Rogov, 2008). It should be noted that although significant Late Jurassic – Early Cretaceous Boreal marine reptile material is described from the Russian platform (Zverkov et al., 2015) and the Canadian Arctic (Maxwell, 2010), the majority of taxa are known from Spitsbergen, Svalbard (Hurum et al., 2012).

As the Northeast Atlantic mainly consisted of a series of rift basins throughout the Jurassic and Cretaceous (Faleide et al., 2008; Faleide et al., 1993; Skogseid, 2010) and the Western-Middle Russian shelf was covered by a shallow epicontinental sea (Middle Russian Sea; Arkhangelsky et al., *in press*), the connectivity between northern and southern regions was direct influenced by sea level fluctuations. Such fluctuations may have influenced faunal exchange (Cecca et al., 2005; Mutterlose et al., 2003), as during periods of regression provincialism may be enhanced, whereas transgressive episodes may have permitted faunal influxes from other regions (Riding et al., 2011). As such, sea-level fluctuations can significantly affect the palaeobiogeographic distribution of marine faunas (Cecca et al., 2005).

Early work on eustatic sea level changes in the Mesozoic, suggested a general transgression through the Jurassic followed by a sea level fall in the Valanginian (Doré, 1992; Hallam, 2001; Haq, 1987). With improved stratigraphic resolution, sea level fall has been identified from the Late Jurassic – earliest Cretaceous, ending with a transgression in the Valanginian (Cecca et al., 2005; Hansen et al., 2012; Miller et al., 2005; Mutterlose et al., 2003). A critical phase in the opening of the Northeast Atlantic was reached in the Mid Jurassic – Early Cretaceous, when rifting progressed northwards reaching the Barents Sea (Hansen et al., 2012; Lundin and Doré, 1997; Sibuet et al., 2007). Such tectonic events coupled with the eustatic fluctuations in the Late Jurassic – Early Cretaceous, make this time interval paramount in understanding marine macrofaunal distributions between higher and lower latitudes. Of the few Boreal localities from the Late Jurassic, the

island of Spitsbergen (Svalbard Archipelago) is the most fossiliferous and is a key locality at which to study the biotic interactions between Tethyan and Boreal faunas, with its location at the northern border of the Northeast Atlantic (60-70° N) during the Mid Jurassic – Early Cretaceous (Doré, 1991; Dypvik et al., 2003). The Volgian (Tithonian-Berriasian) Slottsmøya Member marine Lagerstätte represents ~12 Myr of deposition, with some 58 marine reptile specimens excavated throughout the member (Delsett et al., 2016).

Fluctuating provincialism in the Boreal Region between the Mid Jurassic and the Aptian have been documented for microfauna (Alsen and Mutterlose, 2009; Mutterlose, 1992; Pauly et al., 2012; Rawson, 1993) and also macrofauna such as ammonites (Cecca et al., 2005; Rogov and Zakharov, 2009), bivalves (Rogov and Zakharov, 2009) and mega-onychites (Cephalopod hooks; Hammer et al., 2013), along with the presence of several new taxa of endemic echinoderms (Rousseau and Nakrem, 2012). Due to the high degree of provincialism between the Boreal and Tethyan realms during the Tithonian – Aptian, biochronological correlation has been difficult in the Northern hemisphere. This is reflected in the use of the three separate names for the geological stages that span the Jurassic-Cretaceous boundary, namely the Tithonian, Portlandian and Volgian (Cecca et al., 2005). Phylogenetic analysis has indicated that certain Late Jurassic ophthalmosaurid ichthyosaurs (Delsett et al., 2016; Paparella et al., 2016; Roberts et al., 2014) and cryptoclidid plesiosaurs (Benson and Druckenmiller, 2014; Roberts et al., 2017), were provincial Boreal clades. Some authors have argued that these phylogenetically inferred endemic clades are not sufficient evidence for the existence of a restricted Northeast Atlantic seaway (Paparella et al., 2016). Others have suggested a presence of marine reptiles of Boreal affinity in the Northern Tethys (Tyborowski, 2016), but this is currently unsupported (see Discussion).

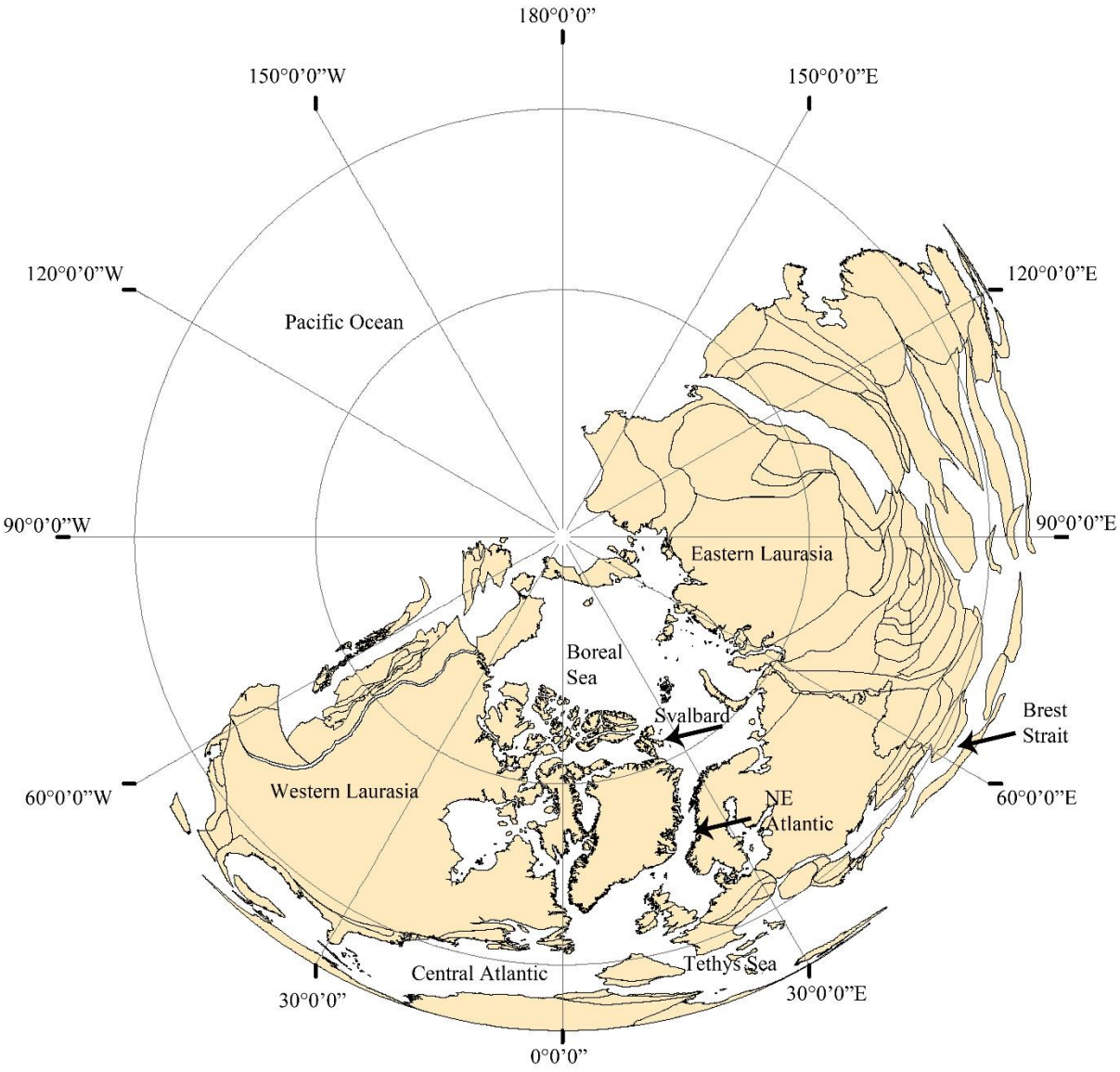

Figure 4.1: Palaeogeographic reconstruction of the polar region (with modern coastlines superimposed) during the latest Jurassic – earliest Cretaceous (145Ma), modified with permission from Torsvik and Cocks (2017).

The distribution and diversity of plesiosaurians and ichthyopterygians in the Mid Jurassic (Callovian) – Early Cretaceous (Valanginian)

Our understanding of marine reptile distribution during the Mid Jurassic – Early Cretaceous has increased with recent research, particularly in the under-sampled Southern Hemisphere (Gasparini et al., 2015b; Schultz et al., 2003;

Stinnesbeck et al., 2014). For plesiosaurians, the Mid – Late Jurassic represented a time of change, as the previously dominant groups of the Early – early Mid Jurassic (e.g. rhomaleosaurids and microcleidids) were replaced by new clades (pliosaurids and cryptoclidids) (Benson and Druckenmiller, 2014). For the ichthyosaurians, this period shows an increase in taxonomic diversity and world-wide distribution for the ophthalmosaurid ichthyosaurs (Maxwell et al., 2016). Here we present the published and previously unpublished occurrence data on the fossil record of ichthyosaurians and plesiosaurians during the Callovian – Valanginian interval, with comparison to changes in climate and eustatic sea level. Individual taxonomic information and relevant references appear in Appendix 7 (Tables A7.1-3).

Callovian – Oxfordian

The mid Callovian eustatic transgression was one of the more significant sea level fluctuations during the Jurassic (Hallam, 2001). This tectonically driven transgression initiated connections between previously isolated marine provinces (Westermann, 1993). This overall transgressional trend, although punctuated by episodic regressions continued into the Oxfordian, (Hallam, 1988, 2001; Sahagian et al., 1996). The most significant of these regressions, occurred in the late Callovian, where a drop in sea level was recorded in most geographical regions (Hallam, 1988; Hallam, 2001) except the Russian platform (Sahaigian et al., 1996). This regression may have been partly due the development of land-fast glaciation at high latitudes (Dromart et al., 2003). A global cooling event lasting for ~2.6 Myr has been recorded from stable isotopic analyses ($\delta^{18}O$) of belemnite rostra and apatite from chondrichthyan fish tooth enamel (Dromart et al., 2003; Veizer et al., 1999). This global cooling event across the Mid – Late Jurassic is also reflected in the influx of large numbers of Boreal ammonites into the Tethyan region (Dromart et al., 2003).

The Callovian yields some of the earliest records of derived plesiosaurs and ichthyosaurs families' world-wide (Fernández, 1999; Gasparini and Spalletti, 1993). However, it should be noted that a clear gap in the marine reptile fossil record in the Tethyan region has been observed during the Oxfordian Stage and is referred to as the "Correlian Gap" (Young, 2014). Globally, the Oxfordian plesiosaur fossil record includes three main clades; the cryptoclidids, rhomaleosaurids and pliosaurids (Benson and Druckenmiller, 2014) (Figure 4.2). The cryptoclidids are a clade of

long-necked (plesiosauroid) plesiosaurs, present during in Mid Jurassic – Early Cretaceous (Benson and Druckenmiller, 2014). The earliest remains of this group are from the Callovian stage (Gasparini and Spalletti, 1993). Cryptoclidid specimens of Callovian – Oxfordian age have been reported in Western Europe (Andrews, 1910; Brown, 1981), North America (O'Keefe and Street, 2009; O'Keefe and Wahl, 2003b), Argentina (Gasparini and Spalletti, 1993) and Cuba (Gasparini et al., 2002), giving the cryptoclidids an almost global distribution at this time (Appendix 7, Table A7.1). The last recorded occurrences of another plesiosaur clade, the rhomaleosaurids, are from mid-high latitudes during the Callovian: *Borealnectes* from Arctic Canada, a possible occurrence in Argentina, along with unidentified fragmentary material from the Oxford Clay Formation (UK) and the Hlebnovka Formation (Russia) (Benson et al., 2015; Gasparini and Spalletti, 1993; Sato and Wu, 2008). While specimens of thalassophonean pliosaurids from the Callovian have been described from the United Kingdom (Oxford Clay Formation) (e.g.Andrews, 1913; Ketchum and Benson, 2011), Oxfordian occurrences are less common: the most complete material is described from Cuba (Jagua Formation; Gasparini, 2009) and Italy (Rosso Ammonitico Veronese Formation; Cau and Fanti, 2015), along with fragmentary material from North America (Sundance Formation; Wahl et al., 2010) and Eastern Europe (Lomax, 2015).

Although the earliest unambiguous ophthalmosaurid ichthyosaur records are from the lower Bajocian deposits of the Chacaico region (Argentina;Fernández and Talevi, 2014), ophthalmosaurids were a taxonomically diverse and widespread distribution during the Callovian – Oxfordian interval. Specimens have been described from Cuba (Fernández and Iturralde-Vincent, 2000), North America (Gilmore, 1905), Western Europe (Andrews, 1910; Moon and Kirton, 2016) and Russia (Arkhangelsky, 1997). The best preserved and most articulated specimens are from the Oxford Clay Formation of the United Kingdom.

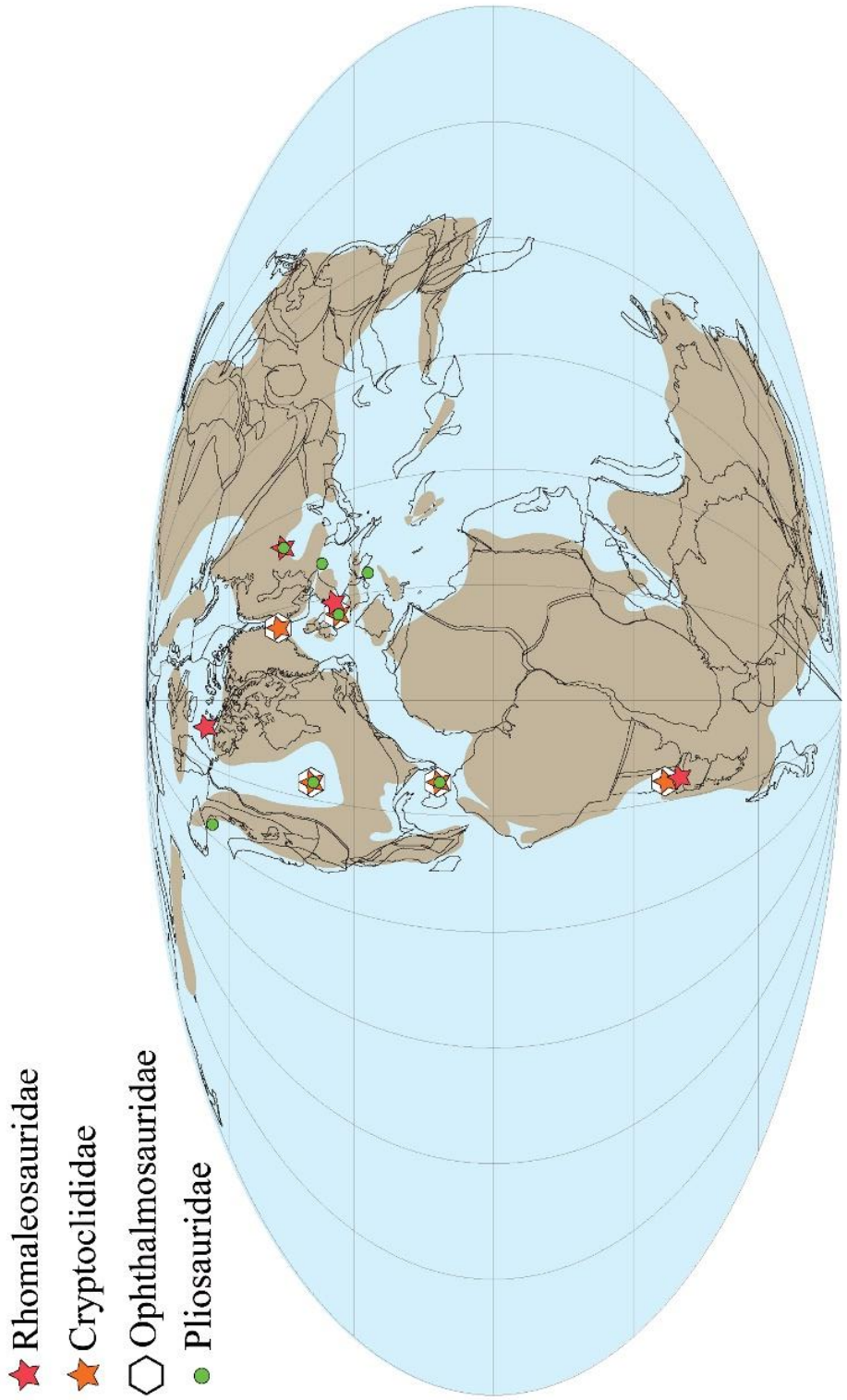

Figure 4.2: The distribution of plesiosaurians and ichthyopterygians during the Callovian – Oxfordian interval, based on data collected for this study (See Appendix 7, Table A7.1 for list). Map modified using GMAP V.2015 (Torsvik and Smethurst, 1999) with palaeocoastline information from Smith et al., 1994.

Kimmeridgian – Tithonian (Volgian)

In the Northern Hemisphere, transgressive conditions continued from the Oxfordian into the Kimmeridgian, with a sea level peak recognised in Kimmeridgian strata from Greenland, in the *eudoxus* zone (Surlyk, 1991). This transgressive event flooded the Russian platform, creating a large, shallow seaway opening into the Tethys via the Brest Strait (Eastern Europe; Arkhangelsky et al., *in press*; Rogov et al., 2008). Although a global warming trend prevailed, from the Late Oxfordian into the Tithonian, there is some evidence for seasonality in the Kimmeridgian from the Arctic Canadian Sverdrup Basin (Galloway et al., 2013), with mean palaeotemperature modelled to be between 0-4°C in winter and 20-24°C in summer during the Late Jurassic (Sellwood and Valdes, 2006). This seasonality may have been a causative factor driving the low marine macrofaunal species richness in the Sverdrup Basin (Embry, 1991). A cooler climate is also evident in Western European lower latitudes: oxygen isotope data from belemnite rostra from Scotland have yielded palaeotemperatures estimates ranging between 10-13°C (Wierzbowski, 2004). Warm palaeotemperatures in the Volga Region have been calculated during this time interval (14-23°C), followed by a slight cooling towards the Jurassic – Cretaceous boundary (Gröcke et al., 2003). The mid Tithonian represented a high level peak in sea level, followed by a regression in the latest – Tithonian - Early Cretaceous (Miller et al., 2005). At this point the Boreal-Tethyan ammonite exchange in Western Europe was severely reduced by comparison to that seen during the Kimmeridgian, possibly the result of a temporary closure of the Brest Strait and/or a restricted Northeast Atlantic (Zakharov and Rogov, 2003).

The Kimmeridgian – Tithonian interval has a rich record of marine reptiles, partly due to the development of a number of marine fossil Lagerstätten (Benson et al., 2010; Figure 4.4).Coinciding with the Kimmeridgian and Tithonian transgressions, plesiosaurian and ichthyosaurian specimens have been described from the Northeast Atlantic seaway (Greenland and Northern Norway) and from the Russian Platform (Volga Region), indicating their presence in these seaways (Smith, 2007a; Storrs et al., 2000). The plesiosaur fossil record from this interval are predominately from the Northern Hemisphere, particularly for cryptoclidid plesiosaurs. Indeed, outside the Northern Hemisphere only two cryptoclidid occurrences are documented from these stages: a vertebral series from the

Kimmeridgian of Western India (Bardet et al., 1991) and a plesiosauroid vertebrae (cf. Cryptoclididae) from the Late Jurassic – Early Cretaceous Chichali Formation of Pakistan (Buffetaut, 1981). Despite this apparently more restricted distribution, cryptoclidid taxonomic diversity remained high (Figure 4.4). A number of taxa are described from the Tethyan Sub-Boreal and Boreal realms, with the majority of them being taxa that are known only from a single specimen (Appendix 7, Table A7.2). The one exception is *Colymbosaurus*, a cryptoclidid genus present in both high and lower latitudes during the Kimmeridgian – Tithonian (Benson and Bowdler, 2014; Roberts et al., 2017). Pliosaurids remain geographically widely distributed through the Kimmeridgian and Tithonian stages, with a well-distributed, but with poorly preserved and fragmentary specimens from the Northern and Southern Hemispheres (Buchy et al., 2006b; Gasparini and Fernández, 2005; Malakhov, 1999). The best preserved and most complete pliosaurid specimens derive from the Kimmeridge Clay Formation of the UK (for summary see Benson et al., 2013).

Ophthalmosaurids increased in generic diversity in the Late Jurassic and retained a dual hemisphere distribution, with a number of cosmopolitan genera: *Arthropterygius* and *Ophthalmosaurus*. Numerous ophthalmosaurid specimens have been described from the Boreal region (Druckenmiller et al., 2012; Maxwell, 2010; Roberts et al., 2014; Sissons et al., 2015), Argentina (Fernández and Maxwell, 2012), Western Europe (Moon and Kirton, 2016), Mexico (Buchy, 2010) and Western Russia (Zverkov et al., 2015). Zverkov et al. (2015) suggested that Late Jurassic ophthalmosaurid ichthyosaur taxa (*Arthropterygius*) had at least three seaways (Boreal-Panthalassaic Seaway, Northeast Atlantic, Middle Russian Sea) for faunal exchange from the Boreal Sea to Western Russia and South America. Additional, undiagnostic material from the Antarctic Peninsula has also been described (Hikuroa, 2009; Schultz et al., 2003).

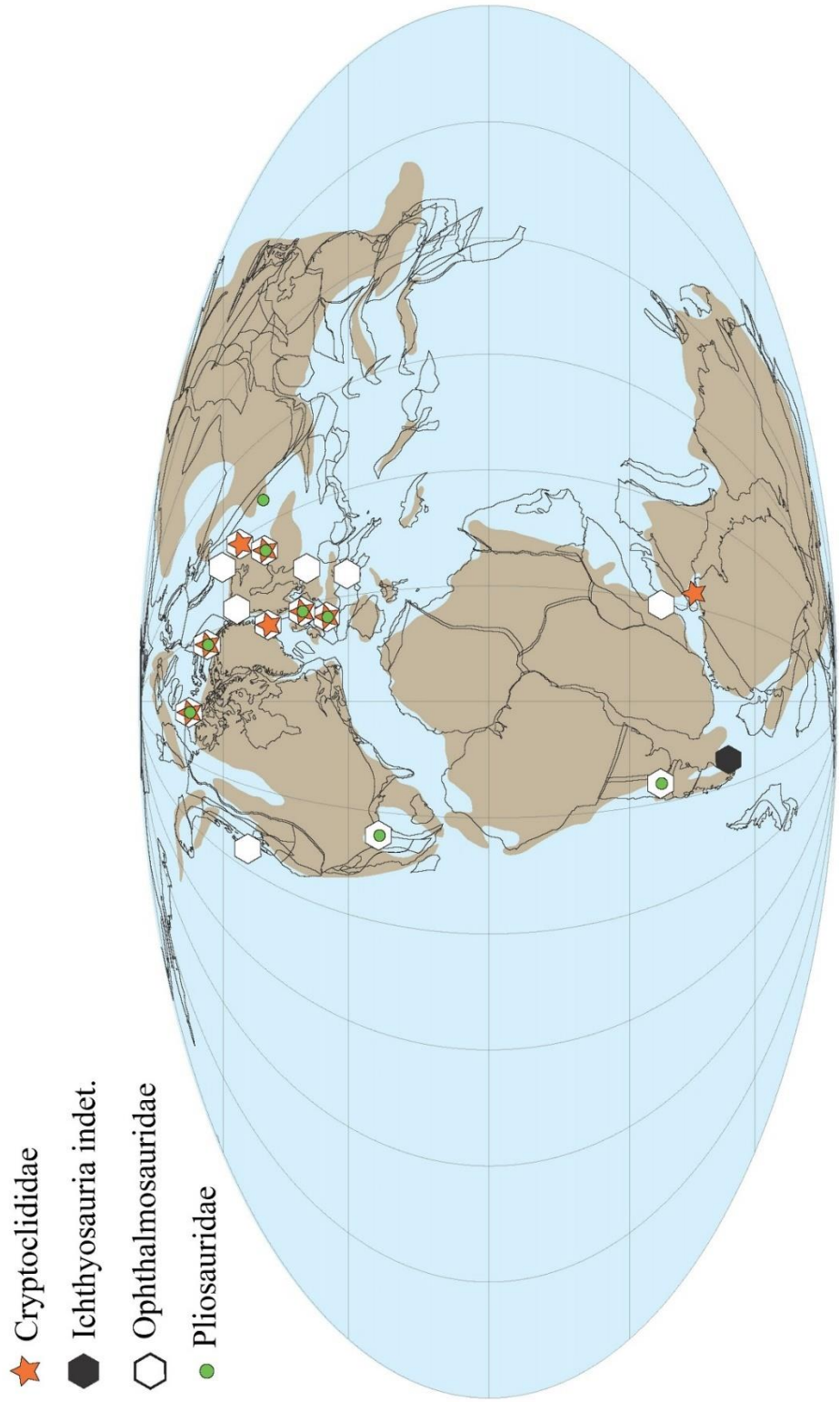

Figure 4.3: The distribution of plesiosaurians and ichthyosaurians during the Kimmeridgian – Tithonian (early – mid Volgian) interval, based on published and unpublished data (see Appendix 7, Table A7.2 for list). Map modified using GMAP V.2015 (Torsvik and Smethurst, 1999), with palaeocoastline information from Smith et al. 1994.

Berriasian-Valanginian

A faunal crisis occurred during the terminal Jurassic – earliest Cretaceous in response to climatic, eustatic and abiotic factors (e.g., volcanism, impact events), causing biodiversity losses in both invertebrate and vertebrate marine faunas, ultimately resulting in a biotic reorganisation (Barash, 2008). Marine reptile faunal composition underwent dramatic changes during the earliest Cretaceous stages, with the introduction of crown-group plesiosauroids (Xenopsaria = Elasmosauridae + Leptoclidia + Polycotylidae; Benson and Druckenmiller, 2014) and a loss of diversity and disparity in cryptoclidid plesiosaurs, pliosauroids, ophthalmosaurids and other groups of marine reptiles (Tennant et al., 2016b). The sea level fall at the Jurassic – Cretaceous boundary reinitiated provincialism in marine flora and fauna (Pauly et al., 2012). South to North directional warm water surface currents, gradients in temperature and palaeogeographic isolation have been used to explain the absence or rarity of Boreal belemnites in the Tethyan region and the presence of Tethyan belemnite fauna in the Boreal region (Alsen and Mutterlose, 2009; Price and Mutterlose, 2004). Oxygen and carbon isotope data from Valanginian belemnites and glendonities from Svalbard (4-7°C) and from Siberia (2-14°C), display a cooler climate in this region than the contemporary recorded Greenhouse global climate (Price and Mutterlose, 2004; Price and Nunn, 2010).

Plesiosauroid remains of uncertain identity are present in Southern England (Kear and Milner, 2009) (Figure 4.4). Basal xenopsarian specimens including the taxon *Brancasaurus*, have been described from the Bükeberg Formation of Germany (Sachs et al., 2016). No unambiguous pliosaurid material is available from this interval.

Few Berriasian – Valanginian ophthalmosaurid taxa are known. *Keilhauia nui* from the Slottsmøya Member (Spitsbergen) represents the most complete such taxon from the Berriasian (Appendix 8, Delsett et al., 2017). Other, more fragmentary remains of ophthalmosaurids are present in the Spilsby Sandstone Formation of Eastern England (Fischer et al., 2012; Forrest and Oliver, 2003), with possible occurrences of *Ophthalmosaurus* in Northern Russia (indeterminate stratigraphy Late Tithonian – Berriasian; Zverkov et al., 2015). From the Valanginian, a fragmentary rostrum of *Aegirosaurus* has been described from France (Fischer et al., 2011a), extending the stratigraphic range of this genus from the

Tithonian. In the Southern Hemisphere, an ichthyosaur “cemetery” preserved in Valanginian strata from Southern Chile preserves numerous ophthalmosaurid ichthyosaur specimens, some of which are referred to *Platypterygius* (Stinnesbeck et al., 2014).

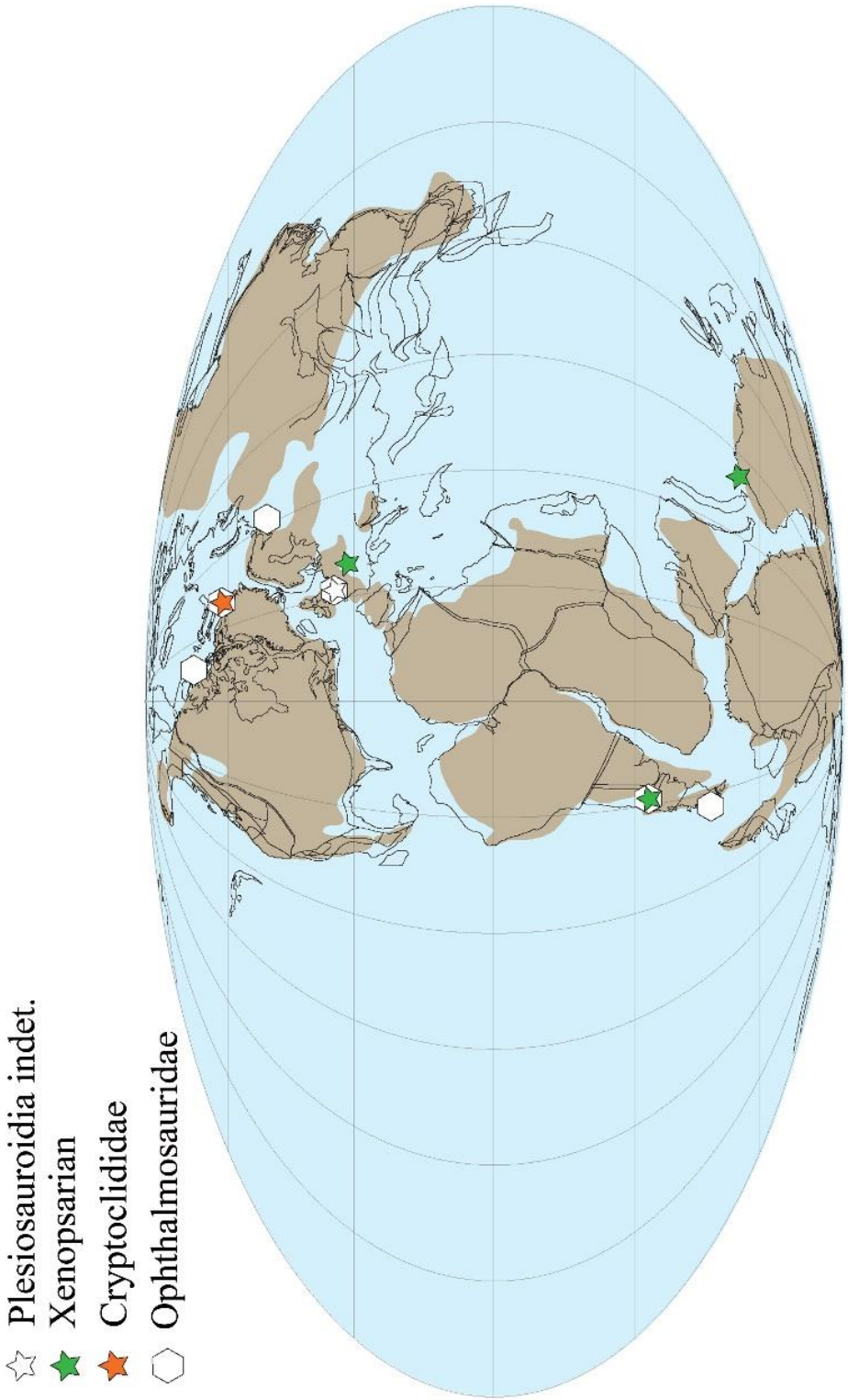

Figure 4.4: The distribution of plesiosaurians and ichthyosaurians during the Berriasian – Valanginian interval, based on published and unpublished data (see Appendix 7, Table A7.3 for list). Map modified using GMAP V.2015 (Torsvik and Smethurst, 1999), with palaeocoastline information from Smith et al. (1994).

Materials and Methods

Palaeobiogeographic analyses and the fossil record

Biogeographical analyses are useful to compare ecosystems or individual clades and their spatial distribution (Cecca, 2002). However, the fossil record is challenging as most biogeographical analyses applied to extant animal groups require assumptions that cannot be met using fossil data (Lieberman, 2000). Although the fossil record is never a completely accurate reflection of reality, palaeobiogeographical analyses can be useful indicators of the amount of recorded taxonomic diversity shared between different regions (Cecca, 2002). Brooks and van Veller (2003) provided a summary of biogeographical analyses, including some of those most commonly applied to fossil datasets such as: parsimony analysis of endemicity (Rosen, 1978; see Methods), latitudinal gradients of species richness (Gaston, 2000) and index measures of faunal similarity (Raup and Crick, 1979; see Methods). Most commonly, biogeographical analyses are performed on presence-absence data for taxa at a species or generic level.

We collected taxonomic, stratigraphic, regional and literature information on the plesiosaurian and ichthyosaurian fossil records from the Callovian – Valanginian, representing the largest and most detailed occurrence matrix from this interval (Appendix 6, Tables A6.1-3). Taxonomic and occurrence data were collected from the literature, museum databases and collections, with supplementary information gathered from the Palaeobiology Database (PBDB). The data were separated into three temporal bins: Callovian – Oxfordian, Kimmeridgian – Tithonian and Berriasian – Valanginian. The purpose of this database is to put Boreal plesiosaurians and ichthyosaurians into a global chronological context. This study does not include other marine reptile groups (e.g. testudines and crocodylomorphs), as these have not yet been described from the Boreal region and the distribution of these groups is more influenced by latitudinal gradients (Tennant et al. 2012a; see Discussion). However, these two groups should be included in future work. The collected data has been subjected to several different analyses in an attempt to identify and illustrate the palaeobiogeographic relationships in cryptoclidid plesiosaurs and ophthalmosaurid ichthyosaurs. These include ancestral states analysis, parsimony analysis of endemicity (PAE) and distance measures. The

purpose of these analyses is to quantitatively display shared taxonomic occurrences, highlight periods of cladogenesis and infer ancestral origin.

The fossil record is severely limited in comparison to the real abundances and diversities at any given time, due to preservation, collection and exposure biases for any given taxon (Benton et al., 2011). Therefore, any analyses of the diversity, abundance and palaeobiogeography of macro fossils should be seen only as an estimation of reality based on the data available. Several factors (expanded from Bardet et al., 2014) should be borne in mind when attempting to reconstruct the biogeographical ranges of extinct animals, namely that:

1) The region of origination cannot be precisely identified, but only inferred on the basis of an incomplete fossil record.
2) The choice of taxonomic rank has implications for the observed distributional patterns and amount of endemism.
3) Differences in faunal distribution over time must be considered: it is difficult to correlate the presence of taxa precisely in time.
4) Larger macro predators are less common in the palaeoecosystem and also less likely to be preserved due to their size.
5) Time periods with a high number of known concentration or conservation Lagerstätte artificially boost general taxonomic diversity compared to periods lacking Lagerstätte (e. the Berriasian Stage for marine reptiles).
6) Regional collection bias – specimen collection in Europe and North America has been extensive in comparison to other regions (e.g. South America, Antarctica, Africa). Specimens are better known from Europe and North due to A) discoveries made as a result of petroleum, stone quarries and mining operations, B) localities have been easily accessible for palaeontologists, C) has received a long historic interest
7) It must be borne in mind that the precise temporal and geographic distribution of an extinct taxon will remain unknown.

To try to compensate for these issues we, 1) use the taxonomic rank of genus for our palaeobiogeographic analyses, with the exception of the ancestral states analysis. Applying the rank of genus will reduce the subjectively high diversity recorded in some Lagerstätte and also eliminate disagreements on alpha taxonomy; 2) use

expanded temporal bins to reduce the impact of low sampling density, single occurrence data bias and the lack of detailed stratigraphic control in some regions.

Phylogenetic methods and ancestral states analysis

Time-calibrated phylogenetic trees yield information regarding closely-related taxa and thereby contribute to understanding palaeobiogeographic distributions and degree of regional provincialism (Maguire and Stigall, 2008). Although fossil data are subject to bias (see above and Benton et al., 2011), for marine fauna biogeographic analyses such as PAE (Parsimony analysis of endemicity) and distance measures when combined with ancestral states analysis, can be useful to illustrate diversification and distribution events with respect to the opening and closing of seaways in response to tectonic movement and eustatic sea level change (Herrera et al., 2015; Paparella et al., 2016).

Time-calibrated phylogenetic trees for Plesiosauroidea (Microcleididae, Cryptoclididae and Xenopsaria) and ophthalmosaurid ichthyosaurs were generated using the most recently published matrices (Delsett et al, 2017; Maxwell et al., 2016; Roberts et al., 2017; Chapter 3, this volume). Of the plesiosaurian clades present during the Callovian – Valanginian interval, only Plesiosauroidea was chosen to be displayed from the Plesiosauria tree, as the taxonomic status of pliosaurid taxa is problematic and their intrarelationships are currently poorly understood (Benson et al., 2013; Fischer et al., 2015; Knutsen, 2012b). The Plesiosauroidea phylogenetic analysis used the character list and matrix for Plesiosauria consisting of 76 operation taxonomic units (OTUs) and 273 characters. This matrix is derived from a characters and states of Benson and Druckenmiller (2014), with modifications and additional characters from this volume (Chapters 2, 3; Appendix 5). For the ophthalmosaurid ichthyosaurs, the data matrix and characters derived from Maxwell et al., (2016) with additional taxonomic information from Delsett et al. (2017). This matrix (Appendix 7), includes 27 taxa and 66 characters. The phylogenetic analyses were run in TNT v1.5 (Goloboff and Catalano, 2016), using Ratchet analysis combined with tree branch bisection reconnection (TBR). All characters were equally weighted and run using 1000 iterations, 10 Random Seed, 10 Random Addition Sequences with all trees kept.

To show lineage ranges, occurrence data was taken from PBDB with updates and additional occurrences from the literature and personal observations. The data for Ichthyosauria and Plesiosauria is currently incomplete and sometimes flawed: PBDB is updated by users and therefore the data is only as good as the contributor, meaning that the database is far from exhaustive in regard to the number of taxa and time ranges and can include errors in the alpha taxonomy (Prothero, 2015). Temporal distributions for single occurrence taxa (e.g. *Janusaurus lundi*) have a maximum-minimum range given by PBDB for the entire stage (in this case Tithonian). Although this is an under- or overestimation, we refrain for changing this for single occurrence taxa and taxa with limited stratigraphic control. As exact stratigraphic position of the taxon (*Gen. et sp. n*ov.) discussed in Chapter 3 of this volume (either Tithonian or Berriasian) is unknown, we increased the range of this taxon to encompass part of the Tithonian and Berriasian (late Volgian). Certain ranges from PBDB for individual taxa were increased from personal observations and publications, or adjusted, based on the updated temporal estimates for some stages (see Appendix 7, Tables A7.4-5; Ogg et al., 2016).

The time-calibrated phylogenies where generated in R (CRAN), using the *paleotree* (Bapst, 2012), *phytools* (Revell, 2012) and *strap* (Bell, 2015) packages. The method *DatePhylo* was used to calibrate the individual cladograms *a posteriori* from the ophthalmosaurid and plesiosauroid strict consensus trees respectively, using information from their temporal ranges. The R-script, tree files and range data for these analyses can be found in Appendix 7. This method only yields an approximate time-calibrated tree and not a "true" time-scaled tree (Bapst, 2014), as rates of branching, extinction and sampling are not incorporated and beyond the scope of the available data and this paper to estimate. As a result, the diversification events are solely based on range data. Due to the poor resolution of the Ophthalmosauridae strict consensus tree, some of the polytomies had to be artificially resolved using the package *ape* to run an ancestral states analysis. The poor resolution of this consensus tree is likely due to the small number of phylogenetic characters used (66) in comparison to the number of taxa (27) included, in addition to the low percentage of completeness for some of the taxa.

The time-calibrated trees from both groups, in addition to their occurrence data were analysed using the package *BioGeoBEARS* (Matzke, 2013, 2014) in R

(CRAN). *BioGeoBEARS* allows for multiple methods of biogeographic analysis to be tested including, DEC (dispersal, extinction and cladogenesis), DEC+J (DEC with founder-event speciation; Matzke, 2014), DIVA-LIKE (maximum likelihood version of Dispersal-Vicariance analysis), DIVA-LIKE + J (DIVA with founder-event speciation), BAYAREALIKE (maximum likelihood version of Bayesian Ancestral Area Estimation), BAYAREALIKE+J (BAYAREA with founder-event speciation). The Ln likelihood of each result can then be compared and the best fitting model (lowest Ln likelihood) can be chosen. This can in turn be informative as to the type of distribution the data displays, for example whether founder events or vicariance are reflected in the data (Matzke, 2014). Eight geographical areas of interest (GAIs) were used in the Plesiosauroidea analysis and seven GAIs in the ophthalmosaurid analysis. These include; the Boreal region, North America (Sundance Sea and Western Interior Seaway), Panthalassa (including the Neuquen Basin and Caribbean Corridor), Sub-Boreal Tethys (including UK and German formations), Tethys (Eastern Tethys), South Africa and the Volga Region in Russia. The GAIs were chosen as they represent either seaways, provinces or larger marine areas separated by land. The limitation of the number of regions is computational, as in theory these could be increased.

Each model was tested using the statistical model selection options in *BioGeoBEARS* (Matzke, 2013). with DEC+J being the befitting model for the data with the highest Ln likelihood and lowest AIC value (see Appendix 7, Table A7.6). The script for *BioGeoBEARS* and data sets are available in the supplementary information (Appendix 7).

Parsimony analysis of endemicity (PAE)

Parsimony analysis of endemicity (PAE) is a commonly used method to identify areas of endemism by using presence-absence data of taxa in geographical units (Morrone, 2014). The geographical units are represented as "taxa" and the individual species or genera are used as "characters", with "0" recording absence and "1" recording presence. Areas of endemism are defined from the strict-consensus tree as "clades" of area units supported by two or more synapomorphic species (i.e. endemic species; Morrone, 1994). Although still widely used, PAE has been criticised for the inherent assumptions required by the method that are not known for the fossil record.

These include the assumption that vicariance is the predominant speciation process, and that the absence of a taxon cannot be interpreted as meaning that the taxon was never present in that region (Brooks and van Veller, 2003; Casagranda et al., 2012). Exclusively endemic taxa result in regional "autapomorphies", which do not yield any information about overlapping distributions. Consequently, only generic taxonomic rank could be used in this case, as individual species are significantly less widespread than the generic distributions. This method has however been thoroughly tested and can be successful with smaller datasets (Morrone, 2014), it has therefore been utilised here, in favour of other more recently developed methods such as Lieberman-modified Brooks Parsimony Analysis (LBPA; Lieberman, 2000), where larger data sets are required (Maguire and Stigall, 2008).

The dataset including Kimmeridgian – Tithonian plesiosaurian and ichthyosaurian genera (17 genera from 9 regions), is by far the largest in comparison to Callovian – Oxfordian and Berriasian – Valanginian data, particularly for the Boreal region. Particularly for the Berriasian – Valanginian interval, a near lack of described material makes PAE impossible to utilise.

The geographical areas of interest (GAIs) used in PAE were separated based on localities bearing diagnostic material of Kimmeridgian-Tithonian in age (Appendix 7, Figure A7.2). These included Arctic Canada, the Moscow Basin, Western Europe (North-western Tethys), Eastern Europe, the Neuquen Basin, Mexico, Madagascar and Svalbard. A hypothetical root was also added into the data set, as is standard for PAE (Morrone, 2014). All GAIs has preserved material that can be identified to at least genus level for either ophthalmosaurid or plesiosaurian taxa. The analysis was performed in TNT V 1.5 using implicit enumeration (Goloboff and Catalano, 2016). The data set utilised for this analysis is available in the supplementary information (Appendix 7, Table A7.7)

Dissimilarity Indices

In addition to PAE, dissimilarity/similarity indices are a useful way of displaying taxa shared between different regions (Shi and Archbold, 1995; Vavrek, 2011). A major challenge with applying these methods to fossil datasets is the assumption that there are equal sampling conditions (each locality is subject to an identical collection effort), which cannot be presumed for fossil data. Despite this,

this type of analyses can provide useful indications of the shared diversity between different localities based on the data available data and/or can support observations from other forms of analysis.

The presence-absence data (Appendix 7; Tables A7.8) was converted into a distance matrix using the package *fossil* in R Studio (Vavrek, 2011) by using the Sørenson (Sorenson) similarity index. Although many other similarity/dissimilarity analyses have been developed, the Sørenson measure is one of the more widely used and works well on both binary and quantitative data (Vavrek, 2011). This method also places more emphasis on the shared taxa present than the unshared taxa, which is more applicable to fossil. In *fossil*, this equation is rewritten to show dissimilarity or distance between two items (in this case GAIs) where a value of 1 signifies that two communities/localities share no taxa and a value of 0 means that the faunas are identical (Vavrek, 2011). To minimise bias of unequal sampling conditions, insufficiently sampled GAIs (Madagascar, Eastern Europe and North-western Russia) were omitted from this analysis.

Results

Time-calibrated phylogenies and ancestral-state analysis

Two time-calibrated trees for the Plesiosauroidea (Figure 4.5) and ophthalmosaurid ichthyosaurs (Figure 4.6) were constructed. When interpreting the phylogenetic results, the strength of individual clades must be taken into account. For the cryptoclidid plesiosaurs, the relationships between the individual subclades are supported by multiple character-states and synapomorphies (Chapter 3, this volume). However, for the ophthalmosaurids, some taxa are poorly supported due to either to incomplete specimens or the fact that key areas of the specimens used as phylogenetic characters are poorly preserved (see Introduction, this volume).

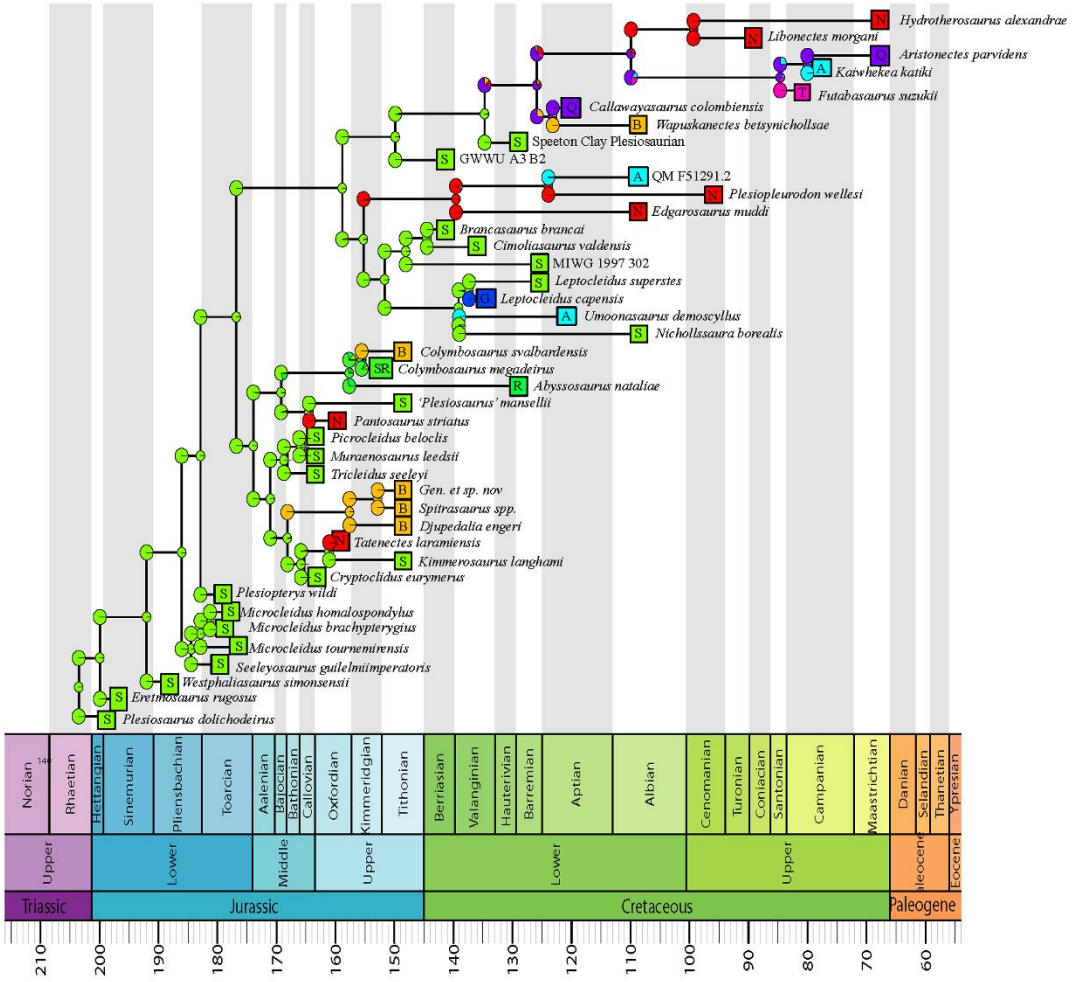

Figure 4.5: DEC + J ancestral states analysis of Plesiosauroidea with 8 geographic regions of interest (colours in brackets). Ln likelihood = -67.62, d = $3e^{-04}$, e = 0, j = 0.0402. The pie-charts shown on the time-calibrated trees indicate the probabilities based on the data that the ancestor of this clade derives from a given GAI. Probabilities are given for branch points and nodes. Abbreviations: **A**, Australia (cyan); **B**, Boreal Region (yellow); **G**, South Africa (dark blue); **N**, North American Sundance Sea and Western Interior Seaway (red); **Q**, Panthalassa and Neuquen (purple); **R**, West Russian Volga Region (green); **S**, sub-Boreal Tethys (lime green); **T**, Eastern Tethys (pink). Additional colours are colur combinations of the combined regions

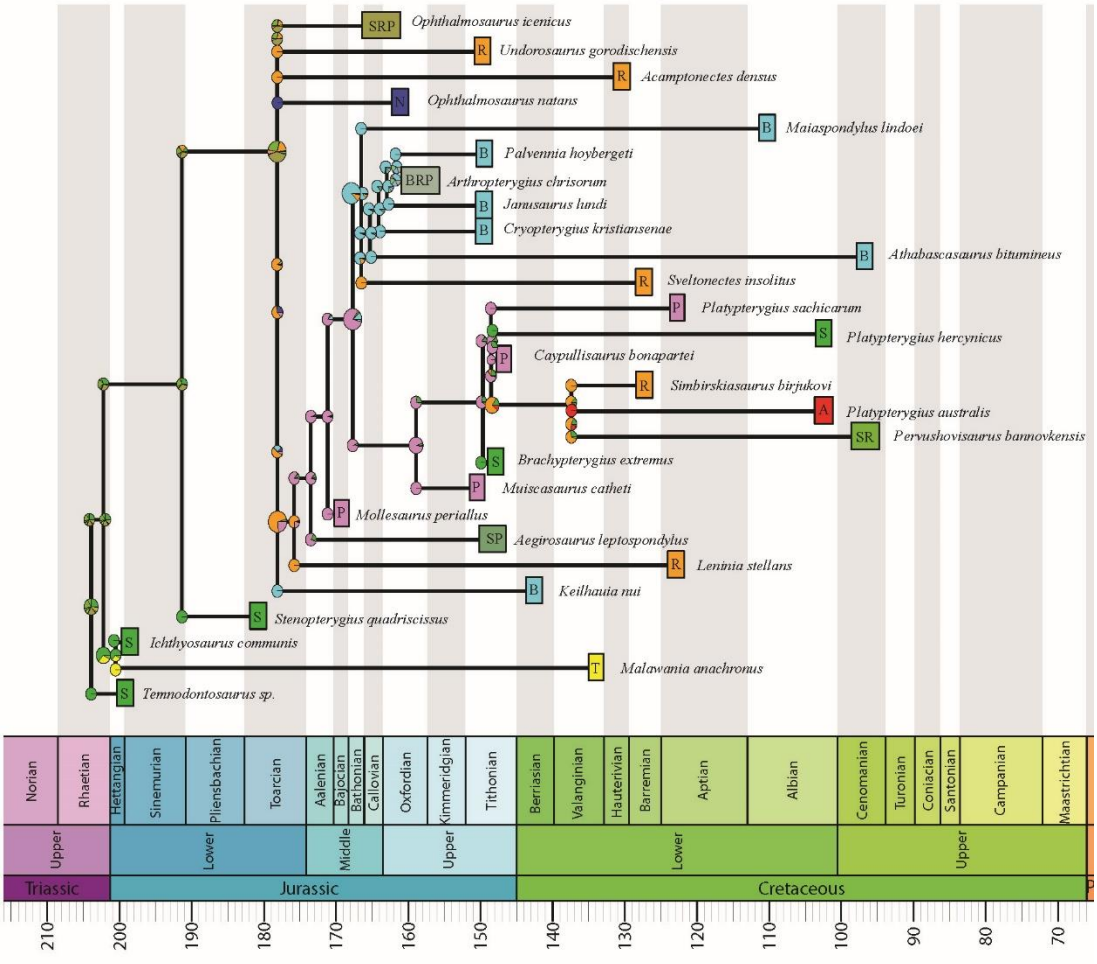

Figure 4.6: DEC + J ancestral states analysis of Ophthalmosauridae with 7 geographric regions of interest (colours in brackets). Ln likelihood = -71.62, d = 0.0044, e = 0.0126, j = 0.086. The pie-charts shown on the time-calibated trees indicate the probablilties based on the data that the ancestor of this clade derives from a given GAI. Probabilities are given for branch points and nodes. Abbreviations: **A**, Australia; **B**, Boreal Region (light blue); **N**, North American Sundance Sea (purple); **P**, Panthalassa and Neuquen (pink); **R**, West Russian Volga Region/Middle Russian Sea (orange); **S**, sub-Boreal Tethys (green); **T**, Eastern Tethys (yellow). Additional colours are colour combinations of the combined regions

Results from the model comparison test (Ln likelihood and AIC, Appendix 7, Table X) show that the DEC+J model displayed the best fit to the data for Plesiosauroidea (Figure 4.5) and Ophthalmosauridae (Figure 4.6). This analysis includes dispersal, extinction, cladogenesis with founder-event speciation.

Plesiosauroidea (Figure 4.5)

The results indicate a Sub-Boreal Tethyan origin for the derived families of Plesiosauroidea including Cryptoclididae. With major cladogenesis events taking place in the Middle Jurassic, Late Jurassic and Early Cretaceous. The parameter describing founder-event speciation (j = 0.04) is positive and displays a larger value than the parameters describing dispersal ($d = 3e^{-04}$) and extinction (e = 0). These results indicate that founder-event speciation is more significant in explaining the palaeobiogeography of Ophthalmosauridae than dispersal and extinction processes.

Ophthalmosauridae (Figure 4.6)

The DEC+J analysis indicate a complex historical distribution throughout the Jurassic – Cretaceous for Ophthalmosaurids. Although some relationships are unclear due to polytomies, a Panthalassic origin is indicated for the large clade of Boreal ophthalmosaurids, as well as some Cretaceous Russian and Sub-Boreal taxa. Major cladogenesis events are suggested in the Mid Jurassic and latest Jurassic. As in the Plesiosauroidea results, the parameter describing founder-event speciation (j = 0.086) is larger than the dispersal (d = 0.0044) and extinction (e = 0.0126) parameters. Again, this indicates that founder-event speciation appears more significant in explaining the palaeobiogeography of Plesiosauroidea than dispersal and extinction processes.

Parsimony analysis of endemicity (PAE) and distances measures

PAE on Kimmeridgian-Tithonian plesiosaurians and ophthalmosaurids

Due to the significant number of endemic genera and single occurrence taxa in many localities, few results could be attained using PAE (See Appendix 7, Figure A7.2). The resulting tree displays a single large polytomy including most of the GAIs except for Western Europe and Western Russia. This result is probably due to a combination of a low sample size and high local endemism (regional "autapomorphies") present at most localities.

Distance measures on Kimmeridgian-Tithonian plesiosaurians and ophthalmosaurids

The distance matrix presented in Table 4.4, shows the dissimilarity between five different GAIs for the Kimmeridgian – Tithonian interval. The low distance values between Western Europe and Western Russia observed in the PAE analysis, are also evident here. In addition, a close relationship between Arctic Canada and Western Russia can be extrapolated. This is as would be expected, as the few genera described from the Canadian Arctic are also present in Western Russia. Svalbard shows a much higher distance value (0.71-0.85) to other regions, due to the high number of single occurrence endemic taxa in this region, which probably represents a Lagerstätten bias. The remaining localities have 0.45 – 0.60 overlap in genera, reflecting a moderate number of shared taxa between these regions.

	SV	**AC**	**WR**	**WE**	**NQ**
AC	0.82				
WR	0.71	0.33			
WE	0.73	0.60	0.38		
NQ	0.85	0.50	0.45	0.50	
MX	0.80	0.60	0.50	0.55	0.43

Table 4.1: Distance matrix using the Sørensen measure for selected GAIs, utilising the *fossil* package (Vavrek, 2011) in R (CRAN core group), 1= no overlapping genera, 0 = identical genera. **Abbreviations: SV**, Svalbard; **AC**, Arctic Canada; **WR**, Western Russia; **WE**, Western Europe; **NQ**, Neuquén Basin, Argentina.

Discussion

In order to estimate historical distributions of extinct macrofauna, several abiotic and biotic factors must be taken into account. These include the drivers of biogeographical distribution and regional extinction (e.g., sea level, climatic change and interspecific competition), the taxonomic status of specimens, as well as taking into account palaeobiogeographic records for invertebrate and microfossil taxa. Here we attempt to objectively address inconsistences surrounding the taxonomic status of recently described marine reptiles, which would exert an affect upon the results of biogeographic distribution analyses. We discuss the taxonomic diversification, survival and extinction of plesiosaurs and ophthalmosaurid ichthyosaurs in light of

the results reported here and suggest possible hypotheses for the origins of major plesiosauroid and ophthalmosaurid clades. In addition, we provide hypotheses for the observed provinciality of Boreal clades of marine reptiles. Finally, we discuss the implications widespread distribution of certain taxa and the effects this may have had on their extended temporal survival.

The taxonomic status of Boreal marine reptiles – relationships, referrals and distribution

Many publications have questioned the endemic nature of the Slottsmøya Member marine reptiles, as there are clear morphological similarities between these taxa and those from other areas (Arkhangelsky and Zverkov, 2014; Benson and Bowdler, 2014; Roberts et al., 2014; Roberts et al., 2017; Tyborowski, 2016; Zverkov et al., 2015). Based on the results of this study and other work (Chapters 2-3, this volume), clarification and taxonomic revision of several cryptoclidid and ophthalmosaurid specimens from lower latitudes.

Few ichthyosaur and plesiosaur specimens from other regions have been deemed referable to the Slottsmøya Member taxa. Cervical material from the Kimmeridge Clay Formation (MANCH LL5519g) has been tentatively referred to the Slottsmøya Member genus cf. *Spitrasaurus* by Benson and Bowdler (2014) on the basis of a lateral ridge on the cervical vertebrae. As this anatomical feature is also present on other cryptoclidid material (Andrews, 1910; Chapter 3, this volume), it is not diagnostic for *Spitrasaurus* and the material referred to this genus should instead be referred to *Cryptoclididae* indet.

It has also been suggested that the ophthalmosaurid ichthyosaur taxa *Cryopterygius kristiansenae* and *Janusaurus lundi*, may be referable to other taxa (Arkhangelsky and Zverkov, 2014; Tyborowski, 2016; Druckenmiller et al., 2012; Zverkov et al., 2015): *J. lundi* to the widespread taxon *Arthropterygius chrisorum* and *C. kristiansenae* to the Russian genus *Undorosaurus*, based on shared appendicular features. However, the limited overlapping cranial material for *A. chrisorum* and *Undorosaurus* with the Slottsmøya Member taxa, makes these referrals problematic (Roberts et al., 2014; Zverkov et al., 2015). This is also reflected in the various positions of *A. chrisorum* and *Undorosaurus gorodischensis* in phylogenetic analyses (summarised in Fernández and Campos, 2015), an issue

which may result from too few descriptive characters versus the number of taxa currently used in ophthalmosaurid phylogenetic analyses. Therefore, until cranial material is available for *A. chrisorum* and *Undorosaurus*, *C. kristiansenae* and *J. lundi* should be regarded as separate taxa (Arkhangelsky and Zverkov, 2014; Druckenmiller et al., 2012; Zverkov et al., 2015).

Tyborowski (2016) described *Cryopterygius kielanae* (GMUL 3579-81), from the Tithonian of Poland, thus of the same age as the Slottsmøya Member. Tyborowski (2016), proposed allocation to the genus *Cryopterygius* on the basis of five post cranial features. However, these features are either variable in the holotype of *C. kristiansenae* (the number of distal facets on the humerus), present in several ophthalmosaurid taxa or ambiguous either on *C. kielanae* or *C. kristiansenae* (see Appendix 7 for full discussion). On the basis of these arguments, GMUL 3579-81 is not referable to *Cryopterygius* and nor is it complete enough to warrant the erection of a new genus and should therefore instead be referred to as *Ophthalmosauridae* indet.

Zverkov et al. (2015) referred a partial ichthyopterygian forelimb to *Ophthalmosaurus* sp. from the North-western Russian part of the Boreal Region, based on similarities of the preaxial accessory element and lack of a posterior torsion of the ulnar facet. Contrary to the views of Zverkov et al. (2015), these features are not diagnostic of *Ophthalmosaurus* and can be found in other taxa (e.g. *Janusaurus lundi*) (Roberts et al., 2014; B. Moon, *pers. comm.*). In addition, the preaxial accessory element facet is clearly separated from the radial facet by a distal dorsal-ventral ridge, a feature not observed in *Ophthalmosaurus* (Moon and Kirton, 2016). Thus, the evidence presented in Zverkov et al. (2015) is not sufficient to warrant a referral to the genus *Ophthalmosaurus* without additional material and should instead be referred to *Ophthalmosauridae* indet. Based on this conclusion, no unambiguous records of *Ophthalmosaurus* are known from the Late Jurassic Russian high latitudes.

Diversification, distribution and extinction events for marine reptiles – a link to eustatic and climatic changes?

Tennant et al. (2016b) demonstrated a correlation between sea level and taxonomic diversity in both terrestrial and marine reptiles, where sea level fall

(regression) contributed to loss of diversity for some reptilian clades across the Jurassic-Cretaceous boundary. The ancestral states analyses described in this paper also show that episodes of sea level fall coincided with taxonomic loss, while increased dispersal and taxonomic diversity coincided with transgressional events, thus supporting the interpretations of Tennant et al., (2016b).

Mid – early Late Jurassic

Based on the time-calibrated phylogenies and ancestral states analysis, the major diversification and dispersal events of the Plesiosauroidea and Ophthalmosauridae appear to have initiated in the late Early - Middle Jurassic. The Early – Mid Jurassic "Ophthalmosaurid Radiation" as described by Fischer et al. (2016) is clearly supported by our new analyses. This diversification event at least partly coincided with the mid Callovian transgression, which allowed migration of taxa between the Tethyan Realm through the Caribbean Corridor into Panthalassa (Barrientos-Lara et al., 2016; Gasparini, 1996; Gasparini et al., 2002; Gasparini and Fernández, 2005), creating a link between the Northern and Southern hemispheres. As the DEC+J model demonstrated the best fit to the data, it suggests that a founder-effect may at least in part describe some of the diversification. This in turn fits with the opening of new dispersal routes during sea level highstands during the Mid Jurassic.

Marine reptile remains from the Mid-Late Jurassic transition in the Boreal Realm during the are rare and often of uncertain taxonomic status, therefore the Boreal distribution of this group is poorly known during this interval. However, a southwards dispersal of Boreal invertebrate genera is evident through the North-eastern Atlantic during this interval, indicating that the North-eastern Atlantic was an open seaway at this stage (Dromart et al., 2003). During the Mid-Late Jurassic climatic cooling (Cecca et al., 2005; Korte et al., 2015: Boreal cephalopods, brachiopods and bivalves manage to colonise lower-latitudes, while a northern migration of warm-water adapted Tethyan taxa appears to be limited (Zakharov et al., 2002). During this interval, numerous cryptoclidid taxa disappear from southern latitudes, however ophthalmosaurids continue to diverge and some genera (e.g. *Ophthalmosaurus*) continue into the Late Jurassic (Moon and Kirton, 2016).

Late Jurassic – earliest Cretaceous

Although several potentially restricted Boreal clades were recovered in the phylogenetic analyses for cryptoclidid plesiosaurs and ophthalmosaurid ichthyosaurs, other taxa closely related to Western European and Panthalassic taxa are also present in this region during the Late Jurassic. The ancestral states analysis indicates multiple dispersal events occurred during the Late Jurassic, with at least two separate diversification events into the Boreal Region for the cryptoclidid plesiosaurs and the ophthalmosaurid ichthyosaurs. For the ophthalmosaurid ichthyosaurs, the large Boreal clade (*Cryopterygius kristiansenae*, *Janusaurus lundi*, *Palvennia hoybergeti*, *Arthropterygius chrisorum* and *Athabascasaurus bituminous*) the analysis indicates a Panthalassic origin, whereas for the large Boreal cryptoclidid clade, a Sub-Boreal Tethyan origin is indicated. Curiously, no high-latitude genera of plesiosaurians or ichthyosaurians have been found in lower-latitude regions during the Late Jurassic, while lower-latitude genera (e.g. *Colymbosaurus*, *Pliosaurus*) appear to have a wider distribution into high-latitude areas. This may suggest a predominately south to north distribution pattern, with origination starting in lower-latitude regions.

The ancestral states analysis show that the Kimmeridgian transgression and flooding of the Russian platform allowed the ophthalmosaurids and cryptoclidids to increase in taxonomic diversity and areal distribution (Benson and Druckenmiller, 2014; Fisher et al., 2016). Northward migration of Tethyan ammonite fauna into the Western Russian Sea through the Brest (Pripyat) Strait, has been correlated with eustatic sea level rise during the Kimmeridgian and Tithonian (Zakharov and Rogov, 2003). and this ammonite migration corresponds well with reported marine reptile distributions. Arkhangelsky et al. (*in press*) proposed a distributional pattern for *Colymbosaurus* through the Brest Strait during the late Kimmeridgian – early Tithonian. This taxon is present in the Kimmeridgian and Tithonian of Western Tethys (*Colymbosaurus megadeirus*; Benson and Bowdler, 2014) and from the Tithonian of the Russian Platform (*Colymbosaurus* indet.) and Boreal Region (*Colymbosaurus svalbardensis*) (Arkhangelsky et al., *in press*; Roberts et al., 2017). Another specimen referable to *Colymbosaurus cf. svalbardensis* from the Late Jurassic – Early Cretaceous deposits of Ellesmere Island is also currently under description (Smith and Roberts, *in prep*.), indicating that this taxon had a wide distribution. A similar distribution pattern has also been described for an

ophthalmosaurid ichthyosaur taxon, *Arthropterygius* (Zverkov et al., 2015). Although not as well sampled as the Russian Platform, indeterminate cryptoclidid and ophthalmosaurid remains from Eastern Greenland and Northern Norway suggest that the Northeast Atlantic Seaway was also utilised by marine reptiles during the Kimmeridgian and Tithonian (AJR *pers. obs.*; PMO and MGUH collections).

In the Boreal Realm, a circumpolar distribution of invertebrate fossils suggests that although partially isolated from other regions during the late Tithonian – earliest Cretaceous, significant invertebrate taxonomic diversity was shared between different Boreal localities as well as with the Russian Platform (Zakharov et al., 2002). Although limited data is currently available for marine reptiles, shared diversity is evident between Arctic Canada and the Russian Platform based on our dissimilarity matrix (0.33). The results from this study show that the Slottsmøya Member Lagerstätte from Spitsbergen does not share a significant number of marine reptile taxa with Arctic Canada (0.82) or the Russian Platform (0.71). In comparison to the contemporaneous Kimmeridge Clay Formation, the Slottsmøya Member has an increased taxonomic diversity at a generic and specific level in both cryptoclidid plesiosaurs and ophthalmosaurid ichthyosaurs, especially when considering the numerous specimens of these groups that are currently under description from the Slottsmøya Member. The high number of endemic marine reptile taxa in the Slottsmøya Member is reflected in the high distance measure observed in this study. However, this could potentially be due to an artefact of preservational bias (Benson et al., 2010). Thereby some or all of the Slottsmøya taxa may be present in other Boreal areas.

Although preservational bias may be the cause of unusually high species richness in the Slottsmøya Member, an additional factor may have influenced the provinciality of the region. Little is known about the Late Jurassic palaeogeography north of Spitsbergen and some palaeogeographic reconstructions have hypothesized the existence of landmasses at this location ("Lomonosov Land"; Doré, 1991; Dypvik et al., 2003). Due to the Svalbard's close proximity to Northern Greenland at this time (Dypvik et al., 2003), additional landmasses may have restricted access to the region during regressional periods and thereby enforced provincialism. Our ancestral states analysis provides evidence for Boreal speciation in some clades, and thus indirectly supports the interpretation of endemism. In contrast, such a localized

endemism of marine reptiles in the Slottsmøya Member is not reflected in the invertebrate fossil record (Zakharov, 1987; Zakharov and Rogov, 2008; Zakharov et al., 2002). However, many of the invertebrate clades included in these studies have a pelagic larval stage, which have been shown to obscure patterns of connectivity (Hansen, 1980; Herrera et al., 2015). Invertebrate larvae may have been able to pass geographical restrictions impassable for large marine macro fauna. A better understanding of the palaeogeography of this region is necessary to clarify whether the area in which the Slottsmøya Member was deposited could have experienced periods of temporary isolation during the latest Jurassic.

The Early Cretaceous was characterized by a drop in taxonomic diversity of both cryptoclidids and ophthalmosaurids, which was likely coupled with major regressions and climatic changes (Tennant et al., 2016b). However, during the terminal Jurassic, a higher generic diversity for cryptoclidid plesiosaurs and ophthalmosaurid ichthyosaurs is recorded from mid-high latitudes as compared to the highly sampled lower-latitude regions. Similar to the last occurrences of the rhomaleosaurid plesiosaurs in the Callovian, the two cryptoclidid taxa which are the only members of Cryptoclididae to cross over into the Cretaceous are described from the Boreal Region (*Gen. et sp. nov*; Chapter 3, this volume) and the Russian Platform (*Abyssosaurus nataliae*; Berezin, 2011a). These taxa are belong to different subclades (the Colymbosaurinae and non-Colymbosaurinae), showing that multiple linages crossed the Jurassic – Cretaceous boundary (Figure 4.7). Through both genetic analysis and studies of fossil assemblages it is well known that organisms may retreat to refugia in times of climatic and environmental change, as exemplified by terrestrial organisms during the last glacial maximum (Provan and Bennett, 2008). The active metabolism of plesiosaurians and ichthyosaurians may have increased their ability to colonise high latitude, cold-water environments (Houssaye, 2013), where there would be no or less competition with ectothermic marine reptiles.

Taxonomic survival of well-dispersed plesiosaurian and ichthyosaurian genera

A wider biogeographic range for a given taxon is considered to reduce the chance of global extinction due to regional climatic and environmental changes, thus the taxon a higher survivability (Mittelbach et al., 2007). This implies that cosmopolitan taxa are expected to show a longer stratigraphic range and a lower

extinction rate compared to endemic taxa. In general, pelagic marine reptiles had a widespread distribution and demonstrate a high dispersal potential, although provincialism is evident in some areas (Bernard et al., 2010; Fischer et al., 2011b; Motani, 2005). The Early-Mid Jurassic "Ophthalmosaurid Radiation", is evidence for rapid diversification and high evolutionary rates for this clade (Fischer et al., 2016). Although an increase in taxonomic diversity is present throughout the Late Jurassic, some of the genera from the Middle and early Late Jurassic have a continued presence throughout the Late Jurassic and into the Cretaceous, demonstrating slow rates of phenotypic evolution (Fischer et al., 2016). Based on the data available from this study, ophthalmosaurid and cryptoclidid genera with wider biogeographic distributions also display longer stratigraphic ranges.

The genus *Ophthalmosaurus* had a recognised range from the Callovian (Moon and Kirton, 2016) to the Berriasian (Fischer et al., 2012; McGowan, 1978; Zverkov et al., 2015), spanning a period of at least 20 million years. The majority of this long temporal range is down to a single species, *Ophthalmosaurus icenicus* (Callovian – Tithonian; Moon and Kirton, 2016). The extreme longevity described for the genus *Ophthalmosaurus* and in particular the species *O. icenicus*, is undoubtedly incorrect, as the taxonomic survival of a single species over such an extended timespan is unlikely. As a result, it has been suggested, that there may be greater - as yet unrecognised taxonomic diversity in *Ophthalmosaurus* than previously estimated (Fernández and Campos, 2015), as ichthyosaurian material is hard to speciate on the sole basis of post-cranial material: complete articulated skeletons of this taxon which include crania are rare in the Late Jurassic (Moon and Kirton, 2016). In addition, much of the material referred to this genus in the literature (particularly from the Berriasian), is fragmentary and taxonomically ambiguous, and could yet represent a different taxon (e.g. Zverkov et al., 2015).

Although not as widespread, specimens referred to *Arthropterygius* are recorded from the Kimmeridgian of Northern Canada (Maxwell, 2010), the Tithonian of Argentina (Fernández and Maxwell, 2012) and the Russian Platform (Zverkov et al. 2015). A third ophthalmosaurid genus *Aegirosaurus*, has a documented distribution in the Northern and Southern hemispheres during the Late Jurassic, continuing into the Early Cretaceous in the Northern Hemisphere (Fischer et al., 2011a; Gasparini et al., 2015a). The paraphyletic Cretaceous ophthalmosaurid

genus *Platypterygius* also display a wide geographic distribution and long stratigraphic range; his genus is problematic to include in palaeogeographic analyses as accurate assignment to this taxon is problematic because of the low (postcranial) phenotypic rates observed in other Cretaceous taxa, resulting in the referral of several unrelated specimens to the genus. Although *Platypterygius* has undergone multiple revisions (Fischer, 2012, 2016), a consensus diagnosis for this genus has yet to be defined, the palaeogeographic range of this genus may currently be exaggerated.

In contrast to ophthalmosaurids, plesiosaurians have a more restricted distribution during the Mid Jurassic – Early Cretaceous. The genus *Colymbosaurus* is the only cryptoclidid plesiosaur to show an extended biogeographic distribution from the Western Tethys to the Boreal region, and is also the only genus with an extended stratigraphic range (Roberts et al., 2017). The genus *Pliosaurus* is also recorded from both the Northern and Southern hemispheres during this interval, but as a "waste-basket" taxon: the genus is difficult to identify, usually described from incomplete and fragmentary specimens, despite long historical interest (Knutsen, 2012b). Therefore, any stratigraphic and biogeographic range estimates for *Pliosaurus* are ambiguous at best.

Although subject to alpha taxonomy disputes, the extended temporal range of some marine reptile taxa during the Late Jurassic – Early Cretaceous interval, may be in part due to the extended palaeobiogeographical distribution known for these taxa. Combined with low rates of phenotypical evolution in some groups (Fischer et al., 2016), extended biogeographic distributions may increase taxon survivability/temporal range. Late Cretaceous bivalves show that a higher dispersal ability had a strong negative correlation with speciation rate (Jablonski and Roy, 2003). The reduced phenotypic rates of evolution observed in ophthalmosaurids, could be the product of a similar phenomenon. However, our current understanding of the speciation process in marine reptiles is limited, but this possibility should be explored in future work. With the discovery of new material and/or the redescription of plesiosaurian and ichthyosaurian genera from this time interval, some or all genera included here may be shown to have longer temporal ranges and wider or more restricted (e.g. *Ophthalmosaurus*) spatial distributions than are currently known. Other groups of pelagic marine vertebrates, such as thalattosuchians, should

be incorporated into in the future, to increase the sample size and test the presence of a positive correlation between temporal distribution and stratigraphic range. In addition, such a relationship between distribution and stratigraphic range may also be strengthened if a more inclusive approach was utilised, including taxa that have been omitted in this study (e.g., *Cryopterygius kielanae*).

Concluding remarks and future work

The clear similarity between the taxonomic make-up of plesiosaurian and ichthyosaurian assemblages in Western Russia, Western Europe and Arctic Canada found in this study suggests an exchange between Boreal and lower latitude faunas during the Kimmeridgian and early-mid Tithonian interval. Results from ancestral states analysis in this study, indicate an origin from lower-latitude regions for Boreal cryptoclidid and ophthalmosaurid clades. Although Tethyan and Boreal marine reptile taxa were both present in the Middle Russian Sea, few taxa present in the Boreal region are recorded in other regions. This likely indicates geographic, climatic or other ecological boundaries existed between these regions that acted against migration. Indeed, latitudinal gradients have been observed for numerous invertebrate taxa and thalattosuchians, indicating that adaptation to cooler climates may have been necessary to colonize the Boreal region. However, this fails to explain the endemic genera found in the Slottsmøya Member of Spitsbergen, especially given its geographical position lying between the northern border of the Middle Russian Sea and Arctic Canada. The high taxonomic diversity in the Slottsmøya Member Lagerstätte is likely at least in part a product of preservational bias, implying that some of these taxa will likely be found elsewhere in the Boreal Region in the future. However, some of the endemism may in part be due to the terminal Jurassic regression. As so little is known of the palaeogeographic configuration of landmasses north of present-day Spitsbergen, shallower areas may have represented a periodic geographical barrier for marine reptiles, preventing migration to the rest of the Boreal Region.

Acknowledgements

The authors wish to thank the museum curators and researchers that assisted AJR during collection visits; S. Chapman and L. Steel (NHMUK), A. S. Smith (NOTNH), M. Riley (CAMSM), E. Howlett (OUM), M. Fernández (MOZ, MLP), G. Wass (PETMG), N. Clark (GLAHM), M. Evans (LEICS), K. Sherburn (MANCHM), S. King (YORKM) and G. Cuny (MGUH). D. Foffa, V. E. Nash, D. Legg, B. Moon, S. Etches, K. Hryniewicz, Ø. Hammer, V. Fischer, J. L. Wujek and E. Martin-Silverstone are thanked for discussion. We appreciate the helpful suggestions provided by V. E. Nash, I. Harding, P. S. Druckenmiller and D. Foffa, which improved the manuscript. We have the utmost gratitude to all the volunteers of the Spitsbergen Mesozoic Research Group, who have spent numerous summer holidays excavating the Slottsmøya marine reptiles. Finally, we thank the funding institution Syntheyes for financially supporting AJR to visit the collections at MGUH.

Chapter 5

Concluding remarks and future work

Concluding remarks and future work

This thesis has provided detailed descriptions of new cryptoclidid material from the Late Jurassic – Early Cretaceous Slottsmøya Member of central Spitsbergen with comparisons to penecontemperanous taxa and demonstrated possible distribution patterns and causes. A brief summary of the results from each chapter is presented here, their ties and implications, as well as recommendations for future work.

5.1 Chapter 1 – Methods for excavation and preparation of the Slottsmøya marine reptiles

The aim of this methodology chapter was to present the techniques and equipment used to excavate and prepare the Slottsmøya Member marine reptiles. The presented methods made the subsequent scientific work of this study possibly and thereby justified documentation in this volume. The main findings of this work were; new excavation techniques in congelifractioned shales and permafrost; the temporary adhesive Mowilith can function as alternative to paraloid for stabilisation; the use of cynoacryloids are necessary for preserving heavily fractured material and that using Computed Tomography can reduce damage to specimens during preparation. CT imagery can be used as a visual guide during manual preparation, as well as offer opportunities of elimination of physical preparation entirely through virtual reconstructions.

5.2 Chapter 2 – The osteology of *Colymbosaurus svalbardensis*

Although numerous specimens of *Colymbosaurus* are available in multiple museum collections, only a few have been described in detail. This chapter presents a new specimen of *Colymbosaurus svalbardensis* from the Slottsmøya Member, adding significant postcranial information to this taxon. Intraspecific variation in specimens of *Colymbosaurus* from the UK and the Slottsmøya Member was documented and resulted in the revision of the diagnostic features of this genus. Several important UK *Colymbosaurus* specimens were also identified in this study, but warrant a more detailed description of their osteology. *Colymbosaurus* remains the only cryptoclidid genus with a confirmed presence in multiple regions during the Late Jurassic.

5.3 Chapter 3 – The description of a new taxon of cryptoclidid plesiosaur

In Chapter 3, the Slottsmøya Member cryptoclidid specimen PMO 224.248 was described as a new genus and species based on a unique character combination and autapomorphies. The specimen is exceptional in that it preserves a complete cranium, contributing significant information to our understanding of the morphology of cryptoclidid crania (Figure 5.1). The inclusion of this new taxon to the phylogenetic data matrix utilised in Chapter 2, as well as the incorporated numerous changes and three additional characters, resulted in an altered topology of the Cryptoclididae phylogenetic tree. This phylogenetic work formed the basis for the cryptoclidid time-calibrated phylogeny presented in Chapter 4.

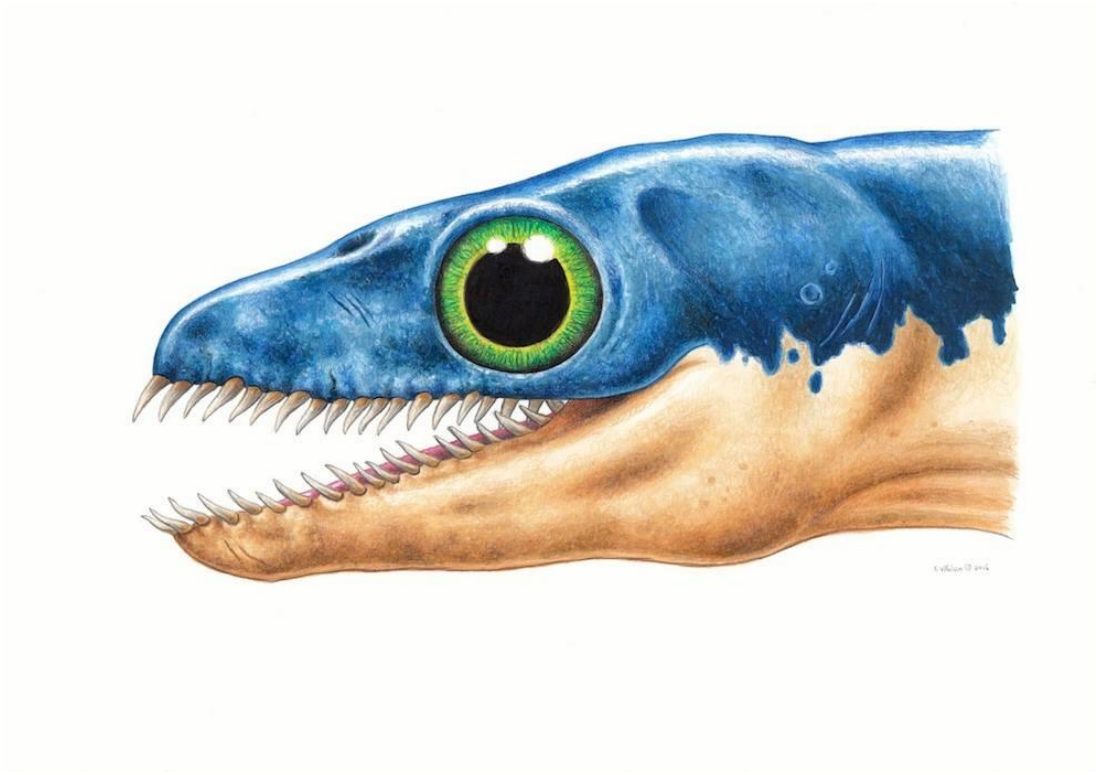

Figure 5.1: A reconstructed profile of PMO 224.248. Illustrated by Esther van Hulsen.

5.4 Chapter 4 – A preliminary report on the palaeobiogeography of Boreal marine reptiles

This paper is an effort to collect all the published records on plesiosaurian and ichthyosaurians during the Callovian – Valanginian interval, supplemented by unpublished material from personal observations. Although flawed due to the limited

data available, we attempted to show more quantitative methods in tackling the hypothesised endemic Boreal marine reptile clades. Results from this study concur with previous work in showing that marine reptile distributions north in to the Boreal Region were heavily dependent on eustatic sea level, due to the geological structure of the seaways connecting to the Tethyan Region. For some marine reptile groups, the cooler climate of the Boreal Region may have restricted colonisation. Certain taxa of marine reptiles which show a global or near-global distribution, also display an extended temporal range beyond that for taxa with a more restricted distribution. This relationship requires further testing with the inclusion of other marine reptile clades. The observed endemicity in some Slottsmøya Member marine reptile taxa may be an artefact of Lagerstätten bias (Benson et al., 2010). However, uplifted regions North of Svalbard, may have played a role in restricting the locality during regressional periods. Further work in the description of other Boreal Realm marine reptile specimens, as well as the detailed palaeogeography work at the highest latitudes are necessary to reach a consensus.

5.5 The implications and impact of this work

In the introduction to this volume, Cryptoclididae is described as a well-known yet enigmatic family of long-necked plesiosaurs. As a result of a long history of description (e.g. Andrews, 1910), previous studies attempting to diagnose genera and species prior to the widespread use of phylogenetic analysis have been challenging (Brown, 1981; Brown et al., 1986). With the redescription of *Colymbosaurus*, the addition of a cryptoclidid taxon and a detailed revision of cryptoclidid character states, this study has provided a strengthened view of cryptoclidid intrarelationships.

The work on palaeobiogeography of the Boreal marine reptiles, compliments the previous works by Arkhangelsky et al. (*in press*), Zverkov et al., (2015) and Bardet (2014), with a summary and more detailed image of the factors behind the observed distributions and intrarelationships in some clades of marine reptiles. Although this work offers a start in interpreting these factors, the study of Mesozoic marine reptile palaeobiogeography is still in its infancy.

5.6 Future work

The Slottsmøya Member marine reptile Lagerstätte has provided a substantial number of new plesiosaurian and ichthyosaurian specimens to the scientific community. However, a significant amount of work remains on the descriptions of the excavated specimens. At least one new cryptoclidid taxon remains to be described (PMO 212.662), along with several specimens awaiting preparation (e.g. PMO 224.247; PMO 222.671 PMO 216.863; PMO 214.452; PMO 222.668). Some of these currently unprepared specimens could represent new genera and/or species, or add morphological information to the described cryptoclidid taxa from the region. In addition, other museum collections from Boreal Region localities (East Greenland, Arctic Russia and Ellesmere Island) hold undescribed material which will add to our current understanding of high latitude cryptoclidids.

The specimen described in Chapter 3 (PMO 224.248), offers multiple opportunities to make new and test existing hypotheses on the palaeobiology of cryptoclidid plesiosaurs. Further studies on the internal cranial anatomy of the specimen could be performed, by virtually decompressing the cranium. As a result, a virtual endocast of the braincase would be available, offering a comparison to similar work to on elasmosaurid plesiosaurs (Zverkov et al., 2017). The exquisite preservation of the cervical vertebral series in PMO 224.248, offers new prospects for interpreting neck flexibility in long-necked plesiosaurs. Although a recent study proposed several hypotheses regarding neck flexibility in cryptoclidids (Noè et al., 2017), these require testing. PMO 224.248 represents a perfect study object for this work, as the neck was preserved in articulation and the original intervertebral spacing documented.

To increase our knowledge of the palaeobiogeography of marine reptiles, significant work remains on the phylogenetic framework for ophthalmosaurid ichthyosaurs, along with further work on the phylogenetic characters in plesiosaurs. For other marine reptile groups to be incorporated in future palaeobiogeographic work (e.g. thalattosuchians), numerous redescriptions of historical specimens are required, as well as a phylogenetic consensus on the interrelationships between individual clades. Although more taxonomic information should be incorporated, other types of palaeobiogeographical analyses could be tested on the existing data. The Simpson similarity measure, also represents an ideal candidate for palaeobiogeographic studies on fossil data, as it can account for variability in sample

sizes (Vavrek, 2011). Further sampling of the Middle Jurassic, early Late Jurassic and Early Cretaceous of Spitsbergen, could shed new light on the complex palaeobiogeographic distribution of marine reptiles in the Boreal Sea during this interval.

The latitudinal gradients observed in some marine reptile groups (Thallatosuchia: Tennant et al., 2016a), requires further testing. Histological sections of thalattosuchian taxa, should be compared in detail to other marine reptile clades present at high latitudes. This may provide insight into how some marine reptile clades where able to colonise colder regions, while others appear restricted. Histological sections of plesiosaurian taxa present at higher and lower latitudes (e.g. *Colymbosaurus*), should also be compared with other contemporaneous taxa only present in a single region. Any differences in the bone microstructure may indicate cold water adaptions necessary for colonising high latitude cold water environments.

In summary, the Slottsmøya Member marine reptile Lagerstätte, in combination with new and redescribed material other Boreal, Sub-Boreal regions and the recently publicly opened Etches Collection (UK), has and will continue to improve our knowledge on Late Jurassic – earliest Cretaceous macro-faunal diversity, temporal ranges and historical distributions in the Northern Hemisphere.

Literature Cited

Aberhan, M. 2001. Bivalve palaeobiogeography and the Hispanic Corridor: time of opening and effectiveness of a proto-Atlantic seaway. *Palaeogeography, Palaeoclimatology, Palaeoecology* 165:375-394.

Alsen, P., and J. Mutterlose. 2009. The Early Cretaceous of North-East Greenland: A crossroads of belemnite migration. *Palaeogeography, Palaeoclimatology, Palaeoecology* 280:168-182.

Andrews, C. W. 1909. On some new Plesiosauria from the Oxford Clay of Peterborough. *Annals and Magazine of Natural History Series VIII* 4:418-429.

Andrews, C. W. 1910. *A descriptive catalogue of the Marine Reptiles of The Oxford Clay Based on the Leeds Collection in the British Museum (Natural History).* British Museum (Natural History), London. 205 pp.+x plates

Andrews, C. W. 1913. *A descriptive catalogue of the marine reptiles of the Oxford Clay, Part 2*.. British Museum (Natural History), London. xix +206 pp

Arkhangelsky, M. S. 1997. On a new ichthyosaurian genus from the lower Volgian substage of the Saratov, Volga Region. *Paleontological Journal* 31:87-90.

Arkhangelsky, M. S., and N. G. Zverkov. 2014. On a new ichthyosaur of the genus *Undorosaurus*. *Proceedings of the Zoological Institute RAS* 318:187-196.

Arkhangelsky, M. S., N. G. Zverkov, M. A. Rogov, I. M. Stenshin, and E. M. Baykina. *in press.* Colymbosaurines from the Upper Jurassic of European Russia and their implication for paleobiogeography of marine reptiles; pp. *i*n B. P. Kear, S. Sachs, A. Smith, and P. D. Druckenmiller (eds.), *Plesiosaurs - Mesozoic Sea Dragons.* Springer - Vertebrate Paleobiology and Paleoanthropology Series.

Avizo ® Fire V.8 – 3D analysis software for materials science, 2013. http://www.vsg3d.com/avizo/fire

Bapst, D. W. 2012. paleotree: an R package for paleontological and phylogenetic analyses of evolution. *Methods in Ecology and Evolution* 3:803-807.

Bapst, D. W. 2013. A stochastic rate-calibrated method for time-scaling phylogenies of fossil taxa. *Methods in Ecology and Evolution* 4:724-733.

Bapst, D. W. 2014. Assessing the effect of time-scaling methods on phylogeny-based analyses in the fossil record. *Paleobiology* 40:331-351.

Barash, M. S. 2008. Evolution of the Mesozoic oceanic biota: response to abiotic factors. *Oceanology* 48:538-553.

Bardet, N., J. Falconnet, V. Fischer, A. Houssaye, S. Jouve, X. Pereda-Suberbiola, A. Pérez-García, J.-C. Rage, and P. Vincent. 2014. Mesozoic marine reptil palaeobiogeography in response to drifting plates. *Gondwana Research* 26:869-887.

Bardet, N., and P. Godefroit. 1998. A preliminary cladistic analysis of the Plesiosauria. *Journal of Vertebrate Paleontology* 18:26A.

Bardet, N., J.-M. Mazin, E. Cariou, R. Enay, and J. Krishna. 1991. Les Plesiosauria du Jurassique supérieur de la province de Kachchh (Inde*). Comptes Rendus de l'Académie des Sciences - Series II* 313:1343-1347.

Barrientos-Lara, J., Y. Herrera, M. Fernández, and J. Alvarado-Otega. 2016. Ocurrence of *Torvoneustes* (Crocodylomorpho, Metriorynchidae) in marine Jurassic deposits of Oaxaca, Mexico. *Revista Brasileira de Paleontologia* 19:415-424.

Benson, R. B. J., and T. Bowdler. 2014. Anatomy of Colymbosaurus megadeirus (Reptilia, Plesiosauria) from the Kimmeridge Clay Formation of the U.K., and high diversity amoung Late Jurassic plesiosauroids. *Journal of Vertebrate Paleontology* 34:1053-1071.

Benson, R. B. J., R. J. Butler, J. Lindgren, and A. S. Smith. 2010. Mesozoic marine tetrapod diversity: mass extinctions and temporal heterogeneity in geological megabiases affecting vertebrates. *Proceedings of the Royal Society B* 277:829-834.

Benson, R. B. J., and P. S. Druckenmiller. 2014. Faunal turnover of marine tetrapods of the Jurassic-Cretaceous transition. *Biological Reviews* 89:1-23.

Benson, R. B. J., M. Evans, and P. D. Druckenmiller. 2012. High Diversity, Low Disparity and Small Body Size in Plesiosaurs (Reptilia, Sauropterygia) from the Triassic-Jurassic Boundary. *PLOS ONE* 7:e31838.

Benson, R. B. J., M. Evans, A. Smith, J. Sassoon, S. Moore-Faye, H. F. Ketchum, and R. Forrest. 2013. A giant pliosaurid skull from the Late Jurassic of England. *PLOS ONE* 8:e65989.

Benson, R. B. J., N. G. Zverkov, and M. S. Arkhangelsky. 2015. Youngest occurrences of rhomaleosaurid plesiosaurs indicate survival of an archaic marine reptile clade at high palaeolatitudes. *Acta Palaeontologica Polonica* 60:769-780.

Benton, M. J., and P. S. Spencer. 1995. *Fossil reptiles of Great Britain*. Chapman and Hall, London.

Berezin, A. Y. 2011a. A New Plesiosaur of the Family Aristonectidae from the Early Cretaceous of the Center of the Russian Platform. *Paleontological Journal* 45:648-660.

Berezin, A. Y. 2011b. Новый плезиозавр семейства Aristonectidae из раннего мела центра Русской платформы. *Палеонтологический журнал* 6:51-61.

Bernard, A., C. Lécuyer, P. Vincent, R. Amiot, N. Bardet, E. Buffetaut, G. Cuny, F. Fourel, F. Martineau, J.-M. Mazin, and A. Prieur. 2010. Regulation of body temperatures by some Mesozoic marine reptiles. *Science* 328:1379-1382.

Bjærke, T. 1980. Mesozoic palynology of Svalbard V. Dinoflagellates from the Agardhfjellet Member (Middle and Upper Jurassic) in Spitsbergen. *Norsk Polarinstitutt Skrifter* 172:145-167.

Bogolyubov, N. N. 1911. *On the history of plesiosaurs in Russia*. Imperial Moscow University Press, Moscow.

Bremer, K. 1994. Banch support and tree stability. *Cladistics* 10:295-304.

Brett, C. E., and G. C. Baird. 1986. Comparative taphonomy: A key to paleoenvironmental interpretation based on fossil preservation. *Palaios* 1:207-227.

Brooks, D. R., and M. G. P. van Veller. 2003. Critque of parsimony analysis of endemicity as a method of historical biogeography. *Journal of Biogeography* 30:819-825.

Brown, D. S. 1981. The English Upper Jurassic Plesiosauridae (Reptilia) and a review of the phylogeny and classification of the Plesiosauia. Bulletin of the British Museum (Natural History), *Geology* 35:253-347.

Brown, D. S. 1984. Discovery of a specimen of the plesiosaur *Colymbosaurus trochanterius* (Owen) on the Island of Portland. *Proceedings of the Dorset Natural History and Archaeological Society* 105:170.

Brown, D. S., and A. R. I. Cruickshank. 1995. The skull of a Callovian plesiosaur Cryptoclidus eurymerus, and the sauropterygian cheek. *Palaeontology* 37:941-953.

Brown, J. H., and A. Kodric-Brown. 1977. Turnover rates in insular biogeography: effect of immigration on extinction. *Ecology* 58:445-449.

Buchholtz, E. A. 2001. Swimming styles in Jurassic ichthyosaurs. *Journal of Vertebrate Paleontology* 21:61-73.

Buchy, M.-C., E. Frey, and S. W. Salisbury. 2006a. The internal cranial anatomy of the Plesiosauria (Reptilia, Sauropterygia): evidence for a functional secondary palate. *Lethaia* 39:289-303.

Buchy, M. C. 2010. First record of Ophthalmosaurus (Reptilia: Ichthyosauria) from the Tithonian (Upper Jurassic) of Mexico. *Journal of Paleontology* 84:149-155.

Buchy, M. C., E. Frey, S. W. Salisbury, W. Stinnesbeck, J. G. López-Oliva, and M. Götte. 2006b. An unsual pliosaur (Reptilia, Sauropterygia) from the Kimmeridgian (Upper Jurassic) of northeasten Mexico. *Neues Jahrbuch für Paläontologie Abhandlungen* 240:241-270.

Buffetaut, E. 1981. A plesiosaur vertebrae from the Chichali Formation (Late Jurassic to Early Cretaceous) of Pakistan. *Neues Jahrbuch für Paläontologie Abhandlungen* 1981:334-338.

Caldwell, M. W. 1997. Limb osteology nd ossification patterens in Cryptoclidus (Reptilia: Plesiosauroida) with a review of sauropterygian limbs. *Journal of Vertebrate Paleontology* 17:295-307.

Carpenter, K. 1996. A review of short-necked plesiosaurs from the Cretaceous of the western interior, North America. Neues Jahrbuch für Geologie und Paläontologie. Abhandlungen 201:259p.

Carpenter, K. 1999. Revision of North American elasmosaurids from the Cretaceous of the western interior. *Paludicola* 2:148-173.

Carpenter, S., and D. Radley. 2010. Discovery and preparation of a large mass of articulated Early Jurassic crinoids from Black Ven (Dorset and East Devon Coast World Heritage Sile, south-west England). *The Geological Curator* 9:103-106.

Casagranda, M. D., L. Taher, and C. A. Szumik. 2012. Endemicity analysis, parsimony and biotic elements: a formel comparison using hypothetical distributions. *Cladistics* 28:645-654.

Cau, A., and F. Fanti. 2015. A pliosaurid plesiosaurian from the Rosso Ammonitico Veronese Formation of Italy. *Acta Palaeontologica Polonica* 59:643-650.

Cecca, F. 2002. *Palaeobiogeography of marine fossil invertebrates - concepts and methods*. 273 pp. Taylor and Francis, London.

Cecca, F., B. Vrielynck, T. Lavoyer, and H. Gaget. 2005. Changes in the ammonite taxonomical diversity gradient during the Late Jurssic-Early Cretaceous. *Journal of Biogeography* 32:535-547.

Cheng, Y.-N., T. Sato, X.-C. Wu, and C. Li. 2006. First complete pistosaurid from the Triassic of China. *Journal of Vertebrate Paleontology* 26:501-504.

Cicimurri, D. J., and M. J. Everhart. 2001. An elasmosaur with stomach contents and gastroliths from the Pierre Shale (Late Cretaceous) of Kansas. *Transactions of the Kansas Academy of Science* 104:129-143.

Cnudde, V., and M. N. Boone. 2013. High-resolution X-ray computed tomography in geosciences: A review of the current technology and applications. *Earth-Science Reviews* 123:1-17.

Collignon, M., and Ø. Hammer. 2012. Petrography and sedimentology of the Slottsmøya Member at Janusfjellet, central Spitsbergen. *Norwegian Journal of Geology* 92:89-101.

Conroy, G. C., and M. W. Vannier. 1984. Noninvasive three dimensional computer imaging of matrix-filled fossil skulls by high resolution computed tomography. *Science* 226:456-458.

Cox, B. M., J. D. Hudson, and D. M. Martill. 1992. Lithostratigraphic nomenclature of the Oxford Clay (Jurassic*). Proceedings of the Geologists' Association* 103:343-345.

Cruickshank, A. R. I., P. G. Small, and M. A. Taylor. 1991. Dorsal nostrils and hydrodynamically driven underwater olfaction in plesiosaurs. Nature 352:62.

Dallmann, W. K. 1999. *Lithostratigraphic Lexicon of Svalbard. Upper Palaeozoic to Quaternary Bedrock. Review and Recommendations for Nomenclature Use.* . 318 pp. Norsk Polarinstitutt, Tromsø.

Dallmann, W. K., H. Major, P. Haremo, A. Andresen, T. Kjærnet, and A. Nøttvedt. 2001. Geological map of Svalbard 1:1000,000, sheet C9G Adventdalen. With explanatory text.. *Norsk Polarinstitutt Temakart* 31/32:4-55.

Dalseg, T. S., H. Nakrem, and M. Smelror. 2016. Dinoflagellate cyst biostratigraphy, palynofacies, depositional environment and sequence stratigraphy of the Agardhfjellet Formation (Upper Jurassic–Lower Cretaceous) in central Spitsbergen (Arctic Norway). *Norwegian Journal of Geology* 96:119-133.

de Blainville, H. D. 1835. Description de quelques espèces de reptiles de la Californie, précédée de l'analyse d'un système général d'Erpétologie et d'Amphibiologie. *Nouvelles Annales du Muséum (National) d'Histoire Naturelle, Paris* 4:233-296.

Delsett, L. L., L. K. Novis, A. J. Roberts, M. J. Koevoets, Ø. Hammer, P. D. Druckenmiller, and J. H. Hurum. 2016. The Slottsmøya Member marine reptile *Lagerstätte*: depositional environments, taphonomy and diagenesis; pp. *i*n B. P. Kear, J. Lindgren, J. H. Hurum, J. Milàn, and V. Vajda (eds.), *Mesozoic Biotas of*

Scandinavia and its Arctic Territories. Geological Society Special Publications, London.

Delsett, L. L., A. J. Roberts, P. D. Druckenmiller, and J. H. Hurum. 2017. A new ophthalmosaurid (Ichthyosauria) from Svalbard, Norway and evolution of the ichthyopterygian pelvic girdle. *PLOS ONE* 12:e0169971.

Ditchfield, P. W. 1997. High northern palaeolatitude Jurassic-Cretaceous palaeotemperature variation: New data from Kong Karls Land, Svalbard. *Palaeogeography, Palaeoclimatology, Palaeoecology* 130:163-175.

Doré, A. G. 1991. The structural foundation and evolution of Mesozoic seaways between Europe and the Arctic. *Palaeogeography, Palaeoclimatology, Palaeoecology* 87:441-492.

Doré, A. G. 1992. Synoptic palaeogeography of the Northeast Atlantic Seaway: late Permian to Cretaceous; pp. 421-446 *i*n J. Parnell (ed.), *Basins on the Atlantic Seaboard: Petroleum Geology, Sedimentology and Basin Evolution*. Geological Society Special Publication.

Dromart, G., J.-J. Garcia, S. Picard, F. Atrops, C. Lécuyer, and S. M. F. Sheppard. 2003. Ice age at the Middle - late Jurassic transition. *Earth and Planetary Science Letters* 213:205-220.

Druckenmiller, P. S. 2002. Osteology of a new plesiosaur from the Lower Cretaceous (Albian) Thermopolis Shale of Montana. *Journal of Vertebrate Paleontology* 22:29-42.

Druckenmiller, P. S., J. H. Hurum, E. M. Knutsen, and H. A. Nakrem. 2012. Two new ophthalmosaurids (Reptilia: Ichthyosauria) from the Agardhfjellet Formation (Late Jurassic: Volgian/Tithonian), Svalbard, Norway. *Norwegian Journal of Geology* 92:311-339.

Druckenmiller, P. S., and A. P. Russell. 2008. A phylogeny of Plesiosauria (Sauropterygia) and its bearing on the systematic status of Leptocleidus Andrews, 1922. *Zootaxa* 1863: 120 pp.

Dunton, K. 1992. Arctic Biogeography: The paradox of the marine bethic fauna and flora. *Trends in Ecology and Evolution* 7:183-189.

Dypvik, H., E. Håkansson, and C. Heinberg. 2003. Jurassic and Cretaceous palaeogeography and stratigraphic comparisons in the North Greenland–Svalbard region. *Polar Research* 21:91-108.

Dypvik, H., J. Nagy, T. A. Eikeland, K. Backer-Owe, A. Andresen, H. Johansen, A. Elverhoi, P. Haremo, and T. Bjaerke. 1991. The Janusfjellet Sugroup (Bathonian to Hauterivian) on central Spitsbergen: a revised lithostratigraphy. *Polar Research* 9:21-43.

Dypvik, H., J. Nagy, T. A. Eikeland, K. Backer-Owe, and H. Johansen. 1992. Depositional conditions of the Bathonian to Hauterivian Janusfjellet Subgroup, Spitsbergen, Norway. *Sedimentary Geology* 72:55-78.

Dypvik, H., and V. Zakharov. 2012. Late Jurassic-Early Cretaceous fine-grained epicontinental Arctic sedimentation – mineralogy and geochemistry of shales from the Late Jurassic-Early Cretaceous transition. *Norwegian Journal of Geology* 92: 65-87.

Efron, B., E. Halloran, and S. Holmes. 1996. Bootstrap confidence levels for phylogenetic trees. *Proceedings of the National Acadomy of Sciences* 93:7085-90.

Embry, A. F. 1991. Mesozoic history of the Arctic Islands; pp. 369-433 *i*n H. P. Trettin (ed.), *Inuitian Orogen and Arctic Platform: Canada and Greenland*. Geologicak Survey of Canada, Geology of Canada.

Everhart, M. J. 2000. Gastroliths associated with plesiosaur remains in the Sharon Springs Member of the Pierre Shale (Lat Cretaceous), Western Kansas. *Transactions of the Kansas Academy of Science* 103:64-75.

Faleide, J. I., F. Tsikalas, A. J. Breivik, R. Mjelde, O. Ritzmann, Ø. Engen, J. Wilson, and O. Eldholm. 2008. Structure and evolution of the continental margin off Norway and the Barents Sea. *Episodes* 31:82-91.

Faleide, J. I., E. Vågnes, and S. T. Gudlaugsson. 1993. Late Mesozoic-Cenozoic evolution of the south-western Barents Sea in a regional riftshear tectonic setting. *Marine and Petroleum Geology* 10:186-214.

Fernández-Javlo, Y., and M. D. M. Monfort. 2008. Experimental taphonomy in museums: Preparation protocols for skeletons and fossil vertebrates under the scanning electron microscopy. *Geobios* 41:157-181.

Fernández, M., and M. Talevi. 2014. Ophthalmosaurian (Ichthyosauria) records from the Aalenian–Bajocian of Patagonia (Argentina): an overview. *Geological Magazine* 151:49-59.

Fernández, M. S. 1999. A new ichthosaur from the Los Molles Formation (Early Bajocian), Neuquen Basin, Argentina. *Journal of Paleontology* 73:677-681.

Fernández, M. S., F. Arcguby, M. Talevi, and R. Evner. 2005. Ichthyosaurian eyes: paleobiological information content in the sclerotic ring of *Caypullisaurus* (Ichthyosauria, Ophthalmosauria). *Journal of Vertebrate Paleontology* 25:330-337.

Fernández, M. S., and L. Campos. 2015. Ophthalmosaurids (Ichthyosauria: Thunnosauria): alpha taxonomy, clades and names; pp. 20-30 *i*n M. S. Fernández, and Y. Herrera (eds.), *Reptiles Extinctos - Volumen en Homenaje a Zulma Gasparini.* Publicación Electrónica de la Asociación Paleontológica Argentina.

Fernández, M. S., and M. Iturralde-Vincent. 2000. An Oxfordian Ichthyosauria (Reptilia) from Viñales, western Cuba: paleobiogeographic significance. *Journal of Vertebrate Paleontology* 20:191-193.

Fernández, M. S., and E. E. Maxwell. 2012. The genus *Arthropterygius* Maxwell (Ichthyosauria:Ophthalmosauridae) in the Late Jurassic of the Neuqúen Basin, Argentina. *Geobios* 45:535-540.

Fischer, V. 2012. New data on the ichthyosaur Platypterygius hercynicus and its implictions for the validity of the genus. *Acta Palaeontologica Polonica* 57:123-134.

Fischer, V. 2016. Taxonomy of *Platypterygius campylodon* and the diversity of the last ichthyosaurs. *PeerJ* 4:e2604.

Fischer, V., M. S. Arkhangelsky, I. M. Stenshin, G. N. Uspensky, N. G. Zverkov, and R. B. J. Benson. 2015. Peculiar macrophagous adaptations in a new Cretaceous pliosaurid. *Royal Society Open Science* 2:150552.

Fischer, V., N. Bardet, R. B. J. Benson, M. S. Arkhangelsky, and M. Friedman. 2016. Extinction of fish-shaped marine reptiles associated with reduced evolutionary rates and global environmental volatility. *Nature Communications* 7:10825.

Fischer, V., A. Clément, M. Guiomar, and P. Godefroit. 2011a. The first definite record of a Valanginian ichthyosaur and its implications on the evolution of post-Liassic Ichthyosauria. *Cretaceous Research* 32:155-163.

Fischer, V., M. Guiomar, and P. Godefroit. 2011b. New data on the palaeobiogeography of Early Jurassic marine reptiles: the Toarcian ichthyosaur fauna of the Vocontian Basin (SE France). *Neues Jahrbuch Fur Geologie Und Palaontologie-Abhandlungen* 261:111-127.

Fischer, V., M. W. Maisch, D. Naish, R. Kosma, J. Liston, U. Joger, F. J. Krüger, J. P. Pérez, J. Tainsh, and R. M. Appleby. 2012. New ophthalmosaurid ichthyosaurs

from the European Lower Cretaceous demonstrate extensive ichthyosaur survival across the Jurassic–Cretaceous boundary. *PLOS ONE* 7:e29234.

Forrest, R., and N. Oliver. 2003. Ichthyosaurs and plesiosaurs from the lower spilsby sandstone member (Upper Jurassic), north Lincolnshire. *Proceedings of the Yorkshire Geological Society* 54:269-275.

Galloway, J. M., A. R. Sweet, G. T. Swindles, K. Dewing, T. Hadlari, A. F. Embry, and H. Sanei. 2013. Middle Jurassic to Lower Cretaceous paleoclimate of Sverdrup Basin, Canadian Arctic Archipelago inferred from the palynostratigraphy. *Marine and Petroleum Geology* 44:240-255.

Gasparini, Z. 1996. Biogeographic evolution of the South American crocodilians; pp. 159-184 *i*n G. Arratia (ed.), *Contributions of Southern South America to Vertebrate Paleontology*. Müncher Geowissenschaftliche, Abhanflungen.

Gasparini, Z., N. Bardet, and M. Iturralde-Vincent. 2002. A new cryptoclidid Plesiosaur from the Oxfordian (Late Jurassic) of Cuba. *Geobios* 35:201-211.

Gasparini, Z., N. Bardet, J. E. Martin, and M. S. Fernández. 2003. The elasmosaurid plesiosaur Aristonectes Cabrera from the latest Cretaceous of South America and Antarctica. *Journal of Vertebrate Paleontology* 23:104-115.

Gasparini, Z., and M. S. Fernández. 2005. Jurassic marine reptiles of the Neuquén Basin: records, faunas and their palaeobiogeographic significance. *Geological Society Special Publications* 252:279-294.

Gasparini, Z., M. S. Fernández, M. de la Fuente, Y. Herrera, L. Cordorniú, and A. Garrido. 2015a. Reptiles from lithographic limestones of the Los Catutos Member (Middle-Upper Tithonian), Neuquén Province, Argentina: An essay on its taxonomic composition and preservation in an environmental and geographic context. *Ameghiniana* 52:1-28.

Gasparini, Z., and L. Spalletti. 1993. First Callovian plesiosaurs from the Neuquen Basin, Argentina. *Ameghiniana* 30:245-254.

Gasparini, Z., J. Sterli, A. Parras, J. P. O'Gorman, L. Salgado, J. Varela, and D. Pol. 2015b. Late Cretaceous reptilian biota of the La Colonia Formation central patagonia, Argentina: Occurences, preservation and paleoenvironments. *Cretaceous Research* 54:154-168.

Gaston, K. 2000. Global patterns in biodiversity. *Nature* 405:220-227.

Gilmore, C. W. 1905. Osteology of Babtanodon (Marsh). *Memoirs of the Carnegie Museum* 2:77-129.

Ginsburg, L., and P. Janvier. 1974. Un nouveau gisement à Plésiosaures dans le Jurassique du Spitsbergen (Archipel du Svalbard). *Årbok - Norsk Polarinstitutt* 1974:262-265.

Goloboff, P. A., and S. A. Catalano. 2016. TNT version 1.5, including a full implementation of phylogenetic morphometrics. *Cladistics* 32:221-238.

Goloboff, P. A., J. Farris, and K. C. Nixon. 2010. T.N.T. 1.1: Tree Analysis Using New Techology Available at http://www.zmuc.dk/public/phylogeny/TNT/.

Grange, D. R., G. W. Storrs, K. Carpenter, and S. Etches. 1996. An important marine vertebrate-bearing locality from the Lower Kimmeridge Clay (Upper Jurassic) of Westbury, Wiltshire. *Proceedings of the Geologists' Association* 107:107-116.

Gray, J. E. 1825. A synopsis of the genera of reptiles and Amphibia, with a description of some new species. *Annals of Philosophy* 26:193-217.

Gröcke, D. R., G. D. Price, A. H. Ruffell, J. Mutterlose, and E. Baraboshkin. 2003. Isotopic evidence for Late Jurassic–Early Cretaceous climate change. *Palaeogeography, Palaeoclimatology, Palaeoecology* 202:97-118.

Hallam, A. 1988. A re-evaluation of Jurassic eustasy in the light of new data and the revised Exxon curve; pp. 261-271 *i*n C. K. Wilgus, B. S. Hastings, C. G. S. C. Kendall, H. W. Posamatir, C. A. Ron, and J. C. van Wager (eds.), *Sea-Level changes - An intergrated approach*, SEPM Pecial Publication.

Hallam, A. 2001. A review of the broad pattern of Jurassic sea-level changes and their possible causes in the light of current knowledge. *Palaeogeography, Palaeoclimatology, Palaeoecology* 167:23-37.

Halstead, L. B. 1989. Plesiosaur locomotion. Journal of the Geological Society 146:37-40.

Hammer, Ø., M. Collignon, and H. A. Nakrem. 2012. Organic carbon isotope chemostratigraphy and cyclostratigraphy in the Volgian of Svalbard. *Norwegian Journal of Geology* 92:103-112.

Hammer, Ø., D. A. T. Harper, and P. D. Ryan. 2001. PAST: Paleontological Statistics Software Package for Education and Data Analysis. *Palaeontologia Electronica* 4:9pp.

Hammer, Ø., K. Hryniewicz, J. H. Hurum, M. Høyberget, E. M. Knutsen, and H. A. Nakrem. 2013. Large onychites (cephalopod hooks) from the Upper Jurassic of the Boreal Realm. *Acta Palaeontologica Polonica* 59:827-835.

Hammer, Ø., H. A. Nakrem, C. T. S. Little, K. Hryniewicz, M. R. Sandy, J. H. Hurum, P. Druckenmiller, E. M. Knutsen, and M. Høyberget. 2011. Hydrocarbon seeps from

close to the Jurassic-Cretaceous boundary, Svalbard. *Palaeogeography, Palaeoclimatology, Palaeoecology* 306.

Hampe, O. 1992. Ein großwüchsiger Pliosauride (Reptilia:Plesiosauria) aus der Unterkreide (oberes Aptium) von Kolumbien. *Courier Forschunginstitut Senckenberg* 145:1-32.

Hampe, O. 2013. The forgotten remains of a leptocleidid plesiosaur (Sauropterygia: Plesiosauroidea) from the Early Cretaceous of Gronau (Mu¨nsterland, Westphalia, Germany*). Paläontologisches Zeitschrift* 87:473-491.

Hansen, J.-A., S. G. Bergh, and T. Henningsen. 2012. Mesozoic rifting and basin evolution on the Lofoten and Vesterålen Margin, North-Norway; time constraints and regional implications. *Norwegian Journal of Geology* 91:203-228.

Hansen, T. A. 1980. Influence of larval disperal and geographic distribution on species longevity in neogastropods. *Paleobiology* 6:193-207.

Haq, B. U., Hardenbol, J. & Vail, P. R. 1987. Chronology of fluctuating sea levels since the Triassic (250 million years ago to present). *Science* 235:1156-1167.

Harland, W. B. 1997. *The Geology of Svalbard*. Geological Society, London.

Herrera, N. D., J. J. ter Poorten, R. Bieler, P. M. Mikkelsen, E. E. Strong, D. Jablonski, and S. J. Steppan. 2015. Molecular phylogenetics and historical biogeography amid shifting continents in the cockles and giant clams (Bivalvia: Cardiidae). *Molecular Phylogenetics and Evolution* 93:94-106.

Hikuroa, D. C. H. 2009. Second Jurassic marine reptile from the Antarctic Peninsula. *Antarctic Science* 21:169-170.

Hillis, D. M., and J. J. Bull. 1993. An empirical test of Bootstrapping as a method for assessing confindence in phylogenetic analysis. *Systematic Biology* 42:182-192.

Hjálmarsdóttir, H. R., H. A. Nakrem, and J. Nagy. 2012. Foraminifera from Late Jurassic – Early Cretaceous hydrocarbon seep carbonates, central Spitsbergen, Svalbard – preliminary results. *Norwegian Journal of Geology* 92:157-165.

Houssaye, A. 2013. Bone histology of aquatic reptiles: what does it tell us about secondary adaptation to an aquatic life? *Biological Journal of the Linnean Society* 108:3-21.

Hryniewicz, K., Ø. Hammer, H. A. Nakrem, and C. T. S. Little. 2012. Microfacies of the Volgian-Ryazanian (Jurassic-Cretaceous) hydrocarbon seep carbonates from Sassenfjorden, central Spitsbergen, Svalbard. *Norwegian Journal of Geology* 92:113-131.

Hryniewicz, K., C. T. S. Little, and H. Nakrem. 2014. Bivalves from the latest Jurassic-earliest Cretaceous hydrocarbon seep carbonates from central Spitsbergen, Svalbard. *Zootaxa* 3859:001–066

Hryniewicz, K., H.-A. Nakrem, Ø. Hammer, C. T. S. Little, A. Kaim, M. R. Sandy, and J. H. Hurum. 2015. The palaeoecology of the latest Jurassic - earliest Cretaceous hydrocarbon seep carbonates from Spitsbergen, Svalbard. *Lethaia* 48:353-374.

Hulke, J. W. 1870. Note on some Plesiosaurian Remains obtained by J. C. Mansel Esq. F.G.S., in Kimmeridge Bay, Dorset. *Quarterly Journal of the Geological Society of London* 26:611-622.

Hulke, J. W. 1873. Memorandum on some fossil vertebrate remains collected by the Swedish expedition to Spitzbergen in 1864 and 1868. *Bihang till Kungliga Svenska Vetenskapsakademiens Handlinger, 1, Afdelning IV* 9:1-11.

Hurum, J. H., H. A. Nakrem, Ø. Hammer, E. M. Knutsen, P. S. Druckenmiller, K. Hryniewicz, and L. K. Novis. 2012. An Arctic lagerstätte – the Slottsmøya Member of the Agardhfjellet Formation (Upper Jurassic – Lower Cretaceous) of Spitsbergen. *Norwegian Journal of Geology* 92:55-64.

Hurum, J. H., A. J. Roberts, G. J. Dyke, S.-T. Grundvåg, H.-A. Nakrem, I. Midtkandal, K. K. Sliwinska, and S. Olaussen. 2016. Bird or maniraptoran dinosaur? A femur from the Albian strata of Spitsbergen. *Palaeontologica Polonica* 67:137-147.

Imlay, R. W. 1980. Jurassic paleobiogeography of the conterminous United States in its continental setting. *US Geological Survey Professional Paper* 1232:44.

Iturralde-Vincent, M. 2003. *A brief account of the evolution og the Carbbean seaway: Jurassic to present*; pp. 386-396 *i*n: The marine Eocene - Oligocene transition. Columbia University Press, New york.

Jablonski, D., and K. Roy. 2003. Geographical range and speciation in fossil and living molluscs. *Proceedings of the Royal Society B* 270:401-406.

Jungers, W. L., and R. J. Minns. 1979. Computed tomography and biomechanical analysis of fossil long bones. *Physical Anthropology* 50:285-290.

Kear, B. P. 2006. Plesiosaur remains from Cretaceous high-latitude non-marine deposits in Southeastern Australia. *Journal of Vertebrate Paleontology* 26:196-199.

Kear, B. P., J. Lingren, J. H. Hurum, J. Milàn, and V. Vajda. 2016. An introduction to the Mesozoic biotas of Scandinavia and its Arctic territories: In *Mesozoic biotas of Scandinavia and its Arctic territories*, Vol. 434, B. P. Kear, J. Lingren, J. H.

Hurum, J. Milàn, and V. Vajda eds, pp. 1-14. Geological Society of London Special Publications, London.

Kear, B. P., and E. E. Maxwell. 2013. Wiman's forgotten plesiosaurs: the earliest recorded sauropterygian fossils from the High Arctic. *GFF* 135:95-103.

Kear, B. P., and A. R. Milner. 2009. Plesiosaur remains from the Jurassic-Cretaceous Purbeck Limestone Group of southern England. *Proceedings of the Geologists' Association* 120:121-125.

Ketchum, H. F., and R. B. J. Benson. 2010. Global interrelationships of Plesiosauria (Reptilia: Sauropterygia) and the pivotal role of taxon sampling in determining the outcome of phylogenetic analyses. *Biological Reviews* 85:361-392.

Ketchum, H. F., and R. B. J. Benson. 2011. The cranial anatomy and taxonomy of *Peloneustes philarchus* (Sauropterygia, Pliosauridae) from the Peterborough member (Callovian, Middle Jurassic) of the United Kingdom. *Palaeontology* 54:639-665.

Kihle, J., J. H. Hurum, and D. Liebe. 2012. Preliminary results on liquid petroleum occurring as fluid inclusions in intracellular mineral precipitates in the vertebrae of *Pliosaurus funkei*. *Norwegian Journal of Geology* 92:341-352.

Knight, W. C. 1900. Some new Jurassic vertebrates. *American Journal of Science Series IV* 10:115-119.

Knutsen, E. M. 2012a. Late Jurassic plesiosaurians (Sauroptyergia - Plesiosauria) from the Agardhfjellet Formation on Svalbard: In *Faculty of Mathematics and Natural Sciences*, Vol. PhD thesis, pp. 250. University of Oslo, Oslo.

Knutsen, E. M. 2012b. A taxonomic revision pf the genus *Pliosaurus* (Owen, 1841a). *Norwegian Journal of Geology* 92:259-276.

Knutsen, E. M., P. S. Druckenmiller, and J. H. Hurum. 2012a. A new plesiosaurid (Reptilia-Sauropterygia) from the Agardhfjellet Formation (Middle Volgian) of central Spitsbergen, Norway. *Norwegian Journal of Geology* 92:213-234.

Knutsen, E. M., P. S. Druckenmiller, and J. H. Hurum. 2012b. A new species of *Pliosaurus* (Sauropterygia: Plesiosauria) from the Middle Volgian of central Spitsbergen, Norway. *Norwegian Journal of Geology* 92:235-258.

Knutsen, E. M., P. S. Druckenmiller, and J. H. Hurum. 2012c. Redescription and taxonomic clarfication of '*Tricleidus' svalbardensis* based on new material from the Agardhfjellet Formation (Middle Volgian). *Norwegian Journal of Geology* 92:175-186.

Knutsen, E. M., P. S. Druckenmiller, and J. H. Hurum. 2012d. Two new species of long-necked plesiosaurians (Reptilia-Sauropterygia) from the Upper Jurassic (Middle Volgian) Agardhfjellet Formation of central Spitsbergen. *Norwegian Journal of Geology* 92:187-212.

Koevoets, M. J., T. B. Abay, Ø. Hammer, and S. Olaussen. 2016. High-resolution organic carbon–isotope stratigraphy of the Middle Jurassic–Lower Cretaceous Agardhfjellet Formation of central Spitsbergen, Svalbard. *Palaeogeography, Palaeoclimatology, Palaeoecology* 449:266-274.

Koevoets, M. J., Ø. Hammer, S. Olaussen, K. Senger, and M. Smelror. *in prep*. Facies, bio- and sequence stratigraphy of the Middle Jurassic to Lower Cretaceous Agardhfjellet Formation in central Spitsbergen: Integration of borehole and outcrop data.

Koevoets, M. J., J. H. Hurum, and M. Friedman. *in prep*. The rediscovery of Late Jurassic teleosts from the Agardhfjellet Formation, Spitsbergen, Svalbard.

Korte, C., S. P. Hesselbo, C. V. Ullmann, G. Dietl, M. Ruhl, G. Schweigert, and N. Thibault. 2015. Jurassic climate mode governed by ocean gateway. *Nature Communications* 6:10.1038/ncomms10015.

Kubo, T., M. T. Mitchell, and D. M. Henderson. 2012. *Albertonectes vanderveldei*, a new elsamosaur (Reptilia, Sauropterygia) from the Upper Cretaceous of Alberta. *Journal of Vertebrate Paleontology* 32:557-572.

Larkin, N., S. O'Connor, and D. Parsons. 2010. The virtual and physical preparation of the Collard plesiosaur from Bridgwater Bay, Somerset, UK. *Geological Curator* 9:107-116.

Launis, A., C. Pott, and A. Mørk. 2014. A glimpse into the Carnian: Late Triassic plant fossils from Hopen, Svalbard. *Norwegian Petroleum Directorate Bulletin* 11:129-136.

Law, I. A., R. A. Houseley, N. Harmmond, and R. E. M. Hedges. 1991. Cuello: resolving the chronology through direct dating of conserved and low-collagen bone by AMS. *Radiocarbon* 33: 303-315.

Lieberman, B. S. 2000. *Paleobiogeography*. 208 pp. Kluwer Academic/Plenum Publishers, New York.

Lippmann, H. G. 1986. Konservierung des interglazialen waldelefanten-skelettes von Crumstadt und perspektiven seiner Ausstellung. *Cranium* 3:14-16.

Lomax, D. R. 2015. The first plesiosaurian (Sauropterygia, Pliosauridae) remains described from the Jurassic of Poland. *Palaeontologia Electronica* 18.2.29A:8pp.

López-Polin, L. 2012. Possible interferences of some conservation treatments with subsequent studies on fossil bones: A conservator's overview. *Quaternary International* 275:120-127.

Lundin, E. R., and A. G. Doré. 1997. A tectonic model for the Norwegian passive margin with implications for the NE Atlantic: Early Cretaceous to breakup. *Journal of the Geological Society of London* 154:545-550.

Lydekker, R. 1889. On the remains and affinities of five genera of Mesozoic reptiles. *Quartely Journal of the Geological Society* 45:41-59.

Maddison, W. P., and D. R. Maddison. 2017. Mesquite: a modular system for evolutionary analysis.

Maguire, K., and A. L. Stigall. 2008. Paleobiogeography of Miocene Equinae of North America: A phylogenetic biogeographic analysis of the relative roles of climate, vicariance, and dispersal. *Palaeogeography, Palaeoclimatology, Palaeoecology* 267:175-184.

Malakhov, D. V. 1999. Giant Pliosaur (Reptilia; Sauropterygia) from the Late Jurassic of Kazakhstan and some remarks on the systematics of Pliosauridae. *Russian Journal of Herpetology* 6:241-246.

Marsh, O., C. 1893: Congress Geologique International, Compte Rendu de la 5me Session, Washington D.C., 1893.

Martill, D. M. 1993. Soupy substrates: a medium for the exceptional preservation of ichthyosaurs of the Posidonia Shale (Lower Jurassic) of Germany. *Kaupia: Darmstädter Beiträge zur Naturgeschichte* 2:77-97.

Martill, D. M., S. Earland, and D. Naish. 2006. Dinosaurs in marine strata: evidence from the British Jurassic, including a review of the allochthonous vertebrate assemblage from the marine Kimmeridge Clay Formation (Upper Jurassic) of Great Britain; pp. 1-31 *i*n E. *ColectivoArqueológico-Paleontológico Salense* (ed.), Actas de las III Jornadas sobre Dinosaurios y su Entorno, Salas de los Infantes, Burgos, España.

Martill, D. M., M. A. Taylor, and K. L. Duff. 1994. The trophic structure of the biota of the Peterborough Member, Oxford Clay Formation (Jurassic), UK. *Journal of the Geological Society* 151:173-194.

Massare, J. A. 1987. Tooth morphology and prey preference of Mesozoic marine reptiles. *Journal of Vertebrate Paleontology* 7:121-137.

Massare, J. A. 1994. Swimming capabilities of Mesozoic marine reptiles: a review; pp. 133-149 *i*n Q. B. L. Maddock, J. M. V. Rayner (ed.), *Mechanics and Physiology of Animal Swimming*. Cambrige University Press, Cambride.

Massare, J. A., R. W. Wahl, M. Ross, and M. V. Connely. 2014. Palaeoecology of the marine reptiles of the Redwater Shale Member of the Sundance Formation (Jurassic) of central Wyoming, USA. *Geological Magazine* 151:167-182.

Matzke, N. J. 2013 . BioGeoBEARS: BioGeography with Bayesian (and likelihood) evolutionary analysis in R scripts. R package, Version 0.2.

Matzke, N. J. 2014 . Model selection in historical biogeography reveals that founder-event speciation is a cruial process in island clades. *Systematic Biology* 63:951-970.

Maxwell, E. E. 2010. Generic reassignment of an ichthyosaur from the Queen Elizabeth Islands, Northwest Territories, Canada. *Journal of Vertebrate Paleontology* 30:403-415.

Maxwell, E. E., D. Dick, S. Padilla, and M. L. Parra. 2016. A new ophthalmosaurid ichthyosaur from the Early Cretaceous of Colombia. *Papers in Palaeontology* 2:59-70.

Maxwell, E. E., and B. P. Kear. 2013. Triassic ichthyopterygian assemblages of the Svalbard archipelago: a reassessment of taxonomy and distribution. *GFF* 135:85-94.

McCoy, E. D., and K. L. Heck. 1987. Som observations on the use of taxonomic similarity in large-scale biogeography. *Journal of Biogeography* 14:79-87.

McGowan, C. 1978. Further evidence for the wide geographical distribution of ichthyosaur taxa (Reptilia, Ichthyosauria). *Journal of Paleontology* 52:1155-1162.

McGowan, C., and R. Motani. 2003. Ichthyopterygia; pp. *i*n H. Sues (ed.), *Handbook of Paleoherpetology*. Verlag Dr. Friedrich Pfeil, München.

McHenry, C. R., A. G. Cook, and S. Wroe. 2005. Bottom-feeding plesiosaurs. *Science* 310:75.

Miller, K. G., M. A. Kominz, J. V. Browning, J. D. Wright, G. S. Mountain, M. E. Katz, P. J. Sugarman, B. S. Cramer, N. Christie-Blick, and S. F. Pekar. 2005. The Phanerozoic Record of global sea-level change. *Science* 310:1293-1298.

Mittelbach, G. G., D. W. Schemske, H. V. Cornell, A. P. Allen, J. M. Brown, M. B. Bush, S. P. Harrison, A. H. Hurlbert, N. Knowlton, H. A. Lessios, C. M. McCain, A. R. McCune, L. A. McDade, M. A. McPeek, T. J. Near, T. D. Price, R. E. Ricklefs, K. Roy, D. F. Sax, D. Schluter, J. M. Sobel, and M. Turelli. 2007. Evolution and the

latitudinal graident: speciation, extinction and biogeography. *Ecology Letters* 10:315-331.

Moon, B. C., and A. M. Kirton. 2016. Ichthyosaurs of the British Middle and Upper Jurassic. Part 1. *Ophthalmosaurus*, Vol. 170, pp. 84. *Monography of the Palaeontographical Society*, London.

Morgans-Bell, H. S., A. L. Coe, S. P. Hesselbo, H. C. Jenkyns, G. P. Weedon, J. E. A. Marshall, R. V. Tyson, and C. J. Willams. 2001. Integrated stratigraphy of the Kimmeridge Clay Formation (Upper Jurassic) based on exposures and boreholes in south Dorset, UK. *Geological Magazine* 138:511-539.

Mørk, A., W. K. Dallmann, H. Dypvik, E. P. Johannessen, G. B. Larssen, J. Nagy, A. Nøttvedt, S. Olaussen, T. M. Pcelina, and D. Worsley. 1999. Mesozoic lithostratigraphy; pp. 127-214 *i*n W. K. Dallmann (ed.), *Lithostratigraphic lexicon of Svalbard. Upper Palaeozoic to Quaternary bedrock. Review and recommendations for nomenclature use*. Norsk Polarinstitutt, Tromsø.

Morrone, J. J. 1994. On the indentification of areas of endemism. *Systematic Biology* 43:438-441.

Morrone, J. J. 2014. Parsimony analysis of endemicity (PAE) revisited. *Journal of Biogeography* 41:842-854.

Motani, R. 2002. Scaling effects in caudal fin propulsion and the speed of ichthyosaurs. *Nature* 415:309-312.

Motani, R. 2005. Evolution of fish-shaped reptiles (Reptilia : Ichthyopterygia) in their physical environments and constraints; pp. 395-420, *Annual Review of Earth and Planetary Sciences*. Annual Reviews, Palo Alto.

Motani, R., B. M. Rothschild, and W. Wahl. 1999. Large eyes in deep diving ichthyosaurs. *Nature* 402:747.

Mutterlose, J. 1992. Migration and evolution patterns of floras and faunas in marine Early Cretaceous sediments of NW Europe. *Palaeogeography, Palaeoclimatology, Palaeoecology* 94:261-282.

Mutterlose, J., H. Brumsack, S. Flögel, W. Hay, C. Klein, U. Langrock, M. Lipinski, W. Ricken, E. Söding, and R. Stein. 2003. The Greenland-Norwegian Seaway: A key area for understanding Lat Jurassic to Early Cretaceous paleoenvironments. *Paleoceanography* 18:10.1029/2001PA000625

Nagy, J., and V. A. Basov. 1998. Revised foraminiferal taxa and biostratigraphy of Bathonian to Ryazanian deposits in Spitsbergen. *Micropaleontology* 44:217-255.

Nixon, K. C. 1999. The Parsimony Ratchet, a new method for rapid parsimony analysis. *Cladistics* 15:407-414.

Noè, L. L., M. A. Taylor, and M. Gómez-Pérez. 2017. An integrated approch to understanding the role of the long neck in plesiosaurs. *Acta Palaeontologica Polonica* 62:137-162.

O'Keefe, F. R. 2001. A cladistic analysis and taxonomic revision of the Plesiosauria (Reptilia: Sauropterygia). *Acta Zoologica Fennica* 214:1-63.

O'Keefe, F. R., and L. M. Ciappe. 2011. Vivipary and K-selected life history in a Mesozoic marine plesiosaur (Reptile, Sauropterygia). *Science* 333:870-873.

O'Keefe, F. R., and H. P. Street. 2009. Osteology of the cryptocleidoid plesiosaur *Tatenectes laramiensis*, with comments on the taxonomic status of the Cimoliasauridae. *Journal of Vertebrate Paleontology* 29:48-57.

O'Keefe, F. R., H. P. Street, C. D. R. Wilhelm, and H. Zhu. 2011. A new skeleton of the cryptoclidid plesiosaur *Tatenectes laramiensis* reveals a novel body shape among plesiosaurs. *Journal of Vertebrate Paleontology* 31:330-339.

O'Keefe, F. R., and W. Wahl. 2003a. Preliminary report on the osteology and relationships of a new aberrant cryptocleidoid plesiosaur from the Sundance Formation, Wyoming. *Paludicola* 4:48-68.

O'Keefe, F. R., and W. J. Wahl. 2003b. Current taxonomic status of the plesiosaur *Pantosaurus striatus* from the Upper Jurassic Sundance Formation, Wyoming. *Paludicola* 4:37-46.

Ogg, J. G., G. M. Ogg, and F. M. Gradstein. 2016. *A concise geological time scale 2016*. 234 pp. Elsevier, Cambridge.

Owen, R. 1860. *Palaeontology; or, a systematic summary of extinct animals and their geologic remains*. Adam and CHarles Black, Edinburgh.

Padilla, C. B., M. E. Páramo, L. L. Noè, M. Gómez Pérez, and M. Luzm Parra. 2010. Acid Preparation of Large Vertebrale Specimens. *The Geological Curator* 9:213-220.

Paparella, I., E. E. Maxwell, A. Ciproani, S. Roncacè, and M. W. Caldwell. 2016. The first ophthalmosaurid ichthyosaur fromt he Upper Jurassic of the Umbrian-Marchean Apennines (Marche, central Italy). *Geological Magazine*:1-22.

Parker, K. R. 1967. The Jurassic and Cretaceous sequence in Spitsbergen. *Geological Magazine* 104:487-505.

Pauly, S., J. Mutterlose, and P. Alsen. 2012. Early Cretacous palaeoceanography of the Greenland-Norwegian Seaway evidenced by calcareous nannofossils. *Marine Micropaleontology* 90-91:72-85.

Persson, P. O. 1962. Plesiosaurians from Spitsbergen. *Norsk polarinstitutt* 1962:62-68.

Phillips, J. 1871. *Geology of Oxford and the Valley of the Thames*. Oxford University Press, Oxford.

Pipiringos, G. N. 1968. Correlation and nomenclature of some Triassic and Jurassic rocks in south-central Wyoming. *US Geological Survey Professional Paper* 594-D:26.

Price, G. D., and J. Mutterlose. 2004. Isotopic signals from late Jurassic–early Cretaceous (Volgian–Valanginian) sub-Arctic belemnites, Yatria River, Western Siberia. *Journal of the Geological Society* 161:959-968.

Price, G. D., and E. V. Nunn. 2010. Valanginian isotope variation in glendonites and belemnites from Arctic Svalbard: Transient glacial temperatures during the Cretaceous greenhouse. *Geology* 38:251-254.

Prothero, D. R. 2015. Garbage in, garbage out: the effect of immature taxonomy on database compilations of north American fossil mammals. *New Mexico Museum of Natural History and Science Bulletin* 68:257-264.

Provan, J., and K. D. Bennett. 2008. Phylogeographic insights into cryptic glacial refugia. *Trends in Ecology and Evolution* 23:564-571.

Raup, D. M., and R. E. Crick. 1979. Measurement of faunal similarity in paleontology. *Journal of Paleontology* 53:1213-1227.

Rawson, P. F. 1993. The influence of sea-level changes on the migration and evolution of early Cretaceous (pre-Aptian) ammonites; pp. 227-242 *i*n M. R. House (ed.), *The Ammonoidae: environment, ecology and evolutionary change*. Systematic Assosiation Clarendon Press, Oxford.

Revell, L. J. 2012. Phytools: An R package for phylogenetic comparative biology (and other things). *Methods in Evolution and Ecology* 3:217-223.

Riding, J. B., M. E. Quattrocchio, and M. A. Martínez. 2011. Mid Jurassic (Late Callovian) dinoflagellate cysts from the Lotena Formation of the Neuquén Basin, Argentina and their palaeogeographical significance. *Review of Palaeobotany and Palynology* 163:227-236.

Rieppel, O., P. M. Sander, and G. W. Storrs. 2002. The skull of the Pistosaur *Augustasaurus* from the Middle Triassic of North-western Nevada. *Journal of Vertebrate Paleontology* 22:577-592.

Roberts, A. J., P. D. Druckenmiller, G.-P. Sætre, and J. H. Hurum. 2014. A New Upper Jurassic Ophthalmosaurid Ichthyosaur from the Slottsmøya Member, Agardhfjellet Formation of Central Spitsbergen. *PLOS ONE* 9:e103152.

Roberts, A. J., P. S. Druckenmiller, L. L. Delsett, and J. H. Hurum. 2017. Osteology and relationships of Colymbosaurus Seeley, 1874, based on new material of C. svalbardensis from the Slottsmøya Member, Agardhfjellet Formation of central Spitsbergen. *Journal of Vertebrate Paleontology*:e1278381.

Rogov, M. 2004. The Russian platform as a key for a Volgian/Tithonian correlation: A review of the Mediterranean faunal elements and ammonite biostratigraphy of the Volgian Stage. *Rivista Italiana di Paleontologia e Stratigraphia* 110:321-328.

Rogov, M. 2012. Latitudinal gradient of taxonomic richness of ammonites in the Kimmeridgian–Volgian in the northern hemisphere. *Paleontological Journal* 46:148-156.

Rogov, M. 2013. Ammonites and Infrazonal Subdivision of the Dorsoplanites panderi Zone (Volgian Stage, Upper Jurassic) of the European Part of Russia. *Doklady Earth Sciences* 451:803-808.

Rogov, M., and V. Zakharov. 2009. Ammonite- and bivalve-based biostratigraphy and Panboreal correlation of the Volgian Stage. S*cience in China Series D: Earth Sciences* 52:1890-1909.

Rogov, M., V. Zakharov, and D. Kiselev. 2008. Molluscan immigrations via biogeographical ecotone of the Middle Russian Sea during the Jurassic. *Volumina Jurassica* VI:143-152.

Rosen, D. E. 1978. Vicariant patters and historical explaination of biogeography. *Systematic Zoology* 27:159-188.

Rousseau, J., and H. A. Nakrem. 2012. An Upper Jurassic Boreal echinoderm lagerstätte from Janusfjellet, central Spitsbergen. *Norwegian Journal of Geology* 92:133-161.

Sachs, S., J. J. Hornung, and B. P. Kear. 2016. Reappraisal of Europe's most complete Early Cretaceous plesiosaurian: Brancasaurus brancai Wegner, 1914 from the "Wealden facies" of Germany. *PeerJ* 4:e2813.

Sachs, S., and B. P. Kear. 2015. Postcranium of the paradign elasmosaurid plesiosaurian *Libonectes morgani* (Welles, 1949). *Geological Magazine* 152:694-710.

Sachs, S., and B. P. Kear. 2017. Redescription of the elasmosaurid plesiosaurian *Libonectes atlasense* from the Upper Cretaceous of Morocco. *Cretaceous Research* 74:205-222.

Sachs, S., B. P. Kear, and M. J. Everhart. 2013. Revised Vertebral Count in the "Longest-Necked Vertebrate" *Elasmosaurus platyurus* Cope 1868, and Clarification of the Cervical-Dorsal Transition in Plesiosauria. *PLOS ONE* 8:e70877.

Sahagian, D., O. Pinous, A. Olferiev, and V. Zakharov. 1996. Eustatic curve for the Middle Jurassic-Cretaceous based on Russian Platform and Siberian stratigraphy: zonal resolution. *AAPG Bulletin* 80:1433-1458.

Sandy, M. R., K. Hryniewicz, Ø. Hammer, H. A. Nakrem, and C. T. S. Little. 2014. Brachiopods from Late Jurassic-Early Cretaceous hydrocarbon seep deposits, central Spitsbergen, Svalbard. *Zootaxa* 3884:501-532.

Sassoon, J., R. Vaughan, S. Carpenter, and L. L. Noè. 2010. The second Westbury Pliosaur: excavation, collection and preparation *The Geological Curator* 9:117-126.

Sato, T., Y. Hasegawa, and M. Manabe. 2006. A new elasmosaurid plesiosaur from the Upper Cretaceous of Fukushima, Japan. *Palaeontology* 49:467-484.

Sato, T., and X.-C. Wu. 2008. A new Jurassic pliosaur from Melville Island, Canadian Arctic Archipelago. *Canadian Journal of Earth Science* 45:303-320.

Schultz, M. R., A. Fildani, and M. Sarez. 2003. Occurrence of the Southernmost South Americn Ichthyosaur (Middle Jurassic - Lower Cretaceous), Parque Nacional Torres del Paine, patagonia, Southernmost Chile. *Palaios* 18:69-73.

Seeley, H. G. 1869. *Index to the Fossil Remains of Aves, Ornithosauria, and Reptilia in the Woodwardian Museum of the University of Cambridge*. 143 pp. Deighton, Bell and Co., Cambridge.

Seeley, H. G. 1874a. Note on some of the generic modifications of the plesiosaurian pectoral arch. *Quarterly Journal of the Geological Society of London* 30:436-449.

Seeley, H. G. 1874b. On *Muraenosaurus leedsii*, a plesiosaurian from the Oxford Clay. Part 1. *Quarterly Journal of the Geological Society of London* 30:197-208.

Sellwood, B. W., and P. J. Valdes. 2006. Mesozoic climates: general circulation modeals and the rock record. *Sedimentary Geology* 190:269-287.

Sennikov, A. G., and M. S. Arkhangelsky. 2010. On a Typical Jurassic Sauropterygian from the Upper Triassic of Wilczek Land (Franz Josef Land, Arctic Russia). *Paleontological Journal* 44:567-572.

Serratos, D. J., P. D. Druckenmiller, and R. B. J. Benson. 2017. A new elasmosaurid (Sauropterygia, Plesiosauria) from the Bearpaw Shale (Late Cretaceous, Maastrichtian) of Montana demonstrates multiple evolutionary reductions of neck

length within Elasmosauridae. *Journal of Vertebrate Paleontology*:10.1080/02724634.2017.1278608.

Shelton, S. Y., and D. S. Chaney. 1994. An evaluation of adhesives and consolidants recommended for fossil vertebrates; pp. *i*n P. Leiggi, and P. May (eds.), *Vertebrate Paleontological Techniques*. Cambridge University Press, Cambridge.

Shi, G. R., and N. W. Archbold. 1995. Palaeobiogeography of Kaxanian-Midian (Late Permian) western Pacific bachiopod faunas. *Journal of Southeast Asian Earth Sciences* 12:129-141.

Shimada, K., T. Kamoshida, M. Iroh, S. Nishino, E. Carmack, F. McLaughlin, S. Zimmermann, and A. Proshutinsky. 2006. Pacific Ocean inflow: Influence on catastrophic reduction of sea ice cover in the Arctic Ocean. *Geophysical Research Letters* 33: 0.1029/2005GL025624

Sibuet, J.-C., S. Srivastava, M. E. Enachescu, and G. Karner. 2007. Early Cretaceous motion of Flemish Cap with respect to North America: implications on the formation of Orphan Basin and SE Flemish Cap-Galicia Bank conjugate margins; pp. 63–76 *i*n G. Karner, Manatschal G., & Pinheiro, L. (ed.), *Imaging, mapping and modelling continental lithosphere extension and breakup.* Geological Society of London, Special Publications.

Sissons, R. L., M. W. Caldwell, C. A. Evenchick, D. B. Brinkman, and M. J. Vavrek. 2015. An Upper Jurassic ichthyosaur (Ichthyosauria: Ophthalmosauridae) from the Bowser Basin, British Columbia. *Canadian Journal of Earth Science* 53:34-40.

Skogseid, J. 2010. The Orphan Basin - a key to understanding the kinematic linkage between North and NE Atlantic Mesozoic rifting. 2nd Central & North Atlantic Conjugate Margins Conference Keynotes 2:13-23.

Smith, A. 2007a. The back-to-front plesiosaur *Cryptoclidus* (*Apractocleidus*) aldingeri from the Kimmeridgian of Milne Land, Greenland. *Bulletin of the Geological Society of Denmark* 55:1-7.

Smith, A. G., D. G. Smith, and B. M. Funnell. 1994. *Atlas of Mesozoic and Cenozoic coastlines*. Cambridge University Press, Cambridge.

Smith, A. S. 2007b. Anatomy and Systematics of the Rhomaleosauridae (Sauropterygia: Plesiosauria), PhD thesis. *National University of Ireland*, University College Dublin, Dublin.

Smith, A. S. 2013. Morphology of the caudal vertebrae in *Rhomaleosaurus zetlandicus* and a review of the evidence for a tail fin in Plesiosauria. *Paludicola* 9:144-158.

Smith, A. S., and R. B. J. Benson. 2014. Osteology of *Rhomaleosaurus thorntoni* (Sauropterygia: Rhomaleosauridae) from the Lower Jurassic (Toarcian) of Northamptonshire, England. *Monograph of the Palaeontographical Society* 168:40pp, 35 pls.

Smith, A. S., and A. J. Roberts. *in prep*. A specimen of Colymbosaurus svalbardensis from the 'Reptile Creek Formation' (Upper Jurassic/ lower Cretaceous?) of Ellesmere Island, Canada.

Stephan, E. 2000. Oxygen isotope analysis of animal bone phosphate: method refinement, influence of consildants, and reconstruction of palaeotemperatures for Holocene sites. *Journal of Archaeological Science* 27:523-535.

Stinnesbeck, W., E. Frey, L. Rivas, J. M. Pardo Pérez, M. L. Cartes, C. S. Soto, and P. Z. Lobos. 2014. A Lower Cretaceous ichthyosaur graveyard in deep marine slope channel deposits at Torres del Paine National Park, southern Chilie. *Geological Society of America Bulletin* 126:1317-1339.

Storrs, G. W. 1993. Function and phylogeny in sauropterygian (Diapsida) evolution. *American Journal of Science* 293-A:63-90.

Storrs, G. W. 1994. Fossil vertebrate faunas of the British Rhaetian (latest Triassic). *Zoological Journal of the Linnean Society* 112:217-259.

Storrs, G. W. 1997. Morphological and taxonomic clarification of the genus Plesiosaurus; pp. 145-190 *i*n J. M. C. E. Nicholls (ed.), *Ancient Marine Reptiles*. Academic Press, San Diego.

Storrs, G. W., M. S. Arkhangelsky, and E. V. M. 2000. Mesozoic marine reptiles of Russia and other former Soviet republics; pp. *i*n M. J. Benton, M. A. Shishkin, D. M. Unwin, and E. N. Kurochkin (eds.), *The age of Dinosaurs in Russia and Mongolia.* Cambridge University press, Cambridge, United Kingdom.

Surlyk, F. 1991. Sequence stratigraphy of the Jurassic - lowermost Cretaceous in East Greenland. *Bulletin of the American Association of Petroleum Geology* 75:1468-1488.

Sutton, M. D. 2008. Tomographic techniques for the study of exceptionally preserved fossils. *Proceedings of the Royal Society B* 275:1587-1593.

Sutton, M. D., I. Rahman, and R. Garwood. 2014. *Techniques for Virtual Palaeontology*. 208 pp. Wiley, New York.

Takeda, Y., K. Tanabe, T. Sasaki, K. Uesugi, and M. Hoshino. 2016. Non-destructive analysis of in situ ammonoid jaws by Synchotron radiation X-ray micro-computed tomography. *Palaeontologia Electronica* 19.3.46A:1-13.

Taylor, M. A., and A. R. I. Cruikshank. 1993. A plesiosaur from the Linksfield erratic (Rhaetian, Upper Turassic near Elgin, Morayshire). *Scottish Journal of Geology* 29:191-196.

Taylor, M. P., and M. J. Wedel. 2013. The effect of intervertebral cartilage on neutral posture and range of motion in the necks of sauropod dinosaurs. *PLOS ONE* 8:e78214.

Tennant, J. P., P. D. Mannion, and P. Upchurch. 2016a. Environmental drivers of crocodyliform extinction across the Jurassic/Cretaceous transition. *Proceedings of the Royal Society B* 283:20152840.

Tennant, J. P., P. D. Mannion, and P. Upchurch. 2016b. Sea level regulated tetrapod diversity dynamics through the Jurassic/Cretaceous interval. *Nature Communications* 7:12737

Thulborn, R. A., and A. Warren. 1980. Early Jurassic plesiosaurs from Australia. *Nature* 285:224-225.

Torsvik, T. H., D. Carlos, J. Mosar, L. R. M. Cocks, and T. N. Malme. 2002. Global reconstructions and North Atlantic palaeogeography 400 Ma to Recent; pp. 18-39 *i*n E. EA. (ed.), *BATLAS - Mid Norway plate reconstructions atlas with global and Atlantic perspectives.* Geological Survey of Norway, Trondheim.

Torsvik, T. H., and M. A. Smethurst. 1999. Plate tectonic modeling: Virtual reality with GMAP. *Computers and Geosciences* 25:395-402.

Tyborowski, D. 2016. A new ophthalmosaurid ichthyosaur from the Late Jurassic of Owadów-Brzeziniki Quarry, poland. *Acta Palaeontologica Polonica* 61:791-803.

Vavrek, M. J. 2011. *Fossil*: palaeoecological and palaeogeographical analysis tools. *Palaeontologia Electronica* 14.1.1T:16p.

Veizer, J., D. Ala, K. Amzy, P. Bruckschen, F. Buhl, C. G. A. F., A. Diener, S. Ebneth, Y. Godderis, T. Jasper, C. Korte, F. Pawllek, O. G. Podlaha, and H. Strauss. 1999. 87Sr/86Sr, N18O and N13C Evolution of Phanerozoic seawater. *Chemical Geology* 161:59-88.

Vincent, P., and R. B. J. Benson. 2012. *Anningsaura*, a basal plesiosaurian (Reptilia, Plesiosauria) from the Lower Jurassic of Lyme Regis, United Kngdom. *Journal of Vertebrate Paleontology* 32:1049-1063.

Vinn, O., K. Hryniewicz, C. T. S. Little, and H. A. Nakrem. 2014. A Boreal serpulid fauna from Volgian-Ryazanian (latest Jurassic-earliest Cretaceous) shelf sediments and hydrocarbon seeps from Svalbard. *Geodiversitas* 36:527-540.

Wadewitz, E. 1977. Mowilith, an ideal conservation material for fossilized bone (Ein ideales Konservierungsmittel fur fossiles Knochenmaterial). *Der Praparator* 23:42-46.

Wahl, R. W., J. A. Massare, and M. Ross. 2010. New material from the type specimen of *Megalneusaurus rex* (Reptilia: Sauropterygia) from the Jurassic Sundance Formation, Wyoming. *Paludicola* 7:170-180.

Westermann, G. E.G.1993. Global bio-events in the mid-Jurassic ammonites controlled by seaways; pp. 187-226 *i*n M. R. House (ed.), *The Ammonoidea: Environment, Ecology and Evolutionary Change*. Oxford University Press, Oxford.

Wiens, J. J. 2006. Missing data and the design of phylogenetic analyses. *Journal of Biomedical Informatics* 39:34-42.

Wiens, J. J., and M. C. Morill. 2011. Missing data in phylogenetic analysis: reconciling results from simulations and empirical data. *Systematic Biology* 60:719-731.

Wierzbowski, A., K. Hryniewicz, Ø. Hammer, H. A. Nakrem, and C. T. S. Little. 2011. Ammonites from hydrocarbon seep carbonate bodies from the uppermost Jurassic - lowermost Cretaceous of Spitsbergen and their biostratigraphical importance. *Neues Jarbuch Geologie und Paläontologie Abhandlungen* 262:267-288.

Wierzbowski, H. 2004. Carbon and oxygen isotope composition of Oxfordian-Early Kimmeridgian belemnite rostra: palaeoenvironmental implications for Late Jurassic seas. *Palaeogeography, Palaeoclimatology, Palaeoecology* 203:153-168.

Wierzbowski, H., and M. Rogov. 2011. Reconsructing the palaeoenvironment of the Middle Russian Sea during the Middle - Late Jurassic transition using stable isotope ratios of cephalopod shells and variations in faunal assemblages. *Palaeogeography, Palaeoclimatology, Palaeoecology* 299:250-264.

Wilhelm, B. C. 2010. Novel anatomy of Cryptoclidid plesiosaurs with comments on axial locomotion, Master of Science thesis, pp. 70. *Marshall University*, Huntington, West Virginia.

Wilhelm, C. B., and F. R. O'Keefe. 2010. A new partial skeleton of a cryptocleidoid plesiosaur from the Upper Jurassic Sundance Formation of Wyoming. *Journal of Vertebrate Paleontology* 30:1736-1742.

Williston, S. W. 1925. The osteology of the reptiles. 300 pp, Cambridge.

Wiman, C. 1914. Ein Plesiosaurierwirbel aus dem juengeren Mesozoicum Spitsbergens. Bulletin - Uppsala Universiteter, *Mineralogisk-geologiska Instiut* 12:201-204.

Yakowlew, V. N. 1903. Neue Funde von Trias-Saurier auf Spitzbergen. *Verhandlungen der Russisch-Kaiserlichen Minerlogischen Gesellschaf* 40:179-202.

Young, M. T. 2014. Filling the 'Corallian Gap': re-description of a metriorhynchid crocodylomorph from the Oxfordian (Late Jurassic) of Headington, England. *Historical Biology* 26:80-90.

Young, M. T., and L. Steel. 2014. Evidence for the teleosaurid crocodylomorph genus *Machimosaurus* in the Kimmeridge Clay Formation (Late Jurassic) of England. *Historical Biology* 26:472-479.

Young, M. T., L. Steel, and H. Middleton. 2014. Evidence of the metriorhynchid crocodylomorph genus *Geosaurus* in the Lower Kimmeridge Clay Formation (Late Jurassic) of England. *Historical Biology* 26:551-555.

Young, M. T., L. Steel, M. P. Rigby, E. A. Howlett, and S. Humphrey. 2015. Largest known specimen of the genus *Dakosaurus* from the Kimmeridge Clay Formation (Late Jurassic) of England, and an overview of Dakosaurus specimens discovered from this formation (including reworked specimens from the Woburn Sands Formation). *Historical Biology* 27:947-953.

Žák, K., M. Košťák, O. Man, V. A. Zakharov, M. A. Rogov, P. Pruner, J. Rohovec, O. Dzyuba, and M. Mazuch. 2011. Comparison of carbonate C and O stable isotope records across the Jurassic/Cretaceous boundary in the Tethyan and Boreal Realms. *Palaeogeography, Palaeoclimatology, Palaeoecology* 299:83-96.

Zakharov, V. A. 1987. The bivalve Buchia and the Jurassic-Cretaceous boundary in the Boreal Province. *Cretaceous Research* 8:141-153.

Zakharov, V. A., and M. A. Rogov. 2003. Boreal-Tethyan mollusk migrations at the Jurassic-Cretaceous boundary time and biogeographic ecotone position in the Northern Hemisphere. *Stratigraphy and Geological Correlation* 11:152-171.

Zakharov, V. A., and M. A. Rogov. 2008. The Upper Volgian Substage in Northeast Siberia (Nordvik Peninsula) and its panboreal correlation based on ammonites. *Stratigraphy and Geological Correlation* 16:423-436.

Zakharov, V. A., B. N. Shurygin, N. I. Kurushin, S. V. Meledina, and B. L. Nikitenko. 2002. A Mesozoic Ocean in the Arctic paleontological evidence. *Russian Geology and Geophysics* 43:143-170.

Zhang, J., D. A. Rothrock, and M. Steele. 1998. Warming of the Arctic Ocean by a strengthen Atlantic inflow: Model results. *Geophysical Research Letters* 25:1745-1748.

Zverkov, N. G., M. S. Arkhangelsky, J. M. Pardo Pérez, and P. A. Beznosov. 2015. On the Upper Jurassic ichthyosaur remains from the Russian North. *Proceedings of the Zoological Institute RAS* 319:81-97.

Zverkov, N. G., A. O. Averianov, and E. V. Popov. 2017. Basicranium of an elasmosaurid plesiosaur from the Campanian of European Russia. *Alcheringa*:10.1080/03115518.2017.1302508

Appendix 1

Additional information for the introduction

Additional information for the introduction

Table A1.1: A general overview of the cryptoclidid fossil record, based on published and unpublished specimens in museum collections.

Country	Genus	Species	Time/Stage	Reference
Argentina				
	cf. *Muraenosaurus*	indet.	Callovian	Gasparini and Spalletti 1993
	cf. *Cryptoclidus*	indet.	Callovian	Gasparini and Spalletti 1993
Canada				
	Colymbosaurus	cf. *svalbardensis*	Late Jurassic	pers. obs. AJR
Cuba				
	Vinialesaurus	*caroli*	Oxfordian	Gasparini et al. 2002
East Greenland				
	indet.	indet.	Kimmeridgian	Smith 2007
France				
	Tricleidus	*seeleyi*	Oxfordian	Sauvage 1873
India				
	indet.	indet.	Kimmeridgian - Tithonian	Bardet et al. 1991
Pakistan				
	indet.	indet.	Late Jurassic	Buffetaut 1981
Russia				
	Colymbosaurus	indet.	Tithonian	Arkhagelsky et al. (accepted)
Svalbard				
	Spitrasaurus	*wensaasi*	Tithonian	Knutsen et al. 2012c
	Spitrasaurus	*larseni*	Tithonian	Knutsen et al. 2012c
	Djupedalia	*engeri*	Tithonian	Knutsen et al. 2012b
	Colymbosaurus	*svalbardensis*	Tithonian	Chapter 2, this volume Knutsen et al. 2012a
	Gen .nov	*sp. nov*	Tithonian - Berriasian	Chapter 3, this volume
United Kingdom				
	Colymbosaurus	*megadeirus*	Kimmeridgian - Tithonian	Benson and Bowdler 2014
	Colymbosaurus	indet.	Kimmeridgian - Tithonian	Roberts et al. 2017
	Kimmerosaurus	*langhami*	Tithonian	Brown, 1981
United States				
	Tatenectes	*laramiensis*	Oxfordian	O'Keefe and Street 2009
	Pantosaurus	*striatus*	Oxfordian	O'Keefe and Wahl 2003

Table A1.2: Collected specimens (2004-2012) and historical specimens from the central Spitsbergen. If not otherwise stated all specimens are from the Slottsmøya Member, Agardhfjellet Formation. Stratigraphic positions and references are included where available. Specimens described in this thesis are highlighted. **Abbreviations: Fm**, Formation; **NA**, not available; **PMO,** Paleontological Museum Oslo, University of Oslo, Oslo, Norway; **SVB**, Svalbard Museum, Longyearbyen, Norway.

Number	Group	Position	Species	References
PMO 222.655	Ichthyosaur	44.8m	*Keilhauia nui*	Delsett et al. 2017
PMO 222.658	Ichthyosaur	39.1m		Under study
PMO 224.248	Plesiosaur	38.5m		Chapter 3
PMO 222.665	Ichthyosaur	30.4m		
PMO 219.718	Plesiosaur	29.3m	*Spitrasaurus wensaasi*	Knutsen et al. 2012c
PMO 212.662/ SVB1452	Plesiosaur	27.0m		
PMO 222.671	Plesiosaur	22.5m		
PMO 214.578	Ichthyosaur	20.8m	*Cryopterygius kristiansenae*	Druckenmiller et al. 2012
PMO 224.250	Ichthyosaur	19m		Under study
PMO 224.251	Ichthyosaur	19m		
SVB 1450	Plesiosaur	17.8m	*Spitrasaurus larseni*	Knutsen et al. 2012c
PMO 222.672	Plesiosaur	17.5m		
PMO 222.673	Plesiosaur	17m		
PMO 224.247	Plesiosaur	16.5m		
PMO 227.932	Ichthyosaur	15.65 m	Ophthalmosauridae indet.	Delsett et al. 2017
PMO 222.669	Ichthyosaur	15.5m		Under study
PMO 222.670	Ichthyosaur	14.5m	Ophthalmosauridae indet.	Delsett et al. 2017
PMO 222.663	Plesiosaur	14m	*Colymbosaurus svalbardensis*	Chapter 2; Roberts et al. 2017
PMO 214.135	Pliosaur	14m	*Pliosaurus funkei*	Knutsen et al. 2012d
PMO 214.136	Pliosaur	14m	*Pliosaurus funkei*	Knutsen et al. 2012d
PMO 216.863	Plesiosaur	14m		
PMO 216.838	Plesiosaur	14m	*Colymbosaurus svalbardensis*	Knutsen et al. 2012a; Liebe & Hurum 2012

SVB 1451	Ichthyosaur	11.8m	*Palvennia hoybergeti*	Druckenmiller et al. 2012
PMO 222.668	Plesiosaur	11.8m		
PMO 222.659	Ichthyosaur	9.5m		
PMO 216.839	Plesiosaur	7m	*Djupedalia engeri*	Knutsen et al. 2012b; Liebe & Hurum 2012
PMO 224.252	Ichthyosaur	7m		Under study
PMO 222.662	Ichthyosaur	-0.2	Ophthalmosauridae indet.	Delsett et al. 2017
PMO 224.166	Ichthyosaur	-0.2m		
PMO 222.654	Ichthyosaur	-4m	*Janusaurus lundi*	Roberts et al. 2014
PMO 222.664	Plesiosaur	-4.4m		
PMO 222.667	Ichthyosaur	-7m		Roberts et al. 2014; under study
PMO 214.452	Plesiosaur	-8m		Under study
PMO 222.666	Plesiosaur	-11m		
PMO 218.377	Plesiosaur	-31-22 or -15-11 m	*Colymbosaurus svalbardensis*	Andreassen 2004; Knutsen et al. 2012a
PMO 224.249	Ichthyosaur	-51m		
PMO 222.657	Plesiosaur	NA		
PMO 222.660	Ichthyosaur	NA		
PMO A 27745	Plesiosaur	NA	*Colymbosaurus svalbardensis*	Persson 1962; Andreassen 2004; Knutsen et al. 2012a
PMO 222.661	Plesiosaur	NA		
PMO 227.931	Ichthyosaur	~-1 m Dorsoplanites bed		
PMO 219.572/ PMO 220.401	Plesiosaur	NA		Liebe & Hurum 2012
PMO 229.925	Ichthyosaur	NA		
PMO 229.926	Plesiosaur	-7m Dorsoplanites bed		
PMO 229.927	Plesiosaur	NA		
PMO 217.564	Ichthyosaur	Seep 8		Hryniewicz et al. 2015
PMO 230.083	Plesiosaur	NA		
PMO 230.084	Plesiosaur	NA		

PMO 230.085	Plesiosaur	~17.5m		
PMO 230.086	Reptilia indet.	Carolinefjellet Fm.		
PMO 230.087	Ichthyosaur	0?		
PMO 230.088	Pliosaur	0?		
PMO 230.089	Ichthyosaur	0?		
PMO 230.090	Plesiosaur	NA		
PMO 230.091	Plesiosaur	NA		
PMO 230.092	Ichthyosaur	NA		
PMO 230.093	Ichthyosaur	NA		
PMO 230.094	Ichthyosaur	NA		
PMO 230.095	Ichthyosaur	~31m		
PMO 230.096	Ichthyosaur	NA		
PMO 230.097	Ichthyosaur	NA		

Literature Cited

Andreassen, B. H., 2004. Plesiosaurs from Svalbard. Unpublished MSc thesis, University of Oslo, 109 pp.

Arkhangelsky, M. S., Zverkov, N. G., Rogov, M. A., Stenshin, I. M. and E. M. Baykina. *in press*. Colymbosaurines from the Upper Jurassic of European Russia and their implication for paleobiogeography of marine reptiles. *In* Kear, B. P., Sachs, S., Smith, A. and P. S. Druckenmiller (eds.). *Plesiosaurs - Mesozoic Sea Dragons*. Springer - Vertebrate Paleobiology and Paleoanthropology Series

Bardet, N., Mazin, J-M., Carious, E., Enay, R and J. Krishna. 1991. Les Plesiosauria du Jurassique supérieur de la province de Kachchh (Inde). *Comptes Rendus de l'Académie des Sciences - Series II* 313: 1343-1347.

Benson, R. B. J and T. Bowdler. 2014. Anatomy of Colymbosaurus megadeirus (Reptilia, Plesiosauria) from the Kimmeridge Clay Formation of the U.K., and high diversity among Late Jurassic plesiosauroids. Journal of Vertebrate Paleontology 34: 1053-1071

Brown, D. S. 1981. The English Upper Jurassic Plesiosauridae (Reptilia) and a review of the phylogeny and classification of the Plesiosauria. *Bulletin of the British Museum (Natural History), Geology* 35: 253-347.

Delsett, L. L., Roberts, A. J., Druckenmiller, P. S. and J. H. Hurum, 2017. A new ophthalmosaurids (Ichthyosauria) from Svalbard Norway, and Evolution of the ichthyopterygian pelvic girdle. *PLOS ONE* 12: e0169971.

Druckenmiller, P. S., Hurum, J. H., Knutsen, E. M. And H-A. Nakrem, 2012. Two new ophthalmosaurids (Reptilia: Ichthyosauria) from the Agardhfjellet Formation (Upper Jurassic: Volgian/Tithonian), Svalbard, Norway. *Norwegian Journal of Geology* 92: 311-229.

Gasparini, Z., Bardet, N. and M. Iturralde-Vincent. 2002. A new cryptoclidid Plesiosaur from the Oxfordian (Late Jurassic) of Cuba. *Geobios* 35: 201-211

Gasparini, Z., and L. Spalletti. 1993. First Callovian plesiosaurs from the Neuquén Basin, Argentina. *Ameghiniana* 30: 245-254

Hryniewicz, K., Nakrem, H-A., Hammer, Ø., Little, C. T. S., Kaim, A., Sandy, M. R. and J. H. Hurum, 2015. The Palaeoecology of the latest Jurassic – earliest Cretaceous hydrocarbon seep carbonates from Spitsbergen, Svalbard. *Lethaia* 48, 353-374.

Knutsen, E. M., Druckenmiller, P. S. and J. H. Hurum, 2012a. Redescription and taxonomic clarification of '*Tricleidus' svalbardensis* based on new material from the Agardhfjellet Formation (Middle Volgian). *Norwegian Journal of Geology* 92: 175-186.

Knutsen, E. M., Druckenmiller, P. S. and J. H. Hurum, 2012b. Two new species of long-necked plesiosaurians (Reptilia: Sauropterygia) from the Upper Jurassic (Middle Volgian) Agardhfjellet Formation of central Spitsbergen. *Norwegian Journal of Geology* 92: 187-212

Knutsen, E. M., Druckenmiller, P. S. and J. H. Hurum, 2012c. A new plesiosauroid (Reptilia: Sauropterygia) from the Agardhfjellet Formation (Middle Volgian) of central Spitsbergen, Norway. *Norwegian Journal of Geology* 92: 213-234.

O'Keefe, F. R. and J. R. Wahl. 2003. Current taxonomic status of the plesiosaur *Pantosaurus striatus* from the Upper Jurassic Sundance Formation, Wyoming. *Paludicola* 4: 37-46

O'Keefe, F. R. and H. P. Street, 2009. Osteology of the cryptocleidoid plesiosaur *Tatenectes laramiensis*, with comments on the taxonomic status of the Cimoliasauridae. *Journal of Vertebrate Paleontology* 29: 28-57

Sauvage, H.-E. 1873. Notes sur les reptiles fossils. *Bulletin de la Société Géologique de France, série 3* 1: 365-386

Smith, A. 2007. The back-to-front plesiosaur Cryptoclidus (Apractocleidus) aldingeri from the Kimmeridgian of Milne Land, Greenland. *Bulletin of the Geological Society of Denmark* 55: 1-7

Appendix 2

Published article Delsett et al. 2016

The Slottsmøya marine reptile *Lagerstätte*: depositional environments, taphonomy and diagenesis

LENE L. DELSETT[1]*, LINN K. NOVIS[2], AUBREY J. ROBERTS[3], MAAYKE J. KOEVOETS[1], ØYVIND HAMMER[1], PATRICK S. DRUCKENMILLER[4] & JØRN H. HURUM[1]

[1]*Natural History Museum, University of Oslo, 0318 Oslo, Norway*

[2]*Tromsø University Museum, 9037 Tromsø, Norway*

[3]*Ocean and Earth Science, National Oceanography Centre Southampton, University of Southampton, Southampton SO14 3ZH, UK*

[4]*University of Alaska Museum and Department of Geosciences, University of Alaska Fairbanks, Fairbanks, Alaska 99775, USA*

**Corresponding author (e-mail: l.l.delsett@nhm.uio.no)*

Abstract: The Late Jurassic Slottsmøya Member *Lagerstätte* on Spitsbergen offers a unique opportunity to study the relationships between vertebrate fossil preservation, invertebrate occurrences and depositional environment. In this study, 21 plesiosaurian and 17 ichthyosaur specimens are described with respect to articulation, landing mode, preservation, and possible predation and scavenging. The stratigraphic distribution of marine reptiles in the Slottsmøya Member is analysed, and a correlation between high total organic content, low oxygen levels, few benthic invertebrates and optimal reptile preservation is observed. A new model for 3D preservation of vertebrates in highly compacted organic shales is explained.

Supplementary material: A taphonomic description of each marine reptile specimen is available at https://doi.org/10.6084/m9.figshare.c.2133549

Mesozoic marine reptiles have been known from the Svalbard archipelago for more than 150 years, particularly from Triassic units (Maxwell & Kear 2013; Hurum *et al.* 2014). However, it was not until 1914 that Wiman described the first Jurassic marine reptile, a plesiosaur, from the island of Spitsbergen (Wiman 1914; Kear & Maxwell 2013). Beginning in 2004, an extensive new field survey for Jurassic marine reptiles was undertaken by the Spitsbergen Jurassic Research Group (SJRG), an international team of palaeontologists and geologists. During eight field seasons (2004 and 2006–12) on Spitsbergen, SJRG collected more than 40 marine reptile skeletons from the dark marine shales of the Upper Jurassic–Lower Cretaceous Slottsmøya Member of the Agardhfjellet Formation (Fig. 1). Given the sheer abundance of material and quality of preservation, we have characterized this unit as a *Lagerstätte* (Hurum *et al.* 2012).

In the course of this work, detailed taphonomical data have been collected, permitting a rare insight into plesiosaur and ichthyosaur taphonomy. Previous studies were limited primarily to two other Jurassic units: the Oxford Clay and the Posidonienschiefer Formation (Martill 1985, 1986, 1993). However, the material upon which these studies were based was collected decades ago, and the specimens were not adequately stratigraphically constrained or contextualized geologically: thus, taphonomical interpretations presented in these studies are somewhat contentious. Efimov (2001) also analysed the taphonomy of a large number of Upper Jurassic and Lower Cretaceous ichthyosaurs from two parts of the Ulyanovsk Section in the Volga Region.

Here, for the first time, we address plesiosaur and ichthyosaur taphonomy based on a large sample size ($n = 38$) with many articulated specimens from a site where stratigraphic, sedimentological and palaeontological data were collected simultaneously (Table 1; Figs 2 & 3). In this paper, we describe the preservational modes of the skeletons, and attempt to interpret the major physical and biotic factors affecting skeletal preservation. We incorporate new surface and well-log data to document the stratigraphic distribution of skeletons in the unit, especially in relation to the total organic

From: KEAR, B. P., LINDGREN, J., HURUM, J. H., MILÀN, J. & VAJDA, V. (eds) 2016. *Mesozoic Biotas of Scandinavia and its Arctic Territories*. Geological Society, London, Special Publications, **434**, 165–188. First published online December 16, 2015, updated December 17, 2015, http://doi.org/10.1144/SP434.2

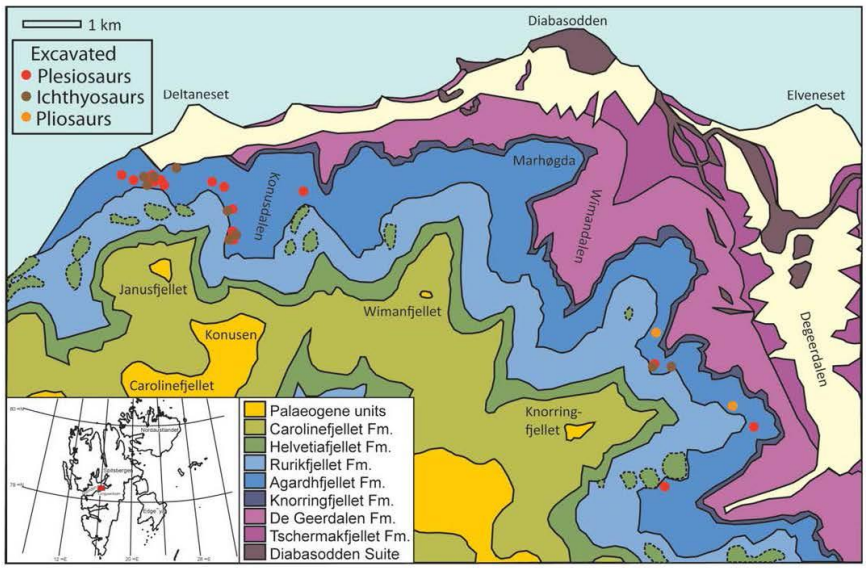

Fig. 1. Geological map of the study area in central Spitsbergen, with the main marine reptile locations marked with red, brown and yellow circles. Redrawn and adapted from Dallmann *et al.* (2001).

content (TOC). The causes for the exceptional abundance of marine reptile skeletons found in the Slottsmøya Member compared to other members is beyond the scope of this paper.

Geological setting

The Svalbard archipelago is located between latitudes 74–81° N and longitudes 10–35° E, in the northwestern corner of the Barents Sea shelf. The Middle Jurassic–Lower Cretaceous succession forming the Janusfjellet Subgroup comprises the Agardhfjellet and Rurikfjellet formations. The Agardhfjellet Formation consists of black shales and siltstones deposited in an open-marine, oxygen-deficient shelf setting (Dypvik *et al.* 1991; Collignon & Hammer 2012). The Myklagardfjellet bed, a distinct thin marker horizon of weathering clays, marks the boundary between the two formations (Birkenmajer 1980).

The marine reptiles and invertebrates discussed in this study occur in the Slottsmøya Member, the uppermost member of the Agardhfjellet Formation (Figs 1 & 2). The Slottsmøya Member rests on the Oppdalsåta Member and is overlain by the Wimanfjellet Member of the Rurikfjellet Formation (Mørk *et al.* 1999). The Slottsmøya Member was deposited in an open-marine shelf (Hammer *et al.* 2012). The thickness ranges from 70 to 100 m, and consists of black to grey shales and siltstones with siderite interbeds (Dypvik *et al.* 1991). Shelf conditions were slightly dysoxic with periodical oxygenation of the bottom water, which might have been a result of influx of clastic sediments (Collignon & Hammer 2012). The shales of the mid-section show little alternation in mineralogy, suggesting a stable depositional environment, while the sediments in the silty intervals were transported into the basin by turbidity currents (Collignon & Hammer 2012). This interpretation is supported by taphonomical and ecological evidence. Some crinoids and echinoids were situated in the sediment as if they were transported, while other echinoderms like asteroids and ophiuroids were found *in situ* (Rousseau & Nakrem 2012). TOC values of the Slottsmøya Member show considerable fluctuation, with the largest excursion reaching 9.7% (Hammer *et al.* 2012).

In the uppermost part (39–49 m) of the Slottsmøya Member, several cold-seep communities have been discovered. From these, a diverse and low-dominance invertebrate fauna has been described (Hammer *et al.* 2011, 2013; Wierzbowski *et al.* 2011; Hryniewicz *et al.* 2012, 2014). The non-seep fauna invertebrate diversity was probably also quite high. This assumption is based on a study of the

Slottsmøya Member from East Spitsbergen by Birkenmajer *et al.* (1982), the echinoderm fauna in the section (Rousseau & Nakrem 2012) and field observations in the area.

Abbreviations

PMO, Natural History Museum, University of Oslo (Palaeontological collection); SJRG, Spitsbergen Jurassic Research Group; SVB, Svalbard Museum, Longyearbyen.

Materials and methods

The 38 marine reptile skeletons used in this study were excavated during eight field seasons (2004 and 2006–12) by the SJRG. For each skeleton, the locality information, stratigraphic position and taphonomical data (e.g. orientation, nature and degree of articulation, and associated invertebrates) were recorded in the field at the time of collection (Table 1; Figs 2 & 3). During preparation, additional information was obtained concerning the articulation and association of skeletal elements, quality of preservation, completeness and bone modification. Field drawings and photographs before and during preparation were utilized in constructing skeletal maps of 28 of the specimens (Figs 4–8). The remaining specimens were relatively incomplete, poorly preserved or very disarticulated and, consequently, were not illustrated.

The marine-reptile-rich Jurassic deposits in the Oxford Clay Formation and the Posidonienschiefer Formation were used for comparative purposes in this study. The lowermost unit of the Oxford Clay Formation, the Peterborough Member, contains fossiliferous, organic-rich mudstone (Tang 2002). The clay was deposited in a shallow epicontinental seaway, and it is suggested that the seafloor substrate was soupy (Martill *et al.* 1994). The Posidonienschiefer Formation of Holzmaden is known for its well-preserved marine reptiles and fish. The formation comprises finely laminated bituminous shale, and is regarded as the archetype for stagnant deposition (Seilacher *et al.* 1985).

Martill (1985, 1986, 1993) collected vast amounts of information in his descriptions of marine reptiles from the Oxford Clay and the Posidonienschiefer Formation. In his studies of the preservation of the marine reptiles from the Peterborough Member (Martill 1985), he classified five preservation types based on the degree of skeletal articulation and the elements preserved: (1) articulated skeletons; (2) disarticulated skeletons; (3) isolated bones and teeth; (4) rolled and worn skeletal elements; and (5) coprocoenosic accumulations. Two types of disarticulation were observed. In the first type, bones were disarticulated but associated, and the disarticulation was caused by gravitational collapse of the skeleton. There were no scattered skeletal elements. In the second type, bones were scattered over a considerable distance, and the disarticulation could be a consequence of scavenging, current activity or both (Martill 1993). The five preservational modes of Martill (1985) form the basis for the categorization of the Slottsmøya Member marine reptile skeletons in this study, which we segregate into three different categories:

- Articulated skeleton: this definition (Martill 1985, p. 159) is used to describe a specimen with a true bone to bone relationship. However, parts of the skeleton can be missing due to surface erosion.
- Partly articulated skeleton: this is a new category based on the definition of the first type of disarticulated skeletons used by Martill (1985), which recognizes that some skeletons found in the Slottsmøya Member are intermediate between articulated and disarticulated (also observed by Martill 1993). A partly articulated specimen consists of two or more skeletal elements in articulation: for example, sections of associated vertebrae, ribs still articulated to vertebrae or partly articulated fins, along with disarticulated elements.
- Disarticulated skeleton: the definition (Martill 1985, p. 161) is used to describe a specimen lacking a bone to bone relationship and where the elements are scattered over a limited area. Martill (1985) also included specimens with some articulated elements in the definition, but here we include such specimens in the category of partly articulated skeletons.

To analyse the variation in three-dimensionality of the bones, a computerized tomography (CT) scan of two vertebrae from an ichthyosaur (PMO 222.654: holotype of *Janusaurus lundi* Roberts, Druckenmiller, Sætre & Hurum, 2014) was conducted. The two vertebrae were scanned with a Nikon Metrology XT 225 ST X-ray microtomograph at the Natural History Museum in Oslo, at a voltage of 210 kV, a current of 300 μA and an exposure time of 500 ms (Fig. 9).

The invertebrate fossils analysed here were discovered while conducting detailed stratigraphic logging of two cores: DH2 and DH5R. These cores were obtained by the Longyearbyen CO_2 Laboratory during a full-core drilling campaign (Larsen 2012). Approximately 70 m of the cores are assigned to be part of the Slottsmøya Member. Invertebrate abundances represent qualitative estimates, as the area covered by the cores is minimal and fossils could only be observed on split surfaces

Table 1. *Collected specimens*

Collection No.	Stratigraphic position (m)	Elements preserved	Articulation	Landing mode	References	Taxon	Figure reference
PMO 222.655	44.8	Almost complete	Articulated	Dorsal, then lateral torsion	Under study	I	Figure 4a
PMO 222.658	39.1	Forefin, pectoral girdle, vertebrae	Disarticulated	Unknown	Under study	I	Figure 8d
PMO 224.248	38.5	Skull, forefins, pectoral girdle, vertebrae	Articulated	Ventral	Under study	Pe	Figure 5a
PMO 222.665	30.4	Vertebrae	Partly articulated	Unknown		I	
PMO 219.718	29.3	Almost complete	Articulated	Dorsal	Knutsen *et al.* (2012*b*)	*Pe: Spitrasaurus wensaasi*	Figures 3b and 4e
PMO 212.662/ SVB 1452	27.0	Partial skull, phalanges, vertebrae	Partly articulated	Dorsal		Pe	Figures 3d and 7c
PMO 222.671	22.5	Forefin, pectoral girdle, vertebrae	Partly articulated	Unknown		Pe	Figure 5b
PMO 214.578	20.8	Almost complete	Articulated	Anterior, then twisted laterally	Druckenmiller *et al.* (2012)	*I: Cryopterygius kristiansenae*	Figures 3a and 4b
PMO 224.250	19	Forefins, pectoral girdle	Partly articulated	Ventral	Under study	I	Figure 5d
PMO 224.251	19	Forefins, girdle elements, vertebrae, hindfin	Partly articulated	Dorsal		I	Figure 5c
SVB 1450	17.8	Partial skull, forefin, vertebrae	Partly articulated	Ventral	Knutsen *et al.* (2012*b*)	*Pe: Spitrasaurus larseni*	Figure 7d
PMO 222.672	17.5	Vertebra, pelvic girdle	Disarticulated	Unknown		Pe	Figure 8e
PMO 222.673	17	Vertebrae	Disarticulated	Unknown		Pe	
PMO 224.247	16.5	Forefins, girdle elements, vertebrae	Partly articulated	Ventral		Pe	Figure 6d
PMO 222.669	15.5	Skull, vertebrae, pectoral girdle, forefin	Partly articulated	Anterior, then twisted laterally	Under study	I	Figures 3c and 7e
PMO 222.670	14.5	Hindfins, vertebrae, pelvic girdle	Articulated	Left lateral	Under study	I	Figure 4c
PMO 222.663	14	Forefins, pectoral girdle, vertebrae, hindfins	Partly articulated	Ventral	Under study	Pe	Figure 7f
PMO 214.135	14	Partial skull, vertebrae, humerus, phalanges, coracoid	Partly articulated	Dorsal	Knutsen *et al.* (2012*d*)	*Pi: Pliosaurus funkei*	Figure 6f
PMO 214.136	14	Partial skull, vertebrae	Disarticulated	Unknown	Knutsen *et al.* (2012*d*)	*Pi: Pliosaurus funkei*	
PMO 216.863	14	Forefin, pectoral girdle, vertebrae, pelvic girdle, hindfin	Partly articulated	Unknown		Pe	

PMO 216.838	14	Hindfins, vertebrae, pelvic girdle, phalanges	Partly articulated	Unknown	Knutsen *et al.* (2012*a*); Liebe & Hurum (2012)	Pe: *Colymbosaurus svalbardensis*	Figure 6c
SVB 1451	11.8	Skull, ribs, vertebrae, phalanges, clavicle	Partly articulated	Dorsal	Druckenmiller *et al.* (2012)	I: *Palvennia hoybergeti*	Figure 6e
PMO 222.668	11.8	Vertebrae, pelvic girdle	Disarticulated	Unknown		Pe	Figure 8c
PMO 222.659	9.5	Skull	Disarticulated	Unknown		I	
PMO 216.839	7	Almost complete	Partly articulated	Ventral	Knutsen *et al.* (2012*c*); Liebe & Hurum (2012)	Pe: *Djupedalia engeri*	Figure 6a
PMO 224.252	7	Partial skull, ribs	Partly articulated	Dorsal	Under study	I	Figure 5e
PMO 222.662	−0.2	Pelvic girdle, femur, tail bend	Partly articulated	Unknown		I	Figure 7b
PMO 224.166	−0.2	Humerus, vertebrae	Disarticulated	Unknown		I	Figures 3c and 8a
PMO 222.654	−4	Partial skull, appendicular skeleton, vertebrae	Partly articulated	Right ventrolateral	Roberts *et al.* (2014)	I: *Jansusaurus lundi*	Figure 6b
PMO 222.664	−4.4	Propodial, vertebrae	Disarticulated	Unknown		Pe	Figure 8b
PMO 222.667	−7	Partial skull, vertebrae, pectoral girdle, forefin	Partly articulated	Ventral	Roberts *et al.* (2014); under study	I	Figure 7a
PMO 214.452	−8	Forefins, hindfins, pelvic girdle, vertebrae	Disarticulated	Ventral	Under study	Pe	Figures 3f and 8f
PMO 222.666	−11	Vertebrae	Disarticulated	Unknown		Pe	
PMO 218.377	−31 to −22 or −15 to −11	Propodial, hindfin	Partly articulated	Unknown	Andreassen (2004); Knutsen *et al.* (2012*a*)	Pe: *Colymbosaurus svalbardensis*	
PMO 224.249	−51	Partial skull, vertebrae, partial fin	Disarticulated	Unknown		I	
PMO 222.657	Unknown	Vertebrae	Articulated	Unknown		Pe	
PMO 222.660	Unknown	Vertebrae	Disarticulated	Unknown		I	
PMO A27745	Unknown	Hindfins, pelvic girdle, vertebrae	Articulated	Dorsal	Persson (1962); Andreassen (2004); Knutsen *et al.* (2012*a*)	Pe: *Colymbosaurus svalbardensis*	Figure 4d

Slottsmøya Member marine reptile specimens collected 2004–2012 in stratigraphic order. Stratigraphic position measured above or below (−) the yellow layer (see sedimentary log in Fig. 2). I, ichthyosaur; Pe, plesiosauroid; Pl, pliosaurid. Figure references are to figures in this paper.

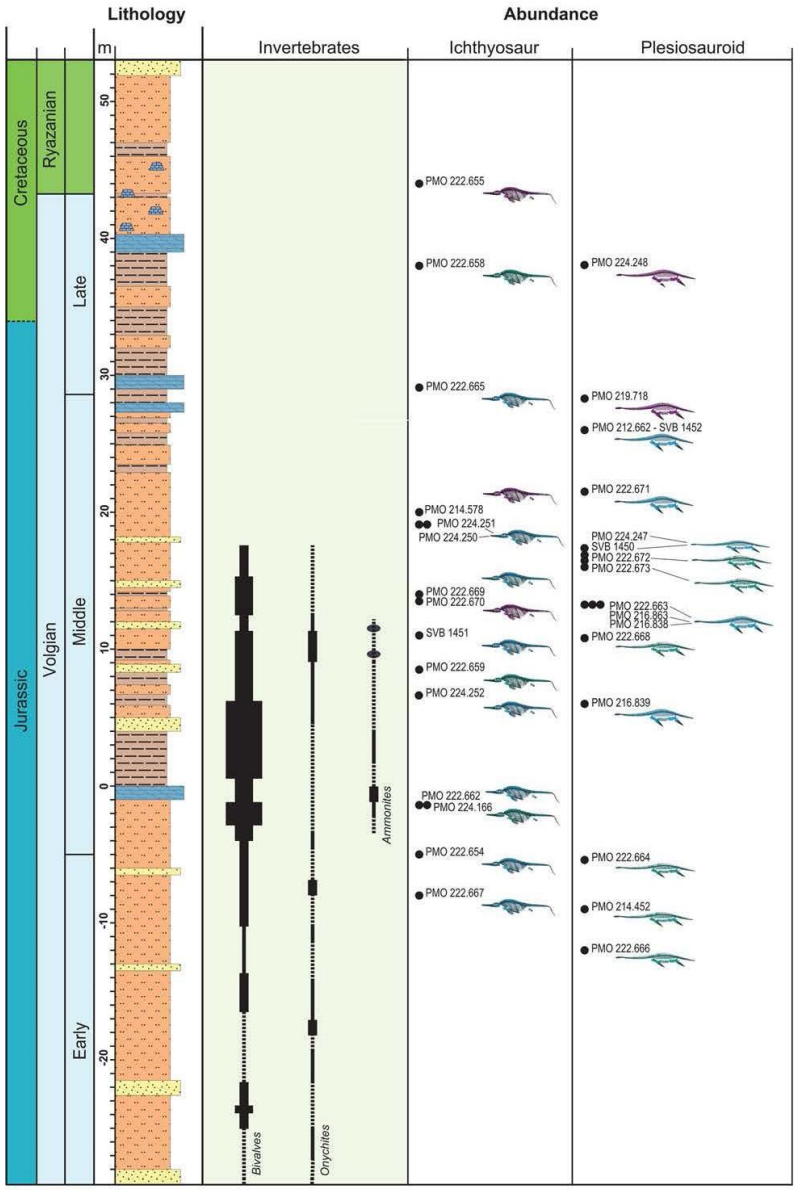

Fig. 2. Composite log of the marine reptile interval in the Slottsmøya Member in the Janusfjellet–Knorringfjellet area. Lithology based on Collignon & Hammer (2012); isotope and TOC data from Hammer *et al.* (2012); foraminiferal zones from Hjalmarsdottir (2012) and Nagy & Basov (1998); all from Janusfjellet sections. Invertebrate abundance (qualitative) from the DH2 core, Longyearbyen.

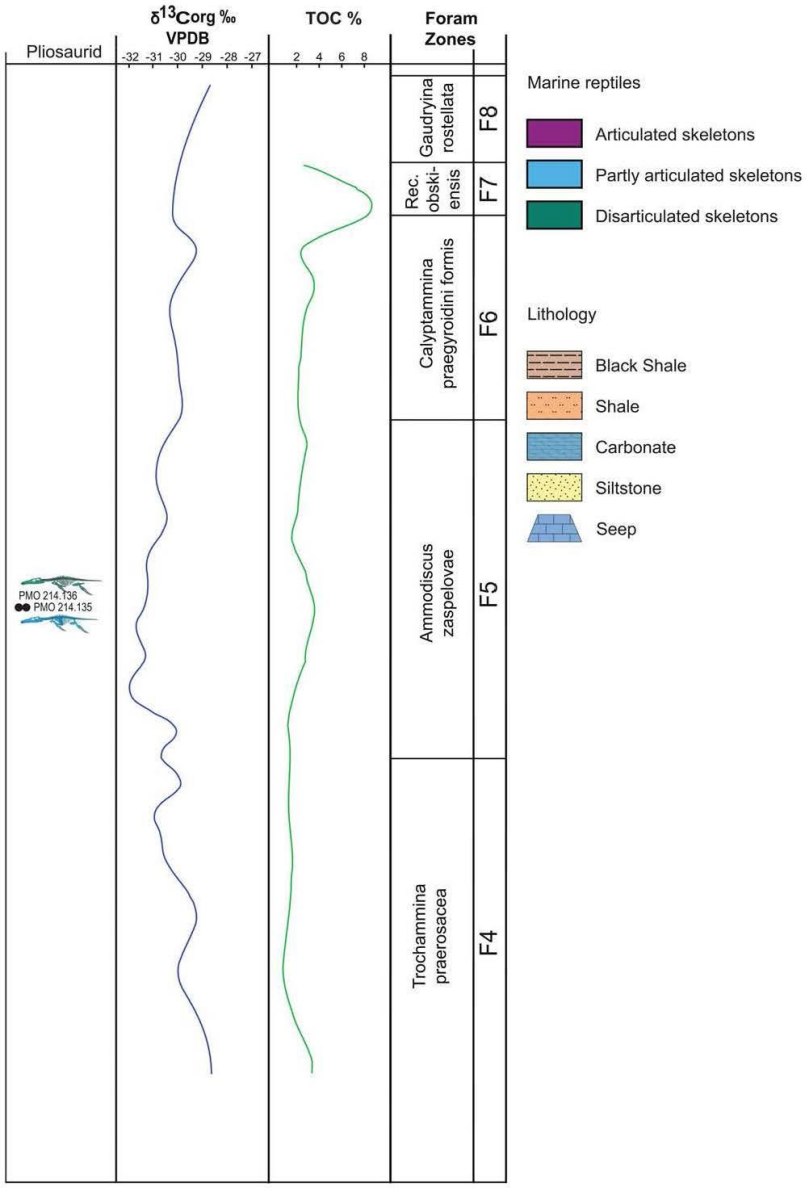

Fig. 2. *Continued.*

Fig. 3. Field photographs of selected specimens with different articulation status: (**a**) PMO 214.578, articulated ichthyosaur; (**b**) PMO 219.718, articulated plesiosauroid; (**c**) PMO 222.669, partly articulated ichthyosaur; (**d**) PMO 212.662/SVB 1452, partly articulated plesiosauroid; (**e**) PMO 224.166, disarticulated ichthyosaur; and (**f**) PMO 214.452, disarticulated plesiosauroid. Photographs by the SJRG.

that were unevenly distributed. TOC measurements were obtained from the DH2 core samples.

Results and discussion

Articulation of marine reptile specimens

Articulated skeletons. There are seven articulated skeletons among the Slottsmøya marine reptiles: ichthyosaurs ($n = 3$) and plesiosauroids ($n = 4$) (Figs 3a, b, 4 & 5a). Two ichthyosaurs (PMO 214.578, holotype of *Cryopterygius kristiansenae* Druckenmiller *et al.*, 2012: Figs 3a & 4b; PMO 222.655: Fig. 4a) and one plesiosauroid (PMO 219.718: holotype of *Spitrasaurus wensaasi* Knutsen *et al.*, 2012*b*: Figs 3b & 4e) are nearly complete. PMO 214.578 lacks only the posterior portion of the tail, while PMO 219.718 lacks the skull in addition to the posterior portion of the skeleton lost to erosion. PMO 222.655 has only a few displaced vertebrae and neural arches, in addition

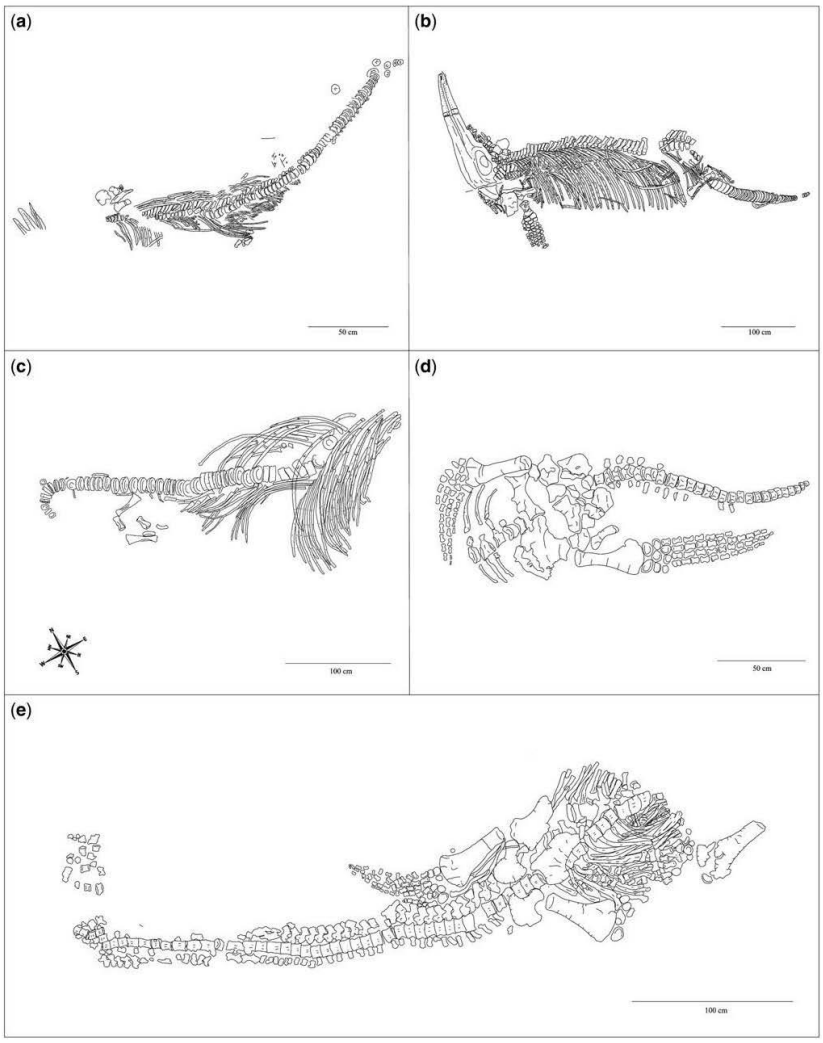

Fig. 4. Outlines of articulated marine reptile specimens from the Slottsmøya Member, Agardhfjellet Formation, Svalbard. The specimens are drawn from the side stratigraphically up unless otherwise stated. See Table 1 for more information on each specimen. (**a**) PMO 222.655, ichthyosaur, drawn from the side stratigraphically down. (**b**) PMO 214.578, holotype of the ichthyosaur *Cryopterygius kristiansenae*, drawn from the side stratigraphically down. (**c**) PMO 222.670, ichthyosaur. (**d**) PMO A27745, holotype of the plesiosauroid *Colymbosaurus svalbardensis*. (**e**) PMO 219.718, holotype of the plesiosauroid *Spitrasaurus wensaasi*.

to the pelvic girdle, which was moved anteriorly from its original position. The rostrum was divided from the body by a fault, and was found about 30 cm deeper. The preservation of the specimen is poor in the anterior part and improves posteriorly. PMO A27745 (Fig. 4d) is an articulated posterior

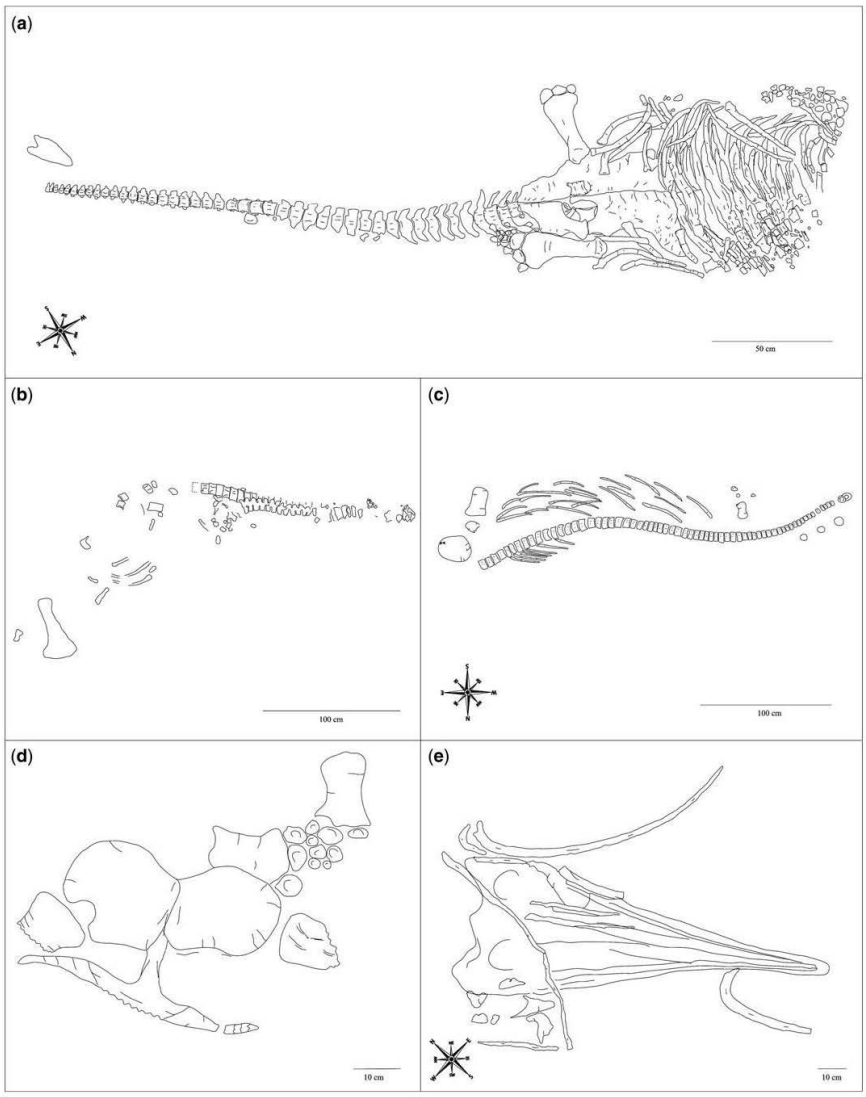

Fig. 5. Outlines of articulated and partly articulated marine reptile specimens from the Slottsmøya Member, Agardhfjellet Formation, Svalbard. The specimens are drawn from the side stratigraphically up unless otherwise stated. See Table 1 for more information on each specimen. (**a**) PMO 224.248, plesiosauroid. (**b**) PMO 222.671, plesiosauroid. (**c**) PMO 224.251, ichthyosaur. (**d**) PMO 224.250, ichthyosaur. (**e**) PMO 224.252, ichthyosaur.

portion of a plesiosauroid, collected in 1931 and described by Persson (1962) as *Tricleidus svalbardensis* and then later redescribed as *Colymbosaurus svalbardensis* by Knutsen *et al.* (2012*a*). PMO 224.248 (Fig. 5a) is the only plesiosauroid skeleton from the Slottsmøya Member that preserves a

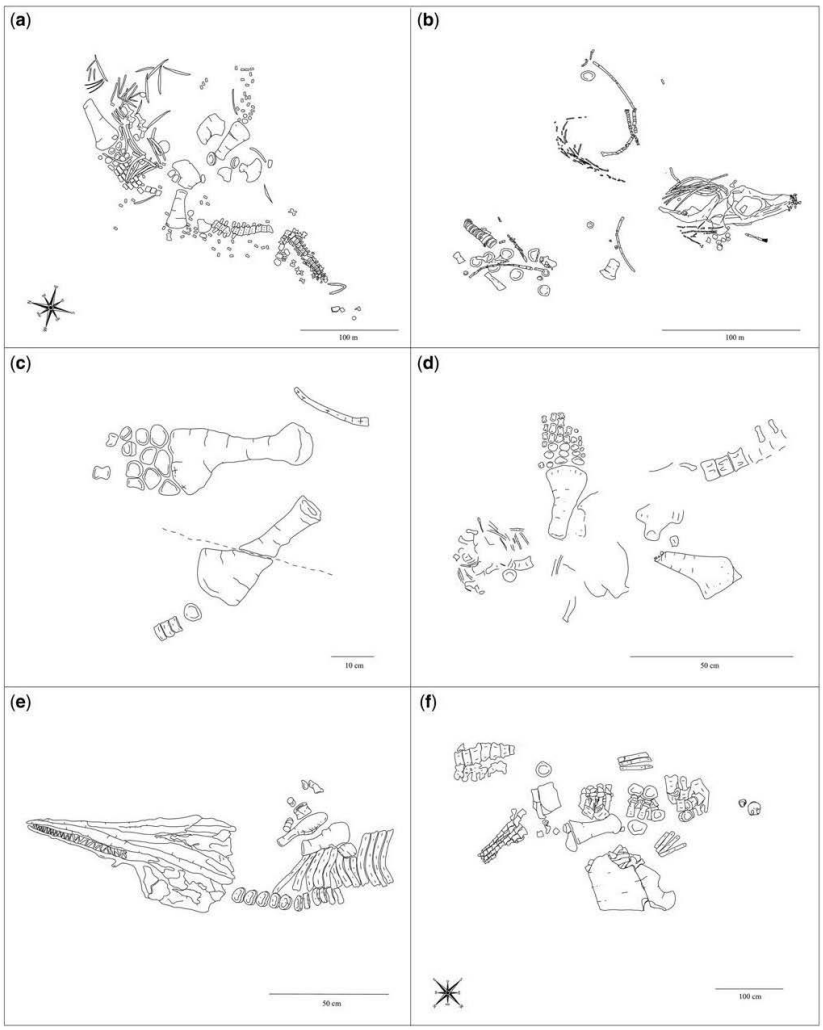

Fig. 6. Outlines of partly articulated marine reptile specimens from the Slottsmøya Member, Agardhfjellet Formation, Svalbard. The specimens are drawn from the side stratigraphically up unless otherwise stated. See Table 1 for more information on each specimen. (**a**) PMO 216.839, holotype of the plesiosauroid *Djupedalia engeri*. (**b**) PMO 222.654, holotype of the ichthyosaur *Janusaurus lundi*. (**c**) PMO 216.838, plesiosauroid, referred to *Colymbosaurus svalbardensis*. (**d**) PMO 224.247, plesiosauroid. (**e**) SVB 1451, holotype of the ichthyosaur *Palvennia hoybergeti*. (**f**) PMO 214.135, holotype of the pliosaurid *Pliosaurus funkei*.

complete and articulated skull. It is slightly displaced from the neck. PMO 222.670 (Fig. 4c) is the posterior half of a large ichthyosaur, while PMO 222.657 is an unfigured articulated series of cervical vertebrae from a plesiosauroid. For PMO 222.670, PMO 224.248 and PMO A27745, approximately half of the skeleton is missing, probably due to erosion of the hillside.

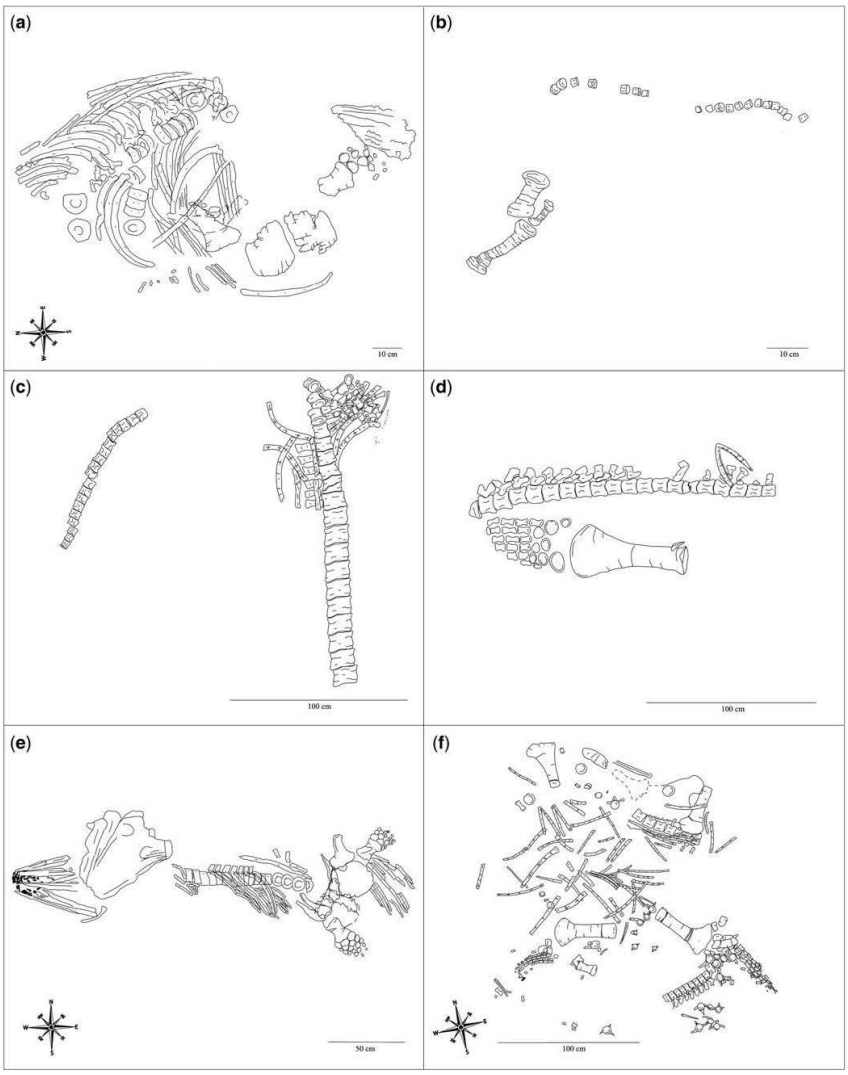

Fig. 7. Outlines of partly articulated marine reptile specimens from the Slottsmøya Member, Agardhfjellet Formation, Svalbard. The specimens are drawn from the side stratigraphically up unless otherwise stated. See Table 1 for more information on each specimen. (**a**) PMO 222.667, ichthyosaur. (**b**) PMO 222.662, ichthyosaur. (**c**) PMO 212.662/SVB 1452, plesiosauroid. (**d**) SVB 1450, holotype of the plesiosauroid *Spitrasaurus larseni*. (**e**) PMO 222.669, ichthyosaur. (**f**) PMO 222.663, plesiosauroid.

Some elements of the articulated skeletons have also undergone other types of post-mortem taphonomical alteration. In the ichthyosaur PMO 214.578, the skull is dorsoflexed at an angle of 90° relative to the long axis of the skeleton. In the pelvic area, there are some crushed vertebrae; in the

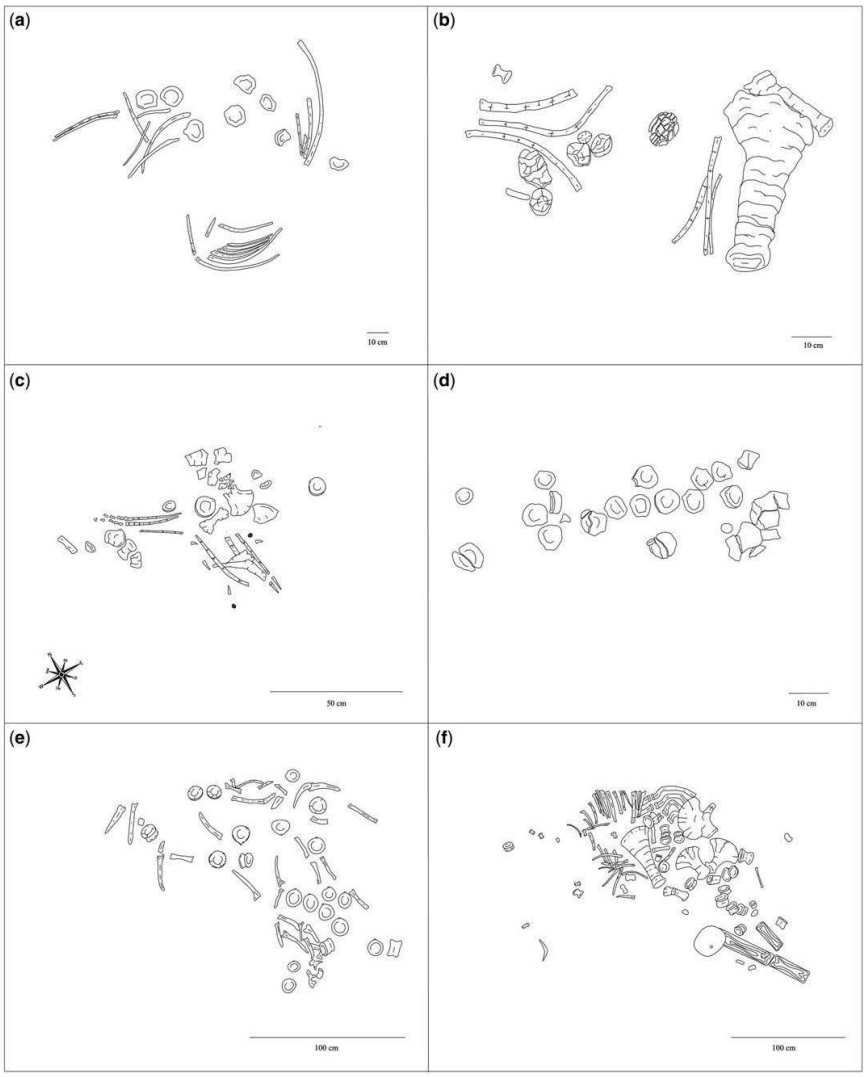

Fig. 8. Outlines of disarticulated marine reptile specimens from the Slottsmøya Member, Agardhfjellet Formation, Svalbard. The specimens are drawn from the side stratigraphically up unless otherwise stated. See Table 1 for more information on each specimen. (**a**) PMO 224.166, ichthyosaur. (**b**) PMO 222.664, plesiosauroid. (**c**) PMO 222.668, plesiosauroid. (**d**) PMO 222.658, ichthyosaur. (**e**) PMO 222.672, plesiosauroid. (**f**) PMO 214.452, plesiosauroid.

stomach area, the ribs on the right-hand side are bent inwards. The left forefin is completely articulated, while the right is partly disarticulated and displaced along the dorsal side of the skull. The left hindfin is articulated, and is flipped posterodorsally on top of the sacral vertebral region. In the plesiosauroid PMO A27745, the right hindfin is articulated and lies parallel to the vertebral column, while the left

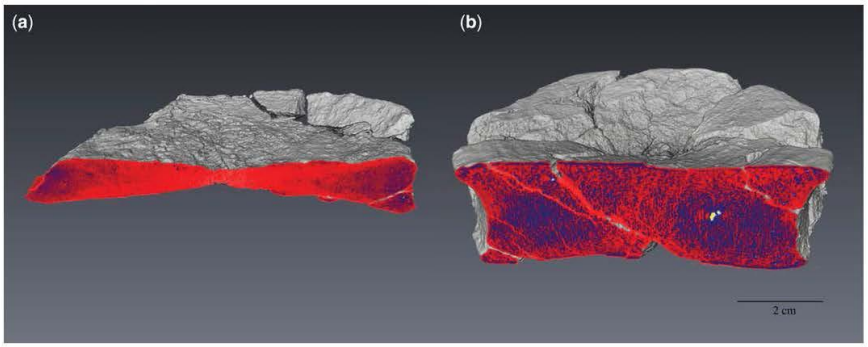

Fig. 9. Compressed and uncompressed vertebrae from ichthyosaur PMO 222.654, CT scan: (**a**) compressed vertebra; and (**b**) uncompressed vertebra. Colours show the X-ray density, with blue (pore-filling) denser than red (bone).

hindfin was rotated 180° and lies articulated in the opposite direction. The left forefin of the plesiosauroid PMO 219.718 is articulated with almost all of the phalanges in life position. In contrast, the right forefin is disarticulated, with the phalanges scattered along the left lateral part of the skeleton. The right femur is found at the posterior end of the specimen, close to the exposed surface, and the phalanges are scattered on top of the left lateral side.

Partly articulated skeletons. There are a total of 19 partly articulated skeletons including plesiosauroids ($n = 9$), pliosaurid ($n = 1$) and ichthyosaurs ($n = 9$) (Figs 3c, d, 5b–e, 6 & 7). The plesiosauroid PMO 216.839 (holotype of *Djupedalia engeri* Knutsen, Druckenmiller & Hurum, 2012*c*) (Fig. 6a) is nearly complete, but lacks the skull, left hindfin and caudal vertebral series. The ichthyosaur SVB 1451 (Fig. 6e) is the holotype of *Palvennia hoybergeti* Druckenmiller, Hurum, Knutsen & Nakrem, 2012, and consists of a skull articulated to cervical vertebrae and ribs, associated with a partial clavicle, a partial humerus and some phalanges. SVB 1450 (Fig. 7d) is a plesiosauroid, and the holotype of *Spitrasaurus larseni* Knutsen, Druckenmiller & Hurum, 2012*b*. The specimen consists of an articulated fin, a partial vertebral series articulated to the neural arches, as well as the lower jaw, teeth and a few skull fragments.

Several of the skeletons were spread over large areas. PMO 222.654 (holotype of the ichthyosaur *Janusaurus lundi*) (Fig. 6b), with an estimated body length of 3–4 m (Roberts *et al.* 2014), had body elements scattered over an area of 2 × 2.5 m, in four distinct clusters. The plesiosauroid PMO 222.663 (Fig. 7f), estimated body length of 6–7 m, was spread over an area of 2.5 × 3 m. PMO 214.135 (holotype of the pliosaurid *Pliosaurus funkei* Knutsen, Druckenmiller & Hurum, 2012*d*) (Fig. 6f), with an estimated body length of 10–13 m (Knutsen *et al.* 2012*d*), had groups of elements scattered over an area of 4.6 × 2.7 m.

PMO 216.838 (Fig. 6c) is a plesiosauroid, referred to *Colymbosaurus svalbardensis* (Persson, 1962) in Knutsen *et al.* (2012*a*). The specimen had an unusual preservation as it was found in a siderite concretion, and is partially deformed. The plesiosauroid PMO 216.863 (unfigured) was found in a slumped block and tilted nearly vertically.

Disarticulated skeletons. Twelve disarticulated skeletons were collected from the Slottsmøya Member, including ichthyosaurs ($n = 5$), a pliosaurid ($n = 1$) and plesiosauroids ($n = 6$) (Figs 3e, f & 8). Vertebrae, ribs and fins are the most frequently preserved body elements, while pelvic girdle elements, teeth and neural arches are less common. The plesiosauroid PMO 214.452 (Figs 3f & 8f) preserves both ischia closely associated with the right pubis, while elements from the body, particularly ribs and vertebrae, have been scattered around the pubis–ischia cluster. PMO 214.136, a referred specimen of *Pliosaurus funkei,* includes cranial remains that were probably articulated prior to burial, but were later displaced by slumping due to solifluction.

Currents

Bottom currents can be responsible for the disarticulation of skeletons and loss of skeletal elements (Beardmore *et al.* 2012*a*), and the position of skeletal elements can be used to evaluate water movement and direction of flow (Barnes & Hiller 2010). Small light bones have the highest potential to be moved by currents. For the partly articulated and disarticulated specimens in this study, there is no clear pattern of sorting. Some of the ribs seem

to lie perpendicular to one another, which could indicate changes in current direction. In several of the skeletons, many of the distal phalanges lie scattered around the skeleton, although other phalanges in the same skeleton are articulated, possibly due to stronger ligaments in proximal parts of the fins. This is especially visible in the plesiosauroids PMO 216.839 (Fig. 6a) and PMO 222.663 (Fig. 7f). The phalanges of the plesiosauroid PMO 219.718 (Fig. 4e), all located in the body area of the animal, seem to have been orientated by a dominant current direction crossing the vertebral column. The torso of the plesiosauroid PMO 219.718 most probably hit the seafloor before the rest of the body, and sank down in the sediments. This left the lighter cervical vertebrae and skull on the sea bottom, and they were likely to have been exposed to current activity. Teeth from the skull of the plesiosauroid PMO 224.248 (Fig. 5a) drifted from the skull over the cervical vertebrae in a similar direction, while distal phalanges from one of the forefins were disarticulated in a different direction. This could be indicative of a difference in current direction.

Distribution of the skeletons in the section

In general terms, the sedimentary environment of the Slottsmøya Member shale is interpreted to be a dysoxic shelf with periods of oxygen influx to the sea bottom when coarser clastic sediments (silt and sand) were deposited as turbidites or by storm events (Collignon & Hammer 2012). TOC content is an important indicator of the environment near the seafloor. Hammer *et al.* (2012) found fluctuating TOC values in the Slottsmøya Member, with a distinct peak at the base of the member (−25 m, TOC value 3.6%), followed by a second peak (12 m, TOC value 4.2%) and a third peak (42 m, TOC value 9.7%) (Fig. 2). The 12 m peak falls within the zone of highest marine reptile abundance in the section, from approximately 10 to 20 m. Two of the seven articulated skeletons are also found in this interval. Nickel–vanadium measurements indicate conditions at the seafloor varying within the dysoxic range throughout the section, with a minimum value at approximately 5–10 m in the section (Collignon & Hammer 2012). No articulated skeletons were found in the interval below 10 m, which is lower in organic carbon content. TOC levels remain relatively high (ranging from 2.7 to 4.4%) from 20 m to the top of the interval prospected for vertebrates. Four articulated skeletons are found in this upper interval, the uppermost (PMO 222.655) close to the maximum TOC value at 42 m.

Figure 2 presents qualitative invertebrate fossil abundance from cores drilled for the CO_2 storage project in Longyearbyen, Svalbard, approximately 12 and 19 km from the excavation sites at Janusfjellet and Knorringfjellet, respectively. Correlation between outcrop and core is based on lithostratigraphy, biostratigraphy and organic carbon isotope curves. The majority of the benthic fauna consists of bivalves, but gastropods, brachiopods and scaphopods are also quite common in the Slottsmøya Member. There is a tendency for a negative correlation between bivalve and marine reptile abundance, with relatively few bivalves but some skeletons below 0 m, followed by maximum bivalve abundance and a gap in the vertebrate record from 0 to 6 m, then a gradual reduction in bivalve abundance as the vertebrates become more common around the second TOC peak at 12 m. The benthic faunal record therefore supports the hypothesis of poor oxygenation contributing to the high preservational potential of skeletons.

Hjalmarsdottir (2012) identified foraminiferal morphogroups in the Slottsmøya Member according to the classification scheme of Nagy *et al.* (2009). The main interval of vertebrate finds in the Slottsmøya Member is found between approximately −10 and 30 m in the sections. Hjalmarsdottir (2012) did not extend her study below −1.3 m, but from that level to 30 m she found a dominance of epifaunal species, with subordinate surficial/shallow infauna and occasional deep infauna, indicating a generally dysoxic environment. However, there is considerable stratigraphic variation: for example, Hjalmarsdottir (2012) recorded practically no infauna (i.e. highly dysoxic to anoxic according to Nagy *et al.* 2009) at −1.3, 0.8 and 10.9 m, while at 8.4, 14–18 and 30 m the infauna ranges from 20 to 40% (dysoxic). Together with the stratigraphic variation in lithology and geochemistry (Collignon & Hammer 2012), this indicates that while the seafloor was dysoxic in the vertebrate interval, there was considerable variation throughout the member, with excursions into both highly dysoxic/anoxic and low oxic conditions at the seafloor.

Floating and sinking

Whether the marine reptiles floated after death, or sank immediately, is a question under debate (Reisdorf *et al.* 2012). It is density that controls whether a carcass sinks or refloats, but refloating might also be prevented by increased hydrostatic pressure, if the water is sufficiently deep (Allison *et al.* 1991). In modern cetaceans, the drift and refloating pattern varies with fat content: a whale carcass with a high fat content will drift in the surface waters immediately after death, while one with a low fat content will first sink, then possibly refloat as decay gases accumulate. Ichthyosaurs are regarded as sustained high-speed swimmers in the Mesozoic seas, and they were probably negatively buoyant (Holger 1992). Data obtained from studies on Recent cetaceans

show that a carcass may rise from water depths up to 50 m (Reisdorf *et al.* 2012). The Slottsmøya Member is regarded as an open-marine shelf environment (Dallmann 1999), with water depths estimated at between 100 and 150 m (Collignon & Hammer 2012). Similar conditions are also observed in the Posidonienschiefer Formation, with a shelf depth of 50–100 m (Röhl *et al.* 2001). Thus, the ichthyosaur carcasses preserved in these two *Lagerstätten* probably did not resurface.

Schäfer (1972) argued that marine mammals that die by natural causes might, under some circumstances, drift for weeks at the sea surface. When the connective tissue decayed, the skeletal elements would be spread over a large area by ocean currents and finally land on the seafloor as disarticulated bones or groups of bones (Schäfer 1972). Observations of decaying dolphins show that the integument tears first where the mechanical stress is strongest. These areas include the roof of the skull, the margins of the lower jaw, above the scapula and in the tail section. The trachea sometimes supports the connection between the skull and the body for a while (Schäfer 1972). The pliosaurid PMO 214.135 (Fig. 6f) is thought to have been partly disarticulated before it landed on the seabed (Knutsen *et al.* 2012*d*), and probably decayed whilst floating in the ocean. The porous structure of its vertebrae suggests that they were oil-filled, similar to those of some cetaceans (Kihle *et al.* 2012). This could explain the preservation of only parts of the skeleton, as a longer floating period would advance the decay. The disarticulated specimens PMO 224.166 (Figs 3e & 8a), PMO 222.664 (Fig. 8b), PMO 222.668 (Fig. 8c), PMO 222.658 (Fig. 8d), PMO 222.672 (Fig. 8e) and PMO 214.452 (Figs 3f & 8f) might all represent parts from carcasses that floated for a prolonged period of time post mortem.

Most of the marine reptile skeletons in the Posidonienschiefer Formation are complete but partially disarticulated. The slight disarticulation was for a long time explained by the expansion of internal gases in the gut region, causing the carcass to explode, ejecting bones and internal organs, and leaving a disarticulated carcass (Keller 1976; Martill 1993). However, Reisdorf *et al.* (2012) showed that it is unlikely that skeletal elements from a vertebrate could have been scattered in this way only by the release of putrefaction gases under hydrostatic or atmospheric pressures.

While the ichthyosaur neck and skull resemble those of dolphins, plesiosauroids possess a greatly elongated neck, which narrows towards the skull, so that less connective tissue supports the head. The connection between the atlas–axis complex and the basioccipital was small, and the skull was probably one of the first elements to detach from a decaying animal floating in the water. The majority of the plesiosauroid skeletons from Slottsmøya were found without cranial material, as is the case for several other localities, such as from the Upper Cretaceous Pembina and Sharon Spring members in the USA (Carpenter 2006). While some of the crania were likely to have been lost due to surface erosion prior to discovery, several skeletons appear to have lost the cranium prior to burial, during the 'bloat and float' decompositional phase described by Schäfer (1972). The plesiosauroid PMO 219.718 (Figs 3b & 4e) possesses an articulated skeleton, including all but the anteriormost cervical vertebrae, but lacks a skull. The skull must have been lost during early decay, either in the floating phase or just after settling at the seafloor. The specimen must have had a short post-mortem floating period, since most of the skeletal elements are present. A single plesiosauroid specimen, PMO 224.248 (Fig. 5a), has a complete, articulated skull, while PMO 212.662/SVB 1452 (Figs 3d & 7c) and SVB 1450 (Fig. 7d) retain some skull elements. The skull of PMO 224.248 has disarticulated from the atlas–axis and drifted 10–20 cm away from the anterior cervicals. This is highly unusual and could illustrate the earliest stage of post-mortem skull drifting. An Upper Cretaceous elasmosaurid plesiosauroid from North Canterbury, New Zealand described by Barnes & Hiller (2010) was discovered missing the skull. They suggested that it probably disarticulated prior to the carcass reaching the seafloor, either being removed by a predator or scavenged shortly after death. It could have also been detached during the early stage of the 'bloat and float' phase, an interpretation also suggested for the Pembina and Sharon Spring plesiosaurs (Carpenter 2006) and the Triassic sauropterygian *Serpianosaurus* (Beardmore *et al.* 2012*b*). Barnes & Hiller (2010) also suggested that the head and neck could be transported for a distance after it detached from the torso. This is true for sauropod dinosaurs, where articulated necks are often found without the rest of the skeleton (e.g. Wedel *et al.* 2000), but this is not observed in the Slottsmøya specimens, where the necks are usually associated with the body.

Landing

The original body shape and the decompositional state of the carcass upon hitting the seafloor affect the orientation of the preserved skeleton (Martill 1986). Complete or near-complete carcasses land in five different positions: dorsally, laterally, ventrally, anteriorly and posteriorly (Martill 1993). Esperante *et al.* (2002) studied fossil whales from the Miocene–Pliocene Pisco Formation in Peru, and found an equal number of dorsally and ventrally landed skeletons. Of more than 500 specimens, only

two skeletons were found in a lateral position, which could be related to the instability of the whale carcass on the seafloor (Esperante *et al.* 2009). Skeletons may also land laterally and secondarily be moved into a dorsal or ventral position. Martill (1993) observed that ichthyosaurs from the Posidonienschiefer Formation more often had lateral than dorsal landings, and suggested that specimens landing dorsally often rolled over to a lateral position.

Dorsal landings. Specimens landing dorsally often possess a perfectly articulated vertebral column (Martill 1993). Decaying whales floating in the water tend to rotate, leaving the heavier dorsal side down due to intestinal gas build-up in the abdominal cavity (Schäfer 1972), but whether this affects the final mode of deposition is difficult to predict. Three plesiosauroids (PMO 219.718: Figs 3b & 4e; PMO 212.662/SVB 1452: Figs 3d & 7c; PMO A27745: Fig. 4d), one pliosaurid (PMO 214.135: Fig. 6f), and four ichthyosaurs (PMO 222.655: Fig. 4a; PMO 224.251: Fig. 5c; SVB 1451: Fig. 6e; PMO 224.252: Fig. 5e) from the Slottsmøya Member are interpreted to have landed dorsally. The ichthyosaur PMO 222.655 probably landed dorsally, and later experienced lateral torsion.

Lateral landings. Two ichthyosaur specimens (PMO 222.670: Fig. 4c; PMO 222.654: Fig. 6b) from the Slottsmøya Member are preserved laterally. PMO 222.654 had a ventrolateral landing. In a lateral landing, there is often a distinct preservation difference between the upper and lower surface of the skeleton, and the preservation of the limbs on the stratigraphically down side is usually better preserved than on the opposite side (Martill 1993). This is seen in the ichthyosaur PMO 222.654 (Fig. 10b–d).

Ventral landings. In a ventral landing, the skeleton often shows all four limbs articulated. Because of decomposition of the ligament of the vertebral column, the vertebral centra will drop to the seabed, often resulting in a partly or completely disarticulated vertebral column (Martill 1993). Six plesiosauroids (PMO 224.248: Fig. 5a; SVB 1450: Fig. 7d; PMO 224.247: Fig. 6d; PMO 222.663: Fig. 7f; PMO 216.839: Fig. 6a; PMO 214.452: Figs 3f & 8f) and two ichthyosaurs (PMO 224.250: Fig. 5d; PMO 222.667: Fig. 7a) from the Slottsmøya Member show this mode of preservation.

Anterior landings. In an anterior landing, the skull lands first and can penetrate into the sediment. Two ichthyosaur specimens (PMO 214.578: Figs 3a & 4b; PMO 222.669: Figs 3c & 7e) in this study are interpreted to have had an anterior landing. The anterior part of the rostrum of PMO 222.669 is damaged and filled with more than 50 teeth, most of which have been displaced. This specimen probably experienced a head-first landing, where the rostrum penetrated the sediment and broke, and its pieces and teeth were pressed posteriorly into the remaining parts of the jaw. An anterior landing was also found in an *Ophthalmosaurus* specimen from the Redwater Shale Member, with its skull at a 90° angle to the bedding. The rostrum was split open and broken (Wahl 2009), in contrast to the specimens in this study. In the Lower Jurassic of the Jura Mountains in Switzerland, a vertically emplaced skull was found connected to the postcranial skeleton. The fins restricted further penetration of the animal into the sediment (Wetzel & Reisdorf 2007).

For most of the specimens collected from the Slottsmøya Member, the landing mode cannot be easily assessed owing to a high degree of disarticulation. In specimens where this can be analysed, dorsal ($n = 8$) and ventral ($n = 8$) landings are the most common modes. For plesiosauroids, dorsal ($n = 4$) and ventral ($n = 6$) landings are the only types experienced. The reason for this is probably the plesiosauroid body shape, with large flat fins on the sides of the body, a torso that is broader than high and a small head. Ichthyosaurs, however, in addition to ventral and dorsal landings, experienced lateral ($n = 2$) and anterior ($n = 2$) landings. This is also thought to be related to a large head, taller body, fewer large fins and a dorsoventrally expanded tail. None of the specimens landed posteriorly, nor are such landings known for ichthyosaurs (Martill 1993), nor, to our knowledge, for plesiosaurians. The cause for this, presumably, is the heavier anterior part in ichthyosaurs and the above-explained body shape for plesiosaurians.

Predation, scavengers and associated invertebrates

The cause of death of any fossil organism is often difficult to assess. Normal causes of death for whales and dolphins are related to predators, parasites and hazards at birth. Death by old age or illness is rare (Schäfer 1972). Evident bite marks, scars on the bones or missing skeletal elements are observed in many of the Oxford Clay Formation specimens, and this could indicate predation or scavenging (Martill 1986). Evidence for predation or scavenging is also seen in whales: for example, in the occurrence of bite marks on the skull of a baleen whale skeleton in the Lower Pliocene Huelva Sands Formation (Corral *et al.* 2004). Most ichthyosaurs and plesiosauroids were not predators of large-bodied vertebrates in the Mesozoic seas, and were certainly a target for predation by pliosaurids and chondrichthyans (Martill 1996). In the Upper Jurassic Kimmeridge Clay, ichthyosaur vertebrae are

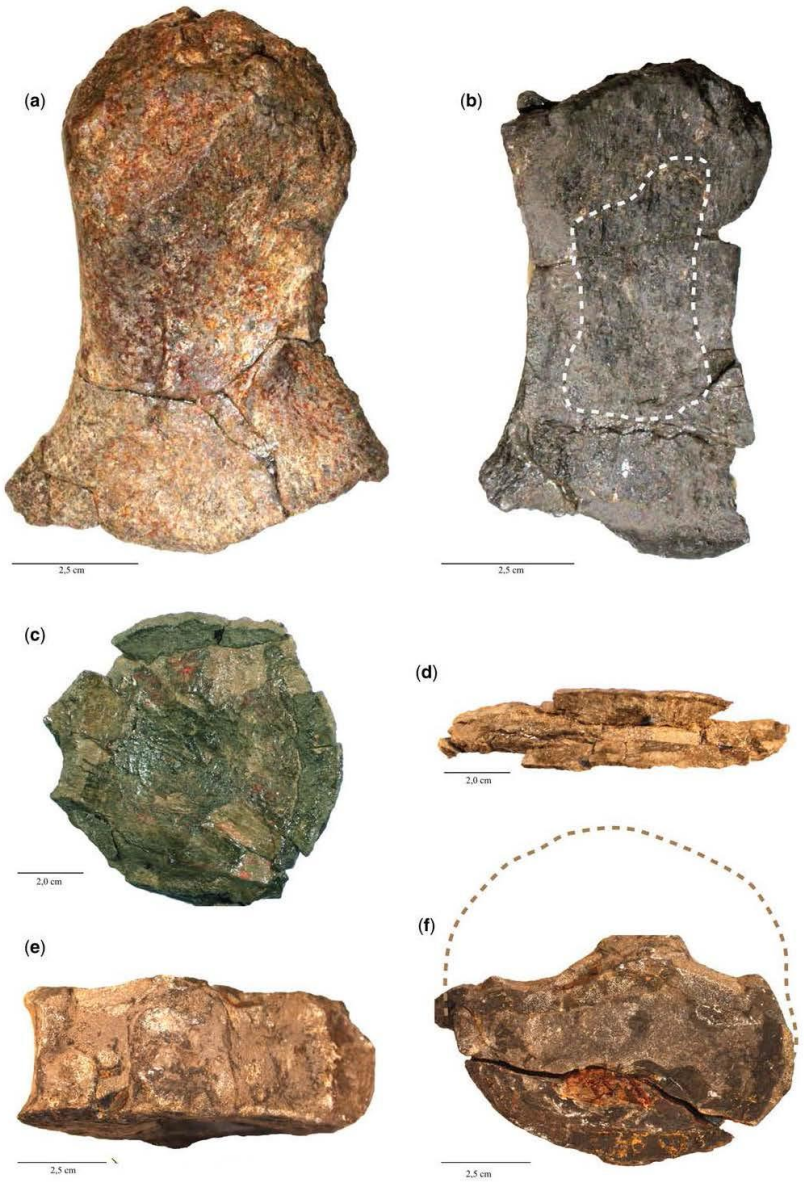

Fig. 10. Compaction and erosion of bones: (**a**) lateral view of the left femur of PMO 214.578; (**b**) lateral view of the left femur of PMO 222.654 with the outline of the eroded area; (**c**) anterior surface of the compressed vertebra of PMO 222.654; (**d**) ventral side of the compressed vertebra of PMO 222.654; (**e**) right lateral side of the eroded vertebra from PMO 214.578; and (**f**) anterior side of vertebra of PMO 214.578 with the outline of the eroded bone mass.

frequently found with bite marks, some of which are thought to be from pliosaurids (Martill 1996), as is the case for one skull of the Early Cretaceous elasmosaur *Eromangasaurus australis* (Sachs, 2005) (Thulborn & Turner 1993). Interestingly, chondrichthyans have not been found in the Slottsmøya Member.

To predict whether elements are missing as a result of scavenging or predation is difficult (Martill 1986). Most of the *Lagerstätten* with marine vertebrates were deposited in anoxic seafloor environments, which potentially limit the ability for macro-organisms to scavenge carcasses (Allison 1988). Whether the carcass is floating or settled on the seabed, scavengers are often responsible for its disarticulation (Martill 1986). Fragmented remains found near articulated specimens are believed to be the result of scavenging, and some of the marine reptile specimens from the Oxford Clay are possible examples (Martill 1985).

Few of the Slottsmøya marine reptiles show traces of predation or scavenging. In the plesiosauroid PMO 222.663, a belemnite was observed beside its articulated vertebral column, and an ammonite was found in the stomach area of the ichthyosaur PMO 214.578. Both of these findings could indicate scavenging by invertebrates during the 'mobile scavenger stage' (Smith & Baco 2003). The plesiosauroid SVB 1450 had an ichthyosaur tooth lying on top of a neural arch in the cervical region. The plesiosauroid PMO 224.248 had several ichthyosaur teeth located on top of and next to the cervical vertebrae, but the vertebrae were not displaced in any way. In the ichthyosaur PMO 222.654, a gracile plesiosauroid tooth was found close to the disarticulated humerus, but no obvious bite marks are visible, and the observed tooth is more adapted for feeding on soft-bodied organisms such as cephalopods (Roberts *et al.* 2014).

The bivalve *Buchia* is by far the most common invertebrate found close to the skeletons. It is found on the plesiosauroids PMO 212.662/SVB 1452, PMO 224.248 and PMO 222.663, and the ichthyosaurs PMO 222.670 and PMO 222.669. On PMO 222.670, some serpulids were also found. In the plesiosauroid PMO 219.718 and in the pliosaurid PMO 214.135, segments of ophiuroids were lying close to the bones. These associations could indicate part of the enrichment/opportunist stage, which often involves smaller organisms such as invertebrates and bacteria (Smith & Baco 2003), but it is uncertain as we do not know whether the organisms used the bones as a substrate.

Oxygenation

When a carcass lands on the seabed, sediment firmness, sedimentation rate, presence of currents, scavengers, epifauna and the oxygen level at the seafloor affect the preservation of the carcass. Rapid burial and low oxygen levels are often regarded as key elements for excellent preservation of skeletons (Seilacher *et al.* 1985; Brett & Baird 1986; Allison 1989).

The Posidonienschiefer Formation contains many well-preserved marine reptiles, together with more disarticulated specimens (Martill 1993). The sediment is described as a laminated organic-rich mud rock with a TOC ranging from 2 to 15% (Littke *et al.* 1991; Martill 1993). The marine reptiles preserved with soft tissue and body outlines are thought to have been exposed to rapid burial, either in soupy sediments or by episodic sedimentation followed by early diagenesis (Allison 1989; Martill 1993). Whether the Posidonienschiefer Formation was oxic or anoxic is debated. Kaufmann (1981) argued that the seafloor and the first few centimetres of the water column were anoxic, and only the part of the animal reaching above this anoxic level would be fed on. In contrast, Seilacher (1982) believed that the seafloor was occasionally oxic, with an anoxic water column.

The Oxford Clay Formation shows excellent preservation of marine reptiles. Most of the specimens were deposited in the Peterborough Member, described as an organic-rich mudstone (Tang 2002) with a TOC of 0.5–16% (Kenig *et al.* 1994). The Peterborough Member is thought to represent a soupy sediment, owing to the lack of burrowing organisms (Tang 2002), and this has been invoked to explain the preservation of soft parts (Martill 1985).

The Posidonienschiefer Formation and the Oxford Clay Formation in many ways resemble the Slottsmøya Member in being deposited on a dysoxic shelf with some beds consisting of reworked sediments such as siltstones to very-fine-grained sandstones with a low sedimentation rate (Collignon 2011). In the Oxford Clay Formation, a positive correlation between the articulation of marine reptiles and the TOC content in the sediments is observed, as in the Slottsmøya Member. It was suggested that high productivity in the water column and low oxygenation levels at depth in the Oxford Clay Formation prevented scavenging and decay (Martill 1985). Except for a thin coal seam observed around some parts of the pliosaurid PMO 214.135, and possible stomach content in the plesiosauroids PMO 214.452 and PMO 222.663, no soft tissue or body outline has been observed on the Slottsmøya Member marine reptiles.

Bone preservation

The stratigraphic up and down sides of marine reptile specimens from the Posidonienschiefer

Formation demonstrate two very different preservation styles. While the down side (typically the visible prepared surface) is well preserved, the upper side is comparatively eroded by sediment particles in suspension and partly disarticulated by currents (Martill 1993; Reisdorf *et al.* 2012, 2014). The same pattern is also shown in a mysticete cetacean carcass from the Lower Pliocene (Esperante *et al.* 2009).

For the ichthyosaur PMO 222.654, a similar distinct difference in preservation can be seen. The lower side of the bones is better preserved than the upper surface. For example, the left femur is eroded with a flattened upper surface and, when comparing it to that of a well-preserved femur of the ichthyosaur PMO 214.578 (Fig. 10a), the damage is clearly evident. A vertebra from PMO 214.578 is eroded on its right lateral side, the one stratigraphically up (Fig. 10e, f). These specimens indicate soupy sediment where the skeleton partly sank into the sea bottom, but the reason for the erosion is not known.

Burial, compaction and diagenesis

The deformation and flattening of the bones of marine reptiles from the Posidonienschiefer Formation has been studied by several authors (e.g. Martill 1993). This shale has a high organic content and a sedimentation rate of 4 mm ka^{-1} (compacted state: Reisdorf *et al.* 2014). The specimens are usually severely flattened during the compaction of the sediment, but early formations of calcareous concretions around fossils prevent the compaction in rare cases (Martill 1993; Reisdorf *et al.* 2012).

Some compaction is observed in the skeletons from the Slottsmøya Member, but to a lesser extent than in the Posidonienschiefer. Within the same specimen, the skeletal elements range from some being almost completely flattened to others retaining their original 3D shape. This is clearly evident in the plesiosauroid PMO 219.718, in which the skeleton has undergone dorsoventral compression: some neck vertebrae are flattened, whereas others are elongated to more than twice the normal length through brittle deformation and regrowth of barite in the cracks. Several of the compacted vertebrae of the ichthyosaur PMO 222.654 were deposited flat on the bedding plane, with one of their articular surfaces facing stratigraphically down, and experienced strong anteroposterior compaction (Figs 9 & 10c, d). This is also present in the plesiosauroid PMO 222.663, where areas of the pectoral girdle and vertebrae are significantly compacted, whereas other regions are completely uncompacted. CT scans of vertebrae from PMO 222.654 (Fig. 9) indicate that the 3D vertebrae contain early precipitated minerals like calcite and barite in the pores, while the compressed vertebrae lack this.

A study of three-dimensionally preserved bones of *Pliosaurus funkei* (PMO 214.135 and PMO 214.136) in thin sections revealed that the pore structures of the bones are mineralized mainly by barite, and to a lesser extent by calcite (Kihle *et al.* 2012). The earliest phase of permineralization is calcite followed by barite in these specimens. The unusually large amount of early diagenetic barite in the pore structure of bones from Slottsmøya Member seems to be crucial for their 3D preservation. Barite in the ocean is known to precipitate in the water column, on the seafloor or within marine sediments. The barite solubility increases with pressure and temperature up to 100°C (Griffith & Paytan 2012). Fluids enriched in barite may be driven out of the sediment and into the pore structure of the buried bones during compaction or tectonic processes. Large volumes of remobilized barite in highly reducing, organic-rich sediments are mostly related to cold fluid seepage (Torres *et al.* 2003). The presence of cold-seep carbonates *in situ* at the top of Slottsmøya Member (Hryniewicz *et al.* 2012) is evidence for methanogenesis, which could be the mechanism for the remobilization of barite by lowering of porewater sulphate concentration.

Collignon & Hammer (2012) published inductively coupled plasma mass spectrometry (ICP-MS) results that revealed two stratigraphic levels with a high content of barium in the Slottsmøya Member. The first one at the base level (0 m) occurs as a white to yellowish coating of barite on macroinvertebrate fossils. The second is in the uppermost part of the section at approximately 48 m. Collignon & Hammer (2012) interpreted this as either an indicator of a high influx of biogenic material into the sediments or, alternatively, due to cold-seep venting.

Evidence for a very early precipitation of barite in the bones of PMO 214.135 and PMO 214.136 are the major sections of recrystallization of the barite showing weak autofluorescence due to tension or stress from deep burial and tectonics on the skeleton after mineralization (Kihle *et al.* 2012). Aqueous and hydrocarbon-bearing fluid inclusions (HCFI) occur in both calcite and barite, and provide information on burial depth and temperature. Kihle *et al.* (2012) performed microthermometry on 115 inclusions, of which 65 were HCFI. Most primary aqueous inclusions in barite homogenize within a temperature of homogenization (T_h) of 105–107°C, with Gaussian tails in the range of T_h 101–115°C. This is exactly the temperature where barite solubility starts to decrease, following Griffith & Paytan (2012). The secondary aqueous inclusions tend to homogenize at somewhat lower temperatures than their primary counterpart, at a T_h

range of 89–91°C. Later trains of hydrocarbon-bearing fluid inclusions were found to homogenize within 47–71°C (Kihle *et al.* 2012) and are formed during the brittle deformation of the primary barite crystals during the uplift. The primary aqueous inclusions and the hydrocarbon-bearing fluid inclusions revealed a continuous lowering of the minimum trapping temperature, indicative of an uplift scenario with a maximum burial of 2800–3000 m (Kihle *et al.* 2012).

Conclusions

This paper provides a description of the taphonomy of marine reptiles found in the Slottsmøya Member from the Upper Jurassic on Svalbard. The taphonomical descriptions of the specimens were divided into three preservation categories, where seven skeletons were categorized as articulated, 19 skeletons as partly articulated and 12 skeletons categorized as disarticulated. Eight of the marine reptiles landed dorsally, eight ventrally, two anteriorly and two laterally.

The distribution of marine reptiles in the section is analysed, and a correlation between high total organic content, low oxygen levels, few benthic invertebrates and good reptile preservation is observed. A TOC peak centred at 12 m (TOC value of 4.2%) correlates with the highest abundance of marine reptiles, from approximately 10 to 20 m in the section (Fig. 2).

The Slottsmøya Member preserves the marine vertebrates with a high degree of three-dimensionality, in contrast to several other *Lagerstätten*. In this paper, we suggest a new explanatory model for vertebrates in shale with a high compaction rate under the influence of cold-seep venting:

(1) landing of marine reptiles at the dysoxic sea bottom at a water depth of about 150 m (Collignon & Hammer 2012);
(2) slow burial with a sedimentation rate of 11 mm ka^{-1} (compacted state: Hammer *et al.* 2012), with erosion of exposed parts and partial disarticulation by currents;
(3) large accumulation of organic-rich mud leading to microbial degradation of organic carbon and, hence, methanogenesis (Torres *et al.* 2003). Cold seepage starts;
(4) porewater sulphate is consumed by oxidation of methane and organic carbon (Suess & Whiticar 1989);
(5) barite dissolves owing to sulphate depletion;
(6) fluid migration and dissolution of calcite/aragonite due to the early compaction of sediments, with some calcite precipitated in the pores of the bones;
(7) barite precipitated in the pore structure of the bones;
(8) the seepage ends;
(9) the formation of siderite nodules in layers with more sand (Collignon & Hammer 2012);
(10) large amounts of sediments from the Cretaceous and Lower Cenozoic bury the skeletons to a maximum depth of 3000 m;
(11) secondary trains of fluid inclusions formed during the uplift state. Brittle deformation of the bones and recrystallization of the barite and calcite occurs.

May-Liss Knudsen Funke, Bjørn Lund, Lena Kristiansen and Victoria Engelschiøn Nash are thanked for their assistance in the preparation of the specimens. Sincere thanks are also due to the Spitsbergen Jurassic Research Group, which aided in the excavation of the specimens, with a special thanks to the volunteers Magne Høyberget, Øyvind Enger, Stig Larsen, Tommy Wensås and Bjørn Funke. Grants for the excavations were provided by the Polar Institute, the Norwegian Research Council, the Ministry of Education and Research, and National Geographic (EC-0435-9 and EC-0425-09). The sponsors for the excavations are thanked: Spitsbergen Travel, ExxonMobil, Fugro, the Norwegian Petroleum Directorate, Statoil, Bautas, PowerShop, OMV, Helsport, Nexen, Bayerngas, Lividi, Telenor, Simula, forskning.no, Directconnect and livestream.com. This study is, in part, based on a Master thesis by Linn K. Novis. LLD and MJK are supported by PhD grants from the Ministry of Education and Research via the Natural History Museum, University of Oslo. LKN is supported by a PhD grant from the University in Tromsø. AJR is supported by PhD grants from Tullow Oil, NERC and the University of Southampton. Two anonymous reviewers added valuable comments that helped to improve the manuscript.

References

ALLISON, P. A. 1988. The role of anoxia in decay and mineralization of proteinaceous macrofossils. *Paleobiology*, **14**, 139–154.

ALLISON, P. A. 1989. Konservat-*Lagerstätten*: cause and classification. *Paleobiology*, **14**, 331–334.

ALLISON, P. A., SMITH, C. R., KUKERT, H., DEMING, J. W. & BENNETT, B. A. 1991. Deep-water taphonomy of vertebrate carcasses: a whale skeleton in the bathyal Santa Catalina basin. *Paleobiology*, **17**, 78–89.

ANDREASSEN, B. H. 2004. *Plesiosaurs from Svalbard*. Master thesis, University of Oslo.

BARNES, K. M. & HILLER, N. 2010. The taphonomic attributes of a Late Cretaceous plesiosaur skeleton from New Zealand. *Alcheringa*, **34**, 333–344.

BEARDMORE, S. R., ORR, P. J., MANZOCCHI, T. & FURRER, H. 2012*a*. Float or sink: modelling the taphonomic pathway of marine crocodiles (Mesoeucrocodylia, Thalattosuchia) during the death–burial interval. *Palaeobiodiversity and Palaeoenvironments*, **92**, 83–98.

BEARDMORE, S. R., ORR, P. J., MANZOCCHI, T., FURRER, H. & JOHNSON, C. 2012*b*. Death, decay and disarticulation: modelling the skeletal taphonomy of marine reptiles demonstrated using *Serpianosaurus* (Reptilia; Sauropterygia). *Palaeogeography, Palaeoclimatology, Palaeoecology*, **337–338**, 1–13.

BIRKENMAJER, K. 1980. Jurassic–Lower Cretaceous succession at Agardhbukta, East Spitsbergen. *Studia Geologica Polonica*, **66**, 35–52.

BIRKENMAJER, K., PUGACZEWSKA, H. & WIERZBOWSKI, A. 1982. The Janusfjellet Formation (Jurassic–Lower Cretaceous) at Myklegardfjellet, East Spitsbergen. *Palaeontologica Polonica*, **43**, 107–140.

BRETT, C. E. & BAIRD, G. C. 1986. Comparative taphonomy: a key to paleoenviromental interpretation based on fossil preservation. *Palaios*, **1**, 207–227.

CARPENTER, K. 2006. Comparative vertebrate taphonomy of the Pembina and Sharon Springs Members (Middle Campanian) of the Pierre Shale, Western Interior. *Paludicola*, **5**, 125–149.

COLLIGNON, M. 2011. *Sedimentological analysis of the Slottsmøya Member, Agardhfjellet Formation (Late Jurassic–Early Cretaceous) in the Janusfjellet area, Spitsbergen*. Master thesis, University of Oslo.

COLLIGNON, M. & HAMMER, Ø. 2012. Lithostratigraphy and sedimentology of the Slottsmøya Member at Janusfjellet, central Spitsbergen: evidence for a condensed section. *Norwegian Journal of Geology*, **92**, 89–101.

CORRAL, J. C., PEREDA-SUBERBIOLA, X. & BARDET, N. 2004. Shark bite marks in a mosasaur vertebra from the Late Cretaceous of Álava (Basque–Cantabrian Region). *Revista Española de Paleontología*, **19**, 23–32.

DALLMANN, W. K. 1999. Outline of the geological history of Svalbard. *In*: DALLMANN, W. K. (ed.) *Lithostratigraphic Lexicon of Svalbard. Upper Palaeozoic to Quaternary Bedrock. Review and Recommendations for Nomenclature Use*. Norwegian Polar Institute, Tromsø, 17–24.

DALLMANN, W. K., MAJOR, H., HAREMO, P., ANDERSEN, A., KJÆRNET, T. & NØTTVEDT, A. 2001. *Geological Map of Svalbard 1:100,000, Sheet C9G Adventdalen*. Norwegian Polar Institute, Temakart, **31/32**, 4–55.

DRUCKENMILLER, P. S., HURUM, J. H., KNUTSEN, E. M. & NAKREM, H. A. 2012. Two new ichthyosaurs (Ichthyosauria: Ophthalmosauridae) from the Agardhfjellet Formation (Upper Jurassic: Volgian), Svalbard, Norway. *Norwegian Journal of Geology*, **92**, 311–339.

DYPVIK, H., NAGY, J. *ET AL.* 1991. The Janusfjellet Subgroup (Bathonian to Hauterivian) on Central Spitsbergen: a revised lithostratigraphy. *Polar Research*, **9**, 21–43.

EFIMOV, V. M. 2001. On the taphonomy of Late Jurassic and Early Cretaceous Ichthyosaurs from the Volga Region near Ulyanovsk. *Paleontological Journal*, **35**, 188–190.

ESPERANTE, R., BRAND, L. R., CHADWICK, A. & POMA, O. 2002. Taphonomy of fossil whales in the diatomaceous sediments of the Miocene/Pliocene Pisco Formation, Peru. *In*: DE RENZI, M., PARDO ALONSO, M. V., BELINCHÓN, M., PEÑALVER, E., MONTOYA, P. & MÁRQUEZ-ALIAGA, A. (eds) *Current Topics on Taphonomy*. Ayuntamiento de Valencia, Valencia, 337–343.

ESPERANTE, R., GUINEA MUNIZ, F. & NICK, K. E. 2009. Taphonomy of a mysticeti whale in the Lower Pliocene Huelva Sands Formation (southern Spain). *Geologica Acta*, **4**, 489–505.

GRIFFITH, E. M. & PAYTAN, A. 2012. Barite in the ocean – occurrence, geochemistry and palaeoceanographic applications. *Sedimentology*, **59**, 1817–1835.

HAMMER, O., NAKREM, H. A. *ET AL.* 2011. Hydrocarbon seeps close to the Jurassic-Cretaceous boundary, Svalbard. *Palaeogeography, Palaeoclimatology, Palaeoecology*, **306**, 15–26.

HAMMER, Ø., COLLIGNON, M. & NAKREM, H. A. 2012. Organic carbon isotope chemostratigraphy and cyclostratigraphy in the Volgian of central Spitsbergen. *Norwegian Journal of Geology*, **92**, 103–112.

HAMMER, Ø., HRYNIEWICZ, K., HURUM, J. H., HØYBERGET, M., KNUTSEN, E. M. & NAKREM, H. A. 2013. Large onychites (cephalopod hooks) from the Upper Jurassic of the Boreal Realm. *Acta Palaeontologica Polonica*, **58**, 827–835.

HJALMARSDOTTIR, H. R. 2012. *Foraminifera from Upper Jurassic–Lower Cretaceous hydrocarbon seep carbonates and adjacent shales in the Slottsmøya Member, central Spitsbergen*. Master thesis, University of Oslo.

HOLGER, J. A. 1992. Taphonomy and paleoecology of *Shonisaurus popularis* (Reptilia: Ichthyosauria). *Palaios*, **7**, 108–117.

HRYNIEWICZ, K., HAMMER, Ø., NAKREM, H. A. & LITTLE, C. T. S. 2012. Microfacies of the Volgian–Ryazanian (Jurassic–Cretaceous) hydrocarbon seep carbonates from Sassenfjorden, central Spitsbergen, Svalbard. *Norwegian Journal of Geology*, **92**, 113–131.

HRYNIEWICZ, K., NAKREM, H. A., HAMMER, Ø., LITTLE, C. T. S., KAIM, A., SANDY, M. R. & HURUM, J. H. 2014. The palaeoecology of the latest Jurassic–earliest Cretaceous hydrocarbon seep carbonates from Spitsbergen, Svalbard. *Lethaia*, **48**, 353–374, http://doi.org/10.1111/let.12112

HURUM, J. H., NAKREM, H. A., HAMMER, Ø., KNUTSEN, E. M., DRUCKENMILLER, P. S., HRYNIEWICZ, K. & NOVIS, L. K. 2012. An Arctic *Lagerstätte* – the Slottsmøya Member of the Aghardfjellet Formation (Upper Jurassic–Lower Cretaceous) of Spitsbergen. *Norwegian Journal of Geology*, **92**, 55–64.

HURUM, J. H., ROBERTS, A. J., NAKREM, H. A., STENLØKK, J. A. & MØRK, A. 2014. The first recovered ichthyosaur from the Middle Triassic of Edgeøya, Svalbard. *Norwegian Petroleum Directorate Bulletin*, **11**, 97–110.

KAUFMANN, E. G. 1981. Ecological reappraisal of the Posidonienschiefer (Toarcian) and the stagnant basin model. *In*: GRAY, J. (ed.) *Communities of the Past*. Hutchinson Ross Publishing, Stroudsburg, PA, 311–381.

KEAR, B. & MAXWELL, E. E. 2013. Wiman's forgotten plesiosaurs: the earliest recorded sauropterygian fossils from the High Arctic. *GFF*, **135**, 95–103.

KELLER, T. 1976. Magen- und Darminhalte von Ichthyosauriern des süddeutschen Posidonienschiefers. *Neues Jahrbuch für Geologie und Paläontologie Monatshefte*, **5**, 266–283.

KENIG, F., HAYES, J. M., POPP, B. N. & SUMMONS, R. E. 1994. Isotopic biogeochemistry of the Oxford Clay Formation (Jurassic), UK. *Journal of the Geological*

Society, London, **151**, 139–152, http://doi.org/10.1144/gsjgs.151.1.0139

KIHLE, J., HURUM, J. H. & LIEBE, L. 2012. Preliminary results on liquid hydrocarbons occurring as fluid inclusions in intracellular mineral precipitates in bones of the Late Jurassic *Pliosaurus funkei*, central Spitsbergen. *Norwegian Journal of Geology*, **92**, 341–352.

KNUTSEN, E. M., DRUCKENMILLER, P. S. & HURUM, J. H. 2012*a*. Redescription and taxonomic clarification of '*Tricleidus*' *svalbardensis* based on new material from the Agardhfjellet Formation (Middle Volgian), central Spitsbergen, Norway. *Norwegian Journal of Geology*, **92**, 175–186.

KNUTSEN, E. M., DRUCKENMILLER, P. S. & HURUM, J. H. 2012*b*. Two species of long-necked plesiosaurians (Reptilia-Sauropterygia) from the Upper Jurassic (Middle Volgian) Agardhfjellet Formation of central Spitsbergen, Norway. *Norwegian Journal of Geology*, **92**, 187–212.

KNUTSEN, E. M., DRUCKENMILLER, P. S. & HURUM, J. H. 2012*c*. A new plesiosauroid (Reptilia–Sauropterygia) from the Agardhfjellet Formation (Middle Volgian) of central Spitsbergen, Norway. *Norwegian Journal of Geology*, **92**, 213–234.

KNUTSEN, E. M., DRUCKENMILLER, P. S. & HURUM, J. H. 2012*d*. A new species of *Pliosaurus* (Sauropterygia: Plesiosauria) from the Middle Volgian, central Spitsbergen, Norway. *Norwegian Journal of Geology*, **92**, 234–258.

LARSEN, L. 2012. Summary of well test results from DH4, DH5, DH6, DH5R and DH7a. Paper presented at the Longyearbyen CO_2 Lab International Workshop, 17–20 September 2012, Longyearbyen, Norway.

LIEBE, L. & HURUM, J. H. 2012. Gross internal structure and microstructure of Late Jurassic plesiosaur limb bones, central Spitsbergen. *Norwegian Journal of Geology*, **92**, 285–310.

LITTKE, R., LEYTHAEUSER, D., RULLKÖTTER, J. & BAKER, D. R. 1991. Keys to the depositional history of the Posidonia Shale (Toarcian) in the Hils Syncline, Northern Germany. *In*: TYSON, R. V. & PEARSON, T. H. (eds) *Modern and Ancient Continental Shelf Anoxia*. Geological Society, London, Special Publications, **58**, 311– 333, http://doi.org/10.1144/GSL.SP.1991.058.01.20

MARTILL, D. M. 1985. The preservation of marine vertebrates in the Lower Oxford Clay (Jurassic) of central England. *Philosophical Transactions of the Royal Society of London*, **311**, 155–165.

MARTILL, D. M. 1986. The stratigraphic distribution and preservation of fossil vertebrates in the Oxford Clay of England. *Mercian Geologist*, **10**, 161–186.

MARTILL, D. M. 1993. Soupy substrates: a medium for the exceptional preservation of ichthyosaurs of the Posidonia Shale (Lower Jurassic) of Germany. *Kaupia: Darmstädter Beiträge zur Naturgeschichte*, **2**, 77–97.

MARTILL, D. M. 1996. Fossils explained 17: ichthyosaurs. *Geology Today*, **12**, 194–196.

MARTILL, D. M., TAYLOR, M. A., DUFF, K. L., RIDING, J. B. & BOWN, P. R. 1994. The trophic structure of the biota of the Peterborough Member, Oxford Clay Formation (Jurassic), U.K. *Journal of the Geological Society, London*, **151**, 173–194, http://doi.org/10.1144/gsjgs.151.1.0173

MAXWELL, E. E. & KEAR, B. P. 2013. Triassic ichthyopterygian assemblages of the Svalbard archipelago: a reassessment of taxonomy and distribution. *GFF*, **135**, 85–94.

MØRK, A., DALLMANN, W. K. *ET AL.* 1999. Mesozoic lithostratigraphy. *In*: DALLMANN, W. K. (ed.) *Lithostratigraphic Lexicon of Svalbard. Upper Palaeozoic to Quaternary Bedrock. Review and Recommendations for Nomenclature Use*. Norwegian Polar Institute, Tromsø, 127–214.

NAGY, J. & BASOV, V. A. 1998. Revised foraminiferal taxa and biostratigraphy of Bathonian to Ryazanian deposits in Spitsbergen. *Micropaleontology*, **44**, 217–255.

NAGY, J., REOLID, M. & RODRÍGUEZ-TOVAR, F. J. 2009. Foraminiferal morphogroups in dysoxic shelf deposits from the Jurassic of Spitsbergen. *Polar Research*, **28**, 214–221.

PERSSON, P. O. 1962. Plesiosaurians from Spitsbergen. *In*: *Norwegian Polar Institute Yearbook 1961*. Tromsø, 62–68.

REISDORF, A. G., BUX, R. *ET AL.* 2012. Float, explode or sink: postmortem fate of lung–breathing marine vertebrates. *Palaeobiodiversity and Palaeoenvironments*, **92**, 67–81.

REISDORF, A., ANDERSON, G. *ET AL.* 2014. Reply to 'Ichthyosaur embryos outside the mother body: not due to carcass explosion but to carcass implosion' by van Loon (2013). *Palaeobiodiversity and Palaeoenvironments*, **94**, 487–494, http://doi.org/10.1007/s12549-014-0162-z

ROBERTS, A. J., DRUCKENMILLER, P. S., SÆTRE, G.-P. & HURUM, J. H. 2014. A New Upper Jurassic Ophthalmosaurid Ichthyosaur from the Slottsmøya Member, Agardhfjellet Formation of Central Spitsbergen. *PLoS ONE*, **9**, e103152, http://doi.org/10.1371/journal.pone.0103152

ROUSSEAU, J. & NAKREM, H. A. 2012. An Upper Jurassic boreal echinoderm *Lagerstätte* from Janusfjellet, central Spitsbergen. *Norwegian Journal of Geology*, **92**, 133–148.

RÖHL, H-J., SCHMID-RÖHL, A., OSCHMANN, W., FRIMMEL, A. & SCHWARK, L. 2001. Erratum to 'The Posidonia Shale (Lower Toarcian) of SW-Germany: an oxygen-depleted ecosystem controlled by sea level and palaeoclimate'. *Palaeogeography, Palaeoclimatology, Palaeoecology*, **169**, 273–299.

SACHS, S. 2005. *Tuarangisaurus australis* sp. nov. (Plesiosauria: Elasmosauridae) from the Lower Cretaceous of northeastern Queensland, with additional notes on the phylogeny of the Elasmosauridae. *Memoirs of the Queensland Museum*, **50**, 425–440.

SCHÄFER, W. 1972. *Ecology and Paleoecology of Marine Environments*. Oliver & Boyd, Edinburgh.

SEILACHER, A. 1982. Ammonite shells as habitats in the Posidonia Shale of Holzmaden-floats or benthic islands? *Neues Jahrbuch für Geologie und Paläontologie Monatshefte*, **2**, 98–114.

SEILACHER, A., REIF, W. E. & WESTPHAL, F. 1985. Sedimentological, ecological and temporal patterns of fossil *Lagerstätten*. *In*: WHITTINGTON, H. B. & CONWAY MORRIS, S. (eds) *Extraordinary Fossil Biotas: Their Ecological and Evolutionary Significance*. Cambridge University Press, Cambridge, 5–23.

SMITH, C. R. & BACO, A. R. 2003. Ecology of whale falls at the deep-sea floor. *Oceanography and Marine Biology*, **41**, 311–354.

SUESS, E. & WHITICAR, M. J. 1989. Methane-derived CO_2 in pore fluids expelled from the Oregon subduction zone. *Palaeogeography, Palaeoclimatology, Palaeoecology*, **71**, 119–136.

TANG, C. M. 2002. Oxford Clay: England's Jurassic marine park. *In*: BOTTJER, D. J., ETTER, W., HAGADORN, J. W. & TANG, C. M. (eds) *Exceptional Fossil Preservation. A unique View on the Evolution of Marine Life*. Columbia University Press, New York, 307–325.

THULBORN, T. & TURNER, S. 1993. An elasmosaur bitten by a pliosaur. *Modern Geology*, **18**, 489–501.

TORRES, M. E., BOHRMANN, G., DUBRÉ, T. E. & POOLE, F. G. 2003. Formation of modern and Paleozoic strati form barite at cold methane seeps on continental margins. *Geology*, **31**, 897–900, http://doi.org/10.1130/G19652.1

WAHL, W. R. 2009. Taphonomy of a nose dive: bone and tooth displacement and mineral accretion in an ichthyosaur skull. *Paludicola*, **7**, 107–116.

WEDEL, M. J., CIFELLI, R. L. & SANDERS, R. K. 2000. Osteology, paleobiology, and relationships of the sauropod dinosaur *Sauroposeidon*. *Acta Palaeontologica Polonica*, **45**, 343–388.

WETZEL, A. & REISDORF, A. G. 2007. Ichnofabrics elucidate the accumulation history of a condensed interval containing a vertically emplaced ichthyosaur skull. *In*: BROMLEY, R. G., BUATOIS, L. A., MÁNGANO, G., GENISE, J. F. & MELCHOR, R. N. (eds) *Sediment–Organism Interactions: Multifaceted Ichnology*. SEPM Special Publications, **88**, 241–251.

WIERZBOWSKI, A., HRYNIEWICZ, K., HAMMER, Ø., NAKREM, H. A. & LITTLE, C. T. S. 2011. Ammonites from hydrocarbon seep carbonate bodies from the Uppermost Jurassic–Lowermost Cretaceous of Spitsbergen and their biostratigraphical importance. *Neues Jahrbuch für Geologie und Paläontologie, Abhandlungen*, **262**, 267–288.

WIMAN, C. 1914. Ein Plesiosaurierwirbel aus dem jüngeren Mesozoicum Spitzbergens. *Bulletin of the Geological Institute, Upsala*, **12**, 201–204.

Appendix 3

Supplementary data for Chapter 2

Supplementary data for Roberts et al., 2017

Original published online as supplementary information for: Roberts, A. J., Druckenmiller, P. S., Delsett, L. L. and J. H. Hurum, 2017. Osteology and relationships of *Colymbosaurus* Seeley, 1874, based on new material of *C. svalbardensis* from the Slottsmøya Member, Agardhfjellet Formation of central Spitsbergen. *Journal of Vertebrate Paleontology* 37, e1278381. Reformatted for inclusion in this thesis.

Additional information on PMO 222.663

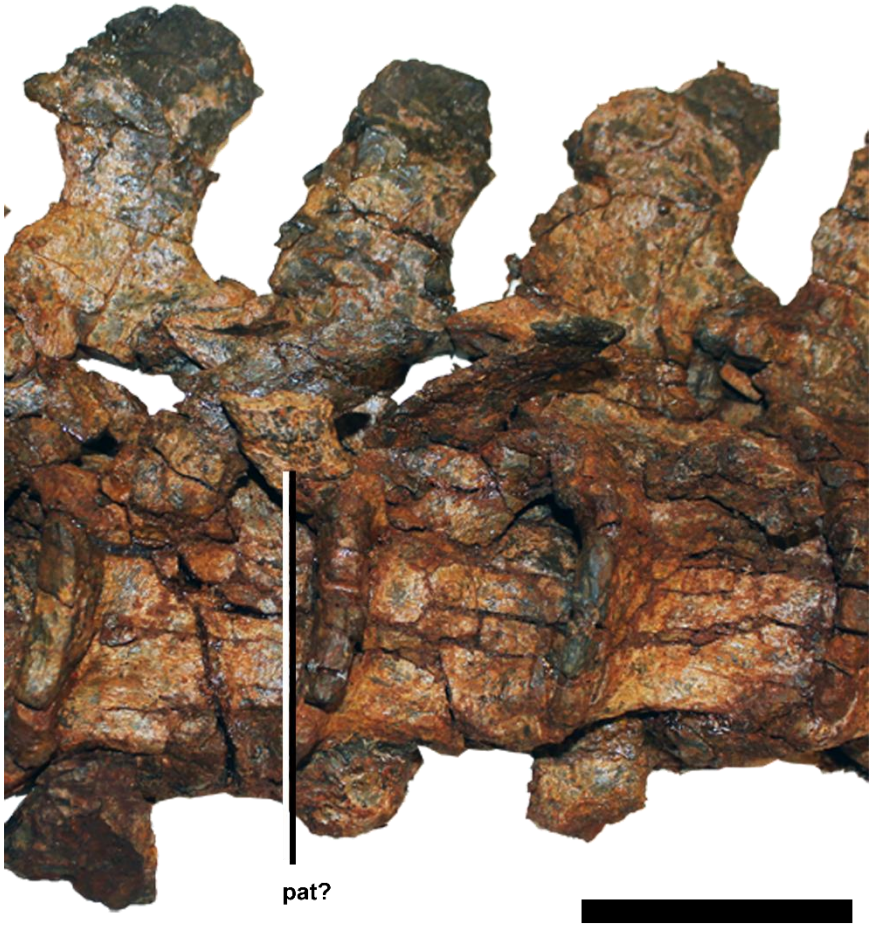

Figure A3.1: A detailed image of the anterior process on the sixth caudal vertebra in the articulated series of PMO 222.663 in lateral view. **Abbreviations**: **pat?**, pathology? Scale bar equals 5cm.

***Colymbosaurus* specimens in UK museums**

Eighteen propodials from the Kimmeridge Clay Formation were measured at UK museums, the measurements are summarized in Table S1. Note that two propodials where included for a single individual (OUM J.3300) and was included to show individual variability and differences if any between the humerus and femur.

Table A3.1: A selection of observations on cryptoclidid propodials from the Kimmeridge Clay Formation (United Kingdom) examined in this study. The presence/absence and extent of a bisecting anteroposteriorly oriented ridge on the distal end of the propodials are noted, along with other remarks. **Abbreviations**: **CAMSM**, Sedgwick Museum of Earth Science, Cambridge University, Cambridge, UK, **MANCH**, The Manchester Museum, Manchester, UK, **NHMUK**, Natural History Museum, London, UK, **OUM**, Oxford University Museum of Natural History, Oxford, UK, **PMO**, Paleontological Museum Oslo, University of Oslo, Oslo, Norway, **YORKM**, York Museum and Art Gallery, York, UK.

Specimen number	**Humerus**	**Ridge observations**	**Remarks**
NHMUK R31787	Right	Present	Postaxial flange broken
NHMUK R10062	Right	Absent	
OUM J.13815	Left	On ulna facet	Reconstructed middle
OUM J.3300/38	Left	Present	
OUM J.9290	Right	On radius facet	
CAMSM J68344	Left	Absent	Juvenile?
YORKM 2005.2224.2	Left	Present	Compressed distal end

PMO 222.663	Right	Absent	Ulna fused to distal end
	Femur		
OUM J.13827	Right	Absent	
OUM J.3300/45	Left	Present	
CAMSM J29654-91	Left	Present	Postaxial flange broken
CAMS J.59736-43	Right	Present	Postaxial flange and proximal edge broken
CAMSM J29740	Right	On fibula facet	
CAMSM J.29738	Left	Present	
MANCH LL.5513	Right	Absent	
MANCH LL.5514	Left	On fibula facet	
PMO 222.663	Right	Absent	
PMO A27745	Right	Absent	
PMO 216.838	Left	Absent	
	Unidentifiable		
OUM J.13826	X	Present	Proximal end missing
OUM J.13841	X	Present	Proximal end missing
YORKM 2005.2223.1	X	Absent	Proximal end missing

Phylogenetic Methods

As the character list is the same as that used in Benson and Druckenmiller (2014), it is not included here. The character list and original matrix is available freely as online supplementary material with that publication. A number of scores were changed for the cryptoclidid plesiosaur taxa examined by *AJR* and *PSD* from the Slottsmøya Member, Kimmeridge Clay Formation (UK) and Oxford Clay Formation. Following Benson and Druckenmiller (2014), *Spitrasaurus* spp. was scored as a composite of the two species *S.* wensaasi and *S. larseni*. The following changes were made in these taxa (char/original score→new score):

- *Muraenosaurus leedsii*: (183/1→0) coding mistake.
- *Kimmerosaurus langhami*: (151/1→0) based on own observations of referred material and holotype (NHMUK R)
- *Colymbosaurus megadeirus*: (142/?→1) (Benson and Bowdler, 2014), (144/?→1) (Benson and Bowdler, 2014), (189/0→1), (234/1→0) no preaxial element preserved, (240/1→0) the curvature of the long axis of the femur is straight or almost straight. (243/2→0) not a valid character state due to significant variation
- *Djupedalia engeri*: (7/0→?), (13/0→?), (200/1→0) do not meet along the midline.
- *Spitrasaurus spp.*: (13/0→?), (159/1→?) Not possible to confirm due to the preservation of the vertebrae, (200/1→0) do not meet along the midline.

Settings used in TNT (V1.1) —The original data matrix by Benson and Druckenmiller (2014) was run in TNT (V1.1 – Goloboff et al., 2008), using first the New Technology analysis – Ratchet. The "random addition sequences" was set to 5000, four iterations where utilized, random seed was set at 1 and all trees were kept. The resulting trees from this initial analysis was then analyzed using TBR. The consistency and retention indexes were generated using the "stats.run" script and the bremer support values were found using the "bremer.run" script, both of which can be found on (http://phylo.wikidot.com/tntwiki) webpage for TNT. A resampling analysis was run on all data sets using bootstrap set at 1000 replicates, which yielded poor (<50) support values within Cryptoclididae.

Literature Cited

Benson, R. B. J., and T. Bowdler. 2014. Anatomy of *Colymbosaurus megadeirus* (Reptilia, Plesiosauria) from the Kimmeridge Clay Formation of the U.K., and high diversity among Late Jurassic plesiosauroids. Journal of Vertebrate Paleontology 34:1053–1071.

Benson, R. B. J., and P. S. Druckenmiller. 2014. Faunal turnover of marine tetrapods of the Jurassic-Cretaceous transition. Biological Reviews 89:1–23.

Goloboff, P., S Farris and K. Nixon. 2008. TNT, a free program for phylogenetic analysis. Cladistics 24:774–786.

Supplementary information S2

Yunguisaurus_liae
0001000??10000000??0010010?000010010?000?000110??200??00?????01020??????????????02?1
0???????0?0?0010020???10011001100?1001?1????13??0??????1??????????41000??00?000000?001
??0??01210?0?00(23)??0??????0?000?200????????????0?00122011?0000002000??11000?000?0?00
0000010000100000

Pistosaurus_postcranium
??
??200111000000000011010010110
0010????101110?00?001?202100??0??001????0122210???1??????01?1?00000000???0???0?10?????
???0

Augustasaurus_hagdorni
010100?0010?00000??0010010000000000000100?001001210100001O??????0???0?0000??????02?
?000?0110000?0010000????0?1100?10??1001??1???01010002100???00??21??41?01??000000200?0
?10000011??0000???????????00?000?102?020000?0?????????????????000??00???100000000???0?
100?1000???0?00

Bobosaurus_forojuliensis
????????????????0???
???02?0?00?00??01?2100000??110?12?000?00??001221
100?10(2
3)1????????????????????????????????0122010?001??????0???1?000????????0???0?0??0??????

Anningasaura_lymense
111000?0120?00??10000100?0010000100000?1000001011200100O?10?0?1020?0110111010010?00
211?1000000011?00?000?111??1110?100?1010?110??00010011000?0?00??0?0??10010??3?0?1201
00?031?1???
????????????

Stratesaurus_taylori
001000?0100100100??0110010000010?0?000010000010001001000010101101012002000010?0010
2211???01000010110?000000?2?111?11000110001?0?001000011000?0?00??2001?1001001110012
0100003101??1????00?0?????????????1?????????????????????01022111??????????????????????????
1???010??010??10

Avalonnectes_arturi
??????????01??10????????10?????01??000010000010011001000010l0???????????????????1??????
0??(12)??????????2100?00211001??100?0110
001101101200?0110?00????1?01201??????????????0102?110??1?????????11020?000?110110?101
000010?100

Meyerasaurus_victor
10?00?0?21??00??11??0100??0000???0??????????????????10?0??0101??(01)0????????0??????022?
0?1?01010111122?11000101?0111100?02110211???01?1001010?0???0???1?120?01?????00?20????
0???0011211012002?110?0?0111?0?1????0201000?0001000102011?0011002100??12020?00021??1
1011010001101100

Maresaurus_coccai

110100?1220?1???1120(02)1001?0?00?????????????00001120?10???10?0110?0?????0?????????0??
11?000101010?122?1000???200111?00??2100?11???01?1?011100????0???????0001???2?0?(01)??1
???030??
????????????

Borealonectes_russelli 11010?1?210?102011100?00(1
2)0?0000??010?0010010000?(0
1)??1?000??0?0???20???12000???????022?1?0???????0??2???201?????111??00???1?0?110??0(1
2)?1?01?10?00100??21?120001???2?0??20?????30?0????????1??????????????????????????????????
?????????????100??00?????1101012???2?011?0001???11?1

Rhomaleosaurus_megacephalus
100101212201121010002100100100?000?000010000010012001000110101???0?201?000???0??100
21110001000110l1???00?0002001111?0??20?0?11??0??00001020?0???0???10120001???1100?201
????10?00111?1012001??20?0?0??????????1??????????????01022110????????00??1?0201001?110?
1??1010??0?????0

Archaeonectrus_rostratus
1002002???0?102?1111??00?????????0?000?10000010012011000?1??01?????????????????????????
????????????????????????11??1????1?????????????11120?0??????????2100100111000201???0?11?
0110110110010??????0?????0?20?1??????????????01?2?1100?10001000??1?020?00??11011011010
001101100

Rhomaleosaurus_cramptoni
10000021220?1020100121101?00001?1000000???0001001201100011110?10?0???1?000???????02?
1110?01010110122?1000000200?11?00??2100?11???01?1?01020?00?????????200???1211000??1?0
?01?1?0002110?100?0????0?????1??????????????1??????0102?11000?10???00??1?021?001?1??110
110100?11?1?00

Rhomaleosaurus_zetlandicus
11000??1220?102010012110??00001??000???????001001?0110?0?1110110?????1?0?0????????221
1??0?1????1?1?2??0??0??20011110000210021100000??1001020?0??????????200010??110?020100?
010?00??2110?1???01201000??????????????????????????????????????1?0??00121202100012110l101
101001?????0?

Rhomaleosaurus_thorntoni
11??0????2?0?10??1021?1101?00?????0??0001000?????????????1??????????????????????????????1?
?01??01?????????????200111??10?11???11000?11100101000??????????0001???110?000100??10?
?01?21101?00?0110100??01100120210?0?000100?10001220110001??????0111?02100002110?????
????????????

Thalassiodracon_hawkinsii
0010000111010011112 0??0?1000???0000000?10020000001011000010110101010002000011000101011?00011001??100?000????0?11101100010000?1200?00100111001 0000??2101310010011100120100002100011101000001011000002011011001?0000000 1000?00010201110010002000001101000 00010?11001010000101100

Hauffiosaurus_longirostris
00?20??0?1??12111120??00???2?????????????????????02???????????01001??0???1?0?????1110?????????????110?0??0?????1001?100?1100?11?0023010011200??

Hauffiosaurus_tomistomimus
00020?10210?1?110??0100?0?0210100100??????00?00010100?0?101?01011??????1001???111011?0?0100010?100?010??????1000?100?1100?1120023010011 20?1100???(02)?1231001?11110?100100002000011101010001??10???0???1??1?0?0?????????????00????????00???0?1000012010000121?01101?1?0?11201?00

Hauffiosaurus_zanoni
00?2??1??1??????????????0?0???????????0?10????????????00?001???010?????????????????11101101?0100010?100?010????20100??100?1100??12002301(01)01120000?00??????310011?11100100100?020?00?????????0?011000002011011 20??0020000?010?0001020?2?0001001000??11010?00121??11011010001101100

Marmornectes_candrewi
0???????????00??0?????00????????????????????????0????10???0???0???10100110?0000?1110002010210200000 00??21?1?0001???1200100100?200?1001??1?00?1?0010000??????1?0??000?00???00????00220111??2000??0011000100001210 0?1??1110??011???1

Peloneustes_philarchus
10020120211100210??010001000101?0100000100200100031211000 10?0010100001100001 1?10102211100110(0
1)010?12110200???21101101100000011110002110010200010 00??21?110001?1212001101000000110012011 00?1?0010001?00?101100001000000201 0??1002301111022000?01??000210001220022101110111101111

Simolestes_vorax
110101???21?10210??010001??010??0100000100200?0003111?000?0?0010100??11000????1???221110???????0?121?0210???210111??10?0000?111000??1?01010?0??00???1111000111 21?0?1000001200110????11?????0????0??20?10012010?02?000?0????000230??1102201??010100021010122001110111001110????

Pliosaurus_BRSMG_Cc332
110101?0221110210??0100110?0111?110000010020010023111100020100101 0???1????01???0?012111001???????12110200???1?101?0010?200???13?00(12)11011011?????????????0001???1?00?00?????00???00??1100??

Pliosaurus_brachydeirus
11?1?????2??102?0??01001???0????????????????00?0???1??????????01010??????????????0?????????1?????0?12110200?????101??010?2000??13000(12)11101021?0???????????0001???110??10???0?00?2010??1100??0???00????0?????1?1???3???1?0??10????1

Gallardosaurus_iturraldei
??0?01?022?1??21????????10??????11?000010020010?31?1100020?01101????1?????????????1211
10???0?010?12110300???211?????1???0?????????????????1????00??2?11?00011??1?0?110?0??201
???
?????

Liopleurodon_rossicus
11?1?1??????10210??01000????1?1?11000001??200?0??3121?????????????????????????????????????
?????????????????????????1????????0???????????1?01011?????????????????????????????????????
?????????????????????1000200?2?????0?2???

Pliosaurus_andrewsi

01020?2021??10210??0??00??00?????????????????00?00?3(01)211?0??0?00??10?????????????102?
11?00110?010?1211020????21111?011000010111100021100101000100110 2??21000101211001000
0002001100120110??1?0010000?????????????????????????????0023011 0???200??01??0202101012200
3210?100011001211

Liopleurodon_ferox
11010120221110210??0100010001 01?11?000010020000003121100020100101000?1100001??1010
22111001101110?12110210???2111110010?0010?111000111101010001100??01101000111212001
00101000011000?0110????2010100????1??0?000?????0??01???1????????10320???010???02101012
?0?2?101?0001???1?11

Kronosaurus_MCZ_1285
??0?0?20?2??????0???01000?(01)?00011000?01110?111?0
???????????12110(23)10??????????0????001????0??????01010?011?0??2??00000?11?3211?0?000?
0001??0?20?1??0??2?10000?00?10?0?????02??0020????1????????103?????????????????????????
???????1????

Brachauchenius_eulerti
010200?0211100210??1100010?0200?11100001012001002312100012??00?????????????????011?
0?000110001012110310 10?21110?0010?0001?11???00000010100?????????????????1???????????
??
???????

Brachauchenius_lucasi
000201202111002 10??010001000200?111?000101200100031210001 2??00?????????????????011
?0100?1011?0??2100310???211???001?00001(12)11????????010?0?0???0?????000002????211?00?
????????00??001???
???????11111

Brachauchenius_MNA_V9433

0102?????1?100210??0100010?0????????0001???00?002(23)1210?0?20?0????0????????????????
???00????110??2110210???211100001 0?0001?111000000001 0100???????????0000211?321110000
0?200?2?0???01?????????????????0?1???????22200002?????11??0011?10????????????????????????
?????????????

QM_F51291
????01??2?????210??010?????0210?1110000????0010???12?????????????????????????????????0?0
0?????????????(23)??????????????????????????????????????10????????????????????????????????
??
?

Attenborosaurus_conybeari
00010010???110??112???0010?0?????0??0001002???????2??10000???11?????????????????????1?2????
????????????????????????0110??0???0?????????10100???0?2??????????310??011110????1???0(0
3)00??11101100?0???1???1?20?10?1????0220000?000?310?02??1?0010001000??1??10?00?????1?0
01?100???01101

Plesiosaurus_dolichodeirus
001100?0110?00100??0010010?0000100100000100?00100010010000101010110(01)010?02000?1111?
10?01100?01000110100?000?1110?0100?100?1000???????10000111O?2???0????01410010121(01)0
0100101003(01)000111111000010000010(01)?2111011001100000000?000?000002012100100020000
?1102010000200110(0 1)1010000?01100

Eopleiosaurus_antiquior
??
??2??????????4100?0111?0?12?1???03??0???????
???01000?11?02??1001002?0?0??00???????0??2?11?00110020000?11010100??1?0110?1010000101
100

Eretmosaurus_rugosus
??
??(12)??????????(34)100110?100?12010000?0001
11??11?0???0000?01????1???????(01)?0??0???????00102012000110000000??11021?1000200110110
10000201100

Westphaliasaurus_simonsensii
??
??2???????????0011021?0??0010?103100011l?1
?0010?0000101?211100120??00000001??10000??20?20001?????000110021000111001101101000l
1?1??1

Seelyosaurus_guilelmiimperatoris
00000?00?10?02?????0???????0?????0??0011001????1?1?01000?0??11????????????????????????
????????????????????????10??100?1010???????100001100?2??????????3100?1221000???1???00?00
?1200110010(23)10000110110100l201?10030?1?0???300?02??20001100010??11020?100?200110
11000011201101

Microcleidus_tournemirensis
0000000?120102100??00100100000000010111100100100020010001l0?1???(12)1?????000?????01
12?110000??00?0?12100100???20????????????????????1100011001l?????????142101112100?20?1
00?00100112001110l0?????????20110012021101301O?010?300122012000110????0??1?020?100?2
?0110110100012?1??1

Microcleidus_brachypterygius
0011000?110102100??00100100000001010111100100101020010001001?????1?????????????101?
?100?0010000?12100000???20????????????????????0000110012?????????232101112l?00??1????
00100?12011110?03100011?0210???1????20130?0?01???101220?10??01002000??11021?100?2??1
1010010011101101

Microcleidus_homalospondylus
000000001101021O???0010020?000?010?0111100100101020010001??111101100102000012?00102
1?1?00????000??2100100???2001001??00?0???102???10000??0012??????????42101112100020110
0100100112011110l0?1000011??1011110001?01?010101???00122012000010?200000110211?10011
0011011010011201101

Plesiopterys_wildi
00100?0?1???00????????00???00??1?0?0???10??01?000100100?00?0?10101110200001001010110

???1????0011?00??00?100???20??100?1000?0?2??0?00?01110?????????024200111211O1?001??00
01001111?1100003000000?01?11?01201??0??0???010?3?0102012?001???00?00011020010l?2??11
001010011101110

Cryptoclidus_eurymerus
00100?0010?101100??0010010100001000002010020100101101000000010?1011101101?1110111
11??00101100011?00?0????000?02001100?1000?0021?020000111012111110l?0131001112320110
011100000001110110000000100011210110010102012010202001?1002101101120l0?10111303201
0122101300110(1 2)2(0 1)(0 1)001211

Tricleidus_seeleyi

01100???????011010?00?0010?000?100????????(12)01001?3001000?000010?00?0111111?????111
110?????????011200?000?1100?02011100010000?0021?01110011001?11?1101?0221001112320110
0111000100?11?01100???????????110110000002012010202?13?????????????210??10111302101012
21023001101111101211

Muraenosaurus_leedsii
00????????0?01100??001001??000?10??????????010?0?????1???0???10?00?0????11?????11011???
???????????0???????????020101000200O?0021?01010011001?1?1101??1421011223201200111000
1001??11110000?200?111???????0???0(12)????1?2020?3?1012?021??12????100123031110122102
3001100111001210

Kimmerosaurus_langhami
??1??0?1??0?0????????????0?????10??0??????201000001020000000111010102011O1?10111111??
???????????200?0????????020011000100O?002??0?00?01220???1?1001?00?00011??3?01100111???
1?0??
??????

Pantosaurus_striatus
??
??(34)100111?320??00???000100??1?
??110000?2000111?????????????????????????????01001?021011200??10????0210101??1?1?10???211??
?1211

Picrocleidus_beloclis
??0????0?010?(0
1)0?????????????10012?????????????????????????????????????1100?1000????2??2?????11?????1?1101?024
1101122320120011100010011l?011?0?0?200?10100101100201020120102020l?01?12?021112200
??101???02111012210110010011111?1?10

Tatenectes_laramiensis
???????0?????????????????0??????0??????1??(12)?????????2000?0000????????????????????????
???????11????????0?1?????????????????????????????11??????01001????00011??32011001?1000100?
110?110000?????????1011??????(12)01??1020101?10?11002101121O??10????0210101??1?2?001?
0211??01??1

Plesiosaurus_mansellii
??
??1111101??2(34)1101???320??00?????01?01??
1111?????1010011??0????????????2??1?202??2???????
??

Colymbosaurus_megadeirus
??
??????????????????????????100?1000??????0???????????1111110??2410012??320?200111??01?01??1

011??00?2110101??0???????????2??102?2??????????????200??10101?021010122102210110 2?11101211

Djupedallia_engeri
??00???????0?01111?????????????????????????????????????020?????????????????????00?0??1??2011???100?5100121132012001110301001102??1100?????????????10?0???0?0??01???(12)??3?????????????2?0??????1?02?0?012?1???101102???1?1211

Spitrasaurus_spp
??????0??0???00??1010????????????1????????????????0???????????0201?100?1000???2??0?00?01110?20111111??2521012 2?32012001110301001 10?01100?????????????10?0???0?0??01???2?????????????????2?11?????1?02(1 2)0?012?1???101102?1???1(1 2)11

Abyssosaurus_nataliae
??2???1110??1(45)1001???32012001 11??01?01??1011??0??(1 2)0???????0010000100??2??10?0?001?1?1101110??2?1??1????10???10?22?0?3??110(0 2)??1001211

Umoonasaurus_demoscyllus
000001001 12??1101020??00??00????0??????????0?002222?10???10?11????1??12?11?0??0??022????0?????11122?1211000????????0??1111??????1111010?01????????????1001????20?1??1010??00?1101011020002 01?00?1???1?01?010?????????????0???????????21????0111?02001022210?2???1?0??10?1??1

Nichollssaura_borealis
000001001120001010201000110000010 0?0000100100001223010100100 11??211?2??0???00000?0221110101100011122?13110000?0111110??0101?112??02?1001010100100??2002210010013201 1?010??000??1102?101?00000?????????10110020?????????????2?12102?01?2?(01)0000??1??200101?21012101100011101110

Leptocleidus_capensis

010001?1112?10101020020 01?0000?10??0000??01001022(23)201010?0??01??21?????0?????????0221110?01?00011122?12110001?????1110?0111??(12)2?111111010101????????????210010??320?1?0100?0?0?0?????1???2????00????0???????????2???1?0??10?1???

Leptocleidus_superstes

??0?0??1?1?0????10(12)?????1?????????????????????0?10222201010?10001112 1?0011?01???????022 11???????????122??31????1???(12)0?01?0132011001000??00?110?11102???1011001?10110011020??1?10020010 2?????????????????????01???02001012?0?????????????????

Cimoliasaurus_valdensis
??1100???1?1(12)1001002320?110100000001?????1??????1011000???001???02001021?0????????0??????1

MIWG_1997_302
??

??01?01??0?1??1010??00??10??11
02?????????????1???1?02???1??01?10?0??

Brancasaurus_brancai 0010?000100000(0
1)?101002001?00000?0?1000???0101?02223010?0?00?011101101120101000100022?????011000??
?0???????????01???100?1110???2??121100111?120100??200141001002320l2?0101100000110101
102000101?1011???1?01?0201?10?0?210?020101210210112l????011100200102220032l?11???110
?1???

GWWU_A3_B2
??
??01?12?20?2001111?000?111001
1100002011101????1?????????????0?210???0101210210102l????0112?02000022210?1???1?0??????
??1

Speeton_Clay_plesiosaurian
??
??2???????????2101012320120011110010011201
111000?20?1111??1011?1??20??1??002?????0101210110112l0??0010210300102l?1021001100011
101?11

Wapuskanectes_betsynichollsae
??
??1??1??
0????????????2101(0
1)2?110?1110110?10??3?????????????200???01???03000022?????????????????????0

Futabasaurus_suzukii
00??000?1?0?00??0??00?0?2?0000?????????????????????0???1????????????????????????????????
0110000?????????????????100??????0????(12)????100001100?????????????????11?22?2022001111?01
0?11110111000?????????????????????????????????????01301?1??01?0?1100200000220300102221122101l
00011101(1 2)10

Callawayasaurus_colombiensis

000010?0?10000(12)?10100?0020?000?10????????0101000022010101000111101l?(12)02?1010??1
?002211001????0?0???2?1100???1?1101(01)?0??20?????2??0100001100l2?????????52101022320
22001111(01)0100111211110????????????200100?1100112001010?10?01?????????00??0(01)??100?22
0300102?3101200?10(0 1)0111??2?1

Kaiwhekea_katiki
00001010??000???1020020020?000?????????11????0?0?32?2111000?00????????????????????????
????????????????????????0101?10??1000??????0300001120?2??????????5101112232l?2?0111?1010
0?11111?10???2????0??000??00??11?32?11??3?12110100(0
1)0012?1??0

Aristonectes_parvidens

00?010??1?0000201??00200200000??00???(01)?11??01010?3212?1?0000?00?1?01212010????????
???????0?10000?????????????????0101010??1000???????3000011200?1101101?02?1111???3???20011
1??01?0??
???????????

Libonectes_morgani
010010?0110000201020020020000000?00110001001110??0?21??111?00010?010?20201010?001002
21100101?00?0?122?1200???2101000101?2000?112000101001?0012???1?????1621?122?320?2001

11??01??1??????????????????????21011??????11100?0?100?1?????????????00??00????????10??????2
00??01?1???????

Hydrotherosaurus_alexandrae
000010?0??0000201(12)100?002??0000?00110001001111?????2121?111??01??????????????????????
????????????????????????????????100010?1?01??112???10000110012???1?????1521112223202200111
?10100111001110000201 1?11?1001(0
1)00001011200?020????120111011000100?000??120310101231023001 10(0 1)011101211

Edgarosaurus_muddi
100101?021001020111010001??0?0??00100001 0?200102220011101000110?01?02?2?1?0????1002
211?01??????10122?130010020110001101111 0?120011(23)110111100?010100000121001?113201
120100000000???01??00?00??????0010?2?0
?3?10??0101??01211

Plesiopleurodon_wellesi
000100?0?100102?1120?000???2?0?????????????1???222201010?10?11??????????????????????????
????????????????????????0001?11???110?1????1(12)000210?0?????????????100?011320?120100?0?
0?0??0??110(02)???(01)0??101?????????????20110?1?01?????????????????????????????(23)(01)?1012
?1??????????????????

QM_F51291.2

000100201100112011 20?000(12)???2?0??00??01010??1???222201010110011110 1?????????????1?0
22??001???00???1?2?100????1??001??????1???11????10001102 0?11101000?0210001(01)02320?12
0100100010010 0?1100?00101010011??1???????20?1??????????2010012101120011011011120010 1
2210221011000111 01(1 2)10

Colymbosaurus_svalbardensis
??
??1????1??
???211?101?????????????????????????????1?1?1???2?0?????0??????????21??????1?2??11?????

PMO_222.663
??
??1?0
000?21101011?0??????????0??????0??0??1?1101?1???200??1010120?10101211023101102111101211

Supplementary Information S3

Yunguisaurus_liae
0001000??10000000??0010010?000010010?000?000110??200??00????01020??????????????02?1
0???????0?0?0010020???10011001100?1001?1????13??0??????1??????????41000??00?000000?001
??0??01210?0?00(23)??0??????0?000?200????????????0?00122011?0000002000??11000?000?0?00
0000010000100000

Pistosaurus_postcranium
??
??2001110000000000011010010110
0010????101110?00?001?202100??0??001????0122210???1??????01?1?00000000???0???0?10?????
???0

Augustasaurus_hagdorni
010100?0010?00000??00100100000000000000100?00100121010000010??????0???0?0000?????02?
?000?0110000?0010000????0?1100?10??1001??1???01010002100???00??21??41?01??000000200?0
?10000011??0000???????????00?000?102?020000?0?????????????????000??00???100000000???0?
100?1000???0?00

Bobosaurus_forojuliensis
????????????????0??
??02?0?00?00??01?2100000??110?12?000?00??001221
100?10(23)1?????????????????????????????????0122010?001??????0???1?000????????0???0?0??0??
????

Anningasaura_lymense
111000?0120?00??10000100?0010000100000?100000101120010000?10?0?1020?0110111010010?00
211?1000000011?00?000?111??1110?100?1010?110??00010011000?0?00??0?0??10010??3?0?1201
00?031?1??
????????????

Stratesaurus_taylori
001000?0100100100??0110010000010?0?00001000001000100100001010110101200200010?0010
2211???01000010110?000000?2?111?11000110001?0?001000011000?0?00??2001?1001001110012
0100003101??1????00?0????????????1?????????????????????01022111??????????????????????????
1???010??010??10

Avalonnectes_arturi
??????????01??10????????10?????01??00001000001001100100001010???????????????????1??????
0??(12)??????????2100?00211001??100?0110
001101101200?0110?00????1?01201???????????????0102?110??1?????????11020?000?110110?101
000010?100

Meyerasaurus_victor
10?00?0?21??00??11??0100??0000???0??????????????????10?0??0101??(01)0????????0??????022?
0?1?01010111122?11000101?0111100?02110211???01?1001010?0???0???1?120?01?????00?20????
0???0011211012002?110?0?0111?0?1????0201000?0001000102011?0011002100??12020?00021??1
1011010001101100

Maresaurus_coccai

110100?1220?1???1120(02)1001?0?00?????????????00001120?10???10?0110?0?????0?????????0??
11?000101010?122?1000???200111?00??2100?11???01?1?011100????0???????0001???2?0?(01)??1
???030???
????????????

Borealonectes_russelli

11010?1?210?102011100?00(12)0?0000??010?0010010000?(01)??1?000??0?0???20???12000??????
?022?1?0???????0??2???201?????111??00???1?0?110??0(12)?1?01?10?00100??21?120001????2?0??
20?????30?0????????1???100??00?????1101012???
2?011?0001???11?1

Rhomaleosaurus_megacephalus
10010121220112101000210010010?000?000010000010012001000110101???0?201?000???0??100
211100010001101l???00?0002001111?0??20?0?11??0??00001020?0???0???10120001???1100?201
????10?00111?1012001??20?0?0??????????1?????????????01022110????????00??1?0201001?110?
1??1010??0?????0

Archaeonectrus_rostratus
1002002???0?102?1111??00?????????0?000?10000010012011000?1??01?????????????????????????
?????????????????????????11??1????1?????????????11120?0??????????2100100111000201???0?11?
011011011001O??????0?????0?20?1?????????????01?2?1100?10001000??1?020?00??11011011010
001101100

Rhomaleosaurus_cramptoni
10000021220?1020100121101?00001?1000000???000100120110001111O?10?0???1?000???????02?
1110?01010110122?1000000200?11?00??2100?11???01?1?01020?00?????????200???1211000??1?0
?01?1?0002110?100?0????0?????1?????????????1??????0102?11000?10???00??1?021?001?1??110
110100?11?1?00

Rhomaleosaurus_zetlandicus
11000??1220?102010012110??00001??000???????001001?0110?0?1110110?????1?0?0????????221
1??0?1????1?1?2??0??0??2001111000021002110000??1001020?0??????????200010??110?020100?
010?00??2110?1???01201000??????????????????????????????????????1?0??0012120210001211011O1
101001?????0?

Rhomaleosaurus_thorntoni
11??0???2?0?10??1021?1101?00?????0??0001000?????????????1????????????????????????????1?
?01??01?????????????200111??10?11???11000?11100101000??????????0001???110?000100??10?
?01?21101?00?0110100??01100120210?0?000100?10001220110001??????0111?02100002110?????
???????????

Thalassiodracon_hawkinsii
00100001110100111120??0?1000???0000000?100200000010110000101101010100020000110001O
1011?00011001??100?000????0?11101100010000?1200?00100111001000O??2101310010011100l2
010000210001110100000101100000201101100l?00000001000?000102011100100020000011010O0
00010?11001010000101100

Hauffiosaurus_longirostris
00?20??0?1??12111120??00???2?????????????????????02???????????01001??0???1?0?????1110????
?????????110?0??0?????1001?100?1100?11?00230101120O?????????????????????????????????????
??
??

Hauffiosaurus_tomistomimus
00020?10210?1?110??0100?0?0210100100???????00?00010100?0?101?01011??????1001????11101
1?0?0100010?100?010??????1000?100?1100?1120023010011120?1100???(0
2)?1231001?11110?100100002000011101010001??10???0???1??1?0?0?????????????00????????00??
?0?10000120100001210?1101?1?0?11201?00

Hauffiosaurus_zanoni
00?2??1??1?????????????????0?0??????????0?10???????????00?001???010?????????????????111011011?0100010?100?010????20100??100?1100??12002301(01)01120000?00??????310011?11100100100?020?00?????????0?0110000020110112O??0020000?010?0001020?2?0001001000??11010?00121??11011010001101100

Marmornectes_candrewi
0???????????00??0?????00?????????????????????????0????10???0???0???10100110?0000?11100020102102000000??21?1?0001???120010010O?200?11001??1?00?1?0010000??????1?0??000?00???00????00220111??2000??00110001000012100?1??1110??011???1

Peloneustes_philarchus
10020120211100210??010001000101?0100000100200100031211000l0?00101000011000011?101022111001l0(01)010?12110200???2110110110000001111000211001020001000??21?110001?12120011010000001100120110O?1?0010001?00?10110000100000020l0??100230111102200O?01??000210001220022101110111101111

Simolestes_vorax
110101???21?10210??010001??010??0100000100200?0003111?000?0?0010100??11000????1???2211110???????0?121?0210???210111??10?0000?111000??1?01010?0??00???111100011121?0?10000012001100????11?????0????0???20?10012010?02?000?0????000230??1102201??0101000210101220011101110011110????

Pliosaurus_BRSMG_Cc332
110101?0221110210??0100110?0111?1100000100200100231111000201001010???1????01???0?012111001???????12110200???1?101?0010?200???13?00(12)11011011?????????????0001???1?00?00?????00???00??1100???

Pliosaurus_brachydeirus
11?1?????2??102?0??01001???0?????????????????00?0???1??????????01010?????????????0?????????1?????0?12110200?????101??010?2000??13000(12)11101021?0???????????0001???110??10???0?00?2010??1100???0???00????0?????1?1???3???1?0??10????1

Gallardosaurus_iturraldei
??0?01?022?1??21????????10??????11?000010020010O?31?1100020?01101????1?????????????121110???0?010?12110300???211?????1???0?????????????????1????00??2?11?00011??1?0?110?0??201???

Liopleurodon_rossicus
11?1?1??????10210??01000????1?1?1100000l??200?0??3121???1????????0???????????1?01011???1000200?2?????0?2???

Pliosaurus_andrewsi
01020?2021??10210??0??00??00?????????????????00?00?3(01)211?0??0?00??10?????????????102?11?00110?010?1211020????21111?011000010111100021100101000100110O??21000101211001000000200110012011O??1?0010000?????????????????????????????0023011O???200??01??0202101012200321O?100011001211

Liopleurodon_ferox
11010120221110210??010001000101?11?000010020000003121100020100101000?1100001??101022111001101110?12110210???2111110010?0010?111000111101010001100??01101000111212001

00101000011000?0110????2010100????1??0?000?????0??01???1????????10320???010???02101012
?0?2?101?0001???1?11

Kronosaurus_MCZ_1285
??0?0?20?2??????0??01000?(01)?00011000?01110?111?0
???????????12110(23)10??????????0????001????0??????01010?011?0??2??00000?11?3211?0?000?
0001??0?20?1??0??2?10000?00?10?0?????02??0020????1????????103??????????????????????????
???????1????

Brachauchenius_eulerti
010200?0211100210??1100010?0200?11100001012001002312100012??00??????????????????011?
0?00011000101211031010?21110?0010?0001?11???00000010100???????????????????1???????????
??
???????

Brachauchenius_lucasi
00020120211100210??01000100020 0?111?0001012001000312100012??00???????????????????011
?0100?1011?0??2100310???211???001?00001(12)11????????010?0?0???0?????000002????211?00?
????????00??001??
??????11111

Brachauchenius_MNA_V9433
0102?????1?100210??0100010?0????????0001???00?002(23)1210?0?20?0????0??????????????????
???00????110??2110210???2111000010?0001?1110000000010100??????????0000211?321110000
0?200?2?0???01??????????????0?1???????22200002?????11??0011?10??????????????????????????
?????????????

QM_F51291
????01??2?????210??010?????0210?1110000????0010???12?????????????????????????????????0?0
0?????????????(23)???????????????????????????????????10?????????????????????????????????????
??
?

Attenborosaurus_conybeari
00010010???110??112???0010?0?????0??0001002??????2??10000???11???????????????????1?2????
???????????????????????0110??0???0?????????10100???0?2??????????310??011110????1???0(03)0
0??11101100?0???1???1?20?10?1????0220000?000?310?02??1?0010001000??1??10?00?????1?001
?100???01101

Plesiosaurus_dolichodeirus
001100?0110?00100??0010010?0000100100001 00?001000100100001010110(01)010?02000?1111?
10?01100?01000110100?000?1110?0100?100?1000???????100001110?2???0????01410010121(01)0
0100101003(01)0001111110000100 0010(01)?21110110011 0000000?000?000002012100100020000
?1102010000200110(0 1)1010000?01100

Eopleiosaurus_antiquior
??
??2??????????4100?0111?0?12?1???03??0???????
???01000?11?02??1001002?0?0??00???????0??2?11?00110020000?11010100??1?0110?1010000101
100

Eretmosaurus_rugosus
??
??(12)??????????(34)100110?100?12010000?0001
11??11?0???0000?01????1???????(01)?0??0???????0010201200011000000??11021?1000200110110
10000201100

Westphaliasaurus_simonsensii
??
???2????????????0011021?0??0010?10310001 11?1
?0010?0000101?211100120??00000001??10000??20?20001?????00011002100011100110110100 01
1?1??1

Seelyosaurus_guilelmiimperatoris
00000?00?10?02?????0???????0?????0??0011001????1?1?01000?0??11?????????????????????????
??????????????????????10??100?1010???????10000 1100?2??????????3100?1221000???1???00?00
?1200110010(2
3)1000011011010012 01?10030?1?0???300?02??20001 1000100??11020?100?20011011000011201 1
01

Microcleidus_tournemirensis
0000000?120102100??00100100000000010111100100100020010001 10?1???(12)1?????000?????01
12?110000??00?0?12100100???20???????????????????1100011 0012?????????142101112100?20?1
00?001001120011 1010?????????2011001202110130 10?010?300122012000110????0??1?020?100?2
?0110110100012?1??1

Microcleidus_brachypterygius
0011000?110102100??0010010000000101011110010010102001000100?????1???????????????101?
?100?0010000?12100000???20????????????????????0000110012?????????2321011121?00??1????
00100?12011110?03100011?0210???1????20130?0?01???101220?10??01002000??11021?100?2??1
1010010011101101

Microcleidus_homalospondylus
000000001101021 0???0010020?000?010?01111001001010200100 01??11110110010200001??00102
1?1?00????000??2100100???2001001??00?0???102???10000??0012??????????42101112100020110
0100100112011110 10?1000011??1011110001?01?010101???00122012000010?20000011021?10011
0011011010011201101

Plesiopterys_wildi
00100?0?1???00????????00???00??1?0?0???10??01?0001001000?00?0?10101110200001001010110
???1????0011?00??00?100???20??100?1000?0?2??0?00?01110??????????02420011121101?001??00
01001111?1100003000000?01?11?01201??0??0???010?3?0102012?001???00?000110200101?2??11
001010011101110

Cryptoclidus_eurymerus
00100?0010?101100??00100101000010000201002010010110100000000 10?1011101101?1110111
11??00101100011?00?0????000?02001100?1000?0021?0200001110121111101?0131001112320110
01110000000111011000000001000112101100101020120102020 0?11002101101 12010?10111303201
0122101300110(1 2)2(0 1)(0 1)001211

Tricleidus_seeleyi

01100???????011010?00?0010?000?100????????(12)01001?3001000?000010?00?0111111?????111
110?????????011200?000?1100?0201110001000?0021?01110011001?11?1101?0221001112320110
0111000100?11?01100???????????11011000000 2012010202?13????????????210??10111302101012
21023001101111101211

Muraenosaurus_leedsii
00?????????0?01100??001001??000?10??????????010?0?????1???0???10?00?0????11?????11011???
???????????0???????????020101000 2000?0021?010100110012?1?1101??14210112232012001 11000
1001??11110000?200?111???????0???0(12)????1?2020?3?1012?021??12????100123031110122102
3001100111001210

Kimmerosaurus_langhami
??1??0?1??0?0?????????????0?????10??0??????201000001020000000111010102011O1?1011111111??
???????????200?0????????020011000100O?002??0?00?01220???1?1001?00?00011??3?01100111???
1?0??
??????

Pantosaurus_striatus
??
??(34)100111?320??00???000100??1?
?110000?2000111?????????????????????????????01001?021011200??10????0210101??1?1?10???211??
?1211

Picrocleidus_beloclis
??0????0?010?(01)0?????????????10012????
??????????????????????????1100?1000???2??2?????11?????1?1101?024110112232012001110001O
0111?011?0?0?200?10100101100201020120102020l?01?12?021112200??101???021110122101100
10011111?1?10

Tatenectes_laramiensis

???????0??????????????????0??????0??????1??(12)??????????2000?0000????????????????????????????
???????11????????0?1????????????????????????????11??????01001????00011??32011001?1000100?
110?110000??????????1011??????(12)01??1020101?10?11002101121O??10????0210101??1?2?001?
0211??01??1

Plesiosaurus_mansellii
??
??1111101??2(34)1101???320??00?????01?01??
1111?????1010011??0???????????2??1?202??2????????
??

Colymbosaurus_megadeirus
??
??????????????????????100?1000??????0???????????1111110??2410012??320?200111??01?01??1
011??00?2110101??0???????????2??102?2?????????????????200??10101?021010122102210110O?111
01211

Djupedallia_engeri
??00???????0?01111?????????????????
??????????????????020?????????????????????00?0??1??2011???100?5100121132012001110301001l0
??1100?????????????????10?0???0?0??01???(12)???3?????????????2?0??????1?02?0?012?1???101102???
1?1211

Spitrasaurus_spp
??????0??0???00??1010?????????????1????????????
???????0???????????0201?100?1000???2??0?00?01110?20111111??2521012202?3201200111030100l
10?01100?????????????????10?0???0?0??01???2?????????????????2?11?????1?02(1
2)0?012?1???101102?1???1(1 2)11

Abyssosaurus_nataliae
??
??2???1110??1(45)1001???3201200111??01?01??
1011??0??(12)0???????0010000100??2??10?0?001?1?1101110??2?1??1????10???10?22?0?3??110(0
2)??1001211

Umoonasaurus_demoscyllus
00000100112??1101020??00??00????0??????????0?002222?10???10?11????1??12?11?0??0??022??
???0????11122?1211000????????0??1111??????1111010?01???????????1001????20?1??1010??0
0?11010110200020l?00?1???1?01?010?????????????0???????????21????0111?02001022210?2???1
?0??10?1??1

Nichollssaura_borealis
00000100112000101020100011000000100?0000100100001223010100100l1??211?2??0???00000?02
2111010110001l122?13110000?0111110??0101?112??02?100101010010l??200221001001320l1?0
10??000??1102?101?00000?????????10110020??????????????2?12102?01?2?(0
1)0000??1??200101?21012101100011101110

Leptocleidus_capensis
010001?1112?10101020020l1?0000?10??0000??01001022(23)201010?0??01??21?????0??????????0
221110?01?00011122?12110001?????1110?0111??(12)2?111111010101???????????210010??320?1
?0100?0?0?0?????1???2????00????0???????????
2???1?0??10?1???

Leptocleidus_superstes

??0?0??1?1?0????10(12)?????1?????????????????0?10222201010?10001112l?0011?01???????022
11???????????122??31????1???(12)0?01?0132011001000
??00?110?11102???1011001?10110011020??1?100200102?????????????????01???02001012?0????
?????????????

Cimoliasaurus_valdensis
??
??1100???1?1(12)1001002320?110100000001???
??1??????1011000???001???02001021?0????????0??????
??1

MIWG_1997_302
??
??01?01??0?1??1010??00??10??11
02?????????????1???1?02???1??01?10?0??

Brancasaurus_brancai

0010?000100000(01)?101002001?00000?0?1000???0101?02223010?0?00?0111011011201010001O
0022?????011000???0???????????01???100?1110???2??12110011l?120100??20014100100232012?
0101100000110101102000101?1011???1?01?0201?10?0?210?020101210210112l????01110020010
22200321?11???110?1???

GWWU_A3_B2
??
??01?12?20?2001111?000?111001
1100002011101????1?????????????0?210???0101210210102l????0112?02000022210?1???1?0??????
??1

Speeton_Clay_plesiosaurian
??
??2???????????2101012320120011110010011201
111000?20?1111??1011?1??20??1??002?????0101210110112002?00102103001022?1021001100011
101?11

Wapuskanectes_betsynichollsae
??

??1??1??0???????????2101(01)2?110?1110110?10??3?????????????200???01???0300002?????????????????????0

Futabasaurus_suzukii
00??000?1?0?00??0??00?0?2?0000?????????????????????0???1????????????????????????????????0110000?????????????????100??????0????(12)????100001100?????????????????11?22?2022001111?010?11110111000?????????????????????????????????01301?1??01?0?11002000002203001022211221011000111011(1 2)10

Callawayasaurus_colombiensis

000010?0?10000(1 2)?10100?0020?000?10????????0101000022010101000111101 1?(1 2)02?1010??1?002211001????0?0???2?1100???1?1101(01)?0??20?????2??0100001100 12?????????52101022320220011 11(01)0100111211110???????????200100?1100112001 0?10?01?????????00??0(0 1)??100?22030010 2?3101200?10(0 1)0111??2?1

Kaiwhekea_katiki
00001010??000???10200200 20?000?????????11????0?0?32?2111000?00??0101?10??1000??????030000112 0?2??????????5101112232 0?2?0111?10100?11111?10???2????0??000??00??11?32?11??3?12110100(01)0012?1??0

Aristonectes_parvidens

00?010??1?0000201??002002000 00??00???(01)?11??01010?3212?1?0000?00?1?01212010????????????0?10000?????????????????0101010??1000???????3000011200?1101101?02?1111???3???2001111??01?0???

Libonectes_morgani
010010?0110000201020020020000 00?00110001001110??0?21??111?00010?010?20201010?00100221100101?00?0?122?1200???2101000101?2000?1120001010 01?0012???1?????1621?122?320?200111??01??1?????????????????????21011??????11100?0?100?1?????????????00??00????????10???????200??01?1???????

Hydrotherosaurus_alexandrae

000010?0??0000201(12)100?002??0000?00110001001 11?????2121?111??01???100010?1?01??112???10000110012???1?????1521112223202200111?10100111001110000 2011?11?1001(01)00001011200?020????1201110110001 00?000??120310101231023001 10(0 1)011101211

Edgarosaurus_muddi
100101?0210010201110100 01??0?0??00100001 0?2001022200111010001 10?01?02?2?1?0????1002211?01??????10122?1300100201100011011110?120011(23)110111100?0101000001210 01?113201120100000000000???01???00?00??????0010?2?0?3?10??0101??01211

Plesiopleurodon_wellesi
000100?0?100102?1120?000???2?0?????????????1???2222010 10?10?11???0001?11???110?1????1(12)000210?0?????????????100?011320?120100?0?0?0??0??110(02)???(01)0??101????????????20110?1?01?????????????????????????????(2 3)(01)?1012?1?????????????????

QM_F51291.2

000100201100112011 20?000(12)???2?0??00??01010??1???222201010110011110 1?????????????1?0
22??001???00???1?2?100????1??001??????1???11????10001102 0?11101000?0210001(01)02320?12
0100100010010 0?1100?00101010011??1???????20?1??????????2010012101120011011011120010 1
2210221011000111 01(1 2)10

Colymbosaurus_svalbardensis
??
??1???110
000?21101011?0??????????0??????0??0??1?1101?1???200??1010120?101012(1
2)1023101102111101211

Appendix 4

Published paper Roberts et al. 2017

Journal of Vertebrate Paleontology

ISSN: 0272-4634 (Print) 1937-2809 (Online) Journal homepage: http://www.tandfonline.com/loi/ujvp20

Osteology and relationships of Colymbosaurus Seeley, 1874, based on new material of C. svalbardensis from the Slottsmøya Member, Agardhfjellet Formation of central Spitsbergen

Aubrey J. Roberts, Patrick S. Druckenmiller, Lene L. Delsett & Jørn H. Hurum

To cite this article: Aubrey J. Roberts, Patrick S. Druckenmiller, Lene L. Delsett & Jørn H. Hurum (2017): Osteology and relationships of Colymbosaurus Seeley, 1874, based on new material of C. svalbardensis from the Slottsmøya Member, Agardhfjellet Formation of central Spitsbergen, Journal of Vertebrate Paleontology, DOI: 10.1080/02724634.2017.1278381

To link to this article: http://dx.doi.org/10.1080/02724634.2017.1278381

Journal of Vertebrate Paleontology e1278381 (18 pages)
Society of Vertebrate Paleontology
DOI: 10.1080/02724634.2017.1278381

ARTICLE

OSTEOLOGY AND RELATIONSHIPS OF *COLYMBOSAURUS* SEELEY, 1874, BASED ON NEW MATERIAL OF *C. SVALBARDENSIS* FROM THE SLOTTSMØYA MEMBER, AGARDHFJELLET FORMATION OF CENTRAL SPITSBERGEN

AUBREY J. ROBERTS,*[1,2] PATRICK S. DRUCKENMILLER,[3,4] LENE L. DELSETT,[2] and JØRN H. HURUM[2]
[1]The National Oceanography Centre, University of Southampton, Southampton, Hampshire SO14 3ZH, U.K., ajr1g13@soton.ac.uk;
[2]Natural History Museum, University of Oslo, 0562, Norway, l.l.delsett@nhm.uio.no; j.h.hurum@nhm.uio.no;
[3]University of Alaska Museum, 907 Yukon Drive, Fairbanks, Alaska 99775, U.S.A., psdruckenmiller@alaska.edu;
[4]Department of Geoscience, University of Alaska Fairbanks, 900 Yukon Drive, Fairbanks, Alaska 99775, U.S.A.

ABSTRACT—*Colymbosaurus* is a genus of long-necked plesiosaurian represented by two valid species: *C. megadeirus* from the Upper Kimmeridge Clay Formation (Kimmeridgian–Tithonian) of the United Kingdom and *C. svalbardensis* from the Slottsmøya Member of the Agardhfjellet Formation (Tithonian–Berriasian) of Svalbard, Norway. Due to the lack of complete and articulated skeletons and a near absence of cranial material, *Colymbosaurus* has been problematic to characterize morphologically. Here, we describe and conduct a phylogenetic analysis on an informative new specimen referable to *C. svalbardensis* from the Slottsmøya Member, preserving a large portion of the axial and appendicular skeleton. The new material contributes important new osteological data for the species and together with an extensive examination of congeners in British museums, clarifies the diagnostic characters of the genus. We provide two new diagnostic characters of the epipodials for the genus and reevaluate the utility of an anteroposteriorly oriented bisecting ridge on the distal end of the propodials. We also present two new diagnostic features for *C. svalbardensis* regarding the neural canal and femoral morphology. A phylogenetic analysis recovers a monophyletic and well-supported *Colymbosaurus*. The new specimen of *C. svalbardensis* confirms that this species is not synonymous with other described Slottsmøya Member plesiosauroids, demonstrating considerable diversity of the clade at high latitudes close to the Jurassic–Cretaceous boundary.

SUPPLEMENTAL DATA—Supplemental materials are available for this article for free at www.tandfonline.com/UJVP

Citation for this article: Roberts, A. J., P. S. Druckenmiller, L. L. Delsett, and Jørn H. Hurum. 2017. Osteology and relationships of *Colymbosaurus* Seeley, 1874, based on new material of *C. svalbardensis* from the Slottsmøya Member, Agardhfjellet Formation of central Spitsbergen. Journal of Vertebrate Paleontology. DOI: 10.1080/02724634.2017.1278381.

INTRODUCTION

Plesiosauria is a clade of secondarily aquatic reptiles that inhabited the Mesozoic seas (Taylor and Cruickshank, 1993). Their earliest remains are known from the Late Triassic (Norian; Sennikov and Arkhangelsky, 2010), and by the Early Jurassic plesiosaurians had a worldwide distribution and were diversified into several clades exhibiting a wide range of morphotypes (Benson et al., 2012; Bardet et al., 2014). In the wake of recent broad-scale phylogenetic studies (O'Keefe, 2001; Druckenmiller and Russell, 2008; Ketchum and Benson, 2010; Benson and Druckenmiller, 2014), there is increasing consensus regarding the taxonomic relationships among major plesiosaurian clades. However, relationships within these clades remain problematic. One major small-skulled, long-necked plesiosauroid clade is Cryptoclididae, known from the Callovian (Middle Jurassic) to the latest Hautervian (Early Cretaceous) (Benson and Druckenmiller, 2014). Cryptoclidids are predominantly distributed in the northern hemisphere, with the majority of specimens found in the Oxford and Kimmeridge Clay formations of the United Kingdom (Gasparini et al., 2002). Recognizing synapomorphies for Cryptoclididae has proven challenging, because many of the described taxa either lack overlapping material or are known from juvenile specimens (Brown, 1981; O'Keefe et al., 2011; Knutsen et al., 2012a, 2012b, 2012c; Benson and Bowdler, 2014). Following Benson and Druckenmiller (2014), cryptoclidid synapomorphies include large orbits and external nares, a small vertical jugal, the lack of a prefrontal, a strongly emarginated cheek, and reduced tooth ornamentation. Ten cryptoclidid genera are currently recognized (Benson and Druckenmiller, 2014): *Abyssosaurus* (Berezin, 2011), *Colymbosaurus* (Seeley, 1874), *Cryptoclidus* (Phillips, 1871), *Djupedalia* (Knutsen et al., 2012c), *Kimmerosaurus* (Brown, 1981), *Muraenosaurus* (Seeley, 1874), *Pantosaurus* (Marsh, 1893), *Spitrasaurus* (Knutsen et al., 2012b), *Tatenectes* (Knight, 1900), and *Tricleidus* (Andrews, 1909). Other provisionally valid cryptoclidids also included in the Benson and Druckenmiller (2014) analysis include *Picrocleidus beloclis* (Andrews, 1910) and '*Plesiosaurus' manselii* (Hulke, 1870).

Colymbosaurinae (Benson and Bowdler, 2014) is a cryptoclidid subclade diagnosed solely on postcranial features due to the

*Corresponding author.

Color versions of one or more of the figures in this article can be found online at www.tandfonline.com/ujvp.

paucity of cranial material for this group (Benson and Bowdler, 2014). Seven species are referred to this subclade, including British (*Colymbosaurus megadeirus*; Seeley, 1869), North American (*Pantosaurus striatus*; Marsh, 1893; O'Keefe and Wahl, 2003), and Russian (*Abyssosaurus nataliae*; Berezin, 2011) taxa. Notably, all four of the plesiosauroids currently described from the Upper Jurassic Slottsmøya Member Lagerstätten of Spitsbergen (*Colymbosaurus svalbardensis, Djupedalia engeri, Spitrasaurus larseni*, and *S. wensaasi*; Knutsen et al., 2012a, 2012b, 2012c) are also members of this clade.

The high Arctic island of Spitsbergen, part of the Norwegian Svalbard archipelago, has yielded many important remains of marine reptiles from the Upper Jurassic Slottsmøya Member of the Agardhfjellet Formation. At present, a total of three new monospecific genera of ichthyosaurs and two new genera and four species of plesiosaurians have been described, all of which are endemic to this region (Hurum et al., 2012; Delsett et al., 2016). The first cryptoclidid described from the Slottsmøya Member Lagerstätten was '*Tricleidus*' *svalbardensis* (Persson, 1962). An additional 23 cryptoclidid skeletons were excavated from the Slottsmøya Member between 2004 and 2012. Based on new morphological data derived from some of this material, Knutsen et al. (2012a) referred the holotype specimen of '*Tricleidus*' *svalbardensis* (PMO A27745) to the British Kimmeridgian genus *Colymbosaurus*, along with two other partial postcranial skeletons (PMO 216.838, PMO 218.377).

Despite being known from numerous specimens in the Kimmeridge Clay Formation and now the Slottsmøya Member of Spitsbergen, *Colymbosaurus* has proven difficult to diagnose, in part due to the near absence of cranial remains and a scarcity of associated material. This problem was further compounded by the suggestion that *Colymbosaurus* is synonymous with *Kimmerosaurus langhami* (Brown, 1981; Brown et al., 1986), also from the Kimmeridge Clay Formation, an idea that is now discounted (Benson and Bowdler, 2014). Recently, Benson and Bowdler (2014) reexamined and rediagnosed this taxon on the basis of three diagnostic characters: (1) a postaxial flange bearing a single large postaxial ossicle facet of subequal size to the other epipodial facets; (2) an anteroposteriorly oriented ridge bisecting the distal facets on the propodials; and (3) cervical vertebrae that are slightly anteroposteriorly shorter than dorsoventrally high and lack a lateral ridge. Here, we describe the most complete Slottsmøya Member specimen referable to *Colymbosaurus svalbardensis*, PMO 222.663. The new material from the Slottsmøya Member and a reexamination of additional material from the Kimmeridge Clay Formation permit a reevaluation of diagnostic characters for both the genus and *C. svalbardensis*.

Institutional Abbreviations—**CAMSM**, Sedgwick Museum of Earth Science, Cambridge University, Cambridge, U.K.; **GLAHM**, The Hunterian Museum, University of Glasgow, Glasgow, U.K.; **LEICS**, Leicester New Walk Museum, Leicester, U.K.; **MANCH**, The Manchester Museum, Manchester, U.K.; **NHMUK**, Natural History Museum, London, U.K.; **NOTNH**, Wollaton Hall, Nottingham, U.K.; **OUM**, Oxford University Museum of Natural History, Oxford, U.K.; **PETRM**, Peterborough Museum, Peterborough, U.K.; **PMO**, Paleontological Museum Oslo, University of Oslo, Oslo, Norway; **PMU**, Paleontological Collections, Museum of Evolution, Uppsala University, Uppsala, Sweden; **SVB**, Svalbard Museum, Longyearbyen, Norway; **YORKM**, York Museum and Art Gallery, York, U.K.

Geological Setting

The Slottsmøya Member is the uppermost of four members of the Agardhfjellet Formation that spans a Middle Jurassic to Lower Cretaceous marine succession on Spitsbergen. The Agardhfjellet Formation is separated from the overlying Lower Cretaceous Rurikfjellet Formation by a regionally recognizable layer known as the Myklegardfjellet Bed (Dypvik et al., 1991) (Fig. 1). The Slottsmøya Member consists of 55–70 m of dark gray to black silty mudstone, which is often weathered into paper shale. There are discontinuous silty beds with associated siderite and dolomite interbeds and siderite nodules, some of which are interpreted as storm deposits (Rousseau and Nakrem, 2012).

The Slottsmøya Member represents approximately 12 million years of deposition spanning the upper Tithonian to the lower Berriasian (Hammer et al., 2012). As summarized in Delsett et al. (2016), detailed stratigraphic and isotopic work has divided the member into lower (−22–0 m), middle (0–27 m), and upper (27–52 m) units (Fig. 2), using a distinctive echinoderm bed ('yellow layer') as a lower marker bed (0 m; Rousseau and Nakrem, 2012) and the *Dorsoplanites* layer as a second, stratigraphically higher marker bed (27 m; Nagy and Basov, 1998; Collignon and Hammer, 2012; Hammer et al., 2012; Hjálmarsdóttir et al., 2012). The specimen described here (PMO 222.663) is from the middle unit (Fig. 2), a particularly fossiliferous stratigraphic interval (~14 m) from which six ichthyosaur and six plesiosaur specimens have been excavated (Delsett et al., 2016). Specimen PMO 216.838, the recently referred specimen of *Colymbosaurus svalbardensis* (Knutsen et al., 2012a), was also found in this same interval. However, the exact stratigraphic position of the holotype specimen (PMO A27745) is unknown.

MATERIALS AND METHODS

Specimen PMO 222.663 was excavated on the mountain of Janusfjellet over two field seasons (2010–2011). The specimen was mechanically prepared using air scribes, air abrasion, and small manual tools. In addition to this new specimen, the holotype of *Colymbosaurus svalbardensis* (PMO A27745) and the two previously referred specimens (PMO 216.838 and PMO 218.377; Knutsen et al., 2012a) were reexamined in the course of this study. In addition to the *C. svalbardensis* material, Kimmeridge Clay Formation specimens were also examined in several U.K. museums. Two of these specimens, NHMUK R10062 and OUM J.3300, are reasonably complete and can be referred to *Colymbosaurus*. To add to the diagnostic features defined by Benson and Bowdler (2014), 22 propodials referred to or with similar morphology to *Colymbosaurus* were examined and measured (Supplementary Data 1, Table S1). The majority of these are from the Kimmeridge Clay Formation held in U.K. museums, save PMO 222.663 and the holotype of *C. svalbardensis* (PMO A27745) from Spitsbergen (Knutsen et al., 2012a). All specimens that were included in this study, with the exception of CAMSM J68344, are from a mature ontogenetic stage. Some specimens include several propodials (OUM J.3300, PMO 222.663, and MANCH LL.5513/MANCH LL.5514) and were examined to assess variation in humeri and femora. More propodial material resembling *Colymbosaurus* is available in private collections and in unregistered material at other museums; these were examined but not included in this study. Whenever possible, the presence or absence of the distal anteroposteriorly oriented ridge, used as one of the diagnostic features by Benson and Bowdler (2014), was recorded and defined by a distinct ridge extending on both epipodial facets.

SYSTEMATIC PALEONTOLOGY

SAUROPTERYGIA Owen, 1860
PLESIOSAURIA de Blainville, 1835
PLESIOSAUROIDEA Gray, 1825
CRYPTOCLIDIDAE Williston, 1925
COLYMBOSAURINAE Benson and Bowdler, 2014
COLYMBOSAURUS Seeley, 1874

Type Species—*Colymbosaurus megadeirus* (Seeley, 1869).

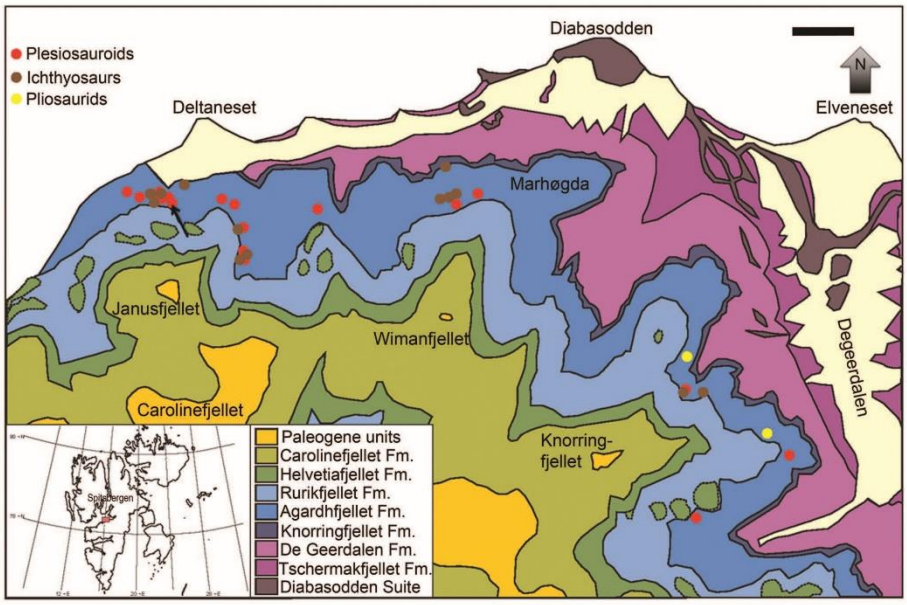

FIGURE 1. Geological map of study area, including the Agardhfjellet Formation and excavation sites. The black arrow indicates the location of PMO 222.663. Modified from Dallmann et al. (2001) and Hurum et al. (2012). Scale bar equals 1 km.

Valid Referred Species—*Colymbosaurus svalbardensis* (Persson, 1962).

Occurrence—Upper Jurassic; Kimmeridge Clay Formation, Kimmeridgian–early Tithonian, U.K.; Agardhfjellet Formation, Tithonian–early Berriasian, Svalbard, Norway.

Emended Diagnosis—A large cryptoclidid with the following features: mid-cervical vertebrae marginally anteroposteriorly shorter than dorsoventrally tall and lacking a longitudinal ridge on the lateral surface (modified from Benson and Bowdler, 2014); middle caudal centra subrectangular due to a flat ventral surface, with widely spaced chevron facets; propodials with a large posterodistal expansion at least twice as large as the preaxial expansion, bearing a single postaxial ossicle facet of subequal size to the epipodial facets (modified from Benson and Bowdler, 2014); ulna conspicuously anteroposteriorly wider than the radius and proximodistally short; fibula symmetrically pentagonal in outline having equally long pre- and postaxial margins and with facets for the fibulare and astragalus subequal in length.

Referred Material—NHMUK R10062, a partial skeleton including cervical, dorsal, and caudal vertebrae, dorsal ribs, a coracoid, ischium and pubis, and a right humerus and some associated limb elements; OUM J.3300, an incomplete skeleton including a partial right mandible, cervical, dorsal, and caudal vertebrae, partial pectoral girdle, four propodials, and disarticulated limb elements.

Remarks—Specimen NHMUK R10062 has not been previously described in detail but was informally referred to *Colymbosaurus* by Brown (1984), whereas OUM J.3300 is currently undescribed but can be confidently referred here to *Colymbosaurus*.

Specimen NHMUK R10062 is one of the most complete specimens referable to *Colymbosaurus*. The preserved mid-dorsal vertebra exhibits a tall neural canal similar to *Colymbosaurus svalbardensis*. The mid-caudals are pentagonal in anterior view, with widely spaced chevron facets as in *Colymbosaurus*. No anteroposteriorly oriented ridge is visible on the distal articular surface of the humerus, similar to some propodials of *Colymbosaurus megadeirus* (Benson and Bowdler, 2014). For this reason, Benson and Bowdler (2014) referred NHMUK R10062 to Plesiosauroidea incertae sedis. The ilia of NHMUK R10062 are nearly identical to those found in PMO 222.663 in their general morphology. They share a subequal expansion of the dorsal end and are mediolaterally compressed.

Specimen OUM J.3300 is the only *Colymbosaurus* specimen to have cranial material, consisting of a partial right mandible along with several possible cranial fragments and the majority of the postaxial skeleton. It is referred to *Colymbosaurus* on the basis of mid-cervical vertebrae that are marginally anteroposteriorly shorter than dorsoventrally tall and lack a longitudinal ridge on the lateral surface. The specimen shares the morphology of the postaxial expansion of the propodials with *Colymbosaurus*, the ulna is conspicuously anteroposteriorly wider than the radius and proximodistally short, and the fibula is pentagonal with subequally large facets for the astragalus and the fibulare.

COLYMBOSAURUS SVALBARDENSIS (Persson, 1962)
(Figs. 3–11)

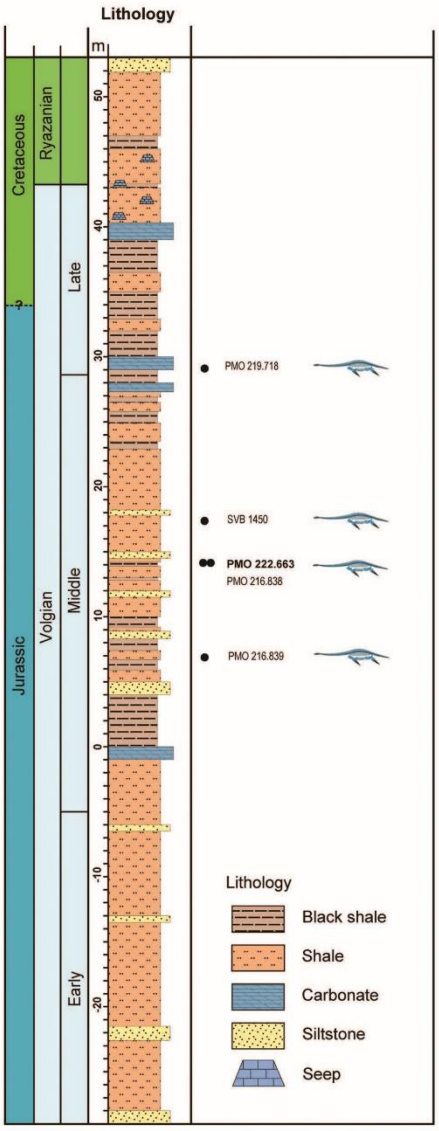

FIGURE 2. The stratigraphic position of PMO 222.663 compared with the referred specimen of *Colymbosaurus svalbardensis* (PMO 216.838) in bold, *Spitrasaurus* (PMO 219.718, SVB 1450), and *Djupedalia* (PMO 216.839). Modified from Delsett et al. (2016).

Holotype—PMO A27745.

Referred Material—PMO 222.663 is an incomplete, partially articulated skeleton preserving 14 dorsal and three sacral vertebrae, a nearly complete caudal series, coracoids, partial interclavicle-clavicle complex, both ilia, four propodials, most of the epipodials, and several more distal limb elements. Other referred material includes PMO 216.838 and PMO 218.377 (Knutsen et al., 2012a).

Emended Diagnosis—A species of *Colymbosaurus* with four sacral vertebrae (three in *C. megadeirus*). Differs from *Colymbosaurus megadeirus* in having proximodistally shorter epipodials in the hind limb (tibia, fibula length/width ratio) (Knutsen et al., 2012a), a dorsoventrally taller neural canal on the mid-dorsal vertebrae (at least twice as tall as wide), a more gracile femoral shaft (PMO 216.838 is excluded here due to preservation), and a posterior margin of the ischium that is abruptly squared-off and relatively broad (Knutsen et al., 2012a).

Diagnostic Remarks on PMO 222.663—This specimen is referred to *Colymbosaurus* on the following basis: (1) the middle caudal centra are subrectangular due to a flat ventral surface, with widely spaced, low chevron facets located ventrolaterally; (2) the propodials possess a large posterodistal expansion at least twice as large as the preaxial expansion and bear a single postaxial ossicle facet of subequal size to the epipodial facets; (3) the ulna is conspicuously anteroposteriorly wider than the radius; and (4) the fibula is symmetrically pentagonal in outline with subequal facets for the fibulare and the intermedium. Specimen PMO 222.663 shares important features with the holotype of *Colymbosaurus svalbardensis* (PMO A27745) and is referred to this taxon on the basis of possessing a neural canal of the middle dorsal vertebrae that is at least twice as tall as wide (maximum internal height/maximum internal width) and relatively short epipodials (tibia length/width ratio).

Occurrence—Upper Jurassic Slottsmøya Member of the Agardhfjellet Formation (upper Tithonian–lower Berriasian). The specimen was found 14 m above the 'yellow layer' marker bed and 13 m below the *Dorsoplanites* marker bed (Delsett et al., 2016); locality coordinates 33X E518470 N8696400.

Taphonomy

Specimen PMO 222.663 consists of a partial axial skeleton with an associated nearly complete appendicular skeleton (Fig. 3). Similar to most of the marine reptile material from the Slottsmøya Member, the specimen has undergone congelifraction (fragmentation due to repeated freeze-thaw cycles) and compaction in certain areas (Delsett et al., 2016). Cranial material, as well as cervical and anterior dorsal vertebrae, is not preserved. In total, 14 partial dorsal vertebrae are preserved, six of which remain in a single articulated series. A total of three compressed sacrals are also present, of which only one preserves an entire neural spine and seven sacral ribs, suggesting the presence of a fourth sacral vertebra. In addition, there are 24 caudal vertebrae, 10 of which are articulated. The majority of these vertebrae are eroded and lack part, if not all, of the neural spine and transverse process. The left pectoral girdle is displaced and lying partially below the right, and is preserved in a more sideritic shale compared with the remainder of the skeleton, resulting in differential compaction of the skeleton in this region. Both femora are preserved, although the left femur is crushed at its proximal end and near the postaxial flange. The right femur has been displaced and shifted 180° relative to the rest of the paddle. The distal limb elements are well preserved and partially articulated in the hind limbs.

Ontogenetic State

Specimen PMO 222.663 is considered an adult on the basis of fused neurocentral sutures throughout the entire preserved portion of the vertebral column, fused caudal ribs, and distinct and

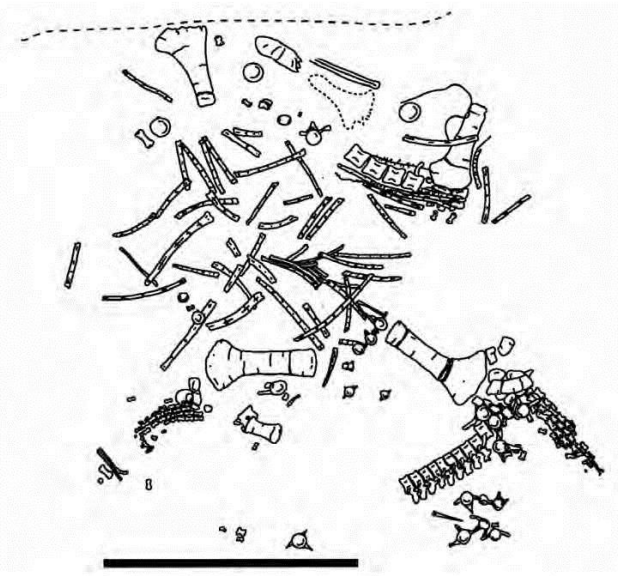

FIGURE 3. Quarry map of PMO 222.663, modified from Delsett et al. (2016). Dashed line indicates erosional slope. Scale bar equals 1 m.

well-formed epipodial facets on the propodials (Brown, 1981). Compared with the syntypes of *Colymbosaurus megadeirus*, PMO 222.663 appears to be slightly smaller based on the size of the vertebrae and propodials (Benson and Bowdler, 2014).

DESCRIPTION AND COMPARISONS

Axial Skeleton

Dorsal Vertebrae—Due to compression of the dorsal vertebrae in PMO 222.663, only certain aspects of the morphology can be described in detail (Fig. 4A–E). The centra are slightly wider than tall in anterior view, similar to *Tatenectes laramiensis* and NHMUK R10062 (*Colymbosaurus* indet.; Brown, 1984; O'Keefe et al., 2011), whereas the centra in *Muraenosaurus leedsii* are more equidimensional (Andrews, 1910; Brown, 1981).

As in *Colymbosaurus svalbardensis*, the neural canal of PMO 222.663 is significantly taller than wide (Fig. 4D, E), although in PMO 222.663 some of this could be attributed to distortion (Knutsen et al., 2012a). This condition differs from the circular neural canal observed in Kimmeridge Clay Formation cryptoclidids (Benson and Bowdler, 2014; A.J.R., pers. observ. of CAMSM J35344 and OUM J.3300). The combined mediolateral width of the zygapophyses is narrower than the centrum, as in *Colymbosaurus megadeirus* (Benson and Bowdler, 2014). Based on the single, undistorted neural arch base, PMO 222.663 lacks an anteroposterior constriction at the base of the neural spine as in all other cryptoclidids (Benson and Druckenmiller, 2014). In the mid-dorsal vertebrae (Fig. 4E), the transverse processes are placed dorsally with respect to the neural canal and gradually shift ventrally in more posterior vertebrae. In anterior view, the transverse processes are inclined at 30–40° with respect to the horizontal plane, as in the holotype of *Colymbosaurus svalbardensis* (Knutsen et al., 2012a). Due to crushing, it is impossible to see if the transverse processes sweep posteriorly in lateral view. The rib facets appear oval and are dorsoventrally taller than anteroposteriorly long, but this could be a taphonomic artifact. The posterior-most dorsal vertebra is more circular than the more anterior vertebrae and has short, rectangular transverse processes in anterior view, but it is still separated from the centrum (Fig. 4C).

Sacral Vertebrae—Three sacral vertebrae are preserved in PMO 222.663 (Fig. 5A–C) and were identified as those vertebrae in which the centrum and neural arch both contribute to the sacral rib facet (Benson and Bowdler, 2014). However, this state can be difficult to determine in well-ossified adults, such as PMO 222.663, where the neurocentral sutures are fused and the centra poorly preserved. Three pairs of sacral ribs were also identified in PMO 222.663, although an additional sacral rib may also be present (see below). Thus, four sacral vertebrae may have been present, but poor preservation and disarticulation in this area makes this difficult to confirm. Four sacrals are present in the holotype of *Colymbosaurus svalbardensis* (PMO A27745) and *Tatenectes laramiensis* (O'Keefe et al., 2011; Knutsen et al., 2012a), whereas three are found in *C. megadeirus* (Benson and Bowdler, 2014).

The order of the sacral vertebrae in PMO 222.663 can be determined by the position of the sacral rib facets, along with other associated vertebrae (O'Keefe et al., 2011). The first sacral was identified by the more dorsal position of the rib facets, compared to the other sacral vertebrae (Fig. 5A). In posterior view, the centrum is mediolaterally wider than dorsoventrally tall. The vertebra interpreted as being the second or third sacral has a more ventrally positioned rib facet than the first (Fig. 5B). The morphology of the sacral rib facets on this vertebra are subcircular rather than dorsoventrally long and anteroposteriorly short, as in the sacrals of one of the syntypes in *Colymbosaurus*

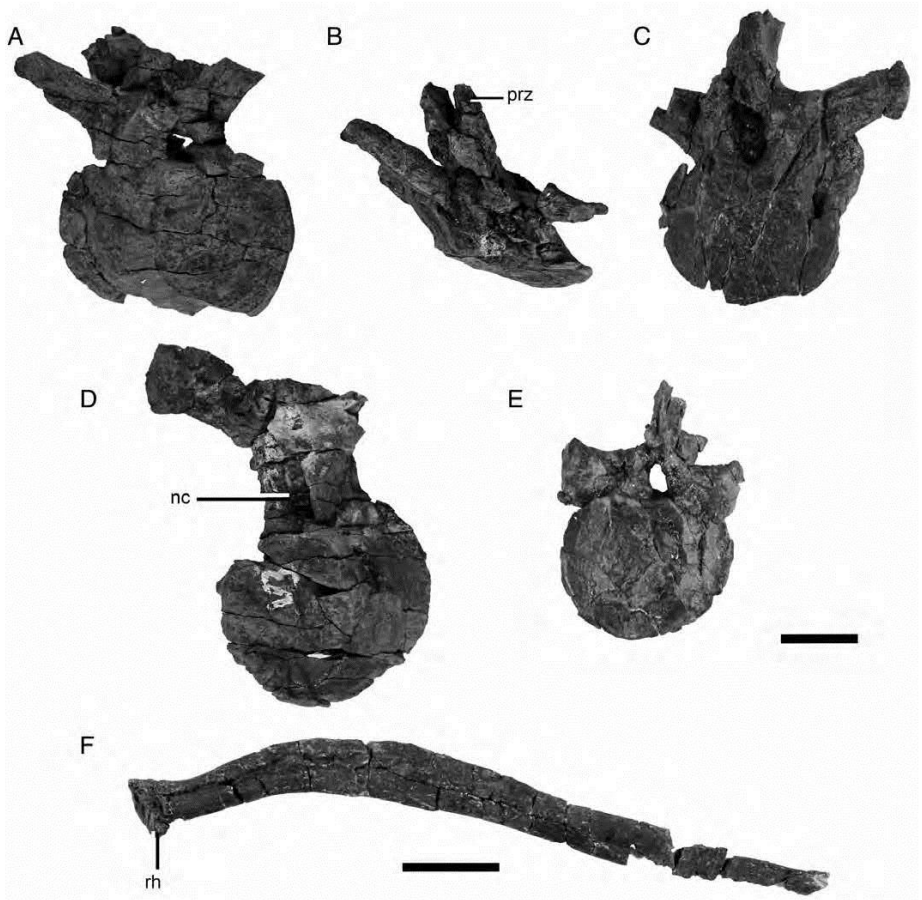

FIGURE 4. Dorsal vertebrae and a partial dorsal rib of PMO 222.663. Mid-dorsal vertebrae in **A**, posterior and **B**, dorsal views; **C**, anterior/mid-dorsal in anterior view; **D**, mid-dorsal in anterior/posterior? view; **E**, posterior-most dorsal in posterior view; **F**, a right dorsal rib in posterior view. **Abbreviations**: **nc**, neural canal; **prz**, prezygapophysis; **rh**, rib head. Scale bars equal 2 cm (**A**–**E**) and 5 cm (**F**).

megadeirus (CAMSM J63919) and NHMUK R10062 (Benson and Bowdler, 2014). The posterior-most sacral is the best preserved of the three and was found in articulation with the first caudal vertebra (Fig. 5C). The neural spine is dorsoventrally shorter and nearly anteroposteriorly as long as the centrum, with a slightly posteroventrally sloping apical margin. As in most cryptoclidids, the sacral neural spines are positioned dorsally from the centrum (O'Keefe et al., 2011). This morphology differs from *Pantosaurus striatus*, where the neural spines are significantly posteriorly inclined (Wilhelm and O'Keefe, 2010). A partial sacral rib was found in articulation with this vertebra (Fig. 5C).

Seven partial to complete sacral ribs are preserved in PMO 222.663. Four are complete, two other proximal rib fragments remain in articulation with the centra, and one is incomplete. The most gracile sacral rib (Fig. 5D) was found adjacent to the second or third sacral vertebra, is straight and trilobate in cross-section proximally, and becomes more oval in cross-section distally. The other sacrals are straight and elongate and exhibit nearly equal expansion of both the proximal and distal ends. The sacral ribs (Fig. 5E–H) are interpreted as two sets, because these were found in close proximity to each other. Each of the sacral ribs preserved in PMO 222.663 is proximodistally extended and exhibits nearly equally expanded proximal and

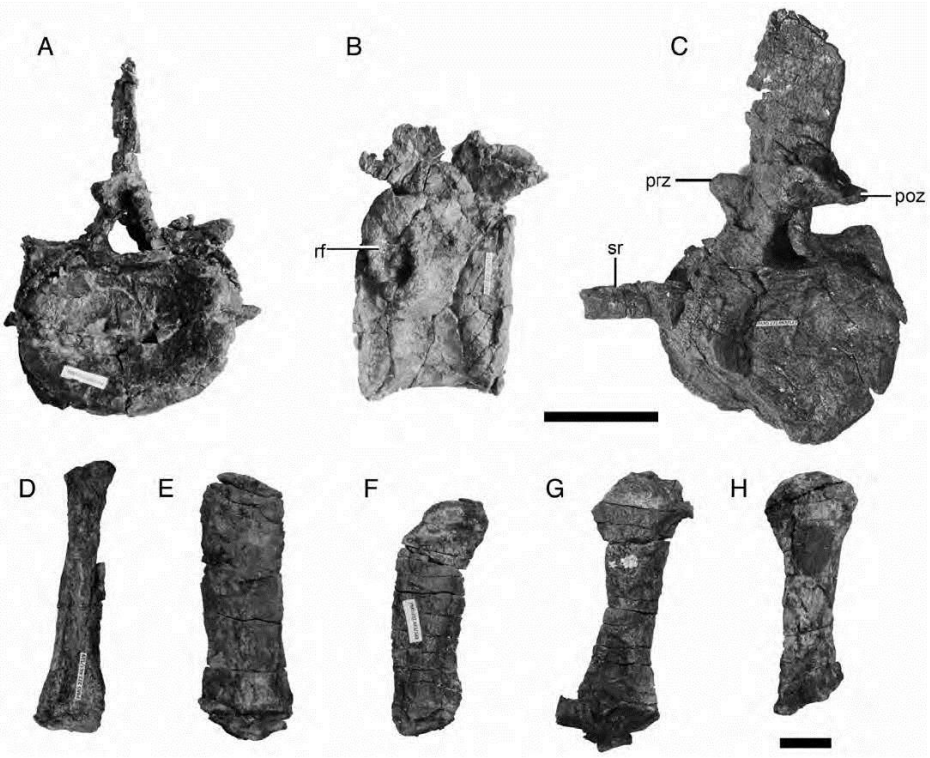

FIGURE 5. Sacral vertebrae and ribs of PMO 222.663. **A**, first sacral vertebra in posterior view; **B**, second or third sacral vertebra in lateral view; **C**, posterior sacral vertebra in posterolateral view; **D**–**H**, sacral ribs. **Abbreviations: poz**, postzygapophysis; **prz**, prezygapophysis; **rf**, rib facet; **sr**, sacral rib. Scale bars equal 5 cm (**A**–**C**) and 2 cm (**D**–**H**).

distal ends. This differs from the spatulate sacral ribs found in *Tatenectes laramiensis* and *Pantosaurus striatus*, which have anteroposteriorly expanded distal ends in dorsal view (Wilhelm and O'Keefe, 2010; O'Keefe et al., 2011). Additionally, PMO 222.663 differs from *Cryptoclidus eurymerus*, in which the proximal end is dorsoventrally thicker than the distal end (Brown, 1981).

Caudal Vertebrae—The 24 caudal vertebrae preserved in PMO 222.663 represent the most complete plesiosauroid tail known from the Slottsmøya Member and consist of an articulated anterior series and several disarticulated mid- and posterior caudals (Fig. 6). In general morphology, the centra are pentagonal and mediolaterally wider than dorsoventrally tall, as in the holotype for *Colymbosaurus svalbardensis* (PMO A27745) and *C. megadeirus* (Knutsen et al., 2012a; Benson and Bowdler, 2014). Paired subcentral foramina are present ventrolaterally. All caudals possess chevron facets, except the first centrum preserved in the series. Similar to the holotype of *C. svalbardensis* (PMO A27745; Knutsen et al., 2012a), the chevron facets are triangular in ventral view, with the apex pointing anteriorly (Fig. 6B), in contrast to oval facets seen in *C. megadeirus* (Benson and Bowdler, 2014). The facets slightly protrude from the ventral surface, but they are recessed in PMU 24781, an historical specimen from the Slottsmøya Member, suggested to resemble *Colymbosaurus* by Kear and Maxwell, (2013). As in both *C. svalbardensis* and *C. megadeirus*, the chevron facets are shared between adjacent vertebrae (Fig. 6E). An anterior ridge on the chevron facet is present in *C. megadeirus* and also NHMUK R10062 (A.J.R., pers. observ.) but is absent in PMO 222.663.

The neural arches on the anterior caudal vertebrae are well preserved (Fig. 6A). These are posteriorly angled, so the posterior margin of the neural spine is dorsal to the anterior third of the succeeding centrum, similar to the holotype specimen of *Colymbosaurus svalbardensis* (PMO A27745; Knutsen et al., 2012a). The neural spine is slightly taller than the dorsoventral height of the centrum (Table 1). On the sixth vertebra in the articulated caudal series, an anteriorly oriented process extends from the pedicel of the neural arch; this structure may be a taphonomic artifact or possibly a pathology (Fig. 6E). This process is fused to the pedicel and appears broken distally (Fig. S1). The

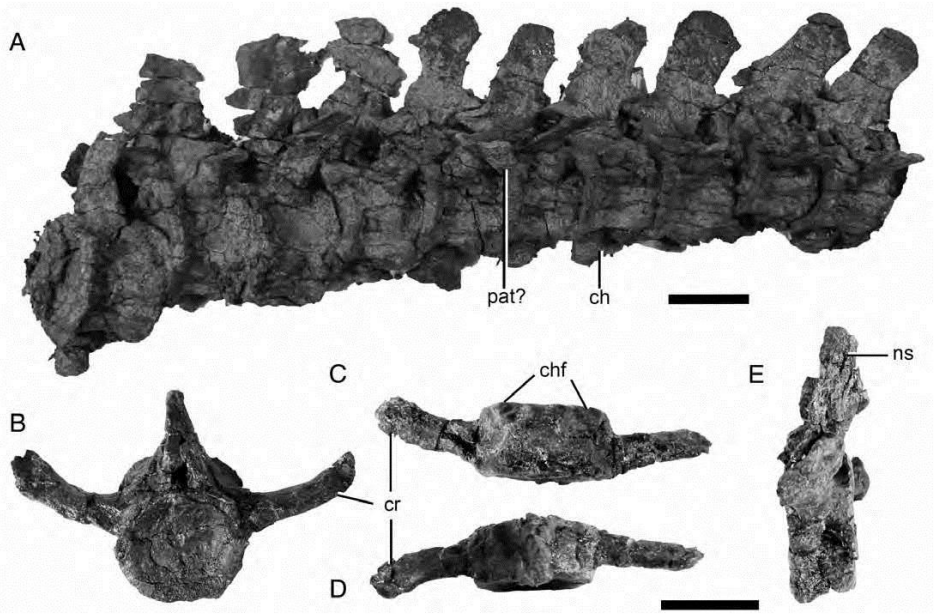

FIGURE 6. Selected caudal vertebrae of PMO 222.663. **A**, the articulated anterior caudal series; mid-caudal vertebra in **B**, anterior, **C**, ventral, and **D**, dorsal views; **E**, mid-caudal in lateral view. **Abbreviations: ch**, chevron; **chf**, chevron facet; **cr**, caudal rib; **ns**, neural spine; **pat?**, pathology? Both scale bars equal 5 cm.

caudal ribs are fused to the centra and are gracile. The ribs terminate in a sharp point, which differs from the spatulate morphology observed in *Cryptoclidus eurymerus* (PETRM R283).

The two posterior-most caudals differ significantly from the rest of the series. The centra are fused via the caudal ribs and part of the neural canal floor (Fig. 7). The posterior-most vertebra is compressed so that the posterior face of the centrum is angled posterodorsally, and the chevrons are fused to the centrum. Unlike the fused posterior caudal vertebrae in *Cryptoclidus eurymerus* NHMUK R8575, those of PMO 222.663 bear caudal ribs, although in the posterior-most vertebra these are significantly reduced. A neural arch is not present, as is often the case in posterior vertebrae (Wilhelm, 2010). This structure may represent a pygostyle-like structure similar to that seen in the posterior caudal series of various plesiosaurians outside Cryptoclididae, such as *Albertonectes* and *Rhomaleosaurus zetlandicus* (Kubo et al., 2012; Smith, 2013). The presence of a fused pygostyle structure in adults has also been suggested to be a synapomorphy of Cryptoclididae (Benson and Druckenmiller, 2014).

The morphological variation throughout the caudal series also provides insight into the possible presence of a tail bend in PMO 222.663. Caudal series are well known from three genera of cryptoclidids: *Cryptoclidus* (e.g., NHMUK R8575), *Muraenosaurus* (e.g., NHMUK R2864), and *Pantosaurus* (USNM 536965; Wilhelm, 2010; Wilhelm and O'Keefe, 2010). The latter has a slight downward bend of the tail starting at the fourth caudal, indicating a tail bend (Wilhelm and O'Keefe, 2010). The presence of a tail bend is difficult to confirm in PMO 222.663 due to the vertebral compression. However, the neural spines angle posteriorly from the mid-caudal vertebrae, resulting in a slight ventral displacement of the vertebrae (Fig. 6E). Following Smith (2013), this morphology could be indicative of a downward tail bend in PMO 222.663.

Dorsal Ribs and Gastralia—Numerous disarticulated dorsal ribs and rib fragments are preserved in PMO 222.663. Five complete or near-complete ribs are preserved, all of which have single-headed proximal ends (although crushed). A single proximal end of an undistorted rib is preserved, bearing an oval facet for articulation with the transverse process (Fig. 4F). The ribs are bilobate in cross-section and gradually become more oval-shaped distally. The most complete and undistorted dorsal rib from PMO 222.663 is likely from the mid-dorsal region and measures approximately 50 cm in total length, lacking the distal-most end. This is slightly longer than those in *Colymbosaurus* indet. (NHMUK R10062; 40–47 cm), which has approximately the same overall body size. The ribs of PMO 222.663 are strongly curved throughout, differing from the weaker curvature observed in NHMUK R10062 (A.J.R., pers. observ.), *Djupedalia engeri*, and *Tatenectes laramiensis* (O'Keefe et al., 2011; Knutsen et al., 2012c).

Several complete gastralia are preserved in PMO 222.663, along with several other probable fragments. These are dorsoventrally curved as in *Cryptoclidus* and *Muraenosaurus* (Andrews, 1910; Brown, 1981) and have grooves along the articulating surfaces of the adjacent gastralia. The majority of these are proximodistally short, curved, and tapering, similar to those

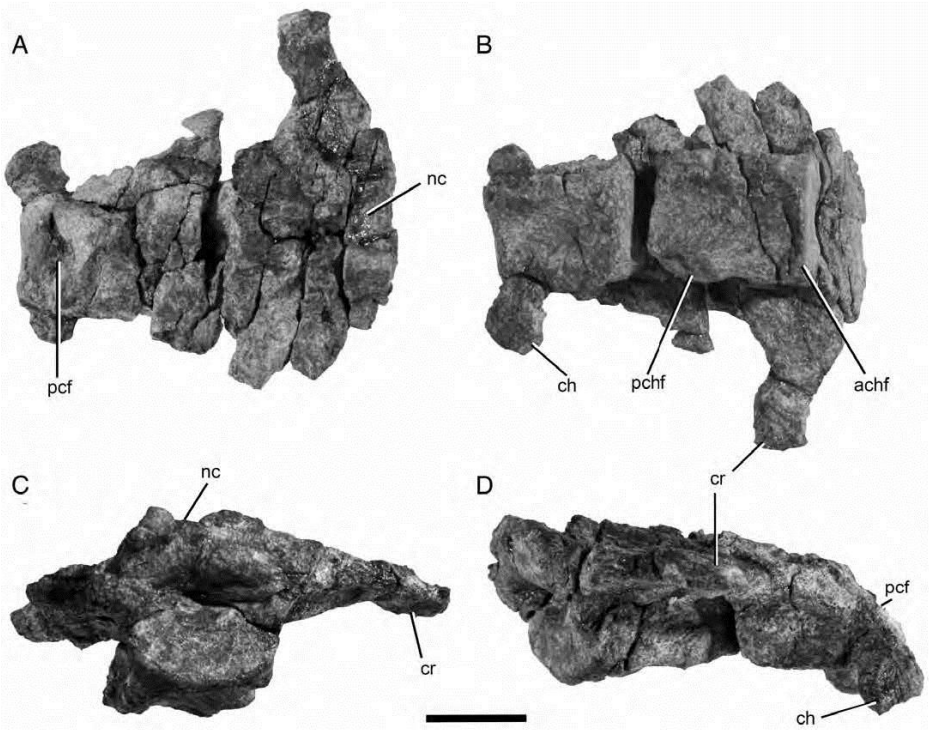

FIGURE 7. Two posterior-most caudal vertebrae of PMO 222.663 in **A**, dorsal, **B**, ventral, **C**, anterior, and **D**, lateral views. **Abbreviations**: **achf**, anterior chevron facet; **ch**, chevron; **cr**, caudal rib; **nc**, neural canal floor; **pcf**, posterior centrum face; **pchf**, posterior chevron facet. Scale bar equals 2 cm.

preserved in other cryptoclidids (Andrews, 1910; O'Keefe et al., 2011). There is no obvious evidence that these are pachyostotic as seen in *Tatenectes laramiensis* (Street and O'Keefe, 2010; O'Keefe et al., 2011).

Appendicular Skeleton

Pectoral Girdle—A partial pectoral girdle is preserved in PMO 222.663. It consists of an incomplete clavicle-interclavicle complex and coracoids (Fig. 8). The fragments interpreted to be the clavicle-interclavicle complex are partially fused, making interpretation difficult (Fig. 8C, D). This complex is rarely preserved in Late Jurassic cryptoclidids, and tentative identifications are based partly on morphology and partly on their proximity to other pectoral elements (Brown, 1981). The nearly complete left clavicle is wing-like, with a smooth ventral surface and a pitted dorsal surface, presumably for articulation with the scapula. The interclavicle is fully fused to the clavicles and appears as a bulge on the visceral surface between the two clavicles. On the left clavicle, the anterior margin is convex and the posterior margin is concave. The medial margin is straight and tapered towards the midline and approaches but does not contact the right clavicle. The lateral margin is more gently rounded than that seen in *Cryptoclidus eurymerus* and *Tricleidus seeleyi* (Andrews, 1909; Brown, 1981). Clavicle-interclavicle complexes are only known from three other Kimmeridgian–Tithonian cryptoclidids and only a single plate-like element is known from the Oxfordian cryptoclidid *Tatenectes laramiensis* (O'Keefe and Street, 2009). In NHMUK R10062 (Brown, 1984), the clavicles differ from those of PMO 222.663 in being triangular and having a foramen perforating one of the elements. The clavicle or interclavicle element preserved in *T. laramiensis* is more square and anteroposteriorly longer in dorsal view than the short and wide element seen in PMO 222.663. However, in the holotype of *Djupedalia engeri* (PMO 216.839), the partial clavicle closely resembles the nearly complete clavicle of PMO 222.663 in being 'wing-like' with a concave anterior margin (Knutsen et al., 2012c).

Portions of the left and right coracoids are preserved and dorsoventrally compressed, obscuring their individual morphology (Fig. 8B). However, they preserve complimentary portions, allowing a more complete reconstruction of their overall shape (Fig. 8A). The element interpreted as the right coracoid, based on its close association with the right humerus, consists of much of the anterior end, including part of the medial symphysis and

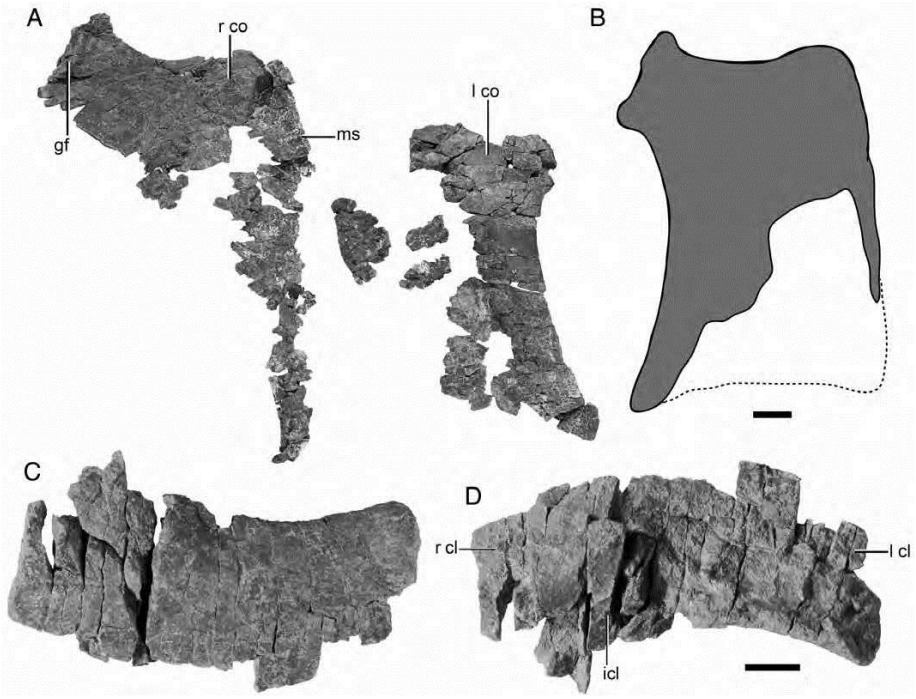

FIGURE 8. The pectoral girdle of PMO 222.663. **A**, the preserved coracoid material reconstructed in approximate life position in ventral view; **B**, reconstructed single coracoid based on the preserved portions of the right and left elements. Clavicle-interclavicle complex in **C**, visceral and **D**, anteroventral views. **Abbreviations**: **gf**, glenoid facet; **icl**, interclavicle; **l cl**, left clavicle; **l co**, left coracoid; **ms**, medial symphysis; **r cl**, right clavicle; **r co**, right coracoid. Scale bars equal 5 cm (**A**, **B**) and 2 cm (**C**, **D**).

glenoid. The left coracoid consists primarily of the lateral margin. There is no clear evidence for the presence of an anteromedial process, but this area is damaged and could have been lost. In anterior view, the region between the glenoid and medial symphysis appears level. The anteroposteriorly oriented platform on the ventral surface of the coracoids observed in other colymbosaurines such as *Colymbosaurus megadeirus* (and possibly *Abyssosaurus*; Benson and Bowdler, 2014) is not present. *Spitrasaurus wensaasi* and *Djupedalia engeri* also lack this trait, although the holotype specimens are not fully mature (Knutsen et al., 2012b, 2012c).

Humerus—The identity and orientation of the humerus is based on the posterior location of the tuberosity relative to the capitulum. The humeri are well preserved but the proximal regions of the right and to some degree the left humerus are dorsoventrally compressed (Fig. 9). The description is largely based on the better preserved left humerus (Fig. 9B–F). In dorsal view, the humeral shaft constricts immediately distal to the proximal head, remains consistently broad for the first one third of the shaft, and then expands distally. Compared with the femur, the humerus is proximally wider, proximodistally shorter, and possesses a more robust shaft (Table 2). In posterior view, the dorsal surface of the humerus is convex along the length of the element and flat to slightly concave along the ventral surface. The postaxial margin of the shaft exhibits coarse rugosities along the majority of its length, with the exception of the postaxial flange. There is a single foramen perforating the left humerus mid-shaft along the postaxial surface that is absent in the right humerus, probably due to deformation in this limb (Fig. 9C). Based on a comparison of the relatively smooth bone surface on the right humerus, in addition to computed tomography (CT) scans of the left taken in this region, the 'swelling' on the left humerus is likely pathological in origin.

The distal articular surface bears three facets for the radius, ulna, and a postaxial ossicle, respectively, the largest being for the ulna. In contrast, there are two epipodial facets in *Muraenosaurus leedsii* and four in *Pantosaurus striatus* (Andrews, 1910; O'Keefe and Wahl, 2003). In dorsal view, the postaxial flange is considerably more developed than the preaxial flange. A reduced preaxial flange is also present in the referred specimen of *Colymbosaurus* (NHMUK R31787), although the postaxial flange is missing (Benson and Bowdler, 2014). In OUM J.3300 (*Colymbosaurus* indet.), the distal margin is similar to that seen in PMO 222.663 in having a reduced preaxial flange and an enlarged postaxial flange. The greatly expanded postaxial

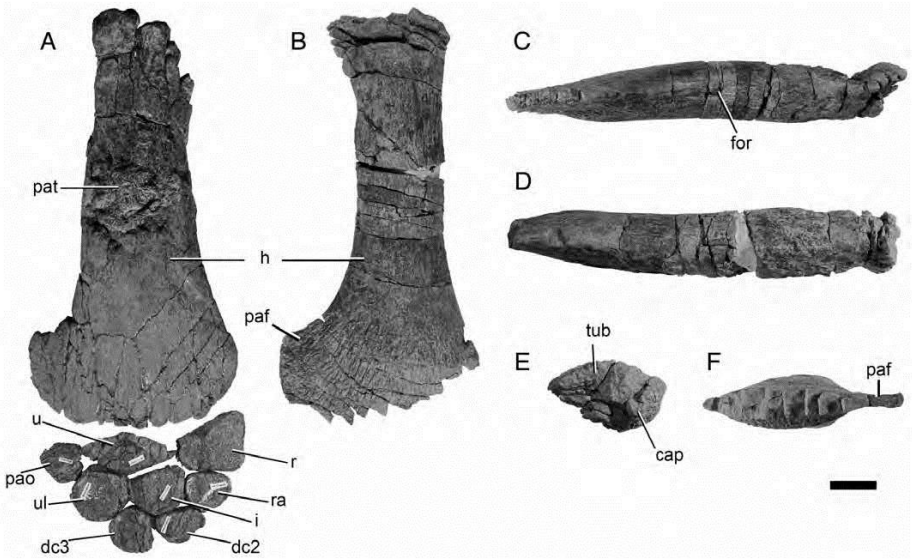

FIGURE 9. Humeri and proximal forelimb elements of PMO 222.663. **A**, right humerus and proximal forelimb elements articulated as found, in dorsal view. Left humerus in **B**, ventral, **C**, anterior, and **D**, posterior views. **E**, proximal and **F**, distal ends of the left humerus. **Abbreviations**: **cap**, capitulum; **dc2**, second distal carpal; **dc3**, third distal carpal; **for**, foramen; **h**, humerus; **i**, intermedium; **paf**, postaxial flange; **pao**, postaxial ossicle; **pat**, pathology; **r**, radius; **ra**, radiale; **tub**, tuberosity; **u**, ulna; **ul**, ulnare. Scale bar equals 5 cm.

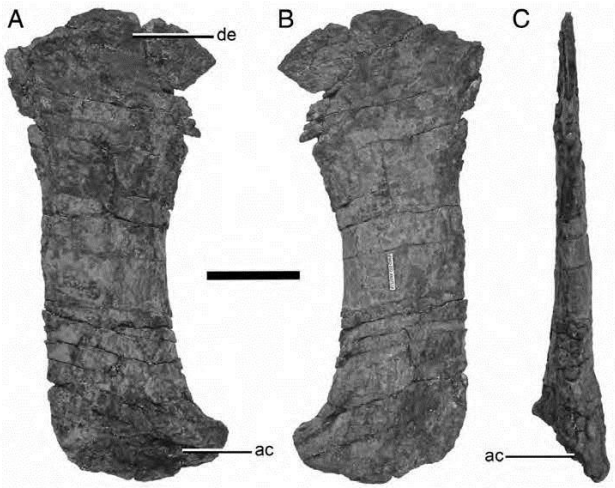

FIGURE 10. Left ilium of PMO 222.663 in **A**, medial, **B**, lateral, and **C**, posterior views. **Abbreviations**: **ac**, acetabular facet; **de**, distal expansion. Scale bar equals 5 cm.

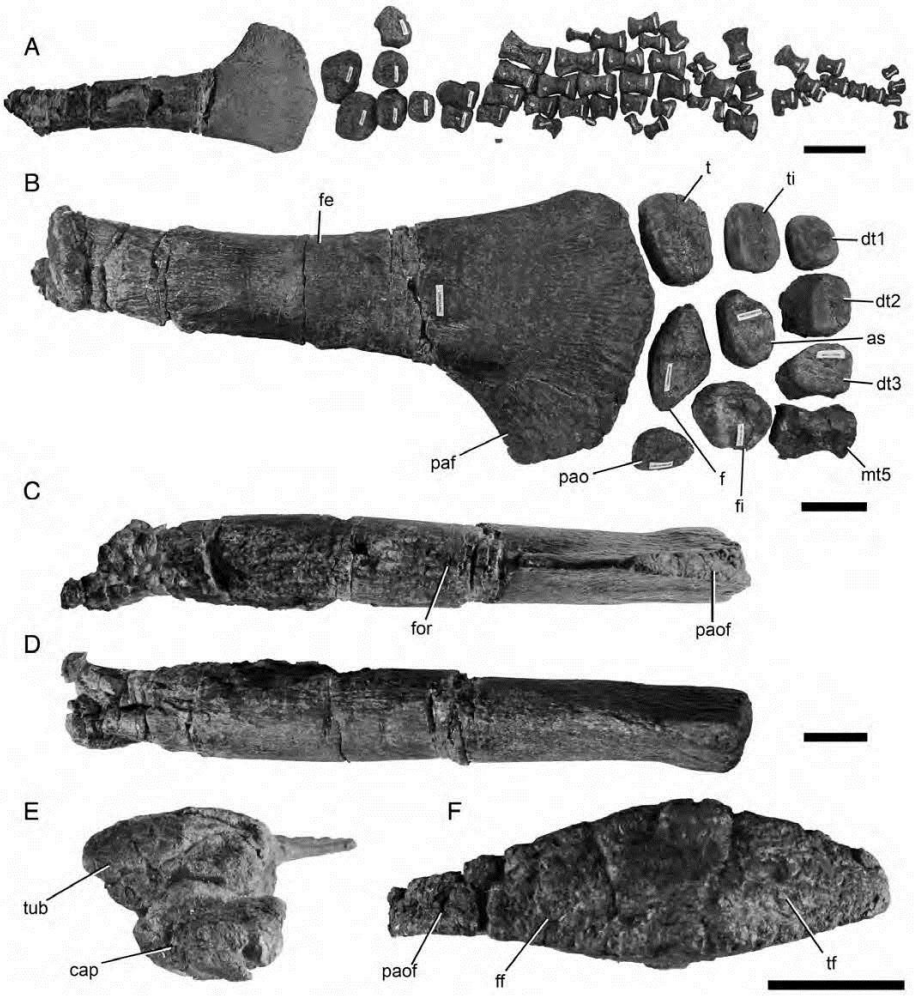

FIGURE 11. Right hind limb of PMO 222.663. **A**, right paddle as preserved in ventral view; **B**, right femur, epipodials, tarsals, and metatarsal IV in dorsal view (reconstructed). Right femur in **C**, posterior, **D**, anterior, **E**, proximal, and **F**, distal views. The identification and position of elements in **B** is based on the more complete paddles of the holotype specimen of *C. svalbardensis* (PMO A27745). **Abbreviations**: **as**, astragalus; **cap**, capitulum; **dt1**, first distal tarsal; **dt2**, second distal tarsal; **dt3**, third distal tarsal; **dt4**, fourth distal tarsal; **f**, fibula; **fe**, femur; **ff**, fibula facet; **fi**, fibulare; **for**, foramen; **mt5**, fifth metatarsal; **paf**, postaxial flange; **pao**, postaxial ossicle; **paof**, postaxial ossicle facet; **t**, tibia; **tf**, tibia facet; **ti**, tibiale; **tub**, tuberosity. Scale bars equal 10 cm (**A**) and 5 cm (**B**–**F**).

morphology seen in PMO 222.663 differs from that seen in Callovian cryptoclidids where the pre- and postaxial flanges are significantly expanded (Andrews, 1910; Brown, 1981). *Spitrasaurus larseni* and *Djupedalia engeri* are also subequally expanded, although this could be due to their younger ontogenetic state (Knutsen et al., 2012b, 2012c).

The right humerus of PMO 222.663 preserves the complete distal edge. It lacks an anteroposteriorly oriented bisecting ridge

TABLE 1. Selected axial skeleton measurements (in cm) for PMO 222.663.

Dorsal vertebrae	DV Height (centrum)	AP Length	ML Width (centrum)	NS Height
Mid-dorsal	7	6	9.2	x
Posterior-most dorsal	7.6	*3.2	9.2	1.9
Sacral vertebrae				
Anterior-most Sacral	6.7	*3.5	9.1	4.9
2/3rd Sacral	*7.4	*5.9	x	x
Posterior-most Sacral	7.1	x	8.0	7.1
Caudal vertebrae				
Anterior-most Caudal	7.0	*2.9	8.7	7.3
Mid-caudal	5.4	x	6.3	5.9
Posterior caudal	2.8	*3.0	3.0	x

*indicates that the number is an estimation (due to compression), and 'x' indicates missing data. **Abbreviations**: **AP**, anterior-posterior; **DV**, dorsal-ventral; **ML**, medial-lateral; **NS**, neural spine.

on the distal epipodial facets, previously considered as a diagnostic character for *Colymbosaurus* (Benson and Bowdler, 2014). The distal end of the right humerus is partially fused with the ulna; however, a groove is absent on the proximal articular surface of the right radius, suggesting that the corresponding ridge on the humerus is absent (Benson and Bowdler, 2014). As in other specimens of *Colymbosaurus*, the ulnar facet of PMO 222.663 is anteroposteriorly longer than the radius, similar to *C. megadeirus* (Benson and Bowdler, 2014). The long ulnar facet preserved in *C. megadeirus* and *C. svalbardensis* differs from other cryptoclidids such as *Pantosaurus striatus, Cryptoclidus eurymerus*, and *Muraenosaurus leedsii*, in which the radial facet is relatively longer (O'Keefe and Wahl, 2003).

Epipodials and Mesopodials—There are three elements in the epipodial row, the radius, the ulna, and a postaxial accessory ossicle, which were preserved in articulation with the right humerus (Fig. 9A). An epipodial foramen (spatium interosseum) is absent in PMO 222.663, unlike Oxford Clay Formation cryptoclidids where an epipodial foramen is present between the radius and the ulna (Andrews, 1910). The radius is trapezoidal in dorsal view, being proximodistally shorter along the posterior margin and in proximal view evenly thick dorsoventrally. The radius is slightly longer than the ulna proximodistally, but approximately 25% shorter anteroposteriorly (Table 2). This morphology is similar to that seen in OUM J.3300 (*Colymbosaurus* indet.) but differs from *Spitrasaurus wensaasi, Djupedalia engeri*, and *Pantosaurus striatus* where, in dorsal view, the radius is twice or more the size of the ulna in volume (O'Keefe and Wahl, 2003; Knutsen et al., 2012b, 2012c). Alternatively, in *Muraenosaurus leedsii* and *Cryptoclidus eurymerus*, the radius is proximodistally longer than the ulna, but nearly identical in anteroposterior width (Brown, 1981). The ulna of PMO 222.663 is anteroposteriorly wider than proximodistally long in dorsal view and has a diamond shape. Specimen OUM J.3300 exhibits a similarly anteroposteriorly elongate ulna, although it is not as pointed as in PMO 222.663. These proportions differ from the proximodistally long ulna of *Pantosaurus striatus* and *Tatenectes laramiensis* (O'Keefe and Wahl, 2003; O'Keefe and Street, 2009). The ulnae in *D. engeri* and *S. larseni* are too poorly ossified for comparison (Knutsen et al., 2012b, 2012c).

TABLE 2. Selected measurements (in cm) of the appendicular elements of PMO 222.663.

Element	PD length	Proximal AP width	Distal AP width	Min. shaft AP width
Left humerus	41	11.5	*20.1	8.3
Right humerus	43.7	11.5	22.2	9.5
Left femur	44.2	10.5	*16.2	6.8
Right femur	45	*5.7	19.9	*5.7
	Max. AP length	Max. PD length	Min. PD length	DV proximal thickness
Right humerus elements				
Radius	8.1	6.1	2.5	2.1
Ulna	9.9	4.9	0	x
Post ax. os.	4.5	4.3	x	x
Right femur elements				
Tibia	7.1	5.1	3.9	3.1
Fibular	8.1	5.5	x	3.6
Post ax. os.	3.8	*4.8	x	2.2
Left femur elements				
Tibia	7.6	5.3	x	3.1
Fibular	3.1	5.2	x	2.9
Post ax. os.	3.9	4.9	x	x

*indicates that the number is an estimation (due to compression), and 'x' indicates missing data. **Abbreviations**: **AP**, anterior-posterior, **DV**, dorsal-ventral; **PD**, proximal-distal.

A postaxial ossicle is preserved in articulation with the humerus and other epipodials in PMO 222.663. This element was positioned directly posterior to the ulna and articulated to the ulnare, giving the element a more distal position than expected for this element. A partial postaxial ossicle is also preserved in *Abyssosaurus nataliae* and resembles the triangular morphology seen in PMO 222.663 (Berezin, 2011). Although a facet for a postaxial ossicle is present in the forelimb of *Pantosaurus striatus* and *Tatenectes laramiensis*, the element is not preserved in the holotypes or referred specimens (O'Keefe and Wahl, 2003; O'Keefe and Street, 2009). A limb element sharing the same morphology as the postaxial ossicle in PMO 222.663 is preserved in OUM J.3300; however, it is not in articulation and whether this postaxial ossicle is from the forelimb or the hind limb cannot be determined.

There are three elements in the proximal mesopodial row: the radiale, intermedium, and ulnare. The radiale is rounded in dorsal view, and is the smallest of the three. It has four facets: for the radius, the intermedium, and first and second carpals. The intermedium and the ulnare are fused, a feature that has been observed in other adult cryptoclidids (Caldwell, 1997). Given that these elements are dorsoventrally compressed, the fusion could possibly also be taphonomic. The intermedium has six facets: for the radius, the radiale, the ulna, the ulnare, and the second and third carpals. The ulnare has five facets: for the intermedium, the ulna, a postaxial accessory ossicle, the third carpal, and the fifth metacarpal. In the distal mesopodial row, the second and third carpals were identified in articulation with the right paddle. Other fragmentary disarticulated metapodial and phalangeal elements were preserved in association with both forelimbs. There is no evidence for a preaxial row as seen in *Spitrasaurus* (Knutsen et al., 2012b).

Pelvic Girdle

Ilium—Both ilia are preserved in PMO 222.663 and were found in the vicinity of their respective limbs (Fig. 10). Other elements of the pelvic girdle were not preserved. The ilia have undergone mediolateral compression, particularly the right ilium. However, because the ilia of PMO 222.663 are compressed, and are incomplete in the holotype specimen of *Colymbosaurus svalbardensis* (PMO A27745), detailed comparative remarks are not possible. In lateral view, the dorsal expansion is only slightly anteroposteriorly wider than the acetabular end, similar to isolated ilia and more complete specimens from the Kimmeridge Clay Formation (e.g., NHMUK R10062, OUM J.3300, CAMSM J29896, and CAMSM J29897). In lateral view, the dorsal margin has subequal anterior and posterior expansions. This differs somewhat from the asymmetrically shaped dorsal portion of the ilium preserved in the holotype of *C. svalbardensis* (PMO A27745), and the more rounded dorsal end of

Tatenectes laramiensis and *Pantosaurus striatus* (Wilhelm and O'Keefe, 2010; O'Keefe et al., 2011; Knutsen et al., 2012a). The anterior margin is concave and displays more of the acetabular facet in medial view, as in the majority of cryptoclidids (Andrews, 1910; A.J.R., pers. observ. of NHMUK R7428). The anterior margin differs somewhat in the holotype of *C. svalbardensis*, where the preserved acetabular end and shaft are straight. A midshaft tubercule is absent in PMO 222.663, similar to other specimens *C. svalbardensis* (Knutsen et al., 2012a), but differing from numerous penecontemporaneous specimens from the Kimmeridge Clay Formation (CAMSM J29896, CAMSM J29897) as well as PMU 24781 from the Slottsmøya Member (Kear and Maxwell, 2013), that possess this feature. The torsion of the shaft seen in *Cryptoclidus eurymerus*, *T. laramiensis*, and *M. leedsii* could not be observed in PMO 222.663 due to crushing (Andrews, 1910; Brown, 1981; O'Keefe et al., 2011).

Femora—Both hind limbs are well preserved, and the majority of the preserved elements are articulated (Fig. 11). In proximal view, the trochanter is situated directly dorsal to the capitulum. As in PMO A27745 (*Colymbosaurus svalbardensis*), the femur of PMO 222.663 retains the same anteroposterior width until approximately midway along the shaft, where it begins to expand (Knutsen et al., 2012a; Table 2). The femoral shaft of PMO 222.663 does not constrict immediately distal to the capitulum (possibly a taphonomic artifact), although there is a slight constriction in the holotype specimen of *C. svalbardensis* (Knutsen et al., 2012a). This differs from *C. megadeirus* and *Muraenosaurus leedsii*, where a clear constriction is present (Andrews, 1910; Brown, 1981; Benson and Bowdler, 2014).

The distal end of the femur bears three distinct facets: for the tibia, the fibula, and a postaxial ossicle. This differs from PMU 24781, which bears additional single pre- and postaxial facets, and *'Plesiosaurus' manselii*, which has two postaxial facets (Hulke, 1870). The tibial and fibular facets are clearly demarcated and pitted and are subequal in anteroposterior length, as in *Abyssosaurus nataliae* (Berezin, 2011), but unlike the larger tibial facet seen in PMU 24781 and in the other referred specimens of *Colymbosaurus svalbardensis* (Knutsen et al., 2012a; Kear and Maxwell, 2013). As in all material referred to *C. svalbardensis* and PMU 24781, an anteroposteriorly oriented ridge bisecting the distal femoral facets is absent in PMO 222.663, unlike some specimens of *C. megadeirus* (Knutsen et al., 2012a; Benson and Bowdler, 2014). Distally, the femur has a well-developed straight-edged postaxial flange, which is angled more posterodistally than in the humeri. The postaxial flange has a relatively shorter postaxial facet than in the humerus.

Epipodials and Mesopodials—There are a total of three elements in the epipodial row, the tibia, the fibula, and a single postaxial ossicle, as in *Colymbosaurus svalbardensis, C. megadeirus, Djupedalia engeri*, and *Spitrasaurus* (Knutsen et al., 2012a, 2012b, 2012c; Benson and Bowdler, 2014), but unlike the two observed in *Cryptoclidus eurymerus, Muraenosaurus leedsii*, and *Tatenectes laramiensis* (Andrews, 1910; Brown, 1981; O'Keefe and Street, 2009). A preaxial epipodial element is not present in either hind limb. The tibia and fibula are nearly equidimensional and are both anteroposteriorly wider than proximodistally long (Table 2). The tibia is suboval in dorsal view, with four facets: for the femur, the fibula, the astragalus, and the tibiale, the largest of which is for the femur. Unlike the well-demarcated astragalar facet of the tibia in both species of *Colymbosaurus*, the astragalar facet of PMO 222.663 is diminutive on the right and indistinguishable from the facet for the tibiale on the left (Knutsen et al., 2012a; Benson and Bowdler, 2014). The fibula is triangular in dorsal view and bears five facets: the longest for the femur, two short facets for the tibia and the postaxial ossicle, respectively, and two subequal facets for the astragalus and the fibulare. The postaxial ossicle is triangular and is similar to that seen in the forelimb (Fig. 11B). This element was removed during excavation of the right hind limb but is preserved articulated on the left. Only an external mold of the postaxial ossicle is known in NHMUK R40640 (*Colymbosaurus* indet.; Brown, 1981; Knutsen et al., 2012a), where it has three subequally sized facets for the femur, the fibula, and the fibulare. Previously, the postaxial ossicle of *C. svalbardensis* was known from the hind limbs of the additional referred specimens, but not the holotype (PMO A27745; Knutsen et al., 2012a). The postaxial ossicle of PMO 222.663 is identical to that in other referred specimens of *C. svalbardensis* (PMO 218.377, PMO 216.838), being triangular and bearing two facets, with the smallest for the fibula.

Three proximal mesopodial elements are preserved; the fibulare is the largest, whereas the somewhat smaller astragalus and tibiale are similar in size, consistent with other specimens of *Colymbosaurus svalbardensis* (Knutsen et al., 2012a). The fibulare and the tibiale are suboval in outline, being anteroposteriorly wider than proximodistally long. The fibulare in *C. svalbardensis* is distinct in being anteroposteriorly broader and bearing two offset distal facets, whereas *C. megadeirus* has a single distal facet for the fifth metatarsal (Knutsen et al., 2012a; Benson and Bowdler, 2014). The first distal tarsal appears similar to other cryptoclidids, being small and bearing three facets. Based on the proximal position of the fifth metatarsal in PMO 222.663, it is possible that this element is shifted entirely into the mesopodial row, as in *Djupedalia engeri* and *C. svalbardensis* (Knutsen et al., 2012a, 2012c).

Metapodials and Phalanges—Five digits are preserved in the hind limb of PMO 222.663. The proximal edges of the metapodials of the hind limb are more convex in dorsal view compared with those in the forelimb. The phalanges are robust with flat articular surfaces, which in dorsal view become more convex distally throughout the hind limb. The distal-most elements are oval to lunate in dorsal view. The longest digit (the third) has a minimum of 11 articulated phalanges and a large number of disarticulated smaller ones distal to the articulated series (Fig. 11A).

DISCUSSION

Phylogenetic Analysis

A modified version of the data matrix of Benson and Druckenmiller (2014) (also used by Benson and Bowdler, 2014) was used in this analysis (Supplementary Data 2, 3). First, we attempted to replicate the results of the original analysis (Benson and Druckenmiller, 2014), which was conducted in PAUP* (Swofford, 2003), using TNT (version 1.1) (Goloboff et al., 2008). The matrix was built in Mesquite (version 3.10; Maddison and Maddison, 2016). In order to most closely replicate the original search algorithm run in PAUP*, a New Technology Search was performed in TNT using a combination of both ratchet and tree bisection reconnection (TBR; see Supplementary Data 1 for specific settings). All characters are unordered and equally weighted, and the same wildcard taxa were removed as in Benson and Druckenmiller (2014). *Yunguisaurus* was defined as the outgroup taxon (Cheng et al., 2006). The search resulted in fewer most parsimonious trees (MPTs; 2016) than in the original analysis, but with the same number of steps (1289) and the strict consensus recovered the same topology (consistency index [CI] = 0.304; retention index [RI] = 0.661).

To the Benson and Druckenmiller (2014) matrix were added the scores for two new operational taxonomic units (OTUs), *Colymbosaurus svalbardensis*, based solely on the holotype specimen, and PMO 222.663. Additionally, a small number of scores for other cryptoclidid taxa were modified (Supplementary Data 2; score changes detailed in Supplementary Data 1). A second matrix was also prepared that combined the scores for *C. svalbardensis* and PMO 222.663 as a single OTU (Supplementary Data 3). Bremer support and a bootstrap percentages were

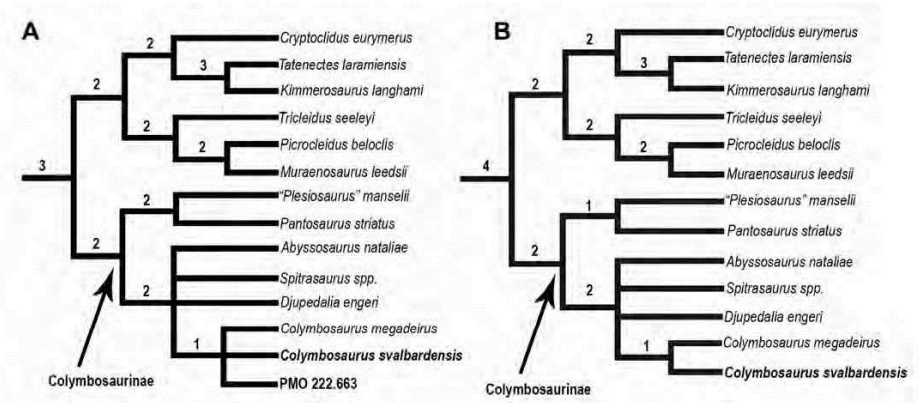

FIGURE 12. The results of the phylogenetic analysis of Cryptoclididae. **A**, strict consensus of 576 MPTs with PMO 222.663 and *Colymbosaurus svalbardensis* scored as separate OTUs (CI = 0.304, RI = 0.661); **B**, strict consensus of 576 MPTs, with a composite scoring of PMO 222.663 and *Colymbosaurus svalbardensis* (CI = 0.303, RI = 0.663). Bremer support values are given above the internodes.

calculated in TNT. Bremer support values are presented in Figure 12; however, bootstrap values for all nodes within Cryptoclididae were less than 50% and are not shown.

The analysis of the first matrix yielded 576 MTPs with 1290 steps. The strict consensus tree recovered PMO 222.663, *Colymbosaurus svalbardensis*, and *C. megadeirus* in a polytomy and as the sister taxon to (*Spitrasaurus* spp. + *Djupedalia* + *Abyssosaurus*) within Colymbosaurinae (Fig. 12A). The analysis of the second matrix yielded 576 MPTs, with 1289 steps and the strict consensus tree recovered the same topology, with *C. svalbardensis* (composite scoring) and *C. megadeirus* as sister taxa (Fig. 12B). The topology for the other cryptoclidids was identical to that presented in Benson and Bowdler (2014).

Diagnostic Characters of *Colymbosaurus*

Multiple Kimmeridge Clay Formation specimens that have been or possibly are referable to *Colymbosaurus* exhibit a large amount of variation in several aspects of their morphology. This variation must be taken into account when reevaluating diagnostic features of the genus.

Characters relating to the length to height ratio and the lack of a lateral ridge on the cervical vertebrae (characters 153 and 154, respectively; Benson and Druckenmiller, 2014) have been studied in *Colymbosaurus megadeirus* (Benson and Bowdler, 2014) but are currently unknown in *C. svalbardensis* (including PMO 222.663). With regards to cervical length to height dimensions, there is a greater degree of intraspecific variation in this character than was previously recognized, particularly regarding which region of the cervical series is measured. In NHMUK R10062, the preserved anterior and posterior cervical vertebrae have a length to height ratio <0.7, but the ratio increases slightly in the mid-cervical vertebra. In OUM J.3300 and the syntype CAMSM J.29596–29691, J.59736–J.59743 (referred to by Benson and Bowdler, 2014 as CAMSM J.29596ect.), this ratio is close to 1.0 in the anterior cervicals, and this value steadily decreases to 0.8 in the mid-cervical vertebrae. This illustrates that more consistent results are found when measurements are limited to the mid-cervical series where there is less variation among specimens referred to *Colymbosaurus*.

One of the most variable features of the genus relates to the morphology of the postaxial flange of the propodials (Fig. 13), defined in the diagnosis of Benson and Bowdler (2014:1054) as "propodials with a large posterodistal expansion bearing a postaxial ossicle facet of subequal size to the epipodial facets." Most other colymbosaurines, including *Abyssosaurus nataliae, Spitrasaurus wensaasi, S. larseni, Djupedalia engeri*, and '*Plesiosaurus*' *manselii*, also possess a postaxial flange (Hulke, 1870; Berezin, 2011; Knutsen et al., 2012a, 2012b, 2012c). Thus, to help further distinguish *Colymbosaurus* from penecontemporaneous taxa, we have modified the diagnosis to denote 'an extended postaxial flange, which is significantly larger than the preaxial flange, bearing a single postaxial ossicle facet of subequal size to the epipodial facets.' Further, the specification of a single postaxial ossicle facet distinguishes *Colymbosaurus* from the taxonomically problematic material of '*P.*' *manselii* (NHMUK PV OR40106), which also has a large postaxial flange but bears discrete facets for two postaxial accessory ossicles on the humerus (Hulke, 1870).

The presence of an anteroposteriorly oriented ridge bisecting the distal articulating facets of the propodials has also been used as a diagnostic character of *Colymbosaurus* (Brown, 1981; Benson and Bowdler, 2014). An anteroposteriorly bisecting ridge on the distal end of the propodials is observed on the propodials of numerous specimens of *Colymbosaurus*, including *C. 'richardsoni'* (NHMUK R1682) and *Colymbosaurus* indet. (OUM J.3300 and NHMUK R31787; Benson and Bowdler, 2014). However, the bisecting ridge shows varying degrees of anteroposterior exposure on other '*Colymbosaurus*-like' propodials from the Kimmeridge Clay Formation, including some that appear to lack the ridge altogether. Eighteen propodials (isolated and associated) from the Kimmeridge Clay Formation that have been either referred to *Colymbosaurus* or otherwise resemble *Colymbosaurus* on the basis of overall propodial morphology or associated material were examined in the course of this study. The left humerus and right femur of PMO 222.663, left femur of PMO 216.838, and the right femur of PMO A27745 were also included for comparison. Of the 22 propodials examined, nine had a well-defined anteroposteriorly oriented ridge present on both epipodial facets, four had a ridge on one of the epipodial facets,

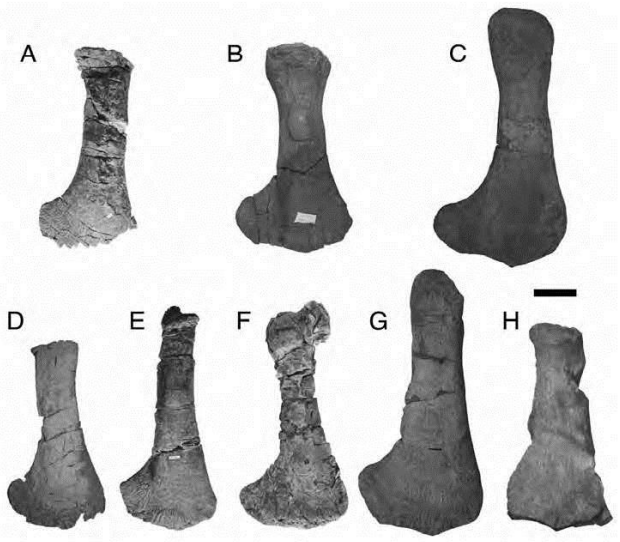

FIGURE 13. Humeri (upper row) and femora (bottom row) of referred specimens of *Colymbosaurus*. **A**, left humerus (reversed) of PMO 222.663 (*C. svalbardensis*); **B**, right humerus of NHMUK 10062 (*Colymbosaurus* indet.; photo used with permission); **C**, right humerus of OUM J.3300 (*Colymbosaurus* indet.); **D**, right femur of PMO A27745 (holotype of *C. svalbardensis*); **E**, right femur of PMO 222.663 (*C. svalbardensis*); **F**, left femur of PMO 216.839 (*C. svalbardensis*) **G**, right femur of OUM J.3300 (*Colymbosaurus indet.*); **H**, right femur of CAMSM H29654 (*C. megadeirus*). Scale bar equals 10 cm.

and nine lacked the ridge altogether (Table S1). Additionally, MANCH LL.5513–14, which preserves both femora, has a recognizable ridge on the left femur, but not on the right.

After reexamination of PMO 218.377, one of the referred specimens of *Colymbosaurus svalbardensis* (Benson and Bowdler, 2014;fig. 10A), the presence of an anteroposteriorly oriented bisecting ridge on the distal humeral facets is equivocal. This ridge is also clearly absent in all other propodials of specimens referable to *C. svalbardensis*, including PMO 222.663. The potential utility of this feature also needs to be judged in the light of other factors, including taphonomic compression (CAMSM J29739, NHMUK R6317) and ontogenetic and/or individual variation (MANCH LL.5513–14). A similar feature has also been observed in other uncompressed cryptoclidid propodials from the Oxford Clay Formation (CAMSM J67072, GLAHM V1807, MANCH LL.14975, LEICS 413.1956/40, NOTNH FS5879) and a non-cryptoclidid propodial from the Kimmeridge Clay Formation (OUM J.13837). These observations suggest that the presence of an anteroposteriorly oriented bisecting ridge may prove valuable in a broader evolutionary context. Given that this character is eqivocal on the holotype of *C. svalbardensis* (PMO A27745), is absent on two of the referred specimens of this species (PMO 222.663, PMO 216.838), and is variable in extent and presence in Kimmeridge Clay Formation specimens of *Colymbosaurus*, we do not consider this to be a reliable diagnostic character for the genus. However, it is possible that the presence of this feature could be diagnostic at a less inclusive taxonomic level, possibly for *C. megadeirus*.

Based on a broad examination of material from both the U.K. and Svalbard, we provide new diagnostic features for *Colymbosaurus* relating to the morphology of the mid-caudal vertebrae and the ulna and fibula.

As described above, the middle caudal centra of *Colymbosaurus* are subrectangular due to the presence of a flat ventral surface with widely spaced, low chevron facets located ventrolaterally (Benson and Druckenmiller, 2014). The middle caudal centra of *Colymbosaurus* are distinctive among cryptoclidids in that their chevron facets project slightly from the ventral surface and are not positioned in a deep groove (PMU 24781) or are not significantly venterolaterally projecting (e.g., *Cryptoclidus eurymerus*; Andrews, 1910; Kear and Maxwell, 2013). The mid-caudal centra of *Colymbosaurus* also have a flat ventral margin in anterior view, compared with the more rounded morphology in *Cryptoclidus eurymerus, Muraenosaurus leedsii*, and *Pantosaurus striatus* (Andrews, 1910; Wilhelm and O'Keefe, 2010).

In referred specimens of *Colymbosaurus* where an ulna is present (PMO 222.663, OUM J.3300), the element is conspicuously anteroposteriorly wider than the radius, and proximodistally short. This differs from the ulna in *Muraenosaurus leedsii* and *Pantosaurus striatus*, where this element is significantly anteroposteriorly shorter than the radius, and from '*Plesiosaurus*' *manselii*, where the ulna and the radius are subequal in length (Hulke, 1870; Andrews, 1910; O'Keefe and Wahl, 2003).

A unique morphology of the fibula is also observed in *Colymbosaurus megadeirus* (CAMSM J29654–91, CAMSM J59736–43), *Colymbosaurus* indet. (OUM J.3300), and *C. svalbardensis* (PMO A27745, PMO 216.383, PMO 218.377, PMO 222.663), in which this element is pentagonal to nearly triangular, with symmetrical preaxial and postaxial margins. The fibula lacks a spatium osseum and has subequal facets for the fibulare and the intermedium, differentiating *Colymbosaurus* from all other cryptoclidids. This particular morphology is noted in Knutsen et al. (2012a) as one of the characters justifying the referral of the *C. svalbardensis* material to *Colymbosaurus*. Although some specimens of *Cryptoclidus eurymerus* also exhibit a pentagonal fibula, these are anteroposteriorly longer than those seen in *Colymbosaurus* and possess a clear spatium osseum (Andrews, 1910; Brown, 1981).

New Autapomorphies for *Colymbosaurus svalbardensis*

In addition to the holotype specimen, PMO A27745, Knutsen et al. (2012a) also included PMO 216.838 and PMO 218.377 in the hypodigm of *Colymbosaurus svalbardensis*. The inclusion of the new specimen described here, PMO 222.663 (also found at nearly the exact same stratigraphic horizon as PMO 216.838), provides the opportunity to recognize two additional autapomorphies from the dorsal vertebrae and the hind limbs.

The neural canal of the dorsal vertebrae in the holotype specimen and PMO 222.663 is conspicuously ovate and dorsoventrally taller than wide when compared with the more rounded, equidimensional neural canals observed in *Colymbosaurus megadeirus* and other plesiosauroids from the Kimmeridge Clay Formation (Benson and Bowdler, 2014; A.J.R., pers. observ. of OUM J.55482). The presence of this character in multiple specimens suggests that this is not simply a taphonomic artifact but is the true morphology and can be recognized as a new autapomorphy of the species. A second possible autapomorphy pertains to the relative anteroposterior expansion of the femoral head relative to the femoral shaft, as seen in either dorsal or ventral view (Fig. 13). In all specimens of *C. svalbardensis*, the anteroposterior width of the femoral shaft is nearly the same as that of the proximal end. In contrast, the anteroposterior width of the shaft is conspicuously less than that of the proximal end in *Colymbosaurus* material from the Kimmeridge Clay (NHMUK R31787, OUM J.3300, NHMUK 10062; Benson and Bowdler, 2014). This feature also does not seem to be the result of a taphonomic bias given that a marked constriction between the humeral head and shaft is present in the newly referred specimen of *C. svalbardensis*, PMO 222.663.

Affinities of NHMUK R10062 to *Colymbosaurus svalbardensis*

Specimen NHMUK R10062, a partial skeleton including much of the vertebral column and associated girdle and limb elements, was originally named *Colymbosaurus 'portlandicus'* by Brown (1984) and was subsequently referred to Plesiosauroidea incertae sedis by Benson and Bowdler (2014). Based on the newly amended diagnosis, NHMUK R10062 shares three diagnostic features of *Colymbosaurus* and can be referred to this taxon: (1) the mid-caudals are pentagonal in anterior view, with widely spaced chevron facets; (2) the humerus has a large postaxial expansion at least twice as large as the preaxial expansion, bearing a single postaxial ossicle facet of subequal size to the epipodial facets; and (3) although the ulna is not preserved, the ulnar facet on the humerus is longer than the radial facet.

It is noteworthy that NHMUK R10062 also shares several features with *Colymbosaurus svalbardensis*. The neural canal of the mid-dorsal vertebrae is taller than wide, although not to the degree observed in specimens of *C. svalbardensis* from the Slottsmøya Member (Knutsen et al., 2012a). Additionally, it shares the same morphology of the posterior margin of the ischium, which is abruptly squared-off and mediolaterally broad. This suggests that NHMUK R10062 is potentially referable to *C. svalbardensis* and, as such, represents the first specimen of this taxon occurring in the upper Kimmeridge Clay Formation. However, in the absence of additional overlapping material, we refrain from formally referring the specimen to *C. svalbardensis*.

Survival of Colymbosaurinae into the Cretaceous

The Slottsmøya Member of central Spitsbergen preserves a high diversity of colymbosaurine plesiosauroids (*Djupedalia engeri, Spitrasaurus larseni, S. wensaasi*, and *Colymbosaurus svalbardensis*) that lived close to or likely across the Jurassic-Cretaceous boundary at high paleolatitudes (>60°; Torsvik et al., 2002). The taxonomic composition differs from the slightly older Kimmeridge Clay Formation in the United Kingdom, where non-colymbosaurine plesiosauroids are also found (e.g., *Kimmerosaurus*). Given that the stratigraphically youngest known colymbosaurine is *Abyssosaurus* from the Lower Cretaceous of boreal Russia (Berezin, 2011), and that colymbosaurines are the only known plesiosauroids from the high-latitude deposits of the Slottsmøya Lagerstätte, we propose that this clade may have persisted across the Jurassic-Cretaceous boundary in the Boreal Realm. Ongoing studies relating to the stratigraphy, the diversity, and the phylogenetic relationships of cryptoclidids from the Slottsmøya Lagerstätte and other sites are needed to better understand the timing and nature of extinctions for the clade at the Jurassic-Cretaceous boundary (Benson and Druckenmiller, 2014).

ACKNOWLEDGMENTS

We thank S. Chapman (NHMUK), M. Riley (CAMSM), E. Howlett (OUM), K. Sherburn (MANCH), A. Smith (NOTNH), S. King (YORKM), M. Evans (LEICS), N. Clark (GLAHM), and G. Wass (PETMG) for access to collections. We acknowledge the reviewers F. R. O'Keefe and P. Vincent for their helpful comments on the manuscript. We thank R. B. J. Benson for comments on an earlier version of the manuscript, D. Legg for advice on using TNT and S. Etches for access to his collection. G. Dyke, E. M. Knutsen, A. H. Roberts, J. S. Roberts, A. Smith, D. Foffa, and R. Forrest are thanked for helpful discussion. M.-L. Funke and V. E. Nash are thanked for their assistance in the preparation of PMO 222.663. Permission to use a photograph of NHMUK 10062 was granted, and the copyright of the image is retained by the Natural History Museum, London, U.K. The Governor of Svalbard provided excavation permits 2006/00528-24 and 2006/00528-32. Field work for the excavation of PMO 222.663 in 2010 and 2011 was funded by Exxon Mobil, Fugro, Spitsbergen Travel, OMV, Nexen, and the National Geographic Society (EC0425_09, EC0435_09). A.J.R. is funded by NERC, GSNOCS University of Southampton, and Tullow Oil. L.L.D. is supported by a Ph.D. grant from the Ministry of Education and Research via the Natural History Museum, University of Oslo.

LITERATURE CITED

Andrews, C. W. 1909. On some new Plesiosauria from the Oxford Clay of Peterborough. Annals and Magazine of Natural History, Series VIII 4:418–429.

Andrews, C. W. 1910. A Descriptive Catalogue of the Marine Reptiles of The Oxford Clay Based on the Leeds Collection in the British Museum (Natural History), London, Part I. British Museum (Natural History), London, xvii + 205 pp.

Bardet, N., J. Falconnet, V. Fischer, A. Houssaye, S. Jouve, X. Pereda Suberbiola, A. Pérez-García, J.-C. Rage, and P. Vincent. 2014. Mesozoic marine reptile palaeobiogeography in response to drifting plates. Gondwana Research 26:869–887.

Benson, R. B. J., and T. Bowdler. 2014. Anatomy of *Colymbosaurus megadeirus* (Reptilia, Plesiosauria) from the Kimmeridge Clay Formation of the U.K., and high diversity among Late Jurassic plesiosauroids. Journal of Vertebrate Paleontology 34:1053–1071.

Benson, R. B. J., and P. S. Druckenmiller. 2014. Faunal turnover of marine tetrapods of the Jurassic–Cretaceous transition. Biological Reviews 89:1–23.

Benson, R. B. J., M. Evans, and P. S. Druckenmiller. 2012. High diversity, low disparity and small body size in plesiosaurs (Reptilia, Sauropterygia) from the Triassic–Jurassic boundary. PLoS ONE 7:e31838. doi: 10.1371/journal.pone.0031838.

Berezin, A. Y. 2011. A new plesiosaur of the Family Aristonectidae from the Early Cretaceous of the center of the Russian Platform. Paleontological Journal 45:648–660.

Blainville, H. D. de. 1835. Description de quelques espèces de reptiles de la Californie, précédé de l'analyse d'un système général d'Erpétologie et d'Amphibiologie. Nouvelles Annales du Museum National d'Histoire Naturelle, Paris 4:233–296.

Brown, D. S. 1981. The English Upper Jurassic Plesiosauridae (Reptilia) and a review of the phylogeny and classification of the Plesiosauria.

Bulletin of the British Museum (Natural History), Geology 35:253–347.
Brown, D. S. 1984. Discovery of a specimen of the plesiosaur *Colymbosaurus trochanterius* (Owen) on the Island of Portland. Proceedings of the Dorset Natural History and Archaeological Society 105:170.
Brown, D. S., A. C. Milner, and M. A. Taylor. 1986. New material of the plesiosaur *Kimmerosaurus langhami* Brown from the Kimmeridge clay of Dorset. Bulletin of the British Museum (Natural History), Geology 40:225–234.
Caldwell, M. W. 1997. Limb osteology and ossification patterns in *Cryptoclidus* (Reptilia: Plesiosauroida) with a review of sauropterygian limbs. Journal of Vertebrate Paleontology 17:295–307.
Cheng, Y.-N., T. Sato, X.-C. Wu, and C. Li. 2006. First complete pistosauroid from the Triassic of China. Journal of Vertebrate Paleontology 26:501–504.
Collignon, M., and Ø. Hammer. 2012. Petrography and sedimentology of the Slottsmøya Member at Janusfjellet, central Spitsbergen. Norwegian Journal of Geology 92:89–101.
Dallmann, W. K., H. Major, P. Haremo, A. Andresen, T. Kjærnet, and A. Nøttvedt. 2001. Geological map of Svalbard 1:1000,000, sheet C9G Adventdalen. Norsk Polarinstitutt Temakart 31/32:3–55.
Delsett, L. L., L. K. Novis, A. J. Roberts, M. J. Koevoets, Ø. Hammer, P. S. Druckenmiller, and J. H. Hurum. 2016. The Slottsmøya Member marine reptile Lagerstätte: depositional environments, taphonomy and diagenesis; pp. 165–188 in B. P. Kear, J. Lindgren, J. H. Hurum, J. Milàn, and V. Vajda (eds.), Mesozoic Biotas of Scandinavia and Its Arctic Territories. Geological Society, London, Special Publications 434.
Druckenmiller, P. S., and A. P. Russell. 2008. A phylogeny of Plesiosauria (Sauropterygia) and its bearing on the systematic status of *Leptocleidus* Andrews, 1922. Zootaxa 1863:1–120.
Dypvik, H., J. Nagy, T. A. Eikeland, K. Backer-Owe, A. Andresen, H. Johansen, A. Elverhøi, P. Haremo, and T. Bjærke. 1991. The Janusfjellet Sugroup (Bathonian to Hauterivian) on central Spitsbergen: a revised lithostratigraphy. Polar Research 9:21–44.
Gasparini, Z., N. Bardet, and M. Iturralde-Vincent. 2002. A new cryptoclidid plesiosaur from the Oxfordian (Late Jurassic) of Cuba. Geobios 35:201–211.
Goloboff, P., S. Farris, and K. Nixon. 2008. TNT, a free program for phylogenetic analysis. Cladistics 24:774–786.
Gray, J. E. 1825. A synopsis of the genera of reptiles and Amphibia, with a description of some new species. Annals of Philosophy 26:193–217.
Hammer, Ø., M. Collignon, and H. A. Nakrem. 2012. Organic carbon isotope chemostratigraphy and cyclostratigraphy in the Volgian of Svalbard. Norwegian Journal of Geology 92:103–112.
Hjálmarsdóttir, H. R., H. A. Nakrem, and J. Nagy. 2012. Foraminifera from the Late Jurassic–Early Cretaceous hydrocarbon seeps, central Spitsbergen, Svalbard—preliminary results. Norwegian Journal of Geology 92:157–166.
Hulke, J. W. 1870. Note on some plesiosaurian remains obtained by J. C. Mansel Esq. F.G.S., in Kimmeridge Bay, Dorset. Quarterly Journal of the Geological Society of London 26:611–622.
Hurum, J. H., H. A. Nakrem, Ø. Hammer, E. M. Knutsen, P. S. Druckenmiller, K. Hryniewicz, and L. K. Novis. 2012. An Arctic Lagerstätte—the Slottsmøya Member of the Agardhfjellet Formation (Upper Jurassic–Lower Cretaceous) of Spitsbergen. Norwegian Journal of Geology 92:55–64.
Kear, B. P., and E. E. Maxwell. 2013. Wiman's forgotten plesiosaurs: the earliest recorded sauropterygian fossils from the High Arctic. GFF 135:95–103.
Ketchum, H. F., and R. B. J. Benson. 2010. Global interrelationships of Plesiosauria (Reptilia, Sauropterygia) and the pivotal role of taxon sampling in determining the outcome of phylogenetic analyses. Biological Reviews 85:361–392.
Knight, W. C. 1900. Some new Jurassic vertebrates. American Journal of Science Series IV 10:115–119.
Knutsen, E. M., P. S. Druckenmiller, and J. H. Hurum. 2012a. Redescription and taxonomic clarification of '*Tricleidus*' *svalbardensis* based on new material from the Agardhfjellet Formation (Middle Volgian). Norwegian Journal of Geology 92:175–186.
Knutsen, E. M., P. S. Druckenmiller, and J. H. Hurum. 2012b. Two new species of long-necked plesiosaurians (Reptilia, Sauropterygia) from the Upper Jurassic (Middle Volgian) Agardhfjellet Formation of central Spitsbergen. Norwegian Journal of Geology 92:187–212.
Knutsen, E. M., P. S. Druckenmiller, and J. H. Hurum. 2012c. A new plesiosaurid (Reptilia-Sauropterygia) from the Agardhfjellet Formation (Middle Volgian) of central Spitsbergen, Norway. Norwegian Journal of Geology 92:213–234.
Kubo, T., M. T. Mitchell, and D. M. Henderson. 2012. *Albertonectes vanderveldei*, a new elsamosaur (Reptilia, Sauropterygia) from the Upper Cretaceous of Alberta. Journal of Vertebrate Paleontology 32:557–572.
Maddison, W. P., and D. R. Maddison. 2016. Mesquite: a modular system for evolutionary analysis. Version 3.10. Available at http://mesquiteproject.org. Accessed March 1, 2016.
Marsh, O. C. 1893. Congress Géologique International, Compte Rendu de la 5me Session, Washington, D.C. 1891:156–159.
Nagy, J., and V. A. Basov. 1998. Revised foraminiferal taxa and biostratigraphy of Bathonian to Ryazanian deposits in Spitsbergen. Micropaleontology 44:217–255.
O'Keefe, F. R. 2001. A cladistic analysis and taxonomic revision of the Plesiosauria (Reptilia: Sauropterygia). Acta Zoologica Fennica 213:1–63.
O'Keefe, F. R., and H. P. Street. 2009. Osteology of the cryptocleidoid plesiosaur *Tatenectes laramiensis*, with comments on the taxonomic status of the Cimoliasauridae. Journal of Vertebrate Paleontology 29:48–57.
O'Keefe, F. R., and W. J. Wahl. 2003. Current taxonomic status of the plesiosaur *Pantosaurus striatus* from the Upper Jurassic Sundance Formation, Wyoming. Paludicola 4:37–46.
O'Keefe, F. R., H. P. Street, C. D. R. Wilhelm, and H. Zhu. 2011. A new skeleton of the cryptoclidid plesiosaur *Tatenectes laramiensis* reveals a novel body shape among plesiosaurs. Journal of Vertebrate Paleontology 31:330–339.
Owen, R. 1860. On the orders of fossil and recent Reptilia, and their distribution through time. Report of the British Association for the Advancement of Science 29:153–166.
Persson, P. O. 1962. Plesiosaurians from Spitsbergen. Norsk Polarinstitutt 1962:62–68.
Phillips, J. 1871. Geology of Oxford and the Valley of the Thames. Oxford University Press, Oxford, U.K., 523 pp.
Rousseau, J., and H. A. Nakrem. 2012. An Upper Jurassic Boreal echinoderm Lagerstätte from Janusfjellet, central Spitsbergen. Norwegian Journal of Geology 92:133–161.
Seeley, H. G. 1869. Index to the Fossil Remains of Aves, Ornithosauria, and Reptilia in the Woodwardian Museum of the University of Cambridge. Deighton, Bell and Co., Cambridge, U.K., 143 pp.
Seeley, H. G. 1874. Note on some of the generic modifications of the plesiosaurian pectoral arch. Quarterly Journal of the Geological Society of London 30:436–449.
Sennikov, A. G., and M. S. Arkhangelsky. 2010. On a typical Jurassic sauropterygian from the Upper Triassic of Wilczek Land (Franz Josef Land, Arctic Russia). Paleontological Journal 44:567–572.
Smith, A. 2013. Morphology of the caudal vertebrae in *Rhomaleosaurus zetlandicus* and a review of the evidence for a tail fin in Plesiosauria. Paludicola 9:114–153.
Swofford, D. L. 2003. PAUP*: Phylogenetic Analysis Using Parsimony (*And Other Methods), version 4. Sinauer Associates, Sunderland, Massachusetts.
Taylor, M. A., and A. R. I. Cruickshank. 1993. A plesiosaur from the Linksfield erratic (Rhaetian, Upper Jurassic near Elgin, Morayshire). Scottish Journal of Geology 29:191–196.
Torsvik, T. H., D. Carlos, J. Mosar, L. R. M. Cocks, and T. N. Malme. 2002. Global reconstructions and North Atlantic palaeogeography 400 Ma to Recent; pp. 18–39 in E. A. Eide (ed.), Batlas–Mid Norway Plate Reconstructions Atlas with Global and Atlantic Perspectives. Geological Survey of Norway, Trondheim, Norway.
Wilhelm, B. C. 2010. Novel anatomy of cryptoclidid plesiosaurs with comments on axial locomotion, M.Sc. thesis, Marshall University, Huntington, West Virginia, 70 pp.
Wilhelm, B. C., and F. R. O'Keefe. 2010. A new partial skeleton of a cryptocleidoid plesiosaur from the Upper Jurassic Sundance Formation of Wyoming. Journal of Vertebrate Paleontology 30:1736–1742.
Williston, S. W. 1925. Osteology of the Reptiles. Harvard University Press, Cambridge, Massachusetts, 300 pp.

Submitted June 3, 2016; revisions received September 22, 2016;
accepted October 31, 2016.
Handling editor: Robin O'Keefe.

Appendix 5

Supplementary phylogenetic information for Chapters 2 - 4

Supplementary phylogenetic information

Phylogenetic characters for Chapters 2-4

The (1-270) characters listed here are the characters complied and published in Benson and Druckenmiller (2014). The new characters (271-273) are used in Chapters 3 and 4.

See the supplementary information available on Dryad for more information on the characters used in Benson and Druckenmiller (2014) and their history of use.

1. Transverse constriction of the rostrum at the premaxilla-maxilla suture: absent (0); present (1).

2. Maxilla, lateral expansion of maxilla posterior to maxilla-premaxilla suture accommodates expanded caniniform bases ['roots']: absent (0); present (1).

3. Ratio of orbit length in dorsal view to temporal fenestra length: 0.3–0.7 (0); >0.8 (1).

4. Ratio of pre-orbital skull length to total skull length measured in dorsal view:

5. Orbit, ventral margin of outline in lateral view: concave, resulting in a suboval orbital outline (0); convex, resulting in reniform orbital outline with prominent lobate anterior extension (1).

6. Dorsal margin of orbit, outline in dorsolateral view: concave, forming part of a suboval orbit (0); convex, skull roof projects into orbit (1).

7. Relative skull length compared to length of dorsal series: 0.20–0.30 (0); 0.31–0.39 (1); >0.40 (2).

8. Inclination of the suspensorium: sub-vertical or weakly inclined (~80–90º) (0); significantly inclined (<70º) (1).

9. Relative positions of external and internal nares: internal naris posterior to external naris (0); nares overlap (1); internal naris anterior to external naris (2).

10. Position of the mandibular glenoid fossa: coplanar with the occipital condyle (0); just posterior to the occipital condyle (1); far posterior to occipital condyle, distance at least equal to basicranial (basioccipital+basisphenoid) length (2).

11. Fluted ornamentation of bone surface around the dorsal orbit margin (on prefrontal or postfrontal): absent (0); striations oblique to orbit margin (1); striations perpendicular to orbit margin (2).

12. Temporal bar, suborbital margin: smoothly curved (0); squared-off posteroventral margin of suborbital skull forms abrupt edge (1).

13. Alveolar margin of upper jaw in lateral view: approximately straight or weakly convex (0); undulating, forming 'scalloped' margin (1).

14. Premaxilla, external surfaces: marked neurovascular foramina but otherwise smooth (0); numerous sharp rugose crests (1); consistently undulating with rounded ridges (2).

15. Premaxilla contact along the dorsal midline: contacts anterior extension of frontals only (0); partially overlaps the frontal along the midline (1); overlaps the entire length of the frontal along the dorsal midline and contacts the parietal (2).

16. Premaxilla, posterior termination: tapering and non-interdigitating or weakly interdigitating (0); broad, deeply interdigitating suture with the frontal or parietal (1).

17. Premaxilla, dorsomedian ridge: absent or indistinct (0); prominent, forming either a narrow crest, a broad bar-like ridge, or a mound-like eminence on the dorsomedian surface of the rostrum (1).

18. Premaxilla, morphology of dorsomedian ridge: narrow and crest-like (taller than wide) (0); broad, occupying most of the internarial width of the rostrum (1); posterior mound (2).

19. Premaxilla, dorsomedian ridge location: anterior (0); posterior (1); elongate, extends from interorbital region to rostral tip (2).

20. Premaxilla dorsomedian foramen: absent (0); present (1).

21. Premaxilla, participation in medial rim of external naris: participates broadly along anteroposterior length of external naris (0); does not participate (1); small contact at anterodorsal corner of external naris (2).

22. Premaxilla, constriction of posteromedian process at level of external naris: absent (0); present, and does not expand to original width posterior to naris (1); present, but premaxilla expands to original width posterior to naris (2).

23. Premaxilla-maxilla sutures: converging posteromedially gradually, for entire length (0); anterior portion extends dorsomedially then abruptly curves posteriorly, resulting in a parallel-sided appearance of the posterior process of the premaxilla (1).

24. Premaxilla-maxilla sutures, morphology anteriorly: curved, but only weakly interdigitating, sinuous, or straight (0); pronounced, anteroposteriorly interdigitating contact with 'zig-zag' appearance (1).

25. Maxilla, posterior extent of maxillary tooth row: around orbital midlength or more anteriorly (0); ventral to postorbital bar (1); ventral to temporal fenestra midlength (2).

26. Maxilla-squamosal contact: absent (0); present (1).

27. Maxilla participation in internal naris: participates (0); does not participate (1).

28. Maxilla, trough or depressed region anterior to external naris: absent (0); present, defined laterally by a longitudinal ridge but does not extend far anteriorly (1); prominent longitudinal trough extends most of the prenarial length of the maxilla (2).

29. Posteromedial extension of the maxilla: extends to anteromedial margin of the external naris (0); extends to midpoint of the medial margin of the external naris (1); extends posteromedial to the external naris (2).

30. Maxilla, posteromedial (=posterodorsal) portion: not subdivided, forms simple sheet of bone (0); subdivided by anteroposteriorly oriented fissures (1).

31. Frontal participation in rim of external naris: does not participate (0); participates (1).

32. Frontal, posterolateral process: present (0); absent (1); inapplicable, premaxilla contacts parietal (?).

33. Frontal participation in orbital margin: participates (0); does not participate, excluded by prefrontal-postfrontal contact (1).

34. Lacrimal: absent, maxilla participates in orbit margin (0); present, maxilla excluded from orbit margin (1).

35. Prefrontal participation in rim of external naris: does not participate (0); participates (1).

36. Postfrontal participation in orbital margin: participates (0); does not participate, excluded by postorbital-frontal contact (1).

37. Jugal participation in orbital margin: participates (0); does not participate, excluded by maxilla-postorbital contact (1).

38. Jugal, size and anteroposterior length: large, with horizontal long axis, extends anteriorly at least one-third of orbital length (0); short, terminates around posterior orbital margin (1); very reduced and anteroposteriorly short with vertical long axis (2).

39. Jugal, shape of anterior margin: tapering, embayed by orbit margin, or contacts 'lacrimal' (0); squared off (1).

40. Jugal-squamosal contact: absent (0); present (1).

41. Jugal-squamosal contact morphology: subvertical and interdigitating (0); subhorizontal for most of length, not interdigitating (1); inapplicable, contact absent (?).

42. Postorbital-squamosal contact: present, excluding jugal from the margin of the supratemporal fenestra (0); absent, and jugal enters margin of the temporal fenestra (1).

43. Postorbital posterolateral process length: long, extending posteriorly for at least two-thirds of the temporal fenestra length (0); prominent, but not elongate, extending approximately one-third of temporal fenestra length (1); short or absent (2).

44. Pineal foramen: present (0); absent (1).

45. Pineal foramen, surrounding elements: enclosed entirely within the parietals (0); contacts the frontals or premaxillae anteriorly (1); inapplicable, pineal foramen absent (?).

46. Pineal foramen-location relative to postorbital bar: level with postorbital bar (0); just posterior to postorbital bar (1).

47. Morphology of pineal foramen: suboval (0); anteroposteriorly elongate and slot-like (1); inapplicable, pineal foramen absent (?).

48. Inter-squamosal suture along the dorsal midline in lateral view: low and rounded (0); raised ~1/3 orbit height dorsally relative to skull table (1); raised abruptly and substantially dorsally relative to skull table (2).

49. Parietal vault in dorsal view: mediolaterally narrow, lateral surfaces weakly concave or slightly sinuous (0); expanded to approximately one-third the mediolateral width of the skull, lateral surfaces convex, forming abrupt 'lateral angle' of Smith & Dyke (2008) (1); strongly expanded, equal to at least half the transverse width of the posterior cranium, lateral surfaces concave (2).

50. Parietal, sagittal crest height: crest absent, dorsal surface of parietal broad and flat (0); low, transversely convex (1); high, transversely compressed sheet (2); very high, forming convex dome in lateral view rising above the skull table (3).

51. Parietal ornamentation adjacent to the pineal foramen: ornamentation absent (0); ornamented with numerous anteroposteriorly oriented ridges that extend from the pineal foramen, surface flat or slightly concave along midline (1); parietal with raised midline ridge (2); 'parietal table' [triangular depression between pineal foramen and sagittal crest; Druckenmiller & Russell, 2008*b*] present (3).

52. Parietal, anterior extension: short or absent, parietal extends to the level of the temporal bar (0); long, parietal extends to orbital midlength or more anteriorly (1); very long, parietal extends to anterior orbit margin or more anteriorly (2).

53. Squamosal arch, posterior margin in dorsal view: dorsal processes extend anterolaterally (0); approximately straight, squamosal dorsal processes extend

laterally from midline contact (1); V-shaped, squamosal dorsal processes extend posterolaterally (2).

54. Squamosal arch, cross section of dorsal process of squamosal: dorsoventral/mediolateral width subequal to or less than anteroposterior width (0); anteroposteriorly compressed (1).

55. Temporal emargination: moderately embayed, temporal bar arches dorsal to a horizontal line drawn through the tooth row (0); weakly embayed, or not embayed, temporal bar does not significantly arch dorsally (1).

56. Temporal bar, dorsoventral thickness: low, significantly less than height of orbit (0); high, subequal to 2/3 or greater than height of orbit (1).

57. Squamosal, anterior extent: ventral to postorbital bar (0); significantly posterior to postorbital bar (1).

58. Inter-squamosal suture along the posterodorsal midline: flat (0); prominent, 'bulb-like' posterior extension (1); low, mediolaterally broad posterior convexity in dorsal view (2).

59. Squamosal-quadrate foramen: absent (0); present (1).

60. Squamosal-quadrate contact, length of ventromedial process of the squamosal: short, approximately half the dorsoventral length of the quadrate shaft or less (0); long, extends further ventrally than half the quadrate shaft length (1).

61. Squamosal, outline of posterior margin in lateral view: approximately straight (0); dorsal portion inflected abruptly anterodorsally (1).

62. Position of tooth row in lateral view: collinear with the mandibular glenoid fossa (0); considerably higher than the glenoid fossa (1).

63. Notochordal pit on occipital condyle: absent (0); present (1).

64. Notochordal pit on occipital condyle, location: centrally or at least partly within ventral two-thirds of condyle (0); comfortably within dorsal one-quarter of condyle (1); inapplicable, notochordal pit absent (?).

65. Occipital condyle constriction: complete, exoccipital facets are separated from the occipital condyle by a groove (0); incomplete because exoccipital facets contact the occipital condyle (1); or constricting groove altogether absent, even ventrally (2).

66. Ventral process of the basioccipital: absent, weakly developed or wide, flat, relatively smooth, with a thin plate present [small 'step' between condyle and ventral surface of basioccipital] (0); very prominent, ventrally projecting plate present (1).

67. Foramen magnum, proportion of foramen enclosed by supraoccipital: less than one-third (0); approximately half (1).

68. Exoccipital-opisthotic body, dorsoventral height:anteroposterior width ratio: <1.1 (0); 1.2–1.3 (1); >1.35 (2).

69. Exoccipital, foramina in lateral surface: one (0); two (1); three/four (2).

70. Opisthotic, paraoccipital process length relative to height of exoccipital body: subequal (0); long, at least 1.3 times as long as body height (1).

71. Opisthotic, orientation of paraoccipital process relative to ventral surface of exoccipital in posterior view: inclined dorsally (0); paraoccipital process oriented parallel to ventral surface of exoccipital (1); inclined ventrally (2).

72. Opisthotic, morphology of articulation with suspensorium: anterior surface of expanded lateral end makes broad contact with suspensorium (0); lateral end unexpanded, lateral/terminal surface makes narrow contact with suspensorium (1).

73. Opisthotic, shaft of paraoccipital process cross section: subcircular, dorsoventral height subequal to anteroposterior width (0); dorsoventrally flattened; anteroposterior width much greater than dorsoventral height (1).

74. Opisthotic, shaft curvature seen in posteromedial view: absent, shaft approximately straight (0); curves dorsodistally (1).

75. Prootic, anteroventral process: long, meaning that ventral anteroposterior length is much greater than dorsal anteroposterior length (0); short, dorsal anteroposterior length is slightly greater than ventral (1).

76. Supraoccipital morphology in lateral view: wider than tall (0); or taller than wide (1).

77. Posteromedian ridge of supraoccipital: present (0); absent (1).

78. Posteromedian process of supraoccipital: present (0); absent (1).

79. Supraoccipital, minimum mediolateral width of exoccipital rami in posterior view: a single ramus is substantially narrower than the foramen magnum (0); subequal to foramen magnum (1).

80. Basisphenoid (or parabasisphenoid) contribution to the basioccipital tuberosities: contributes, enclosing posterior half of tuber and forming part of the articular surface for the pterygoids (0); does not contribute (1).

81. Deep notch in the posterior margin of the body of the basisphenoid ['clivus']: absent (0); present (1).

82. Basisphenoid-basioccipital connection in ventral view: fontanelle absent (0); fontanelle present (1).

83. Parasphenoid (or parabasisphenoid), morphology of ventral surface within interpterygoid vacuity: mediolaterally concave (0); flat or weakly convex (1); bears distinct midline keel (2); inapplicable, parasphenoid does not extend far into posterior interpterygoid vacuity (?).

84. Parasphenoid, posterior extent on midline: terminates within anterior one-third of interpterygoid vacuity or more anteriorly (0); terminates just anterior to basioccipital-basisphenoid contact on ventral surface of basicranium (1); ventrally underlaps basioccipital so basisphenoid-basioccipital contact is not visible in ventral view (2); as state '2' but also underlaps pterygoids ventrally (3).

85. Parasphenoid, cultriform process length: extremely short, effectively absent (0); present forming prominent anterior projection (1).

86. Parasphenoid, ventral surface anteriorly: covered by pterygoids anterior to the posterior interpterygoid vacuities (0); visible through V-shaped notch in posterior pterygoid contact anterior to posterior interpterygoid vacuities (1).

87. Suborbital fenestra bordered by ectopterygoid and maxilla: absent (0); present (1).

88. Lateral palatal fenestration bordered by palatine and pterygoid: absent (0); present (1).

89. Element demarcating the anterior margin of the subtemporal fenestra: the ectopterygoid and pterygoid together (0); exclusively the ectopterygoid (1).

90. Palate, foramina between maxilla and vomer anterior to internal naris: absent (0); present (1).

91. Posterior extent of the vomers: extend to the internal nares (0); extend posterior to the internal nares (1).

92. Pterygoid-vomer contact: pterygoid does not separate vomers along midline (0); pterygoid separates vomers along the midline posteriorly (1).

93. Palatine, participation in the rim of the internal naris seen in ventral view: participates (0); does not participate (1).

94. Palatines, median contact: do not contact (0); contact (1).

95. Pterygoid, anterior termination: tapering (0); transversely broad and interdigitates with vomer (1).

96. Pterygoids, anterior interpterygoid vacuity: absent (0); present (1).

97. Pterygoids, anterior interpterygoid vacuity, mediolateral width: narrow, approximately one-fifth of combined pterygoid width at vacuity midlength (0); broad, at least one-third of combined pterygoid width at vacuity midlength (1); inapplicable, vacuity absent (?).

98. Pterygoids, posterior contact with basicranium: loose, overlapping contact (0); firm sutural contact, ventral surface of pterygoids level with ventral surface of basioccipital (1); narrow anteromedial process of the posterior pterygoid contacts parabasisphenoid primarily or only, forming a butt joint (2).

99. Pterygoids, midline contact posterior to posterior interpterygoid vacuity: absent (0); present posteriorly, but very small (1); present, pterygoid contact

for more than two-thirds of their anteroposterior length posterior to posterior interpterygoid vacuity (2).

100. Pterygoid lateral to the posterior interpterygoid vacuities: flat (0); forms ventrolaterally directed flange with long axis oriented posteromedially (1); relatively broad mediolaterally and forms anteroposteriorly oriented trough or dished, with a marked central depression (2).

101. Pterygoid flange, posterior midline contact: flanges do not contact on midline posterior to posterior interpterygoid vacuity (0); flanges contact on midline, enclosing semicircular fossa posterior to posterior interpterygoid vacuity (1); inapplicable, pterygoid flanges absent (?).

102. Pterygoid, posterolateral portion of pterygoid: does not form squared lappet (0); forms squared lappet that distinctly underlaps quadrate ramus of pterygoid (1).

103. Posterior interpterygoid vacuities, ratio of maximum length to combined width: <1.2 (0); 1.3–1.6 (1); 1.8–2.5 (2); >2.6 (3).

104. Posterior interpterygoid vacuities, location of midpoint relative to anterior margin of subtemporal fossa: posterior to anterior margin of fossa (0); approximately level with anterior margin of fossa or more anterior (1).

105. Basioccipital body, exposure posterior to pterygoid midline contact: absent, pterygoids cover ventral surface of basioccipital anterior to condyle (0); present, semioval portion of basioccipital exposed between pterygoids anterior to condyle (1).

106. Posterior border of anterior interpterygoid vacuity: bordered by pterygoid (0); bordered by parasphenoid (1); inapplicable, anterior interpterygoid vacuity absent (?).

107. Anterior border of anterior interpterygoid vacuity: bordered by pterygoid (0); bordered by vomer (1); inapplicable, anterior interpterygoid vacuity absent (?).

108. Morphology of the posterior border of the anterior interpterygoid vacuity: concave/rounded (0); parasphenoid projects into anterior interpterygoid vacuity

(1); inapplicable, parasphenoid does not contact anterior interpterygoid vacuity, which is thus enclosed posteriorly by the pterygoids (?).

109. Ectopterygoid/pterygoid boss/flange: absent (0); ventrally deflected posterior margin forms flange (1); rugose ventral boss present (2).

110. Ectopterygoid/pterygoid boss, transverse width: approximately as wide mediolaterally as long anteroposteriorly (0); >1.5 times as wide mediolaterally as long anteroposteriorly (1).

111. Shape of the mandible seen in dorsal/ventral view: bowed medially anterior to glenoid (0); not significantly bowed (1).

112. Mandible, symphysis length as measured by the number of alveoli adjacent to the symphysis [relative to the number of maxillary teeth or an estimate thereof]: long symphysis, number of alveoli adjacent to symphysis equals *c*.0.4–0.5 of maxillary alveolar count (0); intermediate, ~0.20–0.30 (1); very short, only 1–2 alveoli adjacent to symphysis (2).

113. Shape of the mandibular symphysis in ventral view: tapers anteriorly (0); laterally expanded (1).

114. Structure of the dentary along the ventral surface of the mandibular symphysis: no ventral elaboration (0); forms raised ventral platform or sharp keel/ridge adjacent to symphysis (1).

115. Contributions to the coronoid eminence laterally: surangular mainly (0); dentary mainly (1).

116. Length of retroarticular process: shorter than or subequal to glenoid anteroposterior length (0); longer than glenoid (1).

117. Orientation of glenoid: articular surface faces dorsally or only slightly dorsomedially (0); strongly inclined dorsomedially (1).

118. Mandible, posterior opening of Meckelian canal on medial surface [anterior margin of the adductor fossa]: dorsoventrally low with V-shaped outline in medial view [anterior margin of adductor fossa 'poorly defined'] (0); dorsoventrally tall [anterior margin of adductor fossa 'well-defined'],

occupying at least half the height of the mandible with curving outline in medial view (1).

119. Mandible, prearticular/splenial-angular contact perforated by anteroposteriorly elongate, oval foramen [lingual mandibular fenestra]: present, emarginates the medial wall of the angular dorsally (0); absent (1).

120. Rounded medial flange formed by articular and prearticular anterior to the glenoid fossa in dorsal view: present (0); absent (1); absent but anterior part of outline of glenoid in ventral view appears 'squared-off' (2).

121. Mandible, prominent longitudinal trough occupies much of the lateral surface anterior to the glenoid [dentary, angular, surangular]: absent (0); present, bounded ventrally by robust longitudinal, ventrolateral ridge (1).

122. Mandible, retroarticular process, dorsoventral orientation of long axis: posterodorsal (0); posteroventral or subhorizontal (1).

123. Mandible, retroarticular process, mediolateral orientation of long axis: directly posterior, in line with 'anteroposterior' long axis of glenoid (0); inflected slightly posteromedially (1).

124. Mandible, dorsal rim of 'lingual mandibular fenestra' formed by: prearticular (0); splenial (1); at prearticular-splenial contact (2); inapplicable, lingual mandibular fenestra absent (?).

125. Splenial participation in mandibular symphysis: does not participate (0); participates (1).

126. Angular relative length and participation in mandibular symphysis: short, extends less than half mandibular length (0); long, extending more than half mandibular length, but does not participate in the symphysis (1); very long, participates in symphysis (2).

127. Surangular, fossa and longitudinal crest on medial surface anterior to glenoid: prominent longitudinal crest forms ventral margin of deep, dorsomedially facing surangular fossa (0); prominent longitudinal crest forms medial margin of mediolaterally expanded dorsal surface of surangular bearing shallow, dorsally facing fossa (1); crest and surangular fossa weak or absent,

dorsal portion of surangular 'blade-like' (2); dorsolaterally facing fossa bounded laterally by a sharp crest (3).

128. Coronoid length and morphology: long, approaching or participating in symphysis (0); small, superficial element that is often disarticulated and thus not preserved, but represented by a facet on the surangular (1).

129. Prearticular, large dorsomedian trough or rugosity: absent or weak (0); present (1).

130. Articular, deep anteroposteriorly oriented cleft [notch] posterior to glenoid: absent (0); present (1); cleft absent, but dorsal surface is strongly concave mediolaterally (2).

131. Number of premaxillary teeth: four (0); five (1); six (2); seven or more (3).

132. Regularity of posterior premaxillary dentition: homodont, distalmost alveolus similar size to more mesial alveoli (0); heterodont, reduced distalmost alveolus (1).

133. Regularity of maxillary dentition: homodont (0); heterodont (1).

134. Diastema at premaxillary-maxillary suture: absent (0); present (1).

135. Spacing between mesial alveoli: narrow, less than mesiodistal length of a single alveolus (0); wide, more than half, or greater than mesiodistal length of a single alveolus and compact bone divides premaxillary and a small number of mesial dentary alveoli (1); one-third of dentary and more than one half of upper tooth row (2).

136. Enamel 'striations' (grooves): present (0); absent (1).

137. Form of apicobasally extending enamel ridges: coarse (0); fine (1); absent (2).

138. Number of maxillary teeth: 12–17 (0); 20–25 (1); >28 (2).

139. Cross sectional shape of teeth in anterior half of tooth row: round or sub-rounded (0); sub-triangular (1).

140. Premaxilla, diameter of first alveolus: not significantly smaller than third alveolus (0); less than half the diameter of third alveolus (1).

141. Relative neck length: the neck is shorter [<0.8 times] (0); subequal to (1); or longer than [>1.2 times] trunk length (2).

142. Axial rib articulation: articulates solely with the axis centrum (0); articulates partly with the atlas centrum (1).

143. Axial rib facet morphology: double-headed (0); single-headed (1).

144. Atlas-axis complex, atlantal centrum [odontoid], participation in anterior rim of atlantal cup: does not participate, excluded by atlantal neural arch–atlantal intercentrum contact (0); participates (1).

145. Atlas-axis complex, hypophyseal ridge: absent or low bulge (0); present and prominent (1).

146. Atlas-axis complex, hypophyseal ridge morphology: longitudinally elongate ventral ridge of approximately equal prominence for its entire length (0); substantially more prominent anteriorly, forming an anteroventral eminence (1); located posteriorly (2).

147. Atlas-axis complex, hypophyseal ridge location: extends across both atlantal centrum, and axial centrum (0); does not contact the axial centrum (1); inapplicable, hypophyseal ridge absent (?).

148. Atlas rib/rib facet or rib-like projection: absent (0); rib present, contacts atlas *via* a distinct rib facet [sometimes co-ossified to atlas] (1); posteroventral projection resembling a fused atlantal rib, but lacking evidence of a rib facet (2).

149. Axial intercentrum, size: small, restricted to ventral surface of atlas-axis complex (0); large, wedge-shaped element that extends dorsally (1).

150. Axial neural spine: transversely narrow (0); transversely broad (1).

151. Axial-atlas-axis complex, length:height ratio of centra: <1.1 (0); 1.15-1.45 (1); >1.5 (2).

152. Number of cervical vertebrae: <15 (0); 18–23 (1); 24–29 (2); 30–36 (3); 37–49 (4); 50–59 (5); >60 (6).

153. Proportions of anterior–middle cervical centra: substantially shorter than high [length <0.7 x height] (0); approximately as long as high (1); substantially longer than high (2).

154. Lateral surfaces of anterior cervical centra: longitudinal ridge absent (0); present (1).

155. Cervical centra, ventral notch: absent, centra subcylindrical (0); present, centra 'dumbell' or 'binocular' shaped (1).

156. Cervical vertebrae, subcentral foramina and foramina on the dorsal surface of the centrum, within the neural canal: both absent (0); both present (1); dorsal foramina present, but subcentral foramina very small or absent (2).

157. Anterior cervical neural spines, morphology: curve posterodorsally (0); inclined straight posterodorsally (1); inflected anterodorsally (2); inapplicable in some pistosaurians that have extremely low neural spines (?).

158. Posterior cervical neural spines, morphology: curve posterodorsally (0); inclined straight posterodorsally (1); inflected anterodorsally (2); inapplicable in some pistosaurians that have extremely low neural spines (?).

159. Posterior cervical neural spines, height relative to centrum: substantially shorter than centrum (0); subequal (1); substantially taller [equal to or greater than 1.2 times centrum height] (2).

160. Rib facets of the anterior–middle cervical vertebrae: rib facets broadly separated (0); two co-joined rib facets (1); mixture of single- and double-headed anterior cervical ribs (2); one rib facet (3).

161. Rib facets of the posterior cervical vertebrae: rib facets broadly separated (0); two co-joined rib facets (1); one rib facet (2).

162. Cervical rib facets location: ventrolaterally on centrum, do not contact neural arch peduncles (0); more dorsally, contact neural arch peduncles (1).

163. Cervical ribs, size and orientation of distal processes: marked anterior and posterior processes throughout cervical rib series, combined long axis of processes oriented approximately anteroposteriorly (0); processes reduced,

especially anterior process, combined long axis oriented posteroventrally (1); large, anteroposteriorly expansive, sheet-like ribs with prominent processes (2).

164. Cervical zygapophyses, combined width: broader than the centrum (0); subequal to the centrum (1); or distinctly narrower than the centrum (2).

165. Cervical centra, median ventral surface: approximately flat or convex (0); bears a rounded midline ridge [*cf.* Tarlo, 1960] (1); or bears a sharp keel (2).

166. Cervical centra, paired lateral ridges on ventral surface: absent (0); present (1).

167. Cervical zygapophyses, orientation: horizontal (0); dorsomedially facing (1).

168. Cervical zygapophyses, median contact between left and right zygapophyseal facets: absent for most/all of length (0); present for most of anteroposterior length (1).

169. Cervical zygapophyseal facets: planar (0); transversely concave/convex (1).

170. Dorsal and posterior cervical neural spines, dorsoventrally elongate groove on posterior surface: absent (0); present (1).

171. Cervical vertebrae, proportions of anterior cervical neural spines: taller than their anteroposterior length (0); longer than tall (1); anteroposteriorly short and 'rod-like', approximately as long anteroposteriorly as the transverse width (2); as long as tall (3).

172. Cervical vertebrae, shape of neurocentral suture in anterior–middle cervical vertebrae in lateral view: rounded, ventrally convex (0); V-shaped (1); extends far ventrally so that neural arch contacts dorsal part of rib facet (2); extends far ventrally but is evenly convex and does not contact rib facet (3).

173. Cervical centrum, proportional width: mediolateral width subequal to height or less (0); at least 1.2 times as wide mediolaterally as high dorsoventrally (1).

174. Cervical neural spines, apices of posteriormost cervical and anterior dorsal neural spines: weakly expanded and convex (0); apex transversely expanded into prominent spine table (1).

175. Anterior cervical centra, small, semi-oval 'lip' extends ventrally from anterior articular surface: no (0); small, transversely narrow lip (1); broad, prominent lip, at least 0.5 times the width of the centrum (2).

176. Posterior cervical rib facets: face laterally (0); or posterolaterally (1).

177. Middle to posterior dorsal transverse processes, distal articular facet: dorsoventrally tall oval, perhaps composed of two weakly divided rib facets (0); composed of only a single subcircular facet (1).

178. Height of dorsal neural spines in lateral view: less than or equal to the height of the centrum (0); conspicuously taller than the centrum (1); more than twice as tall as the centrum (2).

179. Number of dorsal vertebrae: 17–19 (0); 20–23 (1); >24 (2).

180. Number of pectoral vertebrae: 2–4 (0); 5–7 (1).

181. Dorsal neural arch height: tall, base of transverse process located dorsal to midheight of neural canal (0); short, transverse process adjacent to neural canal (1).

182. Dorsal transverse processes, orientation in middle dorsal region: approximately horizontal [laterally oriented] (0); inclined significantly dorsolaterally (1).

183. Dorsal neural spines, strong anteroposterior constriction at base: absent (0); present (1).

184. Dorsal neural spines, mediolateral width of apices in mid–posterior dorsal neural spines: unexpanded, transversely narrow relative to anteroposterior width (0); mediolaterally thick, subequal to anteroposterior width (1); alternate spines expanded laterally to one side (2).

185. Posteriormost dorsal rib facets: prominent transverse process located entirely on neural arch (0); rib facet split between neural arch and centrum ['sacralised'], but bears a typical posterior dorsal rib (1).

186. Sacral ribs: cylindrical and slightly expanded towards distal end (0); transversely expanded, dorsoventrally thin and sheet-like (1).

187. Caudal vertebral count: 25–30 (0); 33–35 (1); 36–40 (2); >40 (3).

188. Caudal ribs facet location in proximal–middle caudal vertebrae: located dorsally, contacting or almost contacting neural arch (0); placed dorsally but neural arch does not form part of facet (1); at midheight of centrum or lower (2).

189. Caudal centra, outline of middle caudal centra in anterior view: suboval (0); subrectangular, chevron facets widely spaced and located ventrolaterally, ventral surface approximately flat giving a subrectangular appearance to centrum in anterior view (1).

190. Caudal centra, length:height ratio of proximal caudal centra: >0.85 (0); 0.6-0.8 (1); <0.55 (2).

191. Caudal centrum, subcentral foramina on ventral surface: paired lateral foramina (0); single midline foramen (1).

192. Caudal vertebrae, chevron facet: located equally on anterior and posterior edges of the centrum (0) or mainly on the posterior edge, low, mound-like eminence may be present on ventrolateral surface of centrum anteriorly (1).

193. Middle and distal caudal vertebrae, chevron facets: flush with level of ventral surface of centrum (0); project significantly ventrally (1).

194. Proximal caudal centra: width to height ratio: 0.9-1.1 (0); >1.1 (1).

195. Distalmost caudal vertebrae, forming 'pygostyle': absent (0); present (1).

196. Ratio of coracoid to scapular length: > or equal to 1.9 (0); 1.6–1.9 (1) < or equal to 1.6 (2).

197. Anteromedial margin of the coracoid: does not contact the scapula (0); contacts the scapula (1).

198. Anteromedial margins of the coracoids: do not contact the dermal girdle elements [clavicle and interclavicle] (0); contact the dermal girdle elements (1).

199. Scapula morphology: dorsal blade expanding ventrally to form acetabular region, lacks expanded ventral plate (0); triradiate with expansive ventral plate (1).

200. Contact of the ventral plates of the scapulae along the midline: do not meet along the midline (0); meet along the ventral midline (1).

201. Scapula blade, outline of anterior margin in lateral view: approximately straight, weakly concave or weakly convex (0); pronounced posterodorsal inflection (1); distinct concave region anterodorsally (2).

202. Shape of the anterolateral margin of the scapula where the dorsal ramus meets the ventral ramus: flat or gently convex (0); forms prominent ridge or shelf (1); inapplicable, ventral plate not developed (?).

203. Scapular blade, anteroposterior width at distal end: subequal to width at midlength (0); narrow, tapering dorsally (1); broad, distal part expanded relative to midlength (2).

204. Scapula blade, length relative to posterior process of scapula: blade longer (0); blade subequal to or shorter than (1).

205. Scapula blade, angle relative to ventral scapula margin: vertical/subvertical [70-90 degrees] (0); intermediate posterodorsal inclination [45-60 degrees] (1); strong posterodorsal inclination [30-45 degrees] (2).

206. Scapula blade, medial surface: smoothly convex or flat (0); robust buttress oriented parallel to long axis of blade (1).

207. Coracoid, posterolateral cornu: does not extend as far laterally as glenoid (0); extends to level of glenoid (1); extends lateral to glenoid (2).

208. Coracoid, median fenestra/large embayment: absent, although intercoracoid contact may be slightly split posteriorly (0); median embayment present (1); posterior processes strongly divergent forming prominent V-shaped or otherwise mediolaterally narrow emargination (2).

209. Coracoid, shape of anterior process: anteroposteriorly long and transversely broad, approximately rectangular (0); anteroposteriorly long and transversely narrow (1); anteroposteriorly short and subtriangular (2).

210. Coracoid, posterior margin, outline in dorsal view: oriented approximately mediolaterally, may be convex, straight or weakly concave (0); anterolaterally oriented (1); possesses a distinct posterior process adjacent to midline (2); oriented posterolaterally (3).

211. Coracoid plate, perforations/large foramina: absent (0); present (1).

212. Coracoid, dorsoventral height of anterior process: dorsoventrally low and thus plate-like (0); taller dorsoventrally than mediolaterally (1).

213. Coracoid, anterior process orientation: extends approximately anteriorly (0); inflected anterolaterally (1).

214. Coracoid, robust buttress on dorsal [visceral] surface connecting glenoid to median symphysis, orientation: posteromedially (0); mediolaterally, and forms posterior margin of an anterior depression (1); mediolaterally oriented, but located anteriorly so anterior depression is absent (2).

215. Coracoid, ventral projection/process extends from intercoracoid symphysis: absent (0); present (1).

216. Coracoid, low, mediolaterally oriented buttress connecting glenoid to median symphysis on ventral surface: present (0); absent (1); mediolaterally oriented shelf or sharp crest extends anteriorly from coracoid surface bounding pectoral fenestra posteriorly (2).

217. Clavicle/interclavicle complex, median fenestra: absent (0): present (1).

218. Contact of the clavicles along the midline: present (0); absent (1).

219. Clavicle/interclavicle complex, shape of anterior margin: markedly concave, mediolateral width of concavity at least 1.25 times the anteroposterior depth (0); anteriorly convex or pointed (1); transversely broad and almost straight (2); small, transversely narrow, weakly concave region (3).

220. Median pelvic bar: present (0); absent (1).

221. Ilium curvature shaft in lateral view: appears straight, pelvic articular end equally expanded anteriorly and posteriorly (0); curves anterodorsally, articular end expanded only anteriorly (1); sigmoidal (2).

222. Ilium, rotation of dorsal blade relative to long axis of proximal articular end: ends perpendicular to one another (0); ends rotated by approximately 45 degrees relative to one another (1).

223. Ilium, shape of dorsal expansion: subequal anterior and posterior expansion, occupies dorsal half of ilium (0); subequal anterior and posterior expansion (or narrowing) confined to dorsal one-third of ilium (1); asymmetrical, extends much further posterodorsally than anteriorly, dorsal surface slopes posterodorsally (2); inapplicable, dorsal expansion absent (?).

224. Ilium, anteroposterior width of dorsal expansion: tapering, less than minimum shaft width (0); slight, just greater than minimum shaft width (1); expanded, between 1.5–2.0 times the minimum anteroposterior width of the shaft (2); large, over 2.5 times minimum shaft width (3).

225. Ilium, tubercle on posterior surface around midlength: absent (0); present as a tubercle (1); rugose, proximodistally oriented crest present (2).

226. Ilium, cross section of shaft around midlength: subcircular (0); mediolaterally compressed, suboval (1).

227. Ilium ratio of length to minimum anteroposterior width: <3.0 (0); 4.0–5.2 (1); >5.3 (2).

228. Ilium, pronounced, broad fossa on medial surface of the dorsal end: present (0); absent or weak (1).

229. Pubis, ratio of anteroposterior length to minimum mediolateral width: < or equal to 1.2 (0); >1.3 (1).

230. Pubis, anterolateral cornu: absent or weak and rounded, extending less far laterally than acetabulum (0); or present, extending further laterally than acetabulum (1).

231. Ischium, length to width ratio: < or equal to 0.9 (0); 1.0–1.3 (1); 1.4–1.8 (2); >1.85 (3).

232. Limbs, postaxial accessory ossicles: absent, or small, round elements appearing late in ontogeny without well-defined articular surfaces (0); present as small elements (1); present as large, well-defined elements contacting other limb bones (e.g. humerus, ulna) *via* well-defined articular surfaces, ossification of these elements is often late but their presence can be inferred by the presence of articular surfaces (2).

233. Second postaxial accessory ossicle articulating with propodial: absent (0); present (1).

234. Limbs, preaxial accessory ossicles: absent (0); present but small (1); present as large, well-defined elements contacting other limb bones (e.g. humerus, radius) *via* well-defined articular surfaces, ossification of these elements is often late but their presence can be inferred by the presence of articular surfaces (2).

235. Forefin, ratio of proximodistal length excluding humerus to maximum anteroposterior width of humerus/proximal epipodials [aspect ratio]: <3.0 (0); 3.1–3.5 (1); >3.6 (2).

236. Ratio of forelimb length to trunk length: <0.8 (0); >0.9 (1).

237. Difference in the axes of propodial and rest of the paddle in the forelimb: proximodistal axis of digits and tarsals/carpals collinear with propodial long axis (0); digits/tarsal/carpal axis extends posterodistally relative to propodial long axis because proximodistal length of radius/tibia is substantially greater than that of the ulna/fibula (1).

238. Propodials, dorsal and ventral surfaces of distal half: uniformly convex or flat with robust pre-and postaxial margins (0); weakly concave region separates central, convex portion from strongly tapering, flange-like pre- and postaxial margins (1).

239. Humerus, long axis curvature in anterior view: straight or almost straight (0); pronounced dorsodistal curve (1).

240. Femur, long axis curvature in anterior view: straight or almost straight (0); pronounced dorsodistal curve (1); pronounced ventrodistal curve (2).

241. Ratio of humerus to femur length: <0.85 (0); 0.9–1.1(1); >1.1 (2).

242. Epipodials, ratio of radius to tibia length: <0.89 (0); 0.9–1.09(1); 1.1–1.3 (2); >1.4 (3).

243. "Tongue-and-groove" articulation between propodial and epipodial: absent, distal articular surfaces of propodials smooth (0); present, deep recesses in distal articular surfaces of propodials accommodate highly convex proximal surfaces of epipodials (1); absent, but a prominent anteroposteriorly oriented ridge bisects the epipodial facets (2).

244. Humerus length *versus* width ratio: >2.9 (0); 2.3–2.7 (1); 1.7–2.2 (2); < 1.6 (3).

245. Preaxial margin of distal humerus in dorsal or ventral view: straight or convex (0); concave [distal humerus expands anteriorly], but anterior expansion relatively small, substantially less than posterior expansion (1); concave, and anterior expansion is large, approaching the size of the posterior expansion (2).

246. Sharp longitudinal ridge on anterior margin of humerus: absent (0); present (1).

247. Shape of the distal end of propodials: uniformly convex (0); propodials distinctly angled for articulation with the epipodials (1).

248. Propodials, angle between long axes of epipodial facets in dorsal view: oblique (0); close to 180 degrees (1).

249. Humerus, inclination of proximal end in dorsal view: inclined posteriorly so that the proximal portion of the anterior margin is convex in dorsal view [often a low mound is located proximally on anterior surface] (0); not inclined, extends proximally so shaft appears straight (1); inclined anteriorly so shaft appears sigmoidal (2).

250. Humerus, shallow groove on ventral surface between epipodial facets (flexor groove): present and prominent (0); present but anteroposteriorly short and shallow (1); absent (2).

251. Femoral length *versus* width ratio: >2.8 (0); 2.1–2.7 (1); 1.55–2.0 (2); < 1.5 (3).

252. Humerus, tuberosity morphology: narrow and projects dorsally (0); broad and projects posterodorsally [tilted] (1).

253. Femur, trochanter morphology: narrow and projects dorsally (0); broad and projects slightly posterodorsally [slightly tilted] (1).

254. Ratio of radius length to maximum width: >2.7 (0); 1.1–1.5 (1); 0.8–1.0 (2); < or equal to 0.75 (3).

255. Ratio of tibia length to maximum width: >2.5 (0); 1.1–1.8 (1); 0.8–1.0 (2); < or equal to 0.75 (3).

256. Radius morphology: preaxial margin concave (0); straight or convex (1).

257. Radius, prominent anterior flange extends from anteroproximal surface: absent (0); present (1).

258. Ulna morphology: postaxial margin concave (0); convex (1).

259. Tibia morphology: preaxial side of tibia concave (0); convex or straight (1).

260. Ulna, expansion of distal end relative to shaft: absent or very weak (0); present (1).

261. Epipodial foramen [=spatium interosseum; =antebrachial foramen]: present, proximodistal length slightly shorter than epipodials (0); present but short, proximodistal length less than half epipodial length (1); absent (2).

262. Ratio of maximum radius length to maximum ulna length: 1.0–1.3 (0); 1.4–1.7 (1); > or equal to 2.0 (2).

263. Radius, posterodistal facet for intermedium: absent (0); present (1).

264. Tibia, posterodistal facet for intermedium: absent (0); present (1).

265. Width of epipodials of the hindlimb: tibia larger (0); widths within 10% of each other (1); fibula larger (2).

266. Anterior (I) and central (II) distal tarsals/carpals: offset relative to proximal tarsals/carpals so distal elements articulate with multiple proximal elements

(0); in line with proximal tarsals/carpals, lacking anteroproximal or posteroproximal articular surfaces (1).

267. Interlocking distal phalanges: absent, digits splayed (0); present, digits parallel (1).

268. Position of the fifth metapodial: lies in the metapodial row (0); shifted proximally so that the proximal half is in the distal mesopodial row (1); shifted proximally so the entire fifth metapodial is in the mesopodial row in manus (2).

269. Metapodials, morphology of proximal ends: all metapodials form straight, anteroposteriorly oriented butt contacts with distal tarsals (0); at least one metapodial possesses a bifaceted proximal articular surface (1).

270. Phalanx proportions: long and slender [~2-3 times as long proximodistally as broad anteroposteriorly] (0); short and robust (1).

271 Frontal, interfrontal vacuity (new character): frontals are loosely connected along the midline (0); frontals are partially separated along the midline by an interfrontal vacuity (1). Absent, frontals split entirely or partially by posterior process of the premaxilla or completely fused (?)

State (0) is present when the frontals are loosely sutured, but lack any emargination along the medial margin of the elements (e.g.*Muraenosaurus leedsii*; Figure A5.1 A)

State (1) is only present in some cryptoclidid plesiosaurs (separate from the frontal foramen observed in some polycotylids) and *Brancasaurus brancai* (Sachs et al., 2016). When present, this state appears to be independent of ontogeny, as it has been confirmed in juvenile (e.g.NHMUK R2853) and adult specimens (e.g.*Tricleidus seeleyi*; Figure A5.1 B).

Scored (0&1) in *Cryptoclidus eurymerus* and *Tatenectes laramiensis*, as a loosely sutured frontal is present, but the presence of a vacuity cannot be confirmed due to the preservation of the specimens.

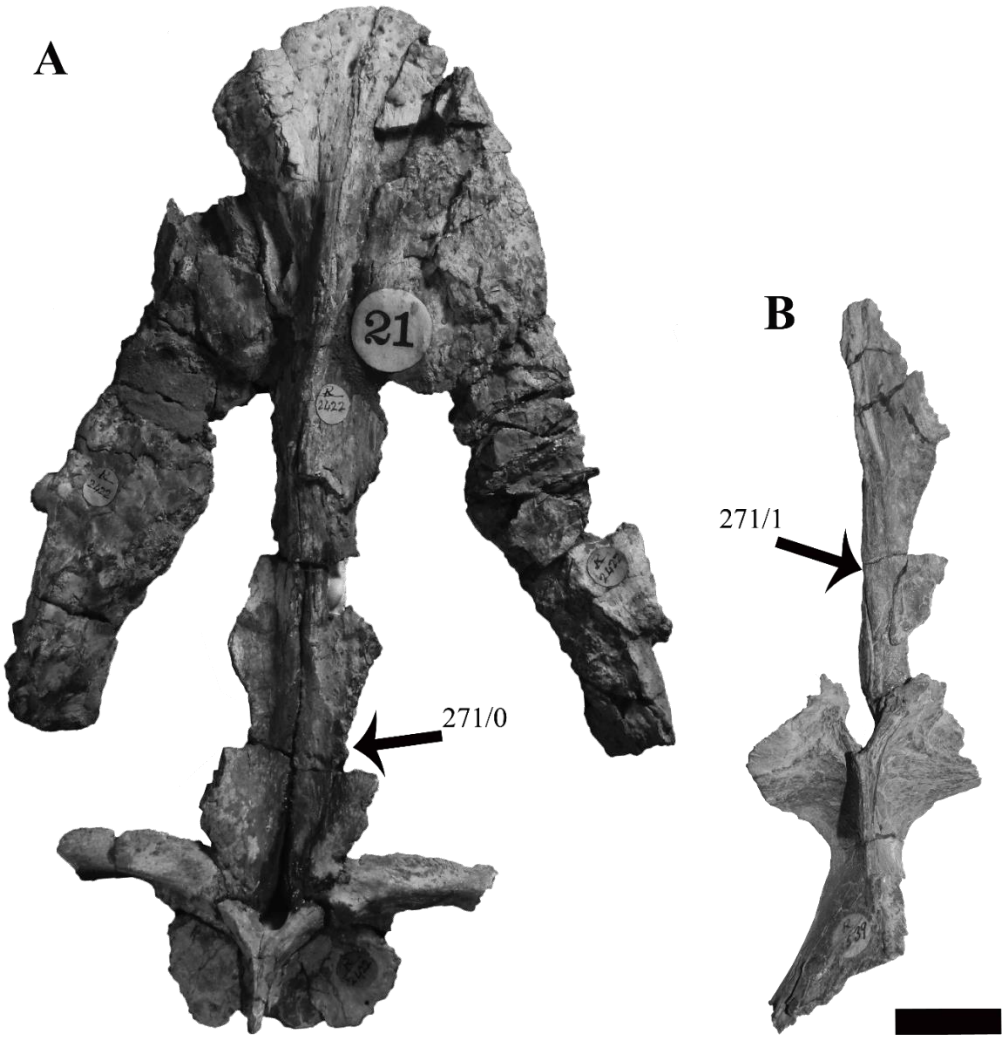

Figure A5.1: Illustration of the character states for character 271, with arrows pointing to the areas of interest. **A**, State 0 illustrated by *Muraenosaurus leedsii* NHMUK R2422 in dorsal view. Photo courtesy of R. Benson. **B**, State 1 illustrated by *Tricleidus seeleyi* NHMUK R3539, in dorsal view. Scale bar equals 2 cm.

<u>272 Dentary, mediolateral expansion of the dorsal surface (new character):</u>

No mediolateral expansion (0); a small lateral expansion present posteriorly; (1) mediolateral expansion, so the alveoli are laterally offset from the centre (2).

State (0) the dorsal surface of the dentary medial and lateral surfaces are uniform or convex and there is no or limited mediolateral expansion of the dentary in dorsal/ventral views (e.g.*Tricleidus seeleyi*; Figure A5.2 A-B).

State (1): Some taxa show a lateral expansion of the dentary dorsal surface, although this is constrained to the posterior region of the dentary (e.g.*Cryptoclidus eurymerus*; Figure A5.2 C).

State (2): some taxa show a mediolaterally extended dorsal surface of the dentary. This expansion is rapidly reduced on the medial and lateral surfaces, giving a triangular cross section at the midpoint of the dentary (e.g.PMO 224.248; Figure A5.2 D-F).

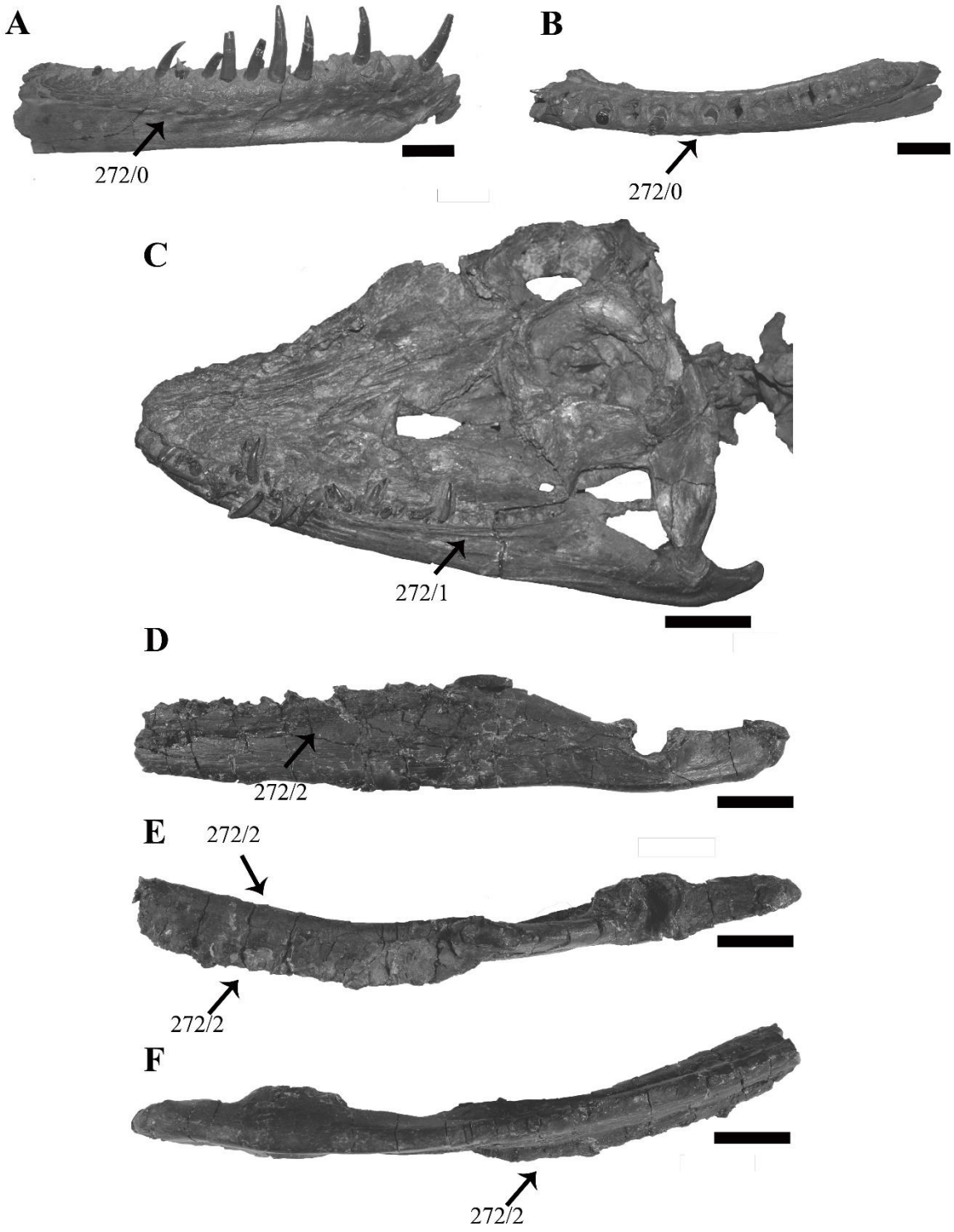

Figure A5.2: Illustration of character 272 in multiple cryptoclidid taxa, with arrows pointing to the areas of interest. State 272/0 illustrated by *Tricleidus seeleyi* NHMUK R3539 in **A**, lateral and **B**, dorsal views. State 272/1 illustrated by *Cryptoclidus eurymerus* PETMG R.283.412 in **C**, lateral view. State 272/2 illustrated by PMO 224.248 in **D**, lateral, **E**, dorsal and F) ventral views. Scale bars equal 2 cm in **A-B**, **D-F**. Scale bar equals 4 cm in **C**.

<u>273 Morphology of the fibula (new character)</u>: Lunate, close to or as proximodistally long as wide (0); pentagonal anteroposteriorly wider than long, with equally sized distal facets for fibulare and astragalus (1)

Edited from character 92 in Smith (2007). It should be noted that although the epipodials from the fore- and hind limbs in most plesiosaurs are similar in morphology, there are some differences in Cryptoclidid and Xenopsarian taxa.

State (0) is observed in most Early – Middle Jurassic plesiosaurians and pliosaurids (e.g.*Hauffiosaurus zanoi*; Figure A5.3 A).

State (1) is observed in Cryptoclidian taxa (e.g.*Colymbosaurus svalbardensis*; Figure A5.3 B)

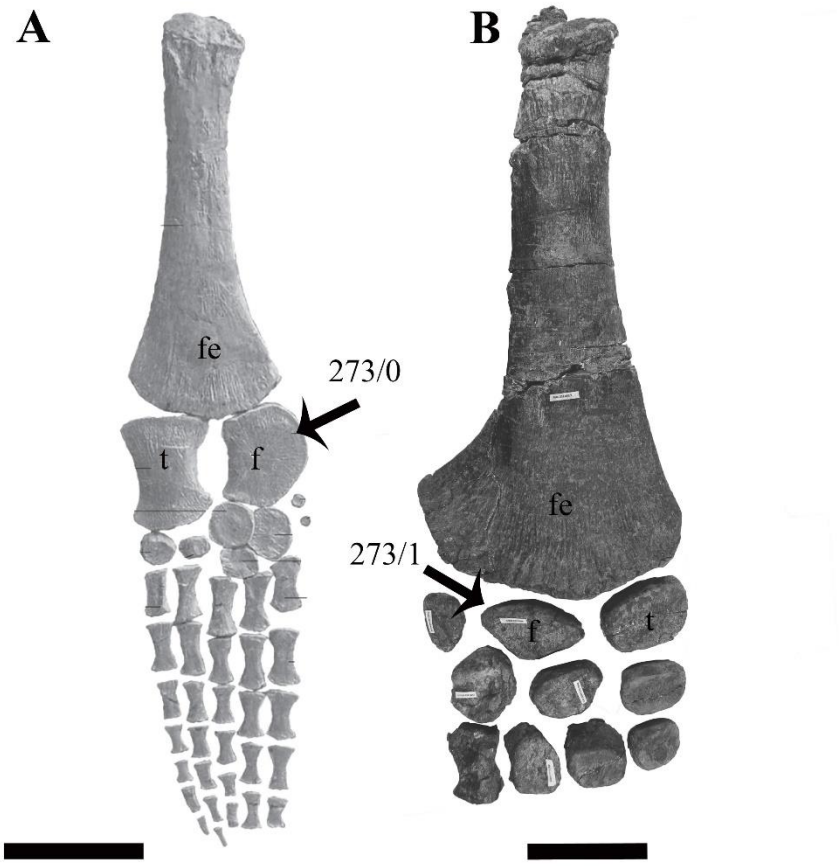

Figure A5.3: Illustration of the different character states for character 273, with arrows pointing to the areas of interest. **A**, State 0 illustrated by *Hauffiosaurus zanoi* modified from Vincent (2011) in dorsal view. **B**, State 1 illustrated by *Colymbosaurus svalbardensis* modified from Roberts et al., (2017) in dorsal view. **Abbreviations: f**, fibula; **fe**, femur; **t**, tibia. Scale bars equal 10 cm.

Changes in character states for individual taxa

The scores for the following cryptoclidid taxa were changed on the basis of personal observation (AJR) if not otherwise stated.

Changed scores in Chapter 2

Muraenosaurus leedsii:
- (183/1→0) coding mistake.

Kimmerosaurus langhami:
- (151/1→0) based on own observations of referred material and holotype (NHMUK R)

Colymbosaurus megadeirus:
- (142/?→1) as described in Benson and Bowdler, (2014)
- (144/? →1) as described in Benson and Bowdler, (2014)
- (189/0→1) as described in Benson and Bowdler, (2014)
- (234/1→0) no preaxial element preserved
- (240/1→0) the curvature of the long axis of the femur is straight or almost straight.
- (243/2→0) not a valid character state due to significant variation

Djupedalia engeri:
- (7/0→?) skull not preserved and mandible incomplete, so an estimation of skull length is not possible
- (13/0→?) upper jaw not preserved
- (200/1→0) do not meet along the midline.

Spitrasaurus spp.:
- (13/0→?) upper jaw not preserved
- (159/1→?) Not possible to confirm due to the preservation of the vertebrae, (200/1→0) do not meet along the midline.

Changed scores in Chapters 3 and 4

Cryptoclidus eurymerus:

- 21/0→2 The premaxillae of PETMG R 283.412 has a small anterodorsal contact with the external naris
- 31/0 →1 frontal does participate in medial/dorsal margin of external naris
- 35/0→ ? prefrontal not visible in any specimens
- 82/1 → 0 based on description in Andrews (1910)

Muraenosaurus leedsii

- 17/0 → 1 dorsomedian ridge of the premaxilla is present in NHMUK R.2422
- 18/0→? The morphology of the dorsomedian ridge does not fit character description
- 27/? → 0 based on description in Andrews (1910)
- 31/? → 1 based on description in Andrews (1910)

- 77/? → 0 based on description in Andrews (1910) and confirmed in Brown et al. (1986)
- 82/1 →0 fontanelle absent, the dorsomedian pit present in this taxon is not homologous
- 91/? → 1 based on description in Andrews (1910)
- 107/? → 0 based on description in Andrews (1910)

Triceidus seeleyi

- 82/1 → 0 fontanelle absent, the dorsomedian pit present in this taxon is not homologous

Kimmerosaurus langhami

- 81/1→ ? due to the poorly preserved basisphenoid
- 82/1 → ? due to the poorly preserved basisphenoid

Picrocleidus beloclis

- 82/2→1 Does not differ from *Muraenosaurus* or *Tricleidus* as described in Andrews (1910) and Brown (1981)

Tatenectes laramiensis

- 43/1&2→? Not preserved for this taxon O'Keefe and Street (2009)

Data matrix utilised in Chapters 3 and 4

The data matrix includes 76 OTUs and 273 characters. Missing data = "?", dual character states = "( )". For the new characters (271-273): the character states for most OTUs were scored from the available literature, with the exception of the cryptoclidid taxa (Table A5.1). These were scored from the literature in combination with personal observations on type and referred material.

Yunguisaurus_liae
0001000??10000000??0010010?000010010?000?000110??200??00?????01020???????????????02?1
0???????0?0?0010020???10011001100?1001?1???13??0??????1??????????41000??00?000000?001
??0??01210?0?00(2
3)??0??????0?000?200?????????????0?00122011?0000002000??11000?000?0?000000010000100000
?0?

Pistosaurus_postcranium
??
???2001110000000000011010010110
0010????101110?00?001?202100??0??001???0122210???1??????01?1?00000000???0???0?10?????
???0???

Augustasaurus_hagdorni
010100?0010?00000??001001000000000000000100?001001210100001 0??????0???0?0000??????02?
?000?0110000?0010000????0?1100?10??1001??1???0101000 2100???00??21??41?01??000000200?0
?10000011??0000???????????00?000?102?020000?0??????????????????000??00???100000000???0?
100?1000???0?00?0?

Bobosaurus_forojuliensis
????????????????0???
???02?0?00?00??01?2100000??110?12?000?00??001221
100?10(23)1????????????????????????????????0122010?001??????0???1?000????????0???0?0??0??
???????

Anningasaura_lymense
111000?0120?00??10000100?0010000100000?10000010112001000?10?0?1020?0110111010010?00
211?1000000011?00?000?111??1110?100?1010?110??00010011000?0?00??0?0??10010??3?0?1201
00?031?1???
?????????????0?

Stratesaurus_taylori
001000?0100100100??0110010000010?0?000010000010001001000010101101012002000010?0010
2211???01000010110?000000?2?111?11000110001?0?001000011000?0?00??2001?1001001110012
0100003101??1????00?0????????????1?????????????????????01022111??????????????????????????
1???010??010??10?00

Avalonnectes_arturi
??????????01??10????????10?????01??0000100000100110010000101 0??????????????????1??????
0??(12)??????????2100?00211001??100?0110
001101101200?0110?00????1?01201???????????????0102?110??1?????????11020?000?110110?101
000010?100??0

Meyerasaurus_victor
10?00?0?21??00??11??0100??0000???0??????????????????10?0??0101??(01)0????????0??????022?
0?1?01010111122?11000101?0111100?02110211???01?1001010?0???0???1?120?01?????00?20????
0???0011211012002?110?0?0111?0?1????0201000?0001000102011?0011002100??12020?00021??1
1011010001101100?00

Maresaurus_coccai
110100?1220?1???1120(02)1001?0?00?????????????00001120?10???10?0110?0?????0?????????0??
11?000101010?122?1000???200111?00??2100?11???01?1?011100????0???????0001???2?0?(01)??1
???030??
?????????????0?

Borealonectes_russelli
11010?1?210?102011100?00(1 2)0?0000??010?0010010000?(0
1)??1?000??0?0???20???12000???????022?1?0???????0??2???201?????111??00???1?0?110??0(1
2)?1?01?10?00100??21?120001???2?0??20?????30?0????????1???????????????????????????????????
?????????????100??00?????1101012???2?011?0001???11?1?0?

Rhomaleosaurus_megacephalus
1001012122011210100021001001 00?000?00001000001001200100011010 1???0?201?000???0??100
2111000100011011???00?0002001111?0??20?0?11??0??00001020?0???0???10120001???1100?201
????10?00111?1012001??20?0?0??????????1??????????????01022110????????00??1?0201001?110?
1??1010??0?????0?00

Archaeonectrus_rostratus
1002002???0?102?1111??00?????????0?000?10000010012011000?1??01??????????????????????????
????????????????????????11??1????1??????????????11120?0??????????2100100111000201???0?11?
0110110110010??????0?????0?20?1??????????????01?2?1100?10001000??1?020?00??11011011010
001101100???

Rhomaleosaurus_cramptoni
10000021220?1020100121101?00001?1000000???00010012011000111 10?10?0???1?000???????02?

1110?01010110122?1000000200?11?00??2100?11???01?1?01020?00??????????200???1211000??1?0
?01?1?0002110?100?0????0?????1?????????????????1??????0102?11000?10???00??1?021?001?1??110
110100?11?1?00?00

Rhomaleosaurus_zetlandicus
11000??1220?102010012110??00001??000???????001001?0110?0?1110110?????1?0?0????????221
1??0?1????1?1?2??0??0??2001111000021002110000??1001020?0??????????200010??110?020100?
010?00??2110?1???01201000???1?0??0012120210001211011011
01001?????0??00

Rhomaleosaurus_thorntoni
11??0????2?0?10??1021?1101?00?????0??0001000?????????????1?????????????????????????????1?
?01??01?????????????200111??10?11???11000?11100101000??????????0001???110?000100??10?
?01?21101?00?0110100??01100120210?0?000100?10001220110001??????0111?02100002110?????
?????????????0?

Thalassiodracon_hawkinsii
00100001110100111120??0?1000???0000000?100200000010110000101101010100020000110001010
1011?00011001??100?000????0?11101100010000?1200?00100111001000??210131001001110012
0100002100011101000001011000002011011001?00000001000?000102011100100020000011010000
00010?11001010000101100?00

Hauffiosaurus_longirostris
00?20??0?1??12111120??00???2?????????????????????02???????????01001??0???1?0?????1110????
?????????110?0??0?????1001?100?1100?11?00230100112 00?????????????????????????????????????
??
?????

Hauffiosaurus_tomistomimus
00020?10210?1?110??0100?0?0210100100???????00?00010100?0?101?01011??????1001????11101
1?0?0100010?100?010??????1000?100?1100?1120023010011 20?1100???(02)?1231001?11110?100
10000200001110101000 1??10???0???1??1?0?0????????????00????????00???0?1000012010000121?
01101?1?0?11201?00?00

Hauffiosaurus_zanoni
00?2??1??1?????????????0?0??????????0?10???????????00?001???010?????????????????11101101?
0100010?100?010????20100??100?1100??12002301(01)01120000?00??????310011?11100100100?
020?00?????????0?0110000020110112 0??0020000?010?0001020?2?0001001000??11010?00121??1
101101000110110 0?00

Marmornectes_candrewi
0???????????00??0?????00?????????????????????????0????10???0???0????????????????????????
?????????????????????10100110?0000?1110002010210200000 00??21?1?0001???120010010 0?200?1
001??1?00?1?0010000??????1?0??000?00???00????00220111??2000??0011000100001210 0?1??111
0??011???1???

Peloneustes_philarchus
10020120211100210??0100010001 01?010000010020010003121100010?0010100001100001 1?1010
2211100110(01)010?12110200???2110110110000001111000211001020001000??21?110001?12120
0110100000011001201100?1?0010001?00?10110000100000020 10??10023011110220 00?01??0002
1000122002210111011110111 1?00

Simolestes_vorax
110101???21?10210??010001??010??0100000100200?0003111?000?0?0010100??11000????1???22
1110???????0?121?0210???210111??10?0000?111000??1?01010?0??00???1111000111 21?0?100000

1200110????11?????0????0??20?10012010?02?000?0????000230??1102201??010100021010122001
1101110011110???????

Pliosaurus_BRSMG_Cc332
110101?0221110210??0100110?0111?1100000100200100231111000201001010???1????01???0?01
2111001???????12110200???1?101?0010?200???13?00(12)11011011?????????????0001???1?00?00
?????00???00??1100??
???????????????

Pliosaurus_brachydeirus
11?1?????2??102?0??01001???0??????????????????00?0???1??????????01010?????????????0?????????
1?????0?12110200?????101??010?2000??13000(12)11101021?0???????????0001???110??10???0?0
0?2010??1100??0???00????0?????1?1???3???1?0?
?10????1???

Gallardosaurus_iturraldei
??0?01?022?1??21????????10??????11?000010020010 0?31?1100020?01101????1?????????????1211
10???0?010?12110300???211?????1???0?????????????????1????00??2?11?00011??1?0?110?0??201
??
??????0?

Liopleurodon_rossicus
11?1?1??????10210??01000????1?1?1100000 1??200?0??3121????????????????????????????????????
?????????????????????????1????????0???????????1?01011????????????????????????????????????
?????????????????????1000200?2?????0?2???
???

Pliosaurus_andrewsi
01020?2021??10210??0??00??00?????????????????00?00?3(01)211?0??0?00??10?????????????102?
11?00110?010?1211020????21111?011000010111100021100101000100110 2??21000101211001000
0002001100120110??1?0010000?????????????????????????????0023011 0???200??01??0202101012200
3210?100011001211???

Liopleurodon_ferox
1101012022111021 0??010001000101?11?000010020000003121100020100101000?1100001??1010
2211100110111 0?12110210???21111100 10?0010?111000111101010001100??01101000111212001
00101000011000?0110????2010100????1??0?000?????0??01???1????????10320???010???02101012
?0?2?101?0001???1?11???

Kronosaurus_MCZ_1285
??0?0?20?2??????0??01000?(01)?00011000?01110?111?0
???????????12110(23)10???????????0????001????0??????01010?011?0??2??00000?11?3211?0?000?
0001??0?20?1??0??2?10000?00?10?0?????02??0020????1????????103????????????????????????????
???????1???????

Brachauchenius_eulerti
010200?0211100210??1100010?0200?111000010120010023121000 12??00?????????????????????011?
0?000110001012110310 10?21110?0010?0001?11???000000101 00?????????????????1???????????
??
????????0?

Brachauchenius_lucasi
000201202111002 10??010001000200?111?000101200100031210001 2??00?????????????????011
?0100?1011?0??2100310???211???001?00001(12)11????????010?0?0???0?????000002????211?00?
????????00??001??
???????11111?0?

Brachauchenius_MNA_V9433
0102?????1?100210??0100010?0????????0001???00?002(23)1210?0?20?0????0?????????????????
???00????110??2110210???2111000010?0001?1110000000010100???????????0000211?321110000
0?200?2?0???01?????????????0?1???????22200002?????11??0011?10?????????????????????????
???????????????

QM_F51291
????01??2?????210??010?????0210?1110000????0010???12?????????????????????????????????0?0
0?????????????(23)????????????????????????????????????10????????????????????????????????
??
????

Attenborosaurus_conybeari
00010010???110??112???0010?0?????0??0001002???????2??10000???11?????????????????1?2????
??????????????????????0110??0???0?????????10100???0?2??????????310??011110????1???0(03)0
0??11101100?0???1???1?20?10?1????0220000?000?310?02??1?0010001000??1??10?00????1?001
?100???01101?0?

Plesiosaurus_dolichodeirus
001100?0110?00100??0010010?0000100100000100?00100010010000101010110(01)010?02000?1111?
10?01100?01000110100?000?1110?0100?100?1000???????10000111O?2???0????01410010121(01)0
0100101003(01)000111111000010000010(01)?2111011001100000000?000?000002012100100020000
?1102010000200110(0 1)1010000?01100??0

Eopleiosaurus_antiquior
??
??2??????????4100?0111?0?12?1???03??0???????
???01000?11?02??1001002?0?0??00???????0??2?11?00110020000?11010100??1?0110?1010000101
100??0

Eretmosaurus_rugosus
??
??(12)??????????(34)100110?100?12010000?0001
11??11?0???0000?01????1???????(0
1)?0??0???????00102012000110000000??11021?1000200110110100002011000???

Westphaliasaurus_simonsensii
??
??2????????????0011021?0??0010?10310001111?1
?0010?0000101?211100120??00000001??10000??20?20001?????000110021000111001101101000l
1?1??1??0

Seelyosaurus_guilelmiimperatoris
00000?00?10?02?????0???????0?????0??0011001????1?1?01000?0??11????????????????????????
??????????????????????10??100?1010???????10000110O?2???????????3100?1221000???1???00?00
?1200110010(23)10000110110100120l?10030?1?0???300?02??20001100010O??11020?100?200110
1100001120110l?0?

Microcleidus_tournemirensis
0000000?120102100??00100100000000010111100100100020010001l0?1???(12)1?????000?????01
12?110000??00?0?12100100???20????????????????????1100011001l?????????142101112100?20?1
00?00100112001110l0?????????20110012021101301O?010?300122012000110????0??1?020?100?2
?0110110100012?1??1??0

Microcleidus_brachypterygius
0011000?110102100??00100100000001010111100100101020010001O0?????1???????????????101?

?100?0010000?12100000???20?????????????????????0000110012?????????2321011121?00??1????
00100?1201111?0?3100011?0210???1????20130?0?01???101220?10??01002000??11021?100?2??1
10100100111011101???

Microcleidus_homalospondylus
0000000011010210???0010020?000?010?0111100100101020010001??111101100102000012?00102
1?1?00????000??2100100???2001001??00?0???102???10000??0012??????????42101112100020110
0100100112011110?0?1000011??1011110001?01?010101???0012201200001?0?20000011021?10011
0011011010011201101?0?

Plesiopterys_wildi
00100?0?1???00????????00???00??1?0?0???10??01?0001001000?00?0?1010111020000100101011?
???1????0011?00??00?100???20??100?1000?0?2??0?00?01110?????????024200111211?01?001??00
01001111?1100003000000?01?11?01201??0??0???010?3?0102012?001???00?0001102001012??11
001010011101110000

Cryptoclidus_eurymerus
0010010010?101100??02100101000110?00201002010010110100000000?10?1011101101?1110110
11??00101100011?00?0????000?02001100?1000?0021?020000111012111110?0131001112320110
0111000000011101100000001000112101100101020120102020?1100210110112010?10111303201
0122101300110(12)2(01)(01)001211(01)11

Tricleidus_seeleyi
011000??????011010?00?0010?000?100????????(12)01001?3001000?000010?00?0111111?????110
110?????????011200?000?1100?02011100010?0021?01110011001?11?1101?0221001112320110
0111000100?11?01100???????????1101100000020120102?13?????????????210??10111302101012
21023001101111101211101

Muraenosaurus_leedsii
00????????0?011010?001001?0000110??????????010?0?????1???0???10?00?0????11??0??11011???
???1???????0???????0???0201010002000?0021?01010011001?1?1101??1421011223201200111000
01001??11110000?200?111???????0???0(1
2)????1?2020?3?1012?021??12????100123031110122102300110011100121012 1

Kimmerosaurus_langhami
??1??0?1??0?0?????????????0?????10??0??????201000001020000000111010102011 01?10111??11??
???????????200?0????????020011000100 0?002??0?00?01220???1?1001?00?00011??3?01100111???
1?0??
??????1(12)?

Pantosaurus_striatus
??
??(34)100111?320??00???000100??1?
?110000?2000111?????????????????????????????01001?021011200??10????0210101??1?1?10???211??
?1211???

Picrocleidus_beloclis
??0????0?010?(01)0?????????????10011????
??????????????????????????1100?1000???2??2?????11?????1?1101?02411011223201200111000100
0111?011?0?0?200?10100101100201020120102020 1?01?12?021112200??101???021110122101100
10011111?1?10?2?

Tatenectes_laramiensis
???????0?????????????????????0??????0??????1?????????????2000?0000?????????????????????????
?????11????????0?1?????????????????????????????11??????01001????00011??32011001?1000100?11

0?110000??????????1011??????(12)01??1020101?10?1100210112l0??10????0210101??1?2?001?02
11??01??1(01)??

Plesiosaurus_mansellii
??
??1111101??2(34)1101???320??00?????01?01??
1111?????1010011??0????????????2??1?202??2????????
????1

Colymbosaurus_megadeirus
??
??????????????????????????100?1000??????0???????????1111110??2410012??320?200111??01?01??1
011??00?2110101??0????????????2??102?2??????????????????200??10101?021010122102210110 2?111
01211??1

Djupedallia_engeri
??00???????0?01111?????????????????
??????????????????020??????????????????00?0??1??2011???100?5100121132012001110301001 10
??1100??????????????10?0???0?0??01???(1
2)??3?????????????2?0??????1?02?0?012?1???101102???1?1211?21

Spitrasaurus_spp
??????0??0???00??1010????????????1????????????
???????0???????????0201?100?1000???2??0?00?01110?20111111??2521012 2?32012001110301001
10?01100??????????????10?0???0?0??01???2?????????????????2?11?????1?02(1
2)0?012?1???101102?1???1(12)11?2?

Abyssosaurus_nataliae
??
??2???1110??1(45)1001???32012001 11??01?01??
1011??0??(1
2)0??????00100001 00??2??10?0?001?1?1101110??2?1??1????10???10?22?0?3??110(02)??100121
1??1

Umoonasaurus_demoscyllus
00000100112??1101020??00??00????0??????????0?002222?10???10?11????1??12?11?0??0??022??
???0?????11122?1211000????????0??1111??????1111010?01???????????1001????20?1??1010??0
0?1101011020002 01?00?1???1?01?010?????????????0???????????21????0111?02001022210?2???1
?0??10?1??1???

Nichollssaura_borealis
000001001120001010201000110000010 0?0000100100001223010100100 11??211?2??0???00000?02
211101011000111 22?13110000?0111110??0101?112??02?100101010010 0??2002210010013201 1?0
10??000??1102?101?00000?????????10110020?????????????2?12102?01?2?(0
1)0000??1??200101?2101210110001110 1110?11

Leptocleidus_capensis
010001?1112?101010200200 1?0000?10??0000??01001022(23)201010?0??01??21?????0?????????0
221110?01?00011122?12110001????1110?0111??(12)2?111111010101?????????? 210010??320?1
?0100?0?0?0?????1??2????00????0????????????
2???1?0??10?1??????

Leptocleidus_superstes
??0?0??1?1?0????10(12)?????1?????????????????0?10222201010?100011121?0011?01??????022
11???????????122??31????1???(12)0?01?0132011001000

??00?110?11102???1011001?10110011020??1?100200102??????????????????01???02001012?0????
?????????????????

Cimoliasaurus_valdensis
??
??1100???1?1(12)1001002320?110100000001???
??1??????1011000???001???02001021?0????????0??????
??1???

MIWG_1997_302
??
??01?01??0?1??1010??00??10??11
02??????????????1???1?02???1??01?10?0???
?

Brancasaurus_brancai
0010?000100000(01)?101002001?00000?0?1000???0101?02223010?0?00?01110110112010100010
0022?????011000???0???????????01???100?1110???2??121100111?120100??20014100100232012?
01011000001101011020000101?1011???1?01?0201?10?0?210?0201012102101121???01110020010
22200321?11???110?1???1?0

GWWU_A3_B2
??
???01?12?20?2001111?000?111001
1100002011101????1????????????0?210???01012102101021????0112?02000022210?1???1?0??????
??1???

Speeton_Clay_plesiosaurian
??
??2???????????2101012320120011110010011201
111000?20?1111??1011?1??20??1??002?????0101210110112OO??00102103001022?1021001100011
101?11???

Wapuskanectes_betsynichollsae
??
??1??1??
0???????????2101(0
1)2?110?1110110?10??3?????????????200???01???03000022???????????????????0???

Futabasaurus_suzukii
00??000?1?0?00??0??00?0?2?0000?????????????????????0???1???????????????????????????????????
0110000???????????????100??????0????(12)????100001100???????????????11?22?2022001111?01
0?11110111000??????????????????????????????01301?1??01?0?1100200000220300102221122101 1
00011101(12)10?01

Callawayasaurus_colombiensis
000010?0?10000(12)?10100?0020?000?10????????010100002201010100011110 11?(12)02?1010??1
?002211001????0?0???2?1100???1?1101(01)?0??20?????2??010000110012??????????52101022320
22001111(01)0100111211110???????????200100?11001120010?10?01?????????00??0(01)??100?22
0300102?3101200?10(01)0111??2?1???

Kaiwhekea_katiki
00001010??000???1020020020?000?????????11????0?0?32?2111000?00?????????????????????????
???????????????????????0101?10??1000??????0300001120?2???????????51011122320?2?0111?1010
0?11111?10???2????0???????????????????????????????????????000??00??11?32?11??3?12110100(0
1)0012?1??0???

Aristonectes_parvidens
00?010??1?0000201??00200200000??00???(01)?11??01010?3212?1?0000?00?1?01212010????????
???????0?10000??????????????0101010??1000???????3000011200?1101101?02?1111???3???20011
1??01?0??
?????????????0?

Libonectes_morgani
010010?0110000201020020020000000?00110001001110??0?21??111?00010?010?20201010?001002
21100101?00?0?122?1200???2101000101?2000?112000101001?0012???1?????1621?122?320?2001
11??01??1???????????????????21011??????11100?0?100?1?????????????00??00????????10???????2
00??01?1????????0?

Hydrotherosaurus_alexandrae
000010?0??0000201(12)100?002??0000?0011000100111?????2121?111??01?????????????????????
????????????????????????????100010?1?01??112???10000110012???1?????1521112223202200111
?101001110011100002011?11?1001(0
1)00001011200?020????120111011000100?000??12031010123102300110(01)011101211???

Edgarosaurus_muddi
100101?02100102011101000 1??0?0??001000010?2001022200111010001 10?01?02?2?1?0????1002
211?01??????10122?1300100201100011011110?120011(23)110111100?010100000121001?113201
1201000000000???01??00?00??????0010?2?0
?3?10??0101??01211?0?

Plesiopleurodon_wellesi
000100?0?100102?1120?000???2?0??????????????1???222201010?10?11??????????????????????????
???????????????????????0001?11???110?1????1(12)000210?0?????????????100?011320?120100?0?
0?0??0??110(0 2)???(0
1)0??101?????????????20110?1?01????????????????????????????(23)(01)?1012?1??????????????????
???

QM_F51291.2
0001002011001120112 0?000(12)???2?0??00??01010??1???222201010110011 1101?????????????1?0
22??001???00???1?2?100????1??001??????1???11????100011020?11101000?0210001(01)02320?12
01001000100100?1100?0010101001 1??1???????20?1??????????201001210112001101101112001 01
221022101100011101(1 2)10???

Colymbosaurus_svalbardensis
???
???1???110
000?21101011?0??????????0??????0??0??1?1101?1???200??1010120?101012(12)102310110211110
1211??1

PMO_224.248
00100000210?0101102021001?1000110??????????010?102102??0000?110?1010?01?1???11110011
0?00?01000011200?000?110??02??010001000???2??0200001100120111111???52001(12)2?320120
011103010011??0110?????????????21011001010201?010202?13????????????201??100???02001022
?1?2?101?0201???121112?

List of references for individual OTUs

Table A5.1: List over references for the operational taxonomic units for adding the character states for new characters.

Operational taxonomic unit	**References**
Yunguisaurus liae	Cheng et al., 2006; Sato et al. 2010; Shang et al., *in press*.
Pistosaurus postcranium	von Huene, 1948; Sues, 1987
Augustasaurus hagdorni	Rieppel et al., 2002; Sander et al., 1997
Bobosaurus forojuliensis	Dalla Vecchia, 2006; Fabbri et al., 2014
Anningsaura lymense	Vincent and Benson, 2012
Stratesaurus taylori	Benson et al., 2012, 2015
Avalonectes arturi	Benson et al., 2012
Meyerasaurus victor	Smith and Vincent, 2010
Maresaurus coccai	Gasparini, 1997
Borealnectes russelli	Sato and Wu, 2008
Rhomaleosaurus megacephalus	Cruickshank, 1994; Smith, 2007, 2015
Archaeonectes	NA
Rhomaleosaurus cramptoni	Smith, 2007; Smith and Dyke, 2008
Rhomaleosaurus zetlandicus	Smith, 2007, 2013; Taylor, 1992a 1992b
Rhomaleosaurus thortoni	Smith and Benson, 2014
Thalassiodrracon hawkinsii	Benson et al., 2011a; Storrs and Taylor, 1996
Hauffiosaurus longirostris	Benson et al., 2011b
Hauffiosaurus tomistomimus	Benson et al., 2011b
Hauffiosaurus zanoni	Vincent, 2011
Marmornectes andrewi	NA
Peloneustes phiarchus	Ketchum, 2008; Ketchum et al., 2011
Simolestes vorax	NA
Pliosaurus BRSMGCs332	NA
Pliosaurus brachydeirus	Knutsen, 2012
Gallardosaurus iturraldei	Gasparini, 2009
Liopleurodon rossicus	Halstead, 1971
Pliosaurus andrewsi	Knutsen, 2012; Tarlo, 1960
Liopleurodon ferox	Barrientos-Lara et al., 2015; Noè et al., 2003
Kronosaurus	Cruickshank et al. 1999; Kear et al., 2006a
Brachauchenius eulerti	Schumacher et al., 2013
Brachauchenius lucasi	Albright et al., 2011; Everhart, 2007; Hampe, 2005
Brachauchenius MNA V9433	NA
QM F51291	Buchy et al., 2006

Attenborosaurus conybeari	Wyse Jackson, 2004
Plesiosaurus dolichodeirus	Vincent and Taquet, 2010
Eoplesiosaurus antiquior	Benson et al., 2012
Eretmosaurus rugosus	Brown, 1994
Westphaliasaurus simonsensii	Schwermann and Sander, 2011
Seeleyosaurus guilelmiimperatoris	Großmann, 2007
Microcleidus tournemirensis	Bardet et al., 1999
Microcleidus brachypterygius	Benson et al., 2012
Microcleidus homospondlyus	Brown et al., 2013
Plesiopterys wildi	O'Keefe, 2004
Cryptoclidus eurymerus	Andrews, 1910; Brown, 1981; Brown et al., 1994
Muraenosaurus leedsii	Andrews, 1910; Brown, 1981
Tricleidus seeleyi	Andrews, 1910; Brown, 1981
Picrocleidus' beloclis	Andrews, 1910; Brown, 1981
Tatenectes laramiensis	O'Keefe et al., 2011; O'Keefe and Street, 2009
Pantosaurus striatus	O'Keefe and Wahl, 2003
Plesiosaurus' mansellii	Hulke, 1970
Spitrasaurus spp.	Knutsen et al., 2012a
Djupedalia engeri	Knutsen et al., 2012b
Colymbosaurus svalbardensis	Knutsen et al., 2012c; Roberts et al., 2017
Colymbosaurus megadeirus	Benson and Bowdler, 2014; Roberts et al., 2017
Abyssosaurus nataliae	Berezin, 2011
Umoonasaurus demoscyllus	Kear et al., 2006b
Nichollssaura borealis	Druckenmiller and Russel, 2008
Leptocleidus capensis	NA
Leptocleidus superstes	Kear and Barrett, 2011
Cimoliasaurus valdensis	Benson et al., 2013
MIWG 1997 302	NA
Brancasaurus brancai	Sachs et al., 2016
GWWU As B2	NA
Speeton Clay plesiosaurian	NA
Wapuskanecttes betsynicholls	Druckenmiller and Russell, 2006
Futabasaurus suzukii	Sato et al., 2006
Callawaysaurus colombiensis	Welles, 1962
Kaiwhekea katiki	Cruickshank and Fordyce, 2002
Aristonectes paridens	Gasparini et al., 2001, 2003
Libonectes morgani	Sachs and Kear, 2017
Hydrotherosaurus alexandrae	Welles, 1943
Edgarosaurus muddi	Druckenmiller, 2002
Plesiopleurodon wellesi	Carpenter, 1996

QM F5191.2	NA

Complete trees for Plesiosauria

The complete consensus tree for Plesiosauria generated for Chapters 3 and 4 (Figure A5.4), and the resampled tree (Figure A5.5).

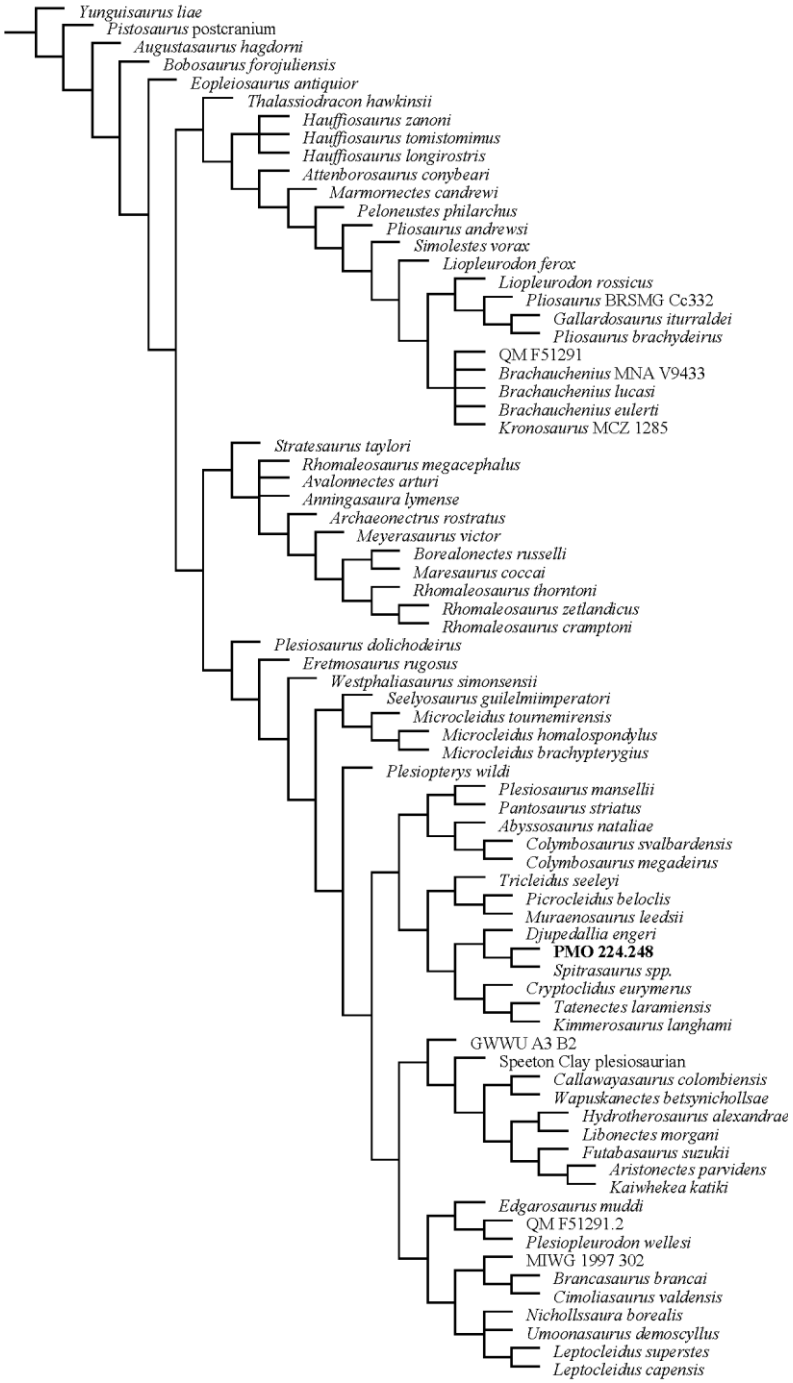

Figure A5.4: The complete consensus tree recovered for Plesiosauria out of 144 MPTs with a score of 1320, with a total of 2190487647 rearrangements made.

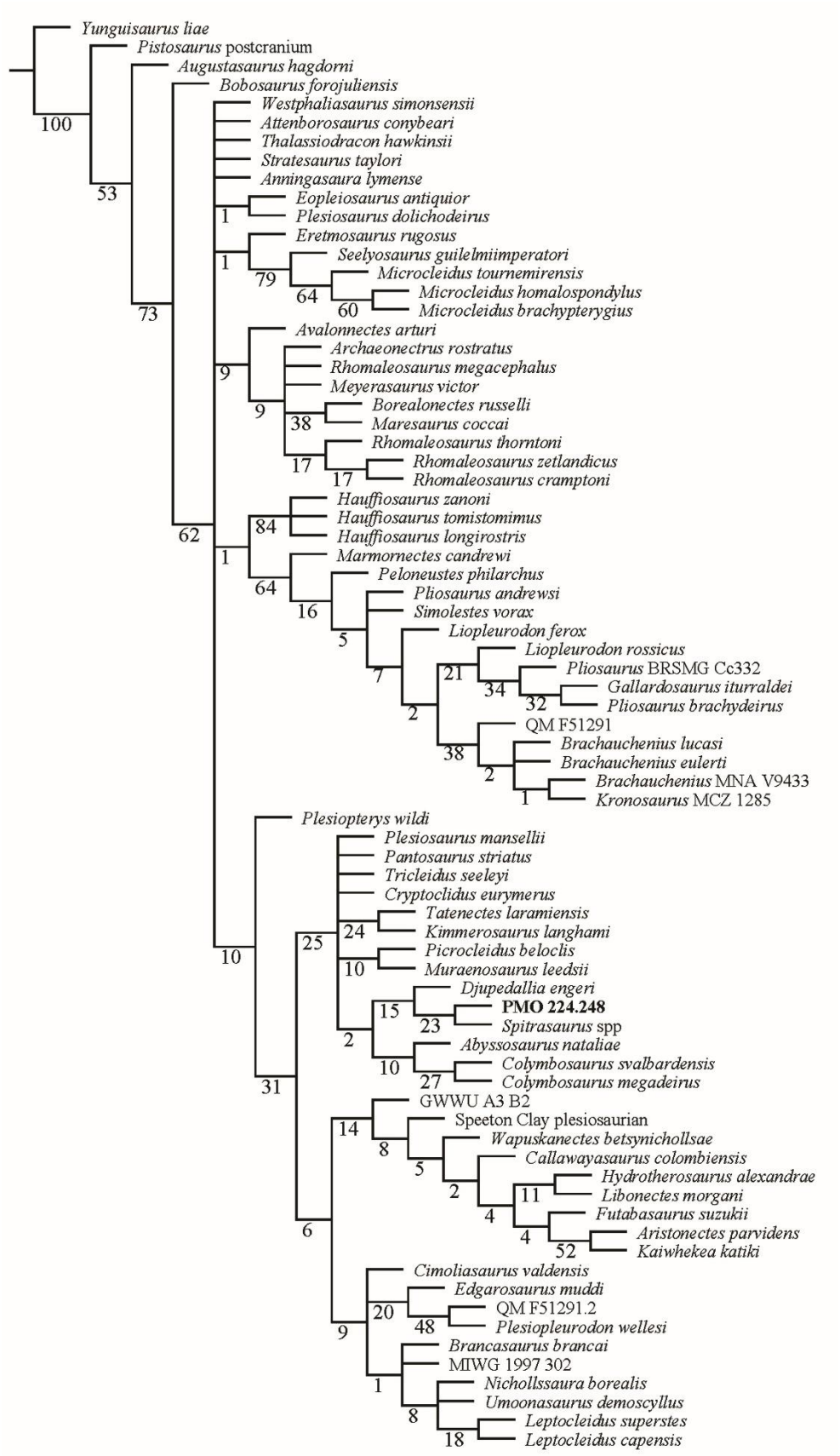

Figure A5.5: Resulting tree of Plesiosauria from bootstrap resampling (1000 replicates). Bootstrap support is reported below the nodes.

Literature cited

Albright III, L. B., Gillette, D. D. and A. L. Titus. 2007. Plesiosaurs from the Upper Cretaceous (Cenomanian–Turonian) Tropic Shale of southern Utah, part 1: new records of the pliosaur *Brachauchenius lucasi. Journal of Vertebrate Paleontology* 27: 31-40.

Andrews, C. W. 1910. A descriptive catalogue of the Marine Reptiles of The Oxford Clay Based on the Leeds Collection in the British Museum (Natural History). *British Museum (Natural History)*. London.

Bardet, N., Godefroit, P. ad J. Sciau. 1999. A new elasmosaurid plesiosaur from the Lower Jurassic of Southern France. Palaeontology 42: 927-952.

Barrientos-Lara, J. I., Fernández, M. S. and J. Alvarado-Ortega. 2015, Kimmeridgian pliosaurids (Sauropterygia, Plesiosauria) from Tlaxiaco, Oaxaca, southern Mexico:*Revista Mexicana de Ciencias Geológicas* 32: 293-304.

Benson, R. B. J., Bates, K. T., Johnson, M. R. and P. J. Withers. 2011a. Cranial anatomy of Thalassiodracon hawkinsii (Reptilia, Plesiosauria) from the Early Jurassic of Somerset, United Kingdom. *Journal of Vertebrate Paleontology* 31: 562-574.

Benson, R. B. J, Ketchum, H. F., Noè, L. F. and M. Gómez-Pérez. 2011b. New information on *Hauffiosaurus* (Reptilia, Plesiosauria) based on a new species from the Alum Shale Member (lower Toarcian: Lower Jurassic) of Yorkshire, UK. *Palaeontology* 54: 547-571.

Benson, R. B. J., Evans, M. and P. S. Druckenmiller. 2012. High Diversity, Low Disparity and Small Body Size in Plesiosaurs (Reptilia, Sauropterygia) from the Triassic–Jurassic Boundary. *PLOS ONE* 7: e31838.

Benson, R. B. J., Ketchum, H. F., Naish, D. and L. E. Turner. 2013. A new leptocleidid (Sauropterygia, Plesiosauria) from the Vectis Formation (Early Barremian–early Aptian; Early Cretaceous) of the Isle of Wight and the evolution of Leptocleididae, a controversial clade. *Journal of Systematic Palaeontology* 11: 233-250.

Benson, R. B. J. and T. Bowdler. 2014. Anatomy of Colymbosaurus megadeirus (Reptilia, Plesiosauria) from the Kimmeridge Clay Formation of the U.K., and high diversity amoung Late Jurassic plesiosauroids. *Journal of Vertebrate Paleontology* 34: 1053-1071

Benson, R. B. J. and P. S. Druckenmiller. 2014. Faunal turnover of marine tetrapods of the Jurassic-Cretaceous transition. *Biological Reviews* 89: 1-23

Benson, R. B. J., Evans, M. and M. A. Taylor. 2015. The anatomy of *Stratesaurus* (Reptilia, Plesiosauria) from the lowermost Jurassic of Somerset, United Kingdom. *Journal of Vertebrate Paleontology* 35: e933739.

Berezin, A. Y. 2011. A New Plesiosaur of the Family Aristonectidae from the Early Cretaceous of the Center of the Russian Platform. *Paleontological Journal* 45: 648-660.

Brown, D. S. 1981. The English Upper Jurassic Plesiosauridae (Reptilia) and a review of the phylogeny and classification of the Plesiosauia. *Bulletin of the British Museum (Natural History), Geology* 35: 253-347

Brown, D. S. 1994. *Plesiosaurus rugos* Owen, 1840 (C'currently *Ertmosaurus rugosus*; Reptilia, Plesiosauria): proposed designation of a neotype. *Bulletin of Zoological Noemclature* 51: 247-249.

Brown, D. S., Milner, A. S. and M. A. Taylor. 1986. New material of the plesiosaur *Kimmerosaurus langhami* Brown from the Kimmeridge clay of Dorset. *Bulletin of the British Museum (Natural History*) 40: 225-234

Brown, D. S., Vincent, P. and N. Bardet. 2013. Oseological redescription of the skull of *Microcleidus homalospondylus* (Sauropterygia, Plesiosauria) from the Lower Jurassic of England. *Journal of Paleontology* 87: 537-549.

Buchy, M-C., Frey, E., Salisbury, S. W., Stinnesbeck, W., López-Oliva, J. G. and M. Götte. 2006. *Neues Jahrbuch für Paläontologie Abhandlungen* 240: 241-270.

Carpenter, K. 1996. A review of short-necked plesiosaurs from the Cretaceous of the western interior, North America. *Neues Jahrbuch für Geologie und Paläontologie. Abhandlungen* 201: 259p.

Cheng, Y-N., Sato, T., Wu, X-C. and C. Li. 2006. First complete pistosauroid from the Triassic of China. *Journal of Vertebrate Paleontology* 26: 501-504

Cruickshank, A. R. I. 1994. Cranial anatomy of the Lower Jurassic pliosaur *Rhomaleosaurus megacephalus* (Stuchbury) (Reptilia: Plesiosauria). *Philosophical Transactions of the Royal Society of London B* 343: 247-260.

Cruickshank, A. R. I., Fordyce, R. E. and J. A. Long. 1999. Recent developments in Australian sauropterygians palaeontology (Reptilia: Sauropterygia). *Records of the Western Australian Museum* 1999: 201-205

Cruickshank, A. R. I. and R. E. Fordyce. 2002. A new marine reptile (Sauropterygia) from new Zeland: further evidence for a Late Cretaceous austral radiation of cryptoclidid plesiosaurs. *Palaeontology* 45: 557-575.

Dalla Vecchia, F. M. 2006. A new sauropterygian reptile with plesiosaurian affinity from the Late Triassic of Italy. *Rivista Italiana si Palenotologia e Stratigrafia* 112: 207-225.

Druckenmiller, P. S. 2002. Osteology of a new plesiosaur from the Lower Cretaceous (Albian) Thermopolis Shale of Montana. *Journal of Vertebrate Paleontology* 22: 29-42.

Druckenmiller, P. S. and A. P. Russell. 2006. A new elasmosaurid plesiosaur (Reptilia: Sauropterygia) from the Lower Cretaceous Clearwater Formation, North-eastern Alberta, Canada. *Paludicola* 5: 184-199.

Druckenmiller, P. S. and A. P. Russell. 2008. Skeletal anatomy of an exceptionally complete specimen of a new genus of plesiosaur from the Early Cretaceous (Early Albian) of north-eastern Alberrta, Canada. Palaeontographica Abt. A, Paläozoologie-Stratigraphie 283: 1-33.

Everhart, M. J. 2007. Historical note on the 1884 discovery of *Brachauchenius lucasi* (Plesiosauria; Pliosauridae) in Ottawa County, Kansas. *Transactions of the Kansas Academy of Science* 110: 255-258.

Fabbri, M., Dalla Vechia, F. M. and A. Cau. 2014. New information on Bobosaurus forojuliensis (Reptilia: Sauropterygia): implications for plesiosaurian evolution. *Historical Biology* 26: 661-669.

Gasparini, Z. 1997. A new pliosaur from the Bajocian of the Neuquen Basin, Argentina. *Palaeontology* 40: 135-147.

Gasparini, Z. 2009. A new Oxfordian pliosaurid (Plesiosauria, Pliosauridae) in the Caribbean Seaway. *Palaeontology* 52: 661-669.

Gasparini, Z., Casadio, S., Fernandez, M. and L. Salgado. Marine reptiles from the Late Cretaceous of northern Patagonia. *Journal of South American Earth Sciences* 14: 51-60.

Gasparini, Z., Bardet, N.m Martin, J. E. And M. Fernandez. The elasmosaurid plesiosaur *Aristonectes* Cabrera from the latest Cretaceous of South America and Antarctica. *Journal of Vertebrate Paleontology* 23: 104-115.

Großmann, F. 2007. The taxonomic and phylogenetic position of the plesiosauroidea from the Lower Jurassic Posidonia Shale of South-West Germany. *Palaeontology* 50: 545-564.

Halstead, L. B. 1971. *Liopleurodon rossicus* (Novozhilov) – A pliosaur from the Lower Volgian of the Moscow Basin. *Palaeontology* 14: 566-570.

Hampe, O. 2005. Considerations on a *Brachauchenius* skeleton (Pliosauroidea) from the lower Paja Formation (late Barremian) of Villa de Leyva area (Colombia). *Mitt. Mus. Nat.kd. Berl., Geowiss. Reihe* 8: 37-51.

von Huene, F. 1948. *Pistosaurus*, a Middle Triassic plesiosaur. *American Journal of Science* 246: 46-52.

Hulke, J. W. 1870. Note on some Plesiosaurian Remains obtained by J. C. Mansel Esq. F.G.S., in Kimmeridge Bay, Dorset. *Quarterly Journal of the Geological Society of London* 26: 611-622

Kear, B. P., Schroeder, N. I., Vickers-Rich, P. and T. H. Rich. 2006a. Early Cretaceous high latitude marine reptile assemblages from Southern Australia. *Paludicola* 5: 200-205.

Kear, B. P., Schroeder, N. I. and M. S. Y. Lee. 2006. An archaic crested plesiosaur in opal from the Lower Cretaceous high-latitude deposits of Australia. *Biology Letters* : doi:10.1098/rsbl.2006.0504.

Kear, B. P. and P. M. Barrett. 2011. Reassessment of the Lower Cretaceous (Barremian) pliosauroid *Leptocleidus superstes* Andrews, 1922 and other plesiosaur remains from the nonmarine Wealden succession of southern England. *Zoological Journal of the Linnean Society* 161: 663-691.

Ketchum, H. F. 2008. The anatomy, taxonomy and systematics of three British Middle Jurassic pliosaurs (Sauropterygia: Plesiosauria), and the phylogeny of Plesiosauria. PhD thesis. University of Cambridge, Cambridge.

Ketchum, H. F. and R. B. J. Benson. 2011. The cranial anatomy and taxonomy of *Peloneustes philarchus* (Sauropterygia, Pliosauridae) from the Peterborough Member (Callovian, Middle Jurassic) of the United Kingdom. *Palaeontology* 54: 639-665.

Knutsen, E. M. 2012. A taxonomic revision of the genus *Pliosaurus* (Owen, 1841a) Owen, 1841b. *Noregian Journal of Geology* 92: 259-276.

Knutsen, E. M., Druckenmiller, P. S. And J. H. Hurum. 2012a. Two new species of long-necked plesiosaurians (Reptilia-Sauropterygia) from the Upper Jurassic

(Middle Volgian) Agardhfjellet Formation of central Spitsbergen. *Norwegian Journal of Geology* 92: 187-212

Knutsen, E. M., Druckenmiller, P. S. And J. H. Hurum. 2012b. A new plesiosaurid (Reptilia-Sauropterygia) from the Agardhfjellet Formation (Middle Volgian) of central Spitsbergen, Norway. Norwegian Journal of Geology 92: 213-234

Knutsen, E. M., Druckenmiller, P. S. And J. H. Hurum. 2012c. Redescription and taxonomic clarfication of '*Tricleidus' svalbardensis* based on new material from the Agardhfjellet Formation (Middle Volgian). Norwegian Journal of Geology 92: 175-186.

Noè, L.F., Liston, J.J. and M. Evans. 2003. The first relatively complete exoccipital-opisthotic from the braincase of the Callovian pliosaur, *Liopleurodon*. *Geological Magazine* 140: 479-486

O'Keefe, F. R. 2004. Preliminary description and phylogenetic position of a new plesiosaur (Reptilia: Sauropterygia) from the Toarchian of Holzmaden, Germany. *Journal of Paleontology* 78: 973-988.

O'Keefe, F. R. and W. J. R. Wahl. 2003. Current taxonomic status of the plesiosaur *Pantosaurus striatus* from the Upper Jurassic Sundance Formation, Wyoming. *Paludicola* 4: 37-46.

O'Keefe, F. R. and H. P. Street. 2009. Osteology of the cryptocleidoid plesiosaur *Tatenectes laramiensis*, with comments on the taxonomic status of the Cimoliasauridae. *Journal of Vertebrate Paleontology* 29: 48-57.

O'Keefe, F. R., Street, H. P., Wilhelm, B. C., Richards, C. D. and H. Zhu. 2011. A new skeleton of the cryptoclidid plesiosaur *Tatenectes laramiensis* reveals a novel body shape among plesiosaurs. *Journal of Vertebrate Paleontology* 31: 330-339.

Rieppel, O. C., Sander, P. M. and G. W. Storrs. 2002. The skull of the pistosaur *Augustasaurus* from the Middle Triassic of North-western Nevada. *Journal of Vertebrate Paleontology* 22: 577-592.

Roberts, A. J., Druckenmiller, P. S., Delsett, L. L. and J. H. Hurum. 2017. Osteology and relationships of Colymbosaurus Seeley, 1874, based on new material of C. svalbardensis from the Slottsmøya Member, Agardhfjellet Formation of central Spitsbergen. *Journal of Vertebrate Paleontology* X: e1278381

Sachs, S., Hornug, J. J. and B. P. Kear. 2016. Reappraisal of Europe's most complete Early Cretaceous plesiosaurian: *Brancasaurs brancai* Wegner, 1914 from the "Wealsen facies" of Germany. *PeerJ* 4: e2813

Sachs, S. and B. P. Kear. 2017. Redescription of the elasmosaurid plesiosaurian *Libonectes atlasense* from the Upper Cretaceous of Morocco, *Cretaceous Research*: doi:10.1016/j.cretres.2017.02.017.

Sander, P. M., Rieppel, O. C. and H. Bucher. 1997. A new pistosaurid (Reptilia: Sauropterygia) from the Middle Triassic of Nevada and its implications for the origin of the plesiosaurs. *Journal of Vertebrate Paleontology* 17: 526-533.

Sato, T., Hasegawa, Y. and M. Manabe. A new elasmosaurid plesiosaur from the Upper Cretaceous of Fukushima, Japan. *Palaeontology* 49: 467-484.

Sato, T. and X-C. Wu 2008. A new Jurassic pliosaur from Melville Island, Canadian Arctic Archipelago. *Canadian Journal of Earth Sciences* 45: 303-320.

Sato, T., Cheng, Y-N., Wu, X-C. and C. Li. 2010. Osteology of *Yunguisaurus* Cheng *et al.*, 2006 (Reptilia; Sauropterygia), a Triassic pistosauroid from China. *Paleontological Research* 14: 179-195.

Schumacher, B. A., Carpenter, K. and M. J. Everhart. 2013. A new Cretaceous Pliosaurid (Reptilia, Plesiosauria) from the Carlile Shale (middle Turonian) of Russell County, Kansas, *Journal of Vertebrate Paleontology* 33: 613-628.

Schwermann, L. and P. M. Sander. Osteologie und Phylogenie von *Westphaliasaurus simonsensii*: Ein neuer Plesiosauride (Sauropterygia) aus dem Unteren Jura (Pliensbachium) con Sommersell (Kreis Höxter), Nordrhein-Westfalen, Deutschland. *Geologie und Paläontologie in Westfalen* 79: 5-60.

Shang, Q-H., Sato, T., Li, C. and X-C. Wu. *in press*. New osteological information from a 'juvenile' specimen of *Yunguisaurus* (Sauropterygia; Pistosauroidea). *Palaeoworld.*

Smith, A. S. 2007. Anatomy and Sytematic of the Rhomaleosauridae (Sauropterygia: Plesiosauria). PHD thesis. National University of Ireland, University College of Dublin. Dublin.

Smith, A. S. 2015. Reassessment of *'Plesiosaurus' megacephalus* (Sauropterygia: Plesiosauria) from the Triassic-Jurassic boundary, UK. *Palaeontologia Electronica* 18.1.20A: 1-19.

Smith, A. S. and G. J. Dyke. 2008. The skull of the giant predatory pliosaur *Rhomaleosaurus cramptomi*: implications for plesiosaur phylogenetics. *Naturwissenschaften* 95: 975-980.

Smith, A. S. and P. Vincent. 2010. A new genus of plesiosaur (Reptilia: Sauropterygia) from the Lower Jurassic of Holzmaden, Germany. *Palaeontology* 53: 1049-1063.

Smith, A. S. and R. B. J. Benson. 2014. Osteology of *Rhomaleosaurus thorntoni* (Sauropterygia: Romaleosauridae) from the Lower Jurassic (Toarchian) of Northamptonshire, England. *Monograph of the Palaeontographical Society* 168: 1-40, pls 1-35.

Storrs, G. W. and M. A. Taylor. 1996. Cranial anatomy of a new plesiosaur genus from the lowermost Lias (Rhaetian/Hettangian) of Street, Somerset, England. *Journal of Vertebrate Paleontology* 16: 403-420.

Sues, H.D. 1987. Postcranial skeleton of *Pistosaurus* and interrelationships of the Sauropterygia. *Zoological Journal of the Linnean Society* 90: 109-131.

Tarlo, L. B. 1960. A review of Upper Jurassic Pliosaurs. *Bulletin of the British Museum (Natural History), Geology* 4:145-189.

Taylor, M. A. 1992a. Functional Anatomy of the Head of the Large Aquatic Predator Rhomaleosaurus zetlandicus (Plesiosauria, Reptilia) from the Toarcian (Lower Jurassic) of Yorkshire, England. *Philosophical Transactions: Biological Sciences* 335: 247-280.

Taylor, M. A. 1992b. Taxonomy and taphonomy of *Rhomaleosaurus zetlandicus* (Plesiosauria, Reptilia) from the Toarcian (Lower Jurassic) of the Yorkshire coast. *Proceedings of the Yorkshire Geological Society* 49: 49-55.

Vincent, P. 2011. A re-examination of Hauffiosaurus zanoni, a pliosauroid from the Toarcian (Early Jurassic) of Germany. *Journal of Vertebrate Paleontology* 31: 340-351.

Vincent, P. and R. B. J. Benson. 2012. *Anningasaura*, a basal plesiosaurian (Reptilia, Plesiosauria) from the Lower Jurassic of Lyme Regis, United Kingdom. *Journal of Vertebrate Paleontology* 32: 1049-1063.

Vincent, P. and P. Taquet. 2010. A plesiosaur specimen from the Lias of Lyme Regis: the second ever discovered plesiosaur by Mary Anning. *Geodiversitas* 32: 377-390.

Welles, S.P. 1943. Elasmosaurid plesiosaurs with a description of the new material from California and Colorado. *University of California Memoirs* 13:125-254, pls.12-29.

Welles, S. P. 1962. A new species of elasmosaur from the Aptian of Colombia and a review of the Cretaceous plesiosaurs. University of California. *Publications of the Geological Society* 44: 1-96.

Wyse Jackson, P. N. 2004. Thomas Hawkins, Lord Cole, William Sollas and all: casts of Lower Jurassic marine reptiles in the Geological Museum, Trinity College, Dublin, Ireland. *The Geological Curator* 8: 11-18.

Appendix 6

Supplementary information for Chapters 3

Supplementary figures for Chapter 3

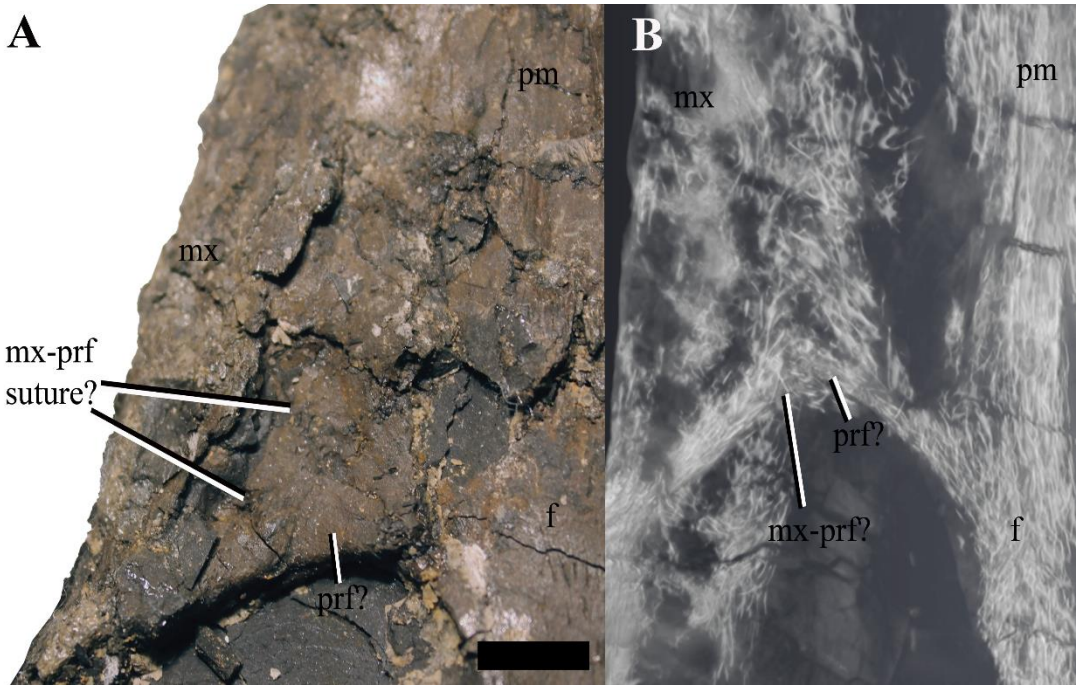

Figure A6.1: The prefrontal of PMO 224.248 as suggested by bone fibre orientation. **A**, a photo of the left preorbital region; **B**, a CT slice of the same area. **Abbreveations:** f, frontal; mx, maxilla; pm, premaxilla; prf, prefrontal. Scale bar equals 2 cm.

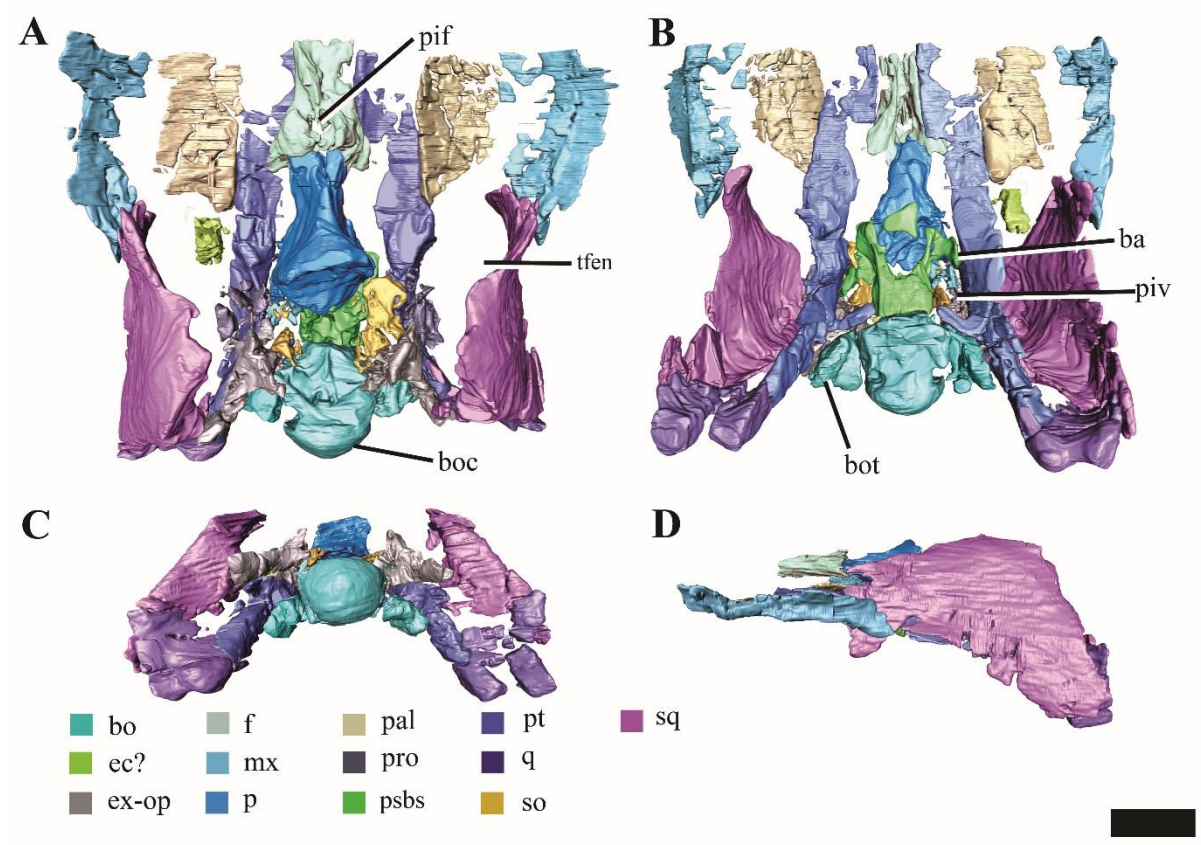

Figure A6.2: The virtual reconstruction of the posterior region of the skull of PMO 224.248, in A) dorsal, B) ventral, C) posterior and D) lateral views. **Abbreveations**: **ba**, basal articulation; **bo**, basioccipital; **boc**, basioccipital condyle; **bot**, basioccipital tuber; **ec**, ectopterygoid?; **ex-op**, exoccipital opisthotic; **f**, frontal; **max**, maxilla; **p**, parietal; **pif**, pineal foramen; **piv**, posterior interpterygoid vacuity; **pro**, prootic; **psbs**, parabasisphenoid; **pt**, pterygoid; **q**, quadrate; **so**, supraoccipital; **sq**, squamosal; **tfen**, temporal fenestra. Scale bar equals 2 cm.

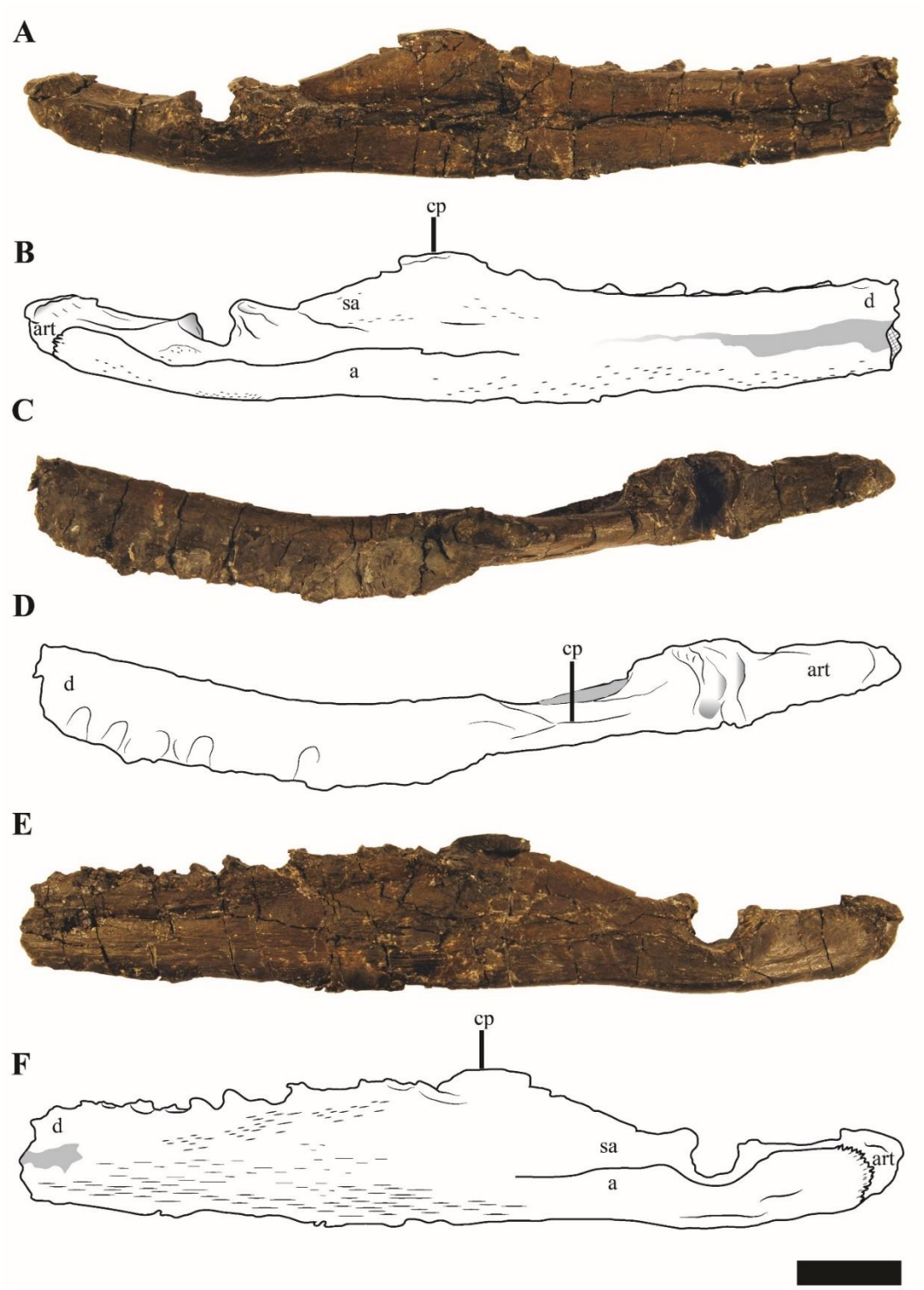

Figure A6.3: The left mandible of PMO 224.248 photographs and interpretations in medial (A-B), dorsal (C-D) and lateral views (E-F). **Abbreviations**: **a**, angular; **art**, articular; **cp**, coronoid process; **sa**, surangular. Scale bar equals 1 cm.

Figure A6.4: The right mandible of PMO 224.248 in A) medial, B) dorsal, C) lateral and D) ventral views. **Abbreviations**: **part**, prearticular; **spl**, splenial.

Figure A6.5: An isolated tooth from PMO 224.248 in A) lingual and B) axial views. **Abbreviations**: **redf**, reabsorption facet; **wf**, wear facet? Scale bar equals 0.5 mm.

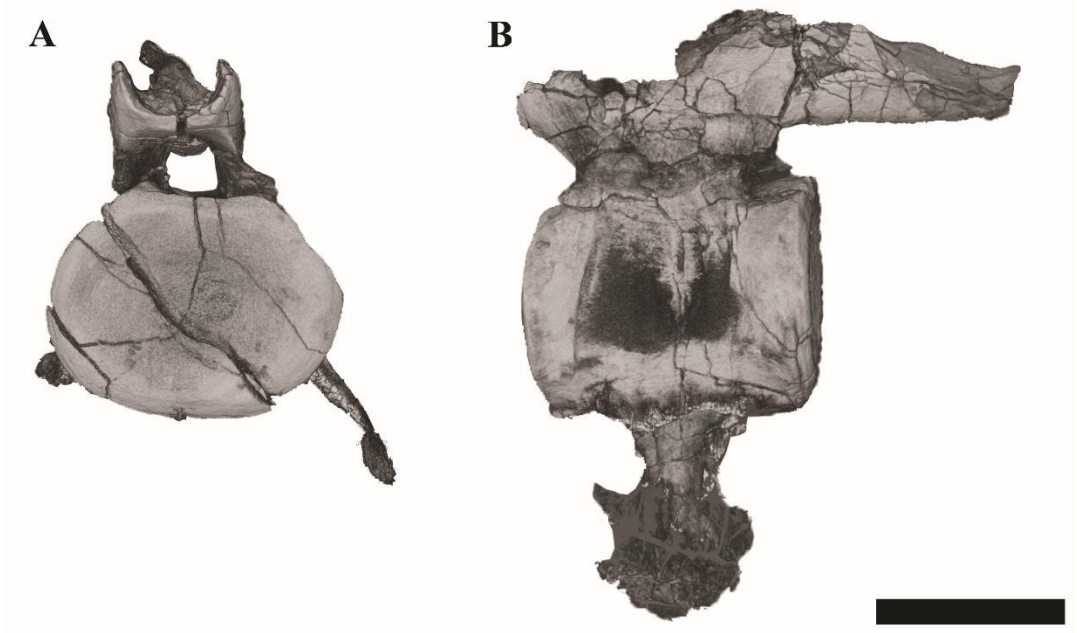

Figure A6.6: The volume rendering of the 8th cervical from PMO 224.248. In **A**, anterior and **B**, lateral views. Scale bar equals 2 cm.

Figure A6.7: The right humerus of PMO 224.248 during preparation. Scale bar equals 5 cm

Figure A6.8: The preaxial accessary elements of the right humerus. Scale equals 3 cm

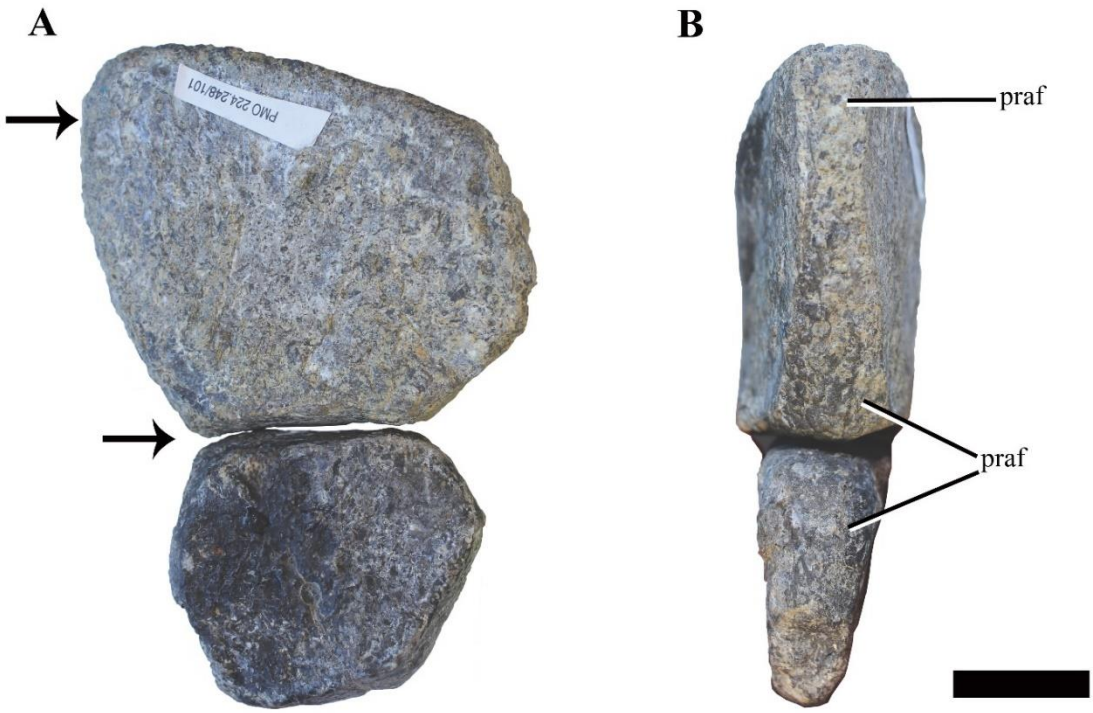

Figure A6.9: The left radius and radiale from PMO 224.248 illustrating preaxial facets. Arrows mark the point of possible insertion. **Abbreviations**: **praf**, preaxial facet. Scale equals 2 cm.

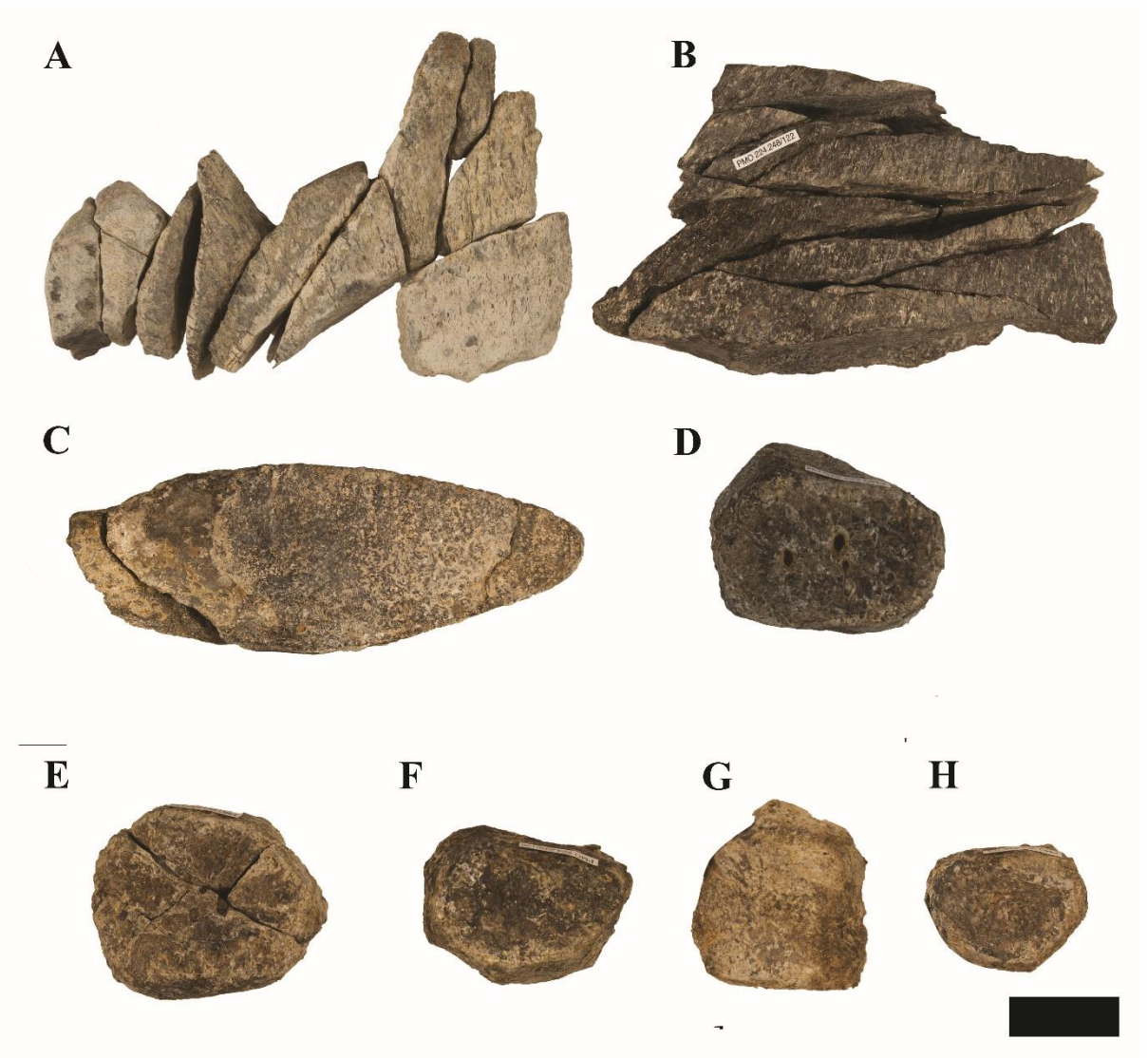

Figure A6.10: The fragmentary femora and selected hind limb elements from PMO 224.248. **A**, the preserved distal portion of the right femur in dorsal view. **T**he left femur in **B**, ventral and **C**, distal views. Mesopodial elements from the left limb: **D**, **a**stragalus; **D**, fibulare; **E-F**, distal tarsal elements. Scale equals 2 cm.

Figure A6.11: The left hindlimb of PMO 224.248 during preparation. Scale bar equals 5 cm.

Measurements for PMO 224.248

Table A6.1: Selected cranial measurements from PMO 224.248 in mm.

Cranial measurements of PMO 224.248	**mm**	
Anteroposterior length of skull	225	
Mediolateral width of skull posteriorly	112	
Mediolateral width of skull over maxilla (max)	120	
Anteroposterior length of premaxilla	82	
Anteroposterior length of frontal	70	
Mediolateral width of frontal (max)	39	
Anteroposterior length of parietal	30	
Dorsoventral height of squamosal	~41	
Anteroposterior length of orbit	60	
Mediolateral width of orbit	55	
Anteroposterior length of skull anterior to orbit	86	
Anteroposterior length of pterygoid	122	
Mediolateral width of left quadrate over condyle	24	
Mediolateral width of basisphenoid posteriorly	16	
Anteroposterior length of antorbital fenestra	80	
Anteroposterior length of posterior interpterygoid	3	
Mediolateral width of vomer	29	
Anteroposterior length of left palatine	~100	
Mediolateral width of basioccipital condyle	21	
Dorsoventral height of basioccipital condyle	~16	
Anteroposterior length (ventral) of basioccipital condyle	26	
Left mandible		
Anteroposterior length (preserved)	175	
Anteroposterior length of retroarticular process	34	
Medial-mesial width (max) of dentary	20	
Mediolateral width of glenoid	18	
Dorsoventral height	31	
Right mandible		
Anteroposterior length (preserved)	140	
Anteroposterior length of retroarticular process	33	
Medial-mesial width (max) of dentary	~12	
Mediolateral width of glenoid	18	

Dorsoventral height	33	

Table A6.2: Selected vertebral measurements from PMO 224.248 in mm. **Abbreviations**: **aa**, atlas-axis complex; **H/L**, height/length ratio; **H/W**, height/width ratio; **na**, not available; **W/L**, width/length ratio.

Vertebral measurements of PMO 224.248						
Number	**Height**	**Width**	**Length**	**H/L ratio**	**H/W ratio**	**W/L ratio**
aa	21.80	22.10	39.00	0.56	0.99	0.57
3	21.00	27.40	24.70	0.85	0.77	1.11
4	22.50	28.40	25.60	0.88	0.79	1.11
5	22.40	29.00	27.70	0.81	0.77	1.05
6	23.10	30.40	27.60	0.84	0.76	1.10
7	23.40	31.60	30.00	0.78	0.74	1.05
8	25.00	31.90	30.40	0.82	0.78	1.05
9	24.80	32.60	32.10	0.77	0.76	1.02
10	25.50	34.50	32.70	0.78	0.74	1.06
11	26.00	35.80	35.10	0.74	0.73	1.02
12	26.10	35.40	36.00	0.73	0.74	0.98
13	26.90	37.80	38.10	0.71	0.71	0.99
14	28.50	38.70	38.30	0.74	0.74	1.01
15	29.20	38.90	39.90	0.73	0.75	0.97
16	30.00	41.40	41.20	0.73	0.72	1.00
17	30.90	43.00	42.30	0.73	0.72	1.02
18	31.70	43.20	43.10	0.74	0.73	1.00
19	33.00	44.00	43.90	0.75	0.75	1.00
20	34.50	45.50	44.20	0.78	0.76	1.03
21	35.60	48.17	45.20	0.79	0.74	1.07
22	35.00	48.40	45.50	0.77	0.72	1.06
23	35.90	49.70	44.00	0.82	0.72	1.13
24	36.00	53.00	46.00	0.78	0.68	1.15
25	37.50	51.00	48.00	0.78	0.74	1.06
26	39.00	53.00	47.00	0.83	0.74	1.13
27	39.00	54.00	50.00	0.78	0.72	1.08
28	39.00	54.00	51.00	0.76	0.72	1.06
29	40.00	56.50	51.00	0.78	0.71	1.11
30	40.60	57.70	52.70	0.77	0.70	1.09
31	39.50	59.00	54.00	0.73	0.67	1.09
32	42.20	60.00	53.20	0.79	0.70	1.13
33	43.40	61.80	53.00	0.82	0.70	1.17
34	42.40	62.00	53.00	0.80	0.68	1.17
35	43.40	61.30	52.90	0.82	0.71	1.16
36	43.20	64.20	52.30	0.83	0.67	1.23
37	44.90	64.90	55.10	0.81	0.69	1.18

38	42.20	65.40	54.80	0.77	0.65	1.19
39	48.40	63.90	54.90	0.88	0.76	1.16
40	46.30	66.40	55.40	0.84	0.70	1.20
41	48.20	67.90	56.30	0.86	0.71	1.21
42	50.10	69.80	57.10	0.88	0.72	1.22
43	47.50	72.20	54.70	0.87	0.66	1.32
44	49.40	71.30	53.60	0.92	0.69	1.33
45	46.70	70.10	53.50	0.87	0.67	1.31
46	45.90	71.00	52.10	0.88	0.65	1.36
47	46.70	74.30	54.50	0.86	0.63	1.36
48	52.50	72.30	na	na	na	na
49	na	na	na	na	na	na
50	na	na	na	na	na	na
51	52.90	78.50	49.5	na	na	na
52	52.60	76.40	57.9	na	na	na
53	na	na	na	na	na	na
54	52.1	73.9	58.1	na	na	na
55	na	76.6	59.2	na	na	na
56	54.4	72.2	59.2	na	na	na
57	55	71	55.5	na	na	na
58	57.5	71.1	na	na	na	na
59	59	68	na	na	na	na

Table A6.3: Selected measurements from the pectoral girdle of PMO 224.248 in mm.

Pectoral elements	**mm**
Interclavicle	
Preserved mediolateral width	~100
Scapulae	
Total mediolateral width	310
Right scapula	
Anteroposterior length	190
Mediolateral width	155
Length of glenoid facet	50
Dorsoventral height of glenoid facet	40
Length of coracoid facet	50
Right coracoid	
Anteroposterior length (preserved)	375

Mediolateral width (at medial symphsis)	175
Dorsoventral height of medial symphsis	60
Anteriorposterior length anteromedial process	70
Mediolateral width anteromedial process (max)	51
Length of glenoid facet	72
Dorsoventral height of glenoid facet	51
Length of scapular facet	~40
Dorsoventral height of scapular facet	51

Table A6.4: Selected forelimb measurements from PMO 224.248. **Abbreviations**: **pao**, postaxial ossicle.

Left Forelimb	**mm**	**Right Forelimb**	**mm**
Left humerus		**Right humerus**	
Proximodistal length	310	Proximodistal length	335
Anteroposteriorwidth proximal end	70	Anteroposteriorwidth proximal end	75
Anteroposteriorwidth midshaft	70	Anteroposteriorwidth midshaft	66
Anteroposterior width distal end	150	Anteroposterior width distal end	150
Anteroposterior width radial facet	60	Anteroposterior width radial facet	60
Anteroposterior width ulnar facet	70	Anteroposterior width ulnar facet	55
Anteroposterior width pao facet	72	Anteroposterior width pao facet	70
Dorsoventral height (max) distal end	39	Dorsoventral height (max) distal end	45
Left radius		**Right radius**	
Proximodistal length	54	Proximodistal length	57
Anteroposterior width	67	Anteroposterior width	70
Dorsoventral height (max)	34	Dorsoventral height (max)	34
Left ulna		**Right ulna**	
Proximodistal length	42	Proximodistal length	45
Anteroposterior width	60	Anteroposterior width	62
Dorsoventral height (max)	37	Dorsoventral height (max)	36
Left postaxial ossicle		**Right postaxial ossicle**	
Proximodistal length	36	Proximodistal length	40
Anteroposterior width	35	Anteroposterior width	35
Dorsoventral height (max)	21	Dorsoventral height (max)	21
		Right preaxial ossicle	
		Proximodistal length	19
		Anteroposterior width	17

Appendix 7

Supplementary data for Chapter 4

Tables of the distribution of ichthyosaurians and plesiosaurians during the Callovian – Valanginian interval

Table A7.1: Global plesiosaurian and ichthyosaurian records from the Callovian – Oxfordian interval

Country	Order	Family	Genus	Species	Time/Stage	Sub region	Formation	Member/Zone	References
Alaska									
	Plesiosauria	Pliosauridae	*Megalneusaurus*	sp.	Oxfordian	SW Alaska	Nanek Fm.		Weems and Blodgett, 1994
Argentina									
	Plesiosauria	Cryptoclididae	cf. Muraenosaurus	indet	Early Callovian	Chacaico	Lajas Fm.	Upper sector	Gasparini and Spalletti, 1993
			cf. Cryptoclidus	indet	Early Callovian	Chacaico	Lajas Fm.	Upper sector	Gasparini and Spalletti, 1993
		Pliosauridae /Rhomaleosauridae?	indet.	indet	Early Callovian	Chacaico	Lajas Fm.	Upper sector	Gasparini and Spalletti, 1993; Benson et al., 2015
Canada									
	Plesiosauria	Rhomaleosauridae	*Boreaonectes*	*russelli*	Callovian	Melville Island	Hiccles Cove Fm.		Sato and Wu, 2008
Cuba									
	Plesiosauria	Cryptoclididae	*Vinialesaurus*	*caroli*	middle-late Oxfordian	near Viñales	Jagua Fm.	Jagua Vieja Mb.	Gasparini et al., 2002
		Pliosauridae	Gallardosaurus	*iturraldei*	middle-late Oxfordian		Jagua Fm.		Gasparini, 2009
	Ichthyosauria	Ophthalmosauridae	indet.	indet.	middle-late Oxfordian		Jagua Fm.		Fernandez and Iturralde-Vinent, 2000
France									
	Plesiosauria	Cryptoclididae	*Tricleidus*	*seeleyi*	Oxfordian	d'Etrochey.			Sauvage, 1873
Italy									
	Plesiosauria	Pliosauridae	indet.	indet	late Callovian - mid Oxfordian	Asiago	Rosso Ammonitico Veronese Fm.	Lithozone 5	Cau and Fanti, 2015
North America									
	Plesiosauria	Pliosauridae	*Megalneusaurus*	*rex*	mid Oxfordian	Wyoming	Sundance Fm.	Redwater Shale Mb.	Wahl et al., 2010
			Tatenectes	*laramiensis*	mid Oxfordian	Wyoming	Sundance Fm.	Redwater Shale Mb.	O'Keefe and Street, 2009
			Pantosaurus	*striatus*	mid Oxfordian	Wyoming	Sundance Fm.	Redwater Shale Mb.	O'Keefe and Wahl, 2003
	Ichthyosauria	Ophthalmosauridae	*Ophthalmosaurus*	*natans*	mid Oxfordian	Wyoming	Sundance Fm.	Redwater Shale Mb.	Gilmore, 1905
Poland									
	Plesiosauria	Pliosauridae	indet.	indet.	Early Oxfordian	Zalas Quarry		*Quenstedtoceras mariae*	Lomax, 2015
Russia									
	Plesiosauria	Rhomaleosauridae	indet.	indet.	Early Callovian	Volograd Region	Hlebnovka Fm.	*Cadoceras elatmae*	Benson et al., 2015
	Ichthyosauria	Ophthalmosauridae	cf. *Ophthalmosaurus*	indet.	Callovian	Saratov Region			Storrs et al. 2000
United Kingdom									
	Ichthyosauria	Ophthalmosauridae	*Ophthalmosaurus*	*icenicus*	Callovian-Oxfordian	England	Oxford Clay Fm.	Peterborough Mb.	Andrews, 1910
	Plesiosauria	Cryptoclididae	*Cryptoclidus*	*eurymerus*	Callovian	England	Oxford Clay Fm.	Peterborough Mb.	Andrews, 1910
			Muraenosaurus	*leedsi*	Callovian	England	Oxford Clay Fm.	Peterborough Mb.	Andrews, 1910
			"Picrocleidus"	*beloiconis*	Callovian	England	Oxford Clay Fm.	Peterborough Mb.	Andrews, 1910
			Tricleidus	*seeleyi*	Callovian	England	Oxford Clay Fm.	Peterborough Mb.	Andrews, 1910
		Pliosauridae	*Marmornectes*	*candrewi*	L. Callovian	Bedfordshire, England	Oxford Clay Fm.	*Sigilocera enodatum*	Ketchum and Benson, 2011a
			Peloneustes	*philarchus*	Callovian	England	Oxford Clay Fm.	Peterborough Mb.	Ketchum and Benson, 2011b
			Liopleurodon	*ferox*	Callovian	England	Oxford Clay Fm.	Stewarby Mb.	Noè et al., 2003
			Simolestes	*vorax*	Callovian	England	Oxford Clay Fm.	Peterborough Mb.	Andrews, 1909
		Rhomaleosauridae	*indet.*	*indet.*	Callovian	Peterborough	Oxford Clay Fm.	Peterborough Mb.	Benson et al., 2015

Table A7.2: Global records of ichthyosaurians and plesiosaurians from the Kimmeridgian – Tithonian interval.

Country	Order	Family	Genus	Species	Time/Stage	Sub region	Formation	Member/Zone	References
Argentina									
	Ichthyosauria	Ophthalmosauridae	*Caypullisaurus*	*bonapartei*	Tithonian	Neuquen	Vaca Muerta Fm.		Fernández, 1997a
			Arthropterygius	*chrisorum*	Tithonian	Neuquen	Vaca Muerta Fm.		Fernández and Maxwell, 2012
			Aegirosaurus	sp.	Tithonian	Neuquen	Vaca Muerta Fm.		Gasparini et al., 2015
	Plesiosauria	Pliosauridae	indet	indet.	Tithonian	Neuquen	Vaca Muerta Fm.		2014
			Pliosaurus	*patagonicus*	Tithonian	Neuquen	Vaca Muerta Fm.		2014
Canada									
	Ichthyosauria	Ophthalmosauridae	*Arthropterygius*	*chrisorum*	Kimmeridgian	Melville island			Maxwell, 2010
		Ophthalmosauridae	indet	indet	Early Kimmeridgian	British Columbia	Bowser Lake Group	Skelhorn assemblage	Sissons et al., 2015
	Plesiosauria	Cryptoclididae	*Colymbosaurus*	cf. *svalbardensis*	Late Jurassic	Melville Island			pers. obs. AJR - MGUH
East Greenland									
	Ichthyosauria	Ophthalmosauridae?	indet.	indet.	Kimmeridgian	Milne Land			pers. obs. AJR - MGUH
	Plesiosauria	Cryptoclididae	indet.	indet.	Kimmeridgian	Milne Land			Smith, 2007
France									
	Ichthyosauria	Ophthalmosauridae	cf. *Ophthalmosaurus*	indet.	Kimmeridgian-Tithonian	Boulonnais	Kimmeridge Clay Fm.		Bardet et al.,
	Plesiosauria	Colymbosaurus	indet.		Kimmeridgian-Tithonian	Boulonnais	Kimmeridge Clay Fm.		Sauvage, 1873
Germany									
	Ichthyosauria	Ophthalmosauridae	*Aegirosaurus*	*leptospondylus*	Tithonian		Solnhofn Fm.		Bardet and Fernandez, 2000
			Ophthalmosaurus	*icenicus*					
India									
	Plesiosauria	Cryptoclididae	indet.	indet	Tithonian	Kutch Provience			Bardet et al., 1991
Italy									
	Ichthyosauria	Ophthalmosauridae	*Gengasaurus*	*nicosiai*	Kimmeridgian - early Tithonian	Genga	Maiolica Fm.	Calcari ad aptici e Saccocoma	Paparella et al., 2016
Madagasgar									
	Ichthyosauria	Ophthalmosauridae	cf. *Brachypterygius*	indet.	Portlandian	Tulear Province			Fernández, 1997b
Mexico									
	Ichthyosauria	Ophthalmosauridae	*Ophthalmosaurus*	*icenicus*	Tithonian	Coahulia	La Caja Fm.		Buchy, 2010, JP 84
	Plesiosauria	Pliosauridae	*Liopleurodon*	indet.					Barrientos-Lara et al. 2016
			indet.	indet.	Kimmeridgian		La Caja Fm.		Buchy et al. 2003
Norway									
	Ichthyosauria	Ophthalmosauridae	*Ophthalmosaurus*	indet.	Kimmeridgian	Andøya	Andøya Fm.		pers. obs. AJR - PMO
Pakistan									
	Plesiosauria	Cryptoclididae?	indet.	indet.	Late Jurassic - Early Cretaceous		Chichali Fm.		Buffetaut, 1981
Poland									
	Ichthyosauria	Ophthalmosauridae	cf. *Cryopterygius*	indet.	Tithonian				Tybowski, 2016

Country	Order	Family	Genus	Species	Time/Stage	Sub region	Formation	Member/Zone	References
Russia									
	Ichthyosauria	Ophthalmosauridae	*Undorosaurus*	*gorodischensis*	Tithonian (MV)	Uljanovsk + Moskow regions			Efimov, 1999a; Arkhangelsky and Zverkov, 2014
			Ophthalmosaurus	indet.	Tithonian (MV)				Efimov, 1999b
			Ostechevia (Brachypterygius)		Tithonian (MV)	Saratov Region			Arkhangelsky, 2000
			Grendelius (Brachypterygius?)	sp.	Tithonian (MV)				Zverkov et al., 2015a
			Paraophthalmosaurus		Tithonian				Arkhangelsky, 1997
			Arthropterygius	indet.	Tithonian (MV)				Zverkov et al., 2015b
	Plesiosauria	Pliosauridae	cf. *Pliosaurus*	indet.	Tithonian	Saratov Region			Halstead, 1971; Storrs et al., 2000
		Pliosauridae	cf. *Pliosaurus*	indet.	Kimmeridgian	Moskow Region			Storrs et al., 2000
		Cryptoclididae	*Colymbosaurus*	indet.	Tithonian	Uljanovsk + Moskow regions			Storrs, et al., 2000; Arkhangelsky et al., (accepted)
Svalbard									
	Ichthyosauria	Ophthalmosauridae	*Cryopterygius*	*kristiansenae*	Tithonian	central Spitsbergen	Agardhfjellet Fm.	Slottsmøya Mb.	Druckenmiller et al., 2012
			Palvennia	*hoeybergeti*	Tithonian	central Spitsbergen	Agardhfjellet Fm.	Slottsmøya Mb.	Druckenmiller et al., 2012
			Janusaurus	*lundi*	Tithonian	central Spitsbergen	Agardhfjellet Fm.	Slottsmøya Mb.	Roberts et al., 2014
		Ophthalmosauridae	indet.	indet.	Tithonian	central Spitsbergen	Agardhfjellet Fm.	Slottsmøya Mb.	Delsett et al. 2017
		Ophthalmosauridae	indet.	indet.	Tithonian	central Spitsbergen	Agardhfjellet Fm.	Slottsmøya Mb.	Delsett et al. 2017
		Ophthalmosauridae	indet.	indet.	Tithonian	central Spitsbergen	Agardhfjellet Fm.	Slottsmøya Mb.	Delsett et al. 2017
	Plesiosauria	Cryptoclididae	*Colymbosaurus*	*svalbardensis*	Tithonian	central Spitsbergen	Agardhfjellet Fm.	Slottsmøya Mb.	Knutsen et al. 2012a; Roberts et al. 2017
			Gen .nov	*sp. nov*	J-K border	central Spitsbergen	Agardhfjellet Fm.	Slottsmøya Mb.	Chapter 3, this volume
			Spitrasaurus	*wensaasi*	Tithonian	central Spitsbergen	Agardhfjellet Fm.	Slottsmøya Mb.	Knutsen et al. 2012b
			Spitrasaurus	*larseni*	Tithonian	central Spitsbergen	Agardhfjellet Fm.	Slottsmøya Mb.	Knutsen et al. 2012b
			Djupedalia	*engeri*	Tithonian	central Spitsbergen	Agardhfjellet Fm.	Slottsmøya Mb.	Knutsen et al. 2012c
		Pliosauridae	*Pliosaurus*	*funkei*	Tithonian	central Spitsbergen	Agardhfjellet Fm.	Slottsmøya Mb.	Knutsen et al. 2012d
United Kingdom									
	Ichthyosauria	Ophthalmosauridae	*Ophthalmosaurus*	*icenicus*	Kimmeridgian - Tithonian	England	Kimmeridge Clay Fm.		Andrews, 1910; Moon and Kirton, 2016
			Nannopterygius	*enthikdon*		England	Kimmeridge Clay Fm.	*aulacostephanus* zones	Kirton, 1983; Moon and Kirton, 2016
			Brachypterygius	*extremus*		England	Kimmeridge Clay Fm.	*pectinatites*	Kirton, 1983; Moon and Kirton, 2016
	Plesiosauria	Cryptoclididae	*Colymbosaurus*	*megadeirus*	Kimmeridgian - Tithonian	England	Kimmeridge Clay Fm.		Benson and Bowdler, 2014; Roberts et al. 2017,
			Colymbosaurus	*indet.*	Tithonian	England	Portland stone	*Titanites giganteus*	Knutsen et al., 2012a
			Kimmerosaurus	*langhami*	Tithonian	England	Kimmeridge Clay Fm.	*pectinatites+ mutablis*	Brown, 1981
			cf. *Spitrasaurus (Colymbosaurinae indet)*	indet.	Tithonian	England	Kimmeridge Clay Fm.		Benson and Bowdler, 2014; Chapter 4, this volume
			Plesiosaurus'	*mansellii*	Tithonian	England	Kimmeridge Clay Fm.	*scitulus*	Hulke, 1870; Benton and Spencer, 1995
		Pliosauridae	*Pliosaurus*	*kevani*	Kimmeridgian	England	Kimmeridge Clay Fm.	*cymodoce*	Benson et al., 2013
			Pliosaurus	*brachydeirus*	Kimmeridgian	England	Kimmeridge Clay Fm.	*cymodoce*	Benson et al., 2013
			Pliosaurus	*westburyensis*	Kimmeridgian	England	Kimmeridge Clay Fm.	*euxodus*	Benson et al., 2013
			Pliosaurus	*carpenteri*	Kimmeridgian	England	Kimmeridge Clay Fm.	*euxodus*	Benson et al., 2013

Country	Order	Family/clade	Genus	Species	Time/Stage	Sub region	Formation	Member/Zone	References
Argentina									
	Plesiosauria	Elasmosauridae	indet.	indet.	Valanginian	Neuquen Basin	Agario Fm.		O'Gorman et al., 2015
Australia									
	Plesiosauria	Leptoclididae	indet.	indet.	Berriasian		Barrow Gr.		Cruickshank and Long, 1998
Canada									
	Ichthyosauria	Ophthalmosauridae	*Ophthalmosaurus*?	indet.	E. Cretaceous	St. Patrick Island			McGowan, 1978
Chile									
	Ichthyosauria	Ophthalmosauridae	*Platypterygius*		Valanginian				Stinnesbeck et al., 2014
France									
	Ichthyosauria	Ophthalmosauridae	*Aegirosaurus*	sp.	Valanginian	Drôme			Fischer et al., 2011
Germany									
	Plesiosauria	Leptoclididae	*Brancasaurus*	*brancai*	Berriasian				Sachs et al. 2016
Russia									
	Ichthyosauria	Ophthalmosauridae							Storrs et al. 2000
Svalbard									
	Ichthyosauria	Ophthalmosauridae	*Keilhauia*	*nui*	Berriasian	central Spitsbergen	Agardhfjellet Fm.	Slottsmøya Mb.	Delsett et al. 2017
United Kingdom									
	Plesiosauria	Leptoclididae	indet.	indet.		England	Splisby Sandstone Fm.		Forrest and Oliver, 2003
		Pliosauridae	indet.	indet.		England	Splisby Sandstone Fm.		Forrest and Oliver, 2003
		Elasmosauridae	indet.	indet.		England	Splisby Sandstone Fm.		Forrest and Oliver, 2003
	Ichthyosauria	Ophthalmosauridae	*Ophthalmosaurus*	indet.	Berriasian	England	Splisby Sandstone Fm.		Fischer et al., 2012

Table A7. 3: Global records of ichthyosaurians and plesiosaurians from the Berriasian – Valanginian interval.

Time-calibrated phylogenies

The data matrix for Plesiosauria can be found in Appendix 4.

The character list from Maxwell et al., (2016) with supplementary data on new taxa from Delsett et al., (2017) was utilised, resulting in a matrix with 27 taxa and 66 characters. Missing data =”?” and multiple character states indicated by “{}”.

Ophthalmosaurid matrix:

Temnodontosaurus_sp.
{01}00000000000000000000000010000?000101000000000000000000000000000000

Malawania_anachronus
??00??110000?0001?00????????

Ichthyosaurus_communis
00000100{01}00000011{12}11010100101000011000000{01}000010000{01}110101100000010

Stenopterygius_quadriscissus
10011100000000001010000101001010011011?1110000000010{01}0000110??0000

Ophthalmosaurus_icenicus
01011111101001001010{01}010{01}000111001111011010101110111111110010100010

Brachypterygius_extremus
0111?0100?110??????011201101?0??1011?????101?100101111110??????????

Maiaspondylus_lindoei
1011?1?01?10????????0??????????????????0??????1?100101?1?0?10????10??

Undorosaurus_gorodischensis
011??????????0????????1??????11?????01??000101110011010100001100 10

Arthropterygius_chrisorum
??????????????????1012011??????????11?1??01001100?1?1010???1100??

Mollesaurus_periallus
11?1?1?0111????0011?101111???010????0??????????????????????????????

Acamptonectes_densus
11?1??1??????1?????0101011101111100100?10101{01}111011??1??0?????????

Caypullisaurus_bonapartei
?????00000?10??1?10????????????????10???111111100011210110??1?0?11

Aegirosaurus_leptospondylus
0001?11011100?10001????????????????1???????1?100101111?1021??0011

Platypterygius_australis
011100210011001012001120110100100011011101111110001121011020110111

Platypterygius_hercynicus
011??100?01??110??1???21?101?010?????1?101111110001121011 0??11101?

Athabascasaurus_bitumineus
10?1?0011?101100110???2???10??11???10?1?????????????????????201?????

Leninia_stellans
??????10?010010?0{01}1???11?0?????????1?????????????????????????????

Sveltonectes_insolitus
1011?1101110111?1??0012111??0?1????100?1110111000??1111110211 10111

Palvennia_hoybertgei

11???00?11???10112????201101???101?1??????????1??????1????????????

Cryopterygius_kristiansenae
111??0001?0001?1121???2?????????0111????0101010000011111100011001?

Janusaurus_lundi
11???010?10011?1121???2111?????1???1??????0100110001?111002011 00??

Muiscasaurus_catheti
1?11?11?0???0????21???20?1????????11??????????????????????????????

Ophthalmosaurus_natans
0??111101000000101???10?001?111?1010?0?110110110??1?13?00????????

Platypterygius_sachicarum
0111??20?1??01?1?20??????????????011??????????????????????????????

Simbirskiasaurus_birjukovi
0?11?0210010???????????2?11??????????????????????????????????????

Pervushovisaurus_bannovkensis
0111?021?????????????????????????1011??????????????????????????????

Keilhauia_nui
????????????????????????????????????01??000100110??1??????2100?0?0

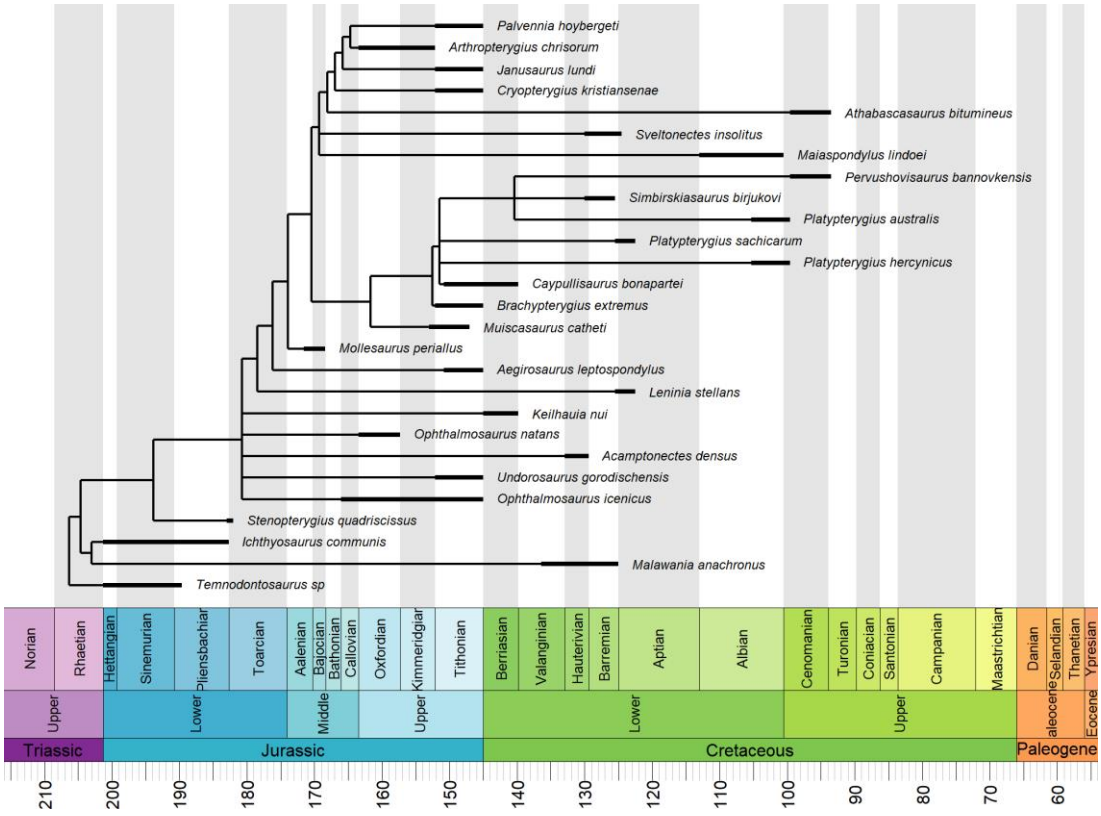

Figure A7.1: The strict consensus tree of 12 MPTs for ophthalmosaurids.

Time calibrate phylogeny in R studio

Program: R studio (R v3.3.2)

R Packages required: *paleotree*, *vegan*, *phytools*, *rread*, *geiger*.

Range data for some taxa from the Palaeobiology Database (PBDB) had to be adjusted in respect to the new Geological Timescale (Gradstein et al., 2016): Callovian taxa (*Ophthalmosaurus icenicus*, *Cryptoclidus eurymerus*, *Muraenosaurus leedsii*, *Tricleidus seeleyi*, '*Picrocleidus' beloclis*); Hauterivian taxa (*Abyssosaurus nataliae*), Barremian taxa (*Muiscasaurus catheti*).

Tree file for ophthalmosaurid tree topology:

(Temnodontosaurus_sp,((Malawania_anachronus,Ichthyosaurus_communis),(Stenopterygius_quadriscissus,(Ophthalmosaurus_icenicus,Undorosaurus_gorodischensis,Acamptonectes_densus,Ophthalmosaurus_natans,Keilhauia_nui,(Leninia_stellans,(Aegirosaurus_leptospondylus,(Mollesaurus_periallus,((Muiscasaurus_catheti,(Brachypterygius_extremus,(Caypullisaurus_bonapartei,Platypterygius_hercynicus,Platypterygius_sachicarum,(Platypterygius_australis,Simbirskiasaurus_birjukovi,Pervushovisaurus_bannovkensis)))),(Maiaspondylus_lindoei,Sveltonectes_insolitus,(Athabascasaurus_bitumineus,(Cryopterygius_kristiansenae,(Janusaurus_lundi,(Arthropterygius_chrisorum,Palvennia_hoybertgei)))))))))));

Table A7.4: Range data for ophthalmosaurid tree. Time set in millions of years.

Taxa	Max	Min
Temnodontosaurus sp.	201.30	189.60
Malawania anachronus	136.40	125.00
Ichthyosaurus communis	201.30	182.70
Stenopterygius quadriscissus	183.00	182.00
Ophthalmosaurus icenicus	166.10	145.00
Undorosaurus gorodischensis	152.10	145.00
Acamtonectes densus	132.90	129.40
Ophthalmosaurus natans	163.50	157.30
Keilhauia nui	145.00	139.80
Leninia stellans	125.45	122.46
Aegirosaurus leptospondylus	150.80	145.00
Mollesaurus periallus	171.60	168.40
Muiscasaurus catheti	129.40	113.00
Brachypterygius extremus	152.10	145.00
Caypullisaurus bonapartei	150.80	139.80
Platypterygius hercynicus	105.30	99.60
Platypterygius sachicarum	125.45	122.46
Platypterygius australis	105.30	99.60
Simbirskiasaurus birjukovi	130.00	125.45
Pervushovisaurus bannovkensis	99.60	93.50
Maiaspondylus lindoei	113.00	100.50

Sveltonectes insolitus	130.00	125.45
Athabascasaurus bitumineus	113.00	100.50
Cryopterygius kristiansenae	152.10	145.00
Janusaurus lundi	152.10	145.00
Arthropterygius chrisorum	163.50	152.10
Palvennia hoybergeti	152.10	145.00

Resulting Ophthalmosaurus tree file with branch lengths:

(Temnodontosaurus_sp:5.02,((Malawania_anachronus:66.58666667,Ichthyosaurus_communis:1.686666667):1.686666667,(Stenopterygius_quadriscissus:10.83666667,(((Keilhauia_nui:35.74,((Leninia_stellans:52.96,(Aegirosaurus_leptospondylus:25.38,(Mollesaurus_periallus:2.3,((Muiscasaurus_catheti:8.741428571,(Brachypterygius_extremus:0.47,((((Pervushovisaurus_bannovkensis:40.82,Platypterygius_australis:35.12):0.02,Simbirskiasaurus_birjukovi:10.42):11.07,(Caypullisaurus_bonapartei:0.67,Platypterygius_hercynicus:46.17):0.02):0.02,Platypterygius_sachicarum:26.02):1.12):9.191428571):8.741428571,((Sveltonectes_insolitus:39.30571429,(Athabascasaurus_bitumineus:68.54857143,(Cryopterygius_kristiansenae:14.89142857,(Janusaurus_lundi:13.73428571,(Arthropterygius_chrisorum:1.177142857,Palvennia_hoybergeti:12.57714286):1.177142857):1.177142857):1.177142857):1.177142857):0.02,Maiaspondylus_lindoei:56.30571429):1.177142857):3.457142857):2.3):2.3):2.3,Ophthalmosaurus_natans:17.24):0.02):0.02,Acamptonectes_densus:47.84):0.02,(Undorosaurus_gorodischensis:28.64,Ophthalmosaurus_icenicus:14.64):0.02):13.11666667):10.83666667):1.686666667);

Tree file for cryptoclidid tree topology:

(((Plesiosaurus_mansellii,Pantosaurus_striatus),(Abyssosaurus_nataliae,(Colymbosaurus_svalbardensis,Colymbosaurus_megadeirus))),((Tricleidus_seeleyi,(Picrocleidus_beloclis,Muraenosaurus_leedsii)),((Djupedalia_engeri,(Ophthalmothule,Spitrasaurus_spp)),(Cryptoclidus_eurymerus,(Tatenectes_laramiensis,Kimmerosaurus_langhami)))));

Table A7.5: Range data for cryptoclidid tree. Time set in millions of years.

Taxa	Min	Max
Cryptoclidus eurymerus	166.10	163.50
Kimmerosaurus langhami	152.10	145.00
Tatenectes laramiensis	163.50	157.30
Djupedalia engeri	152.10	145.00
Spitrasaurus spp.	152.10	145.00
Gen et sp. nov	147.00	139.80
Tricleidus seeleyi	166.10	163.50
Muraenosaurus leedsii	166.10	163.50
Picrocleidus' beloclis	166.10	163.50
Pantosaurus striatus	163.50	157.30
Plesiosaurus' mansellii	155.70	150.80
Abyssosaurus nataliae	132.90	129.40
Colymbosaurus megadeirus	157.30	145.00
Colymbosaurus svalbardensis	152.10	145.00

Resulting Plesiosauroidea tree with branch lengths

(Plesiosaurus_dolichodeirus:5.01,(Eretmosaurus_rugosus:3.51,(Westphaliasaurus_simonsensii:4.26,((Seeleyosaurus_guilelmiimperatori:4.69,(Microcleidus_tournemirensis:5.93,(Microcleidus_brachypterygius:1.57,Microcleidus_homalospondylus:2.57):1.57):1.57):1.57,(Plesiopterys_wildi:3.13,(((((Cryptoclidus_eurymerus:2.826666667,(Kimmerosaurus_langhami:12.71,Tatenectes_laramiensis:1.31):4.126666667):2.826666667,(Djupedalia_engeri:9.343333333,(Spitrasaurus_spp:4.676666667,Gen_nov_sp_nov:4.666666667):4.676666667):10.31):2.826666667,(Tricleidus_seeleyi:5.633333333,(Muraenosaurus_leedsii:2.816666667,Picrocleidus_beloclis:2.816666667):2.816666667):2.816666667):2.826666667,((Pantosaurus_striatus:4.622222222,Plesiosaurus_mansellii:16.02222222):4.622222222,(Abyssosaurus_nataliae:28.53333333,(Colymbosaurus_megadeirus:2.066666667,Colymbosaurus_svalbardensis:7.266666667):2.066666667):11.31111111):4.622222222):2.826666667,(((((Nichollssaura_borealis:30.26666667,Umoonasaurus_demoscyllus:18.26666667):0.1,(Leptocleidus_capensis:1.733333333,Leptocleidus_superstes:12.13333333):1.733333333):12.28333333,(MIWG_1997_302:22.63333333,(Cimoliasaurus_valdensis:8.716666667,Brancasaurus_brancai:3.516666667):3.516666667):3.516666667):3.516666667,(Edgarosaurus_muddi:30.71111111,(Plesiopleurodon_wellesi:27.85555556,QM_F51291.2:15.35555556):15.35555556):15.35555556):3.516666667,(GWWU_A3_B2:8.791666667,(Speeton_Clay_plesiosaurian:6.05,((Wapuskanectes_betsynichollsae:14.63333333,Callawayasaurus_colombiensis:2.633333333):2.633333333,((Futabasaurus_suzukii:4.05,(Kaiwhekea_katiki:0.45,Aristonectes_parvidens:13.25):4.5):24.78333333,(Libonectes_morgani:10.36666667,Hydrotherosaurus_alexandrae:32.16666667):10.36666667):15.63333333):8.683333333):14.84166667):8.791666667):17.6):5.946666667):3.13):5.82):7.76):3.51);

R script for timecalibration

packages required *phytools, strap, paleotree, geiger*

#script for reading tree with singleton nodes. use read.newick instead

#nice feature to check that the range data and the tree data fit: check.names(tree, timedata) using geiger package

```
pt<-read.newick(file="filename.newick",)
pr<-read.csv("filename.csv", header=T, row.names = 1)
plio<-read.csv("filename.csv", header=T, row.names=1)
pt.ts <- DatePhylo(pt, pr, method="equal", rlen=5)
geoscalePhylo(tree=pt.ts, ages=pr, ranges=TRUE, cex.tip=1.5, cex.ts=2, cex.age=2,
x.lim=c(40,210), quat.rm=TRUE, width=4, label.offset=1)
write.tree (pt.ts, file = "filename.newick")
```

Ancestral states analysis in R studio

Program: R studio (R v3.3.2), packages required: *BioGeoBEARS*, *optimx*, *FD*, *parallel*, *phylobase*, *gdata*, *snow*, *phytools*

The code was created by Matzke (2014), more information on the code can be found on phylo.wikidot.com/BioGeoBEARS or in the reference manual for the package.

Presence-absence matrix for Plesiosauroidea

Copy into a text file and save as .data. No changes should be made to the spacing between numerals.

41 8 (N B S R A G Q T)

Plesiosaurus_dolichodeirus 00100000

Eretmosaurus_rugosus 00100000

Westphaliasaurus_simonsensii 00100000

Seeleyosaurus_guilelmiimperatori 00100000

Microcleidus_tournemirensis 00100000

Microcleidus_brachypterygius 00100000

Microcleidus_homalospondylus 00100000

Plesiopterys_wildi 00100000

Cryptoclidus_eurymerus 00100000

Kimmerosaurus_langhami 00100000

Tatenectes_laramiensis 10000000

Djupedalia_engeri 01000000

Spitrasaurus_spp 01000000

Gen_nov_sp_nov 01000000

Tricleidus_seeleyi 00100000

Muraenosaurus_leedsii 00100000

Picrocleidus_beloclis 00100000

Pantosaurus_striatus 10000000

Plesiosaurus_mansellii 00100000

Abyssosaurus_nataliae 00010000

Colymbosaurus_megadeirus 00110000

Colymbosaurus_svalbardensis 01000000

Umoonasaurus_demoscyllus 00001000

Nichollssaura_borealis 00100000

Leptocleidus_capensis 00000100

Leptocleidus_superstes 00100000

MIWG_1997_302 00100000

Cimoliasaurus_valdensis 00100000

Brancasaurus_brancai 00100000

Edgarosaurus_muddi 10000000

Plesiopleurodon_wellesi 10000000

QM_F51291.2 00001000

GWWU_A3_B2 00100000

Speeton_Clay_plesiosaurian 00100000

Wapuskanectes_betsynichollsae 01000000

Callawayasaurus_colombiensis 00000010

Futabasaurus_suzukii 00000001

Kaiwhekea_katiki 00001000

Aristonectes_parvidens 00000010

Libonectes_morgani 10000000

Hydrotherosaurus_alexandrae 10000000

Presence-absemce matrix for Ophthalmosauridae

Copy into a text file and save as .data. No changes should be made to the spacing between numerals.

27 7 (N B S T R A P)

Temnodontosaurus_sp 0010000

Malawania_anachronus 0001000

Ichthyosaurus_communis 0010000

Stenopterygius_quadriscissus 0010000

Ophthalmosaurus_icenicus 0010101

Undorosaurus_gorodischensis 0000100

Acamptonectes_densus 0000100

Ophthalmosaurus_natans 1000000

Keilhauia_nui 0100000

Leninia_stellans 0000100

Aegirosaurus_leptospondylus 0010001

Mollesaurus_periallus 0000001

Muiscasaurus_catheti 0000001

Brachypterygius_extremus 0010000

Caypullisaurus_bonapartei 0000001

Platypterygius_hercynicus 0010000

Platypterygius_sachicarum 0000001

Platypterygius_australis 0000010

Simbirskiasaurus_birjukovi 0000100

Pervushovisaurus_bannovkensis 0010100

Maiaspondylus_lindoei 0100000

Sveltonectes_insolitus 0000100

Athabascasaurus_bitumineus 0100000

Cryopterygius_kristiansenae 0100000

Janusaurus_lundi 0100000

Arthropterygius_chrisorum 0100101

Palvennia_hoybergeti 0100000

#read time-calibrated tree file

clade <-read.newick("clade.newick ")

#read source code for BioGeoBEARS

#Add inn source code

DEC

tipranges = getranges_from_LagrangePHYLIP(lgdata_fn = "filename.data")

```
clade = read.newick (file="filename.newick")

BioGeoBEARS_run_object = define_BioGeoBEARS_run()
BioGeoBEARS_run_object$trfn = clade
BioGeoBEARS_run_object$geogfn = tipranges
BioGeoBEARS_run_object$max_range_size = 8
BioGeoBEARS_run_object$min_branchlength = 0.000001
BioGeoBEARS_run_object$include_null_range = TRUE
BioGeoBEARS_run_object$num_cores_to_use = 5 #edit if number of cores is less
BioGeoBEARS_run_object$force_sparse = FALSE
BioGeoBEARS_run_object = readfiles_BioGeoBEARS_run(BioGeoBEARS_run_o
bject)
BioGeoBEARS_run_object$return_condlikes_table = TRUE
BioGeoBEARS_run_object$calc_TTL_loglike_from_condlikes_table = TRUE
BioGeoBEARS_run_object$calc_ancprobs = TRUE
BioGeoBEARS_run_object$trfn = "filename.newick"
BioGeoBEARS_run_object$geogfn = "filename.data"
#for DEC type following
results_DEC = bears_optim_run(BioGeoBEARS_run_object)
analysis_titletxt = "DEC"
results_object = results_DEC

scriptdir = np(system.file("extdata/a_scripts", package="BioGeoBEARS"))

res2 = plot_BioGeoBEARS_results(results_object, analysis_titletxt,
addl_params=list("j"), plotwhat="text", label.offset=0.45, tipcex=1.5, statecex=0.8,
splitcex=0.8, titlecex=0.8, plotsplits=TRUE, cornercoords_loc=scriptdir,
include_null_range=TRUE, tr=clade, tipranges=tipranges)

plot_BioGeoBEARS_results(results_object, analysis_titletxt, addl_params=list("j"),
plotwhat="pie", label.offset=0.45, tipcex=1.5, statecex=0.8, splitcex=0.8,
titlecex=0.8, plotsplits=TRUE, cornercoords_loc=scriptdir,
include_null_range=TRUE, tr=clade, tipranges=tipranges)



#DEC+J
BioGeoBEARS_run_object = define_BioGeoBEARS_run()

BioGeoBEARS_run_object$trfn = clade

BioGeoBEARS_run_object$geogfn = tipranges

BioGeoBEARS_run_object$max_range_size = 8

BioGeoBEARS_run_object$min_branchlength = 0.000001

BioGeoBEARS_run_object$include_null_range = TRUE

BioGeoBEARS_run_object$num_cores_to_use = 5

BioGeoBEARS_run_object$force_sparse = FALSE
```

```
BioGeoBEARS_run_object =
readfiles_BioGeoBEARS_run(BioGeoBEARS_run_object)

BioGeoBEARS_run_object$return_condlikes_table = TRUE

BioGeoBEARS_run_object$calc_TTL_loglike_from_condlikes_table = TRUE

BioGeoBEARS_run_object$calc_ancprobs = TRUE

BioGeoBEARS_run_object$trfn = "filename.newick"
BioGeoBEARS_run_object$geogfn = "filename.data"

dstart = results_DEC$outputs@params_table["d","est"] estart =
results_DEC$outputs@params_table["e","est"]

BioGeoBEARS_run_object$BioGeoBEARS_model_object@params_table["d","init
"] = dstart
BioGeoBEARS_run_object$BioGeoBEARS_model_object@params_table["d","est"
] = dstart
BioGeoBEARS_run_object$BioGeoBEARS_model_object@params_table["e","init"
] = estart
BioGeoBEARS_run_object$BioGeoBEARS_model_object@params_table["e","est"
] = estart

jstart = 0.0001
BioGeoBEARS_run_object$BioGeoBEARS_model_object@params_table["j","type
"] = "free"
BioGeoBEARS_run_object$BioGeoBEARS_model_object@params_table["j","init"
] = jstart
BioGeoBEARS_run_object$BioGeoBEARS_model_object@params_table["j","est"]
= jstart

results_DECJ = bears_optim_run(BioGeoBEARS_run_object)

analysis_titletxt ="BioGeoBEARS DEC+J on Plesiosauroidea M0_unconstrained"

# Setup
results_object = results_DECJ
scriptdir = np(system.file("extdata/a_scripts", package="BioGeoBEARS"))
res1 = plot_BioGeoBEARS_results(results_object, analysis_titletxt,
addl_params=list("j"), plotwhat="text", label.offset=1, tipcex=1.5, statecex=0.2,
splitcex=0.2, titlecex=0.8, plotsplits=TRUE, cornercoords_loc=scriptdir,
include_null_range=TRUE, tr=clade, tipranges=tipranges)

plot_BioGeoBEARS_results(results_object, analysis_titletxt, addl_params=list("j"),
plotwhat="pie", label.offset=1, tipcex=1.5, statecex=0.2, splitcex=0.3, titlecex=1.5, p
lotsplits=TRUE, cornercoords_loc=scriptdir, include_null_range=TRUE, tr=clade, ti
pranges=tipranges)

#DIVA
```

```
BioGeoBEARS_run_object = define_BioGeoBEARS_run()
BioGeoBEARS_run_object$trfn = clade
BioGeoBEARS_run_object$geogfn = tipranges
BioGeoBEARS_run_object$max_range_size = 8
BioGeoBEARS_run_object$min_branchlength = 0.000001    # Min to treat tip as a
direct ancestor (no speciation event)
BioGeoBEARS_run_object$include_null_range = TRUE
BioGeoBEARS_run_object$on_NaN_error = -1e50    # returns very low lnL if
parameters produce NaN error (underflow check)
BioGeoBEARS_run_object$speedup = TRUE          # shorcuts to speed ML search;
use FALSE if worried (e.g. >3 params)
BioGeoBEARS_run_object$use_optimx = TRUE    # if FALSE, use optim() instead
of optimx()
BioGeoBEARS_run_object$num_cores_to_use = 5
BioGeoBEARS_run_object$force_sparse = FALSE
BioGeoBEARS_run_object =
readfiles_BioGeoBEARS_run(BioGeoBEARS_run_object)
BioGeoBEARS_run_object$return_condlikes_table = TRUE
BioGeoBEARS_run_object$calc_TTL_loglike_from_condlikes_table = TRUE
BioGeoBEARS_run_object$calc_ancprobs = TRUE
BioGeoBEARS_run_object$trfn = "filename.newick"
BioGeoBEARS_run_object$geogfn = "filname.data"


BioGeoBEARS_run_object$BioGeoBEARS_model_object@params_table["s","type
"] = "fixed"
BioGeoBEARS_run_object$BioGeoBEARS_model_object@params_table["s","init"
] = 0.0
BioGeoBEARS_run_object$BioGeoBEARS_model_object@params_table["s","est"
] = 0.0

BioGeoBEARS_run_object$BioGeoBEARS_model_object@params_table["ysv","ty
pe"] = "2-j"
BioGeoBEARS_run_object$BioGeoBEARS_model_object@params_table["ys","typ
e"] = "ysv*1/2"
BioGeoBEARS_run_object$BioGeoBEARS_model_object@params_table["y","typ
e"] = "ysv*1/2"
BioGeoBEARS_run_object$BioGeoBEARS_model_object@params_table["v","typ
e"] = "ysv*1/2"

# Allow classic, widespread vicariance; all events equiprobable
BioGeoBEARS_run_object$BioGeoBEARS_model_object@params_table["mx01v"
,"type"] = "fixed"
BioGeoBEARS_run_object$BioGeoBEARS_model_object@params_table["mx01v"
,"init"] = 0.5
BioGeoBEARS_run_object$BioGeoBEARS_model_object@params_table["mx01v"
,"est"] = 0.5
check_BioGeoBEARS_run(BioGeoBEARS_run_object)
runslow = TRUE
resfn = "Plesiosauroidea_DIVALIKE_M0_unconstrained_v1.Rdata"
```

```
if (runslow)
   {
   res = bears_optim_run(BioGeoBEARS_run_object)
   res

   save(res, file=resfn)
   resDIVALIKE = res
   } else {
   # Loads to "res"
   load(resfn)
   resDIVALIKE = res
   }
analysis_titletxt = "DIVA"
results_object = resDIVALIKE
scriptdir = np(system.file("extdata/a_scripts", package="BioGeoBEARS"))

res2 = plot_BioGeoBEARS_results(results_object, analysis_titletxt, addl_params=lis
t("j"), plotwhat="text", label.offset=1, tipcex=1.5, statecex=0.2, splitcex=0.2, titlecex
=1.5, plotsplits=TRUE, cornercoords_loc=scriptdir, include_null_range=TRUE, tr=c
lade, tipranges=tipranges)

plot_BioGeoBEARS_results(results_object, analysis_titletxt, addl_params=list("j"),
plotwhat="pie", label.offset=1.5, tipcex=1.5, statecex=0.2, splitcex=0.2, titlecex=1.5,
plotsplits=TRUE, cornercoords_loc=scriptdir, include_null_range=TRUE, tr=clade, t
ipranges=tipranges)


##########DIVA+J####

BioGeoBEARS_run_object = define_BioGeoBEARS_run()
BioGeoBEARS_run_object$trfn = clade
BioGeoBEARS_run_object$geogfn = tipranges
BioGeoBEARS_run_object$trfn = "filename.newick"
BioGeoBEARS_run_object$geogfn = "filname.data"

BioGeoBEARS_run_object$max_range_size = 8
BioGeoBEARS_run_object$min_branchlength = 0.000001    # Min to treat tip as a
direct ancestor (no speciation event)
BioGeoBEARS_run_object$include_null_range = TRUE    # set to FALSE for e.g.
DEC* model, DEC*+J, etc.
BioGeoBEARS_run_object$on_NaN_error = -1e50    # returns very low lnL if
parameters produce NaN error (underflow check)
BioGeoBEARS_run_object$speedup = TRUE
BioGeoBEARS_run_object$use_optimx = TRUE    # if FALSE, use optim() instead
of optimx()
BioGeoBEARS_run_object$num_cores_to_use = 5
BioGeoBEARS_run_object$force_sparse = FALSE
BioGeoBEARS_run_object =
readfiles_BioGeoBEARS_run(BioGeoBEARS_run_object)
BioGeoBEARS_run_object$return_condlikes_table = TRUE
BioGeoBEARS_run_object$calc_TTL_loglike_from_condlikes_table = TRUE
```

```
BioGeoBEARS_run_object$calc_ancprobs = TRUE    # get ancestral states from
optim run

# Set up DIVALIKE+J model
# Get the ML parameter values from the 2-parameter nested model
# (this will ensure that the 3-parameter model always does at least as good)
dstart = resDIVALIKE$outputs@params_table["d","est"]
estart = resDIVALIKE$outputs@params_table["e","est"]
jstart = 0.0001
BioGeoBEARS_run_object$BioGeoBEARS_model_object@params_table["d","init
"] = dstart
BioGeoBEARS_run_object$BioGeoBEARS_model_object@params_table["d","est"
] = dstart
BioGeoBEARS_run_object$BioGeoBEARS_model_object@params_table["e","init"
] = estart
BioGeoBEARS_run_object$BioGeoBEARS_model_object@params_table["e","est"
] = estart

# Remove subset-sympatry
BioGeoBEARS_run_object$BioGeoBEARS_model_object@params_table["s","type
"] = "fixed"
BioGeoBEARS_run_object$BioGeoBEARS_model_object@params_table["s","init"
] = 0.0
BioGeoBEARS_run_object$BioGeoBEARS_model_object@params_table["s","est"
] = 0.0


BioGeoBEARS_run_object$BioGeoBEARS_model_object@params_table["ysv","ty
pe"] = "2-j"
BioGeoBEARS_run_object$BioGeoBEARS_model_object@params_table["ys","typ
e"] = "ysv*1/2"
BioGeoBEARS_run_object$BioGeoBEARS_model_object@params_table["y","typ
e"] = "ysv*1/2"
BioGeoBEARS_run_object$BioGeoBEARS_model_object@params_table["v","typ
e"] = "ysv*1/2"


# Allow classic, widespread vicariance; all events equiprobable
BioGeoBEARS_run_object$BioGeoBEARS_model_object@params_table["mx01v"
,"type"] = "fixed"
BioGeoBEARS_run_object$BioGeoBEARS_model_object@params_table["mx01v"
,"init"] = 0.5
BioGeoBEARS_run_object$BioGeoBEARS_model_object@params_table["mx01v"
,"est"] = 0.5


# Add jump dispersal/founder-event speciation
BioGeoBEARS_run_object$BioGeoBEARS_model_object@params_table["j","type
"] = "free"
BioGeoBEARS_run_object$BioGeoBEARS_model_object@params_table["j","init"
] = jstart
```

```
BioGeoBEARS_run_object$BioGeoBEARS_model_object@params_table["j","est"]
= jstart


# Under DIVALIKE+J, the max of "j" should be 2, not 3 (as is default in DEC+J)
BioGeoBEARS_run_object$BioGeoBEARS_model_object@params_table["j","min
"] = 0.00001
BioGeoBEARS_run_object$BioGeoBEARS_model_object@params_table["j","max
"] = 1.99999
check_BioGeoBEARS_run(BioGeoBEARS_run_object)

resfn = "Plesiosauroidea_DIVALIKE+J_M0_unconstrained_v1.Rdata"
runslow = TRUE
if (runslow)
   {
   #sourceall("/Dropbox/_njm/__packages/BioGeoBEARS_setup/")

   res = bears_optim_run(BioGeoBEARS_run_object)
   res

   save(res, file=resfn)

   resDIVALIKEj = res
   } else {
   # Loads to "res"
   load(resfn)
   resDIVALIKEj = res

# Setup
analysis_titletxt = "DIVA+J"
results_object =  resDIVALIKEj
scriptdir = np(system.file("extdata/a_scripts", package="BioGeoBEARS"))
res1 = plot_BioGeoBEARS_results(results_object, analysis_titletxt,
addl_params=list("j"), plotwhat="text", label.offset=1, tipcex=1.5, statecex=0.2,
splitcex=0.2, titlecex=0.8, plotsplits=TRUE, cornercoords_loc=scriptdir,
include_null_range=TRUE, tr=clade, tipranges=tipranges)

plot_BioGeoBEARS_results(results_object, analysis_titletxt, addl_params=list("j"),
plotwhat="pie", label.offset=1, tipcex=1.5, statecex=0.2, splitcex=0.3, titlecex=1.5, p
lotsplits=TRUE, cornercoords_loc=scriptdir, include_null_range=TRUE, tr=clade, ti
pranges=tipranges)

#BAYAREALIKE

 BioGeoBEARS_run_object = define_BioGeoBEARS_run()
 BioGeoBEARS_run_object$trfn = clade
 BioGeoBEARS_run_object$geogfn = tipranges
 BioGeoBEARS_run_object$max_range_size = 8
 BioGeoBEARS_run_object$min_branchlength = 0.000001
 BioGeoBEARS_run_object$include_null_range = TRUE
```

```
 BioGeoBEARS_run_object$trfn = "filename.newick"
 BioGeoBEARS_run_object$geogfn = "filname.data"

 BioGeoBEARS_run_object$on_NaN_error = -1e50
 BioGeoBEARS_run_object$speedup = TRUE
 BioGeoBEARS_run_object$use_optimx = TRUE    # if FALSE, use optim() instead of optimx()
 BioGeoBEARS_run_object$num_cores_to_use = 1
 BioGeoBEARS_run_object$force_sparse = FALSE

 BioGeoBEARS_run_object = readfiles_BioGeoBEARS_run(BioGeoBEARS_run_object)
 BioGeoBEARS_run_object$return_condlikes_table = TRUE
 BioGeoBEARS_run_object$calc_TTL_loglike_from_condlikes_table = TRUE
 BioGeoBEARS_run_object$calc_ancprobs = TRUE    # get ancestral states from optim run


BioGeoBEARS_run_object$BioGeoBEARS_model_object@params_table["s","type
"] = "fixed"
BioGeoBEARS_run_object$BioGeoBEARS_model_object@params_table["s","init"
] = 0.0
BioGeoBEARS_run_object$BioGeoBEARS_model_object@params_table["s","est"
] = 0.0
BioGeoBEARS_run_object$BioGeoBEARS_model_object@params_table["v","typ
e"] = "fixed"
BioGeoBEARS_run_object$BioGeoBEARS_model_object@params_table["v","init
"] = 0.0
BioGeoBEARS_run_object$BioGeoBEARS_model_object@params_table["v","est"
] = 0.0
BioGeoBEARS_run_object$BioGeoBEARS_model_object@params_table["ysv","ty
pe"] = "1-j"
BioGeoBEARS_run_object$BioGeoBEARS_model_object@params_table["ys","typ
e"] = "ysv*1/1"
BioGeoBEARS_run_object$BioGeoBEARS_model_object@params_table["y","typ
e"] = "1-j"
BioGeoBEARS_run_object$BioGeoBEARS_model_object@params_table["mx01y"
,"type"] = "fixed"
BioGeoBEARS_run_object$BioGeoBEARS_model_object@params_table["mx01y"
,"init"] = 0.9999
BioGeoBEARS_run_object$BioGeoBEARS_model_object@params_table["mx01y"
,"est"] = 0.9999
analysis_titletxt = "BAYAREALIKEj on Plesiosauroidea"

results_object = resBAYAREALIKEj

scriptdir = np(system.file("extdata/a_scripts", package="BioGeoBEARS"))

res1 = plot_BioGeoBEARS_results(results_object, analysis_titletxt,
addl_params=list("j"), plotwhat="text", label.offset=1, tipcex=1.5, statecex=0.2,
splitcex=0.2, titlecex=1.5, plotsplits=TRUE, cornercoords_loc=scriptdir,
include_null_range=TRUE, tr=clade, tipranges=tipranges)
```

```
plot_BioGeoBEARS_results(results_object, analysis_titletxt, addl_params=list("j"), plotwhat="pie", label.offset=1, tipcex=1.5, statecex=0.2, splitcex=0.2, titlecex=1.5, plotsplits=TRUE, cornercoords_loc=scriptdir, include_null_range=TRUE, tr=clade, tipranges=tipranges)


#Bayarealike + J

BioGeoBEARS_run_object = define_BioGeoBEARS_run()
BioGeoBEARS_run_object$trfn = clade
BioGeoBEARS_run_object$geogfn = tipranges
BioGeoBEARS_run_object$max_range_size = max_range_size
BioGeoBEARS_run_object$min_branchlength = 0.000001
BioGeoBEARS_run_object$trfn = "filename.newick"
BioGeoBEARS_run_object$geogfn = "filname.data"

BioGeoBEARS_run_object$on_NaN_error = -1e50
BioGeoBEARS_run_object$speedup = TRUE
BioGeoBEARS_run_object$use_optimx = TRUE
BioGeoBEARS_run_object$num_cores_to_use = 1
BioGeoBEARS_run_object$force_sparse = FALSE


BioGeoBEARS_run_object =
readfiles_BioGeoBEARS_run(BioGeoBEARS_run_object)


BioGeoBEARS_run_object$return_condlikes_table = TRUE
BioGeoBEARS_run_object$calc_TTL_loglike_from_condlikes_table = TRUE
BioGeoBEARS_run_object$calc_ancprobs = TRUE

dstart = resBAYAREALIKE$outputs@params_table["d","est"]
estart = resBAYAREALIKE$outputs@params_table["e","est"]
jstart = 0.0001

BioGeoBEARS_run_object$BioGeoBEARS_model_object@params_table["d","init
"] = dstart
BioGeoBEARS_run_object$BioGeoBEARS_model_object@params_table["d","est"
] = dstart
BioGeoBEARS_run_object$BioGeoBEARS_model_object@params_table["e","init"
] = estart
BioGeoBEARS_run_object$BioGeoBEARS_model_object@params_table["e","est"
] = estart
BioGeoBEARS_run_object$BioGeoBEARS_model_object@params_table["s","type
"] = "fixed"
BioGeoBEARS_run_object$BioGeoBEARS_model_object@params_table["s","init"
] = 0.0
BioGeoBEARS_run_object$BioGeoBEARS_model_object@params_table["s","est"
] = 0.0
```

```
BioGeoBEARS_run_object$BioGeoBEARS_model_object@params_table["v","type"] = "fixed"
BioGeoBEARS_run_object$BioGeoBEARS_model_object@params_table["v","init"] = 0.0
BioGeoBEARS_run_object$BioGeoBEARS_model_object@params_table["v","est"] = 0.0
BioGeoBEARS_run_object$BioGeoBEARS_model_object@params_table["j","type"] = "free"
BioGeoBEARS_run_object$BioGeoBEARS_model_object@params_table["j","init"] = jstart
BioGeoBEARS_run_object$BioGeoBEARS_model_object@params_table["j","est"] = jstart

BioGeoBEARS_run_object$BioGeoBEARS_model_object@params_table["j","max"] = 0.99999


BioGeoBEARS_run_object$BioGeoBEARS_model_object@params_table["ysv","type"] = "1-j"
BioGeoBEARS_run_object$BioGeoBEARS_model_object@params_table["ys","type"] = "ysv*1/1"
BioGeoBEARS_run_object$BioGeoBEARS_model_object@params_table["y","type"] = "1-j"

BioGeoBEARS_run_object$BioGeoBEARS_model_object@params_table["mx01y","type"] = "fixed"
BioGeoBEARS_run_object$BioGeoBEARS_model_object@params_table["mx01y","init"] = 0.9999
BioGeoBEARS_run_object$BioGeoBEARS_model_object@params_table["mx01y","est"] = 0.9999
BioGeoBEARS_run_object$BioGeoBEARS_model_object@params_table["d","min"] = 0.0000001
BioGeoBEARS_run_object$BioGeoBEARS_model_object@params_table["d","max"] = 4.9999999

BioGeoBEARS_run_object$BioGeoBEARS_model_object@params_table["e","min"] = 0.0000001
BioGeoBEARS_run_object$BioGeoBEARS_model_object@params_table["e","max"] = 4.9999999

BioGeoBEARS_run_object$BioGeoBEARS_model_object@params_table["j","min"] = 0.00001
BioGeoBEARS_run_object$BioGeoBEARS_model_object@params_table["j","max"] = 0.99999

check_BioGeoBEARS_run(BioGeoBEARS_run_object)

resfn = "Psychotria_BAYAREALIKE+J_M0_unconstrained_v1.Rdata"
runslow = TRUE
if (runslow)
```

```
  {
  res = bears_optim_run(BioGeoBEARS_run_object)
  res

  save(res, file=resfn)

  resBAYAREALIKEj = res
  } else {
  # Loads to "res"
  load(resfn)
  resBAYAREALIKEj = res
  }



resBAYAREALIKEj
scriptdir = np(system.file("extdata/a_scripts", package="BioGeoBEARS"))



# Set up empty tables to hold the statistical results
restable = NULL
teststable = NULL

LnL_2 = get_LnL_from_BioGeoBEARS_results_object(results_DEC)
LnL_1 = get_LnL_from_BioGeoBEARS_results_object(results_DECJ)

 # DIVALIKE, null model for Likelihood Ratio Test (LRT)
 # BAYAREALIKE, null model for Likelihood Ratio Test (LRT)
 res2 = extract_params_from_BioGeoBEARS_results_object
 (results_object=resBAYAREALIKE, returnwhat="table", addl_params=c("j"),
 paramsstr_digits=4)
 # BAYAREALIKE+J, alternative model for Likelihood Ratio Test (LRT)
 res1 = extract_params_from_BioGeoBEARS_results_object
 (results_object=resBAYAREALIKEj, returnwhat="table", addl_params=c("j"),
 paramsstr_digits=4)
 rbind(res2, res1)
 conditional_format_table(stats)
 tmp_tests = conditional_format_table(stats)
 restable = rbind(restable, res2, res1)
 teststable = rbind(teststable, tmp_tests)
 LnL_2 = get_LnL_from_BioGeoBEARS_results_object(resBAYAREALIKE)
 LnL_1 = get_LnL_from_BioGeoBEARS_results_object(resBAYAREALIKEj)
 numparams1 = 3
 numparams2 = 2
 stats = AICstats_2models(LnL_1, LnL_2, numparams1, numparams2)

 LnL_2 = get_LnL_from_BioGeoBEARS_results_object(resBAYAREALIKE)
 LnL_1 = get_LnL_from_BioGeoBEARS_results_object(resBAYAREALIKEj)
 numparams1 = 3
```

```
numparams2 = 2
stats = AICstats_2models(LnL_1, LnL_2, numparams1, numparams2)
# BAYAREALIKE, null model for Likelihood Ratio Test (LRT)
res2 = extract_params_from_BioGeoBEARS_results_object
(results_object=resBAYAREALIKE, returnwhat="table", addl_params=c("j"),
paramsstr_digits=4)
# BAYAREALIKE+J, alternative model for Likelihood Ratio Test (LRT)
res1 = extract_params_from_BioGeoBEARS_results_object
(results_object=resBAYAREALIKEj, returnwhat="table", addl_params=c("j"),
paramsstr_digits=4)
rbind(res2, res1)

conditional_format_table(stats)
tmp_tests = conditional_format_table(stats)
restable = rbind(restable, res2, res1)
teststable = rbind(teststable, tmp_tests)
# ASSEMBLE RESULTS TABLES: DEC, DEC+J, DIVALIKE,
#DIVALIKE+J, BAYAREALIKE, BAYAREALIKE+J
teststable$alt = c("DEC+J", "DIVALIKE+J", "BAYAREALIKE+J")
teststable$null = c("DEC", "DIVALIKE", "BAYAREALIKE")
row.names(restable) = c("DEC", "DEC+J",
 "DIVALIKE", "DIVALIKE+J", "BAYAREALIKE", "BAYAREALIKE+J")
restable = put_jcol_after_ecol(restable)

restable
                LnL numparams          d          e          j
DEC          -87.00829         2 0.0029710467 4.720502e-03 0.00000000
DEC+J         -67.62103         3 0.0002863839 1.000000e-12 0.04018552
DIVALIKE      -79.91633         2 0.0032077346 1.000000e-12 0.00000000
DIVALIKE+J    -68.38179         3 0.0004286939 1.000000e-12 0.03925748
BAYAREALIKE  -108.11982         2 0.0038738386 3.805786e-02 0.00000000
BAYAREALIKE+J -69.37497         3 0.0002104881 6.684676e-04 0.02742695
```

Table A7.6: Model selection table displaying likelihood and AIC values for the Plesiosauroidea data set. The model with highest likelihood for the data is displayed in italics (DEC+J).

		Ln likelihood ratio test		AIC analysis		
Model	**LnL**	**D statistic**	**P value**	**AIC analysis**	**AICwt**	**Ratio**
DEC	-87.00	40.54	1.9e-10	178.01	6.3e-09	2.3e+8
DEC+J	*-67.62*			141.24	0.6	
DIVALIKE	-79.92	29.33	6.1e-08	163.83	7.5e-06	861830
DIVALIKE + J	-68.38			142.7	0.2	
BAYAREALIKE	-108.11	78.97	6.3e-19	220.24	4.2e-18	5.16e+16
BAYAREALIKE+J	-69.37			144.75	0.1	

PAE analysis

Analysis run in TNT V 1.5 (Goloboff and Catalano, 2016), using implicit enumeration. The analysis found six MPTs. Genera which have an uncertain taxonomic status (*Paraophthalmosaurus*, *Ostechevia* and *Grendelius*) were omitted from this analysis. The data matrix (Table A7.6), comprises of 9 geographical areas of interest (GAIs) including a hypothetical root and 17 genera. Format datatype = "01": “0” = absent, “1” = present

Data matrix:

Table A7.7: Data matrix used for the parsimony analysis of endemicity.

	Colymbosaurus	*Kimmerosaurus*	*Spitrasaurus*	*Djupedalia*	*Gen. et sp. nov*	*Pliosaurus*
Root	0	0	0	0	0	0
Svalbard	1	0	1	1	1	1
Eastern_Europe	0	0	0	0	0	0
Arctic Canada	1	0	0	0	0	0
Moscow_basin	1	0	0	0	0	1
NW_Russia	0	0	0	0	0	0
Western_Europe	1	1	0	0	0	1
Neuquén Basin	0	0	0	0	0	1
Mexico	0	0	0	0	0	1
Madagascar	0	0	0	0	0	0

	Ophthalmosaurus	*Brachypterygius*	*Nannopterygius*	*Caypullisaurus*	*Arthtopterygius*
Root	0	0	0	0	0
Svalbard	0	0	0	0	0
Eastern_Europe	1	0	0	0	0
Arctic_Canada	0	0	0	0	1
Moscow_basin	1	1	0	0	1
NW_Russia	1	0	0	0	0
Western_Europe	1	1	1	0	0
Neuquén_ Basin	1	0	0	1	1
Mexico	1	0	0	0	0
Madagascar	0	1	0	0	0

Continued Table A7.7: Data matrix used for the parsimony analysis of endemicity.

	Undorosaurus	*Cryopterygius*	*Palvennia*	*Janusaurus*	*Aegirosaurus*	*Gengasaurus*
Root	0	0	0	0	0	0
Svalbard	0	1	1	1	0	0
Eastern_Europe	0	0	0	0	0	0
Arctic_Canada	0	0	0	0	0	0
Moscow_basin	1	0	0	0	0	0
NW_Russia	0	0	0	0	0	0
Western_Europe	0	0	0	0	1	0
Neuquén_ Basin	0	0	0	0	1	1
Mexico	0	0	0	0	0	0
Madagascar	0	0	0	0	0	0

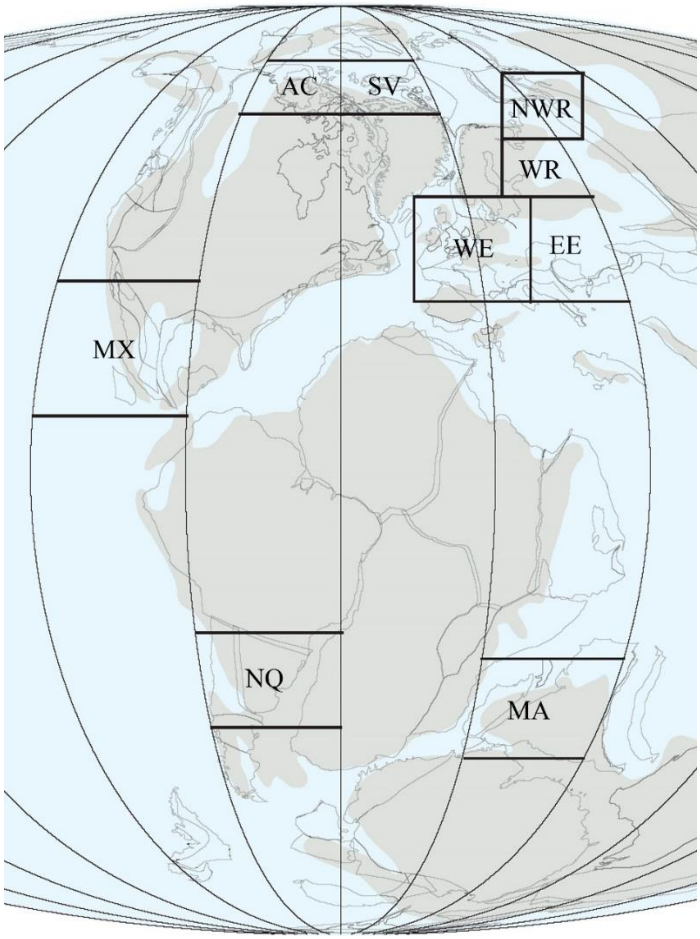

Figure A7.2: Geographic areas on interest included in parsimony analysis of endemicity. **Abbreviations: AC**, Arctic Canada Region; **EE**, Eastern Europe; **MA** Madagascar Region; **MX**, Mexico region; **NQ**, Neuquén Basin; **NWR**, North-western Russian Region; **SV**, Svalbard Region; **WE**, Western Europe Region; **WR**, Western Russian Region.

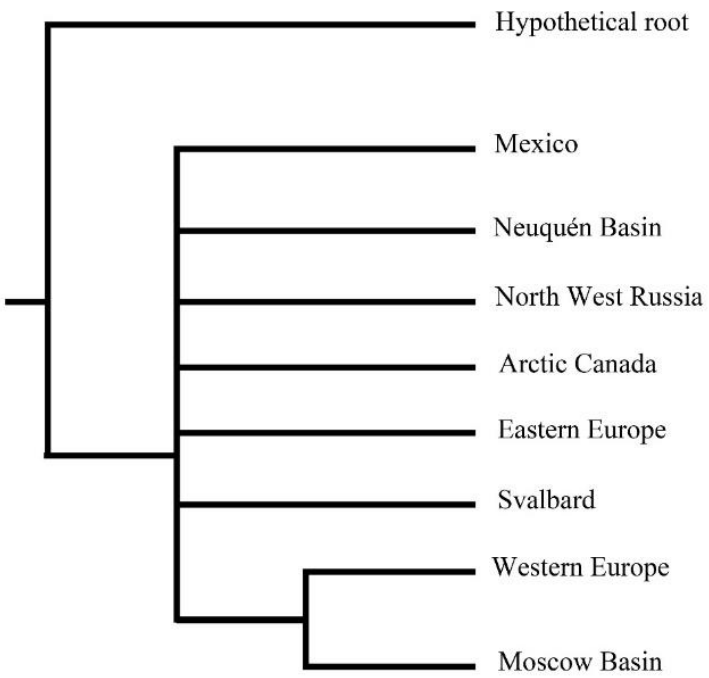

Figure A7.3 Strict consensus tree for the PAE analysis from six MPTs, showing the relationship of shared genera between the different GAIs during the Kimmeridgian - Tithonian interval.

Distance Matrix

Present-absent data for ichthyosaurian and plesiosaurian genera is available in Table A7.7. Genera which have an uncertain taxonomic status (*Paraophthalmosaurus*, *Ostechevia* and *Grendelius*) were omitted from this analysis.

Table A7.8: The presence-absence data for the geographic areas of interest. **Abbreviations**: **AC**, Arctic Canada; **MX**, Mexico region; **NQ**, Neuquén Region; **SV**, Svalbard Region; **WE**, Western Europe; **WR**, Western Russia.

Taxa	**SV**	**AC**	**WR**	**WE**	**NQ**	**MX**
Colymbosaurus	1	1	1	1	0	0
Spitrasaurus	1	0	0	0	0	0
Djupedalia	1	0	0	0	0	0
Kimmerosaurus	0	0	0	1	0	0
Gen et sp. nov	1	0	0	0	0	0
Pliosaurus	1	0	1	1	1	1
Ophthalmosaurus	0	1	1	1	1	1
Nannopterygius	0	0	0	1	0	0
Brachypterygius	0	0	1	1	0	0
Janusaurus	1	0	0	0	0	0
Arthropterygius	0	1	1	0	1	0
Caypullisaurus	0	0	0	0	1	0
Aegirosaurus	0	0	0	1	1	0
Cryopterygius	1	0	0	0	0	0
Undorosaurus	0	0	1	0	0	0
Palvennia	1	0	0	0	0	0

The Sørenson coeffient formulae: 2 x shared taxa/((2 x shared taxa) + species found in sample 1 + species found in sample 2)

R script for the distance matrix using *fossil* in R (CRAN core group).

#packages active: *fossil* (Vavrek, 2011)

```
x<-read.csv("filename.csv", header=T, sep=";")
y<-ecol.dist(x, method=sorenson)
```

	SV	AC	WR	NWR	WE	NQ
AC	0.82					
WR	0.71	0.33				
NWR	1.00	0.50	0.71			
WE	0.73	0.60	0.38	0.75		
NQ	0.85	0.50	0.45	0.66	0.50	
MX	0.8	0.60	0.50	0.33	0.55	0.43

Argumentation for the referral of *Cryopterygius kielanae* to Ophthalmosauride indet.

A more in-depth discussion of the referral of GMUL 3579-81 to Cryopterygius is included here. Cryopterygius kielanae (GMUL 3579-81) is referred to the genus Cryopterygius on the following features (Tyborowski, 2016): 1) proximodistally short humerus in relation to total length (of the animal), with two distal facets (radius and ulna); 2) rectangular-pentagonal proximal phalanges; 3) anteroposteriorly broad femur with two distal facets (fibula and tibia); 4) broad concavity on the proximolateral surface of the scapula and 5) neural arches with V-shaped apical notch in the neural spines. C. kielanae and C. kristiansenae share the number of distal facets (2) on the humerus. This holotype of C. kristiansenae (right bears two facets; left bears a diminutive facet for a preaxial accessory element), illustrating the variability of this character. Arkhangelsky and Zverkov (2014), recognised a similar forelimb architecture in several Late Jurassic ichthyosaurs, indicating a low phenotypical evolution in this region of the skeleton and may represent poor diagnostic features (Fisher et al. 2016). As the vertebral column of C. kielanae and C. kristiansenae are incomplete, making comparisons total length inaccurate. The femora of C. kielanae and C. kristiansenae are similar in general morphology; with and dorsoventrally expanded proximal head and an anteriorly extended tibial facet. There are also numerous differences: C. kristiansenae bears an anteroposteriorly narrower femoral shaft, the tibial facet of C. kielanae faces anterodistally at more of an angle than C. kristiansenae. There are certain unclarified aspects of the scapula feature, if Tyborowski (2016) is referring to the concavity along the ventral margin of the scapula in lateral view; this feature is present in numerous ophthalmosaurids including Ophthalmosaurus icenicus (Kirton, 1983). The final feature regarding the dorsal margin of the neural spines is difficult to compare, as no figure of this feature is provided. Also, the author stated that this neural spine may not come from GMUL 3579-81, which again raises the question of whether this specimen derives from one or multiple individuals.

Literature Cited

Andrews, C. W. 1909. On some new Plesiosauria from the Oxford Clay of Peterborough. Annals and Magazine of Natural History Series VIII 4:418-429.

Andrews, C. W. 1910. A descriptive catalogue of the Marine Reptiles of The Oxford Clay Based on the Leeds Collection in the British Museum (Natural History). British Museum (Natural History), London.

Arkhangelsky, M. S., Zverkov, N. G. and M. A. Rogov, I. M. Stenshin, and E. M. Baykina. *in press*. Colymbosaurines from the Upper Jurassic of European Russia and their implication for paleobiogeography of marine reptiles; pp. *i*n B. P. Kear, S. Sachs, A. Smith, and P. D. Druckenmiller (eds.), *Plesiosaurs - Mesozoic Sea Dragons*. Springer - Vertebrate Paleobiology and Paleoanthropology Series.

Arkhangelsky, M. S. 1997. On a new ichthyosaurian genus from the lower Volgian substage of the Saratov, Volga Region. *Paleontological Journal* 31:87-90.

Arkhangelsky, M. S. 2000. On the ichthyosaur *Otschevia* from the Volgian Stage of the Volga Region. *Paleontological Journal* 34: 549-554.

Arkhangelsky, M. S., and N. G. Zverkov. 2014. On a new ichthyosaur of the genus *Undorosaurus*. *Proceedings of the Zoological Institute RAS* 318:187-196.

Bardet, N., J.-M. Mazin, E. Cariou, R. Enay, and J. Krishna. 1991. Les Plesiosauria du Jurassique supérieur de la province de Kachchh (Inde). Comptes Rendus de l'Académie des Sciences - Series II 313:1343-1347.

Bardet, N. and M. S. Fernández. 2000. A new ichthyosaur from the Upper Jurassic lithographic limestones of Bavaria. Journal of Paleontology 74: 503-511.

Barrientos-Lara, J., Y. Herrera, M. Fernández, and J. Alvarado-Otega. 2016. Ocurrence of *Torvoneustes* (Crocodylomorpho, Metriorynchidae) in marine Jurassic deposits of Oaxaca, Mexico. Revista Brasileira de Paleontologia 19:415-424.

Benson, R. B. J., M. Evans, A. Smith, J. Sassoon, S. Moore-Faye, H. F. Ketchum, and R. Forrest. 2013. A giant pliosaurid skull from the Late Jurassic of England. *PLOS ONE* 8:e65989.

Benson, R. B. J., and T. Bowdler. 2014. Anatomy of Colymbosaurus megadeirus (Reptilia, Plesiosauria) from the Kimmeridge Clay Formation of the U.K., and high diversity amoung Late Jurassic plesiosauroids. *Journal of Vertebrate Paleontology* 34:1053-1071.

Benson, R. B. J., N. G. Zverkov, and M. S. Arkhangelsky. 2015. Youngest occurrences of rhomaleosaurid plesiosaurs indicate survival of an archaic marine reptile clade at high palaeolatitudes. Acta Palaeontologica Polonica 60:769-780.

Benton, M. J., and P. S. Spencer. 1995. Fossil reptiles of Great Britain. Chapman and Hall, London.

Brown, D. S. 1981. The English Upper Jurassic Plesiosauridae (Reptilia) and a review of the phylogeny and classification of the Plesiosauia. *Bulletin of the British Museum (Natural History), Geology* 35:253-347.

Buchy, M. C., Frey, E., Stinnesbeck, W. and J. G. López-Oliva. 2003. First occurrence of a gigantic pliosaurid plesiosaur in the late Jurassic (Kimmeridgian) of Mexico. *Bulletin de la Société Géologique de France* 174: 271-278.

Buchy, M. C. 2010. First record of Ophthalmosaurus (Reptilia: Ichthyosauria) from the Tithonian (Upper Jurassic) of Mexico Journal of Paleontology 84:149-155.

Buffetaut, E. 1981. A plesiosaur vertebrae from the Chichali Formation (Late Jurassic to Early Cretaceous) of Pakistan. Neues Jahrbuch für Paläontologie Abhandlungen 1981:334-338.

Cau, A., and F. Fanti. 2015. A pliosaurid plesiosaurian from the Rosso Ammonitico Veronese Formation of Italy. Acta Palaeontologica Polonica 59:643-650.

Cruickshank ARI & Long JA (1997). A new species of pliosaurid reptile from the Early Cretaceous Birdrong Sandstone of Western Australia. Records of the Western Australian Museum 18, 263-276.

Delsett, L. L., A. J. Roberts, P. D. Druckenmiller, and J. H. Hurum. 2017. A new ophthalmosaurid (Ichthyosauria) from Svalbard, Norway and evolution of the ichthyopterygian pelvic girdle. PLOS ONE 12:e0169971.

Delsett, L. L., A. J. Roberts, P. D. Druckenmiller, and J. H. Hurum. 2017. A new ophthalmosaurid (Ichthyosauria) from Svalbard, Norway and evolution of the ichthyopterygian pelvic girdle. PLOS ONE 12:e0169971.

Druckenmiller, P. S., J. H. Hurum, E. M. Knutsen, and H. A. Nakrem. 2012. Two new ophthalmosaurids (Reptilia: Ichthyosauria) from the Agardhfjellet Formation (Late Jurassic: Volgian/Tithonian), Svalbard, Norway. Norwegian Journal of Geology 92:311-339.

Efimov, V. M. 1999a. A new family of ichthyosaurs, the Undorosauridae fam. nov. from the Volgian Stage of the European part of Russia. Paleontological Journal 33.174-181.

Efimov, V. M. 1999b. Ichthyosaurs of a new genus *Yasykovia* from the Upper Jurassic strata of European Russia. *Paleontological Journal* 35: 91-98.

Fernandez, M. S. 1997a. A new Ichthyosaur from the Tithonian (Late Jurassic) of the Neuquén Basin, North-western Patagonia, Argentina. Journal of Palaeontology 71: 479-484.

Fenández, M. S. 1997b. On the paleogeographic distribution of Callovian and Late Jurassic ichthyosaurs, Journal of Vertebrate Paleontology, 17: 752-754.

Fernández, M. S., and M. Iturralde-Vincent. 2000. An Oxfordian Ichthyosauria (Reptilia) from Viñales, western Cuba: paleobiogeographic significance. Journal of Vertebrate Paleontology 20:191-193.

Fernández, M. S., and E. E. Maxwell. 2012. The genus *Arthropterygius* Maxwell (Ichthyosauria:Ophthalmosauridae) in the Late Jurassic of the Neuqúen Basin, Argentina. Geobios 45:535-540.

Fischer, V. Clément, A., Guiomar, M. and P. Godefroit. 2011. The first definite record of a Valanginian ichthyosaur and its implications on the evolution of post-Liassic Ichthyosauria. *Cretaceous Research* 32: 155-163.

Fischer, V. Maisch, M. W., Naish, D., Kosma, R., Liston, J., Joger, U., Krüger, F. J., Pérez,J. P., Tainsh, J. and R. M. Appleby. .2012. New ophthalmosaurid ichthyosaurs from the European Lower Cretaceous demonstrate extensive ichthyosaur survival across the Jurassic–Cretaceous boundary. *PLOS ONE* 7: e29234.

Forrest and Oliver, 2003. Ichthyosaurs and plesiosaurs from the lower spilsby sandstone member (Upper Jurassic), north Lincolnshire. Proceedings of the Yorkshire Geological Society 54: 269-275.

Gasparini, Z. A new Oxfordian pliosaurid (Plesiosauria, Pliosauridae) in the Caribbean Seaway. Palaeontology 52; 661-669.

Gasparini, Z., and L. Spalletti. 1993. First Callovian plesiosaurs from the Neuquen Basin, Argentina. Ameghiniana 30:245-254.

Gasparini, Z., N. Bardet, and M. Iturralde-Vincent. 2002. A new cryptoclidid Plesiosaur from the Oxfordian (Late Jurassic) of Cuba. Geobios 35:201-211.

Gasparini Z. and J. P. O'Gorman. 2014. A New Species of *Pliosaurus* (Sauropterygia, Plesiosauria) from the Upper Jurassic of North-western Patagonia, Argentina. *Ameghiniana* 51: 269-283.

Gasparini, Z., J. Sterli, A. Parras, J. P. O'Gorman, L. Salgado, J. Varela, and D. Pol. 2015. Late Cretaceous reptilian biota of the La Colonia Formation central patagonia, Argentina: Occurences, preservation and paleoenvironments. Cretaceous Research 54:154-168.

Gilmore, C. W. 1905. Osteology of Babtanodon (Marsh). Memoirs of the Carnegie Museum 2:77-129.

Halstead, L. B. 1971. *Liopleurodon rossicus* (Novozhilov) – A pliosaur from the Lower Volgian of the Moscow Basin. *Palaeontology* 14: 566-570.

Hulke, J. W. 1870. Note on some Plesiosaurian Remains obtained by J. C. Mansel Esq. F.G.S., in Kimmeridge Bay, Dorset. Quarterly Journal of the Geological Society of London 26:611-622.

Ketchum, H. F., and R. B. J. Benson. 2011. The cranial anatomy and taxonomy of *Peloneustes philarchus* (Sauropterygia, Pliosauridae) from the Peterborough member (Callovian, Middle Jurassic) of the United Kingdom. Palaeontology 54:639-665.

Knutsen, E. M., P. S. Druckenmiller, and J. H. Hurum. 2012a. A new plesiosaurid (Reptilia-Sauropterygia) from the Agardhfjellet Formation (Middle Volgian) of central Spitsbergen, Norway. Norwegian Journal of Geology 92:213-234.

Knutsen, E. M., P. S. Druckenmiller, and J. H. Hurum. 2012b. A new species of *Pliosaurus* (Sauropterygia: Plesiosauria) from the Middle Volgian of central Spitsbergen, Norway. Norwegian Journal of Geology 92:235-258.

Knutsen, E. M., P. S. Druckenmiller, and J. H. Hurum. 2012c. Redescription and taxonomic clarfication of '*Tricleidus' svalbardensis* based on new material from the Agardhfjellet Formation (Middle Volgian). Norwegian Journal of Geology 92:175-186.

Knutsen, E. M., P. S. Druckenmiller, and J. H. Hurum. 2012d. Two new species of long-necked plesiosaurians (Reptilia-Sauropterygia) from the Upper Jurassic

(Middle Volgian) Agardhfjellet Formation of central Spitsbergen. Norwegian Journal of Geology 92:187-212.

Lomax, D. R. 2015. The first plesiosaurian (Sauropterygia, Pliosauridae) remains described from the Jurassic of Poland. Palaeontologia Electronica 18.2.29A:1-8.

Matzke, N. J. 2013 . BioGeoBEARS: BioGeography with Bayesian (and likelihood) evolutionary analysis in R scripts. R package, Version 0.2.

Matzke, N. J. 2014 . Model selection in historical biogeography reveals that founder-event speciation is a cruial process in island clades. Systematic Biology 63:951-970.

Maxwell, E. E. 2010. Generic reassignment of an ichthyosaur from the Queen Elizabeth Islands, Northwest Territories, Canada. Journal of Vertebrate Paleontology 30:403-415.

McGowan, C. 1978. Further evidence for the wide geographical distribution of ichthyosaur taxa (Reptilia, Ichthyosauria). Journal of Paleontology 52:1155-1162.

Moon, B. C., and A. M. Kirton. 2016. Ichthyosaurs of the British Middle and Upper Jurassic. Part 1. *Ophthalmosaurus*, Vol. 170, pp. 84. Monography of the Palaeontographical Society, London.

Noe, L.F., Liston, J.J. and Evans, M. 2003. The first relatively complete exoccipital-opisthotic from the braincase of the Callovian pliosaur, *Liopleurodon.* Geological Magazine 140: 479-486.

O'Gorman, J. P, Lazo, D. G., Luci, L. , Cataldo, C. S., Schwarz, E., Lescano, M. and M. B. Aguirre-Urreta. 2015. New plesiosaur records from the Lower Cretaceous of the Neuquén Basin, west-central Argentina, with an updated picture of occurrences and facies relationships. *Cretaceous Research* 56: 372-387.

O'Keefe, F. R., and H. P. Street. 2009. Osteology of the cryptocleidoid plesiosaur *Tatenectes laramiensis*, with comments on the taxonomic status of the Cimoliasauridae. Journal of Vertebrate Paleontology 29:48-57.

O'Keefe, F. R., and W. J. Wahl. 2003. Current taxonomic status of the plesiosaur *Pantosaurus striatus* from the Upper Jurassic Sundance Formation, Wyoming. Paludicola 4:37-46.

Paparella, I., E. E. Maxwell, A. Ciproani, S. Roncacè, and M. W. Caldwell. 2016. The first ophthalmosaurid ichthyosaur fromt he Upper Jurassic of the Umbrian-Marchean Apennines (Marche, central Italy). Geological Magazine:1-22.

Roberts, A. J., P. D. Druckenmiller, G.-P. Sætre, and J. H. Hurum. 2014. A New Upper Jurassic Ophthalmosaurid Ichthyosaur from the Slottsmøya Member, Agardhfjellet Formation of Central Spitsbergen. PLOS ONE 9:e103152.

Roberts, A. J., P. S. Druckenmiller, L. L. Delsett, and J. H. Hurum. 2017. Osteology and relationships of Colymbosaurus Seeley, 1874, based on new material of C. svalbardensis from the Slottsmøya Member, Agardhfjellet Formation of central Spitsbergen. Journal of Vertebrate Paleontology:e1278381.

Sachs, S., J. J. Hornung, and B. P. Kear. 2016. Reappraisal of Europe's most complete Early Cretaceous plesiosaurian: Brancasaurus brancai Wegner, 1914 from the "Wealden facies" of Germany. PeerJ 4:e2813.

Sauvage, H.E. 1873. Notes sur les reptiles fossils. Bulletin de la Société Géologique de France, série 3 1: 356-386.

Sato, T., and X.-C. Wu. 2008. A new Jurassic pliosaur from Melville Island, Canadian Arctic Archipelago. Canadian Journal of Earth Science 45:303-320.

Sissons, R. L., M. W. Caldwell, C. A. Evenchick, D. B. Brinkman, and M. J. Vavrek. 2015. An Upper Jurassic ichthyosaur (Ichthyosauria: Ophthalmosauridae) from the Bowser Basin, British Columbia. Canadian Journal of Earth Science 53:34-40.

Smith, A. S. 2007. Anatomy and Systematic of the Rhomaleosauridae (Sauropterygia: Plesiosauria). PHD thesis. National University of Ireland, University College of Dublin. Dublin.

Stinnesbeck, W., E. Frey, L. Rivas, J. M. Pardo Pérez, M. L. Cartes, C. S. Soto, and P. Z. Lobos. 2014. A Lower Cretaceous ichthyosaur graveyard in deep marine slope channel deposits at Torres del Paine National Park, southern Chilie. Geological Society of America Bulletin 126:1317-1339.

Storrs, G. W., M. S. Arkhangelsky, and E. V. M. 2000. Mesozoic marine reptiles of Russia and other former Soviet republics; pp. *i*n M. J. Benton, M. A. Shishkin, D. M. Unwin, and E. N. Kurochkin (eds.), The age of Dinosaurs in Russia and Mongolia. Cambridge University press, Cambridge, United Kingdom.

Tyborowski, D. 2016. A new ophthalmosaurid ichthyosaur from the Late Jurassic of Owadów-Brzeziniki Quarry, poland. Acta Palaeontologica Polonica 61:791-803.

Wahl, R. W., J. A. Massare, and M. Ross. 2010. New material from the type specimen of *Megalneusaurus rex* (Reptilia: Sauropterygia) from the Jurassic Sundance Formation, Wyoming. Paludicola 7:170-180.

Weems, R. E and R. B Blodgett. 1994. The pliosaurid Megalneusaurus: A newly recognized occurrence in the Upper Jurassic Naknek Formation of the Alaska peninsula. U.S. Geological Survey Bulletin 2152: 169-175.

Zverkov, N. G., M. S. Arkhangelsky, J. M. Pardo Pérez, and P. A. Beznosov. 2015. On the Upper Jurassic ichthyosaur remains from the Russian North. Proceedings of the Zoological Institute RAS 319:81-97.

Appendix 8

Published paper Delsett et al., 2017

PLOS ONE

RESEARCH ARTICLE

A New Ophthalmosaurid (Ichthyosauria) from Svalbard, Norway, and Evolution of the Ichthyopterygian Pelvic Girdle

Lene Liebe Delsett[1]*, Aubrey J. Roberts[1,2], Patrick S. Druckenmiller[3,4], Jørn H. Hurum[1]

1 Natural History Museum, University of Oslo, Oslo, Norway, **2** The National Oceanography Centre, Department of Ocean and Earth Science, University of Southampton, Southampton, Hampshire, United Kingdom, **3** University of Alaska Museum, Fairbanks, Alaska, **4** Department of Geoscience, University of Alaska Fairbanks, Fairbanks, Alaska

* l.l.delsett@nhm.uio.no

OPEN ACCESS

Citation: Delsett LL, Roberts AJ, Druckenmiller PS, Hurum JH (2017) A New Ophthalmosaurid (Ichthyosauria) from Svalbard, Norway, and Evolution of the Ichthyopterygian Pelvic Girdle. PLoS ONE 12(1): e0169971. doi:10.1371/journal.pone.0169971

Editor: William Oki Wong, Institute of Botany, CHINA

Received: June 6, 2016

Accepted: December 24, 2016

Published: January 25, 2017

Data Availability Statement: All relevant data are within the paper and its Supporting Information files.

Funding: LLD is supported by a PhD grant from the Ministry of Education and Research via the Natural History Museum, University of Oslo. AJR is supported by PhD grants from Tullow Oil, NERC and the University of Southampton. Grants for the excavations were provided by the Norwegian Research Council, National Geographic (grant no. EC0425_09 and EC0435_09), the Ministry of

Abstract

In spite of a fossil record spanning over 150 million years, pelvic girdle evolution in Ichthyopterygia is poorly known. Here, we examine pelvic girdle size relationships using quantitative methods and new ophthalmosaurid material from the Slottsmøya Member Lagerstätte of Svalbard, Norway. One of these new specimens, which preserves the most complete ichthyosaur pelvic girdle from the Cretaceous, is described herein as a new taxon, *Keilhauia nui* gen. et sp. nov. It represents the most complete Berriasian ichthyosaur known and the youngest yet described from the Slottsmøya Member. It is diagnosed on the basis of two autapomorphies from the pelvic girdle, including an ilium that is anteroposteriorly expanded at its dorsal end and an ischiopubis that is shorter or subequal in length to the femur, as well as a unique character combination. The Slottsmøya Member Lagerstätte ichthyosaurs are significant in that they represent a diverse assemblage of ophthalmosaurids that existed immediately preceding and across the Jurassic±Cretaceous boundary. They also exhibit considerable variation in pelvic girdle morphology, and expand the known range in size variation of pelvic girdle elements in the clade.

Introduction

Ichthyopterygia is a diverse clade of secondarily aquatic reptiles that lived from the Early Triassic (Olenekian) to the early Late Cretaceous (Cenomanian) [1, 2]. The clade had, by the Late Jurassic, developed into derived ichthyosaurs with a spindle-shaped body, large eyes and a small hind fin. The ichthyosaur body shape and its resemblance to odontocete cetaceans (especially delphinids and phocenids), is often used as a textbook example of convergent evolution among secondarily aquatic vertebrates.

One of the most important trends in ichthyosaur evolution relates to swimming modes and becoming high-speed pursuit predators. This evolutionary pathway is clearly seen in the posterior appendicular skeleton. Among terrestrial tetrapods, the pelvic girdle is necessary to articulate the vertebral column with the hind limbs in order to support the weight of the body and

Education and Research and Brian Snyder. Sponsors for the excavations were Spitsbergen Travel, Exxon Mobil Norway, Fugro, OMV, PowerShop, Nexen, Norwegian Petroleum Directorate, Hydro and Bautas.

Competing Interests: The authors have declared that no competing interests exist.

facilitate locomotion. Typically, the hind limbs are longer than the forelimbs and more commonly used for locomotion [3]. In contrast, it is assumed that derived ichthyosaurs did not use their limbs for locomotion [1, 4, 5]; particularly the hind fins, resulting in a reduction in pelvic girdle size and fusion of the ischium and pubis. Although ichthyosaur hind fins were reduced in size compared to the forefins, there is currently no evidence to suggest complete loss of the hind fin, as occurred among cetaceans [5±7].

An unanswered question is how the body shape evolution through the Jurassic and the Cretaceous affected the relative size and morphology of the pelvic girdle and hind fin. Pelvic girdles are likely important for inferring phylogenetic relationships and have been suggested to show a larger morphological variation than the pectoral girdle [8], but the degree of individual and intraspecific variation is currently not well understood. In spite of their potential importance, ichthyosaur pelvic girdles are relatively understudied (see overviews in dal Sasso and Pinna [9], Motani [10], Maisch and Matzke [11], McGowan and Motani [6]). Traditional descriptions and character matrices used in recent papers are skeletally biased towards the cranium and forefin; in comparison the pelvic girdle has received less attention as a source of useful taxonomic and phylogenetic data (but see new characters in [12]) [6, 13]. Compounding the problem are taphonomic biases, given the relatively small size of the pelvic girdle and hind fin and loose nature of their articulation with other pelvic elements and the vertebral column. Thus, these elements are more easily disarticulated from a rotting carcass during floating or disconnected when landing on the sea bottom [6, 14]. A similar bias exists for the reduced pelvic girdle (innominate) in many cetaceans [15]. Innominates are poorly known in many extinct cetacean species, particularly among fully aquatic taxa, and are virtually unknown in the gap between basilosaurids (late middle Eocene±late Oligocene) and extant species [16].

Many small, fully articulated ichthyosaur specimens from Triassic and Early to Middle Jurassic Lagerstätten have complete pelvic girdles, but this is not the case for the majority of late Middle Jurassic to Cretaceous ophthalmosaurids [8, 17] (S1 Table), in spite of the description of numerous new specimens and taxa in the last decade [18±25]. For five ophthalmosaurid genera, only the ischiopubis is known from the pelvic girdle. The only pelvic girdle material (an ischiopubis) of specimens referred to *Platypterygius* was recently described in *P. australis* [26].

Between 2004 and 2012 the Spitsbergen Mesozoic Research Group excavated the remains of 29 ichthyosaur specimens from the Late Jurassic±Early Cretaceous Slottsmøya Member Lagerstätte [27, 28] (Fig 1). Two previously described ichthyosaurs from the unit have contributed significantly to our knowledge of ichthyosaurian pelvic girdles (Fig 2). The holotype of *Cryopterygius kristiansenae* Druckenmiller, Hurum, Knutsen and Nakrem 2012 preserves the left ischiopubis and ilium together with the majority of an articulated hind fin. The holotype of *Janusaurus lundi* Roberts, Druckenmiller, Sætre and Hurum 2014 preserves the left ischiopubis, both ilia and two disarticulated hind fins [25, 29].

In addition to these previously described specimens, four other Slottsmøya Member specimens have pelvic material, and are described herein. One specimen is Berriasian in age, and consists of a partial skeleton including the most complete pelvic girdle from the Cretaceous known to date. Ichthyosaurs are very poorly known from the Berriasian-Barremian interval [19, 30] with only fragmentary Berriasian material known from a few specimens in England [19, 31, 32], Argentina [17, 33], and possibly from Russia [34] and Chile [35]. The second partial specimen described here is from the Tithonian and is significant because it preserves a complete pelvic girdle with both femora, previously only known from one Late Jurassic specimen except *Ophthalmosaurus icenicus* and the holotype of *Janusaurus lundi* [29], from which it differs substantially. Finally, two additional Tithonian specimens consist of pelvic girdle and hind fin material.

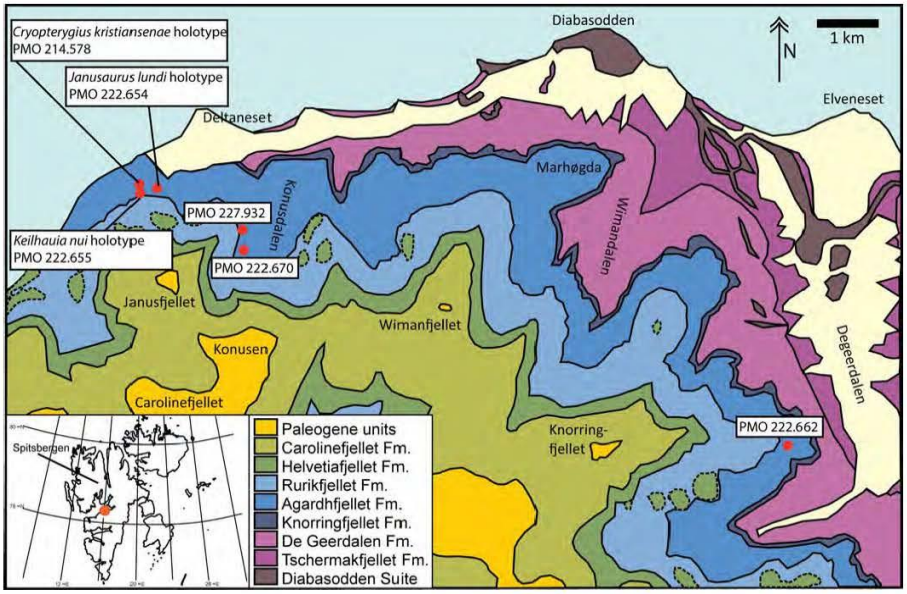

Fig 1. Map showing six ichthyosaur specimens from the Slottsmøya Member Lagerstätte discussed in the text (red dots). Overview map (left corner) shows the Svalbard archipelago and island of Spitsbergen; orange dot corresponds to excavation area. Adapted from Hurum et al. (2012).

doi:10.1371/journal.pone.0169971.g001

The aims of this paper are to: 1) describe four new ichthyosaur specimens from the Slottsmøya Member Lagerstätte; 2) conduct a phylogenetic analysis to determine the position of the most complete specimen, PMO 222.655; 3) use the new material to address size relationships between pelvic girdle elements and femora in Jurassic and Cretaceous taxa and 4) provide an overview of the shape of pelvic girdle elements in ichthyosaurs from the Triassic to their extinction in the Cretaceous and compare this evolution to that of the cetacean innominate.

Institutional abbreviations

SNSB-BSPG, Bayerische Staatssammlung für Paläontologie und Geologie Munich; CAMSM, Sedgwick Museum of Earth Sciences; EP, Paleontological Museum of Undory, Ul'yanovsk Region, Russia; GLAHM, The Hunterian Museum, University of Glasgow; LEIUG, University of Leicester; NHMUK, Natural History Museum, UK; OUMNH, Oxford University Museum; PMO, Natural History Museum, Oslo, paleontological collections; TMP, Royal Tyrrell Museum of Palaeontology, Drumheller, Alberta, Canada.

Geological Setting

The ichthyosaur specimens described in this study were recovered from the Late Jurassic± Early Cretaceous Slottsmøya Member Lagerstätte on Spitsbergen (Fig 2), the largest island in

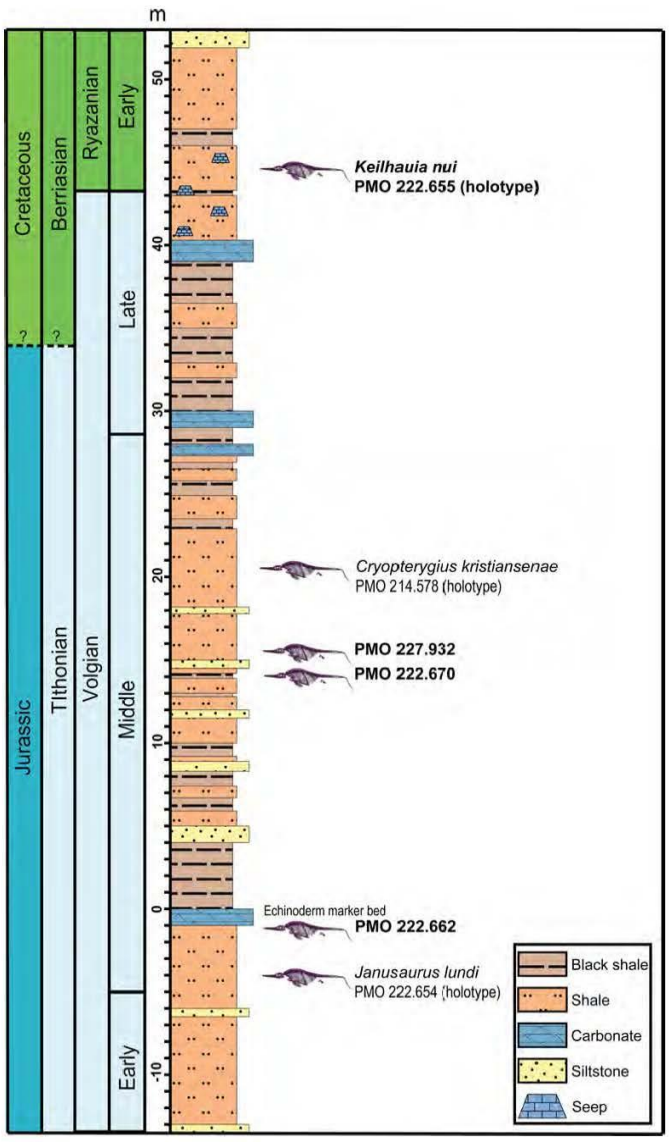
m
Cretaceous
Berriasian
Ryazanian
Early
Late
Middle
Early
Jurassic
Tithonian
Volgian
50
40
30
20
10
0
-10
Keilhauia nui
PMO 222.655 (holotype)
Cryopterygius kristiansenae
PMO 214.578 (holotype)
PMO 227.932
PMO 222.670
Echinoderm marker bed
PMO 222.662
Janusaurus lundi
PMO 222.654 (holotype)
Black shale
Shale
Carbonate
Siltstone
Seep

Fig 2. Stratigraphic section for the Slottsmøya Member Lagerstätte showing the six ichthyosaur specimens with pelvic girdles discussed in the text (newly described material shown in bold). Modified from Delsett et al. (2016).

doi:10.1371/journal.pone.0169971.g002

the Svalbard archipelago (74Ê±81ÊNorth, 10Ê±35ÊEast)(Fig 1). The Slottsmøya Member is the uppermost member in the Agardhfjellet Formation, a 90±350 metres thick unit in the Janusfjellet Subgroup, Adventdalen Group [36]. The Adventdalen Group spans the Middle Jurassic to Lower Cretaceous. During deposition of the Slottsmøya Member, Svalbard was situated at 63± 66ÊNorth [37] and largely covered by an epicontinental sea situated in the Boreal Basin [38, 39].

The Slottsmøya Member is a 70±100 m thick, upwards-coarsening unit made up primarily of dark-grey to black shales and paper shales [38, 40]. Silty and sandy beds also occur, as well as some carbonates. The member was deposited on a slightly dysoxic open marine shelf with periodic oxygenation of the sea bottom [41]. The siltstones and sandstones are interpreted as the result of storms or turbiditic currents [40]. A continuous yellow siltstone bed rich in echinoderm fossils is used as a marker unit and set as 0 m in the section ('echinoderm marker bed') [27]; the position of the specimens described here is given relative to this bed (Fig 2). The distribution of the marine reptiles, invertebrates and total organic content fluctuations in the section is described in detail in Delsett et al. [28].

Based on ammonite and foraminiferal biostratigraphy, the Slottsmøya Member spans the Jurassic±Cretaceous boundary and is upper Tithonian to upper Berriasian in age [42±44]. A regional chronostratigraphic framework for the latest Jurassic and earliest Cretaceous in the Boreal region uses the terms Volgian and Ryazanian to broadly correspond to the Tithonian and Berriasian in wide use elsewhere (Fig 2). Currently, it is unclear whether the Volgian and Ryzanian border corresponds precisely to the Tithonian and Berriasian boundary, i.e. between the Jurassic and the Cretaceous (e.g. [45, 46]). Because Tithonian and Berriasian are more commonly used, these names will be used in this paper.

Material and Methods

Material

Four new ichthyosaur specimens are described here: PMO 222.655 (collected 2010), PMO 222.670 (collected 2011), PMO 222.662 (collected 2007) and PMO 227.932 (collected 2011), which are widely distributed throughout the Slottsmøya Member (Fig 2). The stratigraphic position of each specimen is well constrained and was determined using a total station [27, 40]. Marine reptile specimens from the Slottsmøya Member Lagerstätte display a range of preservation modes from full articulation to disarticulation, and varying preservation of individual elements. Many elements are severely broken and eroded, but compaction and compression is less pronounced than what would usually be expected in these types of sediments. The three-dimensionality is likely a result of early diagenetic barite precipitation in the pore spaces of the bones [28]. The specimens were transported from the field in plaster jackets and mechanically prepared in the lab at the Natural History Museum, University of Oslo.

Calculation of relative lengths of elements

One of the aims of this study is to understand the size relationships between pelvic girdle and limb elements of ichthyosaurs from the Early Jurassic to the Cretaceous. To do this, the length of different elements (humerus, ilium, ischiopubis and femur) were measured and calculated as simple ratios to investigate whether there are any clear evolutionary trends or unique pelvic girdle architecture among the different species. The ratios were also plotted against geological ages for each taxon to test for correlations.

Measurements were taken from Jurassic and Cretaceous specimens that preserve at least two of the following lengths: humerus, ilium, ischiopubis and femur. In specimens with two humeri or femora, the mean proximodistal length was used (measurement details are provided in S1 Text). It should be noted that the time range for comparisons of ilial and femoral length to ischiopubic length is shorter than when compared to other elements, due to the change from tripartite (the pelvic girdle consists of ilium, ischium and pubis) to bipartite (ilium and ischiopubis) pelvic girdles. More complete or near-complete specimens with pelvic girdles are known for Early±Middle Jurassic taxa than from late Middle Jurassic to Cretaceous ophthalmosaurids, and *Stenopterygius* is unique for being known from numerous specimens. Both of these factors skew the dataset to some extent, and a Spearman rs correlation test is used. From Jurassic and Cretaceous taxa with known pelvic girdles (S1 Table), *Excalibosaurus* is the only genus not represented by any specimen in the calculations because we have either not personally examined this material or the necessary measurements are available in the published literature. Triassic taxa are outside the scope of this paper. For geological age a median age was used based on which stages the species is known to occur (see S2 Table for references).

Statistical methods

A Spearman rs correlation test was conducted in PAST 3 [47] for the relationship between geological age and the following length ratios; femur: humerus; ilium: femur; ischiopubis: ilium and ischiopubis: femur. The specimens were grouped into four categories; Early/Middle Jurassic specimens with a tripartite pelvis, Early/Middle Jurassic juveniles with a bipartite pelvis (only *Stenopterygius* specimens), Early/Middle Jurassic adults with a bipartite pelvis, Late Jurassic specimens and Cretaceous specimens.

Pelvic girdle evolution in a phylogenetic framework

To facilitate discussion about the evolution of pelvic girdle shape, illustrations of known pelvic girdles were prepared and plotted onto a recent phylogeny of Ichthyopterygia using the topology of Ji et al. [48] for non-ophthalmosaurids. Because an additional aim of this study is to establish the phylogenetic position of PMO 222.655 using a larger taxon sampling of derived ichthyosaurs than that presented in Ji et al. [48], a new phylogenetic analysis of Ophthalmosauridae was conducted using the matrix of Roberts et al. [29] (S2 Text and S3 Text for character list and data matrix). The new matrix (22 OTUs and 56 characters) was assembled and analyzed in TNT V1.1 and includes PMO 222.655; however the other new material described herein was excluded due to its fragmentary nature. The scores for *Undorosaurus gorodischensis* Efimov 1999 are based on personal observation (LLD at EP) and Arkhangelsky and Zverkov [49]. The matrix of Fischer et al. [50] was not used because only two of the novel post-cranial characters would be possible to score for PMO 222.655. The character matrix for ichthyosaurs is still very volatile, and several different sets are in current use (e.g. [12]). In addition, the slightly smaller data matrix of Roberts et al. [29] permits the use of implicit numeration as a search algorithm. All characters were unweighted and unordered. The analysis was performed in TNT V1.1 [51] and run using the implicit enumeration algorithm with the outgroup taxon specified as *Temnodontosaurus*. Bremer support was calculated using the bremer function in TNT. CI and RI statistics were found using the stats.run script for TNT.

Nomenclatural acts

The electronic edition of this article conforms to the requirements of the amended International Code of Zoological Nomenclature, and hence the new names contained herein are available under that Code from the electronic edition of this article. This published work and the

nomenclatural acts it contains have been registered in ZooBank, the online registration system for the ICZN. The ZooBank LSIDs (Life Science Identifiers) can be resolved and the associated information viewed through any standard web browser by appending the LSID to the prefix [a]http://zoobank.org/[o]. The LSID for this publication is: urn:lsid:zoobank.org:pub:8-E049808-F51A-42C5-916B-D5AE05669596.

The electronic edition of this work was published in a journal with an ISSN, and has been archived and is available from the following digital repositories: PubMed Central, LOCKSS and CRIStin (University of Oslo Library).

Systematic Paleontology

Ichthyosauria de Blainville 1835

Neoichthyosauria Sander 2000

Thunnosauria Motani 1999

Ophthalmosauridae Baur 1887

Keilhauia gen. nov.

urn:lsid:zoobank.org:act:2D45A81F-D4FB-4BA3-8F61-B9BB775389F0

Keilhauia nui sp. nov.

urn:lsid:zoobank.org:act:A48F4CB9-A930-4DB3-A737-004EBC772537

(Figs 3±9, Table 1)

Holotype and only specimen: PMO 222.655, an articulated, partial skeleton consisting of an incomplete rostrum, the dorsal and preflexural vertebrae, the right pectoral girdle and fore-fin, most of the pelvic girdle and both femora.

Etymology: Genus name in honor of Baltazar Mathias Keilhau (1797±1858), the first Norwegian geologist to do fieldwork in the Arctic. He was part of an expedition to Svalbard (Spitsbergen) in 1827. His collection is housed at the Natural History Museum in Oslo, Norway.

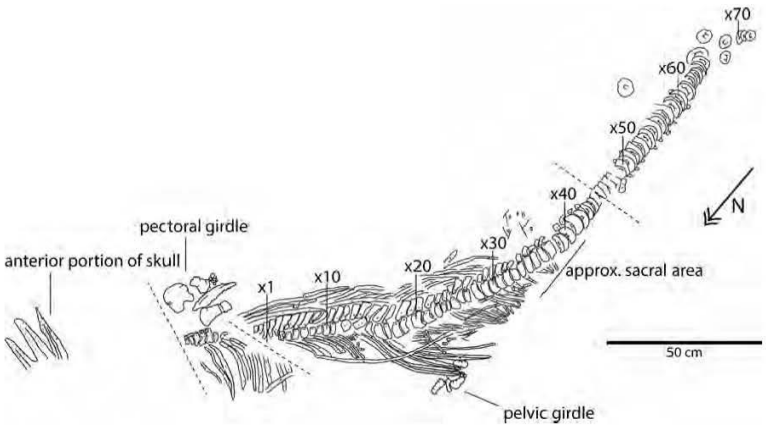

Fig 3. Skeletal map of *Keilhauia nui* (PMO 222.655) viewed from the side stratigraphically down, i.e. the prepared side. Vertebrae numbers (°x#°) indicate position relative to the anterior end of the preserved skeleton and do not correspond to their actual position in the column. Dashed lines show three faults. Scale bar equals 50 cm. Modified from Delsett et al. 2016.

doi:10.1371/journal.pone.0169971.g003

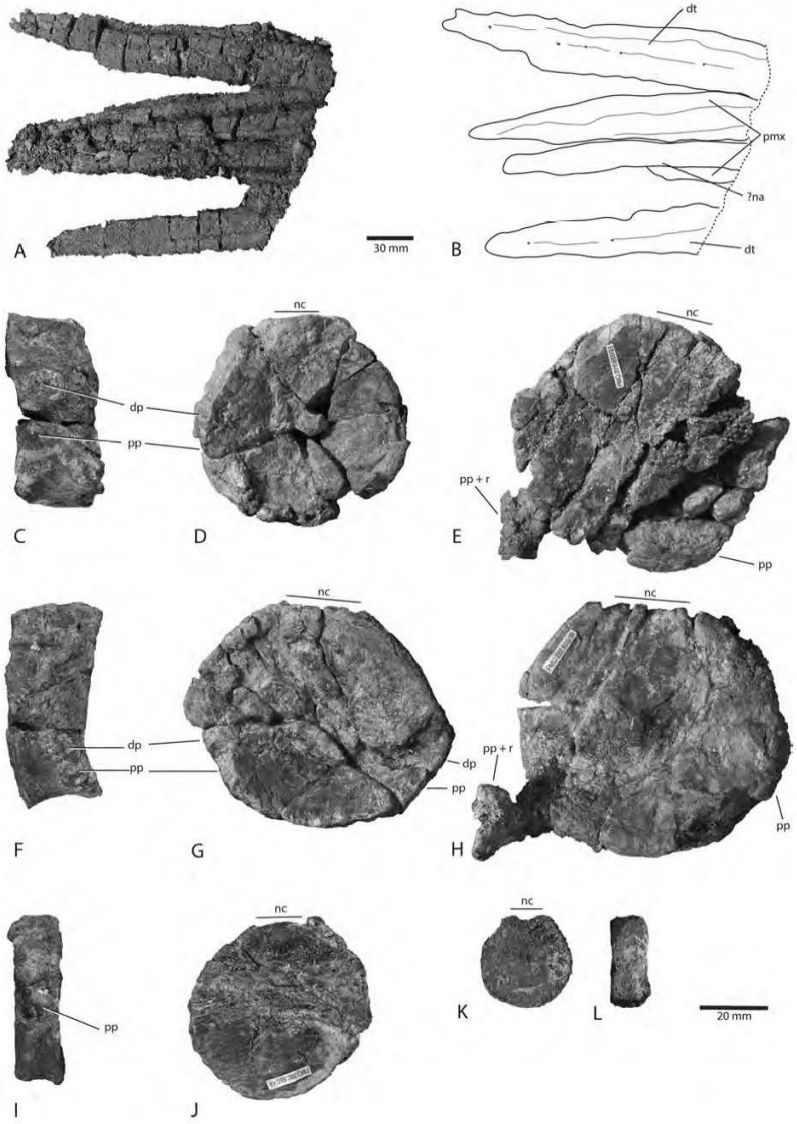
A
30 mm
B
dt
pmx
?na
dt
C
dp
pp
D
nc
E
nc
pp + r
pp
F
dp
pp
G
nc
dp
pp
H
nc
pp + r
pp
I
pp
J
nc
K
nc
L
20 mm

Fig 4. Rostrum and vertebrae of *Keilhauia nui* (PMO 222.655). Rostrum in A and B; dentaries in lateral view and premaxillae in ventral view. Scale bar equals 30 mm. Vertebra x18 (anterior dorsal) in C left lateral and D posterior views. Vertebra x39 (possible sacral) in E anterior view. Vertebra x29 (posterior dorsal) in F right lateral and G anterior views. Vertebra x54 (anterior caudal) in H anterior view. Vertebra x64 (caudal) in I lateral and J? anterior views. Vertebra x72 (fluke) in K anterior or posterior and L lateral views. Vertebrae numbers do not correspond to actual position in the vertebral column. Scale bar for C-L equals 20 mm. Abbreviations: **dp** diapophyses, **dt** dentary, **na** nasal, **nc** neural canal, **pmx** premaxilla, **pp** parapophyses, **r** rib.

doi:10.1371/journal.pone.0169971.g004

where PMO 222.655 is also housed. Species name in honor of Natur og Ungdom (Young Friends of the Earth Norway) working to protect the Arctic environment, who celebrate their 50 year anniversary in 2017.

Holotype locality: Island of Spitsbergen, north side of Janusfjellet, approximately 13 km north of Longyearbyen, Svalbard, Norway. UTM WGS84 33X 0518847 8696044

Holotype horizon and stage: Slottsmøya Member, Agardhfjellet Formation, Janusfjellet Subgroup, early Berriasian, Early Cretaceous. 44.8 metres above the echinoderm marker bed.

Differential diagnosis. An ophthalmosaurid with the following autapomorphies: ilium anteroposteriorly expanded at the dorsal end; ischiopubis shorter or subequal in length to the femur (differs from all other Middle-Late Jurassic and Cretaceous ophthalmosaurids, but found in some specimens of *Stenopterygius* sp).

The species also possesses the following unique character combination: Posterior dorsal and anterior caudal centra less than 3.5 times as high as long (4 times or more in *Ophthalmosaurus icenicus* and *Arthropterygius chrisorum*)[52, 53]; glenoid contribution of the scapula larger than coracoid facet (smaller in *Caypullisaurus bonapartei* and *Sveltonectes insolitus*)[24, 54]; small acromion process of scapula (prominent in *Brachypterygius extremus*, *Acamptonectes densus*, *Platypterygius americanus*, *Caypullisaurus bonapartei* and *Sveltonectes insolitus*)[19, 24, 52, 54, 55]; anteromedial process of coracoid present (not present in *Caypullisaurus bonapartei* and *Platypterygius australis*)[26, 54]; absence of a strongly developed deltopectoral crest of the humerus (present in *Caypullisaurus bonapartei*, *Platypterygius americanus* and *Sveltonectes insolitus*)[24, 54, 55]; humerus with facet for preaxial accessory element anterior to radius

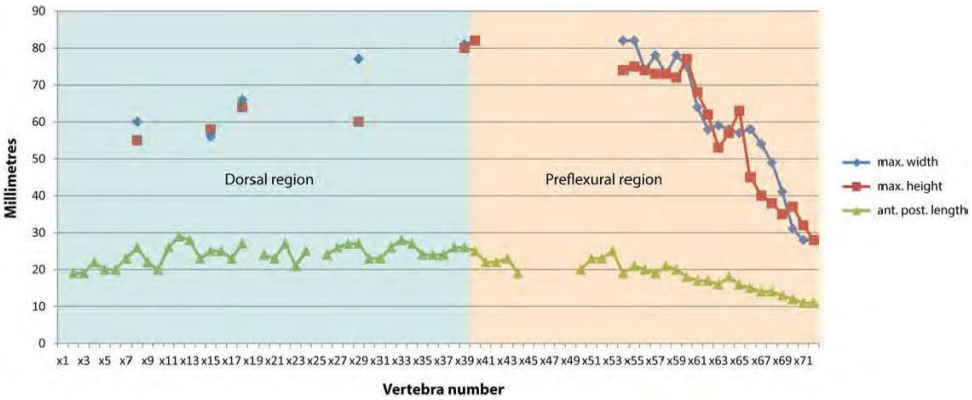

Fig 5. Vertebral dimensions of *Keilhauia nui* (PMO 222.655). Vertebral numbers do not correspond to the actual position in the column, but to those used in the text. Blue area: dorsal region, orange area: preflexural area.

doi:10.1371/journal.pone.0169971.g005

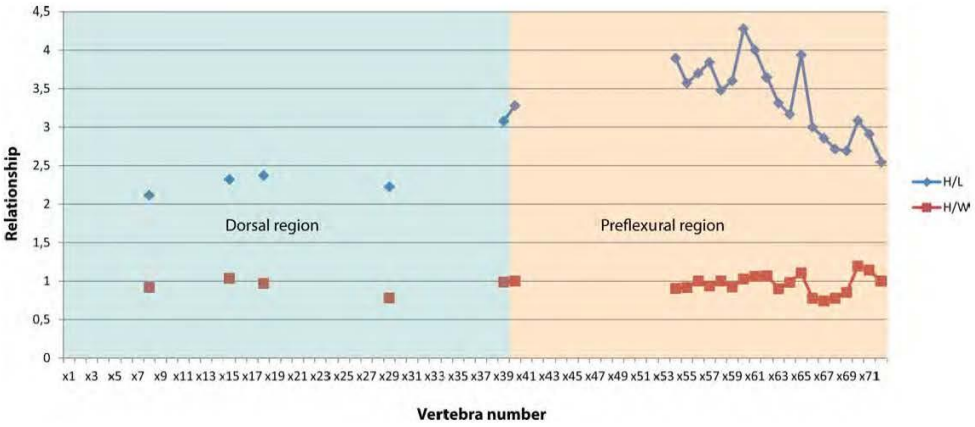

Fig 6. Ratios of vertebral dimensions of *Keilhauia nui* (PMO 222.655) showing the relationship between height to length and height to width. Vertebral numbers do not correspond to the actual position in the column, but to those used in the text. Blue area: dorsal region, orange area: preflexural area.

doi:10.1371/journal.pone.0169971.g006

(absent in *Brachypterygius extremus*, *Maiaspondylus lindoei*, *Aegirosaurus leptospondylus* and *Sveltonectes insolitus*)[24, 52, 56, 57]; posteriorly deflected ulnar facet (absent in *Brachypterygius extremus*, *Maiaspondylus lindoei*, *Caypullisaurus bonapartei*, *Platypterygius australis*, *Aegirosaurus leptospondylus*, *Sveltonectes insolitus* and *Cryopterygius kristiansenae*)[24±26, 52, 54, 56, 57]; lack of a contact between the humerus and intermedium (present in *Brachypterygius extremus*, *Maiaspondylus lindoei* and *Aegirosaurus leptospondylus*)[52, 56, 57]; complete fusion of the ischium and pubis lacking an obturator foramen (only proximal fusion in *Cryopterygius kristiansenae* and *Undorosaurus gorodischensis*, present with foramen in *Ophthalmosaurus icenicus*)[25, 52, 58]; medial margin of ischiopubis straight in dorsal and ventral view (shared

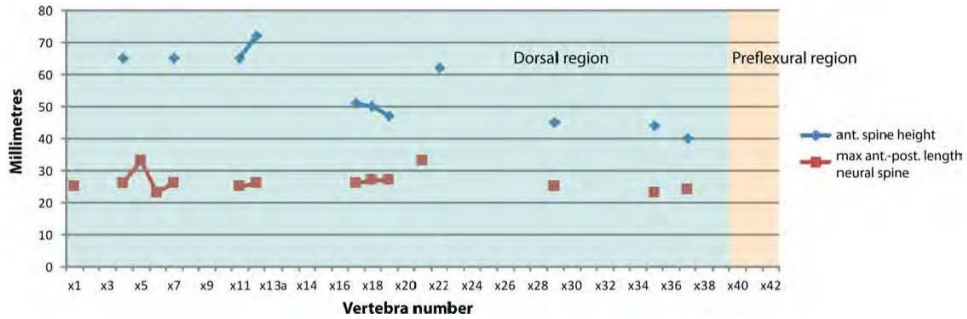

Fig 7. Neural spine dimensions of *Keilhauia nui* (PMO 222.655) showing height and maximum anterior-posterior length. Vertebrae numbers do not correspond to the actual position in the column, but to those used in the text. Blue area: dorsal region, orange area: preflexural area.

doi:10.1371/journal.pone.0169971.g007

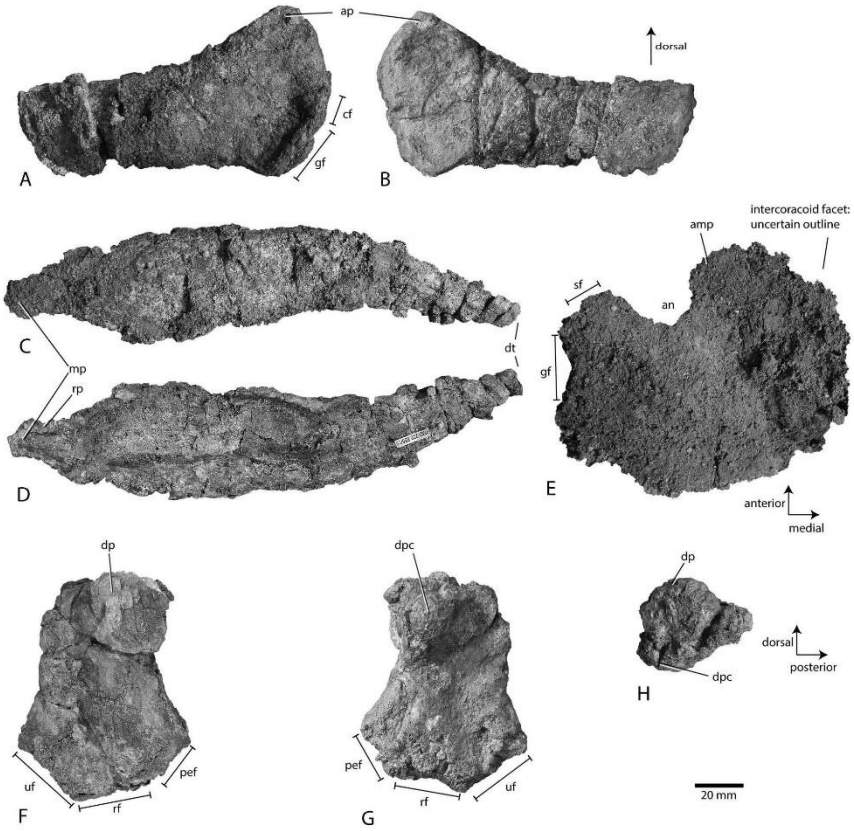

Fig 8. Right pectoral girdle and humerus of *Keilhauia nui* PMO 222.655. Scapula in A lateral and B medial views. Clavicle in C dorsal and D ventral views. Coracoid in E ventral view. Humerus in F dorsal, G ventral and H proximal views. Scale bar equals 20 mm. Abbreviations: **amp** anteromedial process, **an** anterior notch, **ap** acromion process, **cf** coracoid facet **dp** dorsal process, **dpc** deltopectoral crest, **dt** distal tip, **gf** glenoid facet, **mp** medial projection, **pef** preaxial accessory element facet, **rf** radial facet, **rp** rim on posterior side of medial projection, **sf** scapular facet, **uf** ulnar facet.

doi:10.1371/journal.pone.0169971.g008

with *Janusaurus lundi* only)[29]; femur with two distal facets (three in *Platypterygius americanus*, *P. australis*, *P. hercynicus* and *Paraophthalmosaurus saratoviensis*)[26, 55, 59, 60].

Preservation. PMO 222.655 is articulated and partially complete (Fig 3). The individual appears to have landed on the seafloor on its left lateral side. Skeletal preservation improves posteriorly. The only preserved portion of the skull are the tips of the rostral elements (length = 25 cm), including the anterior portions of the dentaries and premaxillae, and a smaller portion of the nasal (Fig 4). A few isolated partial teeth were found in association with

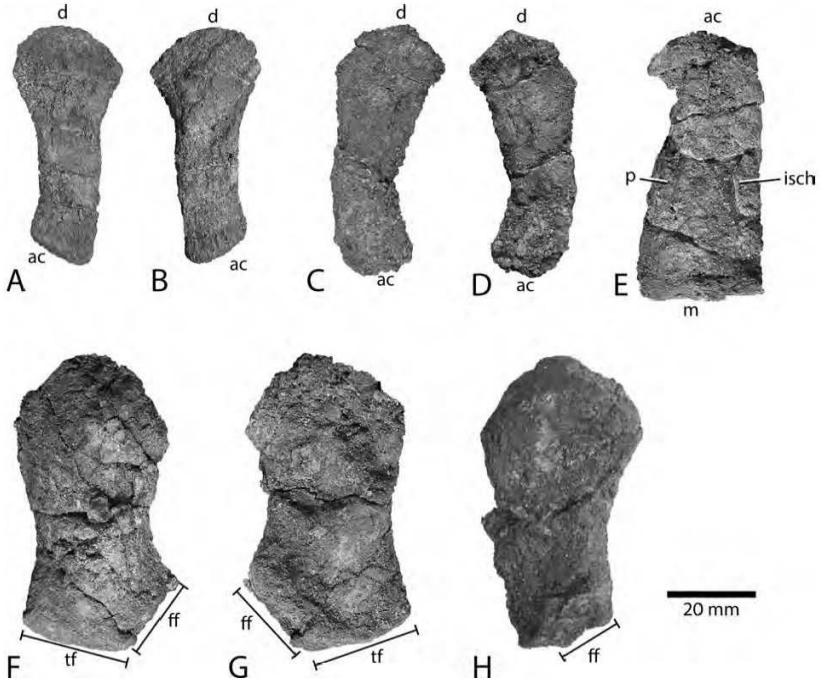

Fig 9. Pelvic girdle and femur of *Keilhauia nui* (PMO 222.655). Ilium in A and B lateral and medial (?) views. Posterior is to the left in A. The other ilium in C and D lateral (?) and medial (?) views. Posterior is to the right in C. Ischiopubis in E lateral or medial view. The better-preserved femur in F and G dorsal (?) and ventral (?) views. The other femur from the best preserved side in H dorsal or ventral view. Scale bar equals 20 mm. Abbreviations: **ac** acetabular end, **d** dorsal end, **ff** fibular facet, **isch** ischium, **m** medial end, **p** pubis, **tf** tibial facet.

doi:10.1371/journal.pone.0169971.g009

fragments of the ribs and gastralia. The teeth most likely originate from the skull of PMO 222.655, and are probably not gut content, judging from their size. Almost the entire vertebral column is preserved in articulation. For the purposes of description, numbers of individual vertebrae (x1-x72) and neural arches (x1-x42) were given during preparation and indicate position relative to the anterior end of the preserved skeleton but do not correspond to their actual position in the column (Figs 5–7). Some vertebrae are probably missing in the cervical region. Anterior to the fault in the anterior dorsal region, the individual vertebrae are difficult to discern, and directly posterior to it, severely crushed. Vertebra x19 is not preserved, but its existence is indicated by a higher number of neural arches than vertebrae in this area. Most of the vertebrae preserve their neural arches. Anterior to the fault in the anterior dorsal region, seven vertebrae have parts of their neural arches. Posterior to this fault 43 neural arches are preserved, the most complete are those belonging to vertebrae x3-x6. Between the body and the preserved part of the tail is a compressed area with fragments of five vertebrae. The entire

Table 1. Selected measurements of PMO 222.655, holotype specimen of *Keilhauia nui*. Lengths given in millimetres.

Right humerus PMO 222.655/1 (Fig 8F±8H)	
Maximum proximodistal length	86
Minimum anteroposterior width, midshaft	44
Maximum anteroposterior width, proximal end	49
Maximum dorsoventral height, proximal end	40
Maximum anteroposterior width, distal end	67
Maximum dorsoventral height, distal end	25
Anteroposterior length of radial facet	30
Anteroposterior length of ulnar facet	26
Anteroposterior length of preaxial element facet	20
Maximum dorsoventral width of radial facet	17
Maximum dorsoventral width of ulnar facet	7
Maximum dorsoventral width of facet for preaxial acc. element	11
Right scapula PMO 222.655/2 (Fig 8A and 8B)	
Maximum proximodistal length	123
Maximum anteroposterior width, proximal blade	67
Minimum anteroposterior width, middle of blade	36
Maximum anteroposterior width, distal blade	34
Dorsoventral length of coracoid facet	17
Dorsoventral length of glenoid facet	24
Coracoid PMO 222.655/17 (Fig 8E)	
Maximum mediolateral width	110 (estimate)
Maximum anteroposterior length	118
Anteroposterior length of glenoid facet	62
Anteroposterior length of scapular facet	28
Clavicle PMO 222.655/15 (Fig 8C and 8D)	
Maximum width	45
Maximum length	204
Ilium PMO 222.655/60 (Fig 9A and 9B)	
Maximum dorsal-acetabular length	54
Maximum anteroposterior width, acetabular end	25
Maximum height (thickness), acetabular end	2
Maximum anteroposterior width, dorsal end	16
Ilium PMO 222.655/61 (Fig 9C and 9D)	
Maximum dorsal-acetabular length	55
Maximum anteroposterior width, acetabular end	24
Maximum height (thickness), acetabular end	3
Maximum anteroposterior width, dorsal end	16
Ischiopubis PMO 222.655/62 (Fig 9E)	
Maximum proximodistal length	59
Maximum anteroposterior width, proximal end	20
Maximum anteroposterior width, distal end	27
Left femur PMO 222.655/58 (Fig 9F and 9G)	
Maximum proximodistal length	64
Maximum anteroposterior width, proximal end	33
Maximum height, proximal end	14
Maximum anteroposterior width, distal end	33

(*Continued*)

Table 1. (*Continued*)

Minimun anteroposterior width of shaft	25
Anteroposterior length of tibial facet	13
Anteroposterior length of fibularfacet	14
Right femur PMO 222.655/59 (Fig 9H)	
Maximum proximodistal length (partly eroded)	60
Maximum anteroposterior width, proximal end	36
Maximum height, proximal end	16

doi:10.1371/journal.pone.0169971.t001

postflexural column is missing. Many ribs are preserved in articulation. Anterior to the fault in the anterior dorsal region, the ribs are in position but fractured. Posterior to this fault they are relatively well preserved, but almost none are complete. Fourty-one ribs are preserved in position on the left lateral side of the specimen and 21 on the right side. The left side of the pectoral girdle (Fig 8) is missing, as well as the left forefin and one of the ischiopubes. The pelvic girdle and hind fin (Figs 3 and 9) appear to have drifted or been moved anteriorly after death because the elements was found at the position of vertebra x20, whereas the sacral vertebra is interpreted to be vertebra x39 (see below).

Ontogeny. The proximal head of the humerus is convex (Fig 8H), which is traditionally considered a criterion for skeletal maturity [61]. The surface texture of the humerus shaft is partly eroded, but is relatively smooth and not "sand paper-like" as would be expected in a juvenile specimen [61]. The degree of ossification (when it is possible to observe) resembles mature finished bone [61]. The closure of the gaps between proximal fin elements could not be assessed because the forefin was not in articulation [61]. Criteria relating to the orbit and sclerotic aperture, the basicranium and the neural spines [62] are not applicable because these parts are not preserved or poorly preserved. Based on available evidence and the size of the animal, we infer that PMO 222.655 reached a late juvenile to adult ontogenetic stage.

Total body length. Estimated total body length is based on a combination of the length of the vertebral column and rostrum, an estimation of missing portions and relative position using the quarry map. The unpreserved part of the skull is assumed to represent two thirds of total skull length (50 cm) based on comparable skull dimensions of *Cryopterygius kristiansenae* (PMO 214.578) [25]. The preserved part of the vertebral column has a length of 260 cm. The missing cervical vertebrae are estimated to represent 10±20 cm, and the compressed caudal area might have extended the measureable body length up to 10 cm. These lengths depend on how many vertebrae are missing and how much the compression expanded the area anterior to the tail. We assume that the missing part is the fluke and that it was approximately 60±80 cm in length, based on the relative size of the fluke of *Ophthalmosaurus icenicus* [7]. This provides an estimated total body length of 3.8±4.3 metres.

Skull. The premaxillae and nasals are not preserved well enough to present any details; however, the rostrum of *Keilhauia nui* (PMO 222.655) (Fig 4A and 4B) becomes dorsoventrally taller compared to the equivalent point in the rostrum of *Aegirosaurus leptospondylus* Wagner 1853 [56], and is more similar to that of *Cryopterygius kristiansenae* [25] and *Caypullisaurus bonapartei* Fernández 1997 [17, 54]. Nutrient foramina are visible on the lateral sides of the dentaries in a shallow longitudinal groove reaching almost to the anterior tip of these elements. Fragments from approximately ten teeth are preserved. None of them are complete, and none preserve the enamel, so that length and possible ornamentation is not possible to describe. The crowns that are preserved are conical, with a narrow crown apex and a slight lingual curvature.

Vertebral column. Thirty-eight more or less well preserved vertebrae are preserved in the presacral region and 33 in the caudal (Figs 3 and 4C±4L). Additionally, poorly preserved remains of 5±7 vertebrae are located in the anteriormost area of the body, which are neither given numbers in the "x" series nor measured. Centrum number x39 (Figs 4E, 5 and 6) marks the approximate position of the sacral vertebra based on the observations that it possesses only one apophysis and thus might represent the transition from bicipital to unicipital ribs, and that rib length rapidly decreases from vertebra x28 (10 cm) to x39 (4 cm). However, the transition from bicipital to unicipital ribs could lie anterior to this because not all of the centra were removed from the matrix for closer examination. An exact presacral vertebral count is not possible to determine; however, based on the preserved centra, the presacral number must have been at least 43. This is more than in *Nannopterygius enthekiodon* Hulke 1871 (41 vertebrae [52]), *Platypterygius americanus* Nace 1939 (37 vertebrae [55]) and *Athabascasaurus bitumineus* Druckenmiller and Maxwell 2010 (42 vertebrae [22]). There is uncertainty regarding the number of presacral vertebrae in *Ophthalmosaurus icenicus* Seeley 1874, with estimates ranging from 38±43 [7, 52]. *Platypterygius australis* McCoy 1867 has 46 presacral vertebrae, [26], and *Cryopterygius kristiansenae*, *Aegirosaurus leptospondylus* and *Platypterygius platydactylus* Broili 1907 have more than 50 presacral vertebrae [25, 56, 63].

The height and width of the centra in the dorsal region increase posteriorly. In vertebra x18 (Fig 4C and 4D), the diapophysis and the parapophysis are situated midway between the dorsal and ventral edges on the lateral side, indicating that this is an anterior dorsal vertebra, and the apophyses on vertebra x29 (Fig 4F and 4G) are situated on the ventral half, typical of a posterior dorsal vertebra. The majority of the vertebrae from the dorsal region are circular in anterior or posterior view.

Generally, the caudal centra in the anterior part of the preflexural stock are the highest and widest in the entire column [7]. In *Keilhauia nui* (PMO 222.655), that is found at vertebra x40 (Figs 5 and 6). Similar to the dorsal vertebrae, the anterior caudal vertebrae are nearly circular in anterior or posterior view [7]. The largest height: length ratio is found in vertebra x59 (Fig 6) and decreases posterior to this. In the posterior part of the preflexural stock the height of the vertebrae decreases rapidly but the width decreases less rapidly. This results in dorsoventrally shortened vertebrae, which can be seen in centra x59-x71 (Fig 4I±4L). Vertebra x72 (Fig 4K and 4L) is higher than wide, an indication of the fluke base [7]. The centrum edges change from being sharp to broadly rounded shortly before the fluke [7], a feature that is observed from vertebra x69 and posteriorly. The apical centra were not preserved. Some small, rounded bones (diameter 10±15 mm) that were found in the region of vertebrae x50-x60 may be chevrons.

The neural spines are posteriorly inclined and of the same anteroposterior length throughout the axial skeleton, although in some cases the length expands slightly in the dorsalmost part (Fig 7). The anteroposterior length is similar to that of their corresponding vertebral centra. This is similar to *Cryopterygius kristiansenae* [25] but differs from *Ophthalmosaurus icenicus*, where the anteroposterior length increases posterior to vertebra 25 [52]. The mediolateral width of the neural spine is narrowest at the dorsal end (approximately 5 mm), and increases ventrally. The dorsal margins of the spines are straight and lack the dorsal notches as seen in *Cryopterygius kristiansenae* [25] or *Platypterygius australis* [64]. Whether the dorsal margins are rugose or have a longitudinal groove as in *Ophthalmosaurus icenicus* [52] for an extension of soft tissue is not possible to determine. The dorsal end of the neural spines in *Aegirosaurus leptospondylus* (SNSS-BSPG 1954 I 608) is smoother than in *Keilhauia nui* (PMO 222.655) and slightly convex. The neural spines are similar in height but the height drops by 30% at vertebra x20, and continues to decrease after that (Fig 7). In *Ophthalmosaurus icenicus* the neural spines decrease rapidly in height in the posterior trunk region. However, the maximum neural spine height is encountered approximately at vertebra 25 in *Ophthalmosaurus icenicus* [52], but this

happens in the anterior dorsal section in *Keilhauia nui* (PMO 222.655). In the anteriormost preserved vertebrae in *Keilhauia nui*, the neural spine height is larger than the corresponding centrum height, and the relationship is reversed posterior to this, resembling the situation in *Gengasaurus nicosiai* Paparella, Maxwell, Cipriani, Roncacè and Caldwell 2016 [65]. For vertebra x39, the centrum height is twice as high as the neural spine height. The transition from the prezygapophysis to the pedicel is smooth, rather than abrupt. The pedicels, where visible, have a triangular shape in lateral view and are not thickened, rather they are mediolaterally narrow.

A single dorsal rib is preserved almost in entirety, probably belonging to vertebra x7, and is 81 cm long. More posterior ribs measure approximately 75 cm as preserved. Posterior to the dorsal-caudal transition, the ribs are between 2 and 5 cm in length until vertebra x60. The ribs are figure eight-shaped in cross section in the proximal portion, but this becomes less pronounced distally. This condition is typical of ophthalmosaurids, except for *Acamptonectes densus* Fischer, Maisch, Naish, Kosma, Liston, Joger, KrÜger, PÂrez, Tainsh and Appleby 2012, in which the ribs have a rounded cross-section with only a small groove on one side of some dorsal ribs [19] and *Mollesaurus periallus* FernÂndez 1999 in which the ribs bear a dorsal crest [66]. A few disarticulated gastralia fragments were preserved close to the caudal region. The fragments have a circular cross-section and are much smaller in diameter than the ribs.

Pectoral girdle. The scapula (Fig 8A and 8B) has a dorsoventrally expanded proximal end and a straight distal blade. The anterior third of the element widens gradually into what we interpret as a relatively small acromion process with a triangular shape in lateral view. It has a partially broken ridge dorsally on the lateral side. The acromion process is small also in *Cryopterygius kristiansenae* [25], *Platypterygius hercynicus* Kuhn 1946 [59] and *Sisteronia seeleyi* Fischer, Bardet, Guiomar and Godefroit 2014 [18]. The acromion process is taller and more prominent in *Acamptonectes densus* [19], *Sveltonectes insolitus* Fischer, Masure, Arkhangelsky and Godefroit 2011[24] and *Platypterygius australis* [26] than in *Keilhauia nui*. The shape and size of the acromion process varies in different specimens of *Ophthalmosaurus* sp. [52] (from small in e.g. OUMNH J48007 to prominent and pointed LEIUG 90986; pers. obs. LLD. Specimens assigned to *Ophthalmosaurus* because of their similarity to published specimens in e.g. [52], and that both were found in the Oxford Clay.). In anterior view, the proximal end consists of the acromion process dorsally, and ventral to it, a mediolaterally narrower section, as well as a wider coracoid facet and a more prominent glenoid contribution ventrally. Similar to *Sveltonectes insolitus* [24] and an indeterminate Albertan ophthalmosaurid specimen (TMP 92.41.01 8]) the glenoid facet does not continue on the ventral side of the scapula in *Keilhauia nui*, as it does in *Cryopterygius kristiansenae* [25].

The scapular blade has its maximum mediolateral thickness approximately midlength between the proximal and distal end. In lateral view, the distal end of the blade is angled diagonally, so that the dorsal edge reaches approximately 5 mm further distally than the ventral portion. The blade has the same dorsoventral height throughout, similar to *Acamptonectes densus* [19]; in contrast, all other ophthalmosaurids have a dorsoventrally expanded distal end. Additionally, *Platypterygius hercynicus* and *Sisteronia seeleyi* have shafts that are more thickened mediolaterally [18, 59].

The right clavicle (Fig 8C and 8D) is nearly complete and not fused to any other pectoral element. The medial margin bears a medially-projecting process along its ventral edge that is squared in anterior view. It widens dorsoventrally at approximately 15 mm from the medial edge. Anteroposteriorly the projection is thin and surrounded by a rim posteriorly. This differs from most other ophthalmosaurids, which are dorsoventrally thicker medially, often with a digitiform outline along the midline in dorsal view [6], although a morphology resembling *Keilhauia nui* has been observed in some specimens of *Ophthalmosaurus* sp. (e.g., GLAHM: V1861, pers. obs. AJR). Distal to the dorsoventral thickening, the clavicle gradually narrows

again towards the distal tip. The posterior side of the clavicle is concave for articulation with the interclavicle, and this part is longer mediodistally than the distal projection, compared to *Ophthalmosaurus icenicus* [52] and *Mollesaurus periallus* [66], where the two parts are approximately equal in length. In *Janusaurus lundi* the concave section is longer than that seen in *Keilhauia nui* [29]. The distal projection is curved posteriorly, and narrows into a 10 mm wide tip, resembling the condition seen in *Ophthalmosaurus icenicus* [52], *Baptanodon natans* Marsh 1879 [67] and *Janusaurus lundi* [29]. This differs from TMP 92.41.01 (Ophthalmosauridae indet.), which is at its anteroposteriorly widest at the distal end [8].

The right coracoid (Fig 8E) is poorly preserved. In ventral view, it is reniform in outline, and as preserved approximately equal in anteroposterior length and mediolateral width. In *Cryopterygius kristiansenae* [25], the coracoid is somewhat anteroposteriorly longer than wide and is subcircular, whereas the coracoid of *Nannopterygius enthekiodon* [52] and *Sveltonectes insolitus* [24] are considerably narrower in mediolateral width than long. The anterior notch is prominent, similar to that in *Arthropterygius chrisorum* Russell 1993 [53] and *Ophthalmosaurus icenicus* [52]. The coracoid also possesses an anteromedial process, as in *Ophthalmosaurus icenicus* [52] and *Acamptonectes densus* [19]. This feature is absent in *Caypullisaurus bonapartei* [54] and in *Platypterygius australis* [26]. The glenoid and scapular facets are well demarcated, similar to *Sveltonectes insolitus* [24], but in contrast to *Acamptonectes densus*, where the two facets are not separated [19]. In *Arthropterygius chrisorum*, the angle between the two facets is less acute than in *Keilhauia nui* [53]. The scapular facet is only 45% of the length of the glenoid facet. In *Cryopterygius kristiansenae* the scapular facet is 50% of the length of the glenoid [25], and they are close to equal length in *Janusaurus lundi* [29]. The thickness of the intercoracoid facet is not possible to assess due to the preservation.

Forefin. The orientation of the humerus (Fig 8F and 8H) is based on McGowan and Motani [6] and Druckenmiller et al. [25]. Because of their position relative to the vertebral column, the pectoral girdle and forefin elements are interpreted to be from the right side. Of the two major processes on the humerus, we interpret the longer and more ridge-like ("plate-like") to be the dorsal process, which makes this process more posteriorly situated than the deltopectoral crest. Following this interpretation, the postaxial edge is dorsoventrally narrower and sharper than the anterior edge in posterior view. The smallest facet is for the preaxial accessory element in most ophthalmosaurids, which also supports the interpretation of the processes. In proximal view (Fig 8H), the dorsal process is placed midway anteroposteriorly, and the more prominent deltopectoral crest is located in a relatively more anterior position. Although a small portion of the dorsal process (Fig 8F) might be lacking dorsally, the process is remarkably small in proximodistal length compared to that seen in other ophthalmosaurids, including *Ophthalmosaurus icenicus* [52] (e.g. OUMNH 48754, OUMNH 68542, LEIUG 90986 pers. obs. AJR, LLD) and *Cryopterygius kristiansenae* [25]. The dorsal process fails to meet the midpoint of the shaft, as in some specimens of *Undorosaurus gorodischensis* [58] and *Aegirosaurus leptospondylus* (SNSB-BSPG 1954 I 608, pers. obs. LLD). In *Ophthalmosaurus icenicus*, *Brachypterygius extremus* von Huene 1922 [52], *Paraophthalmosaurus saveljeviensis* Arkhangelsky 1997 [68] and *Cryopterygius kristiansenae* [25] the dorsal process extends to the humeral midpoint, and it extends further yet in *Arthropterygius chrisorum* [53], *Platypterygius americanus*, *P. australis* and *P. hercynicus* [55, 59, 63, 69]. The deltopectoral crest in *Keilhauia nui* is generally more prominent than the dorsal process (Fig 8G). As preserved, it is placed in the proximal and anterior region of the ventral surface. Similar to *Arthropterygius chrisorum* [53], *Platypterygius hercynicus* [59] and *Janusaurus lundi* [29], the deltopectoral crest of *Keilhauia nui* extends less than half of the total shaft length. In contrast, the deltopectoral crest extends distal to the mid-point in *Ophthalmosaurus icenicus* [52] and nearly reaches the distal end in *Sisteronia seeleyi* [18], *Acamptonectes densus* [19] and *Platypterygius americanus* [55].

The distal end of the humerus is anteroposteriorly wider than the proximal end. The shaft has only a weakly developed mid-shaft constriction, with the minimum width approximately 20% less than the proximal maximum width. The humerus bears three distal facets (Fig 8F and 8G). The anterior facet is partly eroded, but is interpreted to be for the preaxial accessory element, followed by those for the radius and ulna, as in the majority of ophthalmosaurids [25, 29, 30, 52, 65]. Of the three distal facets, that for the preaxial accessory element is the smallest. It is distorted, but a small rim can be seen on its anterior half. The radial facet is slightly longer anteroposteriorly than the ulnar facet and the dorsoventrally tallest of the three facets. The facet for the radius is oval in distal view, but is distorted along the anteriormost edge. The ulnar facet is posteriorly deflected, in contrast to *Gengasaurus nicosiai* [65], with an angle of approximately 120Êto the radius facet. *Sveltonectes insolitus* [24], *Nannopterygius enthekiodon* [70], *Platypterygius hauthali* von Huene 1927 [69] and *Platypterygius platydactylus* [63] bear only two facets. *Maiaspondylus lindoei* Maxwell and Caldwell 2006 [71], *Aegirosaurus leptospondylus* [56], *Brachypterygius extremus* [72] and *Platypterygius americanus* [55] all have three distal facets, but the middle one belongs to the intermedium in the three first; in contrast *Platypterygius americanus* has one postaxial facet for an accessory element. *Cryopterygius kristiansenae* possesses two facets on the left humerus but three on the right [25]. A fourth facet for a postaxial element is seen in *Platypterygius hercynicus* [59] and in some specimens of *Platypterygius australis* [26]. Eight small forefin elements are associated with the humerus, of which the largest two might be the radius and ulna, based on their size and a possible articulation with the humerus.

Pelvic girdle. The ilium (Fig 9A+9D) is mediolaterally narrower than other ophthalmosaurids (with the possible exception of *Aegirosaurus leptospondylus*) and as both ilia are preserved and show the same feature, it is not likely that it is a taphonomic feature. The ilia are oriented similar to those in *Ophthalmosaurus icenicus* [52] with the concave side facing posteriorly. The concavity is more pronounced in *Athabascasaurus bitumineus* [22] and *Janusaurus lundi* [29]. This is probably also the case in *Aegirosaurus leptospondylus*, however the preservation is rather poor (SNSB-BSPG 1954 I 608, pers. obs. LLD). It is not possible to distinguish between the right and the left ilium. The element is equally wide anteroposteriorly and widens dorsally, making the anteroposterior length of the dorsal end 1.5 times the length of the acetabular end, which is autapomorphic among ophthalmosaurids. The end interpreted to be the acetabulum is mediolaterally thicker than the rest of the element and lacks distinct distal facets. The acetabular edge is diagonal with respect to the two parallel sides of the shaft, with the anterior side extending further ventrally.

The ischiopubis (Fig 9E) is a proximodistally short element. It is partly broken and may be slightly flattened, but the proximodistal length appears preserved in its entirety, based on the unbroken medial margin. Notably, and unique among ophthalmosaurids, the ischiopubis is slightly shorter than the femur. The ischium and pubis are completely fused without any trace of a foramen. The portion of the element that is dorsoventrally thicker than the other is interpreted to be the pubis. The complete fusion of the elements is shared with *Janusaurus lundi* [29], *Sveltonectes insolitus* [24], *Athabascasaurus bitumineus* [22], *Aegirosaurus leptospondylus* [56], *Caypullisaurus bonapartei* [17] and possibly *Platypterygius australis* [26]. This differs from *Ophthalmosaurus icenicus* [52], *Cryopterygius kristiansenae* [25], *Undorosaurus gorodischensis* [58] and *Paraophthalmosaurus* (ª*Yasykovia*º) [73], all of which have a foramen or open notch (see also Discussion). The ischiopubis has an elongate trapezoidal shape, and is oriented similar to *Ophthalmosaurus icenicus* [52], *Stenopterygius quadriscissus* [6] and *Cryopterygius kristiansenae* [25], such that the anteroposteriorly widest portion is interpreted as the medial end. The medial end is dorsoventrally thicker than the acetabular end, but whether this is a real or a taphonomic artifact is difficult to determine. Similar to *Janusaurus lundi*, the

medial end of the ischiopubis is straight in dorsal view [29] whereas in other ophthalmosaurids it is typically more rounded (with the possible exception of *Athabascasaurus*) [24±26, 52, 56, 58, 73] (*Caypullisaurus bonapartei*: Fernández pers. comm.). The medial edge is 1.4 times anteroposteriorly wider than the acetabular end. In contrast, in *Aegirosaurus leptospondylus* the medial end is more than twice as long anteroposteriorly than the acetabular end [56] and in *Janusaurus lundi* it is 1.8 times as long [29]. *Ophthalmosaurus icenicus* [52] and *Athabascasaurus bitumineus* [22] are also wider medially, but *Sveltonectes insolitus* is unique in having an ischiopubis equally expanded at both ends [24].

Hind fin. In PMO 222.655 both femora (Fig 9F±9H) are preserved; however, they are eroded and compressed (confirmed by CT-scanning that indicates crushed trabeculae). The more complete femur is used primarily here for description, but because the processes are poorly preserved it is not possible to distinguish the left from the right. The anteroposterior orientation of the femora is based on the distinction between the tibial and fibular facets. Typically in ophthalmosaurids, the tibial facet is oriented perpendicular to the long axis of the femur, and the fibular facet is distinctly angled posterolaterally [14]. The proximal and distal ends are equally wide anteroposteriorly in dorsal view, with a modest mid-shaft constriction. The proximal end is slightly taller dorsoventrally along its anterior edge near the dorsal process. The dorsal and ventral processes are not well preserved, but do seem to have been dorsoventrally and proximodistally short compared to higher and longer processes in most ophthalmosaurids such as PMO 222.670, described below, and many specimens of *Ophthalmosaurus icenicus* ([52] and LEIUG 90986, pers. obs. LLD), as well as Cretaceous isolated femora from the Cambridge Greensand (e.g. CAMSM B58337-61 and TN1753 pers. obs. LLD and "*Platypterygius*" CAMSM B58058, pictured in [18]). However, in *Arthropterygius chrisorum*, the dorsal and ventral processes are poorly developed as in *Keilhauia nui* [53]. The femur bears two distal facets, typical of most ophthalmosaurids [24, 25, 29, 52, 53, 56, 58, 74], although *Platypterygius hercynicus*, *P. americanus*, *P. australis* [26, 55, 59] and *Paraophthalmosaurus saratoviensis* [60] have three. In *Keilhauia nui* the fibular facet faces posterolaterally, approximately 120 degrees relative to the tibial facet. Both facets have the same anteroposterior length. One of the femora was found with three associated, small rounded bones, presumably more distal elements of the hind fin, but of uncertain identity.

Ichthyosauria de Blainville 1835

Neoichthyosauria Sander 2000

Thunnosauria Motani 1999

Ophthalmosauridae Baur 1887

Ophthalmosauridae indet.

Referred material: PMO 222.670; posterior half of a large ichthyosaur, with a complete pelvic girdle and both femora. PMO 222.662; associated ilium, ischiopubis, femur and fibula, and articulated caudal vertebrae. PMO 227.932; a single ischiopubis, lacking only a part in the acetabular end.

PMO 222.670. Figs 10 and 11, Table 2

Locality: Island of Spitsbergen, north side of Janusfjellet, approximately 13 km north of Longyearbyen, Svalbard, Norway. UTM WGS84 33X0519609 8695600.

Horizon and stage: Slottsmøya Member, Agardhfjellet Formation, Janusfjellet Subgroup, early middle Tithonian. 14.5 m above the echinoderm marker bed.

Preservation. PMO 222.670 represents the posterior half of an individual that landed on the seafloor on its left lateral side (Fig 10). The posterior dorsal, preflexural and some postflexural vertebrae are preserved in articulation with the dorsal ribs and associated with a complete pelvic girdle and both femora. The pelvic girdle elements and femora (Fig 11) are three-dimensional and were found close to the vertebral column in a region where the ribs experience a

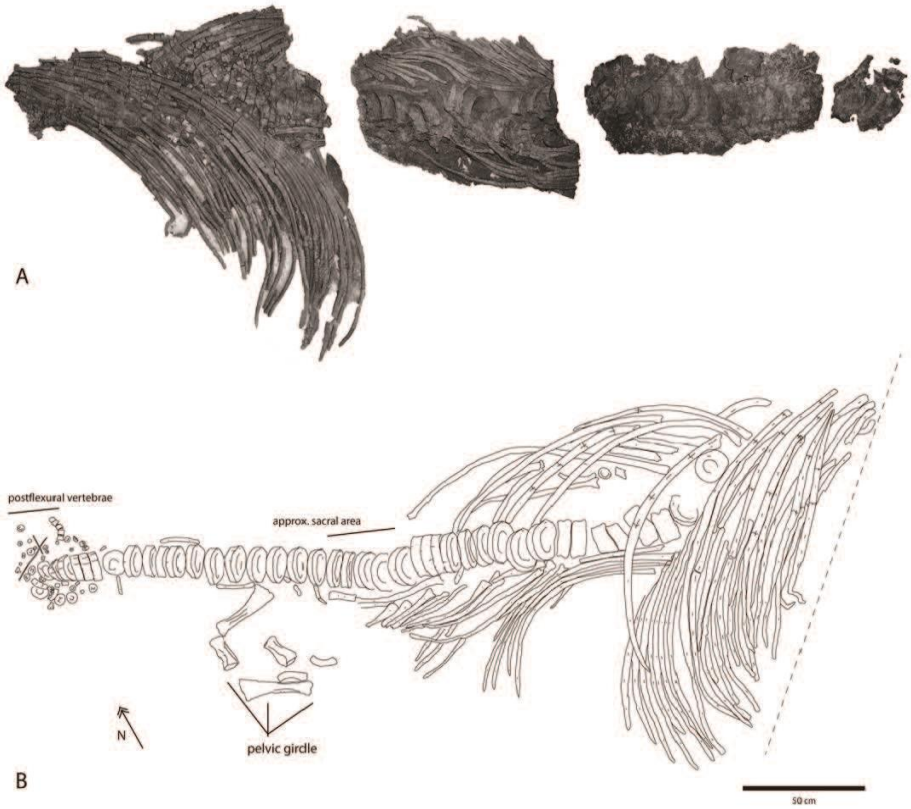

Fig 10. Vertebral column of PMO 222.670 showing A, photograph of stratigraphically down side as preserved and prepared in the four jackets and B, illustration of the complete, restored, articulated series seen from the stratigraphic up side. Dashed line represents the edge of the cliff. Scale bar equals 50 cm. Modified from Delsett et al. 2016.

doi:10.1371/journal.pone.0169971.g010

rapid decrease in length and then disappear (Fig 10B), suggesting that they were preserved nearly in life position. Fragments of gastralia and some severely compressed neural arches are also preserved. The preservation of the rest of the specimen is poor, due in part to compaction, the presence of siderite in the surrounding matrix and the abundant occurrence of the bivalve *Buchia* [75] on and around the skeleton. The skeleton was also covered by a thick layer of calcium sulphate [76], all of which made it difficult to assess bone texture and see facets. Finally, the posteriormost part of the skeleton, which was preserved in permafrost, is better preserved than portions of the skeleton in the active layer.

Total length estimate and ontogenetic status. The preserved length of PMO 222.670 is 279 cm. Based on the vertebral count of *Ophthalmosaurus icenicus* [52] and *Cryopterygius*

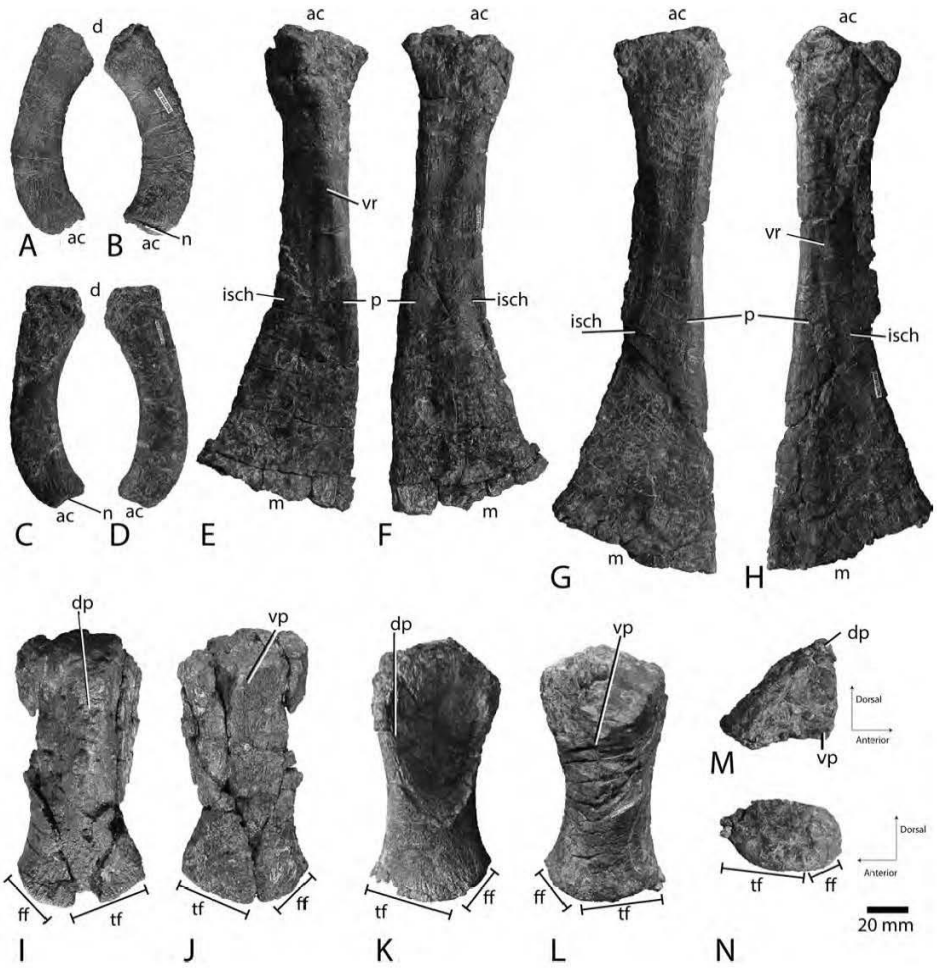

Fig 11. Pelvic girdle and femora of PMO 222.670. Ilium in A and B lateral (?) and medial (?) views. Posterior is to the right in A. The other ilium in C and D lateral (?) and medial (?) views. Posterior is to the right in C. Right ischiopubis in E ventral (anterior to the right) and F dorsal views. Left ischiopubis in G dorsal (anterior to the left) and H ventral views. Right femur in I dorsal (anterior to the right) and J ventral views. Left femur in K dorsal (anterior to the left), L ventral, M proximal and N distal views. Scale bar equals 20 mm. Abbreviations: **ac** acetabulum end, **d** dorsal end, **dp** dorsal process, **ff** fibular facet, **isch** ischium, **m** medial end, **n** notch in acetabular end, **p** pubis, **tf** tibial facet, **vp** ventral process, **vr** ventral ridge.

doi:10.1371/journal.pone.0169971.g011

Table 2. Selected measurements for PMO 222.670, Ophthalmosauridae indet. Lengths are given in millimetres.

Ilium PMO 222.670/5 (Fig 11A and 11B)	
Maximum dorsal-acetabular length (incomplete)	95
Maximum anteroposterior width, widest end	27
Maximum height (thickness), widest end	13
Maximum anteroposterior width, narrowest end	23
Maximum height (thickness), narrowest end	11
Ilium PMO 222.670/3 (Fig 11C and 11D)	
Maximum dorsal-acetabular length	107
Maximum anteroposterior width, dorsal end	31
Maximum mediolateral thickness, dorsal end	13
Maximum anteroposterior width, acetabular end	21
Maximum mediolateral thickness, acetabular end	12
Ischiopubis PMO 222.670/2 (Fig 11E and 11F)	
Maximum proximodistal length	245
Maximum anteroposterior width, medial end	85
Maximum dorsoventral thickness, medial end	11
Maximum anteroposterior width, acetabular end	54
Maximum dorsoventral thickness, acetabular end	28
Minimun anteroposterior width	33
Ischiopubis PMO 222.670/1 (Fig 11G and 11H)	
Maximum proximodistal length	270
Maximum anteroposterior width, medial end	88
Maximum dorsoventral thickness, medial end	9
Maximum anteroposterior width, acetabular end	57
Maximum dorsoventral thickness, acetabular end (element is compressed)	23
Minimun anteroposterior width	35
Left femur PMO 222.670/4 (Fig 11K±11N)	
Maximum proximodistal length	124
Maximum anteroposterior width, proximal end	68
Maximum height, proximal end	49
Maximum anteroposterior width, distal end	59
Anteroposterior length of tibial facet	16
Anteroposterior length of ®bularfacet	40
Right femur PMO 222.670/6 (Fig 11I and 11J)	
Maximum proximodistal length	126
Maximum anteroposterior width, proximal end	59
Maximum height, proximal end	54
Maximum anteroposterior width, distal end	62
Anteroposterior length of tibial facet	12
Anteroposterior length of ®bularfacet	49

doi:10.1371/journal.pone.0169971.t002

kristiansenae [25], we estimate that 25±35 presacral vertebrae are missing, in addition to the skull. The distal end of the tail is curled up and probably not complete. Based on the length of preserved individual vertebrae (25±43 mm in anteroposterior length), the eroded presacral series had a length of 88±123 cm. Based on the body proportions of *Cryopterygius kristiansenae*, the skull was 20±25% of total body length. Assuming approximately 40 cm of the tail is missing the total body length is estimated at 510±590 cm. In *Cryopterygius kristiansenae*,

which has a total length of 5.5 metres, the longest rib is 92 cm. In PMO 222.670 the longest rib exceeds 110 cm. Thus, it is likely the specimen was closer to 6, rather than 5 metres in total length. Based on its large size, the specimen is interpreted as an adult. Other ontogenetic criteria [61, 62] are not easily applicable for this specimen.

Vertebral column. PMO 222.670 preserves a total of 65 vertebrae (Fig 10). Sixteen centra are assumed to belong to the dorsal series and were found articulated to long dorsal ribs, 23 belong to the preflexural series and 26 to the postflexural. The floor of the neural canal is consistently about 35 mm wide at its widest point. The centra in the transition between the dorsal and preflexural series have a diameter of 80±90 mm and their anteroposterior length varies between 32±42 mm as preserved. The vertebrae are compressed to some degree, which might affect the measurements. The preflexural centra associated with the pelvic girdle have a diameter of approximately 80 mm and an anteroposterior length of 25±35 mm. Posterior to this, anteroposterior length decreases gradually.

Eighty-six dorsal ribs were preserved in articulation with the vertebrae. Many ribs are well preserved for almost their entire length. The longest ribs exceed 110 cm in length and the precaudal ribs are double-headed. Some long ribs immediately anterior to the pelvic girdle have a shallow groove on the anterior and posterior surfaces, resulting in a figure eight cross-section, whereas the remaining dorsal ribs do not show this feature. This is unusual among ophthalmosaurids, which normally have figure eight-shaped dorsal ribs. *Acamptonectes densus* and *Platypterygius americanus* also lack the figure eight shape, but *Acamptonectes densus* has a small groove on one side on some dorsal ribs and *Platypterygius americanus* and *Gengasaurus nicosiai* have dorsal ribs with spatulate distal ends [19, 55, 65]. In the few figure eight-shaped ribs in PMO 222.670, the grooves are deeper on the anterior side, and the dorsal portion more robust than the ventral portion. The distal end of all the ribs lacks the groove, as is the case for most ophthalmosaurids. Instead, the distal 25±35% of each rib is longitudinally striated. This feature has not been previously mentioned for any other ophthalmosaurid. A few disarticulated and broken gastralia, with a circular cross-section, were preserved in the caudal region.

Pelvic girdle. In lateral view, the ilium (Fig 11A±11D) is mediolaterally narrow and curved, presumably with the concave side facing posteriorly. The ilium is more curved than *Keilhauia nui* (PMO 222.655), but less so than *Athabascasaurus bitumineus* [22] and *Janusaurus lundi* [29]. The ilium of *Janusaurus lundi* also bears a prominent anterior process that is absent in PMO 222.670. It is not possible to interpret which element is left or right. The dorsoventral orientation of the ilium is interpreted on the basis of a small notch at one end, which is likely for articulation with the ischiopubis and is thus the acetabular end (Fig 11). The dorsal end is anteroposteriorly expanded, but less so than in *Keilhauia nui*. PMO 222.670 resembles TMP 92.41.01 (Ophthalmosauridae indet.) in that the element is anteroposteriorly widest dorsally [8]. The dorsal end is more slender mediolaterally than the rest of the element, and the ilia are in general more flattened mediolaterally than in *Ophthalmosaurus icenicus* (LEIUG 90986, pers. obs. LLD). This might be partly taphonomic, but as the two ilia are similar and other elements from the pelvic girdle are three-dimensional, it is interpreted to be an actual feature.

The ischium and pubis (Fig 11E±11H) are completely fused. The element is anteroposteriorly short, dorsoventrally thin and mediolaterally elongate. The two ischiopubes are identified as right (Fig 11E and 11F) and a left (Fig 11G and 11H). This is based on the observation that one surface is flatter than the other, which is interpreted to be the dorsal and visceral side. The dorsoventrally thicker and more rounded side is interpreted as the pubis, and is thus anterior. The left ischiopubis is longer than the right, which is probably a taphonomic artefact, as it is also less three-dimensional than the right. For the calculations, we used the mean length of each pair of elements, as was done for all other specimens which preserves both sides of a

given element. In dorsal view, the anterior margin is straight, and the posterior margin is broadly concave. A prominent ridge on the ventral surface extends from the mid-point of the acetabular end towards the anterior edge at the approximate mid-length of the element. The acetabular portion is triangular in cross-section and thickened, bearing a rugose acetabular surface. The facet for the ilium is interpreted to be at the dorsoventrally tallest portion of the acetabular end. The medial end of the ischiopubis is anteroposteriorly expanded and dorsoventrally flattened. In medial view, it is slightly curved and bears a groove along its entire length, approximately 5 mm deep. The medial end is straight in dorsal view, as in *Keilhauia nui*, and 1.5 times wider anteroposteriorly than the acetabular end, similar to *Keilhauia nui*.

Hind fin. The femora (Fig 11I±11N) are oriented based on Maxwell et al. [14]. The left femur (Fig 11K±11N) is three-dimensional and almost complete, but slightly compressed on the dorsal side. The right femur (Fig 11I and 11J) is distorted and eroded, missing parts of the posterior margin and the ventral process, but not very flattened due to compression. The dorsal and the ventral process are approximately the same height relative to the shaft, but the dorsal process is narrower than the ventral. The processes are most similar to *Arthropterygius chrisorum* in being distinct, but not large, and approximately of the same height [53], in contrast *Sveltonectes insolitus* has relatively larger processes [24]. In *Athabascasaurus bitumineus* [22] and "*Otschevia zhuralevi*" Efimov 1998 [74] the dorsal process is more prominent, but the ventral process is larger in *Cryopterygius kristiansenae* [25]. In *Keilhauia nui* and *Platypterygius hercynicus* the dorsal process extends a third of its proximodistal length [59], in *Janusaurus lundi* [29] and *Arthropterygius chrisorum* [53], it extends midway, and in *Platypterygius americanus* it covers almost the entire length [55]. The ventral process is straight and extends approximately two-thirds of total femoral length. This morphology differs from *Caypullisaurus bonapartei*, where the ventral process extends midway [17] and less than that in *Platypterygius hercynicus* [59] and *Keilhauia nui*. The anterior margin of the femur is dorsoventrally taller than the posterior margin. The anterior and posterior margins are concave in dorsal view, the posterior more so. A large, concave area posterior to the dorsal process covers two-thirds of the dorsal surface. Where this area ends, the bone is at its narrowest anteroposteriorly. The proximal end is slightly wider anteroposteriorly than the distal. The proximal surface (Fig 11M) is triangular in medial view, with each of the three sides being roughly the same length. The outline of the distal end (Fig 11N) is oval seen in lateral view, bearing two poorly demarcated facets. The tibial facet is more than twice the length of the fibular facet. In dorsal view, the fibular facet faces posterolaterally at almost 45 degrees relative to the tibial facet, similar to *Cryopterygius kristiansenae* [25], but more than *Sveltonectes insolitus* [24] and less than *Keilhauia nui*.

PMO 222.662. Locality: Island of Spitsbergen, east side of Knorringfjellet, approximately 13 km north of Longyearbyen, Svalbard, Norway. UTM: WGS84 33X 528940 8692530.

Horizon and stage: Slottsmøya Member, Agardhfjellet Formation, Janusfjellet Subgroup, early middle Tithonian. 0.2 metres below the echinoderm marker bed.

Fig 12A±12F

PMO 227.932. Locality: Island of Spitsbergen, north side of Janusfjellet, approximately 13 km north of Longyearbyen, Svalbard, Norway. UTM: WGS84 33X 0519622 8695649

Horizon and stage: Slottsmøya Member, Agardhfjellet Formation, Janusfjellet Subgroup, early middle Tithonian. 15.7 metres above the echinoderm marker bed.

Fig 12G and 12H

Ilium. From PMO 222.662, a single ilium (Fig 12A) is preserved. In lateral view, the element is curved, and the concavity is interpreted to be directed posteriorly. The curvature of the element is strongest at the approximate midpoint. Dorsal and posterior to this, the element narrows to the dorsal tip. The shape of the ilium is most similar to that of PMO 222.670, but

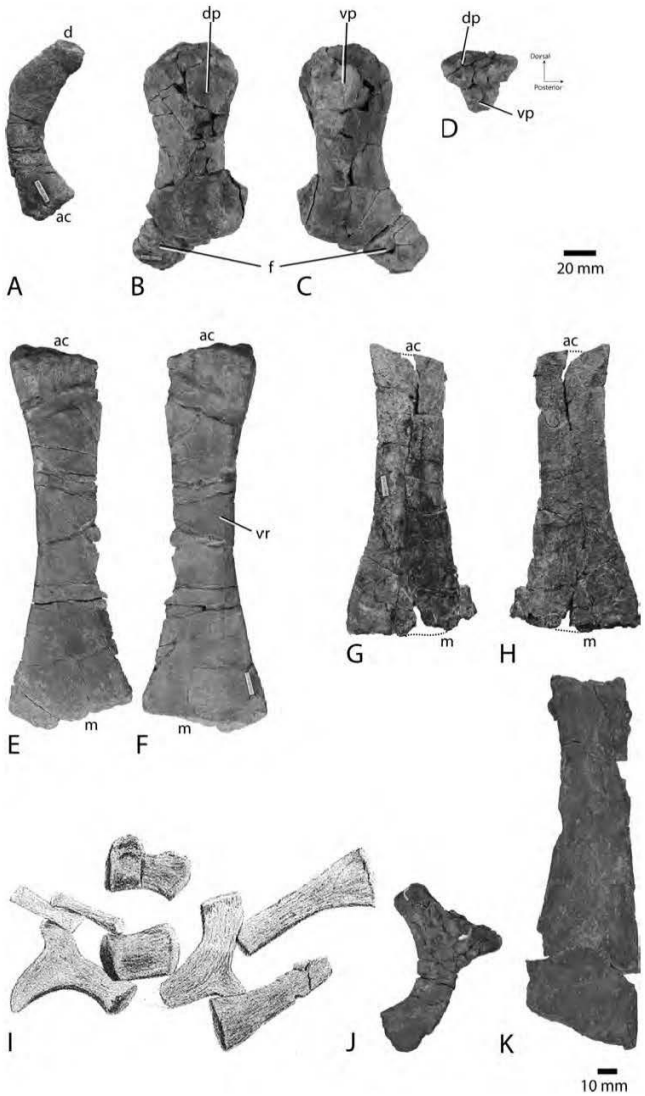

Fig 12. Pelvic girdles and hind fin material. Ilium of PMO 222.662 in A medial or lateral view. Posterior is to the right. Femur and fibula of PMO 222.662 in B dorsal, C ventral and D proximal views. Ischiopubis of PMO

222.662 in E dorsal and F ventral views. Ischiopubis of PMO 227.932 in G and H dorsal (?) and ventral (?) views. Dashed line shows where pieces are missing. Scale bar for A-G equals 20 mm. The Bauer (1898) specimen pelvic girdle in I, not to scale. Compare I to the right ilium of PMO 222.654 *Janusaurus lundi* holotype in J lateral view and the left ischiopubis of PMO 222.654 in K dorsal view. Scale bar for J-K equals 10 mm. Abbreviations: **ac** acetabular end, **d** dorsal end, **dp** dorsal process, **f** fibula, **m** medial end, **vp** ventral process, **vr** ventral ridge.

doi:10.1371/journal.pone.0169971.g012

the acetabular end is more anteroposteriorly expanded, and the posterior curvature more pronounced in PMO 222.662. The acetabular end bears a single large, posterior oval facet and a smaller rounded facet.

Ischiopubis. Both PMO 222.662 and PMO 227.932 preserve a single ischiopubis, which are described and compared together here (Fig 12E±12H). The ischium and pubis are completely fused and lack a foramen. PMO 222.662 (Fig 12E and 12F) is interpreted to be the left based on the criteria used for PMO 222.670 (above), but this is uncertain for PMO 227.932. PMO 222.662 is similar in overall morphology to PMO 222.670, described above. PMO 227.932 shares some features with PMO 222.670; it is anteroposteriorly and dorsoventrally slender and proximodistally elongate, and has one sharp margin and the other thickened and rounded. Based on the orientation of PMO 222.670, the thickened and rounded margin is interpreted to be located posteriorly, even though the thickened part is narrower anteroposteriorly than in PMO 222.670. Compared to the width of the medial end, the minimum anteroposterior width of PMO 227.932 is less narrow than that of PMO 222.670. The anterior margin of PMO 222.662 is sharp and slightly curved in dorsal view, and the posterior margin is dorsoventrally taller and more curved than the anterior. The posterior margin of PMO 227.932 is straight and the anterior margin curves slightly, but less than in PMO 222.670. The acetabular surface of PMO 222.662 is triangular in lateral view and is rugose. Its facets are not well demarcated and the ischiopubis is somewhat eroded in the acetabular end. A triangular area in the posteroventral area is interpreted to be the facet for the femur and the facet for the ilium more dorsally placed. The medial margin of PMO 222.662 is tallest dorsoventrally at the midpoint, and is coarsely rugose. The medial end of PMO 227.932 is expanded, but straighter than in PMO 222.670 and bears a notch along its entire distance, 5±10 mm deep.

Femur. A single femur is preserved in PMO 222.662 (Fig 12B±12D). The femur is constricted at midshaft and the distal end is anteroposteriorly wider than the proximal end. This differs from PMO 222.670, where the proximal end is anteroposteriorly wider, but resembles some specimens of *Ophthalmosaurus icenicus* (e.g. NHMUK 3534 and NHMUK 4531, pers. obs. AJR). It is oriented based on the processes and the facets according to Maxwell et al. [14] and the articulated hind fin of *Cryopterygius kristiansenae* [25]. The element has two processes, of which the smaller and less developed is assumed to be the dorsal process (Fig 12B). This process is barely expressed, but appears to extend past the midpoint of the shaft. The larger ventral process (Fig 12C) is more prominent and extends far past the midpoint of the shaft. Both processes are less developed than in many ophthalmosaurids, including PMO 222.670, but dorsoventrally taller than in *Keilhauia nui*. In proximal view (Fig 12D), the femoral head is an almost equilateral triangle, where the ventral process makes up one of the three corners. The distal end bears three facets, in contrast to *Keilhauia nui*, PMO 222.670 and most ophthalmosaurids, which have two facets, but similar to *Platypterygius hercynicus*, *P. americanus*, *P. australis* [26, 55, 59] and *Paraophthalmosaurus saratoviensis* [60]. One of the facets has a more acute angle relative to the proximodistal axis of the femur and is interpreted to be for the fibula. Thus, the femur is from the right side. The fibular and middle facets are longer anteroposteriorly than the anterior-most facet. The fibula (Fig 12B and 12C), which was found in articulation, is a square-shaped element.

Results and Discussion

Phylogenetic analysis

The holotype specimen of *Keilhauia nui* can be scored for 32% (18/56) of the characters in the Roberts et al. matrix [29]. The phylogenetic analysis resulted in a single MPT (Fig 13) (Length = 132; CI = 0.455, RI = 0.6). *Stenopterygius* was recovered as the sister group of Ophthalmosauridae, as in the topology presented in Ji et al. [48]. A monophyletic Ophthalmosauridae was recovered with robust support (Bremer support = 3) of which *Keilhauia nui* is the basalmost taxon. *Arthropterygius chrisorum* and *Undorosaurus gorodischensis* were the second and third most basal taxa, respectively. The remaining ophthalmosaurids are divided in two clades, Ophthalmosaurinae and Platypterygiinae, as in other analyses [29, 77, 78], although Bremer support for and within these clades is low, especially for Ophthalmosaurinae. The three described Slottsmøya Member taxa (*Janusaurus lundi*, *Cryopterygius kristiansenae* and *Palvennia hoybergeti*) form an unresolved polytomy within Ophthalmosaurinae; however, it is poorly supported (Bremer support = 1).

Taxonomic status of new Slottsmøya Member specimens

Keilhauia nui can be referred to Ophthalmosauridae on the basis of a humerus (Fig 8F and 8G) possessing a facet for an anterior accessory element and the absence of notching on the anterior edge of forefin elements [6, 19]. The phylogenetic analysis also recovered *Keilhauia nui* within Ophthalmosauridae (Fig 13), but as the basalmost taxon and not nested with other Slottsmøya Member species. Given that the holotype specimen of *Keilhauia nui* (PMO 222.655) cannot be scored for any cranial characters (46% of the characters in the matrix are cranial), we interpret this topology to be suspect. Similarly, *Undorosaurus gorodischensis* was recovered as the next most basal ophthalmosaurid; it too is scored primarily on the basis of postcranial remains even though it closely resembles *Cryopterygius kristiansenae* [25, 49] in postcranial morphology, particularly with respect to its forefin.

The holotype specimen of *Keilhauia nui* (PMO 222.655) is not a juvenile form of any other known taxon from the Slottsmøya Member Lagerstätte for which there is overlapping material (*Cryopterygius kristiansenae* and *Janusaurus lundi*; *Palvennia hoybergeti* lacks comparable material). It differs from *Cryopterygius kristiansenae* in having a posteriorly deflected ulnar facet (Fig 8F and 8G) and a fused ischiopubis (Fig 9E). *Keilhauia nui* shares some features with *Janusaurus lundi*, but differs in that the humerus and femur in *Janusaurus lundi* are much more robust and possess a larger dorsal and ventral processes than in *Keilhauia nui* (Fig 9F±9H). In addition, the ilium of *Keilhauia nui* clearly lacks an anterodorsal process (Fig 9A±9D) and is instead uniquely anteroposteriorly expanded in the dorsal end.

Keilhauia nui has a short humerus and femur relative to total body length as well as the least developed dorsal and ventral processes of the humerus and femur compared to almost all other ophthalmosaurids [18, 19, 25, 26, 52, 55, 57, 59, 68]. The presence of two autapomorphies among ophthalmosaurids and a unique character combination in PMO 222.655 warrant the erection of a new taxon. *Keilhauia nui* is also stratigraphically much younger (Berriasian; Fig 2) than other described Svalbard ichthyosaurs and is the youngest ichthyosaur from the Slottsmøya Member described to date.

The more incomplete material, PMO 222.670, PMO 222.662 and PMO 227.932 can only be assigned to Ophthalmosauridae, due to the lack of skull and forefin material. However, the pelvic girdle and femora of PMO 222.670 (Fig 11) are different from any other described taxa, being most similar to PMO 222.662, but differing in the number of distal facets on the femur (Fig 11I±11N). PMO 222.670 preserves approximately half of the vertebral column, displaying

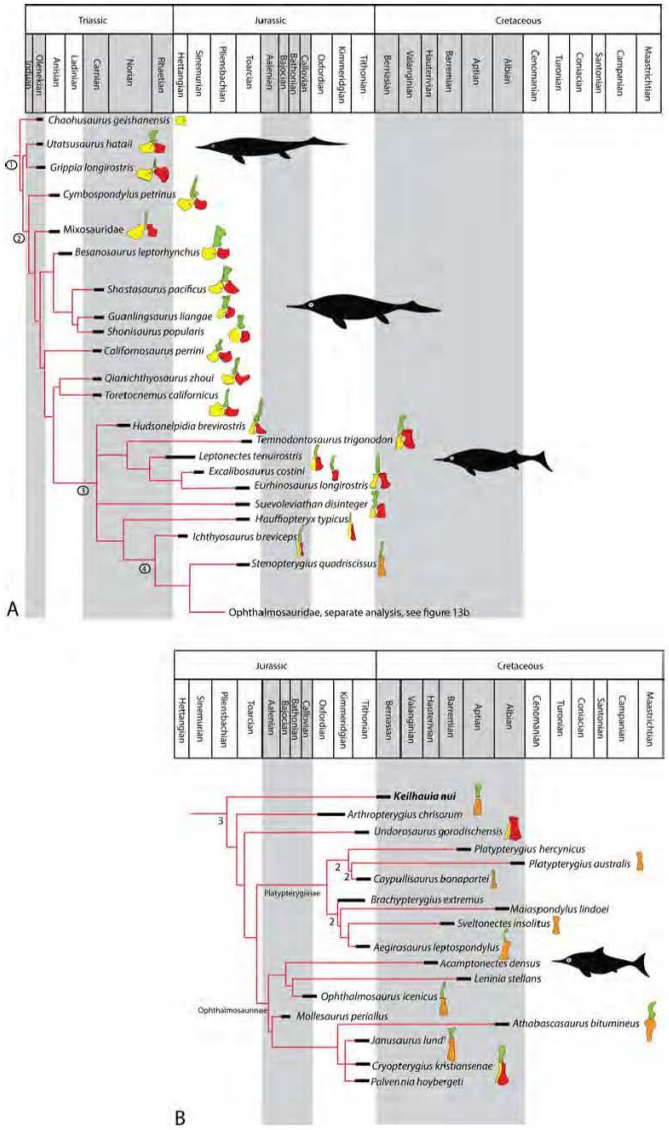
Triassic
Jurassic
Cretaceous
Induan
Olenekian
Anisian
Ladinian
Carnian
Norian
Rhaetian
Hettangian
Sinemurian
Pliensbachian
Toarcian
Aalenian
Bajocian
Bathonian
Callovian
Oxfordian
Kimmeridgian
Tithonian
Berriasian
Valanginian
Hauterivian
Barremian
Aptian
Albian
Cenomanian
Turonian
Coniacian
Santonian
Campanian
Maastrichtian
Chaohusaurus geishanensis
Utatsusaurus hatai
Grippia longirostris
Cymbospondylus petrinus
Mixosauridae
Besanosaurus leptorhynchus
Shastasaurus pacificus
Guanlingsaurus liangae
Shonisaurus popularis
Californosaurus perrini
Qianichthyosaurus zhoui
Toretocnemus californicus
Hudsonelpidia brevirostris
Temnodontosaurus trigonodon
Leptonectes tenuirostris
Excalibosaurus costini
Eurhinosaurus longirostris
Suevoleviathan disinteger
Hauffiopteryx typicus
Ichthyosaurus breviceps
Stenopterygius quadriscissus
Ophthalmosauridae, separate analysis, see figure 13b
A
Keilhauia nui
Arthropterygius chrisorum
Undorosaurus gorodischensis
Platypterygius hercynicus
Platypterygius australis
Caypullisaurus bonapartei
Platypterygiinae
Brachypterygius extremus
Maiaspondylus lindoei
Sveltonectes insolitus
Aegirosaurus leptospondylus
Acamptonectes densus
Leninia stellans
Ophthalmosaurinae
Ophthalmosaurus icenicus
Mollesaurus periallus
Athabascasaurus bitumineus
Janusaurus lundi
Cryopterygius kristiansenae
Palvennia hoybergeti
B

Fig 13. a. Time calibrated phylogeny of non-ophthalmosaurid Ichthyopterygia showing the evolution of the pelvic girdle. Articulated pelvic girdles either redrawn from the literature or based on personal observation (see references in S1 Table). Green = ilium; yellow = pubis; red = ischium; orange = fused ischiopubis. Pelvic girdles shown at different scales. Topology following Ji et al. 2016, showing only those taxa with a preserved pelvis. Clade names represented by circled numbers; 1 = Ichthyopterygia, 2 = Ichthyosauria, 3 = Parvipelvia, 4 = Thunnosauria. b. Time calibrated phylogeny of Ophthalmosauridae showing the evolution of the pelvic girdle. Articulated pelvic girdles either redrawn from the literature or based on personal observation (see references in S1 Table). Green = ilium; yellow = pubis; red = ischium; orange = fused ischiopubis. Pelvic girdles shown at different scales. Relationships following the single tree recovered in the new analysis of the Roberts et al. 2014 matrix (Length = 132; CI = 0.455, RI = 0.6.) Bremer support values for Ophthalmosauridae >2 are shown below the branches.

doi:10.1371/journal.pone.0169971.g013

a morphology rather typical for a large ophthalmosaurid, except the ribs that are rounded in cross-section and longitudinally striated. PMO 222.670 also shares some features with *Janusaurus lundi*, including the complete fusion of the ischiopubis (Figs 11E±11H and 12K) and femoral proportions and morphology (Fig 11I±11N) [29]. However, the ischiopubis of *Janusaurus lundi* is dorsoventrally thinner and less constricted midway than PMO 222.670 (Fig 11E±11H), and the ilium of PMO 222.670 lacks the anterodorsal process found in *Janusaurus lundi* (Fig 11A±11D).

Relative sizes of pelvic girdle and hind fin

The following results summarize the relationship between the ilium, ischiopubis, femur and humerus for Jurassic and Cretaceous ichthyosaur specimens (Fig 14).

Relative femur length

The femur length is 0.7±0.9 of humerus length in adult *Stenopterygius* (n = 30), and it is 0.5± 0.7 of humerus length in Late Jurassic (n = 12) and Cretaceous (n = 5) specimens (S2 Table). A significant correlation is found ($p = 1.55*10^{-5}$; $r^2 = 0.28$) between the femur: humerus length and geological age, with the femur becoming shorter relative to the humerus through time (Fig 14A).

Relative ilium length

No significant trend in the size of the ilium through geological time was found, when compared to either femur length ($p = 0.25$; $r^2 = 0.06$) (Fig 14B) or ischiopubis length (Fig 4C). A specimen of *Ichthyosaurus breviceps* (CAMSMX.50187) differs from other specimens in having a long ilium relative to the femur (1.6 times as long), whereas all the other specimens have an ilium that ranges between 0.7±1.2 of femoral length. The size relationship between the ilium and ischiopubis of *Stenopterygius* is between 0.6±0.8 (n = 8; 1 juvenile) (Fig 14C).

Relative ischiopubis length

Among ophthalmosaurids, a large range of ischiopubis length relative to ilium and femur length is found. Three Slottsmøya Member specimens (the holotype of *Janusaurus lundi* (PMO 222.654); PMO 222.670 and PMO 222.662) are unique in having very long ischiopubes; that are twice or more the length of the ilia (Fig 14C) and 1.8±2.0 times as long as the femur (Fig 14D). In contrast, *Keilhauia nui* (PMO 222.655) and the TMP 92.41.01 (Ophthalmosauridae indet. [8]) have relatively short ischiopubes (S2 Table). In TMP 92.41.01, the ischiopubis is shorter than the ilium, and in *Keilhauia nui* the ischiopubis is slightly shorter than the femur (Fig 14D).

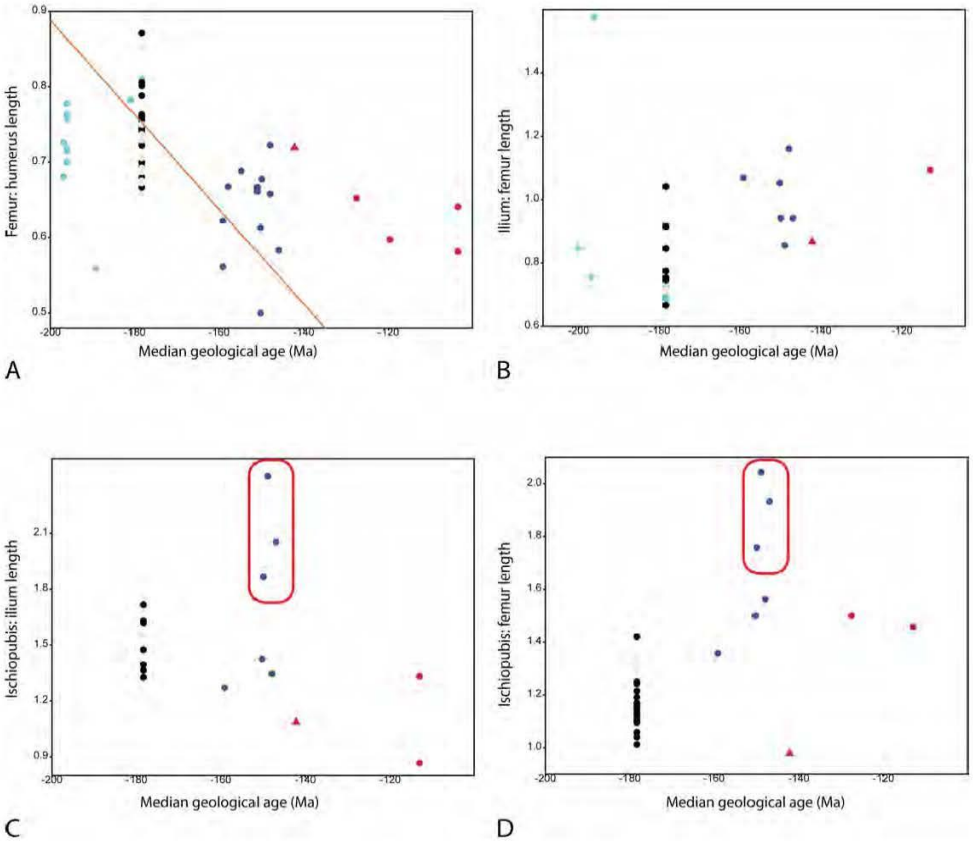

Fig 14. Statistical plots. *Keilhauia nui* (PMO 222.655) represented by a triangle. Light blue = Early/Middle Jurassic specimens with a tripartite pelvis; Beige = *Stenopterygius* juvenile specimens; Black = Early/Middle Jurassic specimens with a bipartite pelvis; Dark blue = Late Jurassic specimens; Red = Cretaceous specimens. See S2 Table for specimens and references. The Slottsmøya specimens with long ischiopubis are shown in the red ellipse. A. Femur: humerus length plotted against age (Ma). There is a significant correlation ($p = 1.55*10^{-5}$; $r^2 = 0.28$ between the femur: humerus length and geological age. Orange line shows linear regression. B. Ilium: femur length plotted against age (Ma). There is no correlation ($p = 0.25$, $r^2 = 0.06$). C. Ischiopubis: ilium length plotted against age (Ma). There is no correlation ($p = 0.29$, $r^2 = 0.07$). D. Ischiopubis: femur length plotted against age (Ma). There is a weak correlation ($p = 0.47*10^{-4}$, $r^2 = 0.07$).

doi:10.1371/journal.pone.0169971.g014

Evolution of the pelvic girdle in ichthyosaurs

Ichthyopterygians are believed to have become aquatic by the Early Triassic [79, 80]. However, the fossil record regarding this transition is still poorly understood, with the exception of *Sclerocormus parviceps* Jiang, Motani, Huang, Tintori, Hu, Rieppel, Fraser, Ji, Kelley, Fu and Zhang 2016 and *Cartorhynchus lenticarpus* Motani, Jiang, Chen, Tintori, Rieppel, Ji and Huang 2014

from the Spathian. The latter has been hypothesized to be able to move both on land and in water [79]. In the Triassic, early ichthyopterygians exhibited long tails and swam with axial undulation (anguilliform) [1, 5]. To obtain a high and efficient swimming speed, an organism must overcome drag, optimized by a spindle-shaped body with few irregularities, and with a ratio for length: maximum diameter of 4.5. Thus, from the Triassic to the Cretaceous, derived ichthyosaurians evolved a thunniform shape and an axial oscillatory swimming style, using a lunate tail on a narrow peduncle as the propulsive organ [1, 4, 5]. Not surprisingly, a similar length: maximum diameter value is seen in the body of extant fast-swimming dolphins and fishes [81]. Here, we attempt to focus on the evolutionary history of one important but understudied component of ichthyosaur locomotion±the pelvic girdle. In the following discussion, we provide an overview of the evolution of the three pelvic bones (Fig 13) taking into account new morphological data from several Slottsmøya Member specimens and the results of the statistical analyses (Fig 14).

Ilium. There are several Triassic genera with anteroposteriorly broad ilia, such as *Guanlingsaurus*, whereas other ilia were relatively straight and simple, such as *Toretocnemus* (Fig 13). *Californosaurus* bears a process on the anterior side of the ventral half of the ilium. In Jurassic parvipelvians, the ilium became narrower and simpler, with a varying degree of posterior curvature. *Suevoleviathan* is a possible exception in that it might have possessed a process (see discussion on orientation in McGowan and Motani 2003 [6]).

One important result from this study is that there is no relative size reduction of the ilium, compared to either femoral length or to ischiopubis length through the Jurassic and Cretaceous. McGowan and Motani [6: 40] noted that the ilium of *Stenopterygius* [a]is often relatively much smaller than it is in *Ichthyosaurus* and *Leptonectes*[o], presumably in relation to the other pelvic elements. Our calculations indicate that that the ilium of *Stenopterygius* is not particularly short relative to the femur or ischiopubis when compared to other Early±Middle Jurassic taxa (Fig 14B and 14C). There is generally little variation in the ilial shape of *Stenopterygius*; the curvature is similar in all investigated specimens, and the acetabular end is somewhat mediolaterally thicker than the dorsal end.

The morphology of the ilia from the Slottsmøya Member ichthyosaurs (Figs 9A±9D, 11A±11D, 12A, 12J and 13) differ from each other and from most other known genera. *Cryopterygius kristiansenae* has an anteroposteriorly broader ilium than most other parvipelvians, whereas PMO 222.670 and PMO 222.662 have simpler, more typical ilia (Figs 11A±11D and 12A). The most unusual ilia are probably those of *Janusaurus lundi*, which have a prominent anterodorsal process (Fig 12J). They resemble a specimen figured (and later lost in WWII) by Bauer [82] as [a]*Ichthyosaurus posthumus*[o] from Solnhofen (Lower Tithonian), which is possibly closely related to *Nannopterygius* [56] (Fig 12I). The element had previously been interpreted as an ischium [56, 82], but judging from its similarity to *Janusaurus lundi*, it is likely an ilium. A specimen of *Ophthalmosaurus icenicus* (NHMUK 3013, pers. obs. AJR) and a Slottsmøya Member specimen (PMO 222.662) (Fig 12A) possess an anterior margin with a distinct dorsal bend, but lack a distinct process as seen in *Janusaurus lundi*.

Ischium and pubis. In Triassic ichthyopterygians, the ischium and pubis consist of two large, rounded bones (Fig 13) [83], similar to some terrestrial squamates. In most genera the obturator foramen is present. In basal ichthyopterygians, cymbospondylids as well as mixosaurids, the pubis is larger than the ischium (Fig 13). In shastasaurids, the two elements are similar in size, whereas among basal parvipelvians with a tripartite pelvis the ischium is the larger element [6, 11]. During the Early Jurassic, the ischium and pubis generally evolved into mediolaterally elongated elements. *Stenopterygius* and *Hauffiopteryx* were the stratigraphically earliest ichthyosaurs with a fused ischium and pubis, a feature also found to be subject to individual variation in *Leptonectes* and *Temnodontosaurus* [84]. In *Hauffiopteryx*, the two elements are fused only at the acetabular end, whereas *Stenopterygius* possesses only a small foramen. In

Stenopterygius, the ischiopubis shows little intraspecific variation except in size. In *Ichthyosaurus* several species possess a pubis that is longer than the ischium, and the genus shows morphological variation in the pelvic girdle that might be important taxonomically [12].

The ischium and pubis are completely fused in the Slottsmøya Member ichthyosaurs (Figs 9E, 11E±11H, 12E±12H, 12K and 13) except for *Cryopterygius kristiansenae*, which shows a medial opening between the two elements. *Undorosaurus gorodischensis* also shows incomplete fusion [58] and an ischiopubis very similar to *Cryopterygius kristiansenae*. It has been suggested that the fusion might have been completed in life by cartilage [58]. Some specimens of *Ophthalmosaurus icenicus* exhibit a medial opening (probably between the two elements) that varies in size intraspecifically, and some specimens possess a foramen (e.g. Andrews 1910: 58; NHMUK 4754, AJR pers. obs.) [52, 85]. The loss of the ischiopubic foramen in Ophthalmosauridae occurred by the Late Jurassic, as shown in the Late Jurassic forms *Aegirosaurus leptospondylus*, *Janusaurus lundi*, *Caypullisaurus bonapartei* (Fig 13), *Paraophthalmos aurus*, PMO 222.670, PMO 222.662 and PMO 227.932.

Maisch and Matzke [11] suggested that complete proximal and distal fusion was a synapomorphy of the clade including *Stenopterygius* and Ophthalmosauridae. This is however not the result of the current phylogenetic analysis, where fusion of the ischiopubis does not appear as a synapomorphy for any clade. The varying degree of fusion of the ischium and pubis within Ophthalmosauridae could result from homoplasy or from intraspecific variation in some species. Complete fusion of the ischiopubis, including the lack of a foramen, can be observed in all known platypterygiine species for which an ischiopubis is known (Fig 13). However, complete fusion is also seen in two out of four known ophthalmosaurine species with a preserved ischiopubis, including *Athabascasaurus bitumineus* (alternatively recovered as a platypterygiine ophthalmosaurid in some studies [19]) and *Janusaurus lundi* [22, 29] and *Keilhauia nui*, whose phylogenetic position is considered uncertain. Thus, it is possible that complete fusion of the ischiopubis may be a valid synapomorphy for Platypterygiinae but not Ophthalmosaurinae [19].

The ischiopubis is long relative to the femur in Late Jurassic ophthalmosaurids, compared to *Stenopterygius*, *Hauffiopteryx* and the few known Cretaceous specimens (Fig 14D). Ischiopubes as large (twice as long or almost twice as long) compared to femur or ilium as those of *Janusaurus lundi* (PMO 222.654), PMO 222.670 and PMO 222.662 have not been described from other localities (Fig 14C and 14D). The large variation in relative size of the ischiopubis in Slottsmøya Member specimens may prove to be an informative new character in phylogenetic analyses, where the states are divided between specimens with an ischiopubis: ilium length ratio $\geq$ 2:1 and those with a lower ratio.

Evolution of the pelvic girdle compared to cetaceans

In contrast to ichthyopterygians, the transition from land to water in early cetaceans is relatively well-documented in the fossil record [79]. Among cetaceans, the small pelvic girdle probably evolved because the hind fin was reduced to minimize drag as their swimming mode evolved from limb paddling to caudal oscillation [86, 87]. Early cetaceans, such as pakicetids and ambulocetids (Early- early Middle Eocene) could walk on land and swim, and had four fully fused sacral vertebrae articulating with the pelvic girdle [88]. Later protocetids (early Middle Eocene) were more aquatic, and taxa such as *Georgiacetus* retained a large pelvic girdle, but without a connection to the sacrum. In Basilosauridae, the first fully aquatic clade, the hind fin was very reduced and not connected to the vertebral column [88]. In extant cetaceans, the pelvis and hind fin is very reduced in size and is often fused into a single element [15, 16].

The evolution of the pelvic girdle and hind fin in cetaceans and ichthyopterygians exhibit a number of similarities, such as loss of contact between the pelvis and the vertebral column and

the loss of the sacrum. *Utatsusaurus hataii*, a basal ichthyopterygian from the Early Triassic (Spathian), has a pelvis that articulates with two sacral ribs, but it does not seem to have been able to bear weight on land [89]. All stratigraphically younger ichthyosaur taxa lack a true sacrum [6] (but see discussion on *Grippia* in Maisch and Matzke 2000) (contra [90, 91]). Cetaceans and ichthyosaurs also reduced the relative size of the pelvic girdle, fused two or more pelvic girdle elements and lost the obturator foramen. There was clearly reduction in the relative size of the pelvic girdle and hind fin from the earliest ichthyosaurs in the Triassic to the more spindle-shaped taxa in the Jurassic, which is reflected in the clade name Parvipelvia ("small pelvis"). However, for most of the investigated length relationships of the pelvic girdle and femur there is no demonstrable trend from the earliest to the latest members of this clade (Fig 14). Although the pelvic girdle and hind fin in ichthyosaurs are not continuously reduced in size throughout their evolutionary history, or disappear entirely, these elements were nonetheless small compared to the total body size. *Keilhauia nui* (PMO 222.655) did possess a relatively small pelvic girdle, as well as a small humerus and femur, but within the range seen in parvipelvians.

Function of pelvis and hind fin in ichthyosaurs

"Doubtless had the ichthyosaurs continued to the present time, they would have lost entirely the hind legs, as have the cetaceans." [83: 117]. Hind fins in vertebrates have been independently lost multiple times throughout the history of life [3]. In secondarily aquatic vertebrates hind limbs have followed multiple different evolutionary pathways, including clades that retained functional limbs throughout their entire history, such as sauropterygians and mosasauroids, and others in which the hind fins have been lost or reduced, namely cetaceans and ichthyopterygians. However, an important difference between ichthyopterygians and cetaceans is that in the latter, some pelvic girdle and hind fin elements are lost completely (at least podial elements and the femur in many taxa), whereas in ichthyosaurs the complete loss of these elements has not been demonstrated [5, 7].

It is interesting to note that cetaceans completely lost their external hind fin in relatively short time span during the transition in becoming fully marine (approximately 8 million years) [88], whereas the ichthyosaurs retained an external hind fin throughout their existence in the marine realm (approximately 150 million years)[5]. That ichthyosaurs did not lose their external hind fin suggests that these elements retained a function in life, and were not only a by-product of obtaining a streamlined shape for fast swimming. Even for the small innominate of cetaceans, its retention suggests that it still had functional significance [16].

The ichthyosaur hind fin possibly had a function related to reproduction or locomotion. Male turtles and crocodilians possess a penis [92], but most fully terrestrial reptiles do not, and it is unknown in ichthyosaurs. Assuming their involvement in reproductive purposes, the hind fins could have played a role in coupling, or the pelvic girdle may have anchored the penis muscles, as in cetaceans [16]. Morphological variation in the large ischiopubes of Slottsmøya Member specimens could also result from variation in pelvic musculature. Small hind fins used in coupling has also been suggested for *Basilosaurus isis* [93]. However, the fused pelvic bones are oriented differently; anteroposteriorly in cetaceans, and mediolaterally in ichthyosaurs. It has been suggested that a flexible pelvic girdle is an adaptation to viviparity in some marine reptiles [94], and this could therefore apply to the viviparous ichthyosaurs. However, whether a flexible pelvic girdle is linked to viviparity is uncertain because most cases of viviparity in reptiles are in terrestrial species [94].

A significant correlation exists in the relationship between femur: humerus length and geological age of the specimen (Fig 14A). This confirms previous research [11], and is interesting

because a larger number of late Middle Jurassic to Cretaceous specimens were included in this study. Through time, the femur becomes shorter in length relative to the humerus. This means that the relationship between the two fin pairs changed through time, possibly related to locomotion. The fins have never been the main propulsion organ in ichthyosaurs, but were probably used for steering and stabilization, with the forefin as the main steering surface [5, 7], which is most common among aquatic animals [95]. Lomax and Massare [96] suggested that the small hind fin of *Ichthyosaurus anningae* played only a minor role in maneuvering. It has also been suggested that hind fins of Late Jurassic ichthyosaurs had no function in steering or locomotion [7]. Strong correlations between serially homologous elements (among them humerus-femur) has however been seen as indirect evidence for a functional role of the hind fin similar to that of the forefin, as control surfaces [97].

Supporting Information

S1 Text. Supporting material and methods information. Supporting material and methods information, including procedure for measurements of the vertebral column, terminology used for the pelvic girdle, method for collecting morphological information about pelvic girdle elements of ichthyosaurs and cetaceans, more information on the method used to calculate the relative lengths of pelvic girdle elements, institutional abbreviations for specimens used in calculations and references for the pelvic girdle drawings in Fig 13, S1 Table and S2 Table.
(DOCX)

S2 Text. Description of characters used in the phylogenetic analysis. The character list is taken from Roberts et al. 2014.
(DOCX)

S3 Text. Data matrix for the phylogenetic analysis.
(DOCX)

S1 Table. Pelvic girdle material from ichthyopterygians Pelvic girdle material from ichthyopterygians, showing for which species either ilium, ischium, pubis or all three are described in the literature, sorted according to time period. The shape of the elements is presented in Fig 13 together with a time-calibrated phylogeny. Comments: * Taxonomic unclearity in the family, example species shown; ** Pubis not preserved; *** Undet. fragments from the pelvic girdle preserved, **** Pelvic material known for more than one species in this genus, ***** Other species in this genus might preserve pelvic girdle material. In addition, the ischiopubis and ilium are known for the Alberta specimen Ophthalmosauridae indet. TMP 92.41.01. References for the pelvic girdles mentioned in S1 Table, see S1 Text for bibliography.
(DOCX)

S2 Table. Specimens used in calculations. Specimens used in calculating relative sizes of pelvic girdle elements, femora and humeri and the measurements. References given for where the measurements are taken from.
(XLSX)

S3 Table. Vertebral measurements for PMO 222.655, holotype of *Keilhauia nui*.
(XLSX)

Acknowledgments

A huge thank you is offered to Spitsbergen Mesozoic Research Group, with a special thanks to H. A. Nakrem, Ø. Hammer and the volunteers M. Høyberget, Ø. Enger, S. Larsen, T. Wensås,

L. Kristiansen and B. Funke. M.-L. K. Funke and V. E. Nash are thanked for their assistance in the preparation of the specimens.

For access to collections with ichthyosaur specimens, thanks to E. Maxwell (SMNS), M. Fernandez (MOZ, MLP), M. Riley (CAMSM), E. Howlett (OUMNH), V. Ward (LEIUG), O. Rauhut (SNSB-BSPG), N. Clark (GLAHM), V.M. Efimov (EP).

For help with measurements and discussion on published specimens; M Fernandez and D. Martill. For discussion on the Russian specimens; N. Zverkov and M. Arkhangelsky.

For access to collections and discussion on cetacean pelvic girdles; Ø Wiig (NHM, Oslo), T. Fredriksen (NHM, Bergen).

Body outline drawings in Fig 13 by Esther van Hulsen.

The following permits were given by the Governor of Svalbard for the excavations in 2007, 2010 and 2011; Sak 2006±00528; RIS ID 3707; RIS ID: 4760. All necessary permits were obtained for the described study, which complied with all relevant regulations.

The reviewers V. Fischer, J. Massare, J. Liu and D. Lomax are sincerely thanked for their suggestions which helped improve the manuscript.

Author Contributions

Conceptualization: LLD AJR PSD JHH.

Formal analysis: LLD AJR.

Funding acquisition: JHH.

Investigation: LLD AJR PSD JHH.

Methodology: LLD.

Project administration: JHH.

Resources: JHH.

Visualization: LLD.

Writing ± original draft: LLD.

Writing ± review & editing: LLD AJR PSD JHH.

References

1. Motani R. Evolution of fish-shaped reptiles (Reptilia: Ichthyopterygia) in their physical environments and constraints. Annu Rev Earth Planet Sci. 2005; 33:395±420.
2. Bardet N. Stratigraphic evidence for the extinction of the ichthyosaurs. Terra Nova. 1992; 4:649±56.
3. Don EK, Currie PD, Cole NJ. The evolutionary history of the development of the pelvic fin/hindlimb. J Anat. 2013; 222(1):114±33. doi: 10.1111/j.1469-7580.2012.01557.x PMID: 22913749
4. Massare JA. Swimming capabilities of Mesozoic marine reptiles: implications for methods of predation. Paleobiology. 1988; 14(2):187±205.
5. Sander PM. Ichthyosauria: their diversity, distribution, and phylogeny. Paläont Z. 2000; 74(1±2):1±35.
6. McGowan C, Motani R. Ichthyopterygia. Sues H-D, editor. München: Verlag Dr. Friedrich Pfeil; 2003. 182 p.
7. Buchholtz EA. Swimming styles in Jurassic ichthyosaurs. J Vert Paleo. 2001; 21(1):61±73.
8. Maxwell EE, Druckenmiller PS. A small ichthyosaur from the Clearwater Formation (Alberta, Canada) and a discussion of the taxonomic utility of the pectoral girdle. Paläont Z. 2011; 85(4):457±63.
9. Dal Sasso C, Pinna G. *Besanosaurus leptorhynchus* n. gen. n. sp., a new shastasaurid ichthyosaur from the Middle Triassic of Besano (Lombardy, N. Italy). Paleontologia Lombarda. 1996; 4:1±21.
10. Motani R. Phylogeny of the Ichthyopterygia. J Vert Paleo. 1999; 19(3):473±96.

11. Maisch MW, Matzke AT. The Ichthyosauria. Stuttgarter Beiträge zur Naturkunde Serie B. 2000(298):1±159.
12. Massare JA, Lomax DR. A new specimen of *Ichthyosaurus conybeari* (Reptilia, Ichthyosauria) from Watchet, Somerset, England, U.K., and a re-examination of the species. J Vert Paleo. 2016; 36(5).
13. Massare J, Lomax DR. An *Ichthyosaurus breviceps* collected by Mary Anning: new information on the species. Geol Mag. 2014; 151(1):21±8.
14. Maxwell EE, Zammit M, Druckenmiller PS. Morphology and orientation of the ichthyosaurian femur. J Vert Paleo. 2012; 32(5):1207±11.
15. Lislevand T. Utviklingen av hvalenes hofter og baklemmerÐDet Iñrebokeks empel i evolusjonsbiologi. Naturen. 2006; 5:196±204.
16. Dines JP, Otárola-Castillo E, Ralph P, Alas J, Daley T, Smith AD, et al. Sexual selection targets cetacean pelvic bones. Evolution. 2014; 68(11):3296±306. doi: 10.1111/evo.12516 PMID: 25186496
17. Fernández M. Redescription and phylogenetic position of *Caypullisaurus* (Ichthyosauria: Ophthalmosauridae). Journal of Paleontology. 2007; 81(2):368±75.
18. Fischer V, Bardet N, Guiomar M, Godefroit P. High Diversity in Cretaceous Ichthyosaurs from Europe Prior to Their Extinction. PLoS ONE. 2014; 9(1):e84709. doi: 10.1371/journal.pone.0084709 PMID: 24465427
19. Fischer V, Maisch MW, Naish D, Kosma R, Liston J, Joger U, et al. New Ophthalmosaurid Ichthyosaurs from the European Lower Cretaceous Demonstrate Extensive Ichthyosaur Survival across the Jurassic±Cretaceous Boundary. PLoS ONE. 2012; 7(1):e29234. doi: 10.1371/journal.pone.0029234 PMID: 22235274
20. Maxwell EE, Dick D, Padilla S, Parra ML. A new ophthalmosaurid ichthyosaur from the Early Cretaceous of Colombia. Pap Palaeontol. 2015; 2(1):59±70.
21. Fischer V, Arkhangelsky MS, Naish D, Stenshin IM, Uspensky GN, Godefroit P. *Simbirskiasaurus* and *Pervushovisaurus* reassessed: implications for the taxonomy and cranial osteology of Cretaceous platypterygiine ichthyosaurs. Zoological Journal of the Linnean Society. 2014; 171(4):822±41.
22. Druckenmiller PS, Maxwell EE. A new Lower Cretaceous (lower Albian) ichthyosaur genus from the Clearwater Formation, Alberta, Canada. Can J Earth Sci. 2010; 47(8):1037±53.
23. Fischer V, Arkhangelsky MS, Uspensky GN, Stenshin IM, Godefroit P. A new Lower Cretaceous ichthyosaur from Russia reveals skull shape conservatism within Ophthalmosaurinae. Geol Mag. 2013; 151(6):60±70.
24. Fischer V, Masure E, Arkhangelsky MS, Godefroit P. A new Barremian (Early Cretaceous) ichthyosaur from Western Russia. J Vert Paleo. 2011; 31(5):1010±25.
25. Druckenmiller PS, Hurum JH, Knutsen EM, Nakrem HA. Two new ophthalmosaurids (Reptilia: Ichthyosauria) from the Agardhfjellet Formation (Upper Jurassic: Volgian/Tithonian), Svalbard, Norway. Norwegian Journal of Geology. 2012; 92(2±3):311±39.
26. Zammit M, Norris RM, Kear BP. The Australian Cretaceous ichthyosaur *Platypterygius australis*: a description and review of postcranial remains. J Vert Paleo. 2010; 30(6):1726±35.
27. Hurum JH, Nakrem HA, Hammer Ø, Knutsen EM, Druckenmiller PS, Hryniewicz K, et al. An Arctic LagerstätteÐthe Slottsmøya Member of the Agardhfjellet Formation (Upper JurassicÐLower Cretaceous) of Spitsbergen. Norwegian Journal of Geology. 2012; 92(2±3):55±64.
28. Delsett LL, Novis LK, Roberts AJ, Koevoets MJ, Hammer Ø, Druckenmiller PS, et al. The Slottsmøya marine reptile Lagerstätte: depositional environments, taphonomy and diagenesis. In: Kear BP, Lindgren J, Hurum JH, Milán J, Vajda V, editors. Mesozoic Biotas of Scandinavia and its Arctic Territories. Geological Society Special Publication. 434. London: Geological Society; 2016. p. 165±88.
29. Roberts AJ, Druckenmiller PS, Sætre G-P, Hurum JH. A New Upper Jurassic Ophthalmosaurid Ichthyosaur from the Slottsmøya Member, Agardhfjellet Formation of Central Spitsbergen. PLoS ONE. 2014; 9(8):e103152. doi: 10.1371/journal.pone.0103152 PMID: 25084533
30. Fernández M, Campos L. Ophthalmosaurids (Ichthyosauria: Thunnosauria): Alpha taxonomy, clades and names. Publicación Electrónica de la Asociación Paleontológica Argentina. 2015; 15(1):20±30.
31. Ensom PC, Clements RG, Feist-Burkhardt S, Milner AR, Chitolie J, Jeffery PA, et al. The age and identity of an ichthyosaur reputedly from the Purbeck Limestone Group, Lower Cretaceous, Dorset, southern England. Cretac Res. 2009; 30(3):699±709.
32. Green JP, Lomax DR. An ichthyosaur (Reptilia: Ichthyosauria) specimen from the Lower Cretaceous (Berriasian) Spilsby Sandstone Formation of Nettleton, Lincolnshire, UK. Proc Geol Assoc. 2014; 125(4):432±6.
33. Fernández M. Ichthyosauria. In: Gasparini Z, Salgado L, Coria RA, editors. Patagonian Mesozoic reptiles. Life of the past. Bloomington: Indiana University Press; 2007. p. 271±91.

34. Zverkov NG, Arkhangelsky MS, Pardo-PÃ©rez J, Beznosov PA. On the Upper Jurassic Ichthyosaur remains from the Russian North. Proceedings of the Zoological Institute RAS. 2015; 319(1):81±97.
35. Pardo-PÃ©rez J, Frey E, Stinnesbeck W, FernÃ¡ndez MS, Rivas L, Salazar C, et al. An ichthyosaurian forefin from the Lower Cretaceous Zapata Formation of southern Chile: implications for morphological variability within *Platypterygius*. Palaeobio Palaeoenv. 2012; 92(2):287±94.
36. Dypvik H, Nagy J, Eikeland TA, Backer-Owe K, Andresen A, Haremo P, et al. The Janusfjellet Subgroup (Bathonian to Hauterivian) in central Spitsbergen: a revised lithostratigraphy. Polar Res. 1991; 9 (1):21±43.
37. Torsvik TH, Van der Voo R, Preeden U, Mac Niocaill C, Steinberger B, Doubrovine PV, et al. Phanerozoic polar wander, palaeogeography and dynamics. Earth Sci Rev. 2012; 114(3±4):325±68.
38. Dypvik H, Zakharov V. Fine-grained epicontinental Arctic sedimentationÐmineral ogy and geochemistry of shales from the Late Jurassic-Early Cretaceous transition. Norwegian Journal of Geology. 2012; 92 (2±3):65±87.
39. Steel RJ, Worsley D. Svalbard's post-Caledonian strataÐa n atlas of sedimentational patterns and palaeogeographic evolution. In: Spencer AM, editor. Petroleum Geology of the North European Margin. Dordrecht: Springer Netherlands; 1984. p. 109±35.
40. Collignon M, Hammer Ø. Petrography and sedimentology of the Slottsmøya Member at Janusfjellet, central Spitsbergen. Norwegian Journal of Geology. 2012; 92(2±3):89±101.
41. Hammer Ø, Collignon M, Nakrem HA. Organic carbon isotope chemostratigraphy and cyclostratigraphy in the Volgian of Svalbard. Norwegian Journal of Geology. 2012; 92(2±3):103±12.
42. Wierzbowski A, Hryniewicz K, Hammer Ø, Nakrem HA, Little CTS. Ammonites from hydrocarbon seep carbonate bodies from the uppermost JurassicÐlo wermost Cretaceous of Spitsbergen and their biostratigraphical importance. Neues Jahrb Geol Palaontol Abh. 2011; 262(3):267±88.
43. Nagy J, Basov VA. Revised foraminiferal taxa and biostratigraphy of Bathonian to Ryazanian deposits in Spitsbergen. Micropaleontology. 1998; 44(3):217±55.
44. Dalseg TS, Nakrem HA, Smelror M. Organic-walled microfossils and palynodebris in cold seep carbonate deposits: The Upper Jurassic±Lower Cretaceous Agardhfjellet Formation on Svalbard (Arctic Norway). Norwegian Journal of Geology. 2016; 96(2).
45. Zakharov VA. In defense of the Volgian Stage. Stratigr Geol Correl. 2003; 11(6):585±93.
46. Ogg JG, Hinnov LA. Jurassic. In: Gradstein FM, Ogg JG, Schmitz MD, Ogg G, editors. The Geologic Time Scale 2012. Oxford: Elsevier; 2012. p. 732±79.
47. Hammer Ø, Harper DAT, Ryan TD. PAST: Paleontological statistics software package for education and data analysis. Palaeontologia Electronica 2001; 4(1).
48. Ji C, Jiang D-Y, Motani R, Rieppel O, Hao W-C, Sun Z-Y. Phylogeny of the Ichthyopterygia incorporating recent discoveries from South China. J Vert Paleo. 2015; 36(1):e1025956.
49. Arkhangelsky MS, Zverkov NG. On a new ichthyosaur of the genus *Undorosaurus*. Proceeding of the Zoological Institute RAS. 2014; 318(3):187±96.
50. Fischer V, Bardet N, Benson RBJ, Arkhangelsky MS, Friedman M. Extinction of fish-shaped marine reptiles associated with reduced evolutionary rates and global environmental volatility. Nat Commun. 2016; 7:1±11.
51. Goloboff PA, Farris JS, Nixon KC. TNT, a free program for phylogenetic analysis. Cladistics. 2008; 24 (5):774±86.
52. Kirton AM. A review of British Upper Jurassic Ichthyosaurs. Unpublished: University of Newcastle upon Tyne; 1983.
53. Maxwell EE. Generic Reassignment of an Ichthyosaur from the Queen Elizabeth Islands, Northwest Territories, Canada. J Vert Paleo. 2010; 30(2):403±15.
54. FernÃ¡ndez MS. A new ichthyosaur from the Tithonian (Late Jurassic) of the Neuquen basin, Northwestern Patagonia, Argentina. Journal of Paleontology. 1997; 71(3):479±84.
55. Maxwell EE, Kear BP. Postcranial anatomy of *Platypterygius americanus* (Reptilia: Ichthyosauria) from the Cretaceous of Wyoming. J Vert Paleo. 2010; 30(4):1059±68.
56. Bardet N, FernÃ¡ndez M. A new ichthyosaur from the Upper Jurassic lithographic limestones of Bavaria. Journal of Paleontology. 2000; 74(3):503±11.
57. Maxwell EE, Caldwell MW. A new genus of ichthyosaur from the lower cretaceous of Western Canada. Palaeontology. 2006; 49:1043±52.
58. Efimov VM. A new family of Ichthyosaurs, the Undorosauridae fam. nov. from the Volgian Stage of the European part of Russia. Paleontological Journal. 1999; 33(2):51±8.

59. Kolb C, Sander PM. Redescription of the ichthyosaur *Platypterygius hercynicus* (Kuhn 1946) from the Lower Cretaceous of Salzgitter (Lower Saxony, Germany). Palaeontographica Abteilung A: Palæozoologie-Stratigraphie. 2009; 288(4±6):151±92.

60. Arkhangelsky MS. On the ichthyosaurian fossils from the Volgian stage of the Saratov region. Paleontologicheskii Zhurnal. 1998(2):87±91.

61. Johnson R. Size independent criteria for estimating age and the relationships among growth parameters in a group of fossil reptiles (Reptilia: Ichthyosauria). Can J Earth Sci. 1977; 14(8):1916±24.

62. Kear BP, Zammit M. *In utero* foetal remains of the Cretaceous ichthyosaurian *Platypterygius*: ontogenetic implications for character state efficacy. Geol Mag. 2014; 151(1):71±86.

63. Broili F. Ein neuer Ichthyosaurus aus der norddeutschen Kreide. Palaeontographica Stuttgart. 1907; 54 (2±3):139±62.

64. Wade M. A review of the Australian Cretaceous longipinnate ichthyosaur *Platypterygius* (Ichthyosauria, Ichthyopterygia). Memoirs of the Queensland Museum. 1990; 28(1):115±37.

65. Paparella I, Maxwell EE, Cipriani A, Roncacè S, Caldwell MW. The first ophthalmosaurid ichthyosaur from the Upper Jurassic of the Umbrian±Marchean Apennines (Marche, Central Italy). Geol Mag. 2016:1±22.

66. Fernández M, Talevi M. Ophthalmosaurian (Ichthyosauria) records from the Aalenian±Bajocian of Patagonia (Argentina): an overview. Geol Mag. 2014; 151(1):49±59.

67. Gilmore CW. The osteology of *Baptanodon* (Marsh). Memoirs of the Carnegie Museum. 1905; 2(2):77± 129.

68. Arkhangelsky MS. On a new Ichthyosaurian Genus from the Lower Volgian Substage of the Saratov, Volga Region. Paleontological Journal. 1997; 31(1):87±91.

69. Fernández M, Aguirre-Urreta MB. Revision of *Platypterygius hauthali* von Huene, 1927 (Ichthyosauria: Ophthalmosauridae) from the Early Cretaceous of Patagonia, Argentina. J Vert Paleo. 2005; 25 (3):583±7.

70. Hulke JW. Note on an Ichthyosaurus (*I. enthekiodon*) from Kimmeridge Bay, Dorset. Quarterly Journal of the Geological Society. 1871; 27:440±1.

71. Maxwell EE, Caldwell MW. A new genus of ichthyosaur from the Lower Cretaceous of Western Canada. Palaeontology. 2006; 49:1043±1052.

72. Boulenger GA. Exhibition of, and remarks upon, a paddle of a new species of ichthyosaur. Proceedings of the Zoological Society of London. 1904; 1:424±6.

73. Efimov VM. Ichthyosaurs of a new genus *Yasykovia* from the Upper Jurassic Strata of European Russia. Paleontological Journal. 1999; 33(1):92±100.

74. Arkhangelsky MS. On the ichthyosaur *Otschevia* from the Volgian Stage of the Volga region. Paleontological Journal. 2000; 34(5):549±52.

75. Hammer Ø, Nakrem HA, Little CTS, Hryniewicz K, Sandy MR, Hurum JH, et al. Hydrocarbon seeps from close to the Jurassic-Cretaceous boundary, Svalbard. Palaeogeography, Palaeoclimatology, Palaeoecology. 2011; 306(1±2):15±26.

76. Novis LKS. A taphonomic study of marine reptiles from the Upper Jurassic of Svalbard. Unpublished: University of Oslo; 2012.

77. Zverkov NG, Arkhangelsky MS, Stenshin IM. A review of Russian Upper Jurassic Ichthyosaurs with an intermedium/humeral contact. Reassessing *Grendelius* McGowan, 1976. Proceeding of the Zoological Institute RAS. 2015; 319(4):558±88.

78. Druckenmiller PS, Maxwell EE. A Middle Jurassic (Bajocian) ophthalmosaurid (Reptilia, Ichthyosauria) from the Tuxedni Formation, Alaska and the early diversification of the clade. Geol Mag. 2013.

79. Motani R, Jiang D-y, Chen G-b, Tintori A, Rieppel O, Ji C, et al. A basal ichthyosauriform with a short snout from the Lower Triassic of China. Nature. 2014; 517:485±8. doi: 10.1038/nature13866 PMID: 25383536

80. Jiang D-Y, Motani R, Huang J-D, Tintori A, Hu Y-C, Rieppel O, et al. A large aberrant stem ichthyosauriform indicating early rise and demise of ichthyosauromorphs in the wake of the end-Permian extinction. Scientific Reports. 2016; 6:26232. doi: 10.1038/srep26232 PMID: 27211319

81. Carroll RL. Patterns and processes of vertebrate evolution. Briggs DEG, Dodson P, MacFadden BJ, Sepkoski J, Spicer RA, editors. Cambridge: Cambridge University Press; 1997. 448 p.

82. Bauer F. Die Ichthyosaurier des oberen weissen Jura. Palaeontographica. 1898; 44(6):283±328.

83. Williston SW. Water reptiles of the past and present. Chicago: The University of Chicago Press; 1914. 251 p.

84. McGowan C. Giant ichthyosaurs of the early Jurassic. Can J Earth Sci. 1996; 33(7):1011±21.

85. Andrews CW. A descriptive catalogue of the marine reptiles of the Oxford clay. Based on the Leeds Collection in the British Museum (Natural History), London. Part I. London: Trustees of the British Museum; 1910. 205 p.

86. Buchholtz EA. Vertebral osteology and swimming style in living and fossil whales (Order: Cetacea). J Zool. 2001; 253(2):175±90.

87. Thewissen JGM, Cooper LN, George JC, Bajpai S. From Land to Water: the Origin of Whales, Dolphins, and Porpoises. Evo Edu Outreach. 2009; 2:272±88.

88. Uhen MD. The Origin(s) of Whales. Annu Rev Earth Planet Sci. 2010; 38:189±219.

89. Motani R, Minoura N, Ando T. Ichthyosaurian relationships illuminated by new primitive skeletons from Japan. Nature. 1998; 393:255±7.

90. Wiman C. Über den Beckengürtel bei *Stenopterygius quadriscissus*. Bulletin of the Geological Insitution of the University of Uppsala. 1921; 18:19±32.

91. Wiman C. Über den Beckengürtel der Triasichthyosaurier. Palaeontologische Zeitschrift. 1922; 5 (3):272±6.

92. Kelly DA. Penile Anatomy and Hypotheses of Erectile Function in the American Alligator (*Alligator mississippiensis*): Muscular Eversion and Elastic Retraction. Anat Rec. 2013; 296(3):488±94.

93. Gingerich PD, Smith BH, Simons EL. Hind Limbs of Eocene *Basilosaurus*: Evidence of feet in whales. Science. 1990; 249(4965):154±7. doi: 10.1126/science.249.4965.154 PMID: 17836967

94. Motani R, Jiang D-y, Tintori A, Rieppel O, Chen G-b. Terrestrial Origin of Viviparity in Mesozoic Marine Reptiles Indicated by Early Triassic Embryonic Fossils. PLoS ONE. 2014; 9(2):e88640. doi: 10.1371/journal.pone.0088640 PMID: 24533127

95. Lighthill MJ. Hydromechanics of aquatic animal propulsion. Annu Rev Fluid Mech. 1969; 1:413±46.

96. Lomax DR, Massare JA. A new species of *Ichthyosaurus* from the Lower Jurassic of West Dorset, England, U.K. J Vert Paleo. 2015; 35(2):e903260.

97. Maxwell EE, Dececchi TA. Ontogenetic and stratigraphic influence on observed phenotypic integration in the limb skeleton of a fossil tetrapod. Paleobiology. 2013; 39(1):123±34.